Numéro d'ordre : 42487

Université des Sciences et Technologies de Lille
Ecole Doctorale Biologie-Santé de Lille

Thèse de Doctorat

Sven POTELLE

En vue de l'obtention du grade de
Docteur de l'Université de Lille Nord de France - Lille I

Discipline : Aspects cellulaires et moléculaires de la biologie
Spécialité : Biochimie et biologie moléculaire

TMEM165: un nouvel acteur de la régulation de l'homéostasie golgienne du Mn2+, impliqué dans les anomalies congénitales de la glycosylation

Présentée le 08 Décembre 2017 devant la commission d'examen

Président :	Dr. Anne Harduin-Lepers (Université de Lille 1)
Rapporteurs :	Pr. Valérie Cormier-Daire (Hôpital Necker-Paris)
	Pr. Hudson Freeze (Sanford Burnham Prebys Medical Discovery Institute, USA)
Examinateurs :	Dr. Sophie Groux-Degroote (Université de Lille 1)
	Pr. Emile Van Schaftingen (Institut de Duve - Belgique)
Directeur de thèse :	Dr. François Foulquier (Université de Lille 1)

Numéro d'ordre : 42487

Université des Sciences et Technologies de Lille
Ecole Doctorale Biologie-Santé de Lille

Doctoral Thesis

Sven POTELLE

To obtain the degree of PhD
Université de Lille Nord de France - Lille I

Discipline : Cellular and molecular aspects of biology
Speciality : Biochemistry and molecular biology

TMEM165: a new regulator of Golgi Mn2+ homeostasis involved in Congenital Disorders of Glycosylation

Presented on the 8th December 2017 in front of the examination board

President :	Dr. Anne Harduin-Lepers (Lille 1 University)
Reporters :	Pr. Valérie Cormier-Daire (Necker hospital-Paris)
	Pr. Hudson Freeze (Sanford Burnham Prebys Medical Discovery Institute, USA)
Examiners :	Dr. Sophie Groux-Degroote (Lille 1 University)
	Pr. Emile Van Schaftingen (De Duve Institute, Belgium)
PhD supervisor :	Dr. François Foulquier (Lille 1 University)

« The seeker after the truth is not one who studies the writings of the ancients and, following his natural disposition, puts his trust in them, but rather the one who suspects his faith in them and questions what he gathers from them, the one who submits to argument and demonstration, and not to the sayings of a human being whose nature is fraught with all kinds of imperfection and deficiency. Thus the duty of the man who investigates the writings of scientists, if learning the truth is his goal, is to make himself an enemy of all that he reads, and, applying his mind to the core and margins of its content, attack it from every side. He should also suspect himself as he performs his critical examination of it, so that he may avoid falling into either prejudice or leniency ».

Alhazen (965-1040)

« La science, mon garçon, est faite d'erreurs, mais d'erreurs qu'il est bon de commettre, car elles mènent peu à peu à la vérité ».

Jules Verne, Voyage au centre de la Terre

REMERCIEMENTS

Je tiens tout d'abord à remercier le **Pr. Christophe d'Hulst** de m'avoir accueilli au sein de l'Unité de Glycobiologie Structurale et Fonctionnelle (UMR8576/CNRS).

Dr. Anne Harduin, merci de m'avoir fait l'honneur de présider le jury de ma thèse. Je vous remercie également pour la curiosité que vous avez manifestée à l'égard de mon projet.

I would like to thank **Pr. Hudson Freeze**, who kindly accepted to be a reviewer for my thesis. Indeed, having you as one of my reviewers is a great honor that I will not forget. Je remercie le **Pr. Valérie Cormier-Daire** d'avoir également gentiment accepté d'examiner mon travail de thèse.

J'aimerais également remercier le **Pr. Emile Van Schaftingen**, qui, en plus d'avoir gentiment accepté d'être examinateur de ma thèse, deviendra dans quelques temps mon directeur de post-doctorat à l'Institut de Duve.

J'adresse un remerciement particulier au **Dr. Sophie Groux-Degroote**, sans qui je ne serais pas en train d'écrire ces lignes dans ma thèse. Sans toi, ta bonne humeur et tes (très) précieux conseils, mon parcours aurait pu être très différent. Merci d'avoir accepté d'être examinatrice de mon travail de thèse.

Je remercie chaleureusement mon directeur de thèse, le **Dr. François Foulquier.** Tout d'abord, je te suis très reconnaissant de m'avoir donné l'opportunité de faire mon Master 2 Recherche dans l'équipe et en particulier à tes côtés. Sans cette opportunité, je ne serais pas là aujourd'hui. Merci François pour tes nombreux conseils et ton écoute. Je te remercie ensuite pour la confiance que tu m'as accordée tout au long du projet de thèse. Les nombreuses discussions pendant lesquelles nous avons pu établir des hypothèses toutes plus farfelues les unes que les autres et pendant lesquelles nous avons pu nous arracher les cheveux sur ce projet ô combien complexe, me manqueront. Je remercie également le **Dr Dominique Legrand**, qui bien que très occupé ces dernières années, a toujours trouvé le temps de venir partager sa précieuse expérience scientifique et sa joie de vivre toute aussi importante.

Un grand merci à l'ensemble de l'équipe "Mécanismes de la N-glycosylation et pathologies associées". **Dr. Geoffroy de Bettignies**, je te remercie entre autres pour tes conseils en biologie moléculaire et pour ton avis toujours critique (dans le bon sens du terme) sur mon travail. Merci

au **Dr. Sandrine Duvet,** ta bonne humeur quotidienne est un gros atout dans une grande équipe de recherche. De plus, tu as été la première personne à m'initier aux CDG quand j'étais en première année de master. Ce fut un plaisir de travailler avec toi. Merci au **Dr. Marie-Ange Krzewinski-Recchi,** qui a toujours été disponible et attentionnée à mon égard. Tes conseils scientifiques et les discussions plus générales que nous avons eues ont toujours été appréciables. Je remercie également le **Pr. Jean-Claude Michalski** et le **Pr. Willy Morelle** pour leur sympathie et leurs précieux conseils tout au long de ma thèse.

Merci au **Docteur** (et oui !!) **Eudoxie Dulary**, qui a su me conseiller grâce à son expérience acquise toujours un an avant moi. Ca y est c'est fini pour toi la recherche alors je te souhaite de voler vers de nouveaux horizons avec l'expérience acquise ces 4 années et de t'épanouir dans l'enseignement. Aie confiance en toi et tu y arriveras.

Merci à **Dorothée**, qui a toujours été disponible pour former tous les nouveaux du labo. Tu es un peu notre maman du labo qui sait à la fois nous féliciter et nous réprimander quand on oublie les tâches communes.

J'adresse également des remerciements à **Marine**, notre petite ingénieure d'étude devenue doctorante toujours de bonne humeur même quand tout n'est pas rose. Merci pour ta gentillesse et ta joie de vivre. J'espère que ton avenir professionnel sera radieux (je n'en doute pas).

Anne-Sophie, je te souhaite bon courage pour ta thèse. Ton M2 a été compliqué mais tu as su tout donner et obtenir ton financement, maintenant à toi de rester solide pendant ces 3 ans. N'oublie pas que les gens autour de toi sont là pour t'aider alors n'hésite pas à t'appuyer sur eux pour demander des conseils. Bon courage et bonne continuation.

Elodie, tu es notre « électron libre à rayonnement international ». A l'heure où j'écris ces lignes, tu pourrais autant être encore au labo, en Guadeloupe sur un bateau, à Solfé pour l'apéro ou dans un karaoké à Tokyo. Ça te rend unique et imprévisible mais toujours partante pour être dans tous les coups. Bonne continuation pour ta thèse et ton avenir professionnel.

Merci au **Dr. André Klein**, avec qui ce fut un plaisir de notamment partager une revue scientifique, même si la journée où l'on a bouclé la revue, tu n'as pas pu avoir ta baguette préférée à ta boulangerie car nous avions terminé trop tard. J'admire ta volonté de toujours aller de l'avant et de rechercher de nouveaux horizons.

Céline, je t'ai connue grâce à une collaboration il y a quelques années pour faire du FRET. Quelques années plus tard, c'est avec une grande joie que j'apprends que tu as obtenu le poste dans notre équipe suite au départ en retraite d'Anne-Marie. Ce fut un grand plaisir de travailler avec toi. Tu apportes et apporteras encore beaucoup à l'équipe. Bonne continuation.

Dounia, encore une petite nouvelle dans l'équipe. Je ne me fais aucun souci sur ta capacité à apporter tes connaissances poussées en spectrométrie de masse dans le labo. Aie plus confiance en toi et bon courage pour la suite.

Enfin merci à ceux qui ont quitté l'équipe pendant mes années dans le labo. **Cindy,** tu as été la première personne à me former aux techniques courantes utilisées dans le laboratoire. Je te remercie beaucoup pour ta patience et ta disponibilité. **Anne-Marie,** merci pour tes nombreux conseils et ta joie de vivre. Tes nombreuses connaissances et ta personnalité manquent beaucoup au laboratoire.

Merci au **Dr. Patricia Nagnan-le Meillour**, de m'avoir fait confiance et de m'avoir laissé apporter mon aide au projet d'Alexandre.

Je tiens à remercier TISBio et en particulier le **Dr Corentin Spriet**, pour son aide apportée dans le projet grâce notamment à ses outils de quantification et ses connaissances en microscopie.

Je remercie le **Pr. Gert Matthijs**, le **Dr Romain Peanne**, ainsi que le reste de l'équipe du « Laboratory for Molecular Diagnostics » à l'UZ Leuven pour leur collaboration de longue date avec notre équipe.

Je tiens à remercier le **Pr. Delphine Allorge** et le **Dr Anne Garat** de nous avoir permis l'accès à la plate-forme de toxicologie, et notamment à l'ICP-MS. Merci également à **Valérie Decool** d'avoir réalisé nos analyses, les résultats furent d'une grande aide pour le projet.

Je remercie les personnes avec qui j'ai pu collaborer au sein du laboratoire PHYCELL. Merci à **Valerio, Dmitri, Kateryna, Pascal.** Merci également au **Dr. Christian Slomianny** et à **Elodie Richard** pour l'accès au microscope confocal et leur disponibilité en cas de problème.

J'adresse un remerciement général à l'ensemble du personnel de l'Unité de Glycobiologie Structurale et Fonctionnelle. Je remercie également tous les étudiants présents ou passés du C9 :

Maxime, Pierre, Clément, Charles, Anne-Sophie, Maxence, Justine, Sumeyye, Alexandre et j'en passe. Bonne continuation à vous.

D'une manière plus personnelle, je remercie tous les membres de ma famille. Merci à mes parents d'avoir fait de moi celui que je suis aujourd'hui et de m'avoir soutenu depuis le début de ma scolarité jusqu'à la fin de ma thèse. J'adresse aussi un grand merci à mes grands-parents qui ont toujours fait preuve d'une grande curiosité concernant ma recherche et qui ont toujours été fier de moi. Merci papy pour tous les « sciences & vie » que tu as achetés quand j'étais plus jeune. Si j'en suis là, c'est un peu grâce à toi.

Enfin, merci à **Clémentine**, je pense que tu n'as pas besoin de ces quelques lignes (dans une thèse que tu ne liras pas…) pour savoir à quel point tu comptes pour moi. Sans toi pour me remotiver quand j'en avais un peu marre (et réciproquement), ce manuscrit n'existerait pas. Tu as su m'épauler (et me supporter) toutes ces années et pour ça je t'en remercie. Les sacrifices n'ont pas toujours été faciles mais au final, j'ai trouvé la personne avec qui je veux partager ma vie. Je m'arrête là car je suis très mauvais quand il s'agit d'exprimer mes sentiments sur papier…

RESUME

Quatre classes de molécules sont nécessaires pour former une cellule fonctionnelle : l'ADN, les protéines, les lipides et les glycanes. Cependant, ces derniers ont longtemps été considérés comme des éléments décoratifs sans activité biologique. En réalité, toutes les cellules portent des glycanes, attachés aux protéines ou aux lipides au cours d'une modification post-traductionnelle fondamentale appelée la glycosylation. La glycosylation implique plusieurs acteurs tels que des glycosyltransférases (GT) et nécessite un environnement spécifique. Les GT sont particulièrement connues pour avoir besoin de cations divalents, principalement de Mn2+, pour être pleinement actives. Bien que le lien entre le Mn2+ et la glycosylation soit connu depuis longtemps, il a fallu attendre 2015 pour qu'une anomalie de la glycosylation humaine dû à un dérèglement de l'homéostasie du Mn2+ soit découverte. Toutes les anomalies génétiques affectant la glycosylation sont regroupées dans un groupe de maladies héréditaires rares appelées anomalies congénitales de la glycosylation (CDG). Les CDG englobent principalement les défauts affectant des enzymes directement impliquées dans la glycosylation, mais un sous-groupe important de CDG affectant l'homéostasie du Golgi à récemment été découvert.

En 2012, notre équipe a identifié TMEM165 comme étant une protéine golgienne impliquée dans les CDG, mais dont les fonctions biologiques demeurent inconnues. Ma thèse porte sur l'élucidation des fonctions de TMEM165 et l'établissement du lien entre le déficit en TMEM165 et les anomalies de la glycosylation observées chez les patients atteints de TMEM165-CDG.

Nous avons tout d'abord montré que l'homéostasie golgienne du Mn2+ était altérée en absence de TMEM165, suggérant un problème d'entrée du Mn2+ au niveau du Golgi. Alors que de forts défauts de glycosylation, en particulier des défauts de galactosylation, ont été observés dans des cellules déficientes en TMEM165, nous avons découvert que la supplémentation en Mn2+ était suffisante pour rétablir une glycosylation normale. Puisque la galactosylation est affectée, la supplémentation orale en galactose a été testée chez des patients TMEM165-CDG et il a été prouvé que ce traitement améliorait significativement la glycosylation ainsi que les paramètres biochimiques et cliniques. De plus, nous avons montré que l'exposition à des concentrations élevées de Mn2+ entraînait une dégradation lysosomale rapide de TMEM165.

Dans l'ensemble, notre étude montre que TMEM165 est (i) un acteur clé de la glycosylation golgienne en régulant finement l'homéostasie du Mn2+ et (ii) une nouvelle protéine de l'appareil de Golgi sensible à de fortes concentrations en manganèse.

SUMMARY

Four classes of molecules are required to build a cell: DNA, proteins, lipids and carbohydrates (also called glycans). However, glycans were first seen as decorative elements without any biological relevance. In fact, all cells carry glycans that are attached to proteins or lipids during a fundamental post-translational modification named glycosylation. Glycosylation involves several actors such as glycosyltransferases (GT), glycosylhydrolases and nucleotide sugar transporters. These proteins also require a specific environment and GT are especially known to require divalent cations, mainly Mn2+, to be fully active. The link between Mn2+ and glycosylation in human was established in 1974, but the discovery of a human glycosylation disorder due to Mn2+ homeostasis defect was only reported in 2015. In fact, defects in genes involved in the glycosylation process are gathered into a group of rare inherited diseases named Congenital Disorders of Glycosylation (CDG). CDG primarily encompass genes defects in enzymes directly involved in glycosylation, but a significant subgroup of newly discovered CDG affect Golgi homeostasis, marking a new era in the CDG field.

In 2012, the discovery of CDG patients with TMEM165 mutations, a putative Golgi Ca2+/H+ antiporter, added a new layer of complexity to the field of CDG. My PhD mainly focused on establishing the link between TMEM165 deficiency and the glycosylation defect observed in TMEM165-CDG patients.

We first highlighted that Golgi Mn2+ homeostasis was impaired in TMEM165 depleted cells, suggesting a Mn2+ entry problem at the Golgi level. We next demonstrated a general glycosylation defect, with galactosylation mainly affected. Interestingly, Mn2+ supplementation totally suppressed the observed glycosylation defect. Therefore, the underlying pathological mechanism of TMEM165 deficiency is linked to Golgi Mn2+ homeostasis defect. Since galactosylation was affected, we tested oral galactose supplementation on TMEM165 deficient cell lines and TMEM165-CDG patients. We demonstrated that Golgi glycosylation defects due to deficiency in TMEM165 also improves on galactose supplementation.

In the last study, we have observed that TMEM165 was rapidly and specifically targeted to lysosomal degradation when cells were exposed to high Mn2+ concentrations. However, the reason behind this phenomenon is still not clear and need to be unravelled.

Finally, we propose a model for TMEM165 transport function, in which TMEM165 is able to import cytosolic Mn2+ inside the Golgi lumen against Ca2+.

AVANT-PROPOS

Ce travail a été réalisé sous la direction du **Dr. François Foulquier** au sein de l'Unité de Glycobiologie Structurale et Fonctionnelle
(UMR8576-CNRS, dirigée par le Pr. Christophe D'Hulst)

Il a été financé par une allocation de Recherche du Ministère de l'Enseignement Supérieur et de La Recherche ainsi que par la région Nord-Pas-De-Calais.

Les travaux réalisés lors de cette thèse ont fait l'objet de publications et de communications scientifiques :

PUBLICATIONS :

Revues scientifiques :

Golgi post-translational modifications and associated diseases. ***Potelle S***, Klein A, Foulquier F. J Inherit Metab Dis. 2015

TMEM165 deficiencies in Congenital Disorders of Glycosylation type II (CDG-II) clues and evidences for roles of the protein in Golgi functions and ion homeostasis. Dulary E*, ***Potelle S*,*** Legrand D, Foulquier F. * Contributed equally to this work. Tissue Cell. 2016 Jun 16.

Articles scientifiques :

Glycosylation abnormalities in Gdt1p/TMEM165 deficient cells result from a defect in Golgi manganese homeostasis. ***Potelle, S***., Morelle, W., Dulary, E., Duvet, S., Vicogne, D., Spriet, C., Krzewinski-Recchi, M.-A., Morsomme, P., Jaeken, J., Matthijs, G., et al. (2016). Hum. Mol. Genet. 2016

A sequential bioorthogonal dual strategy: ManNAl and SiaNAl as distinct tools to unravel sialic acid metabolic pathways. Gilormini, P.A., Lion, C., Vicogne, D., Levade, T., ***Potelle, S***., Mariller, C., Guérardel, Y., Biot, C., and Foulquier, F. (2016). Chem. Commun. Camb. Engl. 2016

Evidence for splice transcript variants of TMEM165, a gene involved in CDG. Krzewinski-Recchi MA, ***Potelle S***, Mir AM, Vicogne D, Dulary E, Duvet S, Morelle W, de Bettignies G, Foulquier F. Biochim Biophys Acta. 2017.

Manganese-induced turnover of TMEM165. ***Potelle S****, Dulary E*, Climer L, Duvet S, Morelle W, Vicogne D, Lebredonchel E, Houdou M, Spriet C, Krzewinski-Recchi MA, Peanne R, Klein A, de Bettignies G, Morsomme P, Matthijs G, Marquardt T, Lupashin V, Foulquier F. Biochem J. 2017. * Contributed equally to this work.

Galactose Supplementation in Patients With TMEM165-CDG Rescues the Glycosylation Defects. Morelle W*, ***Potelle S***, Witters P, Wong S, Climer L, Lupashin V, Matthijs G, Gadomski T, Jaeken J, Cassiman D, Morava E, Foulquier F. * Contributed equally to this work.

COMMUNICATIONS PAR AFFICHE :

Sven Potelle, Willy Morelle, Marie-Ange Krzewinski-Recchi, Geoffroy De Bettignies, Dorothée Vicogne, Dominique Legrand, François Foulquier. "TMEM165 (Transmembrane Protein 165) : a novel actor in Golgi glycosylation process involved in Congenital Disorders of Glycosylation". 25th Joint Glycobiology meeting, September 14-16, 2014. Ghent, Belgium.

S. Potelle, W. Morelle, E. Dulary, S. Duvet, C. Spriet, M.A. Krzewinski-Recchi, G. De Bettignies, D. Vicogne, D. Legrand, F. Foulquier. "TMEM165 (Transmembrane Protein 165): A novel regulator of Golgi Mn2+ homeostasis involved in Congenital Disorders of Glycosylation". Colloque annuel des doctorants, 16e journée André Verbert, 5 Septembre 2016. Lille, France

S. Potelle*,* E. Dulary, L. Climer, W. Morelle, Y. Guerardel, D. Vicogne, MA. Krzewinski-Recchi, S. Duvet, E. Lebredonchel, A. Klein, M. Houdou, D. Legrand, G. de Bettignies, J. Jaeken, E. Morava, V. Lupashin, G. Matthijs F. Foulquier. "Relationship between Golgi glycosylation and Golgi Mn2+ homeostasis: TMEM165 does the job". Gordon Research Conferences, Glycobiology, March 19-24, 2017. Ventura, CA, USA.

LIST OF ABBREVIATIONS

ApoC-III: Apolipoprotein C-III
Asn: Asparagine
ATCC: American Type Culture Collection
ATP: Adenosine triphosphate
ATPase: Adenosine triphosphatase
B4GALT1: β-1,4-galactosyltransferase I
BFA: Brefeldin A
BSA: Bovin Serum Albumin
Ca2+: Calcium ion
CAZY: Carbohydrate-Active enZYmes
CDG: Congenital disorders of glycosylation
CDG-I: Type I CDG
CDG-II: Type II CDG
CFTR: Cystic fibrosis transmembrane conductance regulator
CMD: Congenital Muscular Dystrophy
CNX: Calnexin
Co2+: Divalent cobalt ion
CRT: Calreticulin
CS: Chondroitin Sulfates
Cu2+: Divalent copper ion
DAPI: 4',6'-DiAmidino-2-PhénylIndole
DMEM: Dulbecco's Modified Eagle's Medium
DMT1: Divalent Metal Transporter 1
Dol: Dolichol
Dol-P: Dolichol phosphate
Dol-PP: Dolichol pyrophosphate
DPBS: Dulbecco's Phosphate Buffer Saline
DS: Dermatan Sulfates
ECL: Enhanced ChemiLuminescence
EDTA: Ethylene Diamine Tetraacetic Acid
EE: Early Endosomes
EGF: Epidermal Growth Factor
ER: Endoplasmic reticulum
ERAD: ER Associated Degradation
ERGIC: ER-Golgi intermediate compartment
FRET: Fluorescence Resonant Energy Transfer
Fuc: Fucose
GA: Golgi Apparatus
GAG: Glycosaminoglycans

Gal: Galactose
GalNAc: *N*-acétyl galactosamine
GALNT2: GalNAc transferase 2
GalT: β-1,4-galactosyltransferase I
Gdt1p: Gcr1 Dependent Translation factor 1
GFP: Green fluorescent protein
GH: glycosylhydrolase
GL: Glycolipids
Glc: Glucose
Glc-6-P: Glucose 6 phosphate
GlcNAc: *N*-acetylglucosamine
GlcNAc-T: GlcNAc transferase
GlcUA: Glucuronic Acid
GM130: Golgi Marker protein 130
GPHR: Golgi pH Regulator
GPI: Glycosylphosphatidylinositol
GSL: Glycosphingolipids
GT: Glycosyltransferases
HPLC: High-performance liquid chromatography
HRP: Horse Radish Peroxidase
HS: Heparan Sulfates
ICAM: Intercellular Adhesion Molecule 1
IdoUA: Iduronic Acid
IEF: Iso-electric focusing
IP3: Inositol-3-Phosphate
IP3R: IP3 receptor
KO: Knockout
KS: Keratan Sulfates
LAMP2: Lysosomal-Associated Membrane Protein 2
LDS: Lithium Dodecyl Sulfate
Man: Mannose
MAN2A1: Alpha-mannosidase 2
ManNAl: *N*-(4-pentynoyl) mannosamine
Met: Methionine
Mg2+: magnesium ion
Mn2+: Divalent manganese ion
MOPS: 3-N-morpholino propanesulfonic acid
mRNA: Messenger RNA
NeuAc: *N*-acetyl neuraminic acid
NST: Nucleotide Sugar Transporter
OEC: Oxygen Evolving Complex
O-GlcNAc: O-N-acetylglucosaminylation

OST: Oligosaccharyltransferase
PA: Phosphatidic acid
PBS: Phosphate Buffer Saline
PCR: Polymerase chain reaction
PDI: Protein disulfate isomerase
PFA: Paraformaldéhyde
PI(3)P: Phosphatidylinositol-3-phosphate
PI(4)P: Phosphatidylinositol-4-phosphate
PI(4,5)P2: Phosphatidylinositol-4,5-biphosphate
Pi: Inorganic Phosphate
PI: Phosphatidylinositol
PLA: Proximity Ligation Assay
PLD: Phospholipase D
Pmr1p: Plasma Membrane ATPase Related
PPI: Peptidyl Prolyl Isomerase
PTM: Post-Translational Modification
RT-qPCR : Reverse Transcription – quantitative Polymerase Chain Reaction
RyR: Ryanodine Receptor
SDS-PAGE: Sodium Dodecyl *Sulfate Poly-Acrylamide Gel Electrophoresis*
Ser: Serine
siRNA: Small interfering RNA
SNARE: SNAP (Soluble NSF attachment protein) receptor
SPCA1: Secretory Pathway Ca2+-ATPase isoform 1
ST3Gal1: α2,3-sialyltransferase I
ST6Gal1: α2,6-sialyltransferase I
TBS: Tris Buffer Saline
TGN: *Trans*-Golgi network
TGN46: Trans-Golgi Network protein 46
Thr: Threonine
TM: Transmembrane
TMD: Transmembrane Domain
TMEM165: Transmembrane Protein 165
Trp: Tryptophane
TSR: Thrombospondin Repeat
UDG-Gal: Uridine diphosphogalactose
UDP: Uridine diphosphate
UGGT: UDP-glucose: glycoprotein glucosyltransferase
WB: Western-Blot
XDP: Nucleotide DiPhosphate
XMP: Nucleotide MonoPhosphate
Zn2+: divalent zinc ion

TABLE OF CONTENTS

LIST OF FIGURES

LIST OF TABLES

INTRODUCTION

[1] GENERAL INTRODUCTION

The accepted dogma in science, which is still believed by mainstream audience, is that biological information comes from DNA and ultimately emerges to protein. However, making a completely functional cell also requires two others classes of molecules: lipids, crucial for building cell membranes among other things, and carbohydrates (also called glycans). At the beginning, glycans were only considered as energy source or structural elements without any strong biological importance or activity. In reality, all cells carry glycans that are either found as free molecules or covalently attached to proteins or lipids during a post-translational modification (PTM) named glycosylation, thus forming the glycoconjugates. Glycosylation is a conserved fundamental process found across the entire phylogenetic spectrum, and is even present in all cell type of a given organism. Glycoconjugates are involved in a broad range of functions taking place at the cell-cell, cell-matrix, cell-molecule or host-parasite interfaces, mainly by finely modulating proteins or lipid functions or by acting as specific recognition molecules.

The metabolism of glycans has been intensively studied in the beginning of the 20th century. Combined with biochemistry approaches, these researches led to the rise of the glycobiology field. Glycobiology is defined by Varki as “the study of the structure, biosynthesis, biology, and evolution of saccharides that are widely distributed in nature, and the proteins that recognize them” [1]. Although glycobiology became a recognized scientific field, it was always lagging behind protein and DNA fields. Indeed, the huge diversity of glycan structures and the fact that glycan biosynthesis is not template driven and therefore not predictable made glycans much more difficult to study than other classes of molecules. However, more than 61 000 scientific articles linked to “glycosylation or glycobiology” are now available on PubMed, and the number of articles are increasing each year since the 1980’s. Moreover, since 2005, more than 2000 articles are published each year, revealing the recent expansion of the glycobiology field.

The structural diversity of glycosylation is insured in mammals by nine nucleotide sugar donors, a multitude of glycosylhydrolases (GH) and glycosyltransferases (GT), which generate various glycosidic bonds in α or β stereoisomeric configurations on a wide variety of lipids and protein acceptors. In mammals, protein and lipid glycosylation comprises many different glycosylation types. However, excepted for O-linked N-acetylglucosaminylation (O-GlcNAcylation) that is

performed exclusively in the cytosol, they all take place sequentially in two organelles: the endoplasmic reticulum (ER) and the Golgi apparatus (GA). For some specific glycosylation types discussed later, only one organelle is involved during the glycosylation process. According to the linkage of the first monosaccharides to the amino acid, three major types of glycosylation can be distinguished:

- **N-glycosylation**, when the glycan is linked to the amide group of an asparagine (Asn).
- **O-glycosylation**, defined by the attachment of the glycan to the hydroxyl group of a serine (Ser) or a threonine (Thr).
- **C-glycosylation**, also called C-mannosylation, with a single mannose residue linked to the C2 atom of tryptophan (Trp) on specific proteins.

Besides, a given glycoprotein can exist in different glycosylated forms. These glycoforms are the result of macro- and microheterogeneity, which are especially well characterized for N-glycosylation. Macroheterogeneity is generated by the ER and is defined by the structural diversity due to the presence or the absence of a glycan structure at a given glycosylation site. Microheterogeneity is the presence of different glycan structures at a specific glycosylation site, which is the result of Golgi glycosylation [2]. Therefore, the ER and the Golgi have different but complementary roles in the glycosylation process. In a simplified view, ER glycosylation is involved in the folding and the stability of glycoproteins while Golgi glycosylation is responsible for finely regulating the functionality of a protein. Besides, the GA is mainly responsible for the maturation of glycans. Indeed, final steps of glycosylation occur in the Golgi, thus glycoconjugates acquire their definitive structures during their passage through this organelle.

Glycosylation is not only the result of a dynamic process depending on enzymatic activities, but also relies on external factors such as GT localization and organelle overall environment. For example, the nucleotide sugar donors required for Golgi glycosylation are synthetized in the cytosol and must be imported by specific nucleotide sugar transporters (NST) into the Golgi lumen and in the same Golgi cisternae as the GT that use them. Besides, GT requires a specific environment in terms of pH, inorganic phosphate and divalent cations such as Mn^{2+}, Mg^{2+} and Ca^{2+} [3,4]. Moreover, GT are especially known to require divalent cations, mainly Mn^{2+}, to be fully active [5]. The first link between Mn^{2+} and glycosylation in human was established in 1974 [6], but the connexion between a glycosylation disorder and Mn^{2+} homeostasis defect in human was only reported in 2015, more than 40 years later, highlighting the difficulty of studying

glycosylation [7]. In fact, defects in genes involved in the glycosylation process are gathered into a group of rare inherited diseases named Congenital Disorders of Glycosylation (CDG) [8–11]. Despite the fact that almost 5% of the genome is dedicated to glycosylation, this process has always been underestimated and left behind. Yet, more than 110 different CDG have been identified to date, meaning that mutations in one of these 110 genes can lead to a human disease, emphasizing the crucial importance of glycosylation in human biology. CDG primarily encompass gene defects in enzymes directly involved in glycosylation, but a significant subgroup of newly discovered CDG affect Golgi homeostasis, marking a new era in the CDG field [12]. Since the first discovery of a link between defective Golgi homeostasis and abnormal glycosylation in 2004, researchers doubled their effort to decipher new CDG caused by Golgi homeostasis disturbance. The recent discovery of CDG patients carrying TMEM165 mutations, a putative Golgi cation antiporter, added a new layer of complexity both to the field of Golgi glycosylation and to the research on CDG.

[2] GOLGI GLYCOSYLATION

Although the ER is the initiator of most of the glycosylation types, the Golgi apparatus can be seen as another main organelle for glycosylation, as it is responsible for the maturation and the final steps of glycosylation. Thus, most of the glycoconjugates acquire their final structures during their passage through the Golgi. A simplified overview of the different Golgi glycosylation types that will be presented in this chapter is depicted in Figure 1. Several glycosylation types even occurs only in the Golgi apparatus without the action of the ER such as the mucin-type O-glycosylation or the biosynthesis of glycosaminoglycans (GAG). Besides, there are no less than 8 different nucleotide sugar donors in the Golgi apparatus of mammals. Therefore, one key feature of Golgi glycosylation is the high diversity of glycan structures that arise from this organelle. Indeed, for a given type of glycosylation, the amount of different structures observed on mature glycoproteins is huge. This diversity relies on the abundance, the localisation and the affinity of GT and GH, which can prevent or favour the synthesis of specific glycan structures on acceptors. Indeed, it is possible that the action of one enzyme prevents the action of a second enzyme, giving birth to different structures. Moreover, Golgi glycosylation is a highly regulated process, as GT requires a specific environment in terms of pH, divalent cations and inorganic phosphate. In addition, nucleotide sugar donors must be located in the same compartment than the GT that will use them.

In mammals, there are more than 250 resident GT in the Golgi apparatus. They are all type II transmembrane protein (Figure 2), composed of a short cytoplasmic tail at the N-terminus, a single transmembrane domain (TMD) responsible for their anchoring in the Golgi membrane, a stem region variable in length, and a catalytic domain in the Golgi lumen [13]. These enzymes have multiple layers of substrate specificity. Indeed, they are specific to the donor of nucleotide sugar, to the glycan acceptor and to the linkage of the glycosidic bond they catalyse. Some GT such as polypeptide N-acetylgalactosaminyltransferase 2 (GalNAc-T2) and GalNAc-T4 even possess two functional domains, one lectin domain that strongly binds the acceptor glycan and one catalytic domain that performs the enzymatic reaction [14,15]

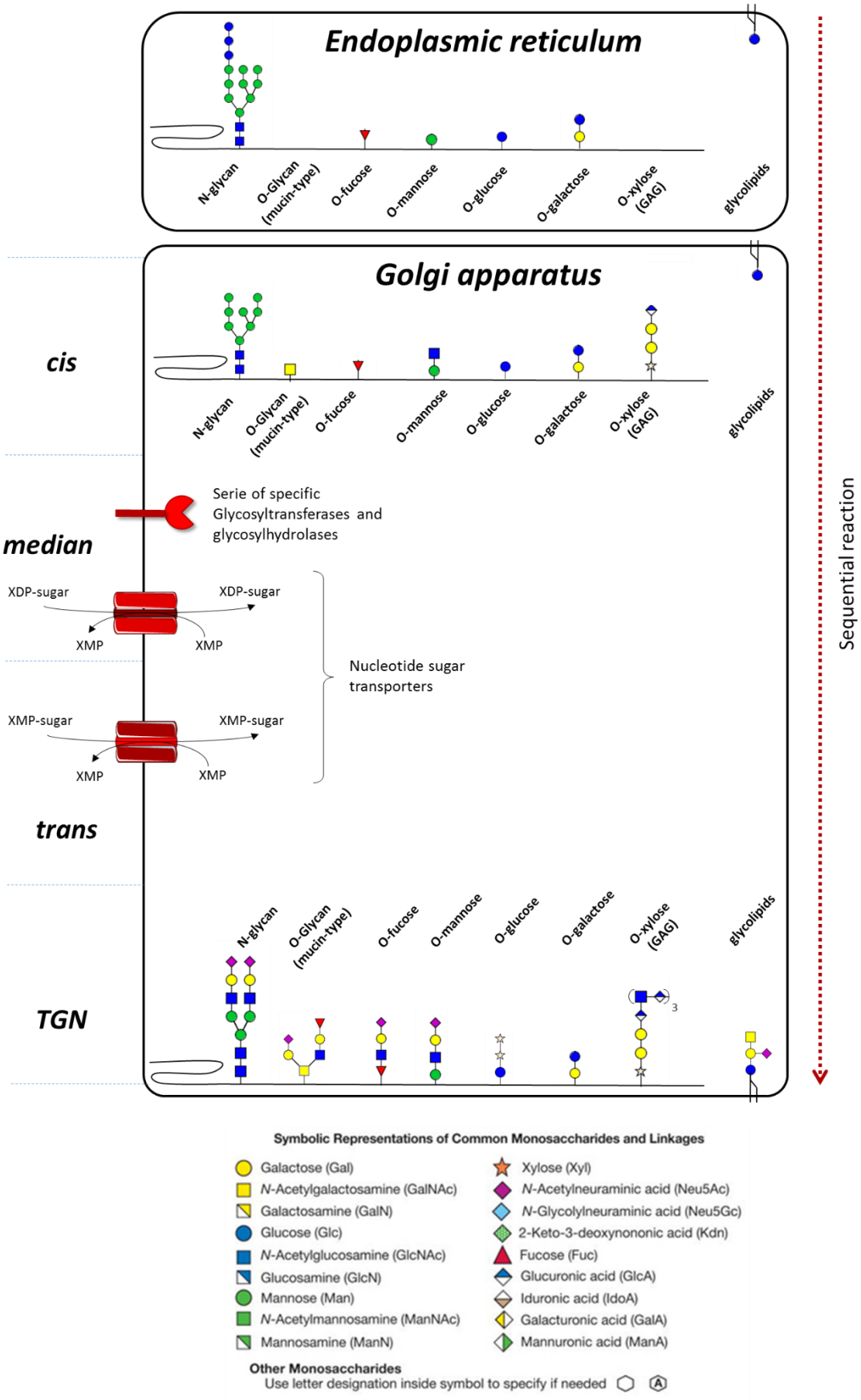

Figure 1. Simplified overview of the different types of glycosylation in mammals, with a focus on Golgi glycosylation. Specific nucleotide sugar transporters , GT and GH are also present in the ER but not depicted here for clarity sake. The glycan structures shown in the TGN are examples but do not fully represent each glycosylation type. C-mannosylation is not shown here since it only takes place in the ER. O-GlcNAcylation is not depicted here since it only occurs in the cytosol.

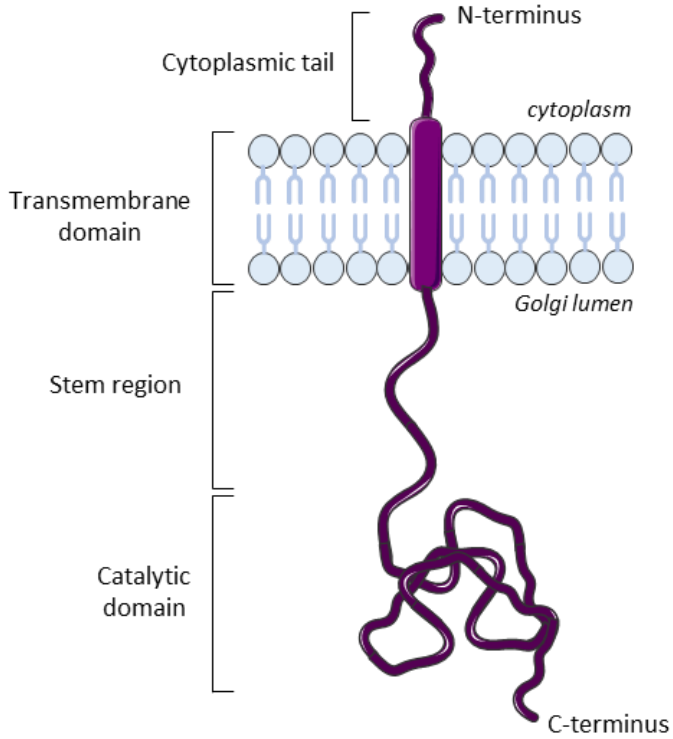

Figure 2. Topology of a Golgi glycosyltransferase. All Golgi glycosyltransferases are type II transmembrane protein. The cytoplasmic tail, the TMD and the stem region are involved in the localisation and the stability of the protein. The catalytic domain is in the Golgi lumen, near the C-terminus of the protein.

Compared to the ER glycosylation that is well conserved among eukaryotes, Golgi glycosylation is very divergent in eukaryote organisms (Figure 3). For example, plants can have xylose residue on their N-glycans, which is not the case in mammals. Yeast N-glycans are also very different from mammalian N-glycans. They are composed of two N-acetylglucosamine (GlcNAc) residues followed by only mannose residues, but their N-glycans can reach up to 200 mannose residues [16]. In human, mannose cannot be added on N-glycans in the Golgi apparatus. This shows that the Golgi is an organelle that has drastically changed during evolution.

An overview of the major glycosylation types will be addressed in this chapter, with a focus on Golgi glycosylation. This section will still not be completely exhaustive, due to the high diversity of Golgi glycosylation.

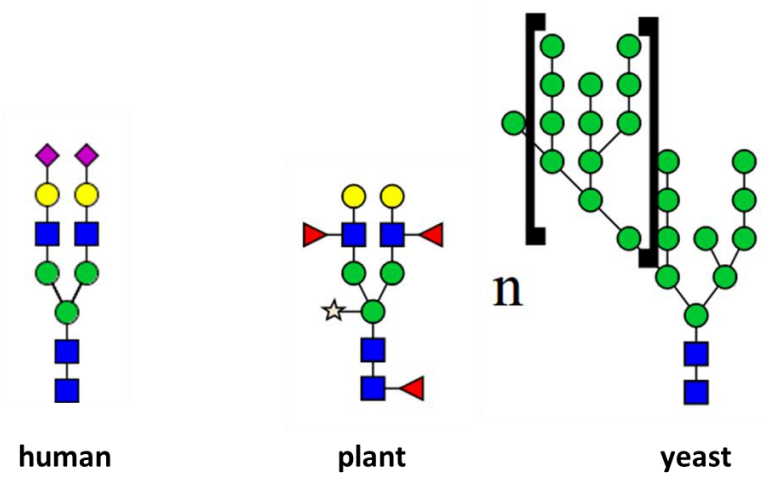

Figure 3. Examples of N-glycosylation differences among eukaryotes. The structures shown here only represent a specific type of N-glycan. Xylose residues in plant N-glycans are absent in human N-glycans. Yeast N-glycan are only composed of mannose and GlcNAc residues.

2.1. N-glycosylation

2.1.1. General introduction

N-glycosylation is a sequential process that occurs in two distinct compartments, the ER and the Golgi apparatus. Since my work mainly focused on the Golgi apparatus, only a quick overview of the ER N-glycosylation will be done. This process is already well-described in literature [1,17,18]. ER N-glycosylation is well conserved during evolution, from yeast to human. It begins with the synthesis of a common oligosaccharidic precursor on a lipid acceptor, the dolichol pyrophosphate, during the dolichol cycle (Figure 4). The structure of the common precursor ($Glc_3Man_9GlcNAc_2$) contains three different sugars and a variety of different linkages (Figure 5). The precursor is then transferred by the oligosaccharyltransferase (OST) all at once on an Asn residue of a consensus sequence Asn-X-Ser/Thr (X being any amino acid excepted proline) on protein regions that have been translocated into the ER lumen. Recently, N-glycosylation has been also observed on non-standard sequons such as Asn-X-Cys, Asn-Gly, and Asn-X- [19–22]. Still, they represent minor N-glycosylation sites compared to the consensus sequence.

After the transfer of the precursor, a series of mandatory processing steps occur (Figure 6). Glucosidase I cleaves the terminal α-1,2 glucose (Glc) residue and glucosidase II next cleaves the newly terminal α-1,3 linked glucose residue, generating a $Glc_1Man_9GlcNAc_2$ N-glycan structure. This structure can be recognised by two specific lectins: calnexin (CNX), and its soluble homolog

calreticulin (CRT). These lectins are associated to Erp-57, a chaperone that will help the folding of the glycoprotein during what is called the CNX/CRT cycle. In addition to this cycle, several chaperones (such as Bip, Protein Disulfide Isomerase (PDI) and Peptidyl Prolyl Isomerase) will help the folding of N-glycoproteins.

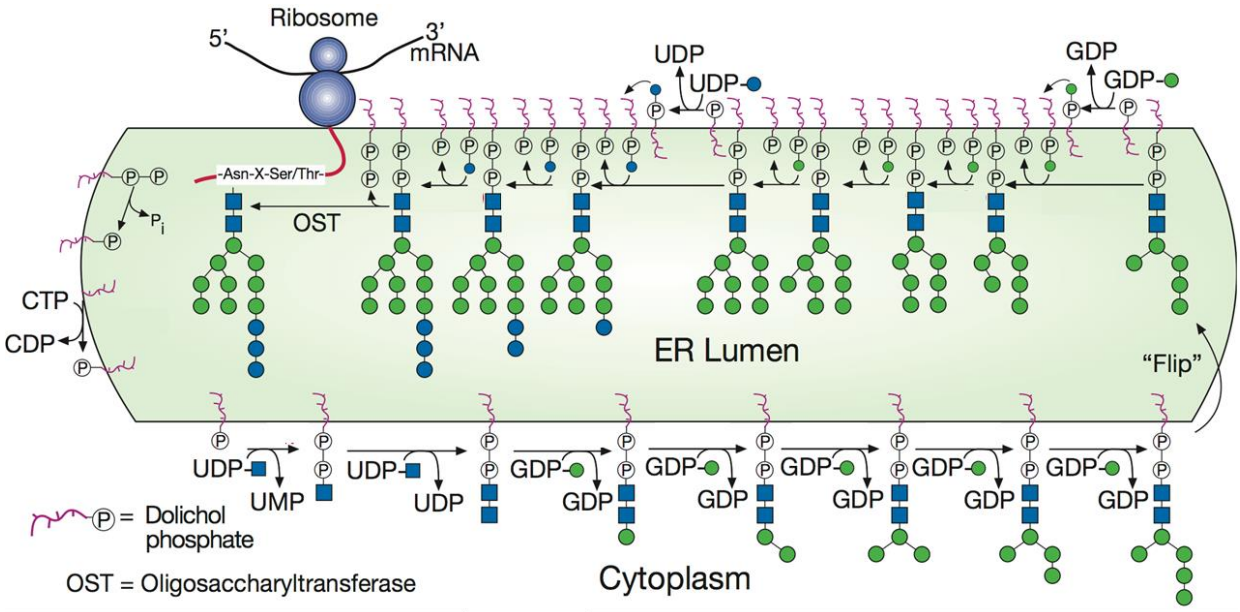

Figure 4. Overview of the dolichol cycle. The dolichol cycle starts in the cytosolic face of the ER with the addition of a GlcNAc phosphate residue on dolichol phosphate. Then, another GlcNAc residue is added, followed by 5 mannose residues. A flippase named RFT1 then translocates the lipid-linked glycan inside the ER lumen where 4 mannose and 3 glucose residues are added. Each step is catalysed by a GT that is specific to the acceptor substrate, the donor substrate and the linkage of the reaction. Finally, the precursor is transferred without the lipid part by the OST on a Asn-X-Ser/Thr of newly synthetized proteins. Adapted from Essentials of glycobiology 2nd edition.

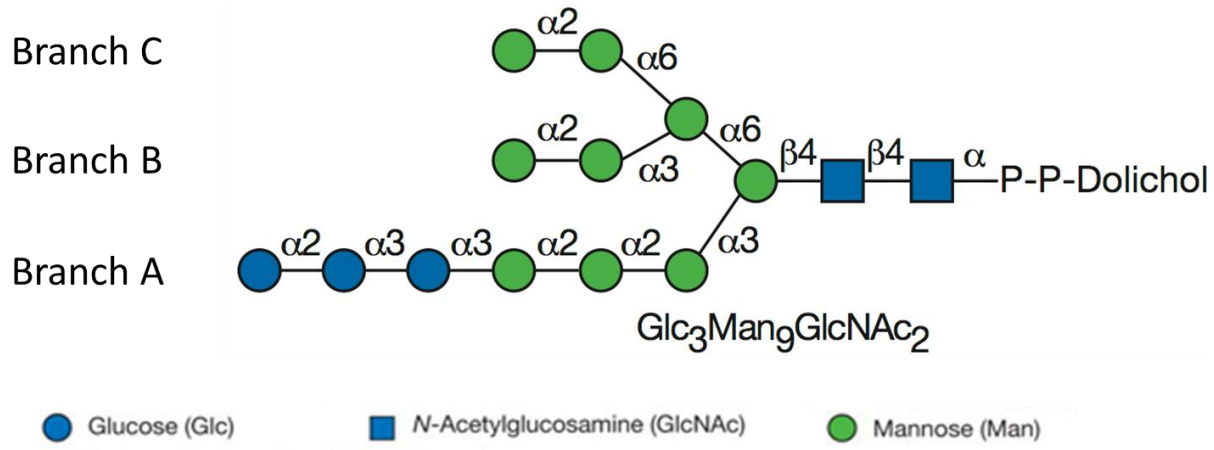

Figure 5. Structure of the oligosaccharidic precursor for N-glycosylation. This precursor is synthetized on a lipid linked acceptor, the dolichol pyrophosphate. The precursor only contains three types of monosaccharides but many different linkages. Monosaccharides are represented according to the nomenclature proposed by Varki and collaborators in 2009. Adapted from Essentials of glycobiology 2nd edition.

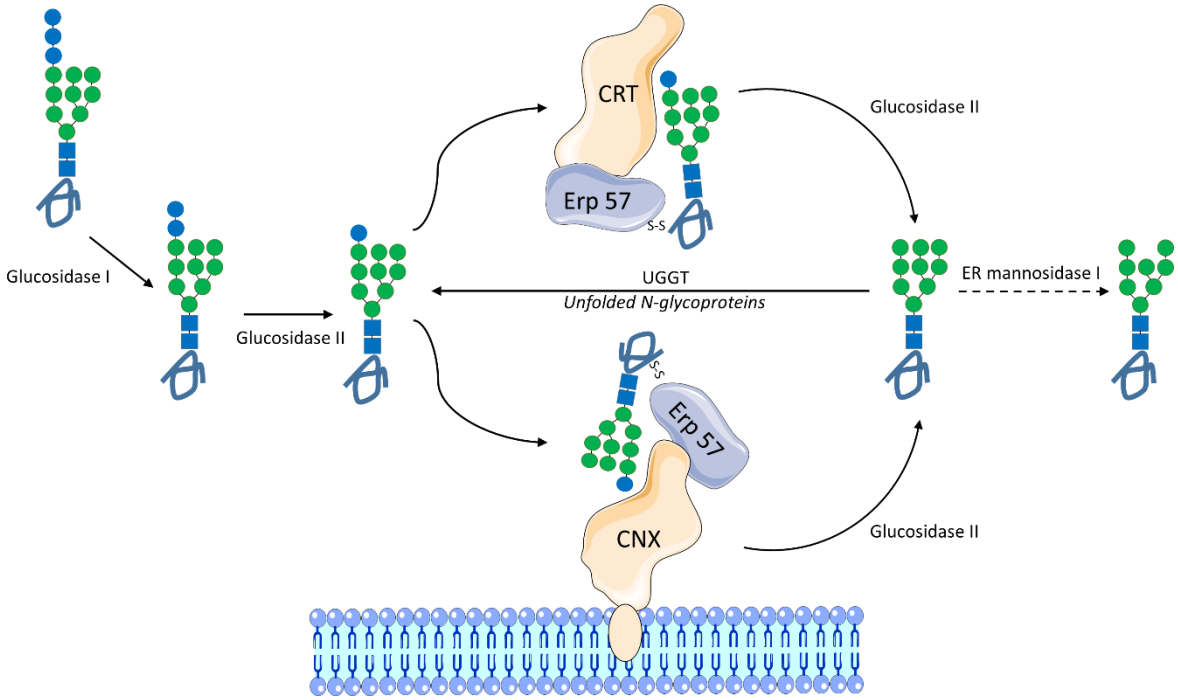

Figure 6. ER N-glycan trimming and quality control. After the trimming of 2 glucose residues, the N-glycan enters the CNX/CRT cycle to help the folding of the protein moiety. If the N-glycoprotein obtains its correct folding, it will be sent to the Golgi apparatus. The ER mannosidase I can additionally remove the terminal α-1,2 linked mannose residue on branch B. If the folding is incorrect or incomplete, the UGGT will add a new glucose residue, allowing the CNX/CRT cycle to start again.

Glucosidase II will finally remove the last α-1,3 linked glucose residue. If the protein is correctly folded, it will be sent to the Golgi apparatus. The ER mannosidase I can additionally remove the terminal α-1,2 linked mannose residue on branch B. Therefore, the majority of N-glycoproteins reaching the Golgi carry N-glycans with 2 GlcNAc residues and either 8 or 9 mannose residues, depending on the action of ER mannosidase I. If the N-glycoprotein is still unfolded, an enzyme named UDP-glucose: glycoprotein glucosyltransferase (UGGT) will add a new α-1,3 linked glucose residue on branch A, allowing the CNX/CRT cycle to start again. However, N-glycoproteins are sometimes still unable to be correctly folded despite all the control points. To avoid any accumulation of unfolded protein that can lead to ER stress, they are targeted to degradation via the ER-Associated Degradation pathway (ERAD). Considering all these control steps, it is not surprising that the ER is seen as a quality control organelle for newly synthesized N-glycoproteins [23].

N-glycoproteins reaching the Golgi will be matured by a combination of glycosylhydrolases (GH) and glycosyltransferases (GT). GH involved in Golgi N-glycosylation are all α-mannosidases and can be classified according to the nature of the glycosidic linkage they cleave. Indeed, mannosidases that cleave α-1,2 linkage form the GH47 family in the CaZY (Carbohydrate-Active

enZYmes) database. Mannosidases that can cleave either α-1,2, α-1,3 or α-1,6 linkages form the family GH38 [24]. The combination of GH and GT will generate the great structural diversity of N-glycans. Nevertheless, N-glycans can be classified into three major categories (Figure 7), with the most abundant N-glycan type found in human being the complex type.

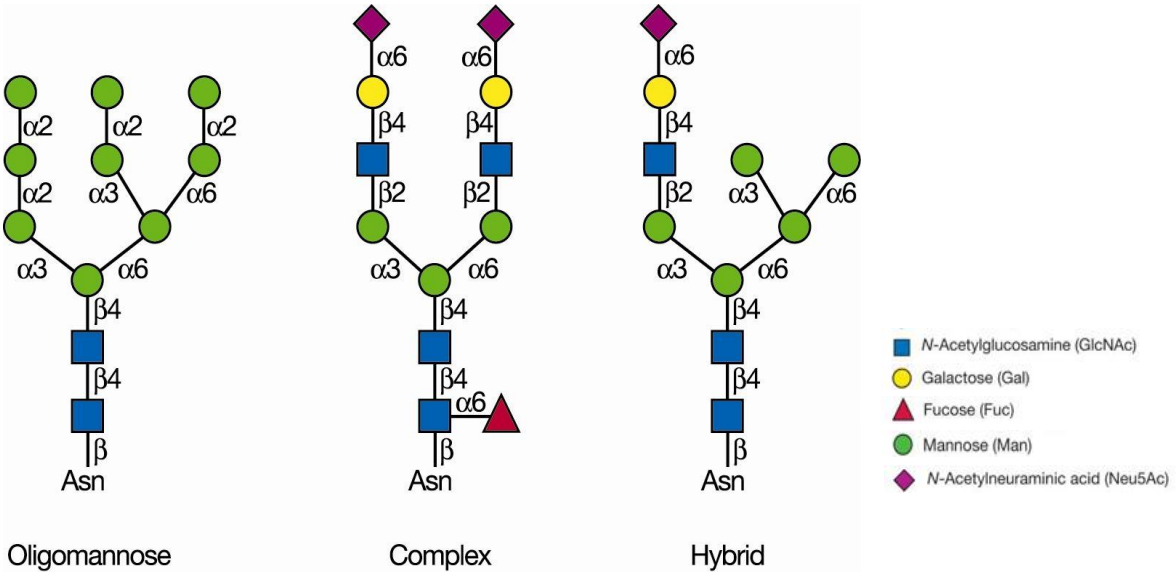

Figure 7. The three types of N-glycans found in mammals. N-glycans added to protein are of three general types in a mature glycoprotein: oligomannose, complex, and hybrid. Each N-glycan contains the common core Man3GlcNAc2. The most common N-glycan type found in human is the complex type. From Essentials of glycobiology, 2nd edition.

2.1.2. N-glycan maturation

Golgi N-glycosylation is a complex process that is not conserved between yeast and human. Yeast N-glycans are only composed of two different sugars (GlcNAc and mannose) as opposed to the five different monosaccharides in human N-glycans that are responsible for the high diversity of the human N-glycome. To generate these glycan structures, N-glycans reaching the Golgi must be finely matured. In this section, only the synthesis of the most common bi-antennary complex structure (the same as the one shown in Figure 7) will be described in details. Indeed, the number of different N-glycans structures is so important that Golgi N-glycosylation is way more intricate than depicted here (Figure 8), but a complete overview of Golgi N-glycosylation is well described in the literature [1,4,25].

Once in the Golgi, the N-glycan is first trimmed by a set of Golgi α-mannosidases. They cleave 4 mannose residues to generate a $Man_5GlcNAc_2$ structure, often called the branched Man_5 structure. N-glycoproteins then reach the medial-Golgi where a GlcNAc transferase named MGAT1 adds a β-1,2 linked GlcNAc residue on the α-1,3 mannose on branch A. This sugar addition is the trigger for the action of Golgi α-mannosidase II, which catalyses the removal of 2

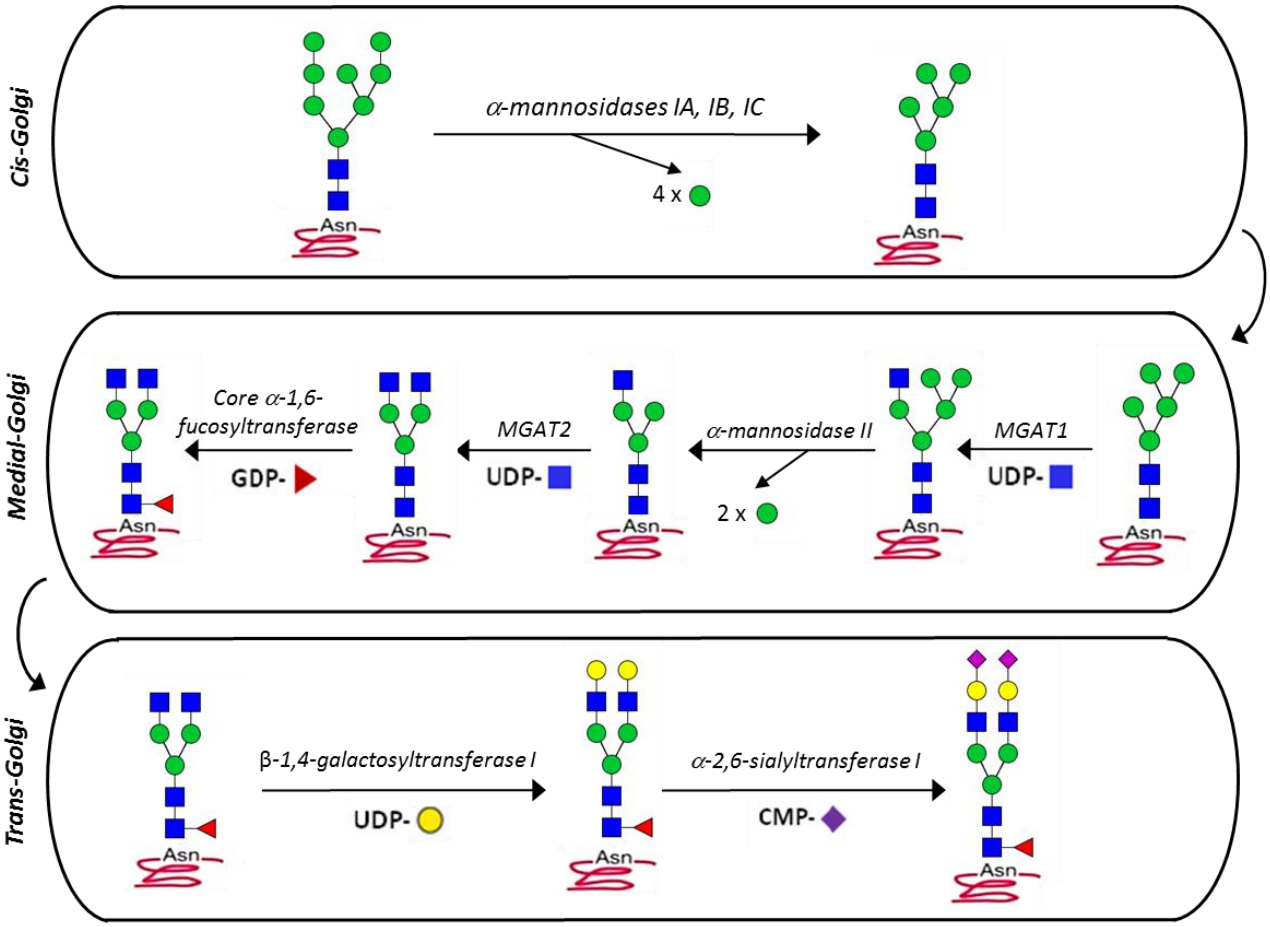

Figure 8. Golgi N-glycan processing and maturation to generate a complex bi-antennary fucosylated N-glycan. This structure is the most common N-glycan found in human.

mannose residues, one α-1,3 linked and the other one α-1,6 linked [26]. This cleavage will distinguish hybrid from complex types N-glycans [27].

Another GlcNAc residue is then added by MGAT2 on the newly-exposed mannose residue. In the medial Golgi, the GlcNAc residue attached to the Asn can also be fucosylated by a core α-1,6 fucosyltransferase. At the trans-Golgi level, two major sugars are added: galactose (Gal) and N-acetylneuraminic acid (Neu5Ac). Galactose is the first sugar to be added in a β-1,4 linkage on the GlcNAc residue, via the action of the β-1,4 galactosyltransferase I. Finally, a terminal Neu5Ac is added on galactose by an α-2,6 sialyltransferase, most notably the α-2,6 sialyltransferase I.

Although the biosynthesis of this structure is already quite elaborated, it does not illustrate the diversity of N-glycan structures. Indeed, complex human N-glycans can be modified by several GlcNAc transferases (MGAT4A, MGAT4B, MGAT4C MGAT5, MGAT5B) that can lead to bi- ; tri- or tetra- antennary N-glycans. MGAT3 can even transfer a GlcNAc residue to the β-linked mannose of the trimannosyl core of N-linked oligosaccharides and produces a bisecting GlcNAc, which is a signal to stop further elongation. β2 linked GlcNAc and β4 linked Gal residues can also be more or less fucosylated in different linkages by a set of fucosyltransferases (FUT1, 2, 3, 4, 5, 6, 7, 9). Finally, terminal sialic acid can also be added in an α-2,6 linkage by ST6Gal-II, or alternatively in an α-2,3 linkage by ST3Gal-IV or ST3Gal-VI. Moreover, N-glycans can be further elongated by polysialic acid structures in specific N-glycoproteins such as Neural cell adhesion molecules (NCAM) [28]. These polysialic acid structures are generated by ST8Sia-II and ST8Sia-IV, which will sequentially add one or several α-2,8 linked Neu5Ac on terminal sialic acid. In addition, Golgi N-glycosylation is not as sequential as presented here, since several enzymes can act together or in a different order as described here. For example, it is possible to find $Man_3GlcNAc_2$ or $Fuc_1Man_3GlcNAc_2$ structures on N-glycans, even if they are still minor species [29].

2.2. O-glycosylation

2.2.1. General introduction

O-glycosylation designates a lot of different types of glycosylation that have in common the attachment of the glycan moiety on a hydroxyl group of an amino acid (Ser, Thr or even Tyr or hydroxylysine for some specific modifications). The different O-glycosylation types are listed in Table 1 and are extensively reviewed in the literature [1,4,19,20]. Since most of these modifications occur in the ER, only mucin-type O-glycosylation will be addressed in details.

- **Mucin-type O-glycosylation** (referred simply as O-glycosylation for the rest of the manuscript) is the most common protein O-glycosylation and will be addressed later in section 2.2.2.

- **O-GlcNAcylation** is the attachment of a single O-linked GlcNAc residue on Ser or Thr of cytoplasmic, nuclear and mitochondrial proteins [30,31]. O-GlcNAcylation is a dynamic PTM catalysed by a couple of enzymes: O-GlcNAc transferase (OGT), the enzyme that adds the sugar using UDP-GlcNAc as donor and O-GlcNAcase (OGA) that removes the sugar. Disturbance in O-

GlcNAcylation homeostasis has been implicated in the pathogenesis of many human diseases, including cancer, diabetes and neurodegeneration. Recently, a novel type of O-GlcNAcylation, catalysed by an ER localised protein named EOGT, has been described on extracellular proteins such as NOTCH [32].

Table 1. Different types of O-glycosylation. ADAMTS, a disintegrin and metalloproteinase with thrombospondin motifs; EOGT, EGF domain-specific O-linked GlcNAc transferase; COLGALT1/2, Collagen Beta(1-O)Galactosyltransferase 1/2 ; OGT, O-linked GlcNAc transferase; POFUT, protein O-fucosyltransferase; POGLUT, protein O-glucosyltransferase; POMT, protein O-mannosyltransferase; TSR, thrombospondin type 1 repeat; XYLT, xylosyltransferase.

Name	linkage	localization of the glycosylation process	enzyme(s) involved in the first step	examples
mucin type O-glycosylation	GalNAc-α-Ser/Thr	Golgi	polypeptide GalNAc transferases	all mucins
O-GlcNAcylation	GlcNAc-β-Ser/Thr	cytosol	OGT	cytosolic, mitochondrial and nuclear proteins
O-GlcNAcylation	GlcNAc-β-Ser/Thr	ER ?	EOGT	O-GlcNAcylation on EGF repeats of extracellular proteins (NOTCH, DUMPY)
O-fucosylation	Fuc-α-Ser/Thr	ER/Golgi	POFUT1, POFUT2	TSR of thrombospondin or ADAMTS family (by POFUT1), EGF domain on NOTCH and clotting factors (by POFUT2)
O-mannosylation	Man-α-Ser/Thr	ER	POMT1, POMT2	a-dystroglycan
O-glucosylation	Glc-β-Ser	ER	POGLUT1	EGF domains on NOTCH and clotting factors
	Glc-α-Tyr	cytosol	Glycogenin	autoglycosylation of glycogenin during glycogen formation
O-galactosylation	Gal-β-Hydroxylysine	ER	COLGALT1, COLGALT2	collagen, adiponectin

- **O-fucosylation** is the attachment of a fucose (Fuc) residue on a Ser or Thr belonging to a consensus sequence on either Thrombospondin Repeat (TSR) domain or Epidermal Growth Factor (EGF) domain on several proteins. Addition on TSR repeats is catalysed by POFUT1 while POFUT2 catalyses the addition of Fuc on EGF repeats. In the case of EGF repeats, the O-fucose may be elongated to a tetrasaccharide in the Golgi apparatus by sequential addition of GlcNAc, Gal and sialic acid. O-fucosylation of TSR may be elongated to a disaccharide by the addition of a Glc residue. Discovered more than 40 years ago, the role of O-fucosylation is still not completely clear in mammals [33–35].

- **O-mannosylation** occurs in the ER, where a mannose residue is transferred by POMT1/POMT2 from dolichol phospho-mannose to Ser or Thr residues on proteins. O-mannosylation existence has been known in mammals for almost 40 years but the only well

documented O-mannosylated protein is the α-dystroglycan [36,37]. O-mannose glycans are known to be elongated in the Golgi apparatus by the addition of different sugars such as Gal, GlcNAc, sialic acid, glucuronic acid (GlcUA), Fuc and xylose (Xyl) [38]. Besides, O-mannosylation has now been implicated in a broad range of human diseases, including cancer and dystroglycanopathies called congenital muscular dystrophy (CMD). Recently, O-mannosylation has been identified on cadherins and protocadherins, expending the field of O-mannosylation [36,39].

- **O-glucosylation** is initiated by the O-glucosyltransferase POGLUT1, with the addition of a β-linked glucose residue to EGF domains on NOTCH or coagulation factors. The glycan can be elongated in the Golgi apparatus with two Xyl residues [1,40]. O-glucosylation is thought to finely tune NOTCH activity by modulating receptor-ligand interactions. In addition, O-glucosylation has also been observed in the cytosol on glycogenin, a glycosyltransferase that catalyses the formation of a short glucose polymer from UDP-Glc in an autoglucosylation reaction during glycogen formation [41].

- **O-galactosylation** only takes place in the ER on proteins carrying collagen like domains such as adiponectin or collagen itself. It consists of the attachment of β-linked galactose residue on a hydroxylysine residue. The glycan can then be elongated with the addition of a glucose residue. Collagen glycosylation is initiated by COLGALT1/2 [42].

2.2.2. Mucin-type O-glycosylation

This section presents a simplified view of the structures, biosynthesis, and functions of mucin-type O-glycans (referred simply as O-glycosylation for the rest of the section). Mucins are highly glycosylated and high molecular weight glycoproteins. They are present in many epithelial surfaces of the body, including the gastrointestinal, respiratory and genitourinary tracts, where they act as a protection against infection by pathogens, physical and chemical damages [1]. Mucin-type O-glycosylation is a widespread heterogeneous PTM of proteins found in the entire animal kingdom, but also in higher plants [43]. In contrast with N-glycosylation, no clear amino acid consensus sequence is known for O-glycosylation [44]. In mucins, O-glycans are covalently α-linked via an N-acetylgalactosamine (GalNAc) to the hydroxyl group of Ser or Thr thus forming an O-glycosidic bond. Three different regions can be distinguished on mucin-type O-glycans:

- **The core region**, located close to the protein chain and basically composed of 2 or 3 sugar residues. Unlike N-glycans, O-glycans have 8 different core glycan structures (Table 2). They all have in common the first α-GalNAc residue attached to the protein. Core 1 to 4 biosynthesis will be addressed in 2.2.2.1. Core 5 to 8 are less common and will not be discussed. However, a full overview is available on the literature [1,45].

Table 2. Structures of the different O-glycan cores. Core 1-4 are the most common structures, with core 1 and core 2 representing the most abundant ones in mammals.

Core 1	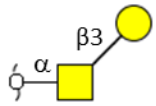 Galβ1-3GalNAcαSer/Thr	Core 5	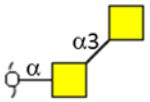 GalNAcα1-3GalNAcαSer/Thr
Core 2	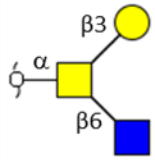 GlcNAcβ1-6(Galβ1-3)GalNAcαSer/Thr	Core 6	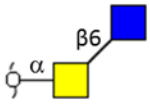 GlcNAcβ1-6GalNAcαSer/Thr
Core 3	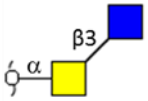 GlcNAcβ1-3GalNAcαSer/Thr	Core 7	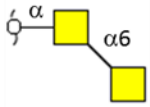 GalNAcα1-6GalNAcαSer/Thr
Core 4	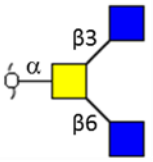 GlcNAcβ1-6(GlcNAcβ1-3)GalNAcαSer/Thr	Core 8	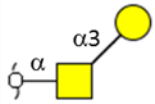 Galα1-3GalNAcαSer/Thr

- **The backbone**, which contributes to the length of the glycan chain. It is mostly composed of disaccharide unit repeats.

- **The peripheral region**, representing glycan antigens. This region is highly diverse in terms of glycan structures. It can be composed of Fuc, sialic acid, or acetyl variant of sialic acid.

2.2.2.1. Biosynthesis

The biosynthesis of O-glycans is a sequential process that only takes place within the Golgi apparatus. It begins with the transfer of a GalNAc residue from UDP-GalNAc onto a Ser or Thr on a fully folded protein. This step is catalysed by polypeptide N-acetyl-α-D-galactosaminyltransferases (ppGalNAc-Ts), a group of well conserved type II transmembrane glycosyltransferases. To date, more than 21 ppGalNAc-Ts localised throughout the Golgi

apparatus have been identified [46]. They are differentially expressed and more or less specific to the protein sequence where the first GalNAc residue is attached. The transfer of this first GalNAc residue generates a structure named the Tn antigen (Figure 9). Tn antigen can also be sialylated by a ST6GalNAc transferases to generate the sialyl-Tn (sTn) antigen. From the Tn antigen, all the different core structures can be synthesized.

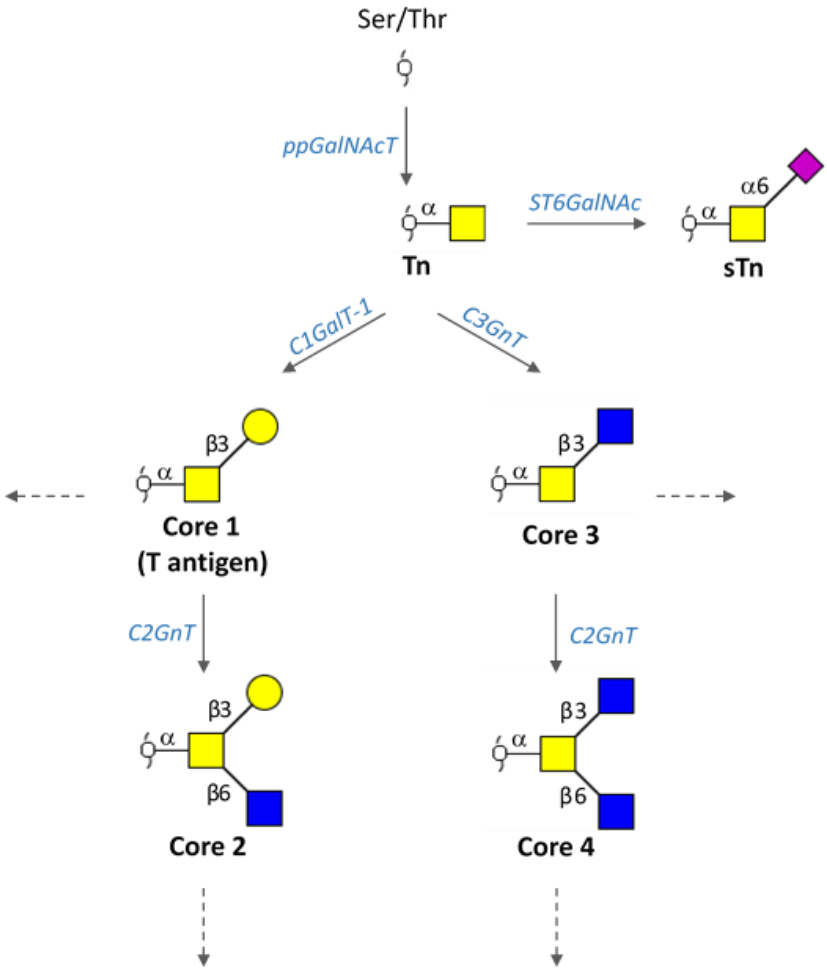

Figure 9. Biosynthesis of core 1 to core 4 O-GalNAc glycans. The attachment of the GalNAc to Ser/Thr is catalyzed by ppGalNAc-Ts and leads to the formation of the Tn antigen. The biosynthesis of core 1 and 2 of O-glycans is controlled by the activity of C1GalT-1 and C2GnT. Core 1 may be substituted with sialic acid or GlcNAc on the Gal residue (not shown), thus preventing the synthesis of core 2. Sulfate or fucose can also extend the core 1 (not shown). The biosynthesis of core 3 and 4 of O-glycans is controlled by the activity of the C3GnT and C2GnT. C2GnT1 and C2GnT3 have restricted activity at core 1, while C2GnT2 also has an activity on core 3 allowing the synthesis of core 4. Core 3 may be substituted with sialic acid in α2-6 linkage to GalNAc or with galactose in β1-4 linkage to GlcNAc. These substitutions prevent the synthesis of core 4. Core O-GalNAc glycans can be extended to form linear or branched structures and substituted with peripheral monosaccharides and/or sulfate groups. Dashed arrows represent the possibility of further elongation of each structures.

Core 1 to 4 biosynthesis is presented in figure 9. Core 1 biosynthesis is carried out by the transfer of a β-1,3 linked Gal residue to the Tn antigen by the core 1 β-1,3-galactosyltransferase 1 (C1GalT-1). The addition of a β-1,6 linked GlcNAc residue to the core 1 by a core 2 β-1,6-N-acetylglucosaminyltransferase (C2GnT) leads to the formation of the core 2. The core 3 is

synthesized by a single β-1,3-N-acetylglucosaminyltransferase (C3GnT) that catalyses the attachment of a GlcNAc residue to the Tn antigen. The core 4 is synthesized from the core 3 by the addition of a GlcNAc residue by the C2GnT2.

Core O-glycans can be extended with monosaccharides including Gal, GlcNAc, Fuc, or sialic acid, but not Man, Glc, or Xyl residues. For example, the backbone of O-glycans is frequently elongated by a subset of GlcNAc-transferases and galactosyltransferases to form repeated GlcNAcβ-1,3-Galβ-1,4 (poly-N-acetyllactosamine) sequences. The terminal part of the O-glycan chains of mucins is highly diverse and generates specific antigenic glycan structures. Important other modifications of mucin O-glycans also include O-acetylation of sialic acid and O-sulfation of Gal and GlcNAc residues.

2.2.2.2. Function(s)

O-glycans have been shown to be involved in a wide range of cellular functions [43,44]. They have a role in sorting and secretion of glycoproteins, on protein conformation, in cell adhesion, angiogenesis, inflammatory responses and autoimmunity. O-glycosylation of mucins is essential to confer their ability to hydrate and protect the underlying epithelium. Besides, the glycan moiety provides almost a complete protection from protease degradation. In addition, alteration of O-glycosylation in animal models leads to pathological phenotypes ranging from embryonic death to developmental defects [44]. Dysregulation of O-linked glycosylation have been associated with a broad range of pathological conditions including familial tumoral calcinosis, Tn syndrome, IgA nephropathy, tumour formation and metastasis.

2.3. Glycosaminoglycans

Glycosaminoglycans (GAG) are polysaccharide side chains of proteoglycans made of linear disaccharide repeating units. These units are composed of an N-sulfated or N-acetylated hexosamine (D-galactosamine (GalN) or D-glucosamine (GlcN)) and an uronic acid (L-iduronic acid (IdoUA) or D-glucuronic acid (GlcUA)) or sometimes a Gal residue. According to the structure of the disaccharide unit, GAG are classified into several families: hyaluronic acid (HA); chondroitin sulfates (CS) and dermatan sulfates (DS); heparan sulfates (HS) and heparin; keratan sulfates (KS).

2.3.1. Structure and biosynthesis of glycosaminoglycans

The final structure of each GAG class is presented in Figure 10. Their biosynthesis will not be addressed since it is beyond the scope of my thesis. However, reviews about their biosynthesis are available in the literature [1,47].

HA is a high molecular weight GAG composed of [GlcUAβ-1,3-GlcNAcβ-1,4-] repeats. Unlike other GAGs, HA is never associated with a protein to form a proteoglycan and does not undergo any modifications. Besides, biosynthesis of HA does not occur in the Golgi apparatus but on the internal surface of the plasma membrane.

The disaccharide component of the CS is the [GlcUAβ-1,3-GalNAcβ-1,4-] unit repeat. It can be sulfated at the C4 and/or C6 positions of the GalNAc residues and at the C2 position of the GlcUA residue [48]. DS are distinguished from CS by the presence of IdoUA residues in their structure. The biosynthesis of CS and DS takes place in the Golgi and is carried out by more than 15 different enzymes [49].

Heparin is exclusively synthesized by mast cells and is composed of the repetition of disaccharide units most often formed of IdoUA residues bound to sulfated GlcN [50]. HS are composed of the repetition of the same disaccharide unit as heparin, with the difference that they preferentially contain GlcUA residues instead of IdoUA. The most represented disaccharide in the HS chains is the [GlcUAβ-1,4-GlcNAcα-1,4-] structure but more than 20 disaccharides with different modifications have been identified. The biosynthesis of HS and heparin occurs in the Golgi apparatus and involved at least 25 enzymes (glycosyltransferases, sulfotransferases, epimerases), thus explaining the high structural diversity of these molecules [47].

KS are N-acetyl-lactosamine [Galβ-1,4-GlcNAcβ-1,3] polymers that can be sulfated at the C6 position on the two monosaccharides. KS are synthesized in the Golgi apparatus and can differ in their type of binding to the protein core. KS of the cornea, called KS-I, are linked via an N-glycan bond to the proteins. KS isolated from the cartilage, called KS-II, are linked via an O-glycosidic bond to serine or threonine residues. A third type of binding via serine-bound mannose has been described, which defines KS-III [51]. KS present a great heterogeneity of length and sulfation. In addition, they may carry sialic acid residues in the non-reducing terminal position.

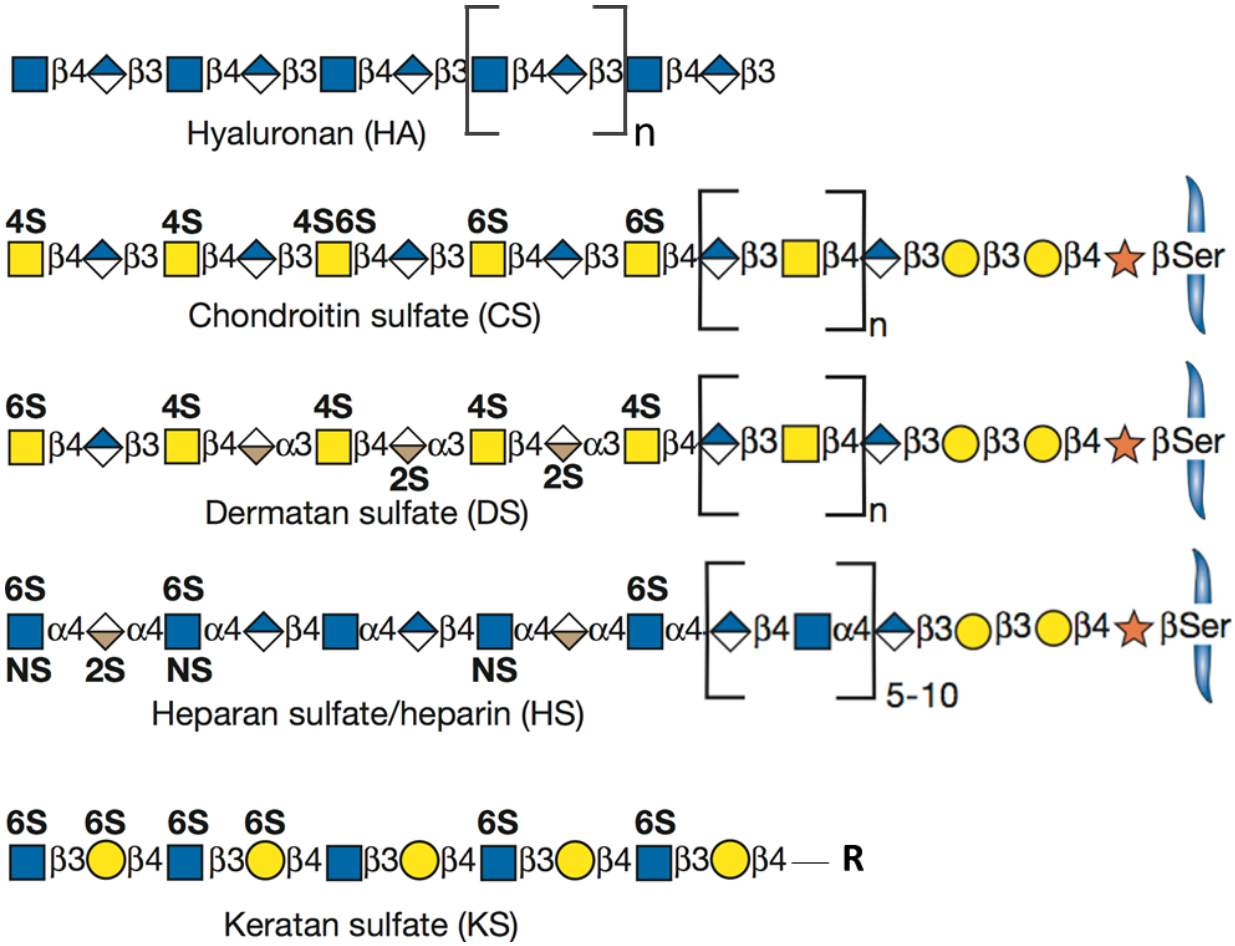

Figure 10. Structures of each glycosaminoglycan class. GAG consist of disaccharide unit repeats composed of an N-acetylated or N-sulfated hexosamine and either an uronic acid (GlcUA or IdoUA) or Gal. DS is distinguished from CS by the presence of IdoUA. KS lack uronic acids and instead consist of sulfated Gal and GlcNAc residues. R can be a N-glycan, O-glycan or a mannose bound to a Ser residue, depending on the type of KS. HS, CS and DS originates from the same tetrasaccharidic core containing 1 Xyl, 2 Gal and 1 GlcUA. Adapted from Essentials of Glycobiology, 2nd edition 2009.

2.3.2. Function(s)

The biological functions of proteoglycans mainly depend on the interaction of the glycosaminoglycan chains with different protein ligands. Due to the high diversity of GAG structures, proteoglycans are involved in a broad range of functions including: cell matrix organization, protein internalization, cell signalling, cell migration and cellular interactions. GAG defects have been linked to a wide range of pathological conditions such as Ehlers-Danlos syndrome, exostoses, and diverse skeletal dysplasias [52].

2.4. Glycolipids

Glycolipid (GL) designates a molecule containing a glycan linked to a lipid moiety. In mammals, most GL are glycosphingolipids (GSL), but glycoglycerolipids, glycophosphatidylinositol and other

types exist. In this section, a focus will be done on GSL as they are synthetized in the Golgi apparatus.

2.4.1. Glycosphingolipids

GSL are plasma membrane glycolipids particularly present in the brain of mammals, where they represent up to 80% of glycoconjugates [1]. They are composed of a hydrophobic lipid part, the ceramide, anchored to the membrane and a hydrophilic glycan moiety exposed at the cell surface [1,53]. The structure of the ceramide can vary in length, hydroxylation or saturation, resulting in significant structural diversity. However, the main structural diversity of GSL is based on the glycan part [53].

2.4.1.1. Biosynthesis

GSL can be divided into two main classes, depending on the first monosaccharide bound to the ceramide. Gal addition forms the galactosylceramide (GalCer) whereas Glc addition forms the glucosylceramide (GlcCer), present in most eukaryotic cells and the precursor to complex GSL. GlcCer is typically substituted by a β-linked Gal residue on the C4 hydroxyl of the Glc to generate the lactosylceramide structure (Galβ-1,4Glcβ-1-O-Cer, LacCer). GlcCer can also substituted by mannose residue to form the mollu- and artho- series of GSL, mainly found in invertebrates [54]. Extension of LacCer can generate 5 different series depending on the substitution, as described in Table 3. In mammals, gangliosides are synthetized in all cells but are still predominant in the brain while GSL of the neolacto series are found in hematopoietic cells. On the contrary, GSL of the lacto series are mostly found in the secretory organs and those of the globo series are the most abundant in erythrocytes [55].

Table 3. Structures of the major GSL series in mammals. The LacCer common structure is depicted in blue.

Series	Structure
Ganglio	GalNAcβ-1,4-Galβ-1,4-Glcβ-1-O-Cer
Neolacto	Galβ-1,4-GlcNAcβ-1,3-Galβ-1,4-Glcβ-1-O-Cer
Lacto	Galβ-1,3-GlcNAcβ-1,3-Galβ-1,4-Glcβ-1-O-Cer
Globo	Galα-1,4-Galβ-1,4-Glcβ-1-O-Cer
Isoglobo	Galα-1,3-Galβ-1,4-Glcβ-1-O-Cer

Since gangliosides are ubiquitous and crucial during brain development, this section will present a brief overview of their biosynthesis. Gangliosides are acidic GSL containing one to five sialic acid residues. Their biosynthesis takes place in the Golgi apparatus and begins with the transfer of sialic acid residues to LacCer by specific sialyltransferases (ST3Gal V, ST8Sia I, ST8Sia V) (Figure 11). LacCer, GM3, GD3, and GT3 are the precursors for 0-, a-, b-, and c-series gangliosides, respectively. GalNAc, Gal, and Neu5Ac residues can be next transferred in a stepwise sequential manner. Similarly to N-glycosylation, the first steps of gangliosides biosynthesis take place in the cis/medial-Golgi and the later ones in the trans-Golgi and TGN [56].

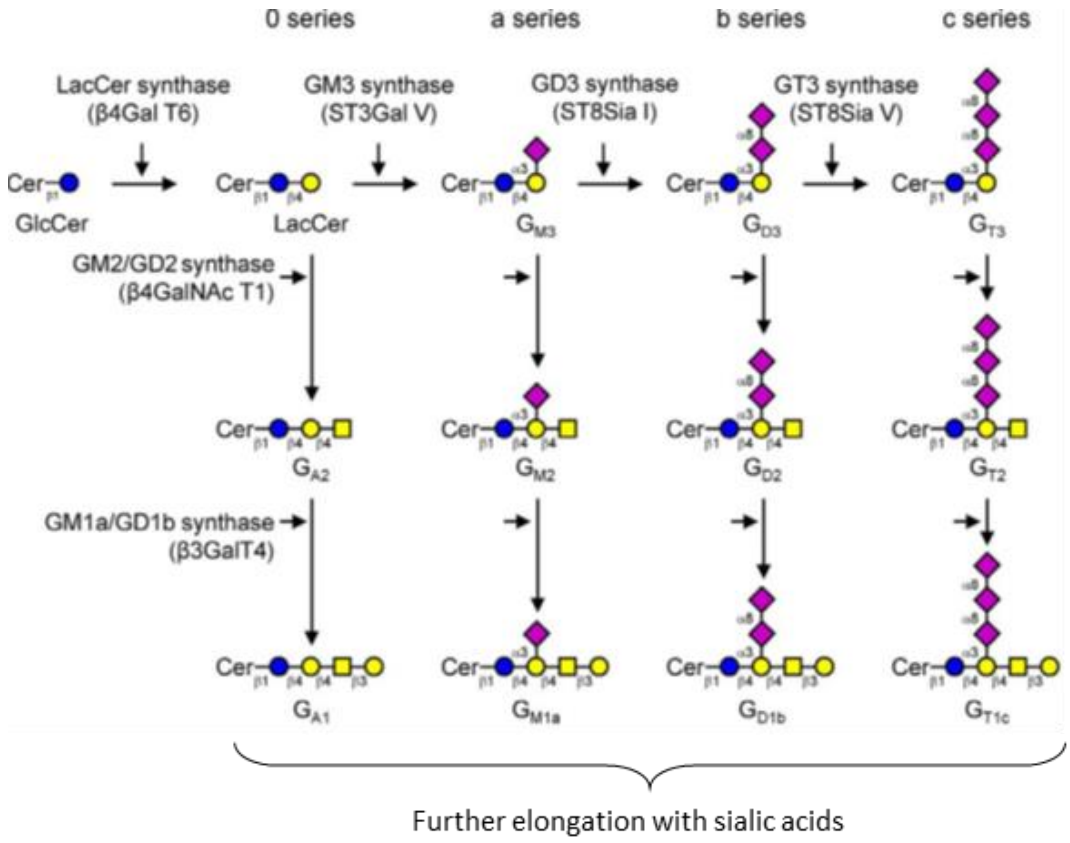

Figure 11. Simplified view of the biosynthesis pathways for gangliosides. Gangliosides are synthesized by the stepwise addition of sugars first to Cer. Cer is the acceptor for UDP-Glc:ceramide β-glucosyltransferase to generate LacCer. The action of ST3Gal V, ST8Sia I and ST8Sia V leads to the precursors of a-, b-, and c-series gangliosides. The 0-series gangliosides are directly synthesized from LacCer. Elongation is then performed by the sequential action of β4GalNAcT1, β3GalT4, ST3Gal II, ST8Sia V and ST6GalNAc V. Adapted from Groux-Degroote and collaborators, ChemBiochem 2017.

2.4.1.2. Function(s)

GSL are essential glycolipids in the nervous system, the immune system, and especially during embryogenesis and early development. They are involved in a wide range of functions such as cell adhesion, cellular interactions, proliferation, and modulation of signal transduction pathways. These functions are mainly governed by the glycan moiety. Moreover, GSL are

required for development at the whole-animal level. Indeed, mice lacking either the gene coding for the GlcCer synthase or the LacCer synthase fail to properly develop [57,58].

2.5. Factors involved in the regulation of the Golgi glycosylation process

Golgi glycosylation relies on many different actors, from enzymes directly related to glycosylation, to proteins involved in the maintenance of the Golgi apparatus homeostasis. Therefore, glycosylation is a highly regulated cellular process that requires a precisely controlled environment to be fully functional (Figure 12). This section describes all the factors known to be involved in the smooth functioning of Golgi glycosylation. Factors that are thought to be regulators of glycosylation will also be discussed. The precise homeostasis controls of some of these factors will be detailed in chapter 3.

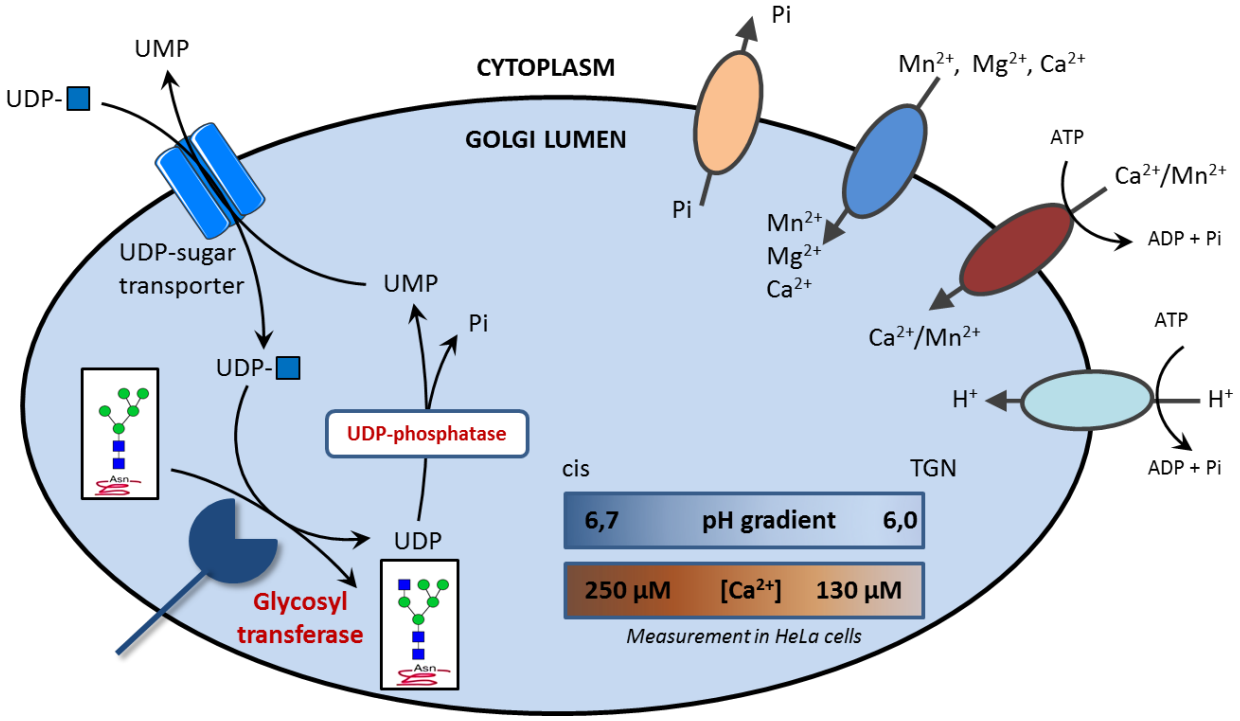

Figure 12. Golgi glycosylation is an extremely regulated process. Example with the addition of a GlcNAc residue to the $Man_5GlcNac_2$ N-glycan by MGAT1. Each step relies on the existence of specific nucleotide sugar transporters and specific glycosyltransferases. Golgi glycosylation also relies on the glycosyltransferase localization which must be the same as the nucleotide sugars they need. Glycosyltransferases also need a particular ionic environment, especially in terms of Mn2+, Ca2+ and Mg2+, H+ and inorganic phosphate. Even slight modifications in the Golgi homeostasis can lead to abnormal glycosylation.

2.5.1. The Golgi apparatus structural organisation

The structural organization of the Golgi apparatus is vital for glycosylation. Actually, the spatial organisation in distinct cisternae and stacks allows the correct sequential glycosylation process [59]. It has recently been highlighted by two proteins involved in the maintenance of the Golgi

stacks, named GRASP55 and GRASP65. Indeed, knocking out these proteins in human cell lines caused the formation of an unstacked Golgi apparatus leading to an impaired glycosylation [60].

The Golgi apparatus is known to be a center of phosphoinositide metabolism and phosphoinositides are non-uniformly distributed throughout the Golgi. Interestingly, the association between the Golgi matrix protein GOLPH, PI4P and actomyosin has been shown to likely be involved in the maintenance of the Golgi structure [61]. In addition, siRNA experiment targeting the human phosphatidylinositol phosphatase SAC1 led to a change in PI4P distribution, resulting in Golgi morphological changes, Golgi GT mislocalization, and ultimately to glycosylation defects [62]. Therefore, the first checkpoint for glycosylation is the maintenance of a correct Golgi structural organization.

2.5.2. Changes in GT expression levels

The total glycan repertoire found in an organism or a cell depends on the level of expression of the enzymes involved in glycosylation. Besides, changes in the expression of genes coding for GT have been reported during early development [63] but also in cancer and inflammation [64–67]. In fact, in such contexts, glycosylation has been shown to be completely modified due to changes in gene expression of one or several GT. Modifications of NST or GH expression levels might also modify Golgi glycosylation, but most of the published studies focused on GT expression rather than NST and GH.

2.5.3. Subcellular localization of Golgi GT, GH and NST

As depicted in Figure 12, the glycosylation reaction requires for each step that a GT, an acceptor substrate, a donor substrate and consequently the corresponding NST, localize in the same Golgi cisternae. If any of these actors is not properly localised in the same cisternae, it could lead to glycosylation defects. In this section, the subcellular localization of GT will be mostly discussed, but GH and NST localization will also be addressed.

Golgi GT are found restricted to a subset of Golgi cisternae, allowing the sequential glycosylation of passing glycoproteins/glycolipids. The potential link between glycosylation and GT localization in mammals was first described by Chaney and collaborators in 1989 [68]. They identified a mutant in CHO (Chinese Hamster Ovary) cell lines that fails to synthetize β-1,6 branched N-glycans, a step catalysed by MGAT5. Interestingly, these cells retain MGAT5 enzymatic activity,

but the enzyme was found in the ER instead of the Golgi. This led scientists to ask an important question: how does a cell retains Golgi proteins? First, although some retention sequences have been identified in Golgi resident proteins such as (F/L)-(L/V)-(S/T) and K-X-D/E, none of them are found in Golgi GT or GH. Therefore, different models have been proposed to explain Golgi GT proper localization:

- **a/ Oligomerization**: oligomerization seems to be a common feature of Golgi GT. By bimolecular fluorescence complementation analyses, authors have demonstrated that GT can form either homo or heterodimers [69,70]. For example, β-1,4-galactosyltransferase I can either form homodimers or heterodimers with α-2,6-sialyltransferase I.

- **b/ Lipid based partitioning:** lipid composition of Golgi membranes is different from cis to trans-Golgi. The idea is that GT/GH oligomerization in the Golgi membrane depends on:
    - Thickness differences between the TMD of the GT/GH and Golgi membrane.
    - GT/GH affinity preferences for sphingo/glycerophospholipids in the Golgi membrane.

In addition, several proteins, such as GOLPH3, regulate localization of glycosyltransferases by working as a coatomer adaptor [71]. Concerning GH localization, their limited number in the Golgi make them harder to study. Thus, less is known about the mechanisms of GH Golgi localization, but one can suggests that some mechanisms resemble the ones described for GT.

GT and the nucleotide sugar donor they need must be localized in the same Golgi compartment. However, all nucleotide sugars are synthetized in the cytosol, excepted for the CMP-Neu5Ac, which also contains a step in the nucleus. Therefore, nucleotide sugars must be imported into the Golgi apparatus by specific NST, which must be properly localised to provide the right nucleotide sugar to GT (Figure 13). It has been shown that the correct localisation of NST probably involves the formation of NST oligomers [72].

2.5.4. Vesicular trafficking

Localization is a balance between retention and recycling, pointing out the importance of vesicular trafficking in maintaining a correct glycosylation [73]. Indeed, defect in vesicular trafficking can lead to an impaired glycosylation as highlighted by defects in the COG complex, a tethering complex involved in Golgi retrograde trafficking. The importance of the COG complex was first observed in CHO ldlc (the ortholog of COG2) null mutant, which show a defect in

multiple glycosylation pathways due to a mislocalization of several GT [74,75]. The link between COG and glycosylation was later strengthened with the discovery of human genetic glycosylation diseases due to COG mutations [76] (see chapter 5).

2.5.5. Nucleotide sugars transporters activity

In addition to their precise localization discussed before, NST transport activity is also a modulating factor of glycosylation. NST are in fact antiporters that always couples the uptake of the nucleotide sugar to the exit of the XMP [77].

All NST share several common kinetic properties [78]:

- Translocation of the nucleotide sugar can be saturated and the apparent Km is in the micromolar range (1-10 µM).
- Translocation is insensitive to the presence of ATP or ionophores.
- Translocation is competitively inhibited by the corresponding nucleoside mono- and diphosphate, but not by the free monosaccharide.

All these features highlight the role of NST activity in regulating Golgi glycosylation. Therefore, modifying NST activity may have significant consequences for glycan structure and NST activity can be a rate-limiting step in the glycosylation process. Consequently, a decrease in nucleotide sugar transport leads to truncated N-glycans among other phenotypes [79]. The first NST mutant was described in *Caenorhabditis elegans*, in the *svq-7* mutant defective in UDP-GlcUA transporter. Toyoda and collaborators have later shown that the biosynthesis of GAG was impaired in this mutant [80]. In CHO cells, a point mutation on Gly189 of the CMP-sialic transporter abolished all transport function. As a result, glycoconjugates found on cell surface lack terminal sialic acid [72]. Finally, the recent discovery of human genetic diseases caused by mutations in genes encoding NST reinforced the tight link between NST activity and glycosylation.

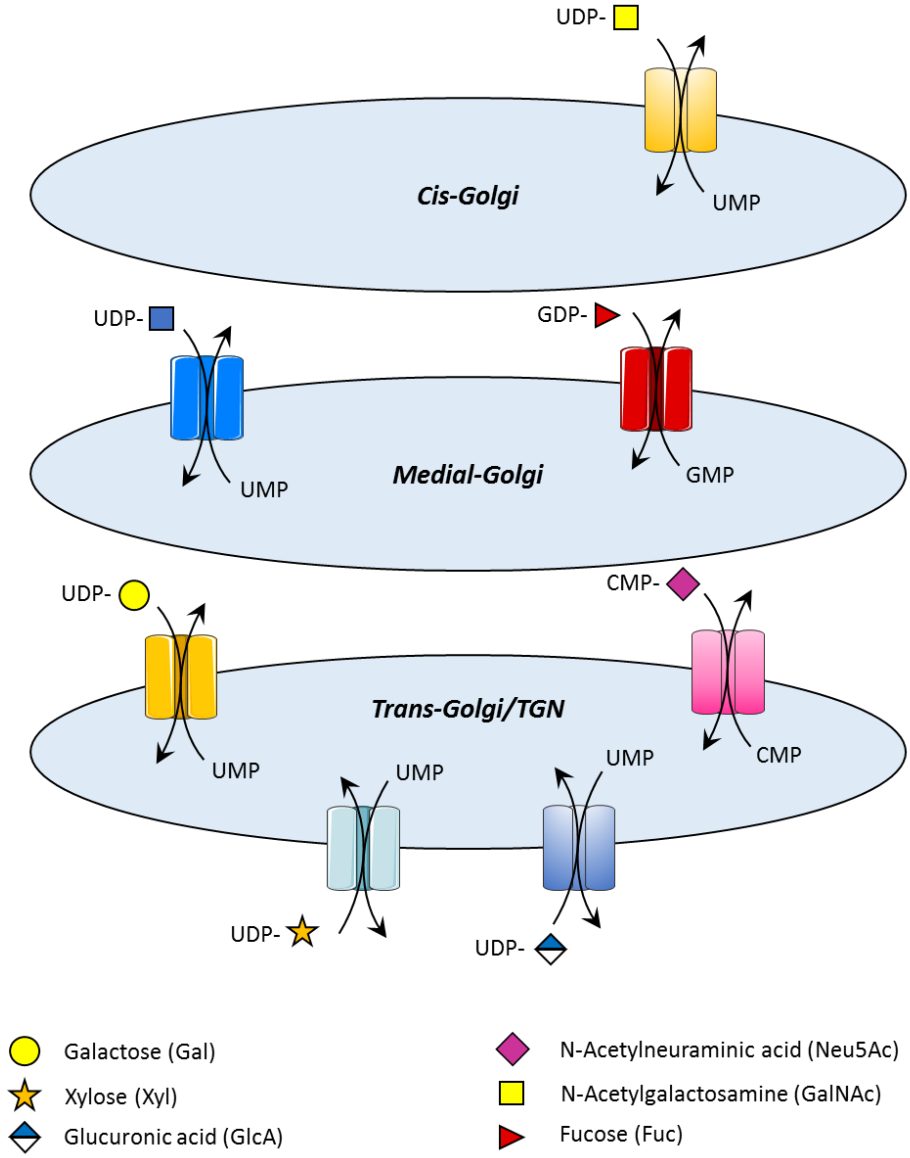

Figure 13. Golgi nucleotide sugar transporters found in mammals. Their precise localization is required for a proper glycosylation. Some transporters are bifunctional. For example, SLC35D1 is able to transport both UDP-GlcUA and UDP-GalNAc. These transporters are not depicted here for clarity. All Golgi NST belong to the SLC35 family.

2.5.6. Luminal nucleoside diphosphatases

As highlighted before, GT using XDP-sugars generate free XDP that are known to inhibit GT activities. Thus, nucleotide sugar diphosphatases exist in the Golgi lumen to catalyse the hydrolysis of XDP to XMP + Pi (inorganic phosphate). These enzymes add another layer of complexity in Golgi glycosylation regulation. Knowledge on Golgi nucleotide sugar diphosphatases is small and only few human Golgi members are discovered (ENTP4, ENTP5, ENTP6) but their activity can affect XMP levels and therefore the nucleotide sugar import into

the Golgi apparatus [72,81]. In yeast, GDA1, a Golgi luminal guanosine diphosphatase is required for proper glycosylation, as GDA1 null mutants display a glycosylation defect [82].

2.5.7. pH

Golgi apparatus is an acidic organelle. In fact, the GA progressively acidifies from cis, where the pH is around 6.7, to trans-Golgi/TGN to reach a value around 6.0 (Figure 14) [83]. Therefore, pH variations have a dramatic effect on cellular processes taking place at the Golgi level such as glycosylation. In 1986, Thorens and Vassalli found that increasing the pH of acidic compartment (Golgi, endosomes, lysosomes) with chloroquine or ammonium chloride, two weak bases, prevented terminal glycosylation of immunoglobulins without affecting their secretion [84]. Besides, in LS174T cells, treatment with bafilomycin A1, an antibiotic that raises intra-Golgi pH, modified mucin glycosylation and decreased mucin sulfation [85]. In fact, pH has a strong effect on Golgi GT localization. Indeed, increasing Golgi pH using ammonium chloride or bafilomycin A1 induces a redistribution of GALNT2, B4GALT1 and POMGNT1. Bafilomycin A1 causes a delocalisation of the GT on the cell surface and ammonium chloride in endosomal compartment [86]. More recently, it was shown that only a 0.2 pH unit increase was sufficient to impair α-2,3 sialylation by redistributing α-2,3 sialyltransferase into endosomes [87].

pH can also possibly have an effect on GT activity, since they require an optimal pH to be fully active, like any other enzyme. However, most of the time, the main consequence of a pH increase is a rapid redistribution of several GT leading to glycosylation changes. Moreover, GH and even NST might also be affected by pH changes but no *in vivo* studies are available in the literature. Finally, the effect of an overacidification of the Golgi is not well known, since tools are lacking to decrease pH of acidic compartments. However, one can think that it could also disrupt glycosylation.

In conclusion, alterations of Golgi pH are associated with glycosylation abnormalities by inducing a mislocalization of Golgi glycosyltransferases and/or interfering with their activity.

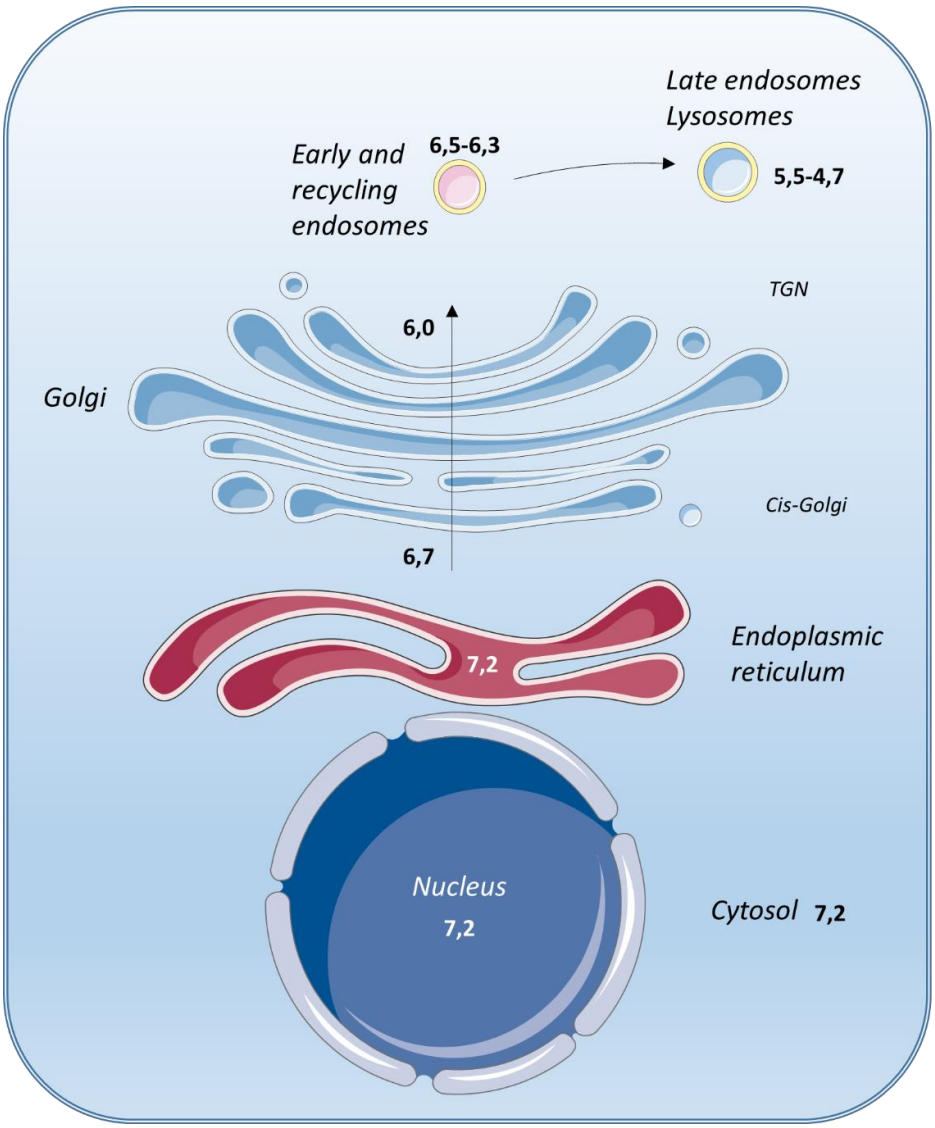

Figure 14. pH values of the secretory pathway. pH values of individual cellular organelles and compartments in a mammalian cell were collected from various sources.

2.5.8. Divalent cations

Although not intensively studies *in vivo*, divalent cations homeostasis play an important role in mammalian glycosylation. Indeed, GT can mainly adopt two types of folding, named GT-A and GT-B, and GT-A enzymes are known to require a divalent metal-ion in their catalytic site as a cofactor for the glycosylation reaction [88].

2.5.8.1. Mn2+

Even if Mn2+ is a trace element, its importance for glycosylation is known for a long time, at least *in-vitro*. Indeed, more than 40 years ago, authors have shown that β-1,4-galactosyltransferase I (B4GALT1; EC 2.4.1.22) activity drastically increased in the presence of Mn2+ in its catalytic site

[6,89]. They also observed a slight activation with other cations, such as Zn2+, Co2+, Cd2+, Fe2+, and Pr3+, but nothing comparable to Mn2+. It was thus confirmed later by structural analysis that this enzyme clearly bound Mn2+ in the catalytic site [90]. Since Mn2+ and glycosylation are at the center of my thesis, a full overview of the link between Mn2+ and glycosylation will be done in chapter 4.

2.5.8.2. Mg2+

Sialyltransferases are known to preferentially bind Mg2+ in their catalytic site compared to Mn2+. In fact, sialyltransferases activation is better with Mg2+, but they can also be activated by Mn2+ and to a lesser extent by Ca2+ [91]. Apart from sialyltransferases, no known Golgi GT preferentially required Mg2+. Strangely, an old paper from 1987 showed that β-1,4-galactosyltransferase 6 required both Mn2+ and Mg2+ to be fully active, since none of the cation alone increased the enzymatic activity [92].

2.5.8.3. Ca2+

To date and to my knowledge, no direct link between Ca2+ and glycosylation has been established *in-vivo*. However, Ca2+ is known to be involved in triggering trafficking events [93,94]. Thus, Ca2+ could be indirectly linked to glycosylation by regulating intra Golgi trafficking for example. In addition, Cheng and DeVries showed in 1985 that a human α-1,2-fucosyltransferase can be greatly activated by Mn2+ and Ca2+ *in-vitro*. They observed a 3-fold enzymatic activity increase after Ca2+ addition by measuring incorporation of fucose from GDP-L-[^{14}C] fucose into a glycoprotein acceptor [95].

Mannosidase Alpha Class 1B Member 1 (Man1b1), is a Golgi class I mannosidase originally thought to be ER-localised [96]. In 2004, structural analysis of the mouse ortholog showed that Man1b1 binds Ca2+ to be fully active and it was then hypothesized that human Man1b1 could also requires Ca2+ as a cofactor [97]. In addition, the nucleoside diphosphatase ENTP4 has been shown to require Ca2+, but can also use Mg2+ and Mn2+ with lower efficiency [81]. Finally, N-acetylglucosamine-1-phosphotransferase (GNPTA/B) is also thought to bind Ca2+ according to the PROSITE database.

2.5.8.4. Other divalent cations

Generally speaking, little is known about other divalent cations required for Golgi glycosylation. However, in addition to Mn2+ and Ca2+, human α-1,2-fucosyltransferase has been shown to be activated by Ba2+ and Mg2+ to a lower extent [95]. On the contrary, Fe2+, Cd2+, Co2+ and Zn2+ decreased its catalytic activity. Besides, α-1,3-fucosyltransferase V is activated by Mn2+, Mg2+ and also slightly by Co2+ and Ca2+ [98]. Moreover, the Golgi α-mannosidase II is thought to bind Zn2+ according to the PROSITE database.

2.5.9. Inorganic phosphate

Pi are generated by XDP-phosphatases during the conversion of the XDP to the XMP in the Golgi apparatus. They are negatively charged molecules (PO_4^{3-}) that must leave the Golgi to avoid any disturbance in overall ion homeostasis. One can easily think that Pi could be indirect regulator of glycosylation. However, no clear link between Pi and glycosylation has been described so far in the literature.

[3] REGULATION OF GOLGI ION HOMEOSTASIS

The concept of homeostasis was introduced more than 150 years ago by Claude Bernard. It was defined as the property of a biological organism to actively regulate variables, such as the concentration of a substance in body fluids, in order to maintain a stable and nearly constant internal environment. Homeostasis can be observed at different levels, from the organism to the organelle inside a cell. Indeed, as described in section 2.5, Golgi homeostasis is crucial for a proper glycosylation. In particular, any disruption in Golgi ionic environment, especially in terms of divalent cations and pH, can lead to glycosylation abnormalities. Therefore, we will focus in this chapter on the precise regulation of these ions in the Golgi apparatus.

The Golgi apparatus is an organelle at the center of the secretory pathway. Therefore, Golgi homeostasis obviously relies on actors localised in the Golgi, but can also be affected by actors at the plasma membrane, endosomes, ER and other organelles, since all these organelles interact with each other to form a hub of vesicular trafficking. In conclusion, Golgi ion homeostasis can be studied independently but whole cellular homeostasis should always be taken into account in such studies.

We previously showed that glycosylation requires a specific and highly regulated environment. However, the field of Golgi ion homeostasis is relatively new and a lot of work remains to be done. Therefore, little is known in mammals and even less in human about Golgi overall ion homeostasis. In this chapter, an overview on Golgi ion homeostasis in human will be addressed with a special focus on Ca2+ and Mn2+ homeostasis. If necessary, information in other organisms (yeast, plants…) will be presented to provide a full overview of Golgi ion homeostasis.

3.1. Ca2+

The average adult body contains approximately 1 kg of calcium, and 99% of total calcium is found in bones [99]. Still, the only source of calcium intake is the diet. Once ingested, calcium is absorbed by epithelial cells in the small intestine where it binds several calcium binding proteins. Ca2+ can finally reach the blood by crossing the basal membrane of epithelial cells. Total plasma Ca2+ concentration is around 2-2.5 mM and approximately 40% is bound to proteins, 10% is engaged in complexes with anions and 50% is ionized free Ca2+ [99]. Intestine, bone and kidney are the three principle organs handling calcium homeostasis. Bone serves as a storage for Ca2+

deposit and kidneys have an important role in Ca2+ reabsorption. Finally, the urine is the main body fluid involved in Ca2+ exit from the body.

At the cellular level, Ca2+ homeostasis is tightly regulated by a large number of Ca2+ pumps, channels and transporters. Ca2+ is involved in several physiological processes, and especially in triggering intracellular signalling events crucial for cell proliferation, survival or apoptosis [100]. Thus, even small changes in cytosolic Ca2+ concentration can drastically modify all the cell metabolism. Therefore, high level of regulation is required to maintain a cytosolic Ca2+ concentration around 100nM. For this reason, several Ca2+ storage organelles exist in human cells. It is known for quite some time that the main organelle for Ca2+ storage is the ER, since ER Ca2+ resting concentration can reach 600µM [101]. In addition to the ER, several secondary Ca2+ storage organelles exist such as mitochondria, lysosomes and also the Golgi apparatus [102]. The Golgi apparatus is able to store 5% of total Ca2+, and is more resistant to Ca2+ depletion than the ER [103]. In addition, a gradient of Ca2+ can be observed in the GA, from around 250-300µM in the cis-Golgi to approximately 130µM in the trans/TGN of HeLa cells [104,105]. These observations proves that the GA is well equipped with a set of proteins capable of regulating Golgi Ca2+ homeostasis (Figure 15).

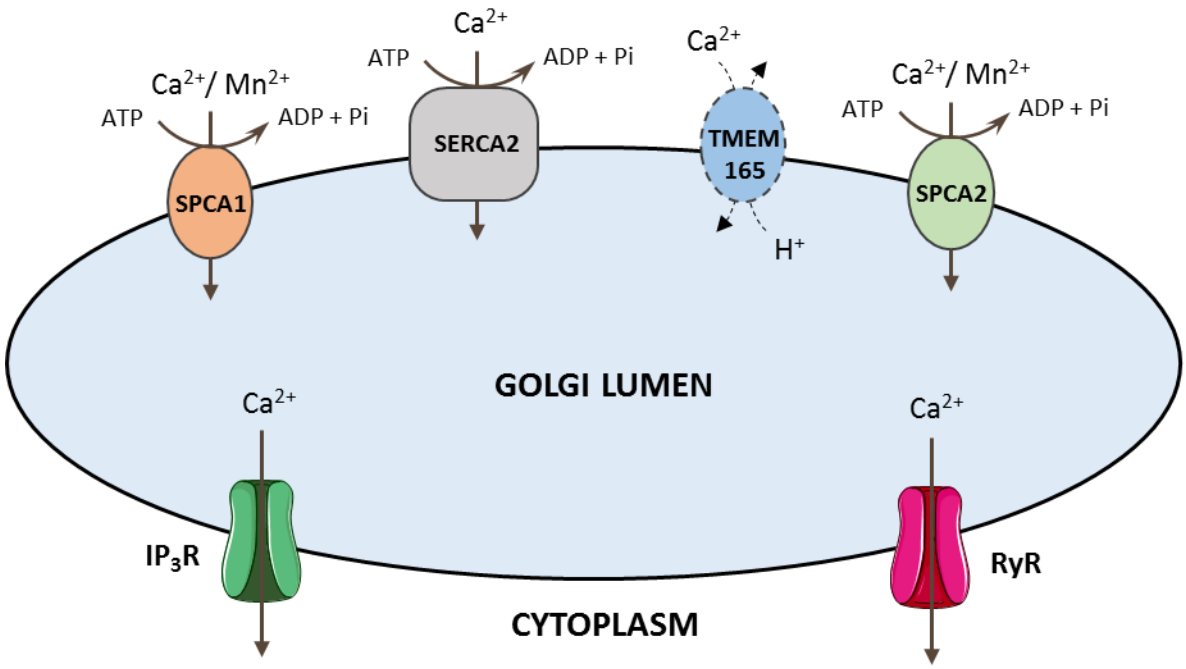

Figure 15. Overview of Golgi Ca2+ homeostasis. Golgi apparatus is equipped with pumps and channels to properly regulate Ca2+ concentration. RyR = Ryanodine Receptor; IP_3R = Inositol-3-phosphate Receptor. In addition, the GA contains several Ca2+ binding proteins (CALNUC, Cab45, calumenin, p54/NEFA) involved in Ca2+ retention inside the organelle. TMEM165 is depicted in dashes, because its involvement in Ca2+ homeostasis in still unclear.

Ca2+ homeostasis at the cellular level is very complex and cannot be summarize easily. Therefore, in this section, only actors directly involved in the maintenance of Golgi Ca2+ homeostasis will be presented (Figure 15). However, several reviews of whole cellular Ca2+ homeostasis are available in literature [100,102,106,107].

3.1.1. Ca2+ uptake in the Golgi

Ca2+ uptake at the Golgi level is mostly done by P-type ATPases:

- **Secretory Pathway Calcium ATPase 1 and 2 (SPCA1 and SPCA2):** SPCA1 is known to be involved in the Ca2+ import into the Golgi lumen [108]. Besides, SPCA1 is more expressed in the trans-Golgi part of the organelle. As a consequence, it has been demonstrated in HeLa cells that Ca2+ uptake at the trans-Golgi level relies almost exclusively on SPCA1 [105]. Although SPCA1 involvement in GA homeostasis is important, it seems to vary depending on the cell line. SPCA2 is not an isoform of SPCA1, as it is encoded by another gene. SPCA2 tissue distribution (brain, gastrointestinal tract, prostate, thyroid, salivary and mammary glands) and cellular expression appears different and more restricted than SPCA1, underlying a more specialized role for this pump [109,110]. SPCA2 is also mostly localized in the trans-Golgi but its role in Golgi Ca2+ homeostasis is less studied. Nevertheless, SPCA2 has been shown to interact with Orai1 at plasma membrane/Golgi contact sites, allowing the coupling of Ca2+ uptake at the plasma membrane to Ca2+ uptake at the Golgi level [111].

- **Sarco/Endoplasmic Ca(2+)-ATPase 2 (SERCA2):** In addition to its well-known role in ER Ca2+ uptake, SERCA2 is also expressed in the Golgi apparatus. SERCA2 is mainly found in the cis-Golgi, slightly in the medial-Golgi but totally absent in the trans-Golgi and TGN.

- **Transmembrane Protein 165 (TMEM165):** TMEM165 belongs to a family of uncharacterized proteins named UPF0016 (Pfam accession number: PF01169). Members of this family are putative cation exchangers, even if their precise functions are unknown. TMEM165 is thought to be a Golgi Ca2+/H+ antiporter involved in Ca2+ uptake, but its contribution in the overall Golgi ion homeostasis is not known [112,113].

In addition, the plasma membrane Ca2+ ATPase (PMCA) was suggested to be involved in GA Ca2+ homeostasis during its trafficking along the secretory pathway [114].

3.1.2. Ca2+ exit from the Golgi

Ca2+ exit from the Golgi can of course be achieved in a non-specific manner by following the secretory pathway. Still, two majors channels directly involved in Ca2+ release from the Golgi to the cytosol have been described:

- **Inositol-3-Phosphate Receptor (IP_3R):** IP_3R was first described in the ER, but it is now clear that the Golgi is the host of IP_3R [115]. In response to IP_3, IP_3R opens and releases intra-Golgi Ca2+ into the cytosol. IP_3R seems to be excluded from the trans-Golgi and TGN, as those cisternae do not release Ca2+ in response to IP_3 [116].

- **Ryanodine Receptors (RyR):** mostly found in the ER, RyR are also localized in the GA. RyR bind various partners that can modulate its Ca2+ release from the Golgi lumen to the cytosol.

Due to all these differences in intra-Golgi localization of Ca2+ transporters, Ca2+ homeostasis is handled differentially between cis and trans/TGN [116].

3.2. H+

Organelles along the secretory pathways progressively acidify their interiors to ensure their optimal functioning. As described in 2.5, pH at the cis-Golgi is around 6.7 and progressively acidified to reach 6.0 at the TGN [101,117–120]. The pH homeostasis in the Golgi is thought to be regulated by proton pump and transporter involved in three main ion transport systems: ATP-mediated proton pumping, counter-ion conductance, and intrinsic proton leakage [121] (Figure 16).

3.2.1. ATP-mediated proton pumping

H+ are pumped into the Golgi apparatus by vacuolar H+-ATPases (V-ATPases), which are found within the membranes of many acidic organelles, including the Golgi apparatus. V-ATPase uses the energy of ATP hydrolysis to transport H+ across membranes, against their concentration gradients. Treatment of cells with inhibitors of V-ATPase (bafilomycin A1 and/or concanamycin A) results in complete neutralization of the Golgi lumen within 10 to 20 min [122].

3.2.2. Counter-ion conductance

The V-ATPase is electrogenic and could affect Golgi membrane potential and therefore the availability of counter-ion such as chloride or potassium. Counter-ion conductance is then used to maintain a low membrane potential via passive influx of anions and/or efflux of another cation [123]. This process is crucial to prevent any increase in membrane potential, which will result in low H+ pumping inside the Golgi. Several counter-ion conductance regulators have been described:

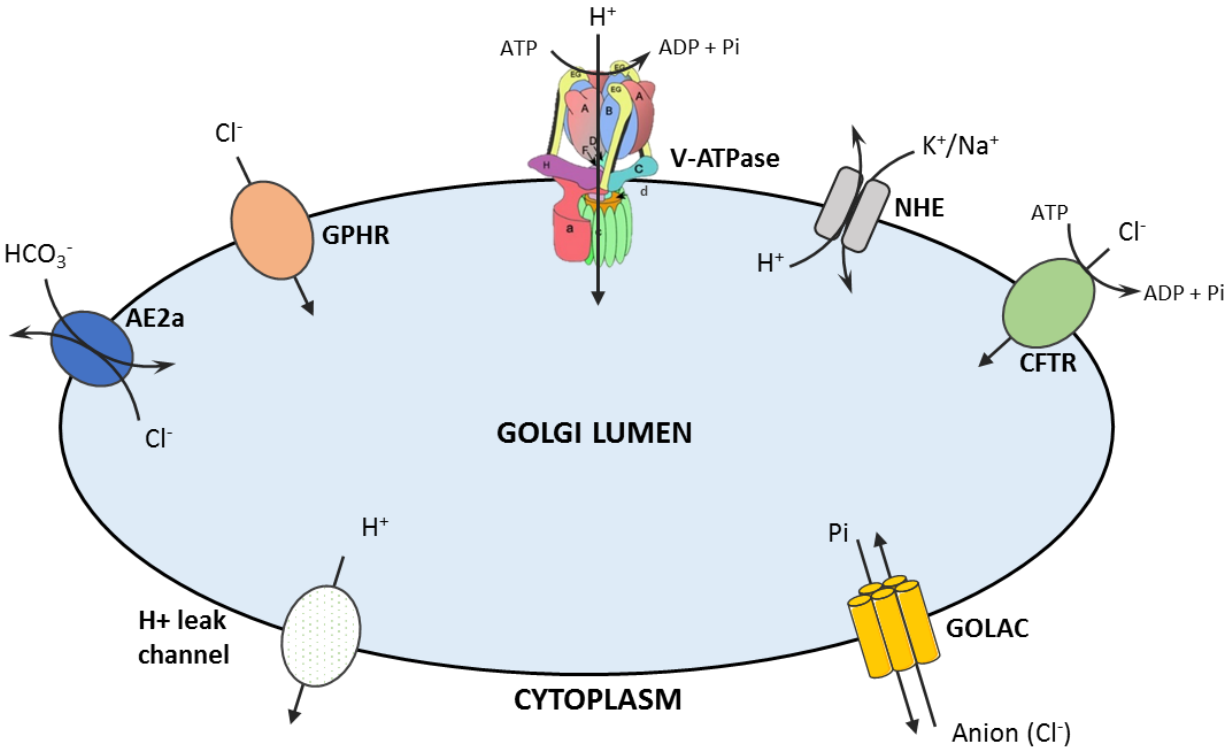

Figure 16. Overview of Golgi pH homeostasis regulation. Golgi apparatus is equipped with pumps and channels to properly regulate pH homeostasis. MCLC, TMEM165 and ClC-3B are not represented since their role in Golgi pH maintenance is not clear. V-ATPase is the major H+ importer inside the Golgi lumen. The proton leak channel is theoretically represented but no proton leak channel have been described to date in the Golgi apparatus.

- **Golgi pH Regulator (GPHR):** described in 2008 by Maeda and collaborators, GPHR is thought to import Cl- to lower the membrane potential created by the V-ATPase. Inactivation of GPHR leads to a specific Golgi pH increase of 0.4-0.5 unit, without affecting lysosomes or endosomes [124].

- **Cystic fibrosis transmembrane conductance regulator (CFTR):** CFTR is localized all along the secretory pathway and could play a role in Golgi counter-ion conductance. Indeed, some mutations of CFTR in cystic fibrosis leads to defective acidification of several intracellular organelles, including the GA [125,126].

- **Golgi anion channel (GOLAC-1 and GOLAC-2):** These channels are thought to be involved in counter-ion conductance, either by importing anion into the Golgi and/or by removing inorganic phosphate from the Golgi apparatus.

- **AE2a:** Golgi is a hub of vesicular transport and a lot of ionic and pH perturbation can happen. Therefore, proteins like AE2a, a HCO_3^-/Cl^- exchanger, act as a buffer to avoid any drastic changes in Golgi pH [117,127].

- **NHE (Na+/H+ exchangers):** several NHE are localized in the GA and therefore are involved in the maintenance of Golgi pH homeostasis. These proteins exchange intraluminal H+ with Na+ or K+ from the cytosol.

Besides, **Mid-1-related** chloride channel (MCLC) is another anion channel (or an activator of anion channels) that localizes to the ER, the Golgi and the nucleus but its role in Golgi pH regulation is unclear [128]. In addition, **ClC-3B** is a voltage-gated chloride channel in the Golgi membrane with no clear role in Golgi pH maintenance [129]. As described before, **TMEM165** is a Ca2+/H+ antiporter in the Golgi apparatus and can thus also be a Golgi pH regulator, although its contribution is not known. Finally, concentrations of anions and cations are interdependent and can be influenced by the transport of Ca2+, Mg2+, and Mn2+.

3.2.3. Proton leakage

The third main way to regulate pH homeostasis is proton leakage. Intrinsic proton leakage across membranes counteracts proton import and prevents excessive over-acidification of the Golgi lumen [130]. However, no proton leak channels have been described to date in the Golgi apparatus.

3.3. Mn2+

3.3.1. Manganese entry in the human body and distribution in fluids

Manganese (Mn) is a trace element essential for life. It is ranked as the twelfth most abundant metal on earth. The primary route of Mn intake is via dietary sources that can normally provide the required amount of Mn for physiological processes, including glycosylation, energy metabolism, immune functions and antioxidant defence. However, Mn can also be inhaled from environmental sources containing high Mn concentrations. The ingested Mn is then absorbed

through the gastrointestinal tract to reach the blood flow. Mn elimination is mainly done by bile excretion in urine. When inhaled, Mn can directly enter the body and bypass the hepatic removal system to cross the blood–brain barrier [131].

Although essential, Mn was also shown to be highly toxic at high concentration or during long time exposure. Indeed, manganese overexposure has been shown to induce neurological symptoms that can result in a Parkinson-like disorder called manganism [132–134]. Moreover, Mn overexposure has been shown to alter neurotransmitter levels. In addition, Mn can inhibit myocardial contraction, dilates blood vessels, and induces hypotension, suggesting that Mn exposure has a significant effect on cardiovascular function [135]. Therefore, the World Health Organization (WHO) and the Agency for Toxic Substances and Disease Registry made some recommendations on Mn exposure. In a public statement in 2012, they stated that normal ranges of manganese levels are about 4–15 µg/L in blood, 1– 8 µg/L in urine, and 0.4–0.85 µg/L in serum. Moreover, the United States Environmental Protection Agency has established that lifetime exposure to 0.3 mg/L manganese is not expected to cause any adverse effects. In addition, the American Food and Drug Administration has established that the manganese concentration in bottled drinking water should not exceed 0.05 mg/L. Finally, the Occupational Safety and Health Administration set a legal limit of 5 mg/m^3 manganese in air averaged over an 8-hour work day. In parallel, Goullé and collaborators developed an method based on ICP-MS to measure several metal elements, including Mn, in blood, plasma, urine and hair [136]. They measured Mn concentrations in blood, plasma and urine of 100 healthy individuals, and hair Mn concentration in 45 healthy individuals. They found reference value ranging from 5-12.8 µg/L in blood, 0.63-2.26 µg/L in plasma, 0.11-1.32 µg/L in urine and 0.016-0.57 µg/L in hair.

In mammals, Mn3+ is the predominant form in blood and is tightly bound to transferrin [137]. Mn2+ in blood is either oxidized to Mn3+ by ceruloplasmin before its binding to transferrin or directly bound to α2-macroglobulin. However, due to the significantly greater abundance of albumin in serum, a large percentage of Mn2+ is presumed to be bound to albumin as well [137,138]. Thus, the proportion of free Mn2+ inside cells is relatively low.

Due to its potential toxicity, regulation of Mn homeostasis is particularly important. Although no strictly specific Mn2+ transporters were described in human, a lot of actors can take part in Golgi manganese homeostasis (Figure 17). Since only few Mn transporters were described in the Golgi, an overview of all the known cellular Mn transporters will be presented in this section.

3.3.2. Manganese uptake at the cellular level

In cells, Mn is mostly found in two oxidation states: Mn2+ and Mn3+, and is distributed within the cytoplasm, the nucleus and microsomes (Golgi, ER…). Although no reliable measurement of cellular Mn concentration were done to date, it is estimated that total manganese concentration is within the nanomolar range. Besides, cytosolic Mn accumulation is in fact the cause of Mn cellular toxicity, since it can impair many fundamental cellular processes. Therefore, Mn2+ homeostasis should be carefully handled to avoid any Mn-induced toxicity. In human, several transporters involved in Mn uptake at the plasma membrane were described (Figure 17):

- **The transferrin receptor:** localized at the plasma membrane, this transporter is involved in the endocytosis of transferrin. Transferrin mostly binds Fe3+ but Mn3+ can also compete for the same binding sites as Fe3+ [139]. As a result, Mn3+ will follow the same pathway as Fe3+ for its entry via transferrin [140–142]. Transferrin is transported to endosomes via receptor mediated endocytosis, where Mn3+ will be released due to the acidic pH of endosomes. Transferrin is then recycled and Mn3+ is reduced to Mn2+. Then, Divalent Metal Transporter 1 (DMT1) can transport Mn2+ from endosomes to the cytosol. This Mn uptake is one of the major pathways for Mn2+ entry inside the cell.

- **DMT1 (Divalent Metal Transporter 1):** DMT1 is found in endosomes but also at the plasma membrane. In addition to his role in Mn2+ uptake via the transferrin, DMT1 also has a role in plasma membrane uptake. DMT1 has the highest transport efficiency for Mn2+, even if it can also transport a wide range of divalent cations, including Fe2+, Zn2+, Mn2+, Cu2+, Co2+, Cd2+, Ni2+, and Pb2+ [143,144].

- **SLC39 family of transporters:** although originally described as Zn2+ transporters, several members of this family localized at the plasma membrane are able to transport Mn2+ [145–148]. SLC39A8 and SLC39A14 are ubiquitously expressed and can transport Mn2+ in addition to Zn2+. SLC39A8 is an electroneutral $Mn2+/HCO_3^-$ or $Zn2+/HCO_3^-$ symporter. In mammals, SLC39A8 has been shown to have a higher affinity for Mn2+ than for Zn2+, with a K_M uptake value of 2.2µM in mice for example [149]. Moreover, authors have shown that SLC39A8 deletion in mice led to severe Mn deficiency, and that hepatic SLC39A8 was mainly responsible for whole-body Mn2+ homeostasis. They also demonstrate that SLC39A8 reclaims Mn2+ from the bile to import the ion inside the cell. More recently, SLC39A8 mutations have been associated to a human glycosylation

disorder due to Mn2+ homeostasis deficiency, strengthening the role of SLC39A8 in Mn2+ homeostasis [7]. With a lower affinity, SLC39A8 can also transport Cd2+, and SLC39A14 can

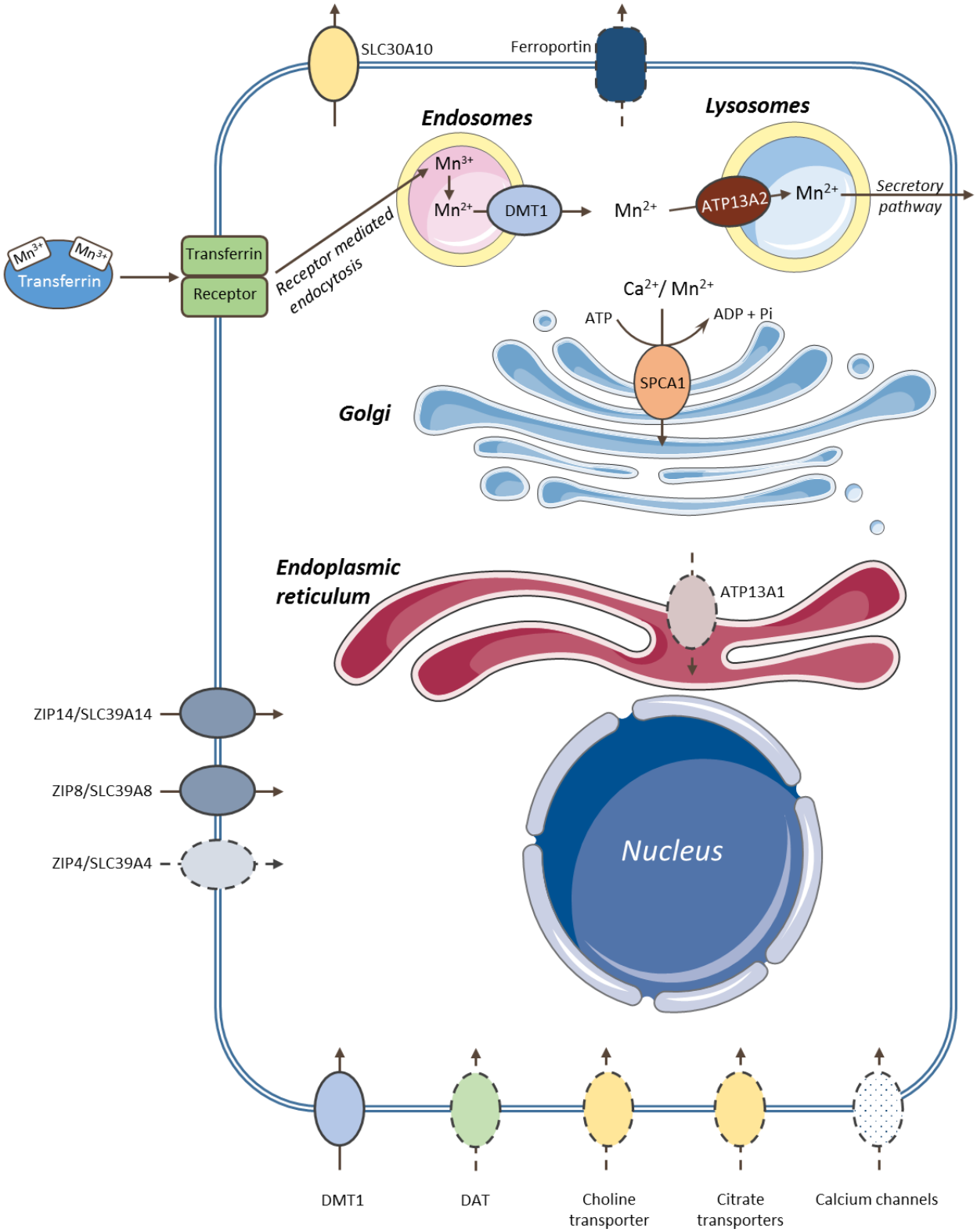

Figure 17. Overview of human manganese transporters. No specific Mn transporters have been found in human. DAT = Dopamine transporter; DMT1 (also called NRAMP2 or SLC11A2) = Divalent Metal Transporter 1; SPCA1 = Secretory pathway Ca2+ ATPase 1. Some transporters are depicted in dashes, because their involvement in manganese homeostasis in still unclear.The major ways of entry are suggested to be via the transferrin receptor and DMT1. The major way of exit is via the secretory pathway.

transport Cd2+ and Fe2+. SLC39A14 role in Mn2+ homeostasis has been recently highlighted in children with hypermanganism and parkinsonism-dystonia [150]. Those patients present a Mn homeostasis disruption due to mutations in SLC39A14. A crucial role of SLC39A14 in maintaining Mn homeostasis was also recently underlined in mice [151]. SLC39A4 is also thought to be able to transport Mn2+ but its role in Mn uptake is totally unclear. Other members of the SLC39 family were not described as Mn2+ transporters.

- **Store-operated calcium channels:** Mn2+ was shown to be transported through plasma membrane SOCs [152]. Still, this pathway is not a major way of entry, as these transporters need to be activated by intracellular calcium stores depletion.

- **Citrate transporters:** their implication in Mn2+ uptake at the plasma membrane was suggested but not experimentally verified in human [153].

- **Choline transporter expressed in neurons:** it is thought to be part of Mn2+ uptake at the plasma membrane, even if its direct involvement in Mn2+ homeostasis is still not clear [146,154].

- **Dopamine transporters:** only expressed in neurons, these transporters are suggested to be involved in Mn2+ uptake at the plasma membrane, even if it was only shown in mice striatum [155].

3.3.3. Transporters involved in the regulation of intracellular manganese homeostasis

Intracellular Mn2+ homeostasis is far from being well known. Nevertheless, several transporters have been shown to be involved in Mn2+ uptake inside organelles:

- **Secretory Pathway Calcium ATPase 1:** despite its name, SPCA1 has been shown to be able to transport Mn2+ inside the Golgi apparatus, with the same affinity as Ca2+ (Kd around 10 nM) [108,156]. However, the Ca2+ concentration inside a cell is way higher than Mn2+ concentration. Therefore, in physiological conditions, SPCA1 is known to mostly transport Ca2+ and not Mn2+. Interestingly, the transport of Mn2+ and Ca2+ is mutually exclusive, suggesting that each ion can occupy the same ion-transport site. Nevertheless, SPCA1 has been shown to be involved in Mn2+ cytosolic detoxification after high Mn exposure [156].

- **ATP13A1:** ATP13A1 is a putative P-type ATPase transporter of Mn2+ into the ER. Spf1, its yeast ortholog, has been described as the only ER Mn2+ transporter in *Saccharomyces cerevisiae* [157].

- **SERCA pumps:** although known as the major Ca2+ pumps in the ER, a weak Mn2+ transport was shown to be possible through SERCA pumps in non-physiological conditions [158–160].

3.3.4. Manganese efflux from the cell

Mn efflux is mostly done via the secretory pathway that will release Mn2+ in the extracellular space. Thus, there are only few transporters involved in Mn export:

- **ATP13A2:** ATP13A2 is a cation transporting ATPase localized in lysosomes. It is thought to be involved in Mn2+ transport from the cytosol to lysosomes, thus participating in Mn2+ efflux via the secretory pathway. However, direct efflux has not been demonstrated yet [146,161].

- **SLC30A10:** originally thought to be a Zn2+ transporter at the plasma membrane, SLC30A10 is in fact involved in Mn2+ efflux, even if the characterization of SLC30A10 function(s) is only at the beginning. Nevertheless, SLC30A10 appears to be physiologically relevant as SLC30A10 deficiencies lead to a Parkinson-like syndrome and affect Mn levels [146,148].

- **Ferroportin:** (or SLC40A1) is the major protein to export Fe2+ from the cell. It has also been described as able to transport Mn2+ but its role in Mn efflux is still unclear [162].

The presence of all those transporters involved in Mn2+ regulation demonstrates the complexity of Golgi Mn2+ homeostasis, which is maintained by a combination of local Golgi pumps and other transporters distributed in the plasma membrane and all along the secretory pathway.

3.4. Other ions: Zn2+, Mg2+, and Cu2+

Zinc cellular homeostasis is highly complex and although Zn2+ concentration is around 0.2 pM in the Golgi, several specific Zn2+ transporters exists in this organelle (Figure 18) [145,163]. Two families of Zn2+ transporters coexists in the Golgi: the ZIP and the ZnT family, with ZIP being more

involved in Golgi Zn2+ exit and ZnT in the Golgi Zn2+ uptake [145,147]. Besides, as presented before, a lot of Mn transporters can transport a broad range of divalent ions, including Zn2+.

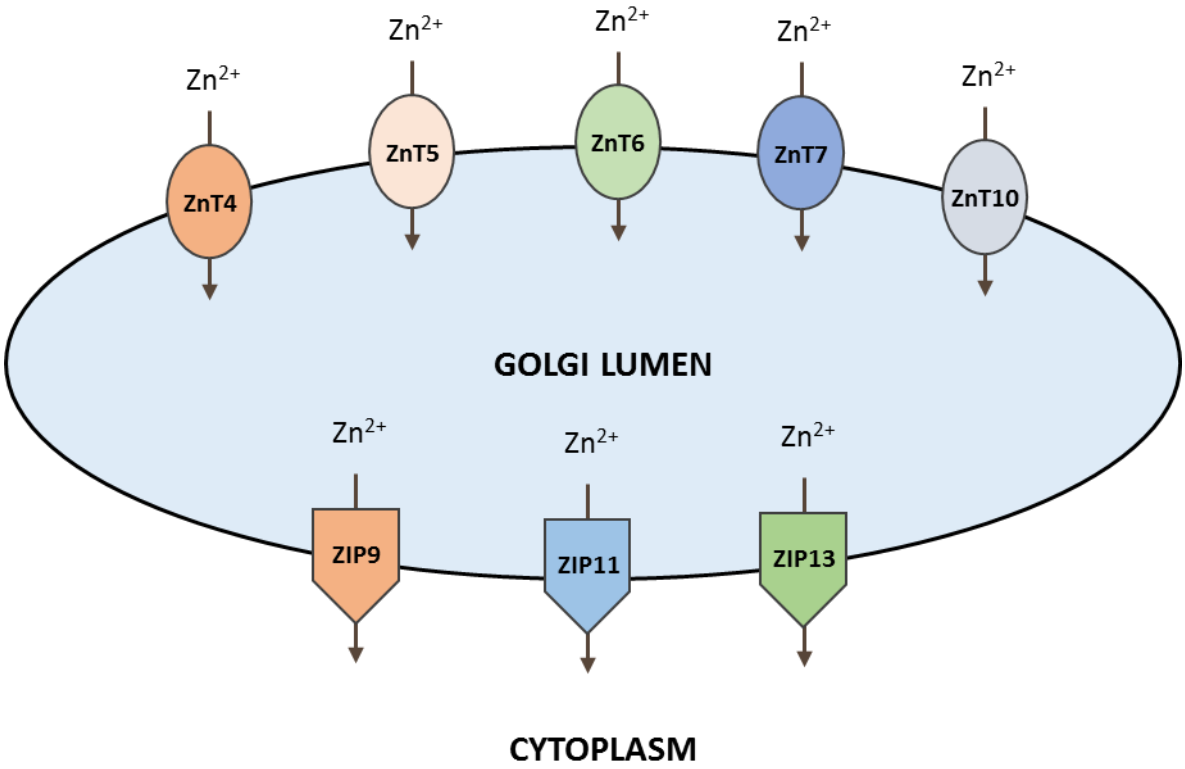

Figure 18. Overview of Golgi Zn2+ homeostasis. This picture illustrates a static view of Zn2+ homeostasis because most ZnT and ZIP transporters dynamically change their subcellular localization in response to various stimuli.

Little is known about Golgi Mg2+ homeostasis. Indeed, no specific Mg2+ transporters have been identified in the GA so far. Only SLC41A1 has been proposed to be a Golgi Na+/Mg2+ exchanger that catches cytosolic Na+ and releases Golgi Mg2+. However, SLC41A1 is also expressed at the plasma membrane and its role in Golgi Mg2+ extrusion was not confirmed in human [164–166].

Concerning Golgi Cu2+ uptake, only ATP7A and ATP7B have been shown to be able to import Cu2+ in the Golgi [167].

[4] Mn2+ AND GLYCOSYLATION

In the previous chapters, we have shown that Mn2+ is an important ion for glycosylation. Besides, Mn2+ homeostasis is crucial for the proper functioning of the cell. In fact, Mn2+ and glycosylation have always been tightly linked. Many studies have been done in prokaryotes, but the large differences between prokaryote and eukaryote glycosylation have led me to focus on Mn2+ and glycosylation in eukaryotes. Moreover, in the eukaryotic reign, the most frequently used organisms to study glycosylation are: *Saccharomyces cerevisiae, Caenorhabtidis elegans, Drosophila melanogaster* and mammals (especially rodent, bovid, and human).

Due to technological advances and the complete sequencing of the human genome, the last twenty years have seen the rise of glycosylation studies in human. Therefore, this chapter will present an exhaustive overview of this link between Mn2+ and human glycosylation.

4.1. Overview of Mn2+ effect on glycosylation in human

4.1.1. Mn2+ and glycosylhydrolases and nucleotide sugar transporters

Little is known about GH requirement for ions. Besides, the only studies available in the literature did not reveal any strict requirement for Mn2+. For example, the human lysosomal α-mannosidase MAN2B1, involved in the catabolism of N-glycans during glycoprotein turnover, was expressed in drosophila and characterized. Authors revealed that MAN2B1 was threefold activated by 1mM Co2+, but only very slightly stimulated by Zn2+, Mg2+ and Mn2+ [168]. However, the other lysosomal class 2B α-1,6-mannosidase MAN2B2 has no clear sensitivity to any metal ion. MAN2A1, the Golgi class II α-mannosidase involved in the trimming of N-glycans, is thought to have a requirement for Zn2+. Its lysosomal homolog MAN2A2 has also been classified as Zn2+ dependent, by similarity with MAN2A1. MAN2C1, a cytosolic class II α-mannosidase involved in the trimming of free oligosaccharides, has been shown to contain Co2+ in its active site. Moreover, a 5-fold increase of its enzyme activity was observed in the presence of 2mM Co2+ [169]. Several glycosylhydrolases have been shown to require Ca2+ as divalent cation. It is for example the case for TMEM2, a cell surface hyaluronidase [170]. MAN1A1, a Golgi α-1,2 mannosidase, is also thought to require Ca2+, by similarity to the mouse ortholog that requires Ca2+ as divalent ion [97]. By similarity, MAN1B1, MAN1C1 and MAN1A2, three α-mannosidases involved in N-glycan trimming, are also classified as Ca2+ dependent

mannosidases. Broadly speaking, glycosylhydrolases rely more on an optimal pH than divalent ions.

To date and to my knowledge, no link between a requirement in divalent cation and nucleotide sugar transporter have been reported.

4.1.2. Mn2+ and glycosyltransferases

4.1.2.1. Mn2+ as an activator of glycosyltransferases

Human GT can be classified into two large families depending on the folding they acquired:

- **GT-A fold**: GT-A consists of an α/β/α sandwich that resemble a Rossmann domain. GT-A have a DXD motif in their structure that is known to coordinate to the phosphates in the nucleotide sugar donor via divalent metal ion, and generally Mn2+. The only exception reported to date is for C2GnT-L glycosyltransferase, an enzyme involved in mucin-type O-glycosylation in leucocytes. This enzyme displays a GT-A fold but lacks a DXD motif in its sequence. It is then thought that Arg378 and Lys401 stabilise the UDP with their positive charges, a role normally played by the divalent cation [171].
- **GT-B fold**: GT-B consists of two separate Rossmann domains with a connecting linker region and a catalytic site located between the domains. GT-B does not contain any DXD motif and most of GT-B glycosyltransferases do not require divalent ion for their activity.

A list of all GT that requires Mn2+ as cofactor is available in Table 4.

4.1.2.1.1. Mn2+ and GT involved in N-glycosylation

The first link between Mn2+ and glycosylation in human date from 1974, when Khatra and collaborators studied properties of the human milk galactosyltransferase [6]. They observed that the synthesis of both lactose and N-acetyl lactosamine involved an enzymatic ordered sequential reaction, with Mn2+ attaching first, then the UDP-Gal and finally the acceptor monosaccharide. They also showed that the enzyme requires Mn2+ to be fully active. Besides, Mg2+ was unable to activate the enzyme, thus demonstrating the specific Mn2+ requirement for the enzyme. This enzyme, later named **β-1,4-Galactosyltransferase-I (B4GALT1),** is one of the most studied GT to date. Knowledge has increased thanks to studies on its bovine ortholog, which shares a lot of homology with the human counterpart [89,172], and by analysing crystal structure obtained from

both human and bovine enzymes [90]. The precise mechanism of the catalytic mechanism involving a Mn2+ divalent ion will be discussed in detail in section 4.2. These first observations led scientists to test divalent metal ion requirement for each new GT identified. Since this first discovery, several GT have been shown to require Mn2+ to be fully active.

Table 4. List of all glycosyltransferases known to require Mn2+ to be fully active. This table only lists GT requiring Mn2+ with strong scientific evidences. GT involved in the same pathway are showed in the same color: gray for N-glycosylation, blue for O-glycosylation, orange for GAG biosynthesis, yellow for glycolipids biosynthesis, no color for other or multiple pathways. GT that are thought to require Mn2+ by similarity to ortholog or other members of the same enzyme family are listed in Table 5.

Enzyme	Gene	Divalent ion co-factor	Glycosylation pathway involved
Beta-1,4-Galactosyltransferase 1	B4GALT1	Mn2+	N-glycosylation
UDP-Glucose Glycoprotein Glucosyltransferase 1 and 2	UGGT1/UGGT2	Mn2+ or Ca2+	N-glycoprotein folding
Polypeptide N-Acetylgalactosaminyltransferase 1, 2 and 3	GALNT1 GALNT2 GALNT3	Mn2+	O-glycosylation (mucin-type)
Polypeptide N-Acetylgalactosaminyltransferase 10	GALNT10	Mn2+	O-glycosylation (mucin-type)
Beta-1,4-glucuronyltransferase 1	B4GAT1	Mn2+	O-mannosylation
LARGE Xylosyl- And Glucuronyltransferase 1	LARGE1	Mn2+ (for xylosyltransferase activity); Mn2+, Mg2+ or Ca2+ (for glucuronyltransferase activity)	O-mannosylation
LARGE Xylosyl- And Glucuronyltransferase 2	LARGE2	Mn2+	O-mannosylation
Xyloside Xylosyltransferase 1	XXYLT1	Mn2+ > Mg2+	O-glucosylation
Fucosyltransferase 3	FUT3	Mn2+	O-glycosylation (terminal antigens)
Fucosyltransferase 5	FUT5	Mn2+ > Ca2+, Co2+, Mg2+	O-glycosylation (terminal antigens)
Fucosyltransferase 7	FUT7	Mn2+, Mg2+ > Co2+, Ca2+	O-glycosylation (terminal antigens)
Beta-1,4-N-Acetyl-Galactosaminyltransferase 2	B4GALNT2	Mn2+	O-glycosylation (terminal antigens)
Alpha 1-3-N-Acetylgalactosaminyltransferase (GTA) And Alpha 1-3-Galactosyltransferase (GTB)	ABO	Mn2+ for both enzymatic activities	O-glycosylation (blood group antigen)
Xylosyltransferase 1	XYLT1	Mn2+	Glycosaminoglycans
Chondroitin Sulfate Synthase 1	CHSY1	Mn2+, Co2+ and Cd2+	Glycosaminoglycans
Chondroitin Polymerizing Factor/Chondroitin Sulfate Synthase 2	CHPF	Mn2+ > Co2+	Glycosaminoglycans
Chondroitin Sulfate Synthase 3	CHSY3	Co2+ > Cd2+ > Mn2+	Glycosaminoglycans
Beta-1,3-Glucuronyltransferase 3	B3GAT3	Mn2+	Glycosaminoglycans

Beta-1,3-Glucuronyltransferase 1	B3GAT1	Mn2+	Glycosaminoglycans
Beta-1,4-Galactosyltransferase 7	B4GALT7	Mn2+	Glycosaminoglycans
Beta-1,4-N-Acetyl-Galactosaminyltransferase 1 (GM2 synthase)	B4GALNT1	Co2+ > Mn2+ > Ni2+	Glycolipids
Beta-1,3-N-Acetylgalactosaminyltransferase 1 (Globoside Blood Group)	B3GALNT1	Mn2+	Glycolipids
Beta-1,4-Galactosyltransferase 6	B4GALT6	Mn2+ and Mg2+, each ion alone do not increase the enzymatic activity	Glycolipids
UDP-GlcNAc:BetaGal Beta-1,3-N-Acetylglucosaminyltransferase 2	B3GNT2	Mn2+	poly-N-acetyllactosamine biosynthesis
Glycogenin 1 and Glycogenin 2	GYG1/GYG2	Mn2+	auto-glucosylation

UDP-Glucose Glycoprotein Glucosyltransferase 1 and (UGGT1 and 2), two homologous enzymes involved in N-glycoproteins folding during ER quality control, were studied in details by Arnold and collaborators [173]. They expressed the cDNA encoding the enzymes in Cos-1 cells, purified the enzymes and measured the incorporation of radioactive glucose on specific acceptor protein. Their results revealed that both enzymes have a preference for Mn2+ or Ca2+.

4.1.2.1.2. Mn2+ and GT involved in O-glycosylation

Polypeptide N-Acetylgalactosaminyltransferases (ppGalNAcT) are GT-A glycosyltransferases that catalyse the first step of mucin-type O-linked glycosylation. A study on recombinant human ppGalNAcT-1, ppGalNAcT-2 and ppGalNAcT-3 showed that these enzymes strictly required Mn2+, since no activity was detected in absence of Mn2+ nor when Mn2+ was substituted by Mg2+ or Ca2+ [174]. Later, it was shown that ppGalNAcT-2 required Mn2+ although it contains a $D^{224}XH^{226}$ motif, different from the classic DXD motif [15]. In 2006, Kubota and collaborators deciphered the mechanism of Mn2+ activation for ppGalNAcT-10 [175]. They first observed that substrate binding (Mn2+, UDP-GalNAc) triggered sequential conformational changes in two loops in the catalytic center of the enzyme. ppGalNAcT-10 does not comprises a DXD motif, but similar to ppGalNAcT-2, it contains a $D^{237}XH^{239}$ motif. Crystal structures of the enzyme showed that Mn2+ binds 6 ligands in an octahedral geometry: two oxygen atoms of the α and β phosphates of UDP, Asp237, His239 and His370, and a water molecule. Therefore, it forms a complex binding

model with UDP-GalNAc, Mn2+ and ppGalNAcT-10. Interestingly, these coordinating amino acid (Asp237, His239 and His370) residues are completely conserved in all pp-GalNAc-Ts.

Beta-1,4-glucuronyltransferase 1 (B4GAT1), an enzyme involved in the O-mannosylation of α-dystroglycan, also specifically required Mn2+ to be fully active [176]. **LARGE1 and LARGE2,** two bifunctional glycosyltransferases involved in O-mannosylation with both xylosyltransferase and β-1,3-glucuronyltransferase activities, can bind divalent ions, one for each enzymatic activity. LARGE1 and LARGE2 xylosyltransferase activity strictly requires a divalent cation, and is most largely increased by Mn2+. LARGE1 β-1,3-glucuronyltransferase activity is detected even in absence of cation, but is doubled by Mn2+, Mg2+ or Ca2+ addition. LARGE2 β-1,3-glucuronyltransferase catalytic activity is increased 4-fold specifically in the presence of Mn2+ [177].

XXYLT1 is the α-1,3-xylosyltransferase 1 that adds a xylose residue to the O-linked Xyl-Glc disaccharide attached to EGF-like repeats in the extracellular domain of NOTCH and factor IX. XXYLT1 from HepG2 cell lines was purified and tested on the Xyl-Glc disaccharide acceptor, then the products of the reaction were analysed using reversed-phase HPLC. They observed that Mn2+ induced a strong increase of the enzymatic activity, but Mg2+ was also able to activate the enzyme with 52% activity compared to Mn2+ as cofactor [178].

Alpha 3/4 fucosyltransferase 3 (FUT3) is a Golgi GT that catalyses α-1,3 and α-1,4 fucosylation during the final step of Lewis antigen biosynthesis (mainly Le^a, Le^b and sLe^a). A soluble version of the human enzyme, composed of amino acid Ala47 to Thr361 and comprising the catalytic domain and a part of the stem, was expressed in *Spodoptera frugiperda* (Sf9) insect cells and intensively studied [179]. Authors have shown that the enzyme was active in the absence of divalent metal ions with still 35% of its maximal activity, but can be activated by several divalent cations *in-vitro*. Mn2+ and Co2+ were the most effective activators leading to 2.7-and 2.8-fold activation of FUT3, respectively. Mg2+ and Ca2+ also enhanced the reaction, leading to a 2.5- and 2.1-fold activation, respectively. Mn2+ is thought to be the divalent metal ion activator *in-vivo* since 50µM Mn2+ already induced a 1.3-fold activation of FUT3 and maximal activity was observed in the range of 5–10 mM Mn2+ concentration, with a 6-fold activation. Adding Mn2+ increases the affinity of the enzyme for GDP-Fuc as they observed a 5-fold decrease of the apparent K_M value (3.3 to 0.7 mM). FUT3 possesses a $D^{162}SD$ motif and the D162N mutant retains

an enzymatic activity to that observed in the absence of divalent ion. Therefore, Mn2+ is an activator of FUT3 but the enzyme does not strictly require Mn2+ to be functional. This characteristic is in fact a key feature of the fucosyltransferase family. **Alpha-(1,3)-fucosyltransferase 5 (FUT5)** is responsible for the terminal step in the biosynthesis of Le^X and sialylLe^X antigens and requires Mn2+ to be fully active [98]. The K_M for Mn2+ in their experimental conditions was determined to be 6.1 mM, and other divalent metal ions were identified as cofactors such as Ca2+ (63% activity compared to Mn2+) , Co2+ (56%), and Mg2+ (53%). **Alpha-(1,3)-fucosyltransferase 7 (FUT7)**, involved in the synthesis of Le^x antigen, has also been shown to be stimulated by the presence of Mn2+ and Mg2+, and to a lesser extent by Ca2+ and Co2+ [180].

Beta-1,4-N-Acetyl-Galactosaminyltransferase 2 (B4GALNT2) is involved in the synthesis of the Sda antigen (GalNAcβ-1,4-[Neu5Acα-2,3]-Galβ). In 1986, Takeya and collaborators observed this enzymatic activity in human blood plasma. They showed that they reached maximal activity when the assay was done with 50 mM MnCl2 [181]. Later in 1989, Malagolini and collaborators showed that when MnCl2 was removed from their assay to measure B4GALNT2 activity in human colonic cells, enzymatic activity was totally abolished [182]. These results demonstrated that Mn2+ is required for B4GALNT2 to be functional.

Human blood group antigens A and B are produced by 2 closely related enzymes with glycosyltransferase activity belonging to the **histo-blood group ABO system transferase**, encoded by the ABO gene [183]:

- An α-1,3-N-acetylgalactosamine transferase (GTA), which catalyzes the transfer of a GalNAc to the Gal residue of the acceptor H antigen (Fucα-1,2-Galβ-O-R), converting the H antigen into A antigen.
- An α-1,3-galactosyl transferase (GTB), which catalyzes the transfer of a Gal to the Gal residue of the acceptor H-antigen, converting the H antigen into B antigen.

Both enzymes are GT-A folded retaining enzymes with a characteristic a characteristic ^{211}DVD^{213} motif belonging to the consensus DXD motif that coordinates to a Mn2+ ion shown to be critical in donor binding and catalysis. A M214R mutant in GTB was shown to be less active than the wild-type GTB. Indeed, kinetic analysis on recombinant M214R revealed a 1200-fold decrease of k_{cat} compared to normal GTB. The UDP-Gal k_{cat} was 5.1 s^{-1} for WT versus 0.0042 s^{-1} for M214R and

the UDP-GalNAc k_{cat} was 0.42 s^{-1} for WT versus 0.00016 s^{-1} for M214R. In fact, the Arg214 prevents the coordination of Mn2+ in the nearby ^{211}DVD^{213} motif by causing displacement of the Mn2+ by a water molecule [183]. In addition, the site stays unavailable even with 10mM MnCl2 addition.

4.1.2.1.3. Mn2+ and GT involved in GAG biosynthesis

Xylosyltransferase 1 (XYLT1) catalyses the first step in GAG biosynthesis by transferring Xyl from UDP-Xyl to specific Ser residues. Studies of XYLT1 catalytic properties have shown that the enzyme requires Mn2+ to bind the UDP of the UDP-Xyl [184]. Besides, XYLT1 comprises two DXD motifs: ^{314}DED^{316} and ^{745}DWD^{747}. However, mutations in the ^{314}DED^{316} have no effect on enzymatic activity [184,185]. On the opposite, the amino acid at the position 745 on the second motif is crucial for XYLT1 function. Indeed, D745G mutation leads to loss of function of the enzyme, but D745E mutant retains enzymatic activity, demonstrating the crucial need of an acidic residue at this particular position. Two mutants D747G and D747E have also been characterized. They displayed a reduced affinity as measured by an increase of their K_M (6.9µM for D747G and 4.4µM for D747E compared to 0.9µM for the WT) but were still able to catalyse the reaction. In addition, changing the W746 to neutral, basic or acid amino acid decreased V_{max} by a 6 fold without altering K_M. However, nucleotide binding was not abolished in those mutants, meaning that alterations in the amino acid sequence of this motif do not abolish the divalent cation-dependent binding of UDP, but alter the rate of the enzymatic reaction. Taken together, these data suggest that Mn2+ is not critical for binding of the nucleotide but clearly enhance the enzymatic reaction.

Several studies have been done on Chondroitin Sulfate Synthases [186,187]. **Chondroitin Sulfate Synthase 1 (CHSY1)** is an enzyme involved in the elongation of CS, with both β-1,3-glucuronic acid and β-1,4-N-acetylgalactosamine transferase activity. In vitro measurement of incorporation of UDP-[^{14}C]GlcUA and UDP-[^{3}H]GalNAc on several acceptors have shown that divalent ions were essential for the enzymatic activities and that this enzyme could be activated by Mn2+, Co2+ or Cd2+ with more or less the same affinity. Precisely, Co2+ addition led to the highest level of β-1,3-glucuronic acid activity, whereas Cd2+ and Mn2+ were 85% and 70% as effective as Co2+, respectively. For β-1,4-N-acetylgalactosamine transferase activity, Mn2+ exhibited the highest activity and Co2+ and Cd2+ were 70 and 53% as effective as Mn2+ [186]. **Chondroitin Sulfate Synthase 3 (CHSY3)** is highly similar to CHSY1 and shares the same GT activities as CHSY1.

Although CHSY3 exhibits enzymatic activities toward the non-reducing terminal residue of CS, CHSY3 is expressed at much lower level than CHSY1 and its specific activity was about 10% of CHSY1. CHSY3 also requires divalent ion to be fully functional but unlike CHSY1, Co2+ seems to be the best activator of CHSY3. CHSY3 can also be activated by Mn2+ or Cd2+, but with less efficiency, especially for the β-1,3-glucuronic acid transferase activity [186]. Finally, **Chondroitin Sulfate Synthase 2 (also named Chondroitin Polymerizing Factor) (CHPF)**, has been shown to require Mn2+ but can also be slightly activated by Co2+. Divalent cations were essential for the two glycosyltransferase activities, since 10 mM EDTA completely abolished both reactions.

Beta-1,3-glucuronyltransferase 3 (B3GAT3) is an enzyme involved in the synthesis of the tetrasaccharide core of GAG. B3GAT3 is responsible for the addition of the GlcUA residue to complete the tetrasaccharide core of GAG. B3GAT3 is composed of a DXD motif ($D^{194}DD^{196}$) that has been shown to be in direct interaction with UDP and Mn2+. **Beta-1,3-glucuronyltransferase 1 (B3GAT1)** is highly similar to B3GAT3 and is involved in the synthesis of HNK-1 antigen, a glycan structure mostly found in neural cell adhesion molecules. B3GAT1 also required Mn2+ for coordination in its $D^{194}DD^{196}$ motif and no enzymatic activity was detected if any D of the motif is mutated to an A [188].

Beta-1,4-galactosyltransferase 7 (B4GALT7) attaches the first galactose residue in the common tetrasaccharide found in GAG. B4GALT7 possesses a $D^{163}XD^{165}$ motif at the *N*-terminal hinge region of the long loop that has been shown to be involved in Mn2+ binding [189]. Besides, the D165E mutant displayed really weak binding to UDP-Gal compared to the WT. Authors also showed using isothermal calorimetric study that specifically in the presence of Mn2+, the enzyme changes its conformation to a so called closed conformation. B4GALT7 undergoes conformational changes upon binding with Mn2+ and UDP, but not in the absence of Mn2+. They observed that one Mn2+ ion and one UDP were located in the catalytic pocket of the enzyme.

4.1.2.1.4. Mn2+ and GT involved in glycolipids biosynthesis

Beta-1,4-Galactosyltransferase 6 (B4GALT6) is involved in the biosynthesis of the LacCer, a precursor of GSL. In normal human proximal tubular cells, the enzyme was shown to require metal ion and was inactive without metal ions [92]. Using membrane-bound enzyme source, maximal activity was obtained in the presence of 1.0 mM Mn2+/Mg2+ (1:1). Surprisingly, each

metal ion alone did not increased significantly the activity, suggesting the need of Mn2+ and Mg2+ in 2 distinct binding sites.

GM2 synthase (Beta-1,4-N-Acetyl-Galactosaminyltransferase 1), an enzyme involved in the early step of GSL biosynthesis, was studied by expressing the human cDNA into CHO cells and by measuring the ability of the enzyme to bind UDP-beads. Using this approach, authors demonstrated that the DXD motif is required for GM2 synthase activity but not critical for nucleotide binding [190]. Indeed, the D356E and D357N mutants retained weak enzymatic activity and nucleotide binding was not altered in the triple mutant D356N/D357N/D358N. They concluded that this motif may function during catalysis in GM2 synthase rather than during the binding to nucleotide sugar. Nevertheless, the enzyme was shown to be dependent to several divalent ions. Indeed, in the presence of 3.5 mM of each metal ion, Co2+ was the better cofactor, followed by Mn2+, which led to 70.1% enzymatic activity compared to Co2+. The enzyme could also be to some extent activated by Ni2+, with 45.7% activity compared to the activation by Co2+.

Beta-1,3-N-Acetylgalactosaminyltransferase 1 (B3GALNT1) is involved in the synthesis of the Gb4 by adding a GalNAc residue to the Gb3 (Figure 19). The cDNA coding the human enzyme was injected into mice lacking endogenous B3GALNT1 but expressing the Forssman synthase, the enzyme responsible for the conversion of Gb4 to Forssman antigen. Thus, they screened mice cells with antibody anti Forssman antigen and purified B3GALNT1 from these cells. Authors have shown that the enzyme strictly require Mn2+ by measuring the incorporation of UDP-[^{3}H]-GalNAc on glycolipids that were extracted and analysed by Thin Layer Chromatography (TLC) immunoblotting [191,192].

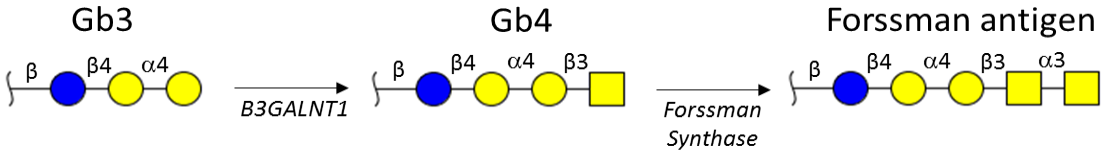

Figure 19. Biosynthesis of the Forssman antigen.

4.1.2.1.5. Mn2+ and GT involved in other or multiple pathways

Other examples of Mn2+ requirement can be found in the literature, such as for the **Beta-1,3-N-acetylglucosaminyltransferase 2 (B3GNT2),** an enzyme involved in the synthesis of poly-N-acetyllactosamine structure with a preference for Gal(β-1,4)Glc(NAc)-based acceptors. Authors have shown that β3GnT2 has an absolute requirement for Mn2+ and a pH optimum at 7.0 [193].

Glycogenin (GYG) is an α-1,4 glucosyltransferase involved in the biosynthesis of glycogen, a storage form of glucose and a polymer of α-1,4 and α-1,6 glucose residues. In fact, glycogenin is able to self glucosylates on Tyr194 through the formation of a glucose 1-O-tyrosyl linkage [194]. Besides, glycogenin can catalyse the subsequent formation of α-1,4-glycosidic linkages, thus initiating the biosynthesis of glycogen. Glycogenin is a retaining enzyme from GT family 8, containing a DXD motif ($D^{101}AD^{103}$) and requires Mn2+ to be fully functional [195]. Indeed, Mn2+ associates with UDP-Glc, then functions as a Lewis acid to stabilize the UDP leaving group and facilitates the transfer of the Glc residue to an intermediate nucleophilic acceptor in the enzyme active site. Finally, the Glc is delivered to Tyr194 [196].

4.1.2.1.6. GT potentially requiring Mn2+

Apart from these GT known to require Mn2+ for their activity, several other GT are thought to require Mn2+ but no solid scientific evidences are available in the literature. Some of these enzymes are listed in Table 5.

Table 5. List of glycosyltransferases thought to require Mn2+ to be fully active. This table lists GT that are thought to require Mn2+ by similarity to ortholog or other members of the same enzyme family. GT involved in the same pathway are showed in the same color: gray for N-glycosylation, blue for O-glycosylation, orange for GAG biosynthesis, yellow for glycolipids biosynthesis, no color for other or multiple pathways.

Enzyme	Gene	Divalent ion co-factor	Glycosylation pathway involved
Mannosyl (Alpha-1,3-)-Glycoprotein Beta-1,2-N-Acetylglucosaminyltransferase	MGAT1	Mn2+ by similarity to the rabbit ortholog	N-glycosylation
Beta-1,4-Galactosyltransferase 2, 3, 4, 5	B4GALT2-5	Mn2+ by similarity to B4GALT1	N-glycosylation
Mannosyl (Alpha-1,3-)-Glycoprotein Beta-1,2-N-Acetylglucosaminyltransferase 4A, 4B, 4C	MGAT4A, 4B and 4C	divalent ion (Mn2+ most likely) by similarity to MGAT1	N-glycosylation
Glycosyltransferase 6 Domain Containing 1	GLT6D1	Mn2+	O-glycosylation (ABO group antigen)
Polypeptide N-Acetylgalactosaminyltransferases	GALNT(X)	Mn2+ by similarity to the family of Polypeptide N-Acetylgalactosaminyltransferases	O-glycosylation (mucin-type)
Beta-1,3-N-acetylglucosaminyltransferase lunatic fringe, manic fringe and radical fringe	LFNG, MFNG, RFNG	Mn2+ by similarity with other Beta-1,3-N-acetylglucosaminyltransferase	O-fucosylation
Protein O-Linked Mannose N-Acetylglucosaminyltransferase 1	POMGNT1	Mn2+ by similarity to B3GALNT1 and B4GALNT1	O-mannosylation
Xylosyltransferase 2	XYLT2	Mn2+ by similarity with XYLT1	Glycosaminoglycans

Exostosin-1 and 2	EXT1/EXT2	Mn2+ by similarity to the mouse ortholog	Glycosaminoglycans
Exostosin-like glycosyltransferases 1, 2 and 3	EXTL1/EXTL2/EXTL3	Mn2+ by similarity to the mouse ortholog	Glycosaminoglycans
Globoside Alpha-1,3-N-Acetylgalactosaminyltransferase 1	GBGT1	Mn2+	Glycolipids
Alpha-1,3-Galactosyltransferase 2	A3GALT2	Mn2+ by similarity to B4GALT family	Glycolipids
Beta-1,3-Glucuronyltransferase 2	B3GAT2	Mn2+ by similarity with B3GAT1 and B3GAT3	multiple pathways
Beta-1,3-Galactosyltransferase 1 and 2	B3GALT1/B3GALT2	Mn2+ by similarity to B4GALT1	multiple pathways

For example, human **Mannosyl (α-1,3-)-Glycoprotein β-1,2-N-Acetylglucosaminyltransferase (MGAT1 or GlcNAcT-I)** has a rabbit ortholog with high similarity, containing a $E^{211}DD^{213}$ motif conserved in the human MGAT1. This motif makes critical interactions with bound UDP-GlcNAc and Mn2+ [197]. **MGAT4A, 4B and 4C** are also thought to require Mn2+ by similarity to MGAT1.

Glycosyltransferase 6 domain-containing protein 1 (GLT6D1) is thought to require Mn2+ due to study on the bovine ortholog GGTA1. GGTA1 catalyzes the transfer of a α-1,3 linked Gal residue, on terminal lactosaminide (Gal-β-1,4-GlcNAc-R) disaccharide. Isothermal titration calorimetry (ITC) revealed that one Mn2+ is required for donor susbtrate binding in the $D^{225}VD^{227}$ motif [198]. **Globoside alpha-1,3-N-acetylgalactosaminyltransferase 1 (GBGT1 or Forssman synthase)** has been suggested to require Mn2+ due to the high similarity with bovine GGTA1.

Exostosin-1 and 2, and exostosin-like glycosyltransferases 1, 2 and 3, which are all involved in the biosynthesis of GAG, are thought to require Mn2+ by similarity to their mouse ortholog [199]. All **ppGalNAc-T and B4GALT2-5** are also classified as Mn2+ dependent, by sequence similarity to other members of the family.

Furthermore, Kaufman and collaborators have shown that Mn2+ depletion within the secretory pathway inhibits O-linked and N-linked glycosylation in CHO cells [200]. They have used A23187, an ionophore that chelates a lot of divalent ions, including Mn2+ with a high selectivity and Mg2+ and Ca2+ to some extent, to induce Mn2+ depletion. They observed that intralumenal Mn2+ is required for O-glycosylation on erythropoietin (EPO) and macrophage colony stimulating factor (M-CSF), 2 well characterized proteins carrying mucin-type O-glycans and few N-glycans. Only

Mn2+ addition reverted the glycosylation defect, with a total normalization for O-glycosylation and a partial normalization for N-glycosylation.

Finally, Mn2+ is also sometimes added in production systems to boost glycosylation of recombinant proteins, thus increasing the yield of the production [201–204].

4.1.2.2. Other effects of Mn2+ on glycosyltransferases

Although known to be an activator for GT, Mn2+ can also have other effect on specific GT or under certain conditions.

For example, Mn2+ indeed activates **Chondroitin Sulfate Synthase 1, 2 and 3**. Nevertheless, above 10mM MnCl2, GlcUA transferase activity was decreased For both CHSY1 and CHSY3 [186]. Above 30mM Mncl2, GalNAc transferase activity decreased for both enzymes. Finally, above 10mM MnCl2, both enzymatic activities decreased for Chondroitin Sulfate Synthase 2 [187]. The same observations were done on **FUT3 and FUT5**, where Mn2+ concentrations higher than 10mM had an inhibitory effect on fucosyltransferase activity, which could be due to the hydrolysis of the GDP-Fuc by Mn2+ [98,179].

Protein O-Mannosyltransferase 1 and 2 (POMT1, POMT2), both catalyse the transfer of a Man residue from dolichol phosphate mannose (Dol-P-Man) to Ser/Thr residues of certain proteins such as α-dystoglycan (α-DG). Using GST-α-DG as the acceptor, Dol-P-[^{3}H]-Man as the sugar donor, and an enzyme extract containing both POMT1 and POMT2, Manya and collaborators have measured the incorporated radioactivity on α-DG after purification on glutathione sepharose column [205]. They observed that neither POMT1 nor POMT2 required divalent cations as the presence of 10mM EDTA led to the best enzymatic activity. Interestingly, they showed that both enzymes were slightly activated by Mg2+ but a 90% decrease of the activity was observed in the presence of Ca2+ or Mn2+, suggesting a role of these ions in POMT inhibition.

In 1990, a protein:glucosyltransferase activity was found in human platelet [206]. The enzyme responsible for the formation of the glucoprotein was found to be inhibited 76% by Mn2+ (5 mM) whereas at lower concentrations Mn2+ had no effect on the activity, pointing out to a role of Mn2+ in GT inhibition. Surprisingly, sialyltransferases do not seem to rely on Mn2+ for their catalytic activity. A study from 1977 has shown that EDTA treatment did not abolished enzymatic

activities of sialyltransferase in the serum nor in the liver. They even observed that Mn2+ strongly inhibited this activity [207]. More recently, studies on ST8Sia II and ST8Sia V, involved in the synthesis of polysialic chains, have no requirement of metal ions [208].

Finally, a strange role of Mn2+ that can possibly have an impact on glycosylation was discovered in 2015. Authors have shown that Mn2+ induced oligomerization leading to lysosomal degradation of several Golgi proteins [209]. They engineered Golgi proteins containing domains that are able to self-interact and self-oligomerize after induction. Among the proteins tested were MAN1A1 and B4GALT1. When oligomerization occurred after Mn2+ induction, these proteins leave the Golgi and are targeted to lysosomal degradation, via the non-canonical Golgi to lysosome pathway.

Altogether, these results show that the role of Mn2+ in glycosylation is not completely understood and far from being simple.

4.1.3. Mn2+ changes can affect all the glycosylation pathways

Interestingly, all the glycosylation pathways include Mn2+ dependent steps that can thus be affected by Mn2+ changes in the cell (Figure 20). Besides, a large majority of Mn2+ dependent GT are localised in the Golgi apparatus (26 out of 29 in Table 4), strengthening the importance of Golgi Mn2+ homeostasis in glycosylation.

As presented in table 5 and figure 19, mucin-type O-glycosylation and GAG biosynthesis can be the most severely affected pathways in case of Mn2+ homeostasis disruption. Indeed, XYLT1, the enzyme that catalyses the first step in HS, CS and DS biosynthesis, strictly requires Mn2+ to be fully active. Therefore, a lack of Mn2+ could prevent the synthesis of these 3 types of GAG. In addition, several polypeptide N-Acetylgalactosaminyltransferases (GALNT), the enzymes that catalyse the first step of mucin-type O-linked glycosylation, are known to be Mn2+ dependent. However, the existence of more than 21 GALNT and their relative redundancy could temper the glycosylation defect when Golgi Mn2+ is lacking.

Moreover, all the Mn2+ dependent enzymes presented in this section have different affinity for Mn2+. Hypothetically, they could be ranked based on their affinity for Mn2+ to detect the most severely affected pathway in case of Mn2+ homeostasis disturbance. However, all the kinetics

analyses available in the studies were performed in different conditions, thus making it impossible to compare Mn2+ affinity for these GT.

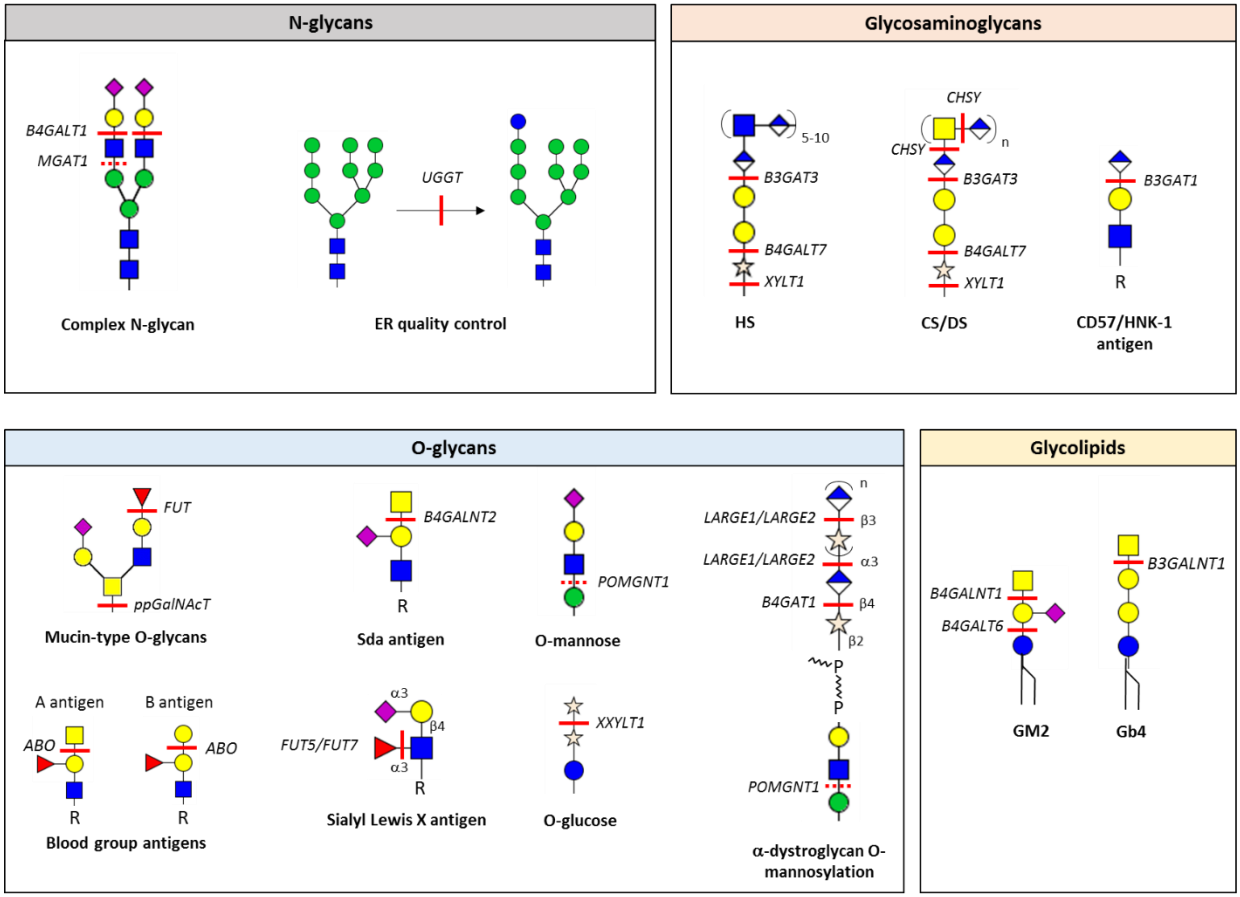

Figure 20. Glycosylation pathways involving Mn2+ dependent glycosyltransferases. Red lines show specific Mn2+ dependent glycosylation steps**.** Glycosylation steps with putative Mn2+ requirement are depicted in red dashes. O-mannosylation of α-dystroglycan requires a ribitol-phosphate linker. Linkage are not always shown for clarity.

4.2. Mechanism of Mn2+ as coordinator for glycosyltransferase catalytic activity

Much has been made on the role of the DXD amino acid sequence in the glycosylation process. In general, for retaining GT-A folded enzymes, the two aspartate residues can interact with the Mn2+ ion, whereas only the last aspartate interacts with the metal cation in inverting GT-A folded enzymes. The X of the motif is usually involved in the ribose binding of the nucleotide sugar donor [5]. Although some insights into the mechanism of Mn2+ coordination for GT have been reviewed in section 4.1, in this section, the mechanism will be addressed in details using β4GalT1 as an example, with a focus on the role of the Mn2+ during the catalysis. Besides, β4GalT1 kinetic pathway represents the general catalytic mechanism for all the inverting GT.

4.2.1. Example with β4GalT1, the most studied glycosyltransferase

β4GalT1 (EC 2.4.1.38), in the presence of Mn2+, catalyses the transfer of Gal from UDP-Gal to the the non-reducing end GlcNAc of complex N-glycans. In the presence of α-lactalbumin (αLA), the acceptor specificity of β4GalT1 is switched from GlcNAc to Glc, thus resulting in the production of lactose [210]. β4GalT1 is a GT-A folded enzyme containing a $D^{248}XD^{250}$ motif located in the cleft of the catalytic domain, which serves as a Mn2+ binding-site [211]. β4GalT1 has two flexible loops, a long and a small one, which are able to undergo conformational changes. The long flexible loop (residues I341-H361) contains residues essential in the closed conformation for the binding of the metal ion, sugar nucleotide, and the acceptor substrate. Among the GT known to date, the catalytic mechanism of β4GalT1 has been the most extensively studied [90,210,211] (Figure 21).

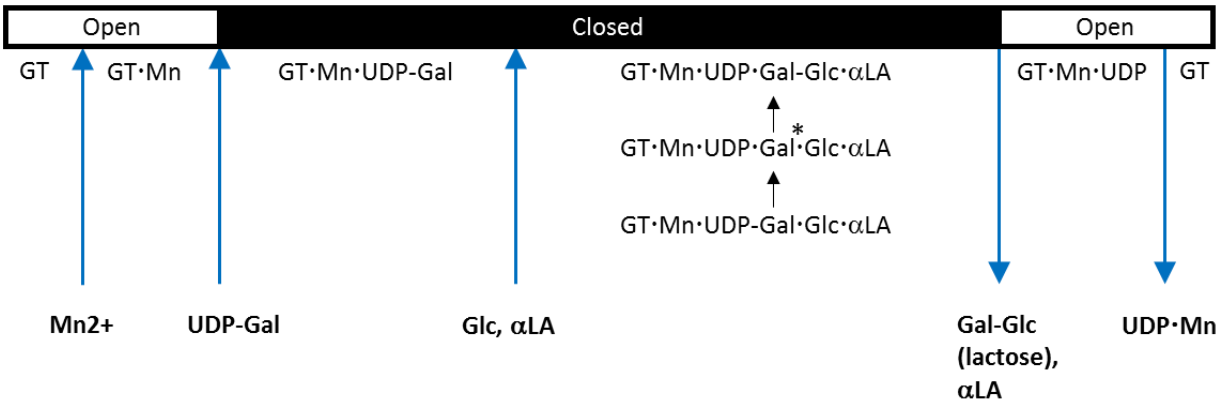

Figure 21. Kinetic catalytic pathway of β4GalT1 in the presence of αLA and with Glc as the acceptor substrate. First, the enzyme is in an open conformation that allow Mn2+ to bind followed by the donor substrate, UDP-Gal. Upon UDP-Gal binding the enzyme undergoes conformational changes from open to closed configuration, exhibiting the acceptor and αLA binding sites. αLA and Glc bind together synergistically to β4GalT1 to form a GT·Mn·UDP-Gal·Glc·αLa complex. During this transition state the Gal residue is cleaved from UDP-Gal and exists as an intermediate oxocarbenium ion, indicated as Gal*. Then, the Gal residue is attached to the Glc acceptor to form the lactose, and is then released from the enzyme along with αLA. Finally, UDP bound with Mn2+ are released together from β4GalT1. Adapted from Ramakrishnan et al., 2006.

4.2.1.1. Mn2+ binding

First, the enzyme is in a so-called open conformation that allows the binding of one Mn2+ ion to the $D^{248}XD^{250}$ motif [90]. The metal ion binding site is located at the N-terminal hinge region of the long flexible loop. Residues Asp250 and Met340 and four water molecules (W1-W4) coordinate the metal ion in this open conformation (Figure 22A). In addition, a conserved water molecule (W5) located in the catalytic pocket, bridges the two Asp residues of the $D^{248}XD^{250}$ motif through hydrogen bonding interactions with their side-chain. The binding of the metal ion is essential and allows UDP-Gal to bind.

4.2.1.2. UPD-Gal binding

Sugar nucleotide then binds to the metal-enzyme complex that is still in the open conformation. Binding of UDP-Gal is impossible if Mn2+ did not bind first to the enzyme. The binding of UDP-Gal induced some changes and bonding. The α-phosphate oxygen atom of the UDP forms a coordination bond with the Mn2+, replacing water molecule W2. The β-phosphate oxygen atom of the UDP forms a coordination bond with the Mn2+, replacing water molecule W3. UDP-Gal binding will trigger a conformational change of the catalytic site, from open to close conformation.

4.2.1.3. Conformational changes

Crystallographic studies on the catalytic domain of β4GalT1 (residues 130–398) have shown that the conformational changes that the enzyme undergoes upon Mn2+/UDP-Gal binding involved the two flexible loops.

The torsion angle of the side chain of His343 changes in a way that it coordinates with the metal ion by replacing W1. With the metal ion now coordinating with residues Asp250, Met340, His343, a water molecule, and two phosphate oxygen atoms of UDP, the long loop is no more flexible. During the conformational changes of the flexible loops, the metal ion moves in such a way that it coordinates with the W5 water molecule, replacing W4 (Figure 22B).

The Trp310 side chain in the small flexible loop, facing away from the binding pocket in an open conformation, moves to face towards the binding pocket. The Trp310 keeps UDP-Gal from being released by making hydrogen bonds with it, and is also involved in the binding of acceptor substrates.

The large loop then undergoes a major conformational change where its carboxyl-terminal hinge region changes from a coil to a helix structure. This allow the loop to cover the pocket with the bound UDP-Gal preventing its escape from the binding cavity and also creates the acceptor binding site. During conformational changes, even the Mn2+ coordination undergoes significant modifications to form a correct and active ground-state structure to facilitate enzyme catalysis.

Altogether, these conformational changes play an important role in the initiation of the catalytic mechanism of the enzyme.

4.2.1.4. Acceptor substrate binding and catalysis

After these conformational changes, the acceptor substrates (here Glc and αLA) can bind to the GT·Mn·UDP-Gal complex and the catalysis can start. The catalysis begins with the cleavage of the UDP-Gal to UDP + Gal. This step includes the existence of an extremely short-lived oxocarbenium intermediate. Then, the Gal residue is attached to the Glc acceptor to form the lactose. The disaccharide product and αLA are both ejected from the enzyme. β4GalT1 then returns to an open conformation state, releases UDP and Mn2+, allowing the reaction to start again. The water molecule W5, by hydrogen bonding interactions with the cleaved β-phosphate oxygen atom of UDP, plays an important role during catalysis in ensuring that the catalytic activity proceeds only forward. Moreover, Met340 is crucial in bonding with Mn2+ during the catalytic cycle of the enzyme. Indeed, when Met340 was mutated to His, the enzyme could not efficiently revert to the open conformation essential for efficient catalysis.

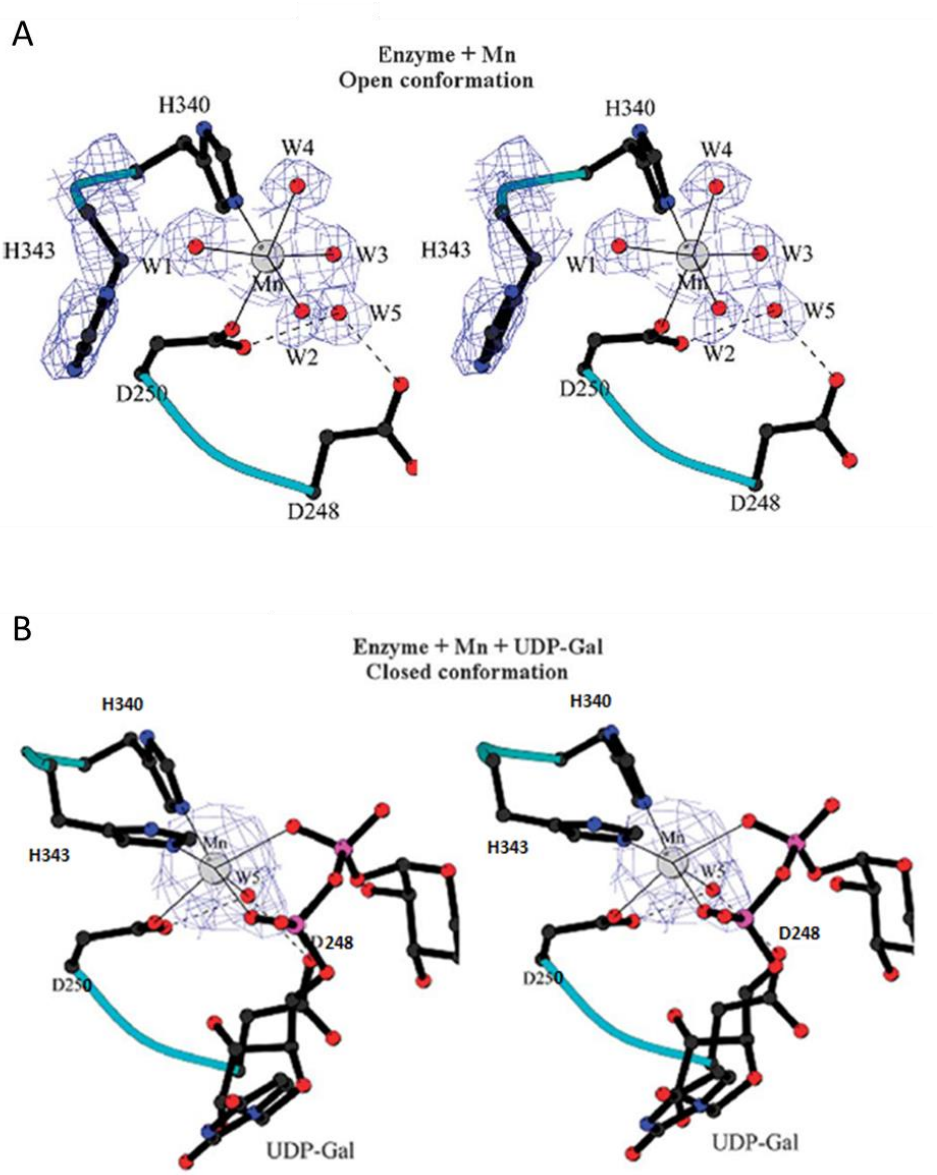

Figure 22. Changes in Mn2+ coordination during UDP-Gal binding to β4GalT1. The coordination bonds with Mn2+ are shown as thin continuous lines and the hydrogen bonds are shown as dotted lines. The final electron density maps comprising Mn2+, the water molecules and the residues of interest are shown as blue lines. (A) Only one Mn2+ is found at the metal-binding site interacting with the H340 and D250 residues. There are also four water molecules, W1–W4, bound to the Mn2+, arranged in an octahedral coordination. The structural water molecule, W5 is found about 3.8A° from the Mn2+. Interestingly, the metal-binding residue H343 does not coordinate with Mn2+. (B) Crystal structure of β4GalT1 in complex with Mn2+ and UDP-Gal, where the enzyme is found in the closed conformation. The Trp310 side-chain is found inside the catalytic pocket and forms a hydrogen bond with the β-phosphate of the UDP. This results in moving the β-phosphate group towards the Mn2+, forming a coordination bond by replacing W3 by the β-phosphate group of UDP. During conformational changes, the sixth coordination bond with W4 is exchanged for a bond with W5. Adapted from Ramakrishnan et al., 2006.

[5] CONGENITAL DISORDERS OF GLYCOSYLATION

5.1. General introduction

Defects in genes involved in the glycosylation process have been identified in human rare inherited diseases named Congenital Disorders of Glycosylation (CDG) [8–11]. The first CDG patient was identified by Professor Jaeken in 1980. A couple of twin sisters had psychomotor retardation and multiple serum glycoproteins abnormalities. These patients were later found deficient in phoshomannomutase (PMM2), an enzyme involved in the conversion of Man-6-P to Man-1-P during the biosynthesis of GDP-mannose, an essential nucleotide sugar for the synthesis of the oligosaccharidic precursor in the ER during N-glycosylation [212–214]. CDG mostly affect N-glycosylation but can also affect other glycosylation types or even multiple pathways. To date, more than 110 different CDGs have been identified that now encompass defects in the synthesis of all glycosylation pathways [215]. Moreover, CDG have been localised to all cellular compartments where glycoconjugates can be synthesized (Figure 23). Due to the importance of the ER and the Golgi in glycosylation, CDG in genes coding for ER or Golgi proteins are logically the most abundant ones. However, CDG are still rare diseases and the number of patients is around 1000, with PMM2-CDG representing more than 700 patients [216,217].

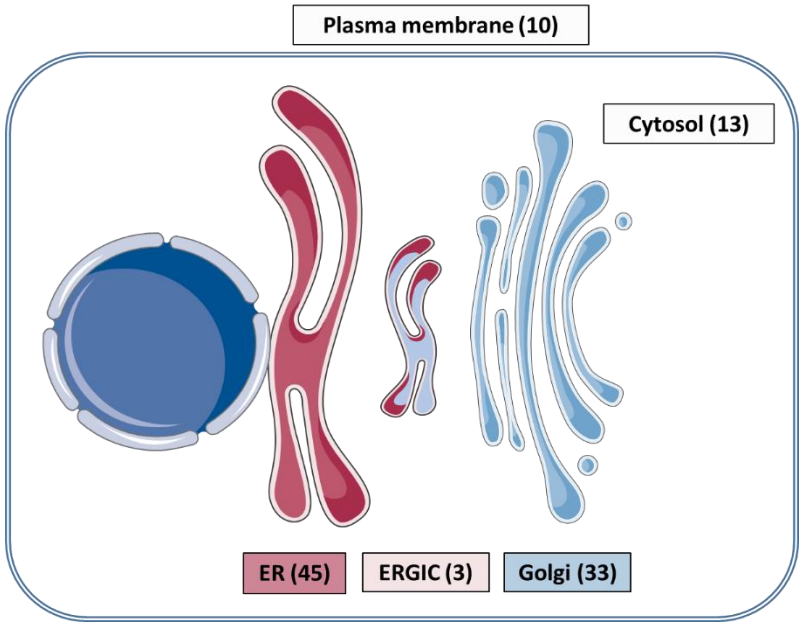

Figure 23. Subcellular localisation of CDG known to date. The number of CDG for each compartment is indicated between brackets. This figure does not include dystroglycanopathies that can be sometimes classified as CDG. Adapted from Peanne and Jaeken, 2017.

Due to the diversity of genes identified in CDG, the clinical spectrum for CDG is broad and all organs can be affected [218–223]. CDG can lead to neurological, immunological, skeletal abnormalities, but also liver, endocrine and skin manifestations. Because of the essential nature of glycosylation, the clinical phenotype of CDG patients ranges from mild mental retardation with

hypoglycemia, protein-losing enteropathy or cardiomyopathy, to profound psychomotor retardation, seizures and blindness in severely affected individuals [216,224].

5.2. A new era in CDGs

Because of the number of enzymes involved in the glycosylation process, it is not surprising that the majority of CDG is caused by mutations in genes encoding protein directly involved the machinery (GT, GH and NST). However, a large number of factors can also modulate glycosylation (see chapter 2.5). Therefore, any disturbance in one of these factors can lead to aberrant protein glycosylation. As a consequence, novel deficiencies have recently emerged, marking a new era in the CDG field. They include deficiencies in vesicular trafficking and/or glycoprotein sorting [225–229]. These new CDGs have been intensively reviewed in the literature [3,230–235]. Another growing class of CDG affects Golgi homeostasis [7,12]. While the impact of such defects on Golgi glycosylation is harder to apprehend, one could think that these defects disturb several factors involved in the regulation of glycosylation (ie pH, divalent cations…) then leading to glycosylation deficiencies. These diseases will be discussed later in section 5.5.

5.3. Identification of CDG patients

The first step to identify CDG patients is to look at the clinical symptoms. Indeed, CDG should be suspected if a patient present any unexplained neurological syndrome, especially when associated with other organs defects. Still, few CDG do not lead to neurological involvement, then one should also screen for CDG any patient with unexplained syndrome [236].

Diagnosis of CDG mostly relies on biochemical analyses. The first test classically used in laboratory is the iso-electrofocalisation (IEF) of the serum transferrin. IEF is an electrophoresis approach based on the separation of proteins according to their isoelectric point. Transferrin is a protein with two N-glycosylation sites, which are occupied most of the time by bi-antennary complex N-glycans (Figure 24). Tetrasialotransferrin (4S) is thus the main serotransferrin isoform. However, those N-glycans can also sometimes be more branched than depicted here. The terminal sialic acid residues carried by complex N-glycans confer positive charges to transferrin.

Therefore, serotransferrin can be analysed by IEF and the migration profile reflects the N-glycosylation efficiency.

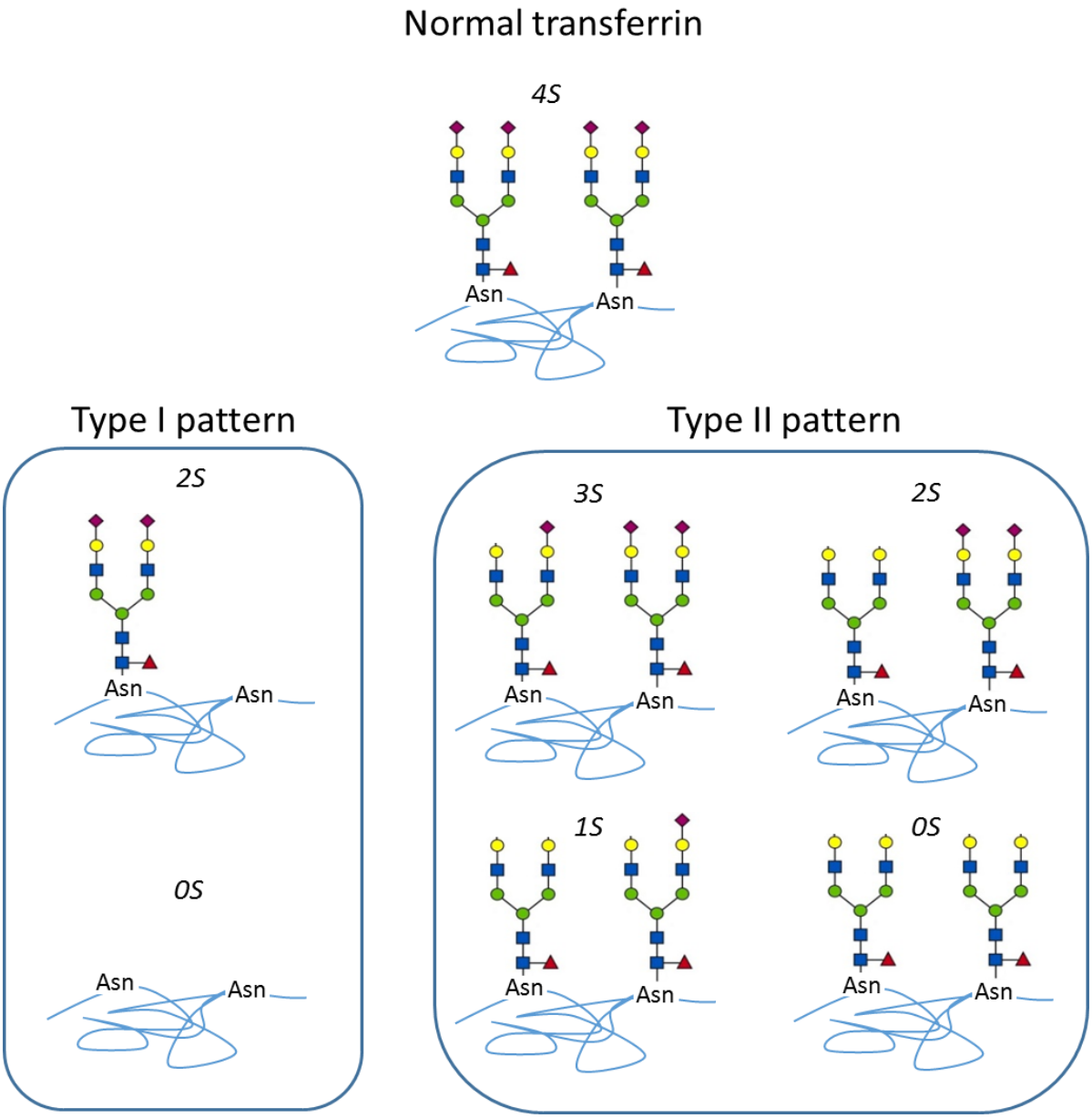

Figure 24. Serum transferrin N-glycans structure. Normal transferrin mostly carries 4 sialic acids (4S). The glycan structures representing the different serum transferrin isoforms are shown (4S: tetrasialotransferrin, 3S: trisialotransferrrin, 2S: disialotransferrin, 1S: monosialotransferrin, 0S: asialotransferrin). Type I pattern reflect an ER glycosylation defect and type II pattern a Golgi glycosylation defect. Serotransferrin from CDG patients can also rarely present a type III pattern that combines the type I and type II pattern.

Thanks to this test, two different CDG groups can be distinguished (Figure 25) [224,237]:

- **Type I CDG (CDG-I):** these patients present a type I pattern of the serotransferrin, with a decrease of 4S and an increase of 2S and 0S isoforms. CDG-I affect ER glycosylation and thus the

synthesis of the precursor. As a result, the in bulk transfer of the precursor will be affected and there will be a loss of glycan on one or two glycosylation sites of the serotransferrin.

- **Type II CDG (CDG-II):** these patients present a type II pattern of the serotransferrin, with a decrease of 4S and a slight increase of all hyposialylated isoforms and especially 3S. CDG-II are due to defects in the glycan processing in the Golgi, leading to abnormal glycan structures on glycoproteins.

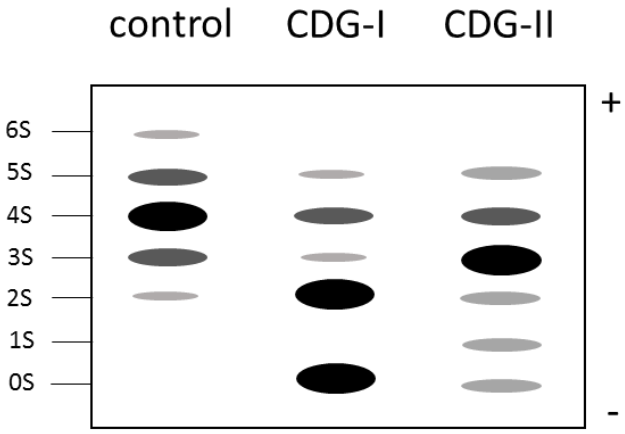

Figure 25. Identification of CDG patients by serotransferrin IEF. Serotransferrin N-glycans can also have more branches (mostly tri-antennary structures) resulting in the presence of 6S and 5S structures. CDG-I pattern shows an increase of 2S and 0S with a decrease of 4S. CDG-II pattern is heterogeneous, with classically a decrease of 4S and an increase of all hyposialylated isoforms. The intensity and the thickness of the band represent its quantity.

However, IEF is a low resolution method with a lot of disadvantages. Indeed, the transferrin glycosylation pattern of some CDG-II appears perfectly normal and some transferrin variants can impair the diagnosis, thus revealing the limitations of this method [238–240]. Moreover, serotransferrin is a circulating blood protein secreted by the liver. Thus, IEF of serotransferrin cannot identify defects in genes coding for proteins that are not expressed in liver. To overcome these limitations, more powerful techniques like electrospray ionization mass spectrometry (ESI-MS) and capillary zone electrophoresis of transferrin or total N-glycans from serum can also be used for CDG diagnosis. However, these methods only detect patients with N-glycosylation defects [241,242]. Recently, a high resolution nano LC-MS analysis was proposed as a glycoprofiling tool to directly diagnose a CDG, but known CDG can only be identified [243,244]. Apolipoprotein C-III (ApoC-III) IEF and mass spectrometry analyses can also be used for CDG diagnosis. ApoC-III is a serum protein with core 1 mucin-type O-glycan carrying one or two sialic acid residues. ApoC-III can thus be used to screen CDG patients having errors in the biosynthesis of mucin type O-glycan. To date, no rapid screening method for the identification of defects in

GL or GAG biosynthesis is available. In any case, all these tests must be followed by genetics analyses (exome sequencing, homozygosity mapping…) to precisely identify the gene and the mutation(s) involved.

Due to the increasing number of CDG identified, the nomenclature as CDG-I and CDG-II followed by a letter was replaced and simplified in 2009. Jaeken and co-authors proposed to use CDG followed by the affected gene name [245]. For instance, CDG-Ia is now designed as PMM2-CDG.

5.4. Treatments

CDG are severe diseases that affect child development. Therefore, finding treatment for CDG is the next critical step. However, once diagnosed, treatment still cannot cure developmental problems and neurological damages.

A treatment with oral mannose supplementation is available for MPI-CDG [246,247]. However, intravenous mannose therapy in patients unable to be fed orally can cause side effects such as seizures and severe depression of consciousness [248]. As the liver is the most affected organ in this CDG and no neurological features were observed, a liver transplantation revealed to be successful for MPI-CDG [249]. Liver transplantation was also proposed for CCDC115-CDG [250]. Oral uridine treatment was proposed for CAD-CDG [251]. D-galactose supplementation has been shown to benefit patients with PGM1-CDG [252]. Interestingly, galactose has also been successful for SLC39A8-CDG [7] and SLC35A2-CDG [253]. Although it is clear that the treatment rescued the impaired galactosylation, the mechanism remained poorly understood. Only heart transplantation was proposed for DOLK1-CDG [254]. Oral-fucose supplementation seems to control infections for SLC35C1-CDG [255]. A treatment with oral butyrate controls seizures in PIGM-CDG [256]. Bone marrow transplantation corrects neutropenia and lymphopenia in PGM3-CDG [257]. For the CDG with a myasthenic syndrome (DPAGT1-CDG, ALG2-CDG, ALG14-CDG, GFPT1-CDG and GMPPB-CDG), cholinesterase inhibitors were proposed as treatment. For GNE-CDG, supplementation with sialic acid may stabilize muscle strength [258]. For PMM2-CDG, a treatment with pharmacological chaperones is promising [259].

5.5. Golgi homeostasis defects leading to CDG

The term homeostasis include many variables. Regarding Golgi glycosylation and homeostasis, three main variables should be carefully maintained (Figure 26):

- protein homeostasis: indeed, the amount of proteins in the Golgi, especially for GT, GH and NST, can severely alter the glycosylation process.
- lipid homeostasis: the structural organization of the Golgi apparatus in stacks and cisternae is very dependent on lipid composition and therefore can be disrupted if lipid homeostasis is not controlled.
- ion homeostasis: as presented earlier, ion homeostasis must also be carefully handled to ensure a proper glycosylation.

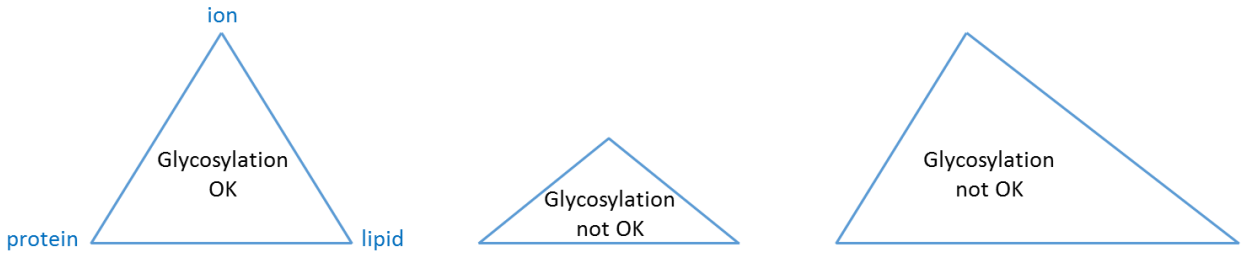

Figure 26. Simplified view of the effect of Golgi homeostasis changes on glycosylation. In the first case, the homeostasis is well maintained and the glycosylation process can occur without any problems. In the second case, the ion concentration is decreased leading to an abnormal glycosylation. In the third case, lipid concentration is increased, leading to alterations in the lipid composition of Golgi membranes and potentially disrupting Golgi structural organization, and then leading to an abnormal glycosylation. Note that some ions such as Mn2+ are more likely to induce glycosylation changes than others.

Although extremely simplified, the view presented here has the advantage to show the importance of a controlled and regulated Golgi homeostasis in glycosylation. Therefore, slight disturbance in this homeostasis can lead to several heterogeneous diseases.

This section will review the defects in Golgi homeostasis leading to CDG, with the most known ones being linked to vesicular deficiencies. Then, defects in ionic homeostasis leading to this new era of CDG will be reviewed. A more detailed focus will be done on ion homeostasis and especially Mn2+ homeostasis defects leading to diseases.

5.5.1. Trafficking defects leading to CDG

Vesicular trafficking is crucial to maintain an equilibrium between the three variables presented before (Figure 26). Indeed, any disturbance in vesicular trafficking can lead to a redistribution of proteins, lipids and ions in the cell. Therefore, it is not surprising that vesicular trafficking defects can lead to CDG. The most described CDG linked to vesicular trafficking defects are the case of COG-CDG, which opened a totally new field in CDG.

5.5.1.1. COG

COG is a multimeric cytoplasmic complex of 8 subunits (Cog1 to Cog8) known to be involved in the tethering of vesicles at the target compartments such as the Golgi apparatus. In 2004, two siblings presented with perinatal asphyxia, dysmorphia (low-set ears, micrognathia, short neck, loose and wrinkled skin), a generalized hypotonia, hepatosplenomegaly, and they developed jaundice shortly after birth [225]. Both patients died from recurrent infections and cardiac insufficiency, the male at age 5 weeks and the female at age 10 weeks. Those patients had a type-II serotransferrin pattern and a general defect in sialylation. In-vitro enzymatic assays showed a decrease activity of core I GalT and ST3Gal-1, meaning that N- and O-glycosylation were impaired. The rate of transport of CMP-Sia and UDP-Gal were also decreased. Finally, FRAP analyses demonstrated that ST3Gal-1 trafficking was specifically slowed down in patient fibroblasts compared to control. COG7 was undetectable in patient skin fibroblasts and genomic DNA sequencing revealed the presence of a homozygous intronic mutation (IVS1+4 A→C). They were the first COG-CDG patients to be characterized. Since then, all COG subunit excepted Cog3 have been described in CDG, thus broadening the spectrum of clinical phenotypes in COG-CDG [225–228,260–262]. Nevertheless, all patients described so far present defects in multiple glycosylation pathways (N- and O-glycoproteins), in the Golgi apparatus ultrastructure, in retrograde intra-Golgi trafficking and in the stability or the localization of several Golgi resident proteins. However, the molecular mechanism responsible for the observed glycosylation defects in those patients has not been clearly determined yet for each case. Broadly speaking, the COG complex has been suggested to be involved in the proper localization of several glycosylation enzymes, including MGAT1, MGAT2, MAN2A1, B4GALT1, and ST6GAL1 [263,264].

5.5.1.2. VPS13B

This gene encodes the **Vacuolar protein sorting-associated protein 13B (VPS13B)**, a transmembrane protein required for GA integrity. Mutations in *VPS13B* are known to cause the Cohen syndrome, a disease that was first described in 1973 [265]. The typical patient phenotype is a truncal obesity, microcephaly, slender extremities, joint hyperlaxity, intellectual disability, and chorioretinal dystrophy with myopia, a phenotype that looks very like CDG phenotypes. Golgi morphology is also strongly disrupted in all of those patients. Therefore, Duplomb, Duvet et al have recently hypothesised that VPS13B deficiency could lead to glycosylation defects responsible for the main clinical manifestations observed in Cohen syndrome [266]. Although no glycosylation defects were observed on transferrin or α1-antitrypsin due to the absence of liver

involvement in the pathology, total N-glycans analysis from serum showed a strong accumulation of agalactosylated and asialylated structures. in peripheral blood mononuclear cells, ICAM-1 and LAMP-2, two heavily glycosylated proteins, were also shown to be hypoglycosylated. Finally, they found that lysosomes were abnormally enlarged in patient fibroblasts, suggesting a crucial role of VPS13B in endosomal/lysosomal trafficking. In conclusion, Cohen syndrome can be also classified as a CDG.

5.5.1.3. TRAPPC11

TRAPPC11 encodes a protein with the same name, which is a subunit of the TRAPPIII complex. This complex is thought to be involved in the anterograde transport from the ER to the ERGIC, in the vesicle export from the Golgi apparatus and in autophagy [267]. In 2016, while authors wanted to work on ER stress using a zebrafish *foie gras* (foigr) mutant, they unexpectedly found a role of TRAPPC11 in glycosylation [268]. Indeed, TRAPPC11 specific depletion, and not the other factors of the TRAPPIII complex, reduced the synthesis of lipid-linked oligosaccharides in the ER. Moreover, TRAPPC11 knockdown in human HeLa cell lines led to protein hypoglycosylation. More recently, TRAPPC11 mutations have been found in a CDG patient with hypotonia, seizures, dysmorphism, cholestasis, nephropathy and osteopathy [269]. Patient fibroblasts were treated with Brefeldin A (BFA), an fungal metabolite known to be able to collapse the GA into the ER, thereby merging all Golgi stacks in a reversible manner [270,271]. Complete disassembly of the Golgi was observed both in control and patient cells upon BFA treatment. After BFA removal, patient cells displayed a delayed in the reassembly of the GA, revealing an anterograde ER to Golgi trafficking defect. Besides, the patient also presented a type II serotransferrin pattern and an increase of non-sialylated forms of ApoC-III, demonstrating defects in both N- and O-glycosylation pathways. TRAPPC11 mutations have been described in other patients in the past but no glycosylation analyses were performed in these patients [215].

5.5.2. Ion homeostasis defects leading to CDG

The field of ion homeostasis disturbance in CDG is relatively new. It was first described in 2008 by Kornak and collaborators in a cutis laxa syndrome caused by mutations in the vesicular H+-ATPase subunit ATP6V0A2 that was later classified as a CDG [12]. These findings about Golgi pH disruption leading to CDG opened a new field of investigation.

5.5.2.1. H+ homeostasis defects

5.5.2.1.1. V-type H+ATPase deficiencies

V-type H+ATPase is composed of 2 multisubunit domains: V0, directly responsible for proton translocation, and V1, involved in the hydrolysis of the ATP. This pump has been shown to be localised in several compartments, including endosomes, lysosomes and Golgi [272]. Thus, V-type H+-ATPase is crucial for the maintenance of the pH homeostasis of all these organelles.

ATP6V0A2 encodes the a2 subunit of the V-type H+-ATPase. Loss of function mutations were identified in several families with autosomal recessive cutis laxa (ARCL) type II [12]. In terms of clinical presentation, patients have a wrinkled skin, varying degrees of growth and developmental delay and central nervous system abnormalities. They also displayed typical facial appearance with downslanding palpebral dissures. All individuals displayed a type II serotranferrin pattern, an ApoC-III IEF with elevated monosialo isoform and decrease disialo isoform, showing a combined defect of N- and O-glycosylation that was confirmed by mass spectrometry analyses. The link between cutis laxa and defective glycosylation was first established in 2005, without knowing the affected gene [273]. Besides, Golgi trafficking was also impaired in patient fibroblasts, without affecting overall Golgi morphology. Indeed, following BFA treatment, significant delay in the retrograde Golgi to ER trafficking was observed. Altogether, this demonstrates a crucial importance of the a2 subunit in Golgi function, especially in glycosylation. Mutations in ATP6V0A2 leading to glycosylation defects are now classified as CDG.

The underlying mechanism of the glycosylation defect is still unclear but two non-exclusive hypotheses emerged:

- pH increase can lead to mislocalization of one or several glycosyltransferases as described by several publications [86,87].
- pH increase can also affect glycosyltransferases activities, because exactly like any other enzymes, they require an optimal pH to be fully active.

ATP6V1A encodes the A subunit of the V1 domain of the V-type H+-ATPase. Whole-exome sequencing identified homozygous mutations in ATP6V1A in three unrelated patients, two patients carrying Gly72Asp mutations and one patient with a Arg338Cys mutation. Patients presented with mild to severe ARCL with neurological impairment and cardiac involvement

(aorta dilatation, hypertrophic cardiomyopathy, septal defects and cardiac failure) [274]. These cardiac features distinguished ATP6V1A-CDG from ATP6V0A2-CDG. Besides, all patients displayed a type II serotransferrin pattern with a consistent loss a 1 sialic acid.

ATP6V1E1 gene encodes the E1 subunit of the V1 domain of the heteromultimeric V-ATPase complex. Mutations in ATP6V1E1 were identified in four patients from 2 different families with ARCL type II with similar phenotype as ATP6V1A-CDG, but without neurological involvement [274]. Besides, a type II Serotranferrin pattern in IEF was observed in these patients.

ATP6AP1 encodes an accessory regulatory subunit of the V-type H+ATPase named ATP6AP1 or Ac45 [275]. In a cohort of unsolved CDG patients, eleven male patients from 6 families have been reported with mutations in the X-linked ATP6AP1 gene [276]. Patients displayed an immunodeficiency syndrome with liver and neurological involvement, associated with abnormal N- and O-glycosylation. Type II serotransferrin pattern was observed in all studied patients, and mucin type O-glycosylation of serum Apo-CIII was abnormal in most patients, showing a decreased sialylation.

5.5.2.1.2. TMEM199

TMEM199 (MIM #616815) encodes TMEM199 (previously called C17orf32), a newly discovered protein involved in Golgi homeostasis [277]. Since TMEM199 is the human ortholog of yeast V-ATPase assembly factor Vph2p (also known as Vma12p), known to play a role in the yeast H+-ATPase functioning, it was thus suggested that TMEM199 could play a role in pH homeostasis via the V-type H+ATPase. TMEM199 partially colocalizes with giantin, a Golgi marker, also with ERGIC marker and COPI vesicles. However, no colocalisation were observed with COPII nor ER markers. Therefore, TMEM199 is considered to be localized to both ERGIC and Golgi compartments. Recently, four patients from three different families have been described with TMEM199-CDG (MIM #616829). Overall, the clinical phenotype is mild and limited to a liver disorder with hepatic steatosis, elevated aminotransferases and alkaline phosphatase, hypercholesterolemia with elevated LDL-C, low serum ceruloplasmin levels. Glycosylation analysis showed a type II serotransferrin pattern with an increase of di- and trisialo isoforms and a decrease of tetrasialo isoform. Nanochip C8 QTOF analysis of intact transferrin confirmed the loss of sialic acid and also revealed a decrease of galactosylation. Metabolic labelling with alkyne-tagged synthetic sugar analogs [278,279] confirmed a clear reduction in sialic acid incorporation in all patients. Apo-CIII

IEF revealed a mucin type O-glycosylation defects in 3 out of 4 patients, showing that TMEM199-CDG leads to a combined N- and O-glycosylation defect. Although its function is still not completely clear, TMEM199 is suggested to play a role in Golgi homeostasis.

5.5.2.1.3. CCDC115

CCDC115 (MIM #613734) encodes CCDC115 (Coiled-Coil Domain-Containing 115), a newly discovered protein suggested to be involved in Golgi homeostasis [277]. CCDC115 shares some homology with the yeast V-ATPase assembly factor Vma22p, known to play a role in the pump functioning. It was thus suggested that CCDC115 could play a role in pH homeostasis at the Golgi level via V-type H+ATPase. Like TMEM199, CCDC115 is localized to ERGIC and Golgi compartments. Eight patients from five different families have been described with CCDC115-CDG (MIM #616828). Seven homozygous mutations (p.Leu31Ser being the most frequent mutation) and one compound heterozygous mutations were found. Patients presented with liver disease (hepatic steatosis, hepatomegaly, fibrosis, cirrhosis) and variable brain involvement (hypotonia, intellectual disability, epilepsy, behaviour problems). Patient sera displayed elevated aminotransferases, alkaline phosphatase, hypercholesterolemia with elevated LDL-C, low serum ceruloplasmin levels. Glycosylation analysis showed a type II serotransferrin pattern with an increase of di- and trisialo isoforms and a decrease of tetrasialo isoform in all patients. MALDI-LTQ analysis of intact transferrin confirmed the loss of sialic acid and also revealed a decrease of galactosylation. Metabolic labelling with alkyne-tagged synthetic sugar analogs [278,279] confirmed a clear reduction in sialic acid incorporation in all patients. Apo-CIII IEF revealed a mucin type O-glycosylation defects in all patients, revealing a combined N- and O-glycosylation defect.

5.5.2.2. SLC39A8: a Mn2+ homeostasis disorder leading to CDG

As described in chapter 3, ***SLC39A8*** encodes SLC39A8 (also named ZIP8), a Zn2+/Mn2+ transporter at the plasma membrane (MIM #608732).

In 2015, Park et al have described the first SLC39A8-CDG patient [7]. A young girl from unrelated German parents was born with short limbs. At the age of 4 months, she presented with dwarfism, cranial asymmetry and malformation of the viscerocranium. Besides, she had brain atrophy but with a normal cerebellum. At the age of 7 months, a liver disease occurred with elevated

transaminase. Mn2+ levels were below the limit of detection both in blood and urine, strongly suggesting a lack of Mn2+ reabsorption in kidney. Whole-exome sequencing revealed a compound heterozygous mutation in SLC39A8: p.Gly38Arg (c.112 G>C), coming from the father, and p.Ile340Asn (c.1019 T>A), from the mother. The I340N mutation is located in a highly conserved residue in transmembrane domain V, which is a part of the ion channel. Glycosylation analysis showed a type II serotransferrin pattern with only 10% of tetrasialo isoform. ESI-MS-TOF detailed analysis of transferrin confirmed the loss of sialic acid but also showed a strong lack of galactose on transferrin N-glycans. Since galactosylation of N-glycans was affected, authors hypothesised that reduced Mn2+ levels impaired β-1,4-galactosyltransferase I activity, known to be a Mn2+-dependent glycosyltransferase. Therefore, the patient was put on oral galactose treatment (up to 3.75 g/kg per day), to increase the pool of UDP-Gal, the nucleotide sugar substrate of β-1,4-galactosyltransferase I. Although serotransferrin glycosylation was corrected, the clinical efficacy of this treatment is however not clear yet. This therapeutic approach with galactose supplementation can indeed only treat symptoms attributable to hypogalactosylation and does not correct malfunction of other manganese-dependent enzymes.

Recently, this patient has been subjected to Mn treatment for more than a year [280]. They have chosen to use $MnSO_4$ monohydrated because of its high solubility. At the beginning of MnSO4 treatment substitution, the girl was 8 months old and already under galactose therapy. They progressively increased $MnSO_4$ monohydrated dosage and decreased galactose treatment. At the end, galactose treatment was ended and the patient was treated with 200mg/day of $MnSO_4$ monohydrated. The transferrin glycosylation was not altered, meaning that Mn2+ can easily replace galactose to normalize transferrin glycosylation. They also observed a normalization of all biochemical parameters that were abnormal. Elevated hypoxanthine and alkaline phosphatase levels decreased to reach normal levels after 31 and 87 days of manganese supplementation, respectively. The levels stayed normal since then. They observed an increase of blood Mn that now ranges in the normal concentrations in blood (7-11 ng/mL) and Mn concentration in cerebrospinal fluid reached 1.8 µg/L, comparable to the concentrations obtained in healthy children. In terms of clinical improvement, the patient stopped having seizures, her ability to swallow increased, and vision and hearing also improved. Motor development was generally favourable although psychomotor disability is still present. Patient presents a reduced hyperextension, since she is now able to grip toys, to control her head and

she can bring her hands to her mouth. In addition, no accumulation of Mn in the brain and no symptoms of manganism were observed after brain MRI.

Another SLC39A8-CDG patient has been subjected to Mn therapy. This 19 years old woman carries three different mutations in SLC39A8 (c.[97G > A;1004G >C]; [610G >T]) but has a milder phenotype. Blood manganese levels increased to physiological values when treated with 600mg/day of $MnSO_4$ monohydrated. Transferrin glycosylation was improved, as observed by a decrease of trisialo isoform (from 12% to around 5%) and an increase of pentasialo (from 1-2 to 6-8%). Tetrasialo isoform was not altered. The patient presented improved motor abilities and muscle strength. Ataxia was also reduced.

Manganese supplementation represents a better therapeutic approach than galactose therapy by its ability to correct all biochemical abnormalities that have been detected so far. However, compared to the normal daily intake of 1-2mg manganese in adults, the therapeutic dose is much higher. Therefore, manganese therapy should be monitored carefully to prevent manganism.

In total, 10 patients (from eight families) were identified with SLC39A8 mutations [215]. The most commonly found mutation is the p.Gly38Arg but other mutations were observed: p.Val33Met, p.Gly204Cys, p.Ser335Thr and p.Cys113Ser [281,282]. Individuals with p.Gly38Arg mutations seems to be less affected, with detectable levels of manganese and thus less severe glycosylation defects. However, all individuals share severe psychomotor retardation, seizures, strabismus and impaired growth. They all have Mn levels reduced in blood, a type II serotransferrin pattern and a loss of galactosylated structure was observed in ESI-MS-TOF. In conclusion, SLC39A8-CDG is a glycosylation disorder of Mn homeostasis disturbance.

5.5.2.3. TMEM165

In 2012, *TMEM165* was identified as a gene involved in a new subgroup of CDG [113] (MIM #614727). A full overview of TMEM165 is presented in chapter 6.

[6] TMEM165: a new player in Golgi glycosylation

6.1. TMEM165: genomic organization

TMEM165 (Transmembrane Protein 165) is a gene located on chromosome 4q12 and spans over 57 kb. *TMEM165* is highly conserved in evolution as homologous sequences can be found in 919 different species of bacteria and 409 eukaryotes [283]. Besides, no pseudo-genes for *TMEM165* in human genome were found. The coding sequence of *TMEM165* is divided into 6 exons (Figure 27) that leads to a 1312 bp fragment corresponding to the mRNA of the most abundant *TMEM165* transcript. This mRNA is then translated to the 324 amino acids TMEM165 proteins described below.

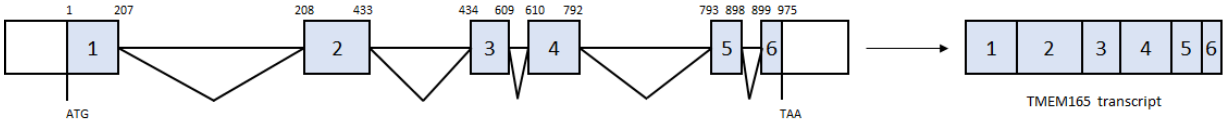

Figure 27. Schematic representation of the predicted genomic structure of TMEM165. Coding exons are shown in blue boxes, and introns (not drawn to scale) are represented by lines. The numbering above each exon is based on coding nucleotides. Adapted from Foulquier et al., 2012.

However, EST database analysis highlighted the existence of *TMEM165* splice transcript isoforms. Two particular isoforms, named Short-Form (SF) and Long-Form (LF) were identified [284]. These variants give rise to proteins isoforms of 129 and 259 amino acids, respectively. SF is a 129 amino acids protein translated from a 732 bp mRNA fragment containing exon E1, E5 and E6 of *TMEM165* gene. SF is expressed at low levels (from 0.5 to 6% compared to the full length TMEM165) in all human cells and tissues tested. LF transcript is a 1124 bp fragment contains Exon E1, E3', E4, E5 and E6 of *TMEM165* gene. Interestingly, the splicing of the gene for this transcript excludes exon E2 and includes an additional exon E3' (a 88 bp shorter version of exon E3). LF transcript was only found in the temporal lobe of human cerebral cortex. This transcript leads to a 259 amino acids sequence. Due to the tissue specific or the extremely low expression of these isoforms, only the most abundant TMEM165 will be detailed in the next sections.

6.2. TMEM165: the protein

6.2.1. The UPF0016 family

TMEM165 belongs to a family of uncharacterized proteins named UPF0016 (Pfam accession number: PF01169). Although uncharacterized, all members of this family share strong sequence

homologies. Besides, members of UPF0016 can be found in almost all organisms, from archaebacteria to human. This family can be divided into 12 subfamilies, with prokaryotes representing subfamilies I to VI and eukaryotes representing subfamilies VII to XII. In addition, plants seems to present the highest diversity in this family, as they possess from 2 to 5 paralogs per genome [283], while only one member for most of the eukaryotic organism was found.

This family is defined by the presence of one or two copies of this consensus pattern: E-Φ-G D-(KR)-(TS), Φ being any hydrophobic residue. Due to the presence of several acidic residue in these motifs, members of the UPF0016 family are presumably cation exchangers, even if their precise functions are unknown. Another feature of the family is the presence of 6 conserved putative transmembrane domains (TMD), which are suggested to be involved in the stability, the folding, the localization or even the function of this family of proteins. Some members of UPF0016 such as TMEM165 also possess a central hydrophilic loop, which is heterogeneous among the family but always contains several acidic residues. On the opposite, there is a strong heterogeneity at the N-terminus level. Its length can vary and some subfamilies members (ie plant subfamily VIII) even lack N-terminal extension. Besides, a site for peptide signal cleavage was identified in the N-terminus tail.

Eukaryotic members of this family contains two copies of the E-Φ-G-D-(KR)-(TS) motifs that are predicted to adopt an antiparallel orientation in the membrane. Moreover, TMHMM prediction leads to a common topology of UPF0016 eukaryotic members in almost all organisms, excepted for some plants (Figure 28).

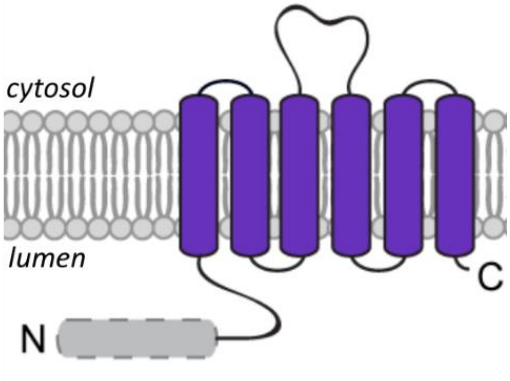

Figure 28. TMHMM predicted a common topology of UPF0016 family members in Metazoa. Adapted from Demaegd et al., 2014. The signal peptide is depicted as a pale grey dotted box.

6.2.2. TMEM165 topology, domains and structure-function relationship

TMEM165 is a 34,9 kDa protein composed of 324 amino acids. TMEM165 expression is ubiquitous and TMEM165 has been described as a Golgi-localized protein that can also be found on endosomes, lysosomes and plasma membrane [113,285]. TMEM165 sequence analysis showed some specific sequences/domains characteristic of the UPF0016 family (Figure 29):

- two copies of the E-Φ-G-D-(KR)-(TS) motifs. The first one is a ELGDK(T) motif in the second TMD, thus facing the cytosol. The second one is a EWGDR(S) motif in the 5th TMD, facing the Golgi lumen. These domains are composed of several acidic amino acids and are thought to form the pore used for ion transport.

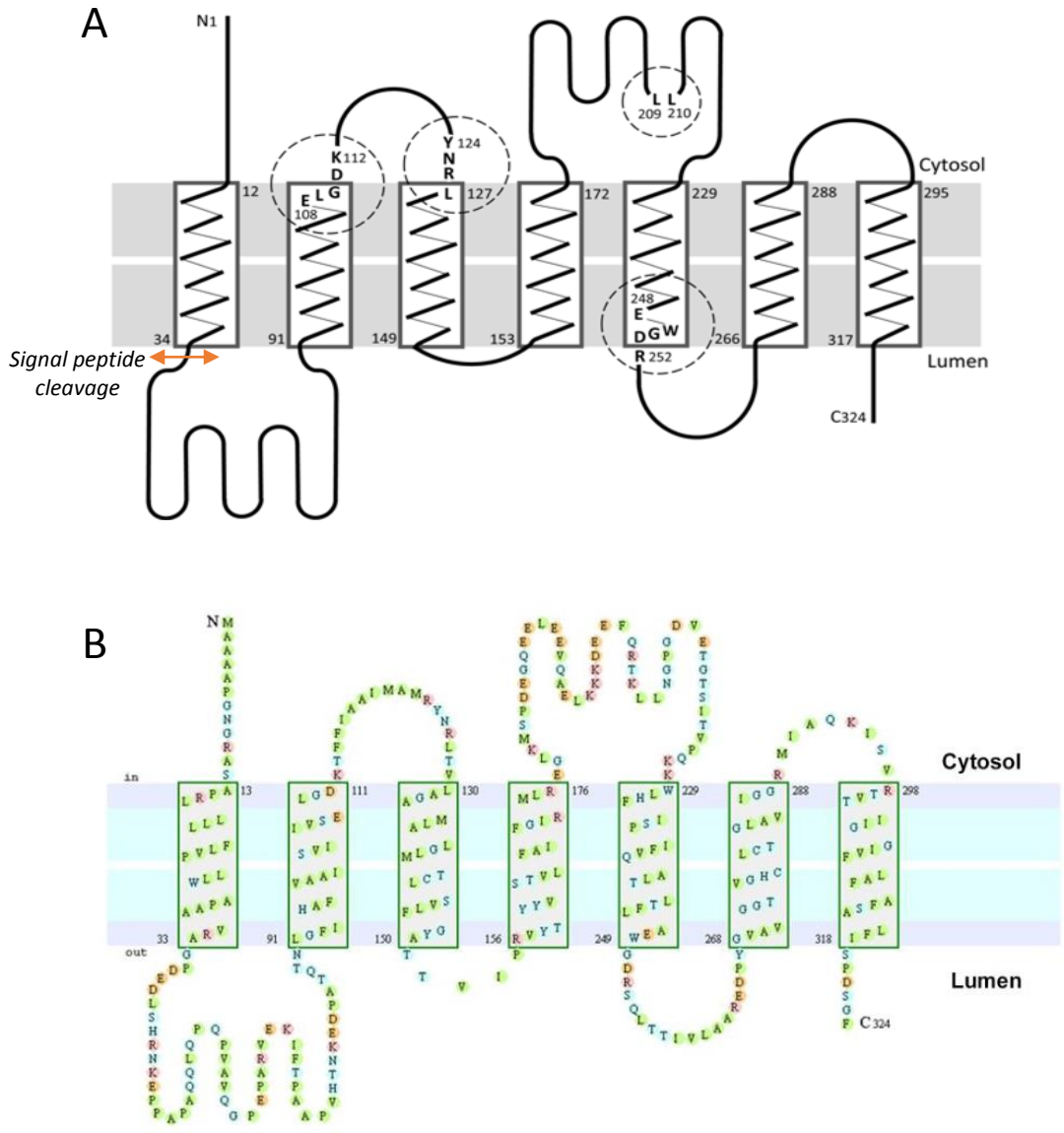

Figure 29. TMEM165 full sequence, topology and conserved domains (A) Prediction of TMEM165 topology and his conserved domains. Dulary, Potelle *et al.,* 2016. (B) TMEM165 full protein sequence (Foulquier *et al.,* 2012).

- A huge central hydrophilic loop, with a lot of acidic amino acids, especially glutamic acids (E). Structural prediction have shown that this loop is organized as a coiled-coil domain, suggesting that the loop is likely involved in protein/protein interactions and/or folding.

Apart from these domains that are conserved in the UPF0016 family, TMEM165 possesses other specific domains:

- A $Y_{124}NRL_{127}$ sequence, located in the first small cytoplasmic loop. This sequence belongs to the YXXΦ consensus sequence described as a sorting motif for lysosomal targeting [286]. Therefore, TMEM165 is able to be sorted at the TGN to be targeted to lysosomes.

- A $L_{209}L_{210}$ sequence in the central hydrophilic loop, originally thought to be another lysosomal targeting signal. Indeed, [DE]XXXL[LI] motif was described as a non-canonical lysosomal targeting signal but for TMEM165, the number of residues between D and LL is actually higher than the motif described. It has been shown that mutations in this motif did not alter TMEM165 localization [285]. This motif is thus not a lysosomal targeting sequence.

6.2.3. TMEM165 orthologs

As described before, TMEM165 is a well conserved protein throughout evolution thus strongly suggesting that TMEM165 function is crucial and ancient. Although a lot of orthologs can be found in databases, only few are studied in details.

TMEM165 mouse ortholog is a 323 amino acid protein with 92% identity with human TMEM165. Zebrafish *tmem165* is predicted to encode a 305 amino acids protein with 79% identity to human TMEM165. A mouse and a zebrafish model to study TMEM165 function exist and will be discussed later in section 6.3.4.

6.2.3.1. PAM71

the UPF0016 protein family in *Arabidopsis thaliana* comprises five members, with PAM71 (Photosynthesis Affected Mutant 71) sharing the most identity with human TMEM165 [287,288]. PAM71 is composed of 370 amino acids and shares 30% identity with its human counterpart.

Besides, PAM71 has been localized to the thylakoid membranes of the chloroplast. PAM71 deletion in *Arabidopsis thaliana* affects the photosystem II of the Oxygen Evolving Complex (OEC) and therefore the light dependent photosynthesis [288]. PAM71 mutants present a disturbance in the Ca2+/Mn2+ partitioning in chloroplasts. Indeed, using radioisotopes (^{45}Ca2+ and ^{54}Mn2+) and intact chloroplasts from WT and PAM71 mutants, authors have measured the amount of radioactivity found in the lumen of thylakoids after Mn2+ or Ca2+ uptake during illumination. They observed that PAM71 mutant thylakoids accumulated about 70% of Ca2+, while only 30% for the WT. On the opposite, that PAM71 mutant thylakoids accumulated about 58% of Mn2+, while more than 80% for the WT. These results show that in absence of PAM71, Ca2+ accumulates in the thylakoid lumen and Mn2+ in the chloroplast stroma. Therefore, this suggests that PAM71 is a Ca2+/Mn2+ antiporter in the thylakoid membrane that imports Mn2+ from the stroma into the thylakoid lumen and exports Ca2+ from the thylakoid lumen to the chloroplast stroma.

Moreover, photosynthesis defects observed in the PAM71 mutant have been shown to be primarily due to Mn2+ deficiency, as Mn2+ supplementation restores the photosynthesis in PAM71 mutants. Therefore, PAM71 has been proposed to be mainly involved in Mn2+ tolerance.

In addition, PAM71 was stably expressed in a *pmr1Δ* yeast strain. Pmr1p is a Golgi Ca2+/Mn2+ATPase that pumps Ca2+ and Mn2+ from the cytosol into the Golgi, and when Pmr1p is defective, yeast cells are more sensitive to high concentrations of Mn2+. Interestingly, PAM71 expression in *pmr1Δ* yeast strain suppressed this sensitivity to high Mn2+ concentrations, thus reinforcing the role of PAM71 in Mn2+ tolerance. The role of PAM71 in Mn2+ homeostasis makes sense since Mn2+ is required in the thylakoid lumen to build up the inorganic Mn_4CaO_5 cluster, which is the catalytic center for water oxidation crucial for the Oxygen Evolving Complex. In conclusion, PAM71 is an integral thylakoid membrane protein that is involved in manganese uptake into the thylakoid lumen.

6.2.3.2. synPAM71

Following the work on PAM71, Gandini and others published a study on synPAM71, the PAM71 ortholog in a cyanobacteria strain named *Synechocystis sp. PCC6803* [289,290]. They observed that ΔSynPAM71 strain displays a Mn-sensitive phenotype and a defect in photosystem II. They

also demonstrated that loss of SynPAM71 induced symptoms of Mn toxicity and thus proposed that SynPAM71 is a putative Mn exporter localised at the plasma membrane of *Synechocystis*.

6.2.3.3. Gdt1p

One of the most studied TMEM165 ortholog is the yeast protein Gdt1p (Gcr1 dependent translation factor 1). Gdt1p is a 280 amino acid membrane protein sharing 38% identity with its human counterpart. Two major differences between TMEM165 and Gdt1p can be observed. Indeed, the first 55 amino acid residues containing the first transmembrane domain is absent in Gdt1p. Besides, whereas TMEM165 is mostly localized in late Golgi compartment (trans and TGN), Gdt1p localizes in the cis- and medial Golgi of yeast [283,291]. Gdt1p is thought to be involved in Ca2+ homeostasis at the Golgi level [291]. Indeed, it was demonstrated that gdt1Δ yeast cells display a strong growth defect when cultured in the presence of 700mM of $CaCl_2$. Patch-clamp experiments also showed that gdt1p is involved in the regulation of the Ca2+ uptake from the cytosol in a yeast strain deleted of Pmr1p, the Golgi Ca2+/Mn2+-ATPase known to be responsible for the Ca2+ supply in the secretory pathway. Besides, Colinet and collaborators have recently shown that acidic conversed residues of the conserved motifs in Gdt1p are required for the calcium transport [292]. In addition to putatively regulate Ca2+ homeostasis, Gdt1p was reported to be likely involved in Golgi pH homeostasis. To support this hypothesis, authors have demonstrated a pH dependent Ca2+ uptake activity using a heterologous expression of Gdt1p in *Lactococus lactis* [293].

6.3. TMEM165-CDG

In 2012, *TMEM165* was identified as a gene involved in a new subgroup of CDG [113] (MIM #614727). To date, 6 patients have been reported as TMEM165-CDG. They all present a type-II serotransferrin isoelectrofocalisation pattern.

6.3.1. Clinical presentation

As described before, CDG phenotype are diverse and most of the time non-specific. TMEM165-CDG patients present a broad range of clinical features. Some of them are found in most of the CDG, for example growth retardation, dysmorphy and failure to thrive. Among the first five TMEM165-CDG patient described, four of them present a major skeletal dysplasia (spondyloepimetaphyseal dysplasia) with spine curvature, joint laxity and short stature. This

skeletal phenotype is a key feature of TMEM165-CDG, as it is not found in other CDG described to date [294]. The last reported patient did not show any clear skeletal abnormalities. However, this patient died at the age of 5 months due to complications and we can presumably think that he was too young to develop a strong skeletal dysplasia [295].

6.3.2. Patient mutations overview

4 different mutations have been found among the 6 reported patients. These mutations are reported in table 6 and their localization on the protein are shown in Figure 30. The first mutation presented in the table is found in three different patients. Two of them are siblings, one is now 24 years old and the other one died at the age of 14 months. The third patient is unrelated to the other two patients and is 9 years old. This mutation causes the activation of a cryptic splice donor site as indicated in table 7, which leads to the production of two different transcripts: the wild-type one and an additional one resulting in the replacement of exon 4 with a 117 bp intronic sequence. If translated, this transcript would lead to a protein shortened by 94 aa and with 27 aa changed at the C-terminus. The three other mutations are missense mutations leading to point mutation on the protein.

Table 6. TMEM165-CDG patient mutations.

Mutations	Type of mutation	TMEM165 protein changes	number of patients	reference
c.792+182G>A	homozygous, activation of a cryptic splice donor site	production of two different protein: the wild-type one and a truncated protein with a 27 aa change at the C-terminal part	3	Foulquier *et al.,* 2012
c.377G>A	homozygous, missense mutation	p.Arg126His	1	Foulquier *et al.,* 2012
c.377C>T and c.910G>A	compound heterozygous, 2 missense mutations	p.Arg126Cys + p.Gly304Arg	1	Foulquier *et al.,* 2012
c.323A>G	homozygous, missense mutation	p.Glu108Gly	1	Althoff *et al.,* 2015

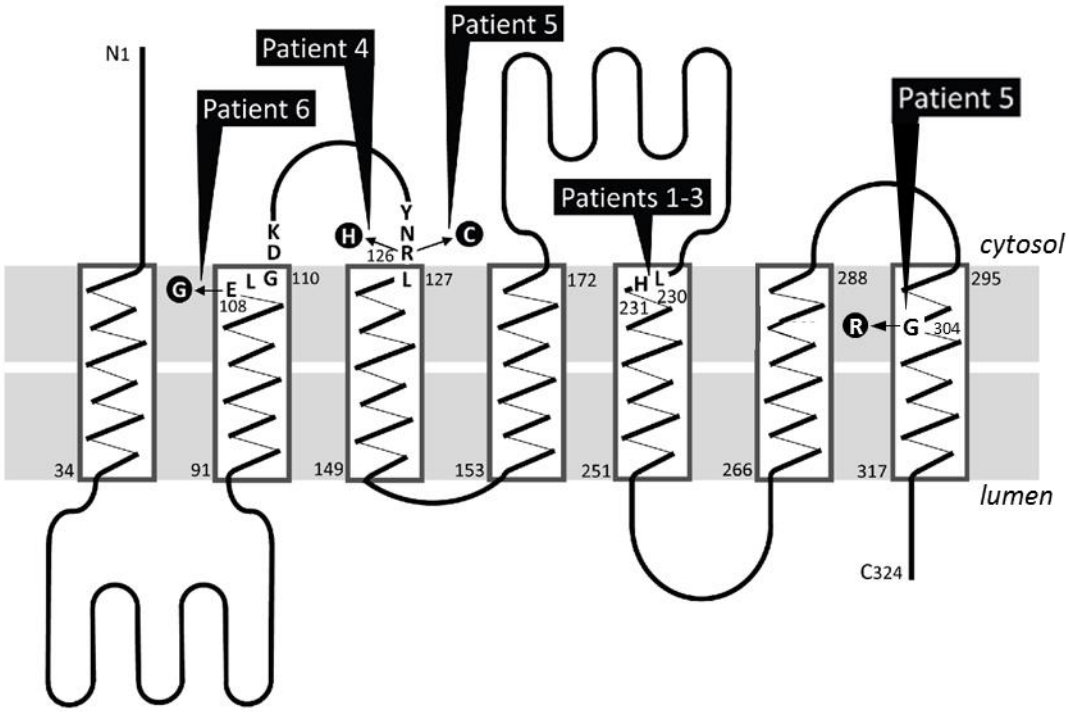

Figure 30. Predicted transmembrane TMEM165 topology showing the protein mutations identified in the six TMEM165-CDG patients discovered so far. The seven predicted transmembrane helices are mapped in rectangles spanning the membrane (in gray). Numbers indicate the positions of amino acid residues on the predicted topology model. The topology model was predicted using the TMHMM v2.0 server tool. From Dulary, Potelle *et al.,* 2016.

6.3.3. Cellular phenotype

In these TMEM165-CDG patients, TMEM165 protein expression is either almost totally abolished (first mutation) or strongly reduced (all the other mutations). However, TMEM165 Golgi localization is not altered. Nevertheless, patients skin fibroblasts present a dilated Golgi apparatus and a fragmented TGN [113]. Besides, an overall overacidification of their endosomes and lysosomes was observed [112].

Golgi glycosylation analyses were performed in patient serum and skin fibroblasts. N-glycosylation analysis revealed a defect in Golgi glycosylation maturation and notably a galactosylation defect and an increase of high-mannose type N-glycans [113,295,296]. O-glycan analyses revealed no major O-glycosylation defects, although Xia and collaborators observed an increase of T antigen (Galβ-1,3-GalNAcα-Ser/Thr) and a decrease of ST antigen (Siaα-2,3-Galβ-1,3-GalNAcα-Ser/Thr) [113,296]. No differences in the ApoC-III migration profile compared to control fibroblasts was observed [113]. No glycosaminoglycans nor glycolipids analysis on patient fibroblasts were performed.

6.3.4. TMEM165-CDG animal models

6.3.4.1. Zebrafish (*Danio rerio*) model

A *tmem165* homolog exists in zebrafish with 35% identity at the nucleotide level compared to human *TMEM165*. Zebrafish *tmem165* is predicted to encode a protein with 79% identity to human TMEM165. The zebrafish protein is predicted to have the same amount of TMD as the human counterpart, and the highly conserved motifs are identical to the human one (ELGDK, EWGDR and YNRL). Besides, tmem165 expression is constant during early development. Therefore, authors have recently developed a tmem165 deficient zebrafish model using a morpholino based approach to reduce tmem165 levels [297].

Morphants embryos appear normal during the first 2 days of development. After 3 days post-fertilization (dpf), morphants appear 8% shorter than WT embryos. They also present a misshapen head and abnormalities in the ventral jaw structures. 87% of the TMEM165 morphants presented a misshapen and slightly retracted Meckel's cartilage, and ceratohyal cartilages were inversely positioned relative to each other (Figure 31). Besides, cartilage were 30% shorter and contained 41% less cells than in the WT embryos. In conclusion, tmem165 morphants present strong alterations in craniofacial morphology.

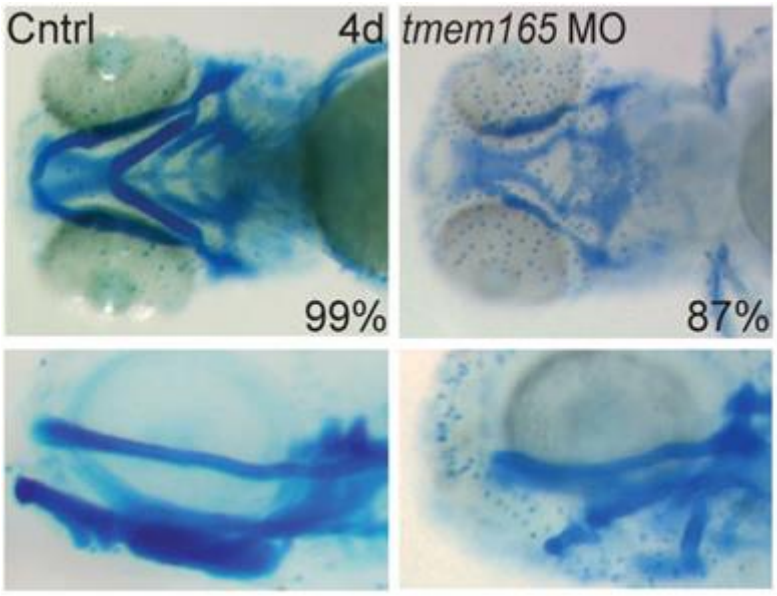

Figure 31. Inhibition of tmem165 expression in zebrafish embryos results in defects in cartilage morphogenesis. Ventral (top panels) and lateral (bottom panels) views of 4 dpf control and tmem165 morphant embryos stained with Alcian Blue revealed altered size and shape of Meckel's cartilage, as well as the palatoquadrate and ceratohyal cartilages. Bammens *et al.*, 2015.

Moreover, 71% of the morphants have a reduced staining, pointing to a decreased CS proteoglycans expression in Meckel's and ceratohyal cartilage. In addition, they observed that CS proteoglycans have smaller GAG chains in morphants compared to control.

They also visualized chondrocyte differentiation using in-situ hybridization (ISH) to measure the expression of several markers:

- Type II collagen (col2a1a), a marker of early differentiation
- Aggrecan, a marker of intermediate differentiation
- Sox9, a transcription factor known to inhibit later stages of chondrocyte differentiation

Interestingly, they observed at 4dpf an increase of col2a1a, a decrease of aggrecan and an increase of sox9. In conclusion, this abnormal cartilage morphology revealed a disruption in chondrogenic maturation program.

Authors have also measured osteoblasts differentiation using type X collagen (col10a1), a marker highly expressed in osteoblasts. Col10a1 was almost undetectable in several morphant structures (dermal parasphenoid and opercle bones). They also showed that osterix, an osteoblast maturation factor, was strongly reduced in multiple morphant structures. Altogether, these results show a problem in osteoblasts differentiation in addition to the chondrocyte differentiation defect. Therefore, TMEM165 seems to reduce bone formation by disrupting osteoblasts maturation. In addition, alizarin red staining revealed a decrease in calcium deposit in bones.

Finally, authors have also analysed N-glycosylation of the morphants compared to control at 4dpf. The total amount of N-glycan was slightly decreased in morphants. They also present a decrease in high mannose trimmed N-glycans, a decrease in $Man_3GlcNAc_3$ and a reduced levels of a broad range of complex N-glycans with or without fucose. Despite the clear skeletal phenotype, the glycosylation defect seems light compared to human. In addition, no differences in O-linked glycans were observed.

To sum up, authors have developed the first TMEM165-CDG animal model that mirrors the morphological and most biochemical phenotypes observed in patients.

6.3.4.2. Mouse (*Mus musculus*) model

A C57BL/6 TMEM165 +/lacz mouse model is available online in the Infrafrontier website (EMMA strain number 05166). These mice harboured only one Tmem165lacz null allele. They displayed an increased mean corpuscular volume and a slightly abnormal iris morphology. No skeletal defects were observed. Therefore, these mice need to be crossed to produce embryos respectively designated as wild-type controls (Tmem165+/+), heterozygous (Tmem165+/-), or homozygous (Tmem165-/-).

6.4. TMEM165 functions

As presented before, TMEM165 belongs to the UPF0016 family whose members are thought to be cation exchangers. In addition, the antiparallel orientation of the ELGDK and EWGDR motifs tend to suggest that TMEM165 is a cation antiporter. In addition to the predicted functions of TMEM165 deduced from the analyses of the protein primary sequence, several early experiments led to hypotheses about TMEM165 functions. It was then proposed that TMEM165 was a putative Ca2+/H+ antiporter, able to import Ca2+ in exchange for intraluminal Golgi protons (Figure 32).

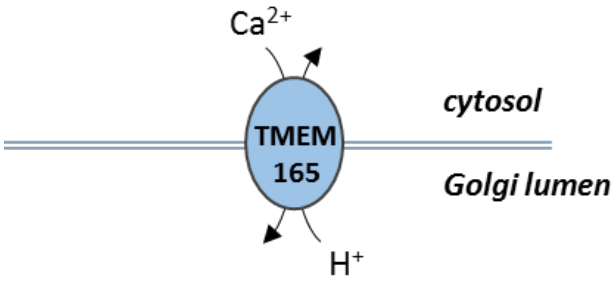

Figure 32. TMEM165 putative model as a Ca2+/H+ antiporter. At the beginning of my PhD, TMEM165 was thought to be able to import cytosolic Ca2+ into the Golgi lumen and to export H+ from the Golgi lumen to the cytosol.

However, although TMEM165 orthologs PAM71 and synPAM71 were recently shown to be linked to Mn2+ homeostasis, no experiments have been performed to address the role of TMEM165 in Mn2+ homeostasis.

6.4.1. Insights into the role of TMEM165 in Ca2+ homeostasis

The possible involvement of TMEM165 in Ca2+ homeostasis originated from studies on gdt1p, the yeast ortholog. Indeed, authors have shown that gdt1p was involved in Ca2+ uptake [291]. Moreover, it was demonstrated that gdt1Δ yeast cells display a strong growth defect when cultured in the presence of 500-700mM of $CaCl_2$. Interestingly, expressing a truncated version of

TMEM165, lacking the first 55 amino acid residues that are absent in yeast gdt1p, partially restored yeast growth in presence of high calcium concentrations. Based on these results, it was suggested that TMEM165 and gdt1p have similar functions in their respective organisms, and that both are involved in Ca2+ homeostasis at the Golgi level where they are localised.

In addition, authors have overexpressed TMEM165 tagged with Red Fluorescent Protein (RFP) in HeLa cells. They showed that a fraction of the total TMEM165-RFP was localized to the plasma membrane after overexpression. Then, they performed whole-cell patch-clamp analyses and observed that TMEM165 was linked to ion transport and probably Ca2+ since the addition of EGTA decreased plasma membrane current. Moreover, using Fura2 as a cytosolic calcium probe, they observed that thapsigargin-induced Ca2+ release was reduced in cells overexpressing TMEM165, showing that TMEM165 was also involved in cytosolic calcium homeostasis [291].

Finally, it was recently shown that TMEM165 expression increased during lactation [298]. Indeed, TMEM165 expression increased in mouse mammary tissues several days before parturition and reached the maximal level of expression during the two weeks after parturition. Since Ca2+ concentration can reach up to 80mM in milk, the cellular Ca2+ homeostasis during lactation must therefore be even more controlled to avoid any Ca2+ toxicity. The increased level of expression of TMEM165 during lactation thus suggests a role in the maintenance of Ca2+ homeostasis in such condition.

6.4.2. Insights into the role of TMEM165 in H+ homeostasis

Several experiments supported a role of TMEM165 in H+ homeostasis. First, deficiency or absence of TMEM165 was shown to decrease the pH of endosomal and lysosomal compartments [291]. Indeed, authors have shown using lysosensor green DND189 that lysosomal pH became more acidic in 3 out the 5 TMEM165-CDG patient fibroblasts and in HeLa siTMEM165 cells. However, no link between TMEM165 and Golgi H+ homeostasis was demonstrated.

The expression pattern of TMEM165 during lactation is also a clue for its role in H+ homeostasis. Indeed, during lactation, the synthesis of lactose in the mammary gland involves the formation of two H+ in the Golgi apparatus. The first one is created during the transfer of Gal onto Glc, and the second one is generated during the hydrolysis of UDP from UDP-gal to UMP and Pi. Besides, since the concentration of lactose in milk can reach up to 100 mM, the number of protons

generated is incredibly high. Moreover, as explained in the chapter 3, there is no Golgi H+ leak channel deciphered to date. Therefore, TMEM165 could play this role as a H+ leak channel to get rid of the accumulation of H+ in the Golgi, especially when the glycosylation rate is high for example during lactation.

OBJECTIVES OF THE PHD PROJECT

The recent discovery of TMEM165-CDG patients added a new layer of complexity both to the field of Golgi glycosylation and to the research on CDG. Despite the intensive work done by our lab and others, a lot of unanswered questions remain and need to be addressed: what is the link between TMEM165 and glycosylation? How does TMEM165 deficiency affect Golgi glycosylation? What is the contribution of TMEM165 in Golgi homeostasis? What are the cellular and molecular functions of TMEM165?

While it is tempting to hypothesize that modifications of the Golgi Ca2+ and pH homeostasis could explain the glycosylation defects observed in TMEM165-deficient patients, the molecular mechanisms by which TMEM165 defects affect Golgi glycosylation is absolutely not known so far.

Thus, **the first and main objective** of my thesis is to decipher the molecular mechanisms leading to a glycosylation defect in TMEM165-CDG patients.

The second objective aims at characterizing the cellular and molecular functions of TMEM165. We will assess TMEM165 contribution to the overall Golgi ionic homeostasis. Moreover, there is no direct evidence that TMEM165 is indeed an ion transporter.

As a whole, this project aims at deciphering the role(s) of TMEM165 in Golgi glycosylation and potentially provide therapeutic targets for TMEM165-CDG patients. Besides, understanding the molecular mechanisms of CDG due to homeostasis defects will potentially lead to many novel breakthroughs regarding Golgi glycosylation regulation.

RESULTS

[1] GLYCOSYLATION ABNORMALITIES IN GDT1P/TMEM165 DEFICIENT CELLS RESULT FROM A DEFECT IN GOLGI MANGANESE HOMEOSTASIS

1.1. Introduction

In 2012, Foulquier and collaborators reported a novel type of CDG due to Golgi homeostasis disturbances: TMEM165-CDG [113] (OMIM entry #614727). The affected patients present a broad range of clinical features, including growth retardation, dysmorphism and failure to thrive, which are frequent symptoms in CDG. They also present the key feature of TMEM165-CDG, which is a major skeletal dysplasia (spondyloepimetaphyseal dysplasia) with spine curvature, joint laxity and short stature.

At the cellular level, patient skin fibroblasts displayed a dilated Golgi apparatus, a fragmented TGN and an overall overacidification of their endosomes and lysosomes. TMEM165-CDG patients displayed a type II serotransferrin pattern and a slight sialylation and galactosylation defect on their N-glycans from sera.

Proposed to be a Golgi Ca2+/H+ exchanger able to catch cytoplasmic calcium and to release Golgi intraluminal protons, the function of TMEM165 was however not yet deciphered. Therefore, TMEM165 was a new actor in Golgi glycosylation but its precise cellular and molecular roles were not yet known.

However, authors did not exhaustively analysed the glycosylation in TMEM165-CDG patients. Besides, although they suggested that TMEM165 deficiencies could disrupt pH homeostasis thus leading to glycosylation defects, they were unable to directly prove the link between TMEM165 deficiency and the glycosylation defect. Therefore, the goal of this first study was to understand and fully characterize the glycosylation defect observed in TMEM165-CDG patients. A lot of unanswered questions also remains to be elucidated: what is the link between TMEM165 and glycosylation? How does TMEM165 deficiency affect Golgi glycosylation? What is the contribution of TMEM165 in Golgi homeostasis? What are the cellular and molecular functions of TMEM165?

To try to address all these issues, we have used different cell models. First, we took advantage of the yeast model, routinely used in our lab. There is indeed a TMEM165 ortholog in yeast named

gdt1p and yeast model has always been a valuable tool to study glycosylation. To study yeast N-glycosylation, we have used a peculiar glycoprotein named invertase. There are 2 types of invertase: one is constitutive, cytosolic and not glycosylated; the other one is secreted and extensively N-glycosylated. Since N-glycosylation is the only PTM carried by the secreted invertase, this protein is a good reporter of Golgi N-glycosylation efficiency *in vivo.* The method consists in doing a zymogram of invertase in native gel that will reflect the glycosylation of the secreted invertase. We will use wild-type (WT), strain deleted of *GDT1 (gdt1Δ*), *PMR1* (*pmr1Δ*) or both *(gdt1Δpmr1Δ*) in this study. Pmr1p is a Ca2+/Mn2+ Golgi ATPase and the ortholog of human SPCA1. *Pmr1Δ* yeast strain has already been well characterized in the literature and shows growth defect in Ca2+ depleted media. *Pmr1Δ* growth defect in absence of Ca2+ can be alleviated by Ca2+ supplementation. Besides, a strong glycosylation defect on invertase was also observed in *pmr1Δ* yeast strain, which can be normalised by Mn2+ supplementation.

To fully characterize the glycosylation defect in TMEM165-CDG patients, it is tempting to use the available patient skin fibroblasts. However, only five patients were available at that time, and they are very heterogeneous in terms of clinical and cellular phenotype. They have a different genetic background, carry different TMEM165 mutations and the expression level of TMEM165 is variable among patients, making these fibroblasts not a reliable model to establish the link between TMEM165 deficiency and glycosylation. Therefore we had to generate mammalian stable cell lines depleted in TMEM165 for the study. We then transfected HeLa and HEK293 cells with the pGIPZ Lentiviral shRNA plasmid (Thermo Scientific) containing either shRNA sequences targeting TMEM165 mRNA or no sequences. Selection was done with puromycine 3µg/mL to get rid of cells that have not got inserted the plasmide in their genome. We then stopped the selection and measured TMEM165 expression in the newly generated polyclonal cell lines.

To study glycosylation in mammalian cells, two different approaches were applied. The first one consists in analysing the migration profile in western-blot of LAMP2 (Lysosomal-Associated Membrane Protein 2) and TGN46 (Trans-Golgi Network protein 46), two heavily glycosylated proteins. Although these proteins are classically used to analyse the N-glycosylation, it is important to note that:

- LAMP2 has 16 N-glycosylation sites and 10 O-glycosylation sites
- TGN46 has 9 N-glycosylation sites and 13 O-glycosylation sites.

This approach remains qualitative but has the advantage to be easyly performed. The second approach more relies on mass spectrometry of total N-glycans extracted from cells. This method is quantitative and gives us data about N-glycan structures differences.

Finally, we have assessed Golgi Mn2+ homeostasis in our cells. To do so, we took advantage of the Golgi protein GPP130 that is known to be a specific Golgi Mn2+ sensor [299]. In mammalian cell lines, it has been shown by several authors that the stability of GPP130 was strictly dependent on Golgi Mn2+ concentration. Indeed, in the presence of 500µM MnCl2, GPP130 was shown to be targeted to lysosomal degradation via a Rab7 dependent mechanism. Besides, GPP130 lumenal stem domain has been shown to be required for this Mn2+ induced degradation, showing that GPP130 strictly responds to Golgi Mn2+ changes.

1.2. Publication

Glycosylation abnormalities in Gdt1p/TMEM165 deficient cells result from a defect in Golgi manganese homeostasis

Sven Potelle[1], Willy Morelle[1], Eudoxie Dulary[1], Sandrine Duvet[1], Dorothée Vicogne[1], Corentin Spriet[1], Marie-Ange Krzewinski-Recchi[1], Pierre Morsomme[2], Jaak Jaeken[3], Gert Matthijs[4], Geoffroy de Bettignies[1] and François Foulquier[1*]

[1] Univ. Lille, CNRS, UMR 8576 – UGSF - Unité de Glycobiologie Structurale et Fonctionnelle, F-59000 Lille, France

[2] Institut des Sciences de la Vie, Université Catholique de Louvain, B-1348, Louvain-la-Neuve, Belgium

[3] Center for Metabolic Diseases, University Hospital Gasthuisberg, KU Leuven, Belgium

[4] Center for Human Genetics, KU Leuven, Leuven, Belgium

*Address correspondence should be sent to: François Foulquier (francois.foulquier@univ-lille1.fr)

Address: Univ. Lille, CNRS, UMR 8576 – UGSF - Unité de Glycobiologie Structurale et Fonctionnelle, F-59000 Lille, France

Tel. + 33 3 20 43 44 30

Fax. +33 3 20 43 65 55

E-mail. Francois.foulquier@univ-lille1.fr

Abstract

Congenital disorders of glycosylation (CDG) are severe inherited diseases in which aberrant protein glycosylation is a hallmark. From this genetically and clinically heterogeneous group, a significant subgroup due to Golgi homeostasis defects is emerging. We previously identified TMEM165 as a Golgi protein involved in CDG. Extremely conserved in the eukaryotic reign, the molecular mechanism by which TMEM165 deficiencies lead to Golgi glycosylation abnormalities is enigmatic. As *GDT1* is the ortholog of *TMEM165* in yeast, both *gdt1Δ* null mutant yeasts and *TMEM165* depleted cells were used. We highlighted that the observed Golgi glycosylation defects due to Gdt1p/TMEM165 deficiency result from Golgi manganese homeostasis defect. We discovered that in both yeasts and mammalian Gdt1p/TMEM165 deficient cells, Mn2+ supplementation could restore a normal glycosylation. We also showed that the GPP130 Mn2+ sensitivity was altered in *TMEM165* depleted cells. This study not only provides novel insights into the molecular causes of glycosylation defects observed in TMEM165-deficient cells but also suggest that TMEM165 is a key determinant for the regulation of Golgi Mn2+ homeostasis.

Introduction

Congenital Disorders of Glycosylation (CDG) are a rapidly growing disease family due to genetic defects of protein and lipid glycosylation [1–4]. In protein N-glycosylation, two different CDG groups can be distinguished. In CDG-I, the molecular defects affect the oligosaccharidic precursor assembly pathway in the endoplasmic reticulum, leading to the presence of unoccupied N-glycosylation sites. CDG-II are due to defects in the glycan processing in the Golgi, giving rise to the presence of abnormal glycan structures on glycoproteins [5,6]. To date, the CDG family comprises nearly hundred disorders [7]. Most are due to defects in the specific glycosylation machinery, such as SLC35A1 [MIM 605634], B4GALT1 [MIM 137060] and MGAT2 [MIM 602616]) [8–10]. However, in the CDG-II group, defects have lately been discovered in proteins that are not only involved in glycosylation but also in other cellular functions. Among these are CDG caused by altered vesicular Golgi trafficking and/or Golgi pH homeostasis marking a new era in the CDG field [11–16].

In 2012, we reported a novel disorder in this group namely TMEM165-CDG [17] (OMIM entry #614727). These patients present a peculiar phenotype including major skeletal dysplasia and hyposialylation and hypogalactosylation of N-glycosylproteins [17,18]. TMEM165 is a

transmembrane protein of 324 amino acids belonging to a well conserved but uncharacterized family of membrane proteins named UPF0016 (Uncharacterized Protein Family 0016; Pfam PF01169). We demonstrated that TMEM165 is a novel Golgi protein that can also be found in endocytic pathways (late endosomes and lysosomes) [19]. We indirectly demonstrated that defects in TMEM165 affect both cytosolic Ca2+ and lysosomal pH homeostasis [20]. Based on these results, we then hypothesized that TMEM165 could be a Golgi-localized Ca2+/H+ antiporter regulating both Golgi Ca2+ and pH homeostasis [20]. Extremely conserved in the eukaryotic reign, *GDT1* is the yeast ortholog of *TMEM165*. We showed that the *gdt1Δ* mutant presents a strong growth defect phenotype in presence of high concentrations of calcium chloride (500-700 mM). In yeast, the Ca2+ Golgi homeostasis mainly results from the activity of Pmr1p, a Golgi P-type ATPase essential to import Ca2+ but also Mn2+ in the Golgi lumen [21–23]. Its activity then maintains very low Ca2+ and Mn2+ concentrations into the cytosol. Interestingly, it has been shown that *PMR1* inactivation leads to strong Golgi glycosylation and trafficking defects [24].

The aim of this study is to decipher the molecular mechanism by which a lack of TMEM165 affects Golgi glycosylation. We used *gdt1* null mutant yeasts and TMEM165 depleted mammalian cells to unravel this mechanism, and present evidence that in both yeasts and mammalian cells, the Golgi glycosylation defects due to a lack of Gdt1p/TMEM165, result from defective Golgi manganese homeostasis.

RESULTS

Mn2+ suppresses the Golgi glycosylation defect of *gdt1Δ* null mutants cultured in presence of high Ca2+ concentrations

We previously reported that *gdt1Δ* null mutants presented a strong growth defect in the presence of high calcium chloride concentrations such as 700mM [25]. To assess whether this growth deficiency was correlated to an abnormal N-linked glycosylation, the gel mobility of secreted invertase, a protein exclusively N-glycosylated and thus a good reporter of Golgi N-glycosylation efficiency *in vivo* was analyzed in the absence and in the presence of increasing Ca2+ concentrations (fig. 1A). In yeast, pmr1p is a Golgi Ca2+/Mn2+ P-type ATPase that is involved in maintaining normal Golgi functions, such as glycosylation [21–23]. Thus, *Pmr1Δ*

strains, known to produce and secrete an aberrant form of invertase, lacking high mannose residues, were taken as positive controls throughout our experiments [21,23].

While invertase isolated from *pmr1Δ* strain migrates on native gels significantly faster than invertase isolated from a wild-type strain, no significant differences in the absence of Ca2+ were observed between *gdt1Δ* and wild type strains. Strikingly and in the presence of increasing Ca2+ concentrations, invertase secreted from *gdt1Δ* strain migrates faster. In wild type strains, increasing Ca2+ concentrations had no effects on invertase mobility (data not shown). As seen in other studies, the increased mobility observed in pmr1p mutant cells cultured in the absence of Ca2+ can partially be reversed in the presence of Ca2+ [22]. These data demonstrate that high environmental Ca2+ concentrations in *gdt1Δ* lead to strong N-glycosylation deficiencies while in *pmr1Δ*, the observed Golgi N-glycosylation defects are markedly restored by Ca2+.

In order to understand how high Ca2+ concentrations in *gdt1Δ* could lead to glycosylation abnormalities, we hypothesized that excess of Ca2+ might interfere with glycosylation processes requiring other metal ions including Mn2+ known to be a cofactor of certain Golgi glycosyltransferases [26]. To test this hypothesis, the invertase mobility was assessed by supplementing the culture medium with 1mM MnCl2 (fig. 1B). While this treatment does not affect the invertase mobility in wild type strain, Mn2+ treatment completely restores the increased invertase mobility in *gdt1Δ* strains cultured in presence of both Ca2+ and Mn2+. As previously reported, the Mn2+ supplementation in *pmr1Δ* mutant also greatly improves the invertase mobility [22]. This complementation is highly specific for Mn2+ as other tested ions do not rescue the glycosylation phenotype (supplementary figure 1). In order to understand the link between gdt1p and pmr1p, invertase mobility was analyzed in the *gdt1Δ*/*pmr1Δ* double knock-out. In normal conditions, the invertase mobility is strongly affected and very similar to the one observed in the *pmr1Δ* strains.

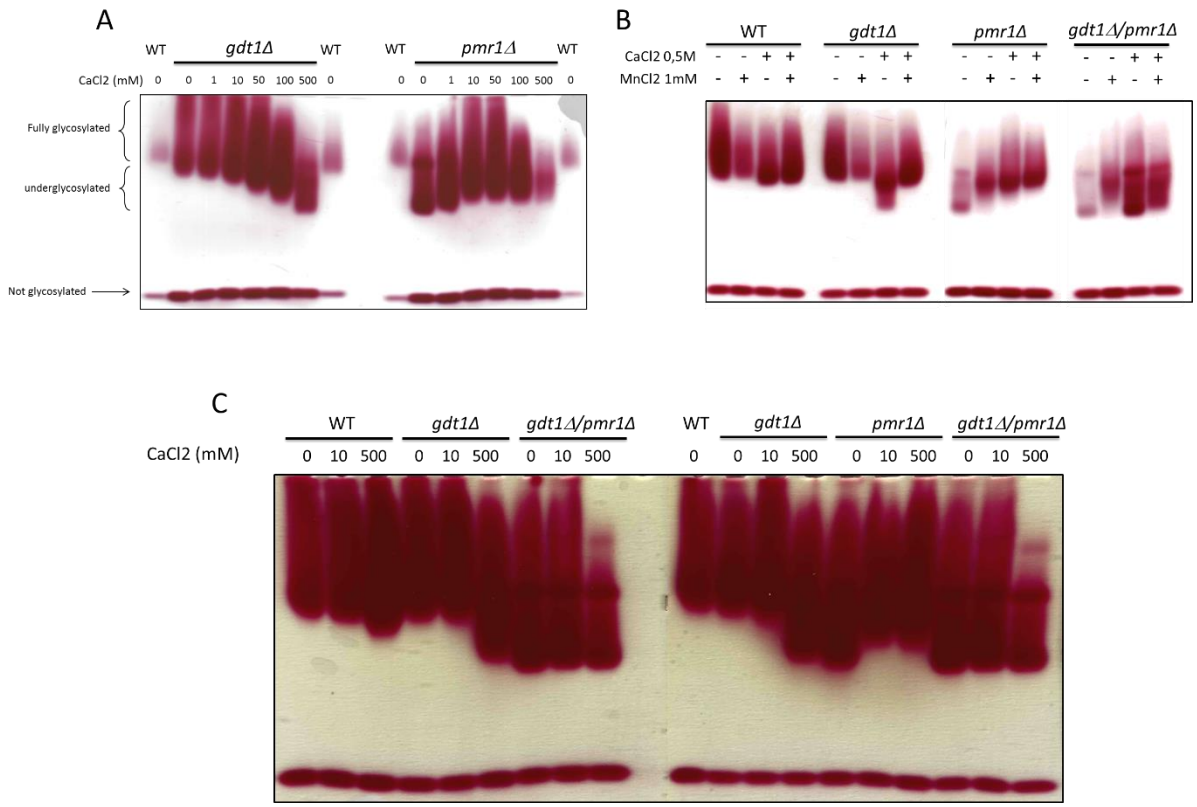

Figure 1: Mn2+ restores the Golgi glycosylation defect of *gdt1Δ* null mutants cultured in presence of high Ca2+ concentrations. (A) High Ca2+ concentrations strongly affect invertase glycosylation in *gdt1Δ* strains and partially suppresses the glycosylation defect in *pmr1Δ* strains. N-glycosylated invertase secreted by wild-type, *gdt1Δ* and *pmr1Δ* mutants with or without the addition of the indicated CaCl2 concentrations in the medium. **(B) Mn2+ suppresses the glycosylation defect of the *gdt1Δ* strains cultured with 0,5M CaCl2.** N-glycosylated invertase secreted by wild-type, *gdt1Δ* strains, *pmr1Δ* and *gdt1Δ/pmr1Δ* strains with or without the addition of 0,5M CaCl2, with or without the addition of Mn2+, or with the addition of both 0,5M Cacl2 and 1mM MnCl2. (C) gdt1p is involved in the suppression of the glycosylation defect in the *pmr1Δ* strains cultured in high Ca2+ concentration. N-glycosylated invertase secreted by wild-type, *gdt1Δ* strains, *and pmr1Δ* and *gdt1Δ/pmr1Δ* strains with or without the addition of 0,5M CaCl2 or 10mM CaCl2.

While Mn2+ slightly suppressed this Golgi N-glycosylation defect, Ca2+ did not. Very interestingly, this result seems to show that gdt1p is then crucial for the suppression of the glycosylation defect in the *pmr1Δ* strains supplemented with Ca2+. However, since 0,5M CaCl2 already leads to a strong invertase mobility defect in *gdt1Δ* strains, a 10mM CaCl2 concentration was used. In these conditions, no glycosylation defect was observed in *gdt1Δ* strains, while in *pmr1Δ* strains 10mM CaCl2 was sufficient to suppress the glycosylation defect (fig 1A and 1C). However, this low concentration was not sufficient to rescue the invertase mobility in the *gdt1Δ/pmr1Δ* double knock-out, demonstrating a crucial need for gdt1p in this rescue (fig 1C).

These unexpected findings not only demonstrate that the observed Golgi N-glycosylation defect in *gdt1Δ* strains cultured in the presence of high Ca2+ concentrations can be suppressed

by the addition of Mn2+ but also that gdt1p is directly involved in the suppression of the glycosylation defect in the *pmr1Δ* strains supplemented with Ca2+. Altogether, one can ask the role of gdt1p in Golgi Mn2+ homeostasis.

Golgi manganese homeostasis is modified in TMEM165 deficient cell line

In order to unravel the link between TMEM165, Golgi Mn2+ homeostasis and Golgi glycosylation defects, TMEM165 expression was depleted using shRNA strategy in HeLa and HEK 293 cells. In order to avoid the issue of clonal variation, polyclonal populations of stably-expressing cells were generated and used for the study. ShRNA depletion of TMEM165 in HeLa and HEK 293 cells was very efficient as 95% of TMEM165 was depleted compared to control cells (fig. 2A, 2C). This decrease was also confirmed by immunofluorescence staining. As shown in Fig 2B and 2D, TMEM165 is absent in TMEM165 depleted cells.

To then assess the Mn2+ Golgi homeostasis in TMEM165 depleted cells, we took advantage of the Golgi protein GPP130 that is known to be a specific Golgi Mn2+ sensor [27,28]. In mammalian cell lines, it has been shown by several authors that the stability of GPP130 was strictly dependent on Golgi Mn2+ concentration. In presence of 500µM MnCl2, GPP130 was shown to be targeted to lysosomal degradation via a Rab7 dependent mechanism [28]. The stability of GPP130 was studied with and without MnCl2 treatment by western blot and immunofluorescence in shTMEM165 HeLa and HEK293 cells (fig. 3 and 4). In accordance with the literature, we showed that the level of GPP130 was significantly reduced when control cells were cultured with Mn2+ (fig. 3A, 4A and quantification in 3B, 4B). Interestingly, this Mn2+-induced degradation is strongly delayed in TMEM165 depleted cells. Quantification indicated that GPP130 loss exceeded 60% in control HeLa cells after 4h Mn2+ treatment while only a 20% decrease is seen in shTMEM165 HeLa cells. We can notice that in HEK293 cells, the effects of Mn2+ on GPP130 stability are less pronounced as GPP130 loss exceeded only 40% in control HEK293 cells after 16h of Mn2+ treatment. Similarly to shTMEM165 HeLa cells, the Mn2+ treatment had no effects on GPP130 stability in shTMEM165 HEK293 cells. Immunofluorescence staining followed by confocal microscopy confirmed the western blot results for both HeLa and HEK293 cells (fig. 3C, 4C and quantification in fig. 3D, 4D). Altogether, these data highly suggest that the Golgi Mn2+ homeostasis is impaired in TMEM165 depleted cells.

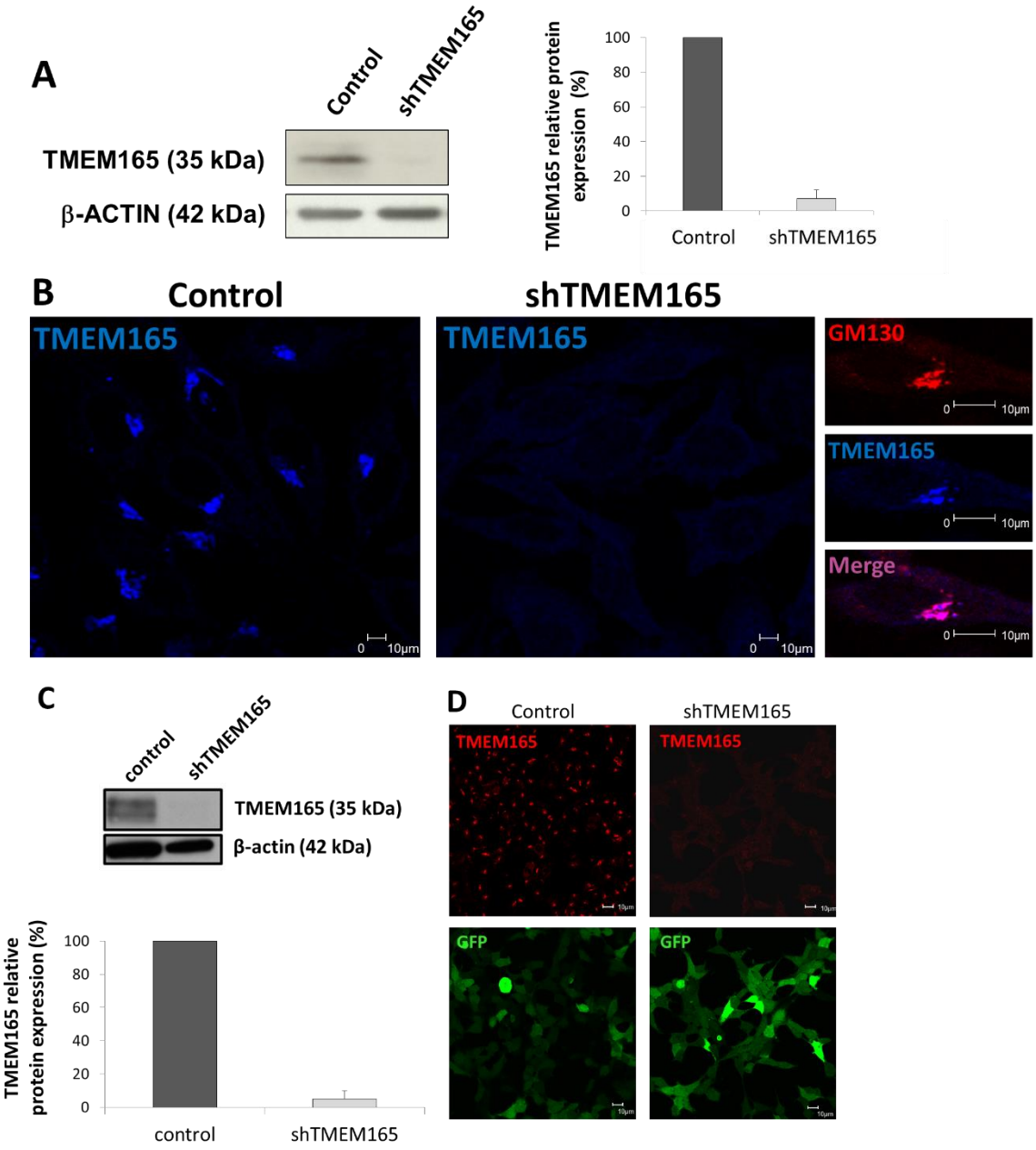

Figure 2: Generation and characterization of shTMEM165 HeLa and HEK293 cells. **(A)** Steady state cellular level of TMEM165. HeLa cells were mock (control) or depleted in TMEM165 (shTMEM165). Total cell lysates were prepared, subjected to SDS-PAGE and Western blot with the indicated antibodies. Right panel represents quantification of TMEM165. **(B)** Control and shTMEM165 HeLa cells were fixed and labeled with antibodies against TMEM165 and GM130 before confocal microscopy visualization. **(C)** Steady state cellular level of TMEM165. HEK293 cells were mock (control) or depleted in TMEM165 (shTMEM165). Total cell lysates were prepared, subjected to SDS-PAGE and Western blot with the indicated antibodies. Lower panel represents quantification of TMEM165. **(D)** Control and shTMEM165 HEK293 cells were fixed and labeled with antibodies against TMEM165 before confocal microscopy visualization. Lower panel shows the GFP, coded by the pGIPZ Lentiviral shRNA plasmid (Thermo Scientific) used for the generation of our cell lines.

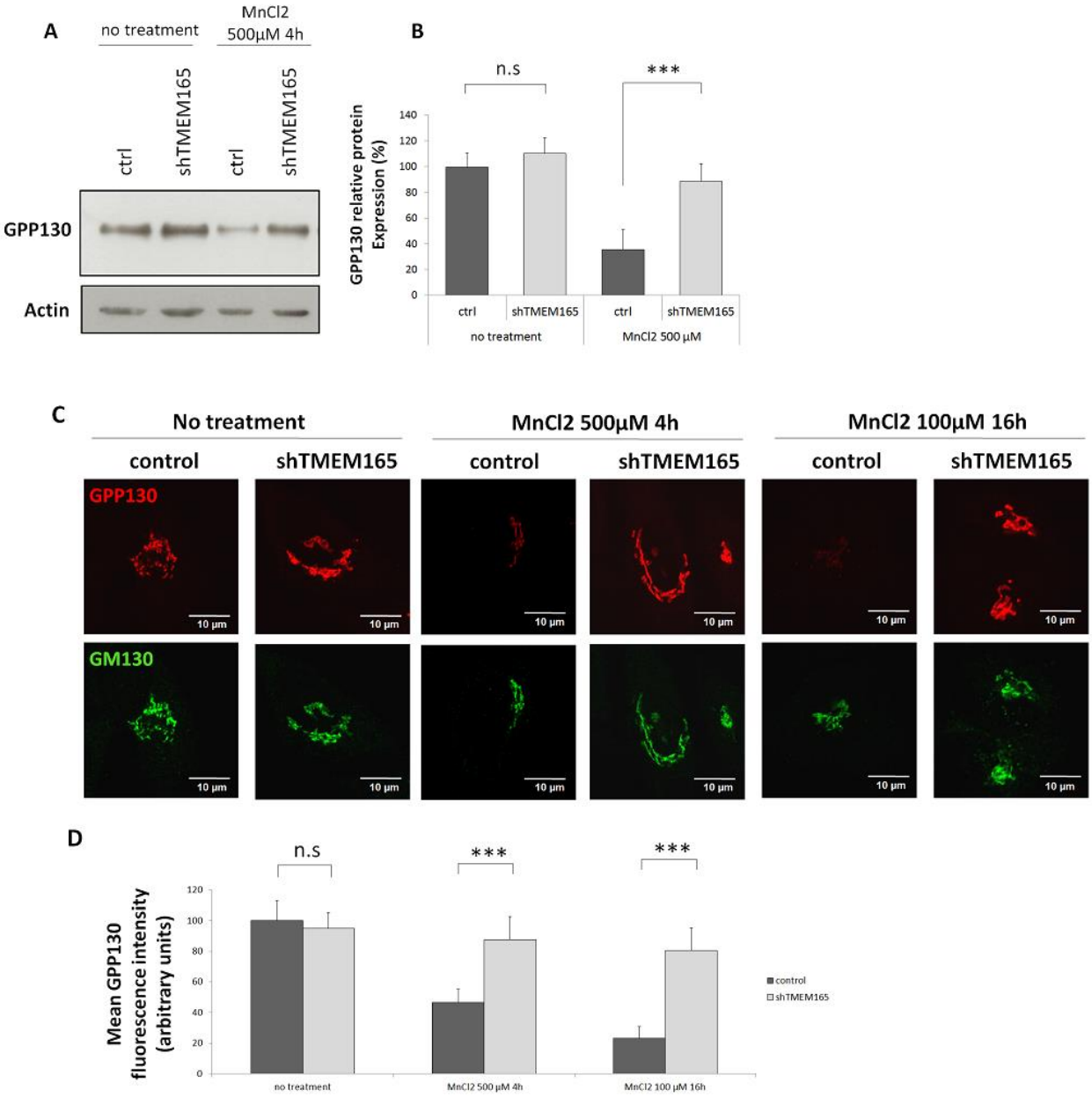

Figure 3. Mn2+ does not alter the stability of GPP130 in TMEM165 deficient HeLa cell lines (A) Steady state cellular level of GPP130. Control and shTMEM165 HeLa cells were treated or not with MnCl2 500 µM during 4h. Total cell lysates were prepared, subjected to SDS-PAGE and Western blot with the indicated antibodies. **(B)** Quantification of GPP130 protein after normalization with actin (N = 3; *** = P value < 0,001). **(C)** Control and shTMEM165 HeLa cells were incubated with MnCl2 500 µM during 4h or 100µM during 16h, fixed and labeled with antibodies against GPP130 (upper panels) and GM130 (lower panels) before confocal microscopy visualization. **(D)** Quantification of the associated GPP130 fluorescence intensity (Number of experiments (N) = 3; number of cells (n) = 50; *** = P value < 0,001).

As shown by Mukhopadhyay and collaborators, high concentrations of extracellular Mn2+ induces rapid redistribution of GPP130 in vesicles before their lysosomal degradation. As HeLa cells were shown to be more sensitive to Mn2+ treatment, we decided to investigate the differential impact of Mn2+ on the vesicular redistribution of GPP130 in shTMEM165 HeLa cells

compared to control cells. The redistribution of GPP130 was followed by immunofluorescence in response to different times of Mn2+ exposure (fig. 5). In the absence of Mn2+, GPP130 is Golgi localized in both control and shTMEM165 HeLa cells (fig. 5A and 5C).

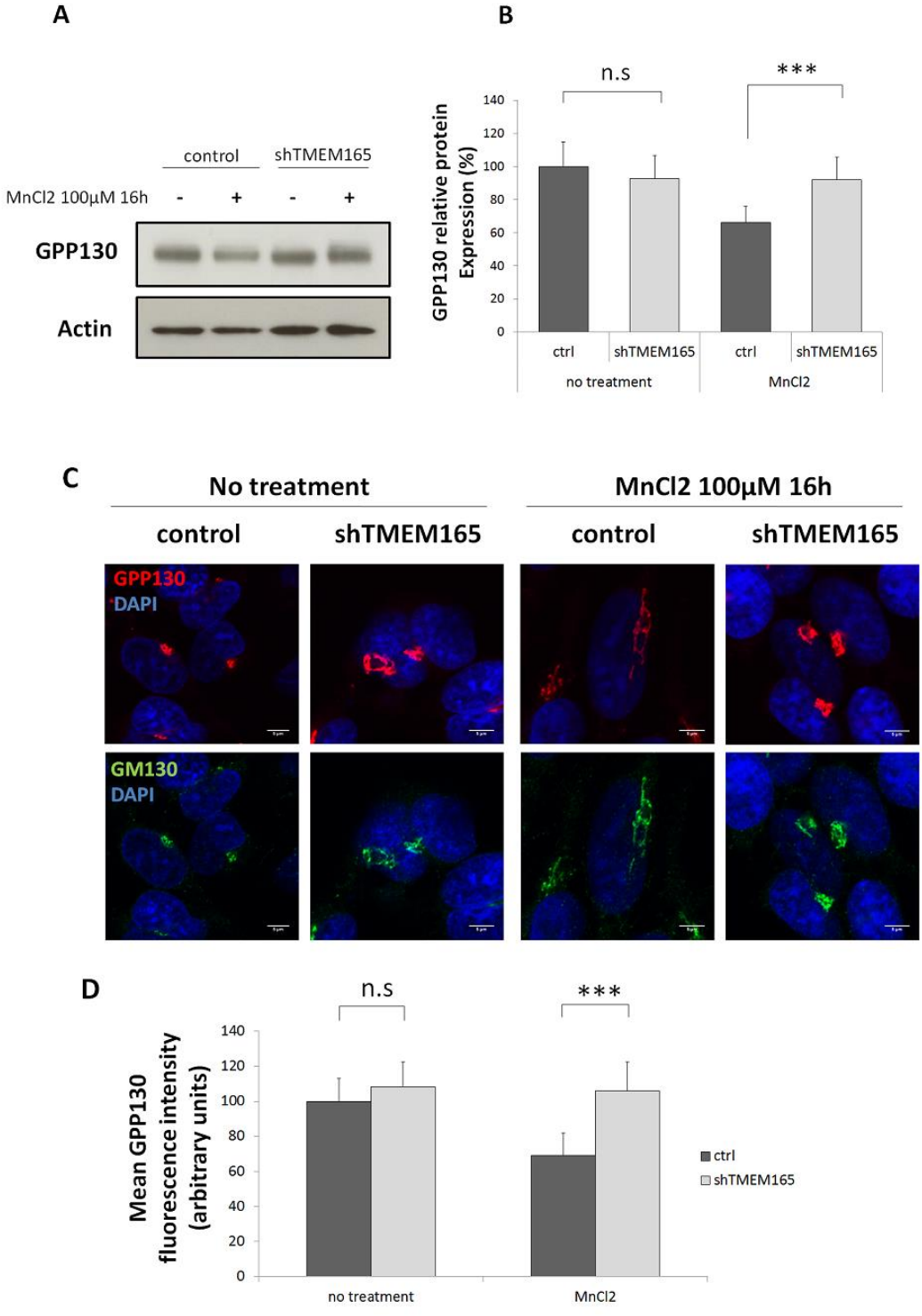

Figure 4. Mn2+ does not alter the stability of GPP130 in TMEM165 deficient HEK293 cell lines (A) Steady state cellular level of GPP130. Control and shTMEM165 HEK293 cells were treated or not with MnCl2 100 µM during 16h. Total cell lysates were prepared, subjected to SDS-PAGE and Western blot with the indicated antibodies. **(B)** Quantification of GPP130 protein after normalization with actin (N = 2; *** = P value < 0,001). **(C)** Control and shTMEM165 HEK293 cells were incubated with MnCl2 100 µM during 16h, fixed and labeled with antibodies against GPP130 (upper panels) and GM130 (lower panels) before confocal microscopy visualization. DAPI staining was performed and shows the nucleus **(D)** Quantification of the associated GPP130 fluorescence intensity (Number of experiments (N) = 2; number of cells (n) = 50; *** = P value < 0,001).

After 1h and 2h of Mn2+ treatment in control cells, GPP130 is delocalized in punctate structures (about 20 GPP130 positive structures per cell have been quantified) decreasing to less than 10 positive structures per cell after 4h of Mn2+ treatment. Remarkably and after Mn2+ exposure, the number of positive GPP130 punctuate structures in shTMEM165 cells is extremely low (about 5 per cell). This confirms the western blot result and demonstrates the insensitivity of GPP130 to Mn2+ treatment in shTMEM165 HeLa cells. As the GPP130 luminal stem domain has been demonstrated to confer this Mn2+ sensitivity, our results highly suggest that TMEM165 is required to regulate Golgi Mn2+ homeostasis.

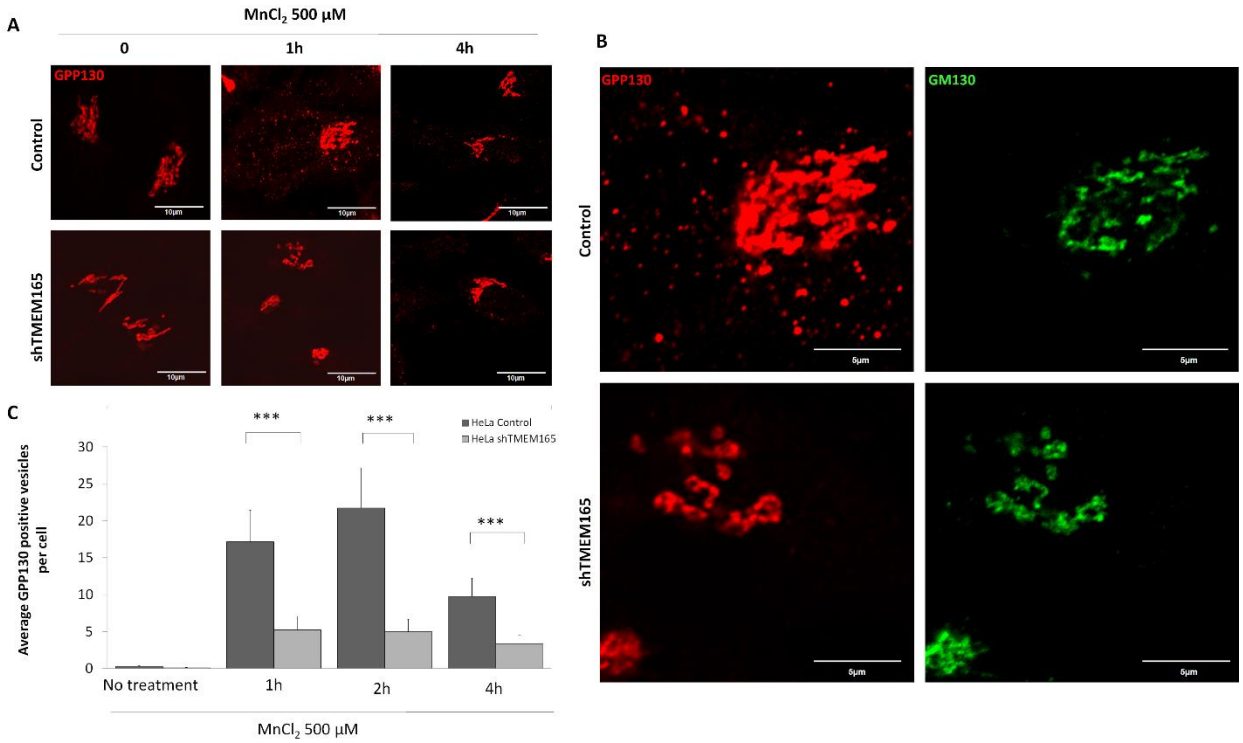

Figure 5. Alteration of the Mn2+ associated GPP130 vesicularization in shTMEM165 cells. (A) Control and shTMEM165 HeLa cells were incubated with MnCl2 500 µM during the indicated times, fixed and labeled with antibodies against GPP130 (upper panels) and GM130 (lower panels) before confocal microscopy visualization. **(B)** Magnification of the 1h panel presented in A. Cells were immunostained with anti-GPP130 (left panels) and anti-GM130 antibodies (right panels). Arrows indicate few examples of GPP130 positive vesicles. **(C)** Quantification of the average number of GPP130 positive vesicles per cell in control and shTMEM165 HeLa cells (N = 2; n = 50; *** = P value < 0,001).

TMEM165 knockdown provokes a glycosylation defect that can be suppressed by manganese supplementation

As we previously showed that Golgi glycosylation deficiency in *gdt1Δ* strains can be suppressed by the addition of MnCl2 in the medium, we wanted to investigate in TMEM165 depleted cells (i) the glycosylation defect and (ii) the impact of Mn2+ supplementation on the suppression of

the glycosylation defect. To evaluate these two aspects, we first determined the steady-state glycosylation status of LAMP2, an extensively N- glycosylated lysosomal resident protein and TGN46, a glycoprotein known to be N- and O-glycosylated. For this, control and shTMEM165 HeLa and HEK293 cells were treated or not with MnCl2 (fig. 6). While a subtle change in the LAMP2 mobility arguing for slight heterogeneity in glycosylation could be observed between control and shTMEM165 HeLa cells (fig. 6A), a more pronounced decrease in TGN46 molecular weight was observed compared to control cells (fig. 6A). Remarkably, when Mn2+ was added to the cell culture, the altered gel mobility of LAMP2 and TGN46 was completely suppressed in shTMEM165 HeLa cells. Comparable with the shTMEM165 HeLa results, a stronger increase in both LAMP2 and TGN46 gel mobility was observed in shTMEM165 HEK293 cells (fig. 6B). Very interestingly, the observed increased gel mobility was also supressed for these two glycoproteins after Mn2+ treatment. To appreciate the specific effect of the Mn2+, shTMEM165 HEK293 cells were treated with MnSO4. Similarly to MnCl2, MnSO4 completely suppresses the observed heterogeneity in gel mobility (supplementary figure 2). To confirm that Mn2+ rescues the glycosylation process, shTMEM165 HEK293 cells treated or not with Mn2+, were subjected to PNGase F treatment (supplementary figure 3). We found that deglycosylation of LAMP2 produced a 40KDa polypeptide for both (supplementary figure 3A). For TGN46 and in absence of Mn2+, PNGase F treatment leads only to a slight increase in gel mobility arguing that among the potential N-glycosylation sites of TGN46, only few of them are N-glycosylated (supplementary figure 3B). We interestingly, found that deglycosylation of TGN46 from shTMEM165 HEK293 cells treated with Mn2+ produces a band with a higher molecular weight than the one obtained in untreated shTMEM165 cells. Altogether these results suggest that Mn2+ rescues the N-glycosylation for LAMP2 and likely the O-glycosylation for TGN46. It is important to note that the glycosylation defect observed for both LAMP2 and TGN46 in shTMEM165 HEK293 cells does not lead to an aberrant subcellular localization for these two proteins (supplementary figure 4).

To confirm the Mn2+ effects, mass spectrometry analysis of N-glycans was performed in control and shTMEM165 HEK293 cells treated or not with Mn2+ (fig. 7). The structures detected at mass-per-charge (m/z) ratios above 2966 were found absent in shTMEM165 HEK293 cells compared to control cells then demonstrating a severe Golgi processing defect.

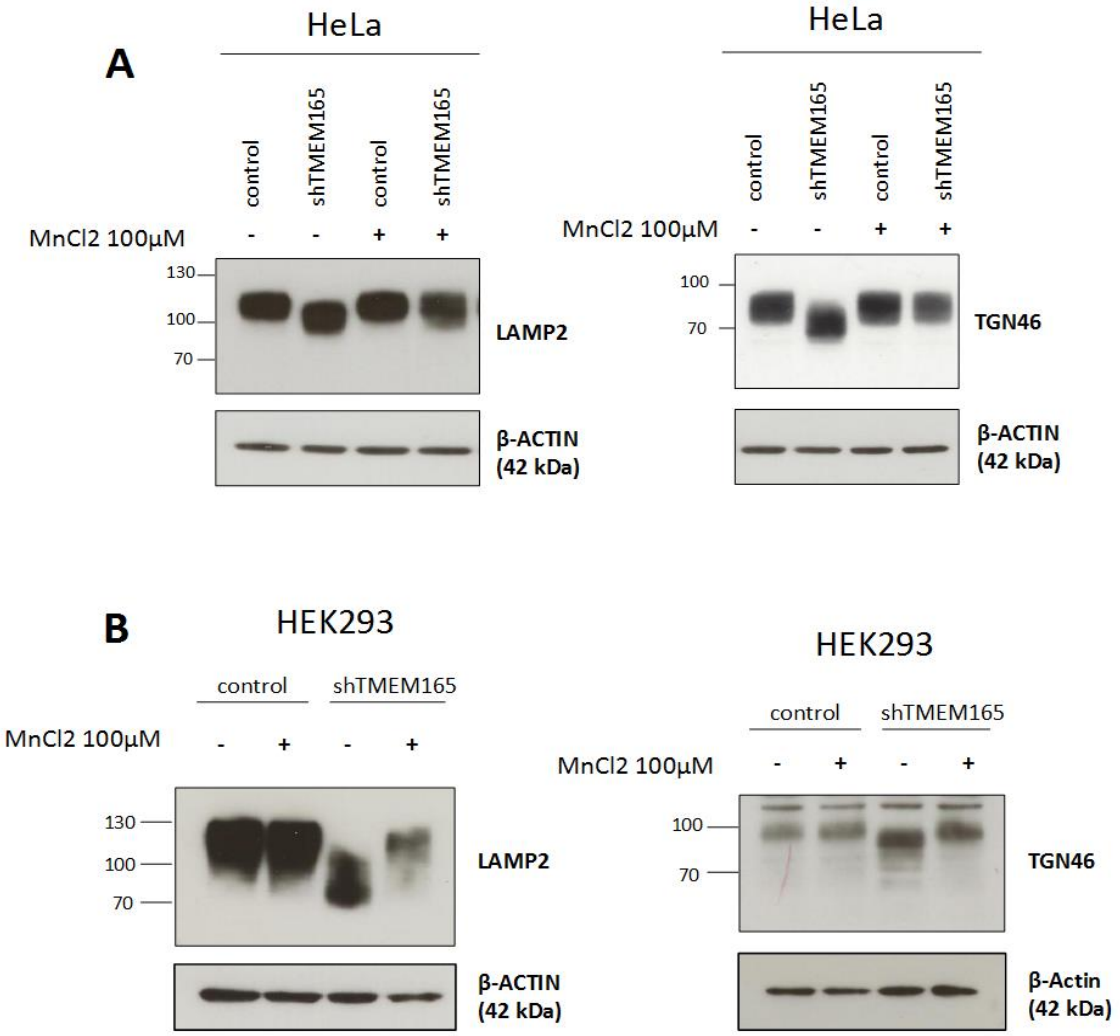

Figure 6. Mn2+ suppresses the observed LAMP2 and TGN46 altered gel mobility in TMEM165 depleted cells. (A) Steady state cellular level and gel mobility of LAMP2 and TGN46 in control and shTMEM165 HeLa cells. (B) Steady state cellular level and gel mobility of LAMP2 and TGN46 in control and shTMEM165 HEK293 cells. Control and shTMEM165 cells were cultured in absence or presence of MnCl2 (100µM) during 18h, cell lysates were prepared, subjected to SDS-PAGE and Western blot with the indicated antibodies.

Remarkably, the structures detected at mass-per-charge (m/z) ratios 1345, 1416, 1591, 1836, 1907, 2040, 2081, 2285, 2326, 2850 and 2891 were found in increased abundance in shTMEM165 cells in comparison to those observed in control cells. These results highlight a strong galactosylation, a moderate GlcNAcylation defect and a very slight sialylation defect in shTMEM165 HEK293 cells. While Mn2+ treatment have no obvious effects on control HEK293

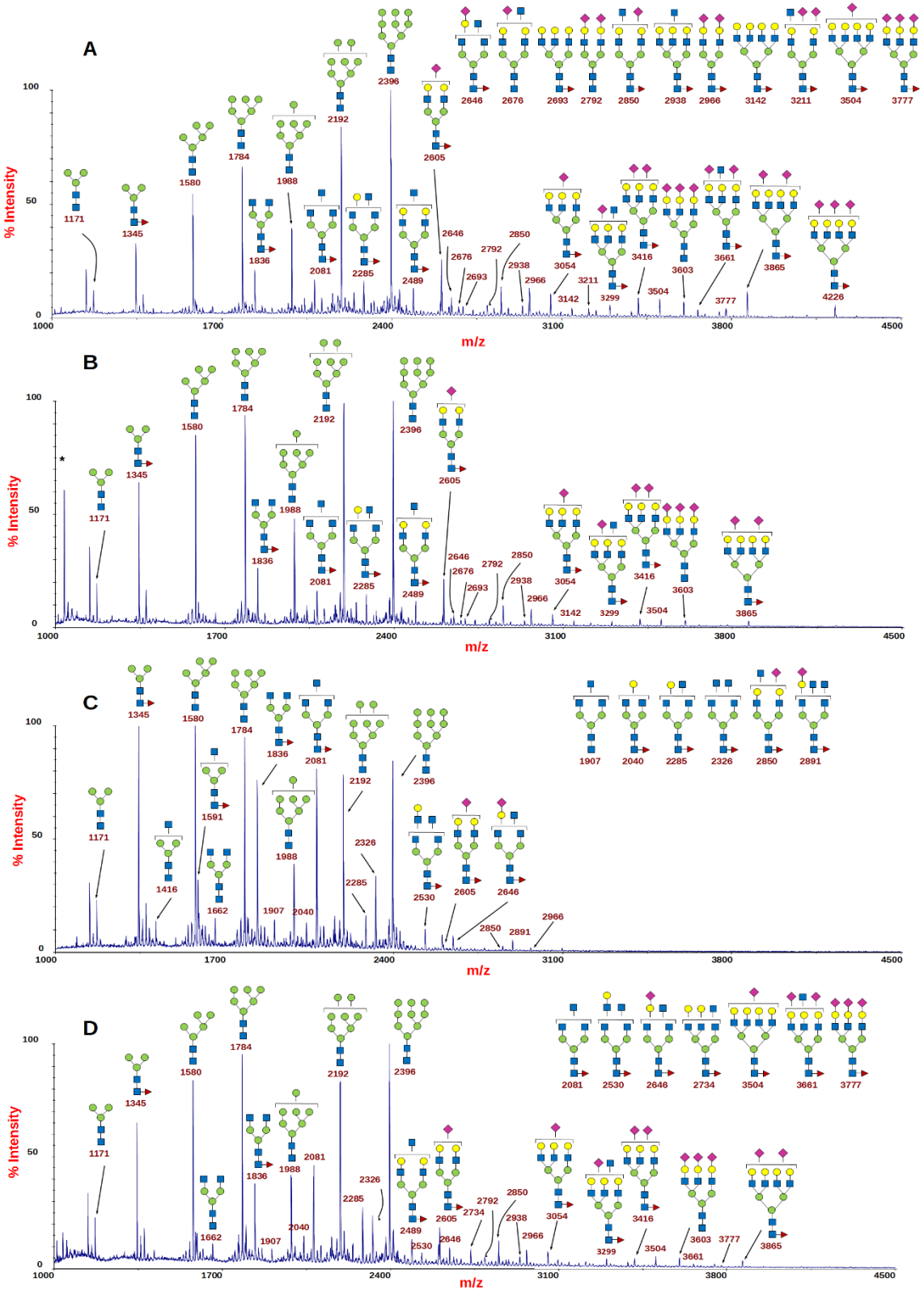

Figure 7. Mn2+ suppresses the observed galactosylation defect in TMEM165 depleted cells. (A) MALDI-TOF-MS spectra of the permethylated N-glycans from control HEK293 cells. (B) MALDI-TOF-MS spectra of the permethylated N-glycans from control HEK293 cells treated with Mn2+ 100µM for 36h. (C) MALDI-TOF-MS spectra of the permethylated N-glycans from shTMEM165 HEK293 cells. (D) MALDI-TOF-MS spectra of the permethylated N-glycans from shTMEM165 HEK293 cells treated with Mn2+ 100µM for 36h. The proposed glycan structures are in accordance with the Golgi biosynthetic pathway. The symbols representing sugar residues are as follows: closed square, N-acetylglucosamine; open circle, mannose; closed circle, galactose; open diamond, sialic acid; and closed triangle, fucose. Linkages between sugar residues have been removed for simplicity.

cells, such treatment largely suppresses the observed glycosylation defects, mainly the galactosylation defect, as observed by the decreased abundance of the structures (m/z) 1836 and 2081. This demonstrates that a defect in TMEM165 impairs the function of Golgi Mn2+ dependent enzymes, mainly the β-1,4-galactosyltransferase I. As Mn2+ supplementation could be considered as a treatment option, different Mn2+ concentrations (1µM to 50µM) have been tested. Interestingly we observe that only 1µM was sufficient to completely suppress the glycosylation defect observed in shTMEM165 HEK293 cells for both TGN46 and LAMP2 (fig. 8). Altogether and in agreement with the yeast results, we demonstrated that (i) the underlying pathomechanism of TMEM165 deficiency is linked to Golgi Mn2+ homeostasis defect and (ii) that the impaired Golgi glycosylation could totally be rescued by the addition of Mn2+.

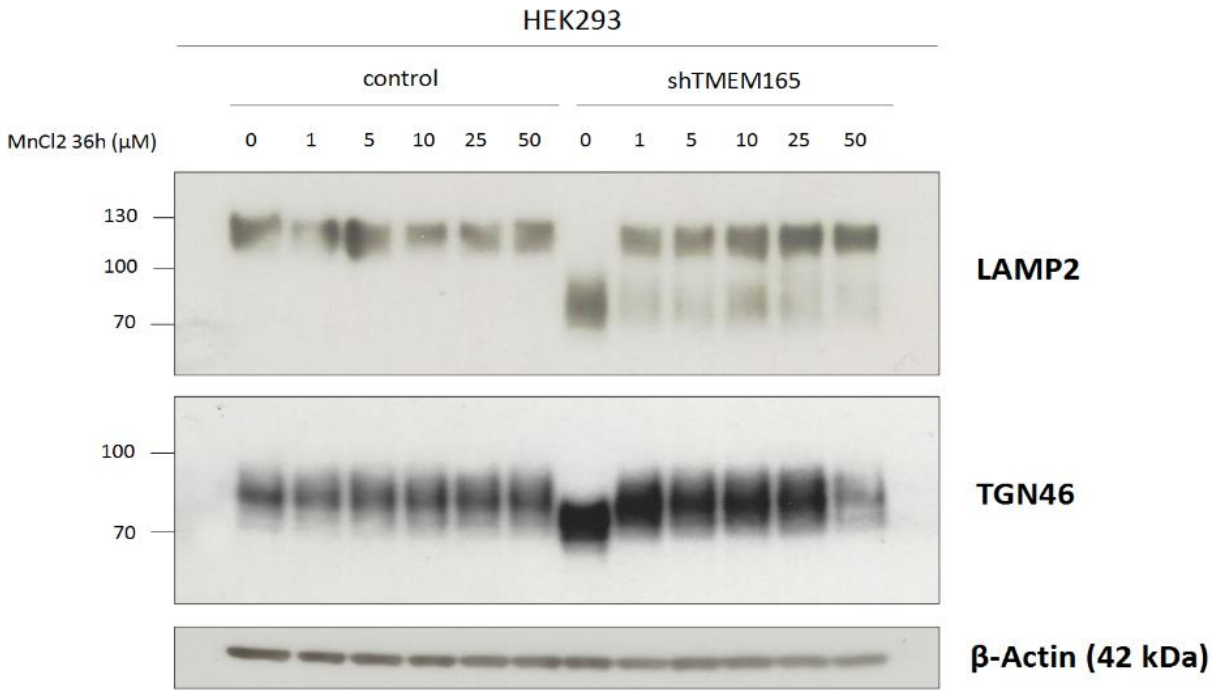

Figure 8. One micromolar MnCl2 is sufficient to suppress the glycosylation defect observed in shTMEM165 HEK293 cells for both TGN46 and LAMP2. Steady state cellular level and gel mobility of LAMP2 and TGN46 in control and shTMEM165 HEK293 cells. Cells were cultured in absence or presence of MnCl2 during 36h, cell lysates were prepared, subjected to SDS-PAGE and Western blot with the indicated antibodies.

DISCUSSION

TMEM165 deficiency was recently found to lead to a type-II CDG associated with defective Golgi N-glycosylation. TMEM165/Gdt1p is extremely conserved during evolution, and has no known direct molecular function. TMEM165/Gdt1p is not directly involved in the Golgi glycosylation process, as it is neither a sugar transporter nor a Golgi glycosyltransferase. Previous work has shown that a lack of Gdt1p leads to a sensitivity to high Ca2+ concentrations and we have demonstrated that TMEM165 is involved in pH homeostasis [20]. These results led us to hypothesize that Gdt1p/TMEM165 could be a Ca+/H+ antiporter involved in the Golgi Ca2+ entrance and exit of H+. In this study, we showed that high environmental Ca2+ concentrations in *gdt1Δ* led to strong N-glycosylation deficiencies while in *pmr1Δ*, the observed Golgi N-glycosylation defects were markedly suppressed in the presence of Ca2+. This antagonistic effect then implied different functions for these two proteins. Interestingly, previous work has also shown that the observed Golgi glycosylation defects in *pmr1Δ* were not due to the lack of Ca2+ uptake but mainly to a lack of Mn2+ uptake. Moreover, adding Mn2+ to the culture medium can rescue the N-glycosylation defect of the *pmr1Δ* strains (22). We therefore hypothesized that the observed glycosylation defect in *gdt1Δ* could also be linked to a decrease in Mn2+ Golgi homeostasis. In that case, the addition of Mn2+ to the culture medium could be sufficient to complement the glycosylation deficiency observed in the presence of high Ca2+ concentrations. In order to explore this hypothesis, Mn2+ and other cations were tested in *gdt1Δ* yeasts. Interestingly, 1mM MnCl2 was sufficient to completely suppress the glycosylation deficiency seen in the presence of high calcium concentration.

Why is the glycosylation deficiency only seen in the presence of high calcium concentration in *gdt1Δ* yeasts? One part of the answer certainly resides in the fact that Pmr1p is a Ca2+/Mn2+ transporter. It is then tempting to hypothesize that a high Ca2+ concentration could prevent the import of Mn2+ via Pmr1p into the Golgi via a dilution phenomenon. In the absence of Gdt1p, the import of Mn2+ into the Golgi compartment would not be sufficient to generate the Mn2+ homeostasis required for Golgi glycosyltransferases activities. The Mn2+ dependent catalytic activity is indeed a characteristic of many Golgi glycosyltransferases in yeasts such as MNN1, MNN2 and MNN5 [29,30]. Therefore and in presence of high Ca2+ concentration, their activities would be likely altered in absence of Gdt1p.

The other possibility that we cannot completely exclude is a direct competition between Ca2+ and Mn2+ inside the Golgi lumen. In that case, Gdt1p would function as an extruder of Ca2+ from the Golgi lumen to lower the competition between Ca2+ and Mn2+. The Mn2+ import into the Golgi could also be indirect. Two Mn2+ transporters exist in the yeast secretory pathway, Smf1p and Smf2p that allows the Mn2+ import in the ER and TGN/endosomes respectively. One can then imagine that the lack of Gdt1p disturbs the functions and/or localization of these transporters in the presence of high Ca2+ concentration then causing indirectly a deficiency of Golgi Mn2+ import [31]. Interestingly, we also showed that gdt1p is directly involved in the suppression of the glycosylation defect in the *pmr1Δ* strains supplemented with Ca2+. This suggests that the presence of Ca2+ increases the Golgi Mn2+ uptake, and that this molecular process is mediated by gdt1p. From these yeast data, we could propose a model where Gdt1p would act as an antiporter or cotransporter of Mn2+/Ca2+. As an abnormal lysosomal pH has been highlighted in TMEM165 deficient CDG patients, we could imagine that the used counterion for Mn2+ entry would be different, H+ for mammalian cells and Ca2+ for yeasts.

As the regulation of Mn2+ homeostasis is highly conserved between yeasts and higher eukaryotes, we assessed the impact of Mn2+ on Golgi glycosylation in TMEM165 depleted cells (HeLa and HEK293). We first wanted to highlight that the Golgi Mn2+ homeostasis was impaired in TMEM165 depleted cells by using GPP130 as an intra-Golgi Mn2+ sensor. We clearly showed that in TMEM165 depleted cells, compared to control cells, the GPP130 Mn2+ sensitivity was altered. As the luminal stem domain was sufficient to confer Mn2+ sensitivity to the protein, our results support a model where the Golgi Mn2+ homeostasis would be disrupted in TMEM165 depleted cells. Interestingly, we observed that the effect of shTMEM165 on GPP130 degradation was stronger in HeLa as compared to HEK293 cells. The Mn2+ concentration inside the Golgi is mainly depending of two factors (i) the uptake of Mn2+ from the cytosol into the Golgi (mainly depending of the Ca2+/Mn2+-ATPase and certainly other transporters) and (ii) the intake of Mn2+ from the extracellular medium into the cytosol (depending of the plasma membrane expression of Mn2+ transporters). As increased Mn2+ concentration in the culture medium has a stronger effect on GPP130 degradation in HeLa cells as compared to HEK293 cells, one can suppose that the Mn2+ intake is very efficient in HeLa compared to HEK293 cells. This could also explain why the glycosylation defect is very subtle in HeLa cells compared to HEK293 cells.

The impact of Mn2+ on Golgi glycosylation was assessed by mass spectrometry and by following the migration profile of two highly glycosylated proteins. While the migration was

shown to be altered for both LAMP2 and TGN46 in both shTMEM165 HeLa and HEK293 cells, the Mn2+ treatment did completely restore a protein mobility comparable to that observed in control cells Analysis of N-linked glycans from glycoproteins using MALDI-TOF mainly showed the accumulation of agalactosylated glycan structures in TMEM165 depleted HEK293 cells arguing for a severe galactosylation defect. In line with the western blot results, Mn2+ treatment almost totally suppressed the observed glycosylation defect. This galactosylation defect is very interesting and seems to be a general characteristic of the cellular Mn2+ impairment. The recent discovery of CDG-patients presenting strong galactosylation defects on serotransferrin and carrying SLC39A8 mutations, a Zn2+/Mn2+ transporter, emphasizes the link between Golgi Mn2+ homeostasis and Golgi galactosylation efficiency process [32]. Two Golgi galactosyltransferases are known to transfer Gal residues from UDP-Gal to terminal N-acetylglucosamine (GlcNAc) residues, the UDP-Gal:N-acetylglucosamine β-1,4-galactosyltransferase I (B4GALT1; EC 2.4.1.22) that synthesizes N-acetyl lactosamine structures on glycoproteins and the UDP-Gal:N-acetylglucosamine β-1,4-galactosyltransferase II (B4GALT2; EC 2.4.1.22) that both act on glycoproteins and glycolipids. From a general point of view, these enzymes as well as the Golgi glycosyltransferases using UDP-sugars as a donor substrate, absolutely require Mn2+ for their activities. This could also explain why the GlcNAcylation process is also impaired in TMEM165 depleted HEK293 cells.

Altogether these experiments confirmed that in both yeasts and mammalian cells, the glycosylation abnormalities due to Gdt1p/TMEM165 defects are rescued by the addition of Mn2+.

In conclusion, we demonstrated that the observed Golgi glycosylation deficiencies in Gdt1p/TMEM165 deficient cells result from a defective Golgi Mn2+ homeostasis. This study provides novel insights into the mechanism of the galactosylation defect observed in TMEM165-deficient cells. These findings also support the potential use of therapeutic trials of Mn2+ in TMEM165 deficient patients.

Material and Methods

Yeast strains and media

Yeast strains originating from BY4741 background used for the experiments are listed

Wild-type (WT) *Mat***a** *his3Δ1 leu2Δ0 ura3Δ0*

pmr1Δ	*Mat**a** his3Δ1 leu2Δ0 ura3Δ0 pmr1Δ::KanMX4*
gdt1Δ	*Mat**a** his3Δ1 leu2Δ0 ura3Δ0 gdt1Δ::KanMX4*
gdt1Δ /pmr1Δ	*Mat**a** his3Δ1 leu2Δ0 ura3Δ0 gdt1Δ::KanMX4 pmr1Δ::KanMX4*

Yeast were cultured at 30°C. Cultures in liquid media are done under a light shaking. Rich media, named YEP media, contains yeast extract (10 $g.L^{-1}$, Difco), Bacto-peptone (20 $g.L^{-1}$, Difco). YPD media is a YEP media supplemented with 2% D-glucose (Sigma-Aldrich). YPR is YEP supplemented with 2% raffinose (Euromedex). Selection antibiotics were added at 100 $\mu g.mL^{-1}$ for nourseothricine and 200 $\mu g.mL^{-1}$ for G418.

Invertase glycosylation analysis

Before any analysis, a preculture in YPD media is done and a volume equivalent to 15 $OD600_{nm}$ units is centrifugated for 3 minutes at 3500 rpm. The supernatant is discarded and the pellet is resuspended in YPR media to induce invertase expression. Calcium, manganese and other ions were added at this step at the indicated concentration. After a 20h culture in YPR, yeasts were centrifugated for 5 minutes at 3500 rpm. Supernatant was discarded and the pellet was kept frozen at -20°C. Invertase glycosylation analysis was performed as described by Ballou et al [33]

Antibodies and other reagents

Anti-TMEM165 and anti-β Actin antibodies were from Sigma–Aldrich (St Louis, MO, USA). Anti-GM130 antibody was from BD Biosciences (Franklin lakes, NJ, USA). Anti-GPP130 antibody was purchased from Covance (Princeton, NJ, USA). Goat anti-rabbit or goat anti-mouse immunoglobulins HRP conjugated were purchased from Dako (Glostrup, Denmark). Polyclonal goat anti-rabbit or goat anti-mouse conjugated with Alexa Fluor were purchased from Thermo Fisher Scientific (Waltham, MA, USA). PNGase F was from Roche Diagnostics (GmbH, Penzberg, Germany). Other chemicals were from Sigma-Aldrich unless otherwise specified.

Cell culture and transfections

All cell lines were maintained in Dulbecco's Modified Eagle's Medium (DMEM) supplemented with 10% fetal bovine serum (Lonza, Basel, Switzerland), at 37°C in humidity-saturated 5% CO_2 atmosphere. We generated polyclonal HeLa and HEK293 stable cell lines knockdown for

TMEM165 by the shRNA technique. Cells were transfected with the pGIPZ Lentiviral shRNA plasmid (Thermo Fisher Scientific) containing either shRNA sequences targeting TMEM165 mRNA or no sequences. The selection was done with puromycine. Thus, we generated two polyclonal cell lines, named control cell line and shTMEM165 for the cell line depleted in TMEM165. For manganese treatment, MnCl2 was added for the times and concentrations described in each figures.

Immunofluorescence staining

Cells were seeded on coverslips for 12 to 24h, washed once in Dulbecco's Phosphate Buffer Saline (DPBS, Lonza) and fixed either with 4% paraformaldehyde (PAF) in PBS pH 7.3, for 30 min at room temperature or with ice-cold methanol for 10 minutes at room temperature. Coverslips were then washed three times with PBS. Only if the fixation had been done with PAF, cells were permeabilized with 0.5% Triton X-100 in PBS for 15 min then washed three times with PBS. Coverslips were then put in saturation for 1h in blocking buffer [0.2% gelatin, 2% Bovin Serum Albumin (BSA), 2% Fetal Bovine Serum (FBS) (Lonza) in PBS], followed by the incubation for 1h with primary antibody diluted at 1:100 in blocking buffer. After washing with PBS, cells were incubated for 1h with Alexa 488-, Alexa 568- or Alexa 700-conjugated secondary antibody (Life Technologies) diluted at 1:600 in blocking buffer. After three washing with PBS, coverslips were mounted on glass slides with Mowiol. Fluorescence was detected through an inverted Leica TCS-SP5 confocal microscope. Acquisition were done using the LAS AF LITE software 2.6.3 (Leica Microsystem, Wetzlar, Germany).

Image Analyses

Immunofluorescence images were analyzed using TisGolgi, an homemade imageJ [36] (http://imagej.nih.gov/ij) plugin developed by TISBio and available upon request. Basically, the program automatically detects and discriminates Golgi and vesicles, based on morphological parameters such as size and sphericity. Then, the program calculates for each image the number of detected objects, their size and mean fluorescence intensity.

PNGase F deglycosylation assay

50µg of cell lysate are vacuum dried with SpeedVac™. Samples are then dissolved in 200µL ammonium bicarbonate 50mM buffer. 5µL of a solution containing 10% SDS and 10% β-mercaptoethanol in ammonium bicarbonate 50mM is added to the samples. Heat for 10min at 100°C. Cool down the samples at room temperature and add 175µL of ammonium bicarbonate 50mM buffer. Add 25 µL of a solution containing 10% NP-40 in ammonium bicarbonate 50mM. To perform the deglycosylation treatment, add 1,5 PNGase F unit to each sample and put the samples at 37°C overnight. Samples are then vaccum dried with SpeedVac™ and then dissolved in NuPAGE LDS sample buffer (Invitrogen) pH 8.4 supplemented with 4% β-mercaptoethanol (Fluka).

Western Blotting

Cells were scraped in DPBS and then centrifuged at 4500 rpm for 3 min. Supernatant was discarded and cells were then resuspended in RIPA buffer [Tris/HCl 50mM pH 7.9, NaCl 120mM, NP40 0.5%, EDTA 1mM, Na_3VO_4 1mM, NaF 5mM] supplemented with a protease cocktail inhibitor (Roche Diagnostics, Penzberg, Germany). Cell lysis was done by passing the cells several times through a syringe with a 26G needle. Cells were centrifuged for 30 min at 20 000g. The supernatant containing protein was estimated with the micro BCA Protein Assay Kit (Thermo Scientific). 20 µg of total protein lysate were put in NuPAGE LDS sample buffer (Invitrogen) pH 8.4 supplemented with 4% β-mercaptoethanol (Fluka). Samples were heated 10 min at 95°C and then separated on 4%-12% Bis-Tris gels (Invitrogen) and transferred to nitrocellulose membrane Hybond ECL (GE Healthcare, Little Chalfont, UK). The membrane were blocked in blocking buffer (5% milk powder in TBS-T [1X TBS with 0.05% Tween20]) for 1 hr at room temperature, then incubated overnight with the primary antibodies in blocking buffer, and washed three times for 5 min in TBS-T. The membranes were then incubated with the peroxidase-conjugated secondary goat anti-rabbit or goat anti-mouse antibodies (Dako; used at a dilution of 1:10,000) in blocking buffer for 1 hr at room temperature and later washed three times for 5 min in TBS-T. Signal was detected with chemiluminescence reagent (ECL 2 Western Blotting Susbtrate, Thermo Scientific) on imaging film (GE Healthcare, Little Chalfont, UK).

Glycan analysis by mass spectrometry

Cells were sonicated in extraction buffer (25 mM Tris, 150 mM NaCl, 5 mM EDTA and 1% CHAPS, pH 7.4) and then dialysed in 6–8 kDa cut-off dialysis tubing in an ammonium bicarbonate solution (50 mM, pH 8.3) for 48 h at 4°C and lyophilized. The proteins/glycoproteins were reduced and carboxyamidomethylated followed by sequential tryptic and peptide N-glycosidase F digestion and Sep-Pak purification. Permethylation of the freeze-dried glycans and MALDI-TOF-MS of permethylated glycans were performed as described elsewhere [35].

Statistical Analysis

Comparisons between groups were performed using Student t-test for 2 variables with equal or different variances, depending on the result of the F-test.

Funding

This work was supported by the French National Research Agency (SOLV-CDG to F.F.); and the Mizutani Foundation for Glycoscience, no. ANR15-CE14-0001 (to F.F.).

Acknowledgements

We are indebted to Dr Dominique Legrand for the Research Federation FRABio (Univ. Lille, CNRS, FR 3688, FRABio, Biochimie Structurale et Fonctionnelle des Assemblages Biomoléculaires) for providing the scientific and technical environment conducive to achieving this work.

Conflict of interests

None.

References

1. Scott,K., Gadomski,T., Kozicz,T. and Morava,E. (2014) Congenital disorders of glycosylation: new defects and still counting. *J. Inherit. Metab. Dis.*, **37**, 609–617.
2. Freeze,H.H. (2013) Understanding human glycosylation disorders: biochemistry leads the charge. *J. Biol. Chem.*, **288**, 6936–6945.
3. Krasnewich,D. (2014) Human glycosylation disorders. *Cancer Biomark. Sect. Dis. Markers*, **14**, 3–16.
4. Jaeken,J. (2013) Congenital disorders of glycosylation. *Handb. Clin. Neurol.*, **113**, 1737–1743.
5. Freeze,H.H. (2007) Congenital Disorders of Glycosylation: CDG-I, CDG-II, and beyond. *Curr. Mol. Med.*, **7**, 389–396.
6. Jaeken,J. and Matthijs,G. (2007) Congenital disorders of glycosylation: a rapidly expanding disease family. *Annu. Rev. Genomics Hum. Genet.*, **8**, 261–278.
7. Freeze,H.H., Chong,J.X., Bamshad,M.J. and Ng,B.G. (2014) Solving glycosylation disorders: fundamental approaches reveal complicated pathways. *Am. J. Hum. Genet.*, **94**, 161–175.
8. Peters,V., Penzien,J.M., Reiter,G., Körner,C., Hackler,R., Assmann,B., Fang,J., Schaefer,J.R., Hoffmann,G.F. and Heidemann,P.H. (2002) Congenital disorder of glycosylation IId (CDG-IId) -- a new entity: clinical presentation with Dandy-Walker malformation and myopathy. *Neuropediatrics*, **33**, 27–32.
9. Jaeken,J., Schachter,H., Carchon,H., De Cock,P., Coddeville,B. and Spik,G. (1994) Carbohydrate deficient glycoprotein syndrome type II: a deficiency in Golgi localised N-acetyl-glucosaminyltransferase II. *Arch. Dis. Child.*, **71**, 123–127.
10. Martinez-Duncker,I., Dupré,T., Piller,V., Piller,F., Candelier,J.-J., Trichet,C., Tchernia,G., Oriol,R. and Mollicone,R. (2005) Genetic complementation reveals a novel human congenital disorder of glycosylation of type II, due to inactivation of the Golgi CMP-sialic acid transporter. *Blood*, **105**, 2671–2676.
11. Wu,X., Steet,R.A., Bohorov,O., Bakker,J., Newell,J., Krieger,M., Spaapen,L., Kornfeld,S. and Freeze,H.H. (2004) Mutation of the COG complex subunit gene COG7 causes a lethal congenital disorder. *Nat. Med.*, **10**, 518–523.
12. Foulquier,F., Vasile,E., Schollen,E., Callewaert,N., Raemaekers,T., Quelhas,D., Jaeken,J., Mills,P., Winchester,B., Krieger,M., *et al.* (2006) Conserved oligomeric Golgi complex subunit 1 deficiency reveals a previously uncharacterized congenital disorder of glycosylation type II. *Proc. Natl. Acad. Sci. U. S. A.*, **103**, 3764–3769.
13. Kranz,C., Ng,B.G., Sun,L., Sharma,V., Eklund,E.A., Miura,Y., Ungar,D., Lupashin,V., Winkel,R.D., Cipollo,J.F., *et al.* (2007) COG8 deficiency causes new congenital disorder of glycosylation type IIh. *Hum. Mol. Genet.*, **16**, 731–741.
14. Paesold-Burda,P., Maag,C., Troxler,H., Foulquier,F., Kleinert,P., Schnabel,S., Baumgartner,M. and Hennet,T. (2009) Deficiency in COG5 causes a moderate form of congenital disorders of glycosylation. *Hum. Mol. Genet.*, **18**, 4350–4356.
15. Reynders,E., Foulquier,F., Leão Teles,E., Quelhas,D., Morelle,W., Rabouille,C., Annaert,W. and Matthijs,G. (2009) Golgi function and dysfunction in the first COG4-deficient CDG type II patient. *Hum. Mol. Genet.*, **18**, 3244–3256.
16. Kornak,U., Reynders,E., Dimopoulou,A., van Reeuwijk,J., Fischer,B., Rajab,A., Budde,B., Nürnberg,P., Foulquier,F., Lefeber,D., *et al.* (2008) Impaired glycosylation and cutis laxa caused by mutations in the vesicular H+-ATPase subunit ATP6V0A2. *Nat. Genet.*, **40**, 32–34.
17. Foulquier,F., Amyere,M., Jaeken,J., Zeevaert,R., Schollen,E., Race,V., Bammens,R., Morelle,W., Rosnoblet,C., Legrand,D., *et al.* (2012) TMEM165 Deficiency Causes a Congenital Disorder of Glycosylation. *Am. J. Hum. Genet.*, **91**, 15–26.
18. Van Scherpenzeel,M., Steenbergen,G., Morava,E., Wevers,R.A. and Lefeber,D.J. High-resolution mass spectrometry glycoprofiling of intact transferrin for diagnosis and subtype identification in the congenital disorders of glycosylation. *Transl. Res.*, 10.1016/j.trsl.2015.07.005.
19. Rosnoblet,C., Legrand,D., Demaegd,D., Hacine-Gherbi,H., de Bettignies,G., Bammens,R., Borrego,C., Duvet,S., Morsomme,P., Matthijs,G., *et al.* (2013) Impact of disease-causing mutations on TMEM165 subcellular localization, a recently identified protein involved in CDG-II. *Hum. Mol. Genet.*, **22**, 2914–2928.
20. Demaegd,D., Foulquier,F., Colinet,A.-S., Gremillon,L., Legrand,D., Mariot,P., Peiter,E., Van Schaftingen,E., Matthijs,G. and Morsomme,P. (2013) Newly characterized Golgi-localized family of proteins is involved in calcium and pH homeostasis in yeast and human cells. *Proc. Natl. Acad. Sci.*, **110**, 6859–6864.

21. Rudolph,H.K., Antebi,A., Fink,G.R., Buckley,C.M., Dorman,T.E., LeVitre,J., Davidow,L.S., Mao,J.I. and Moir,D.T. (1989) The yeast secretory pathway is perturbed by mutations in PMR1, a member of a Ca2+ ATPase family. *Cell*, **58**, 133–145.

22. Dürr,G., Strayle,J., Plemper,R., Elbs,S., Klee,S.K., Catty,P., Wolf,D.H. and Rudolph,H.K. (1998) The medial-Golgi ion pump Pmr1 supplies the yeast secretory pathway with Ca2+ and Mn2+ required for glycosylation, sorting, and endoplasmic reticulum-associated protein degradation. *Mol. Biol. Cell*, **9**, 1149–1162.

23. Antebi,A. and Fink,G.R. (1992) The yeast Ca(2+)-ATPase homologue, PMR1, is required for normal Golgi function and localizes in a novel Golgi-like distribution. *Mol. Biol. Cell*, **3**, 633–654.

24. Cyert,M.S. and Philpott,C.C. (2013) Regulation of Cation Balance in Saccharomyces cerevisiae. *Genetics*, **193**, 677–713.

25. Dudley,A.M., Janse,D.M., Tanay,A., Shamir,R. and Church,G.M. (2005) A global view of pleiotropy and phenotypically derived gene function in yeast. *Mol. Syst. Biol.*, **1**, 2005.0001.

26. Bai,C., Xu,X.-L., Chan,F.-Y., Lee,R.T.H. and Wang,Y. (2006) MNN5 encodes an iron-regulated alpha-1,2-mannosyltransferase important for protein glycosylation, cell wall integrity, morphogenesis, and virulence in Candida albicans. *Eukaryot. Cell*, **5**, 238–247.

27. Masuda,M., Braun-sommargren,M., Crooks,D. and Smith,D.R. (2013) Golgi Phosphoprotein 4 (GPP130) is a Sensitive and Selective Cellular Target of Manganese Exposure. *Synap. N. Y. N*, **67**, 205–215.

28. Mukhopadhyay,S., Bachert,C., Smith,D.R. and Linstedt,A.D. (2010) Manganese-induced trafficking and turnover of the cis-Golgi glycoprotein GPP130. *Mol. Biol. Cell*, **21**, 1282–1292.

29. Ca,W. and S,M. (1998) Activity of the yeast MNN1 alpha-1,3-mannosyltransferase requires a motif conserved in many other families of glycosyltransferases., Activity of the yeast MNN1 α-1,3-mannosyltransferase requires a motif conserved in many other families of glycosyltransferases. *Proc. Natl. Acad. Sci. U. S. Am. Proc. Natl. Acad. Sci. U. S. Am.*, **95, 95**, 7945, 7945–7950.

30. Rayner,J.C. and Munro,S. (1998) Identification of the MNN2 and MNN5 mannosyltransferases required for forming and extending the mannose branches of the outer chain mannans of Saccharomyces cerevisiae. *J. Biol. Chem.*, **273**, 26836–26843.

31. García-Rodríguez,N., Manzano-López,J., Muñoz-Bravo,M., Fernández-García,E., Muñiz,M. and Wellinger,R.E. (2015) Manganese redistribution by calcium-stimulated vesicle trafficking bypasses the need for P-type ATPase function. *J. Biol. Chem.*, **290**, 9335–9347.

32. Park,J.H., Hogrebe,M., Grüneberg,M., DuChesne,I., von der Heiden,A.L., Reunert,J., Schlingmann,K.P., Boycott,K.M., Beaulieu,C.L., Mhanni,A.A., *et al.* (2015) SLC39A8 Deficiency: A Disorder of Manganese Transport and Glycosylation. *Am. J. Hum. Genet.*, **97**, 894–903.

33. Ballou,C.E. (1990) [36] Isolation, characterization, and properties of Saccharomyces cerevisiae mnn mutants with nonconditional protein glycosylation defects. In Enzymology,B.-M. in (ed), Gene Expression Technology. Academic Press, Vol. 185, pp. 440–470.

34. Schneider,C.A., Rasband,W.S. and Eliceiri,K.W. (2012) NIH Image to ImageJ: 25 years of image analysis. *Nat. Methods*, **9**, 671–675.

35. Morelle,W. and Michalski,J.-C. (2007) Analysis of protein glycosylation by mass spectrometry. *Nat. Protoc.*, **2**, 1585–1602.

Supplementary figures

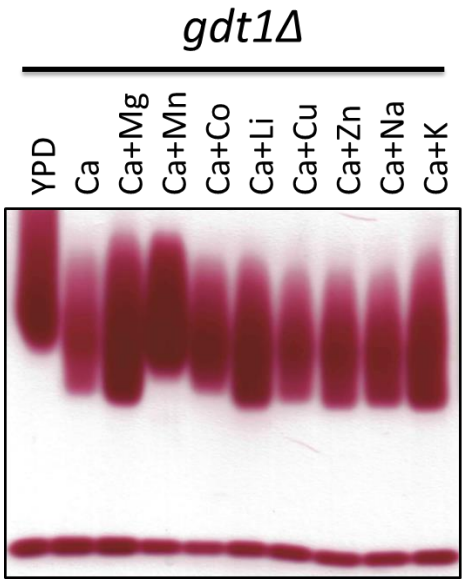

Supplementary figure 1: Sole Mn2+ suppresses the observed glycosylation defect in the *gdt1Δ* strains cultured with 0,5M CaCl2. N-glycosylated invertase secreted by *gdt1Δ* strains. Strains were cultured with 0,5M CaCl2 and 1mM for every other compound.

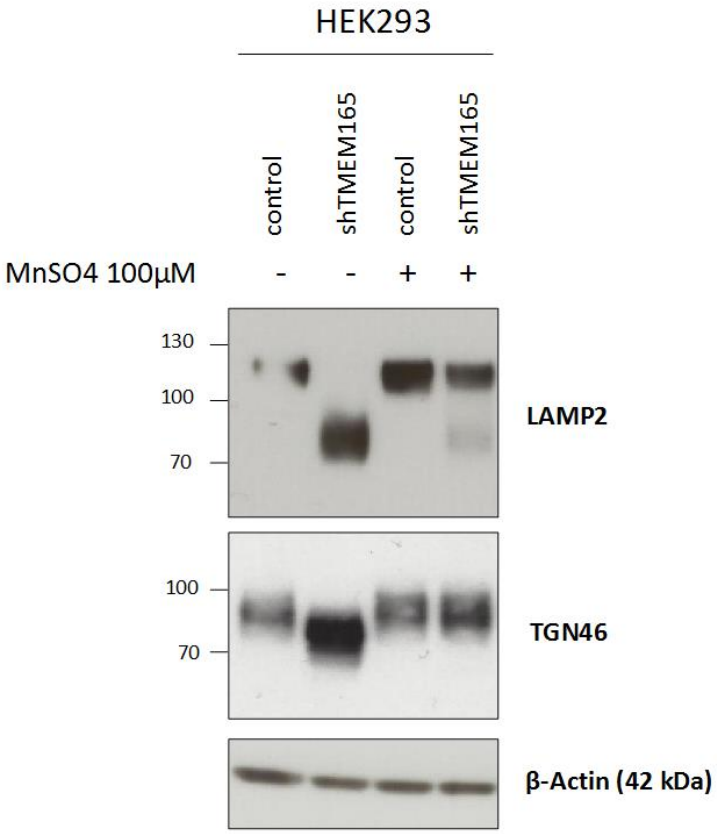

Supplementary figure 2. MnSO4 also suppresses the observed LAMP2 and TGN46 altered gel mobility. Steady state cellular level and gel mobility of LAMP2 and TGN46 in control and shTMEM165 HEK293 cells. Control and shTMEM165 cells were cultured in absence or presence of MnSO4 (100µM) during 18h, cell lysates were prepared, subjected to SDS-PAGE and Western blot with the indicated antibodies.

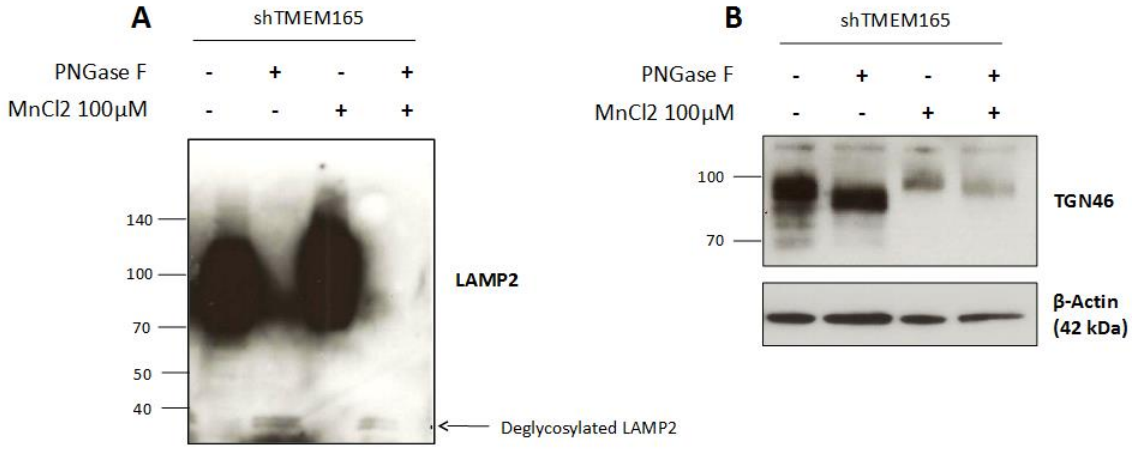

Supplementary figure 3. PNGase F treatment in shTMEM165 HEK293 cells, treated or not with Mn2+. Cell lysates from shTMEM165 HEK293 cells were treated with PNGase F as described in Materials and Methods. Cell lysates were then subjected to SDS-PAGE and Western blot with the indicated antibodies.

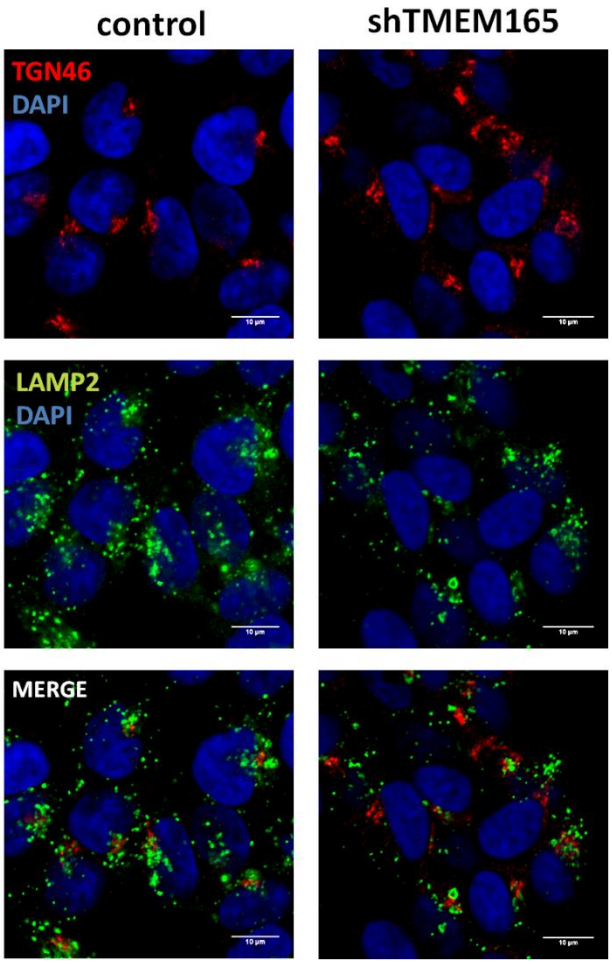

Supplementary figure 4. The observed LAMP2 and TNG46 glycosylation defect in shTMEM165 HEK293 does not lead to an aberrant subcellular localization of LAMP2 and TGN46. Control and shTMEM165 HEK293 cells were fixed and labeled with antibodies against TGN46 (upper panels) and LAMP2 (middle panels) before confocal microscopy visualization. DAPI staining was performed and shows the nucleus. The lower panel shows the merge between LAMP2 and TGN46 staining.

1.3. Complementary results

To complete the results of figure 8, we have also recently shown that 100nM MnCl2 was even sufficient to completely supress the LAMP2 glycosylation defect in HEK KO TMEM165 (Figure 33).

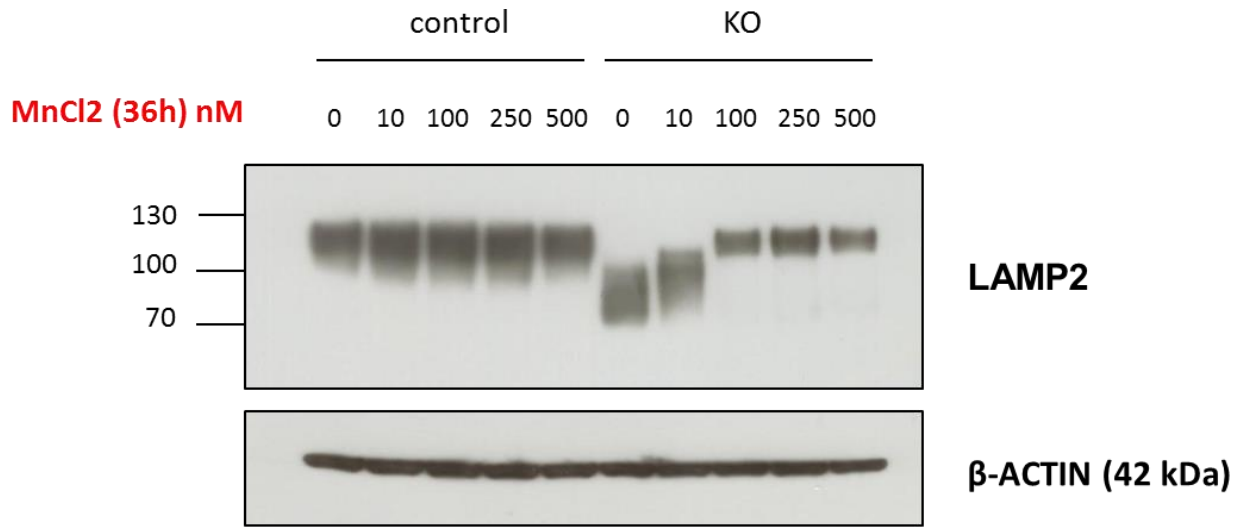

Figure 33. 100nM MnCl2 is sufficient to suppress the LAMP2 glycosylation defect observed in KO TMEM165 HEK293 cells. Steady state cellular level and gel mobility of LAMP2 in control and KO TMEM165 HEK293 cells. Cells were cultured in absence or presence of MnCl2 during 36h, cell lysates were prepared, subjected to SDS-PAGE and analysed by Western blot with the indicated antibodies. HEK293 cells knock-out for TMEM165 by Crispr-Cas9 were kindly provided by Pr. Lupashin (University of Arkansas for Mecidal Sciences, USA).

To go further into the glycosylation analyses, we have also used a metabolic labelling technique with unnatural sialic acid derivatives to monitor sialylation in our cells. This technique is based on the one described by several authors [278,279]. Cells were treated with 500µM *N*-(4-pentynoyl) mannosamine (ManNAl) for the indicated time. This unnatural sugar contains a well tolerated alkyne functional group and is then incorporated into the sialic acid biosynthesis pathway to finally be added onto glycoconjugates in the Golgi apparatus. After incorporation of the modified sugar, a bioorthonogal click chemistry reaction named copper-catalyzed azide alkyne cycloaddition (CuAAC) is performed with a fluorophore containing an azide functional group (here an azido-fluor 568) to reveal the newly synthetised glycoconjugates carrying the unnatural sugar. This reaction is based on the formation of a covalent bond between the alkyne function carried by the sugar and the azide function on the fluorophore. Thus, we obtain a fluorescent signal proportional to the quantity of unnatural sugar added to glycoconjugates. By applying this methodology, we have observed that sialylation is delayed in TMEM165 deficient cell lines (Figure 34). After 8h of labeling, we have observed a dense perinuclear staining in HeLa control cells, which intensifies after 16h of metabolic labeling. It colocalizes with the Golgi marker GM130 and thus correspond to the incorporation of the sugar on glycoconjugates in the Golgi

apparatus. Strikingly, the staining was very weak in HeLa shTMEM165 after 8h of labeling and only a slight increase was observed after 16h of labeling demonstrating a strong sialylation defect or delay in TMEM165 deficient cells. Interestingly, 100µM MnCl2 supplementation suppresses this sialylation defect in HeLa shTMEM165 cells (Figure 35).

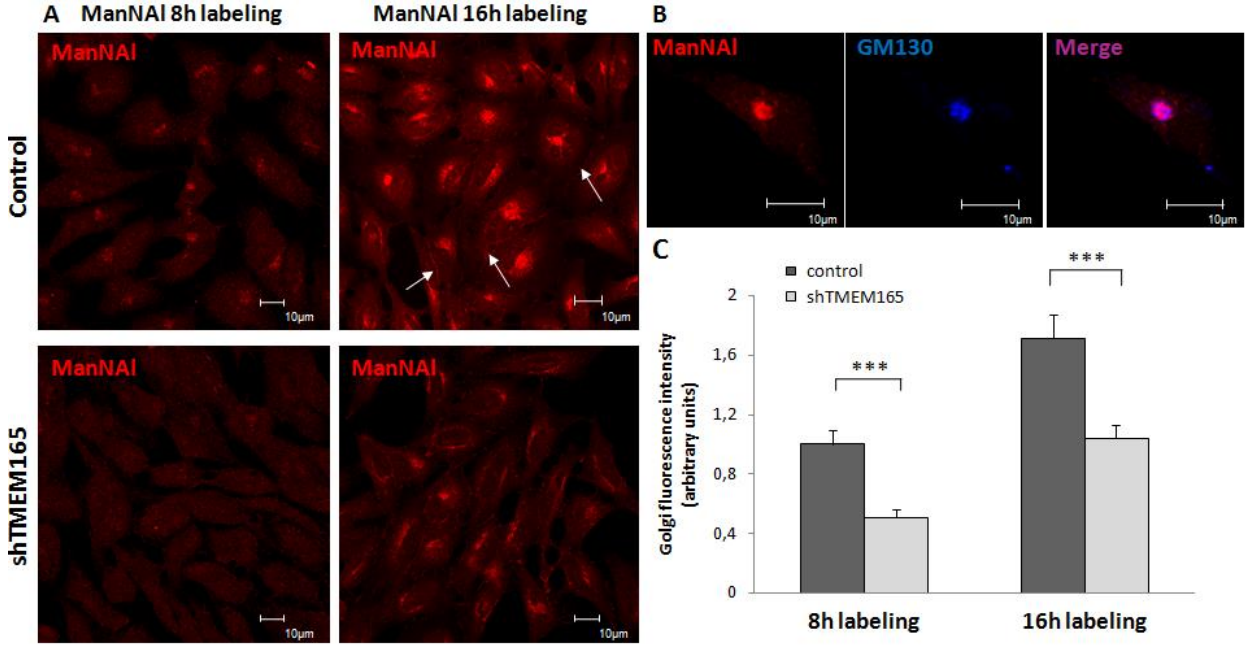

Figure 34. TMEM165 knockdown causes a general sialylation defect. (A) Cells were labeled with ManNAl for 8 or 16h. Click chemistry reaction was then done and the staining was visualized by confocal microscopy. Arrows points to a slight membrane staining. **(B)** Cells were labeled with ManNAl and immunostained with an antibody anti-GM130. (C) Quantification of the Golgi fluorescence intensity. Five independent experiments were done and quantification was done on more than 100 cells each time. *** = P value < 0,001.

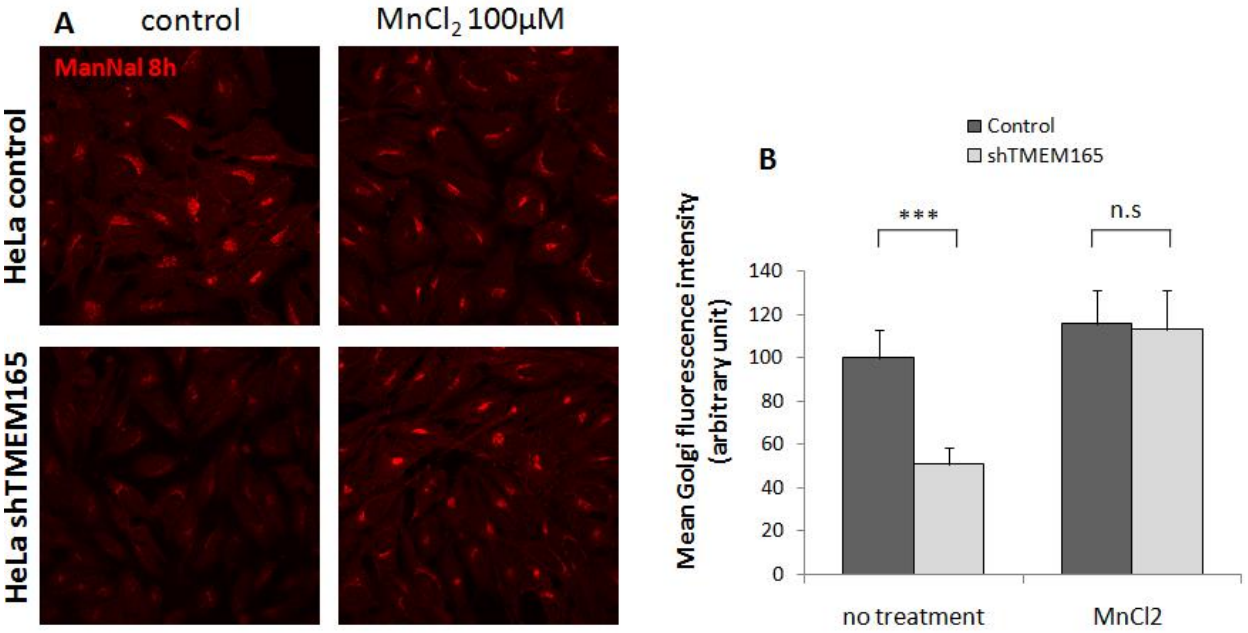

Figure 35. The glycosylation defect in HeLa shTMEM165 is suppressed by the addition of MnCl2. (A) Cells were treated or not by MnCl2 100 µM for 36h, then labeled with ManNAl for 8 in the same MnCl2 concentration. Click chemistry reaction was then done and the staining was visualized by confocal microscopy. **(B)** Quantification of the Golgi fluorescence intensity. Three independent experiments were done and quantification was done on more than 100 cells each time. *** = P value < 0,001.

1.4. Discussion

1.4.1. Gdt1p

In this study, we observed that the *gdt1Δ* mutant presents an N-glycosylation defect only when cultured in the presence of high Ca2+ concentrations (500mM). Since Pmr1p can import both Ca2+ and Mn2+ into the Golgi, we hypothesize that a high Ca2+ concentration could favour Ca2+ uptake and limit Mn2+ entry via Pmr1p. Although high Ca2+ concentration does not leads to a glycosylation defect in a wild-type strain, we suggested that in a *gdt1Δ* strain, the import of Mn2+ into the Golgi compartment would not be sufficient to maintain the Mn2+ homeostasis required for Golgi GT activities. This Mn2+ homeostasis disturbance would then ultimately lead to the glycosylation defect observed in the *gdt1Δ* strain.

In constrast, the observed Golgi N-glycosylation defects in *pmr1Δ* strain were markedly suppressed in the presence of Ca2+. On the opposite, Ca2+ failed to rescue the glycosylation defect in the *gdt1Δpmr1Δ* double mutant, strongly suggesting that the glycosylation rescue by Ca2+ in the *pmr1Δ* mutant comes from the sole activity of gdt1p.

Interestingly, previous works have also shown that the glycosylation defect observed in the *pmr1Δ* strain resulted from a lack of Mn2+ uptake, since Mn2+ supplementation was able to completely normalize the glycosylation. Surprisingly, the addition of 1mM MnCl2 in the cultured media of *gdt1Δ* strain was also sufficient to suppress the glycosylation defect seen in the presence of high Ca2+ concentration. We therefore concluded that the glycosylation defect in *gdt1Δ* is linked to a disturbance in Golgi Mn2+ homeostasis.

We finally propose a model where Gdt1p would act as a Mn2+/Ca2+ antiporter, importing Mn2+ into the Golgi and releasing Ca2+ from the Golgi.

1.4.2. TMEM165

Since the *gdt1Δ* mutant displayed an N-glycosylation defect in high Ca2+ concentrations, we wanted to investigate Golgi glycosylation in TMEM165 depleted cells. We first showed that both LAMP2 and TGN46 glycosylation were strongly affected. Analysis of N-glycans using MALDI-TOF mainly demonstrated a general and severe galactosylation defect. This galactosylation defect seems to be a key feature of Mn2+ homeostasis impairment. Indeed, the recent discovery of

SLC39A8-CDG patients presenting strong galactosylation defects emphasizes the link between Mn2+ homeostasis and Golgi galactosylation efficiency [7].

Interestingly, Mn2+ treatment almost totally suppressed the observed glycosylation defect. As presented in the complementary results section, only 100nM was sufficient to completely suppress the glycosylation defect observed on LAMP2 in KO TMEM165 HEK293 cells, raising the possibility of a therapeutic treatment with Mn2+ in TMEM165-CDG patients. However, mass spectrometry analyses with such low concentrations (100nM to 100µM) should also be done to test whether these concentrations are sufficient to completely suppress the general glycosylation defect.

We also decided to assess the Mn2+ Golgi homeostasis in TMEM165 depleted human cells using GPP130 as Golgi Mn2+ sensor (Figure 36). We highlighted that the Golgi Mn2+ homeostasis was impaired in TMEM165 depleted cells, suggesting a Mn2+ entry problem at the Golgi level in TMEM165 depleted cells and therefore questioning TMEM165 putative function as a Ca2+/H+ antiporter. To date and to my knowledge, this is the second scientific paper using GPP130 as a tool to decipher a pathological mechanism. Although indirect, this first approach has been helpful to understand the underlying mechanism of TMEM165-CDG and familial Parkinsonism due to SLC30A10 mutations [300].

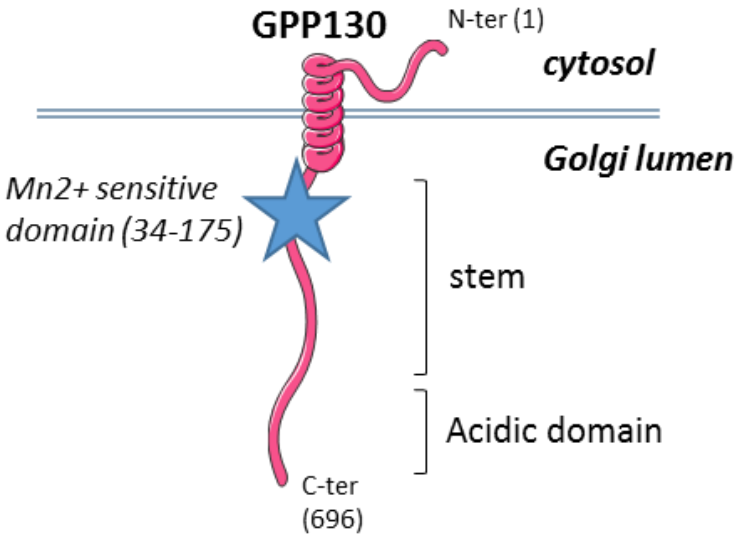

Figure 36. GPP130 topology and domains. GPP130 is a 696 amino acids protein containing a short cytosolic domain, and a long lumenal domain composed of a stem region and an acidic domain near the C-terminus. The Mn2+ sensitive domain, depicted with a blue star, has been mapped to amino acids 34 to 175 of the stem region.

In conclusion, we have demonstrated that the underlying pathological mechanism of TMEM165 deficiency is linked to Golgi Mn2+ homeostasis defect and that the impaired Golgi glycosylation could totally be rescued by the addition of Mn2+.

One main question remains: how does extracellular Mn2+ supplementation rescue the glycosylation in KO TMEM165 cells? Indeed, extracellular Mn2+ could theoretically reach the Golgi stack lumen in two alternate ways: (i) it might be internalized by endocytosis and subsequently reach the Golgi lumen through endosome-to-TGN retrograde trafficking [301,302]; (ii) alternately, it might cross the plasma membrane and eventually the Golgi stack membrane through specific channels or transporters. We cannot exclude that Mn2+ uptake in the ER also play a role in this rescue. This question will be addressed in the next few months in the lab using LAMP2 glycosylation rescue induced by Mn2+ as readout.

1.4.3. The yeast model to study Golgi glycosylation

Yeast and human Golgi glycosylation are very divergent, suggesting that yeast is at first glance not a good model to study Golgi glycosylation and to transfer the knowledge in human. Although it is true most of the time, we demonstrated here the importance of the yeast model to study human Golgi glycosylation defect linked to homeostasis disturbance. Indeed, the regulation of cellular homeostasis is similar in human and in yeast and many Golgi glycosyltransferases in yeasts also require Mn2+ to be fully active. The results obtained on gdt1p helped to orient the study on TMEM165 and therefore reinforced the usefulness of the yeast model in order to understand the pathophysiology of CDG caused by disturbance in actors indirectly involved in glycosylation, such as Golgi ion homeostasis.

1.5. Abstract in French

Les anomalies congénitales de la glycosylation (CDG) sont des maladies héréditaires sévères et rares dans lesquelles une glycosylation anormale des protéines est observée. Dans ce groupe de pathologies génétiquement et cliniquement hétérogène, un nouveau sous-groupe dû à des défauts de l'homéostasie de l'appareil de Golgi vient d'émerger. Notre équipe a identifié en 2012 TMEM165 comme étant une protéine golgienne impliquée dans les CDG. TMEM165 est une

protéine extrêmement conservée dans le règne eucaryote, mais les mécanismes moléculaires par lesquels une perte de fonction de TMEM165 conduit à des défauts de glycosylation golgienne sont énigmatiques. Comme *GDT1* est l'orthologue de TMEM165 chez la levure, des souches de levures dans lesquelles *GDT1* a été retiré ainsi que des cellules de mammifères dans lesquelles TMEM165 est absent ont été utilisées. Nous avons souligné que les défauts de glycosylation dues à une déficience de Gdt1p/TMEM165 résultaient en fait d'un défaut d'homéostasie du manganese au niveau de l'appareil Golgi. Nous avons découvert que dans les levures et les cellules déficientes en Gdt1p/TMEM165, une supplémentation en Mn2+ pouvait rétablir une glycosylation normale. Nous avons également montré que la sensibilité de GPP130 au Mn2+ intra-golgien était diminuée dans les cellules déficientes en TMEM165. Cette étude fournit non seulement de nouvelles informations sur les causes moléculaires des défauts de glycosylation observées dans les cellules déficientes en TMEM165, mais suggère également que TMEM165 est un acteur clé dans la régulation de l'homéostasie golgienne du Mn2+.

[2] GALACTOSE SUPPLEMENTATION IN TMEM165-CDG PATIENTS RESCUES THE GLYCOSYLATION DEFECTS

2.1. Introduction

In 2012, Foulquier and collaborators reported five TMEM165-CDG patients with abnormal N-glycans partially lacking galactose and sialic acid residues. We later fully characterized the glycosylation defect in TMEM165 deficient cell lines [303]. Detailed structural N-linked glycan analysis showed a dramatic hypogalactosylation of N-glycans, thus indicating that a loss of TMEM165 impairs the function of the β-1,4-galactosyltransferase I, a Mn2+ Golgi-dependent glycosyltransferase required for the biosynthesis of complex N-glycan. We also demonstrated that the defect was due to a disturbance in Golgi Mn2+ homeostasis. Interestingly, the glycosylation defect could be suppressed by Mn2+ addition in the cell media.

Recently, galactose oral supplementation has been successful for treating patients with another CDG subtype that is caused by pathogenic variants in SLC39A8, a plasma membrane Zn2+/Mn2+ transporter. SLC39A8-CDG patients also present with severe hypogalactosylation. Galactose therapy in these patients clearly improved glycosylation, but the mechanism remained poorly understood.

Overall, only few CDG subtypes show improved glycosylation following dietary supplementation with monosaccharides. For example, a treatment with oral mannose supplementation is available for MPI-CDG [246] and D-galactose supplementation has been shown to benefit patients with PGM1-CDG and SLC39A8-CDG [7,252].

In this study, we investigated whether galactose supplementation could be beneficial in TMEM165 deficiency. We chose galactose instead of Mn2+ because galactose therapy is easier to setup than Mn2+ therapy and galactose supplementation is already used for several CDG subtypes. The aim of this work was to characterize the effects of galactose supplementation on Golgi glycosylation in TMEM165-depleted HEK293 cells, as well as in two TMEM165-CDG patients and in their cultured skin fibroblasts. HEK293 cells knock-out for TMEM165 by Crispr-Cas9 were kindly provided by Pr. Lupashin (University of Arkansas for Mecidal Sciences, USA).

To study glycosylation in TMEM165 depleted cells, we have analysed the migration profile in western-blot of LAMP2, as decribed in the first publication. In parallel, mass spectrometry of total N-glycans and GSL extracted from cells was performed. For TMEM165-CDG patient fibroblasts, mass spectrometry of total N-glycans was assessed. Besides, InterCellular Adhesion Molecule 1 (ICAM-1) is a heavily N-glycosylated protein whose expression levels at the plasma membrane depends on its glycosylation. ICAM-1 is therefore a good marker of glycosylation and its expression was assessed by immunofluorescence and western blot. Biochemical parameters were measured in two TMEM165-CDG patients by clinicians.

2.2. Publication

Galactose Supplementation in Patients With TMEM165-CDG Rescues the Glycosylation Defects

Willy Morelle,[1]* Sven Potelle,[1]* Peter Witters,[2] Sunnie Wong,[3] Leslie Climer,[4] Vladimir Lupashin,[4] Gert Matthijs,[5] Therese Gadomski,[3] Jaak Jaeken,[2] David Cassiman,[2] Eva Morava,[2,3†] and François Foulquier[1†]

[1]Université de Lille, CNRS, UMR 8576 – UGSF - Unité de Glycobiologie Structurale et Fonctionnelle, F- 59000 Lille, France [2]Metabolic Center, Department of Pediatrics, University Hospitals Leuven, Leuven, Belgium [3]Hayward Genetics Center, Tulane University School of Medicine, New Orleans, Louisiana [4]Department of Physiology and Biophysics, College of Medicine, University of Arkansas for Medical Sciences, Little Rock, Arkansas 72205 and [5]Center for Human Genetics, KU Leuven, Leuven, Belgium

* These authors contributed equally to this study

† These authors contributed equally to this study

all correspondence and requests for reprints to: François Foulquier, Université Lille, CNRS, UMR 8576 – UGSF - Unité de Glycobiologie Structurale et Fonctionnelle, F-59000 Lille, France. E-mail: francois.foulquier@univ-lille1.fr.

Context: TMEM165 deficiency is a severe multisystem disease that manifests with metabolic, endocrine, and skeletal involvement. It leads to one type of congenital disorders of glycosylation (CDG), a rapidly growing group of inherited diseases in which the glycosylation process is altered. Patients have decreased galactosylation by serum glycan analysis. There are >100 CDGs, but only specific types are treatable.

Objective: Galactose has been shown to be beneficial in other CDG types with abnormal galactosylation. The aim of this study was to characterize the effects of galactose supplementation on Golgi glycosylation in TMEM165-depleted HEK293 cells, as well as in 2 patients with TMEM165-CDG and in their cultured skin fibroblast cells

Design and Setting: Glycosylation was assessed by mass spectrometry, western blot analysis, and transferrin isoelectrofocusing.

Patients and Interventions: Both unrelated patients with TMEM165-CDG with the same deep intronic homozygous mutation (c.792+182G.A) were allocated to receive D-galactose in a daily dose of 1 g/kg.

Results: We analyzed *N*-linked glycans and glycolipids in knockout TMEM165 HEK293 cells, revealing severe hypogalactosylation and GalNAc transfer defects. Although these defects were completely corrected by the addition of Mn^{2+}, we demonstrated that the observed *N*-glycosylation defect could also be overcome by galactose supplementation. We then demonstrated that oral galactose supplementation in patients with TMEM165-deficient CDG improved biochemical and clinical parameters including a substantial increase in the negatively charged transferrin isoforms, and a decrease in hypogalactosylated total N-glycan structures, endocrine function, and coagulation parameters.

Conclusion: To our knowledge, this is the first description of abnormal glycosylation of lipids in the TMEM165 defect and the first report of successful dietary treatment in TMEM165 deficiency. We recommend the use of oral D-galactose therapy in TMEM165-CDG.

For this study, SP completely performed and analysed figure 1. SP provided help to Willy Morelle for figure 2 to 5. SP helped with proofreading and editing the paper.

INTRODUCTION

In 2012, we reported pathogenic variants in TMEM165 in 5 patients with abnormal N-glycans partially lacking galactose and sialic acid, establishing TMEM165 deficiency as a new subtype of congenital disorder of glycosylation (CDG; TMEM165-CDG) (1) (phenotypic OMIM #614727). The most severely affected individuals present with severe skeletal symptoms (1, 2). TMEM165 is highly conserved during evolution, but its biological function remains controversial. We recently demonstrated that TMEM165 deficiency disrupts Golgi manganese (Mn^{2+}) homeostasis, resulting in Golgi glycosylation defect and hypoglycosylation, which can be subsequently rescued by Mn^{2+} supplementation (3). Detailed structural N-linked glycan analysis in TMEM165-deficient cells showed a dramatic increase of agalactosylated glycan structures. This indicated that a lack of TMEM165 impairs the function of β-1,4-galactosyltransferase, a Mn^{2+} Golgi-dependent glycosyltransferase required for the biosynthesis of sialylated complex N-glycan structures (4–6).

Currently, only a handful of CDG subtypes shows improved glycosylation following dietary supplementation with monosaccharides. MPI-CDG was the first CDG subtype discovered to be treatable with a few grams of oral mannose (7). Another monosaccharide, D-galactose, has been shown to benefit patients with PGM1-CDG (8).

Interestingly, galactose has also been successful for treating patients with another CDG subtype that is caused by pathogenic variants in SLC39A8, a Zn^{2+}/Mn^{2+} transporter. Patients with defective SLC39A8 present with severe hypogalactosylation of serum transferrin (8), demonstrating the crucial requirement of adequate Golgi Mn^{2+} homeostasis in normal Golgi glycosylation processes. Although it is clear that galactose therapy in these patients rescued the impaired galactosylation, the mechanism remained poorly understood.

In this study, we investigated whether galactose supplementation could be beneficial in TMEM165 deficiency. The aim of this work was to characterize the effects of galactose supplementation on Golgi glycosylation in TMEM165-depleted HEK293 cells, as well as in 2 TMEM165-CDG patients and their cultured skin fibroblast cells.

PATIENTS AND METHODS

Cell culture and transfections

All cell lines were maintained in Dulbecco's Modified Eagle's Medium (DMEM) supplemented with 10% fetal bovine serum (Lonza, Basel, Switzerland), at 37°C in humidity-saturated 5% CO_2 atmosphere. For manganese treatment, MnCl2 was added for the times and concentrations described in each figures.

Skin fibroblast cultures

Skin fibroblasts derived from skin biopsies were maintained in Eagle's minimum essential medium (American Type Culture Collection, Manassas, VA) in a humidified 37 °C incubator. Culture media was supplemented with 10% Fetal Bovine Serum and 1% 100 U Penicillin / 0.1 mg/mL streptomycin. TMEM165 deficient fibroblasts were cultured in the presence of additional galactose in the medium.

In-vitro galactose feeding

Eagle’s minimum essential culture medium was supplemented with 0 mM, 0.75 mM, 2 mM, 5 mM, or 10 mM D-galactose 18 to 24 hours after seeding the cells. D-galactose powder (Sigma-Aldrich, St. Louis, MO) was dissolved in phosphate-buffered saline (PBS) to create a stock solution of 100 mM, which was subsequently diluted to the desired concentration in the culture medium. Cells were fed for 5 to 7 days, with culture medium refreshed every 2 days. On the final day of the feeding experiment, cells were harvested by scraping.

ICAM-1: immunofluorescence staining

Immunohistochemistry was performed on cells seeded on glass coverslips and cultured for 5 days. Samples were fixed with 4% formaldehyde (Sigma-Aldrich) for 10 minutes, and permeabilized with 0.1% saponin (weight-to-volume ratio) and 0.1% bovine serum albumin (weight-to-volume ratio). They were blocked in 5% (volume-to-volume ratio [v/v]) normal donkey serum (Jackson ImmunoResearch Laboratories, West Grove, PA) and incubated with primary antibody against ICAM-1 (1:750; catalog no. MA5-13021; Thermo Fisher Scientific,

Waltham, MA) at 4°C for 3 nights, followed by incubation with biotinylated donkey anti-mouse immunoglobulin G antibody (1:800; catalog no. 715-065-151; Jackson ImmunoResearch Laboratories) and streptavidin-conjuguated Cy3 (1 mg/mL; catalog no. 016-160-084; Jackson Immuno- Research Laboratories) at room temperature for 1.5 hours. The samples were mounted with VectorShield Mounting Medium containing 4',6-diamidino-2-phenylindole (Vector Laboratories, Burlingame, CA). Images were obtained using an Olympus BX51 System microscope with an Olympus DP80 color camera (Olympus, Tokyo, Japan). Particle analysis and manual counting were performed with Fiji (http://imagej.nih.gov/ij) using the Cell Counter plug-in (version 2.0.0-rc-49/1.51a) (9).

LAMP2: actin western blot

Cells were scraped in Dulbecco's PBS and then centrifuged at 4500 rpm for 3 minutes. Supernatant was discarded and cells were resuspended in radioimmunoprecipitation assay buffer (Tris/HCl, 50 mM; pH 7.9; NaCl, 120 mM; NP40 0.5%; EDTA, 1 mM; Na3VO4, 1 mM; NaF, 5 mM) supplemented with a protease cocktail inhibitor (Roche Diagnostics, Penzberg, Germany). Cell lysis was done by passing the cells several times through a syringe with a 26G needle. Cells were centrifuged for 30 minutes at 20,000g. The supernatant containing protein was estimated with the micro BCA Protein Assay Kit (Thermo Fisher Scientific). Total protein lysate (20 µg) was put in NuPAGE lithium dodecyl sulfate sample buffer (Invitrogen), pH 8.4, supplemented with 4% b-mercaptoethanol (Fluka). Samples were heated for 10 minutes at 95°C and then separated on 4% to 12% Bis-Tris gels (Invitrogen) and transferred to nitrocellulose membrane Hybond ECL (GE Healthcare, Little Chalfont, United Kingdom). The membranes were blocked in blocking buffer (5% milk powder in tris-buffered saline and Polysorbate 20 (TBS-T; 1X TBS with 0.05% Tween20 for 1 hour at room temperature, then incubated overnight with the primary antibodies in blocking buffer, and washed 3 times for 5 minutes in TBS-T. The membranes were then incubated with the peroxidase-conjugated secondary goat anti-rabbit or goat antimouse antibodies (1:10,000 dilution; DakoSanta Clara, CA) in blocking buffer for 1 hour at room temperature and later washed 3 times for 5 minutes in TBS-T. Signal was detected with chemiluminescence reagent (ECL 2 Western Blotting Substrate; Thermo Fisher Scientific) on imaging film (GE Healthcare).

ICAM-1: β-integrin Western Blot

Protein expression of ICAM-1 in patients and healthy control subjects was assessed by western blotting. Hydrophobic protein was extracted and enriched by CelLytic MEM Protein Extraction kit (Sigma-Aldrich). Enriched hydrophobic protein (25 µg) of enriched hydrophobic protein was resolved on 10% Bis-Tris Gel (Invitrogen) at 200 V for 55 minutes. After sodium dodecyl sulfate polyacrylamide gel electrophoresis (SDSPAGE), samples were transferred to a 0.45-µm nitrocellulose membrane at 30 V for 2.5 hours on ice. Both running and transfer buffer were supplemented with antioxidant per manufacturer's recommendation (Invitrogen). The membrane was rocked for 1 hour in membrane blocking solution (Invitrogen) at room temperature and incubated overnight with the primary antibodies at 4°C, followed by 6 10-minute washes with 1x PBS supplemented with 0.2% Tween 20 (Sigma-Aldrich). Incubation with secondary antibodies at room temperature for 1 hour was followed by 6 10-minute washes with 0.2% Tween-PBS. Signal was detected by Licor Odyssey CLx IR Imaging System (LI-COR Biosciences, Lincoln, NE). Signal intensity was quantified by Odyssey software (version 2.0).

Primary antibodies were polyclonal rabbit anti-ICAM-1 (1: 4000; catalog no. sc-7891; Santa Cruz Biotechnology, Dallas, TX) and monoclonal mouse anti-integrin-b1 (catalog no. sc-374429; Santa Cruz Biotechnology). Secondary antibodies were DyLight 800-conjugated goat anti-rabbit (1:10000; catalog no. SA5-35571; Thermo Fisher Scientific) and DyLight 680-conjugated goat anti-mouse (1:10,000; catalog no. SA5-10082; Thermo Fisher Scientific). Antibodies were diluted in membrane blocking solution.

Extraction of glycolipids and mass spectrometry analysis

Cells were washed twice with ice-cold PBS; resuspended in 500 µL of water, and sonicated on ice. The material was then dried under N2 and extracted by $CHCl_3/CH_3OH$ (2:1, v/v), $CHCl_3/CH_3OH$ (1:1, v/v) and $CHCl_3/CH_3OH/H_2O$ (1:2:0.8, v/v/v). The supernatants were pooled, dried, and subjected to a mild saponification in 0.1M NaOH in $CHCl_3/H_2O$ (1:1, v/v) at 37°C for 2 hours and then evaporated to dryness. Samples were purified by using a C18 cartridge (Waters, Milford, MA) equilibrated in a CH_3OH/H_2O solvent. The glycosphingolipids (GSLs) were eluted by CH_3OH and $CHCl_3/CH_3OH$ (1:1, v/v) and $CHCl_3/CH_3OH$ (2:1, v/v). Permethylation of the freezedried GSL and matrix-assisted laser desorption/ionization time-of-flight mass spectrometry (MALDI-TOF-MS) of permethylated GSL were performed as described elsewhere (10).

Extraction of cellular and sera N-glycans and mass spectrometry analysis

Cells were sonicated in extraction buffer (25 mM Tris, 150 mM NaCl, 5 mM EDTA, and 1% 3-[(3-cholamidopropyl) dimethylammonio]-1-propanesulfonate [CHAPS], pH 7.4) and then dialyzed in 6- to 8-kDa cut-off dialysis tubing in an ammonium bicarbonate solution (50 mM, pH 8.3) for 48 hours at 4°C and lyophilized. The proteins/glycoproteins were reduced and carboxyamidomethylated, and then underwent sequential tryptic and peptide N-glycosidase F digestion and Sep-Pak purification. Permethylation of the freeze-dried glycans and MALDI-TOF-MS of permethylated glycans were performed as described elsewhere (10). For sera N-glycan analysis, 20 µL of serum was dried and denatured using β-mercaptoethanol and SDS at 100°C during 20 minutes. After adding Nonidet P40, the N-deglycosylation was performed using peptide N-glycosidase F PNGase F. After purification, the permethylation of the freezedried glycans and MALDI-TOF-MS of permethylated glycans were performed as described elsewhere (10).

Patients

In 2 previously described patients, a galactose supplementation trial was initiated (patient 1 and patient 3) (11). Both unrelated patients have the same deep intronic homozygous mutation (c.792+182G.A). The protocol was approved by the institutional review board (IRB; Tulane University Hayward Genetics Center IRB no. 517339-4; Clinicaltrials.gov NCT02955264).

Patient 1 (a 9-year-old boy) has dysmorphism and a severe multisystem disease with neurologic, pulmonary, gastrointestinal, endocrine, and hematological involvement (Table 1), as well as severe skeletal involvement with generalized osteopenia; hypoplasia of the skull base; anterior beaking of T12–L2; broad radial, ulnar, femoral, and tibial metaphyses; and underdeveloped epiphyses.

Patient 2 (a 25-year-old man) has a similar multisystem involvement but to a lesser degree. He has significant endocrine and coagulation anomalies (Table 1). He can walk (with crepitus) and has a normal language (11).

D-galactose supplementation in patients

All procedures were approved by the Tulane University School of Medicine IRB (Tulane IRB no. 517339-3). Two patients with genetically confirmed TMEM165 defect in this observational pilot study received oral D-galactose supplementation (Necese) over 18 weeks. D-Galactose intake was increased in increments, as follows: weeks 0 to 6, 0.5 g/kg/d; weeks 7 to 12, 1.0 g/kg/d; weeks 13 to 18, 1.5 g/kg/d. The purpose of the escalating dosing schedule was to minimize gastrointestinal irritation and metabolic side effects. Laboratory studies in blood (i.e., glucose, lactic acid, ammonia, and galactose-1-phosphate) and in urine (i.e., galactitol excretion) were conducted before the study and at every time point during the study to monitor tolerability to increasing intake of galactose.

Patients were instructed to continue their regular diet in addition to daily oral galactose supplementation. The maximum daily dose of galactose either patient received was 50.0 g (this amount is within the recommended daily intake). Prior studies investigating focal segmental glomerulosclerosis have demonstrated 50.0 g/d of galactose can be safely consumed and tolerated by patients (12).

Before beginning galactose therapy, clinical and metabolic baselines were established. At each time point in the study, each patient underwent a clinical examination, including an assessment for clinical changes, adverse effects, or any concerns regarding the therapy. Blood analysis was performed every 6 weeks to assess glycosylation (isoelectric focusing of serum transferrin and glycomic analysis in blood by mass spectrometry). Additionally, known glycoproteins, such as thyroid hormones, growth hormone, and coagulation and anticoagulation factors, were measured. Other biochemical parameters, including liver function enzymes and creatine kinase, were monitored. Urinary galactose levels were measured as a safety parameter.

RESULTS

Galactose supplementation rescued galactosylation deficiency in TMEM165-depleted cells

Because galactose supplementation in patients with PGM1-CDG and SLC39A8-CDG led to substantial galactosylation improvement, we first investigated the effects of galactose supplementation on Golgi glycosylation in TMEM165-depleted cells. Therefore, TMEM165 knockout (KO) HEK293 cells were generated by the genomic editing technique CRISPR-Cas9

(Supplemental Fig. 1), followed by studies on the steady-state glycosylation status of LAMP2, which is an extensively N-glycosylated lysosomal resident protein. Control and KOTMEM165 HEK293 cells were cultured without or with galactose supplementation in the culture medium (Fig. 1). Consistent with previous reports, a dramatic change in the LAMP2 gel mobility was observed in TMEM165 KO HEK293 cells, indicating a severely defective glycosylation [Fig. 1(A)] (3). As expected, MnSO4 and MnCl2 treatment completely restored normal LAMP2 gel mobility in TMEM165 KO HEK293 cells. Remarkably, 1 mM galactose supplementation achieved the same effect. Other monosaccharides, such as GlcNAc and GlcNH2, were also tested, but none had any effect on the gel mobility of LAMP2 in TMEM165 KO HEK293 cells. These results strongly suggest that D-galactose is the sole monosaccharide capable of rescuing the abnormal LAMP2 gel mobility.

To further characterize the effect of galactose on N-glycosylation, mass spectrometry analysis of total N-glycans was performed in control and TMEM165 KO HEK293 cells that were treated without or with galactose (Fig. 2). Consistent with previous studies, a pronounced hypogalactosylation was seen in TMEM165 KO HEK293 cells, with the accumulation of agalactosylated glycan structures detected at mass-per-charge (m/z) ratios 1836, 2081, and 2326. Although these structures were also found in control cells, the level was detected on a much lower level that is consistent with normal metabolic intermediates generated during normal glycosylation. Of note, the structures detected at m/z ratios greater than 3095 were completely absent in TMEM165 KO HEK293 cells. Altogether, the accumulating glycan structures observed in TMEM165 KO HEK293 cells pointed to a severe galactosylation defect. Although galactose treatment slightly decreased the processing intermediates in control HEK293 cells, its effect on the galactosylation defect observed in TMEM165 KO HEK293 cells was much more pronounced, as indicated by the decreased abundance of the structures with m/z ratios of 1836, 2081, and 2326. After galactose supplementation, N-glycosylation completely normalized. This demonstrated that galactose treatment not only considerably improved N-glycosylation in TMEM165 KO HEK293 cells but also increased N-glycosylation in control cells.

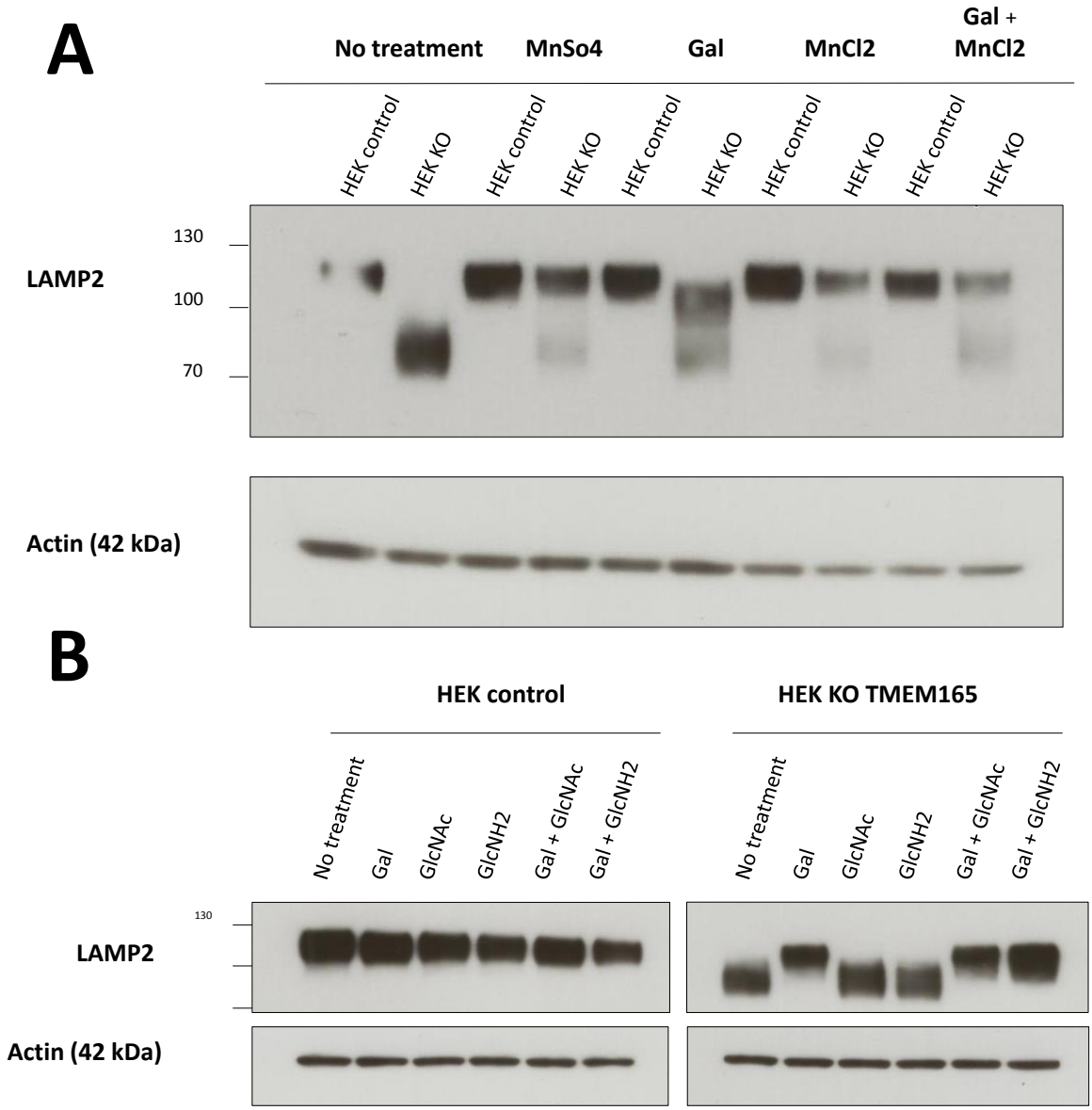

Figure 1. Galactose specifically suppresses the observed LAMP2 glycosylation defect in TMEM165 KO cells. (A) Steady-state cellular level and gel mobility of LAMP2. Control and TMEM165 KO HEK293 cells were cultured in absence or presence of galactose (1 mM), MnCl2 (100 µM), or MnSO4 (100 µM) for 18 hours; cell lysates were prepared, subjected to SDS-PAGE, and western blot with the indicated antibodies. (B) Steady-state cellular level and gel mobility of LAMP2. Control and TMEM165 KO HEK293 cells were cultured in absence or presence of galactose (1 mM), glucosamine (5 mM), or N-acetylglucosamine (5 mM) for 36 hours. Cell lysates were prepared, subjected to SDS-PAGE, and western blot with the indicated antibodies.

Table 1. Hematological and Clinical Parameters in Patients with TMEM165 Receiving Galactose Therapy

	Patient 1				Patient 2			
	Baseline	Week 6	Week 12	Week 18	Baseline	Week 6	Week 12	Week 18
Creatine kinase, IU/L (nl, <190 IU/L)	1470[a]	820[a]	710[a,b]	1184[a]	1223[a,c]	1253[a]	1186[a]	904[a]
PT, s (nl, 9.4–12.5 s)	12.7[a]	11.5[d]	11.3[d]	12.1[d]	13[a,e]	12.4	13.3[a]	13.7[a]
APTT, s (25–36.5 s)	35.0	35.8	31.5	27.2	40.2[a,e]	25.4[d]	38[a]	34.2[a]
Factor IX, % (nl, 70%–130%)	59.2[a]	63.1[a]	66.1[a]	65.3[a]	75[e]	74.8	67[a]	71.8
Factor XI, %(nl, 70%–130%)	83	84.9	89.4	82.7	89.4 §	64.8[a]	51[a]	55.1[a]
Antithrombin, % (nl, 70%–130%)	78	96	88	88	61[a,e]	87[d]	79[d]	85[d]
LH, U/L (nl, 1.7–8.6 U/L)	<0.1[a]	<0.1[a]	<0.1[a]	0.1[a]	2.0	3.1	1.8	2.3
FSH, U/L (nl, 1.2–7.7 U/L)	0.5[a]	0.6[a]	0.3[a]	0.5[a]	0.8[a]	0.8[a]	0.6[a]	0.6[a]
IGF-1, μg/L (nl, 47–251 μg/L)	<35[a]	56[d]	47[d]	64[d]	123	103	125	118
IGFBP3, μg/L (nl, 1995–4904 μg/L)	1848[a]	2172[d]	2149[d]	2129[d]	3219	2494	2931	Pending
TSH, mIU/L (nl, 0.27–4.2 mIU/L)	5.33[a]	4.54[a]	2.98[d]	4.17[a]	5.37[a,e]	4.58[a]	4.26[a]	5.83[a]
Free T4, pmol/L (nl, 12–22 pmol/L)	20.5	19	21.6	22.4[a]	20.5[e]	18.7	17.8	21.1
AST, U/L (<37 U/L)	407[a,b]	409[a,b]	549[a,b]	494[a,b]	319[a,e]	287[a]	265[a]	245[a]
ALT, U/L (nl, <51 U/L)	78[a]	75[a]	131[a]	94[a]	66[a,e]	56[a]	51[d]	43[d]
HDL cholesterol, U/L (nl, >40 U/L)	45	45	38[a]	41	27[a,e]	24[a]	23[a]	24[a]

Abbreviations: ALT, alanine aminotransferase; AST, aspartate aminotransferase; LH, luteinizing hormone; nl, normal limit; PT, prothrombin time.

[a]Outside reference range.

[b]Hemolysis.

[c]5 April 2016.

[d]Corrected.

[e]16 October 2015.

Next, we investigated whether other glycoconjugates were also affected and potentially rescued by galactose supplementation in TMEM165 KO HEK293 cells. Therefore, glycolipids were analyzed by MALDI-MS. As expected, the difference in gangliosides' profiles between control cells and TMEM165 KO HEK293 cells was clear. Although control cells expressed a complex pattern of GSLs, including GM3 (m/z 1372/1484), GM2 (m/z 1617/1729), GM1 (m/z 1821/1933), GD2 (m/z 1978/2090), and GD1 (m/z 2182/2294) species, KO TMEM165 HEK293 cells only showed traces of GM3 and GM2 species (Fig. 3). This indicated a severe glycolipid glycosylation defect that was secondary to a galactosylation defect. Although galactose supplementation did not change the glycolipid glycosylation profile in control cells, glycolipid glycosylation was found partially restored in TMEM165 KO HEK293 cells upon galactose supplementation. The GM3 species were certainly restored but, surprisingly, the GM2 species were not. This result strongly suggested (1) a lack of TMEM165 affected the β-1,4-N-acetylgalactosaminyltransferase (GM2/GD2 synthase) and (2) that galactose supplementation could not rescue the activity of the β-1,4 N-acetylgalactosaminyltransferase. If this was true, then Mn2+ treatment would be expected to rescue both GM3 and GM2 levels in TMEM165 KO HEK293 cells. To test this hypothesis, glycolipid glycosylation was analyzed in TMEM165 KO HEK293 cells treated with Mn2+. Although KO cells presented a drastic change of GM3 and GM2 species compared with control cells, Mn2+ supplementation rescued the synthesis of both GM3 and of GM2 species (Fig. 4). This clearly showed that the transfer of GalNAc on glycolipids was also impaired in the absence of TMEM165.

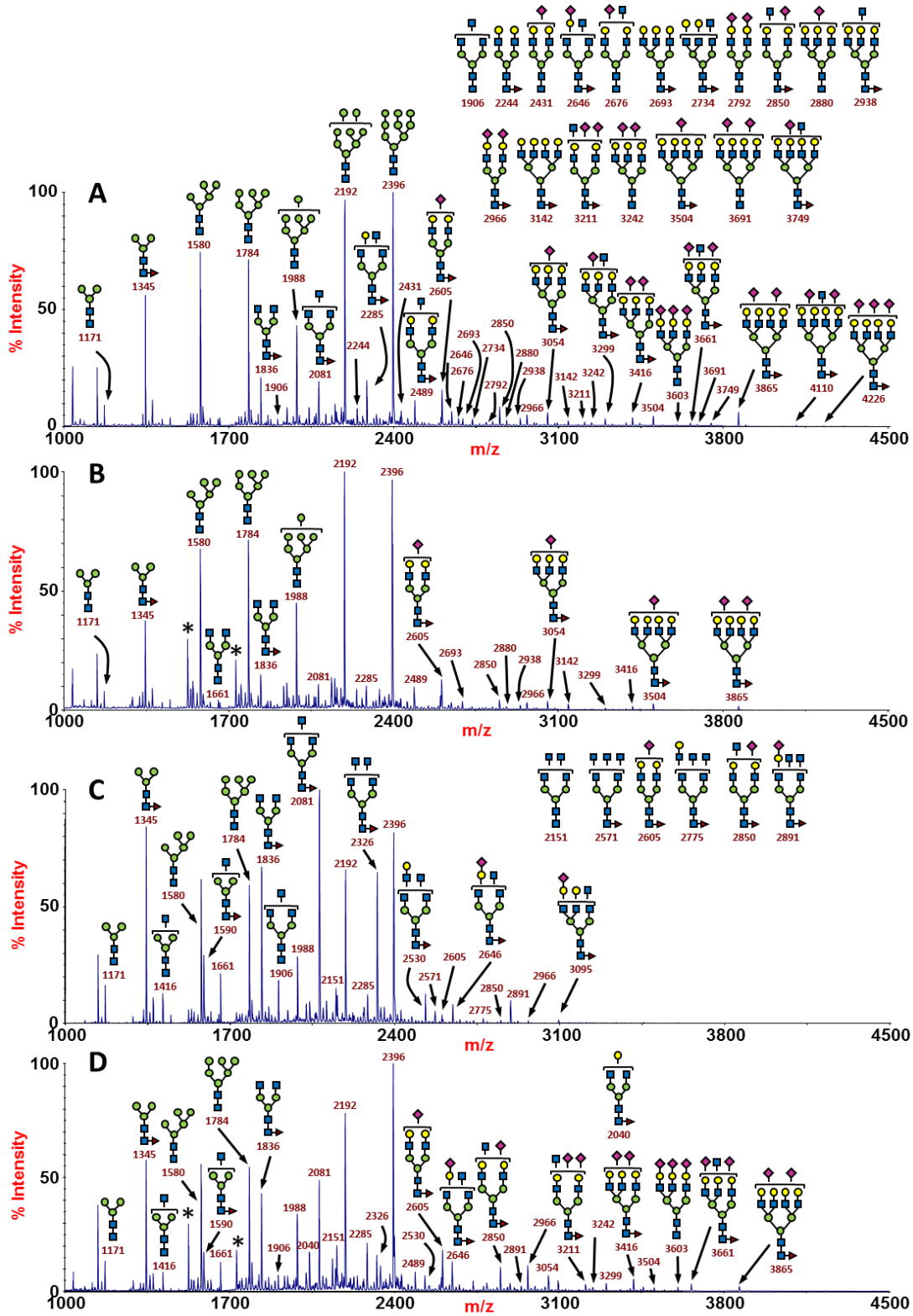

Figure 2. Galactose supplementation suppresses the observed galactosylation defect on N-glycans in TMEM165 KO cells. (A) MALDI-TOF-MS spectra of the permethylated N-glycans from control HEK293 cells. (B) MALDI-TOF-MS spectra of the permethylated N-glycans from control HEK293 cells treated with galactose (1 mM, 36 hours). (C) MALDI-TOF-MS spectra of the permethylated N-glycans from TMEM165 KO HEK293 cells. (D) MALDI-TOF-MS spectra of the permethylated N-glycans from TMEM165 KO HEK293 cells treated with Galactose (1 mM, 36 hours). The symbols representing sugar residues are as follows: closed square, N-acetylglucosamine; open circle, mannose; closed circle, galactose; open diamond, sialic acid; and closed triangle, fucose. Linkages between sugar residues have been removed for simplicity.

ICAM-1 levels increased significantly in vitro on galactose treatment of TMEM165-CDG patient cells

Immunohistochemistry showed a significant decrease in glycosylated InterCellular Adhesion Molecule 1 (ICAM-1) in cultured skin fibroblasts derived from patient 1 carrying the homozygous c.792+182G.A mutation (Supplemental Fig. 2). ICAM-1 has eight N-glycosylation sites and its cell surface expression is known to be markedly diminished in CDG cells. This finding is consistent with the global decrease of cell surface glycoprotein associated with TMEM165 deficiency. Following five days of galactose supplementation in culture media, a slight but significant improvement of ICAM-1 protein expression was observed by immunohistochemistry (Supplemental Fig. 2). This supports the beneficial effect of galactose supplementation in TMEM165 deficiency. The up-regulation of ICAM-1 cell surface expression was significant at 2.0mM and 10 mM D-galactose supplementation, with a 2.5 fold and 3.5 fold increase ($P = 0.006$ and 0.02), respectively. ICAM-1 western blot after 7 days of galactose supplementation also showed a 3.9-, 2-, and 2.8-fold increase at 0.75, 2.0 and 5 mM, respectively (data not shown).

Galactose supplementation is well tolerated and improves biochemical parameters in patients with TMEM165-CDG

Both patients were compliant with D-galactose supplementation during the study. Neither patient had diarrhea or vomiting during the trial. No other adverse effects or galactosuria were reported.

Improved well-being and increased activity levels were reported in both patients. Both, although carrying the same homozygous TMEM165 variant, showed substantial variability between laboratory parameters. The few overlapping abnormalities included increased baseline levels of blood creatine kinase, transaminases, prothrombin time, and thyroid-stimulating hormone. Furthermore, patient 1 had decreased factor IX activity and IGF1 and IGFBP3 levels. These levels were normal in the 16-year-older, adult patient, patient 2. He had decreased activated thromboplastin time (APTT) and antithrombin. Manganese levels were normal in blood samples.

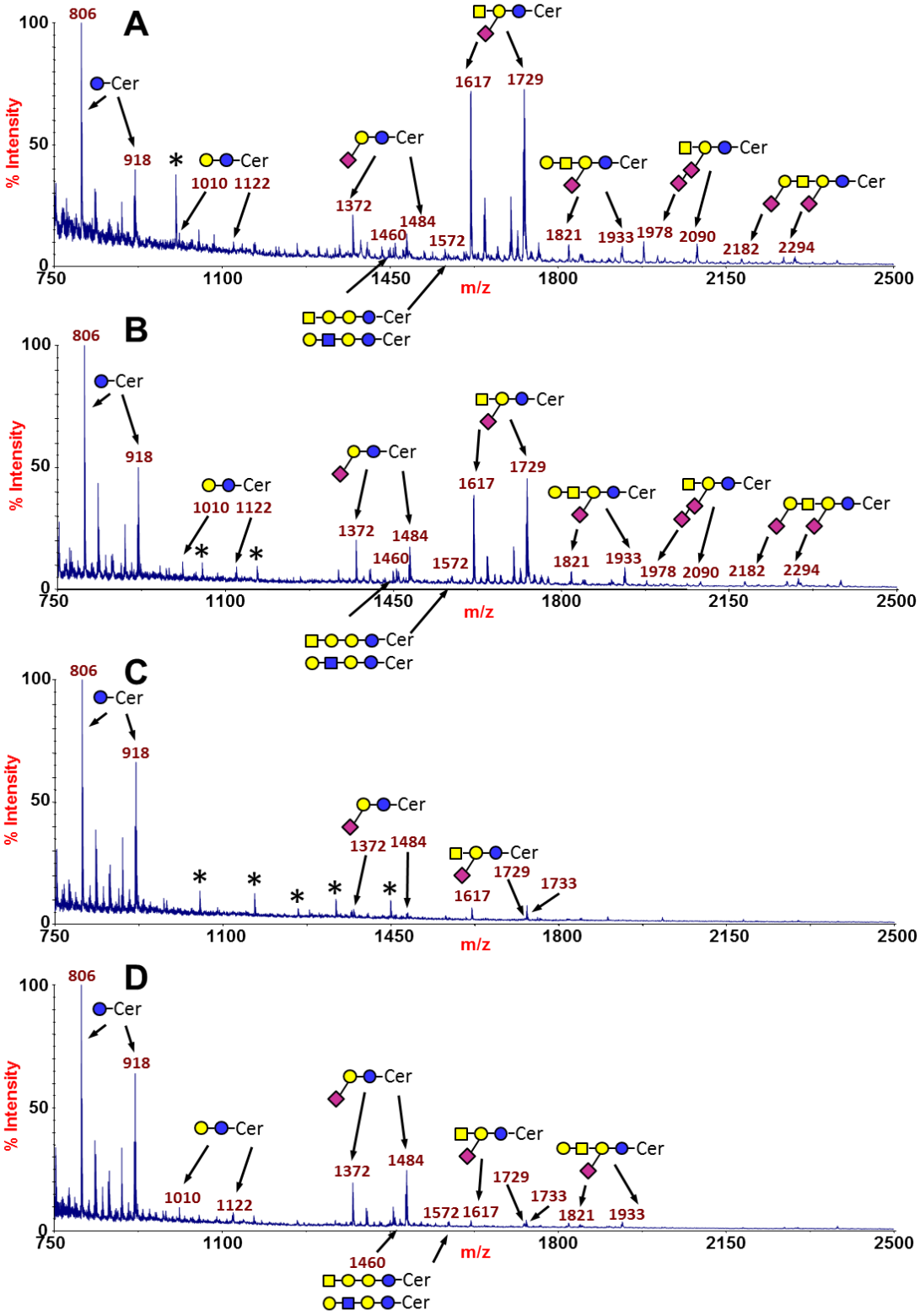

Figure 3. Galactose supplementation only partially suppresses the observed glycosylation defect on glycolipids in TMEM165 KO cells. (A) MALDI-TOF-MS spectra of permethylated glycolipids from control HEK 293 cells. (B) MALDI-TOF-MS spectra of permethylated glycolipids from control HEK 293 cells treated with galactose (1 mM, 36 hours). (C) MALDI-TOF-MS spectra of permethylated glycolipids from TMEM165 KO HEK293 cells. (D) MALDI-TOF-MS spectra of permethylated glycolipids from TMEM165 KO HEK293 cells treated with galactose (1 mM, 36 hours). The symbols representing sugar residues are as follows: yellow closed square, N-acetylgalactosamine; blue circle, glucose; yellow circle, galactose; open diamond, sialic acid. Linkages between sugar residues have been removed for simplicity. All GSLs are present as d18:1/C16:0 and d18:1/C24:0 ceramide isomers.

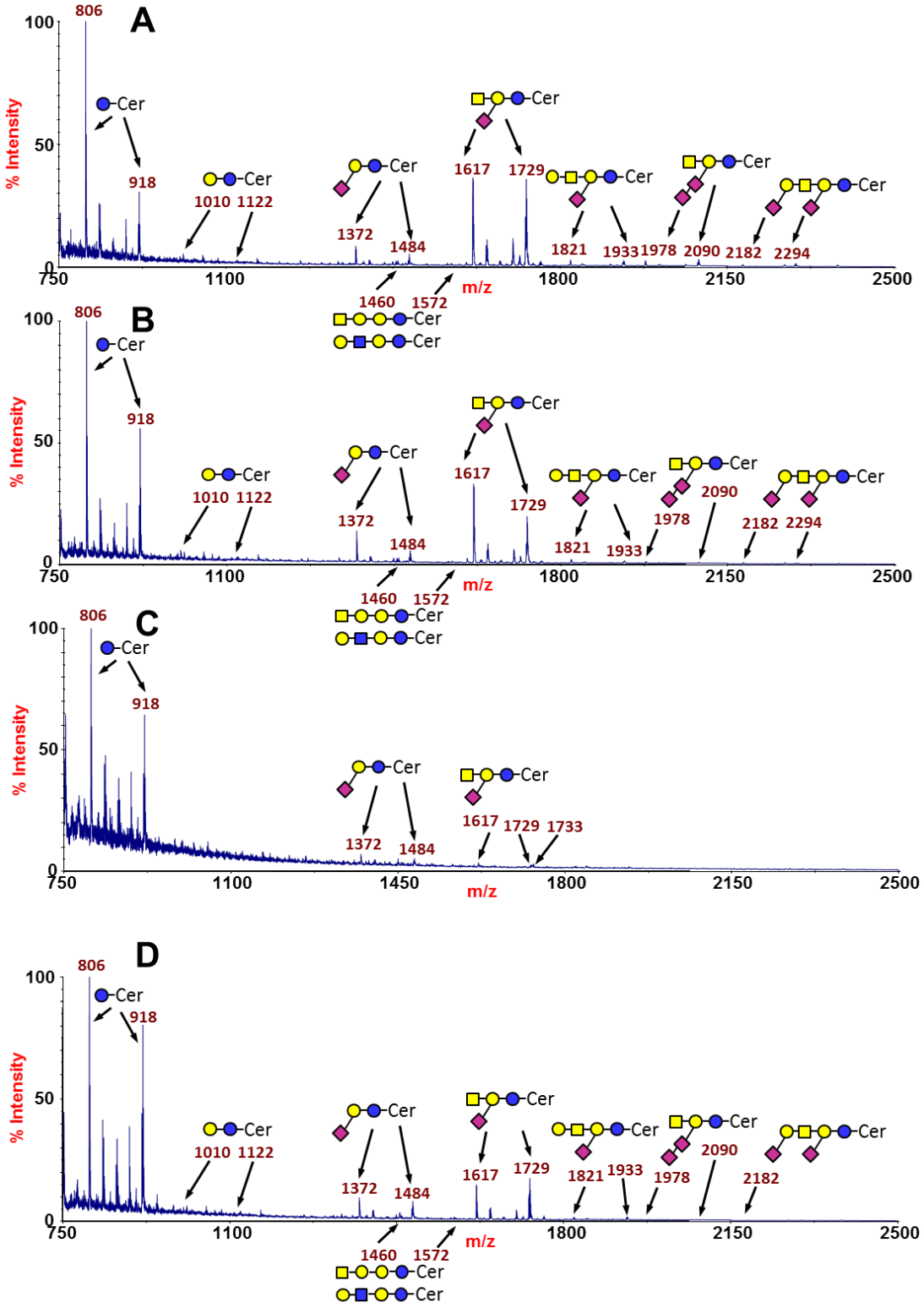

Figure 4. MnCl2 supplementation totally suppresses the observed glycosylation defect on glycolipids in TMEM165 KO cells. (A) MALDI-TOF-MS spectra of permethylated glycolipids from control HEK293 cells. (B) MALDI-TOF-MS spectra of permethylated glycolipids from control HEK293 cells treated with MnCl2 (100 µM, 36 hours). (C) MALDI-TOF-MS spectra of permethylated glycolipids from TMEM165 KO HEK293 cells. (D) MALDI-TOF-MS spectra of permethylated glycolipids from TMEM165 KO HEK293 cells treated with MnCl2 (100 µM, 36 hours). The symbols representing sugar residues are as follows: yellow closed square, N-acetylgalactosamine; blue circle, glucose; yellow circle, galactose; open diamond, sialic acid. Linkages between sugar residues have been removed for simplicity. All GSLs are present as d18:1/C16:0 and d18:1/C24:0 ceramide isomers.

Upon administration of oral D-galactose, there was either a prospective improvement or no substantial effect on the different laboratory parameters. Positive effects of galactose were observed for APTT, antithrombin, IGF1, IGFBP3, and alanine aminotransferase levels in either of the patients. Factor IX deficiency did not normalize in patient 1, but its improvement was apparently sufficient to normalize APTT. Alanine aminotransferase, but not aspartate aminotransferase, improved in patient 2. During the 18 weeks of D-galactose supplementation, there was no effect on creatine kinase, TSH, and cholesterol levels in either patient. To normalize parameters, 1 g/kg/d was sufficient, and no additional benefit was seen from increasing the dosage to 1.5 g/kg/d (Table 1).

Galactose treatment improves N-glycosylation in patients with TMEM165-CDG

To follow changes in N-glycosylation during galactose supplementation, serum N-glycan analysis was performed by mass spectrometry. Figure 5 shows the structures of the N-linked glycans on serum glycoproteins from 2 patients before and after galactose therapy.

Before galactose treatment, a strong presence of undersialylated and undergalactosylated glycans (Hex5HexNAc4 was at m/z 2040, and Hex4HexNAc4 was at m/z 1836) was observed. Interestingly, under galactose therapy, a consistent decrease in the abundance of the structures m/z 1836 (214%) and 2040 (214%) was seen. These results demonstrate the positive effects of the galactose therapy on glycosylation. To confirm these results, analysis was performed of the serum transferrin isoelectric focusing. Patient 1, the most severely affected, presented no substantial changes in 2-, 3-, and 4-sialo transferrin glycoforms under galactose therapy. However, a 15% decrease in 1-sialo and an 8% increase in 5-sialo transferrin glycoforms were observed. For the second patient, a 36% decrease in 1-sialo, a 55% decrease in 2-sialo, a 5% increase in 4-sialo, and a 24% increase in 5-sialo transferrin glycoforms were observed under galactose therapy. Altogether, these results highlight that galactose supplementation reduces the glycosylation defect initially observed in patients deficient in TMEM165.

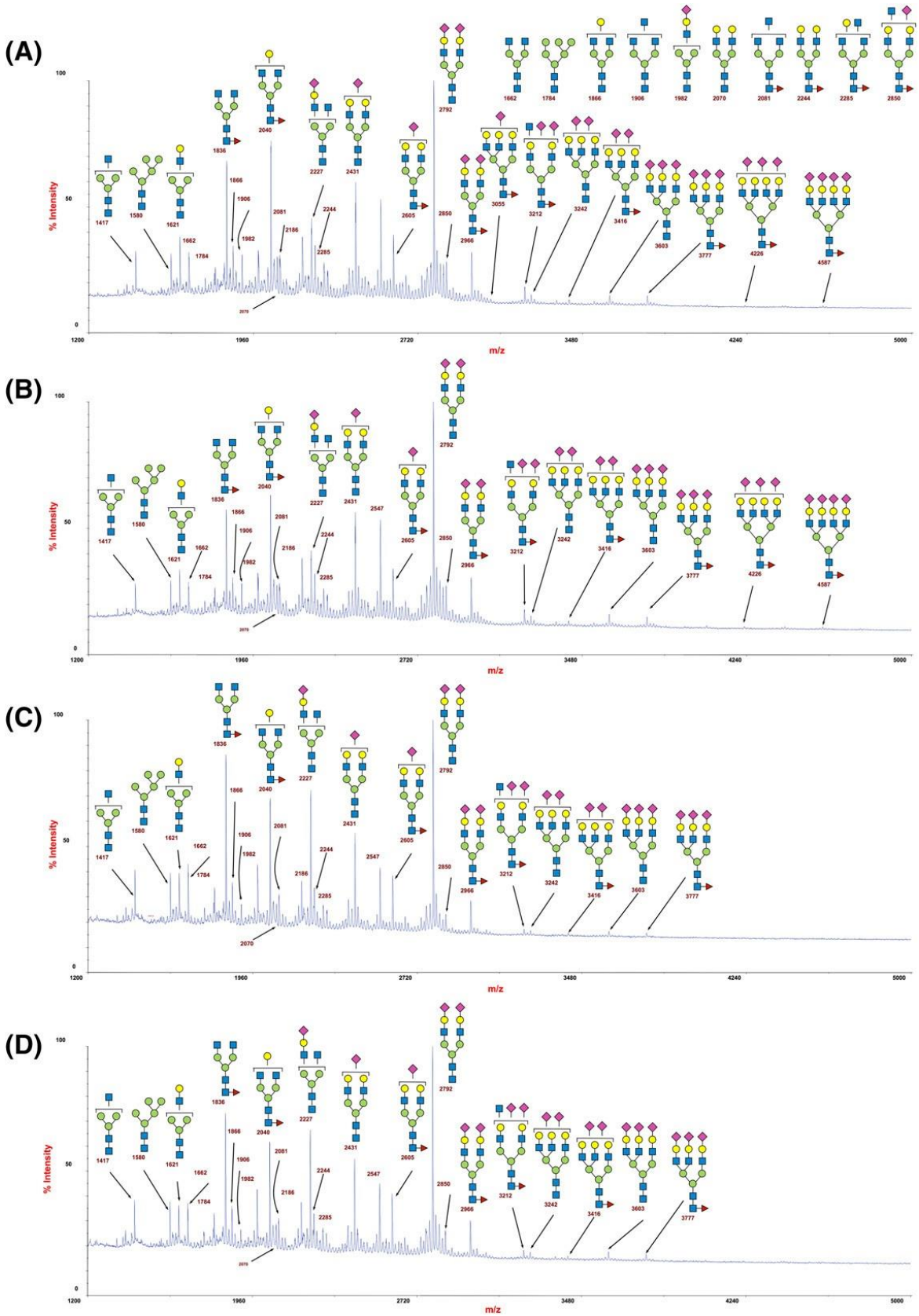

Figure 5. Galactose therapy ameliorates the N-glycosylation in individuals with TMEM165 deficiency. (A and C) MALDI-TOF-MS spectra of the permethylated N-glycans from sera of 2 patients with TMEM165 deficiency who carry the homozygous c.792+182G.A mutation. (B and D) MALDI-TOF-MS spectra of the permethylated N-glycans from sera after 18 weeks of galactose therapy. The symbols representing sugar residues are as follows: closed square, N-acetylglucosamine; open circle, mannose; closed circle, galactose; open diamond, sialic acid; and closed triangle, fucose. Linkages between sugar residues have been removed for simplicity.

DISCUSSION

TMEM165 deficiency is a subtype of CDG, a group of inherited diseases with impaired glycan biosynthesis (13–16). Here, we demonstrate that Golgi hypoglycosylation due to deficiency in TMEM165, a putative Golgi ion transporter and regulator in Golgi Mn2+ homeostasis, improves on galactose supplementation (3).

Recently, mutations have been described in another solute carrier transporter causing CDG, namely, the electroneutral $Mn2+/HCO3^{2-}$ and $Zn2+/HCO3^{2-}$ transporter encoded by SLC39A8 (17). This clearly demonstrates the crucial requirement of ion transporters to provide divalent cations for the activity of Golgi glycosyltransferases. Interestingly, Park and collaborators (17) have shown that oral galactose supplementation resulted in complete normalization of glycosylation in SLC39A8-CDG. Dietary supplementation of galactose has already been reported to be successful in patients with PGM1 deficiency and SLC35A2 deficiency (18, 19, 20). We wanted to test whether galactose treatment is beneficial in both TMEM165 KO cells and in patients with TMEM165-CDG. Oral galactose treatment of our patients was well tolerated and compliance was well achieved. No galactosuria occurred on incremental dosage. Manganese treatment was not attempted, because of normal blood levels of manganese and potential toxicity.

Galactose supplementation improved several, but not all, laboratory results in our patients (Table 1); specifically, coagulation parameters, IGF1, and IGFBP3 were improved in patient 1. The interindividual variability between patients (already at baseline) possibly was due to their different ages (16 years apart). Although most patients with CDG who underwent a trial of D-galactose supplementation in the past because of galactosylation defect showed some biochemical and/or clinical improvement after 2 to 3 months, we cannot rule out that a longer dietary period could have more obvious beneficial effects in patients with TMEM165-CDG. Consistent with these clinical observations, serum N-glycan analysis by mass spectrometry showed improved galactosylation in both patients under galactose therapy.

At the cellular level, a strong galactosylation defect was observed in both N-glycoproteins and glycolipids before treatment. Mn2+ treatment completely suppressed the glycosylation defect. However, differences were observed under galactose treatment, resulting in a complete normalization of N-linked glycans and a partial normalization of glycolipids. In TMEM165 KO cells, Mn2+ supplementation completely rescued the transfer of both Gal and GalNAc on glycolipids, whereas the galactose treatment only rescued the transfer of galactose residues on glycolipids.

This shows that TMEM165 deficiency not only impairs the activities of Golgi galactosyltransferases but also those of Golgi GalNAc transferases. Altogether, this reinforces the idea that the observed impaired Golgi glycosylation in TMEM165-deficient cells results from Golgi Mn2+ disturbances. How does galactose supplementation rescue the galactosylation defect? Galactose is known to be transported into the cells by several glucose transporters such as GLUT1, GLUT3, and GLUT4, the insulin-independent transporter (21). Within the cytosol, galactose is rapidly phosphorylated into galactose-1- phosphate. UDP-galactose (UDP-Gal) is then generated by the galactose-1-phosphate uridyltransferase that catalyzes the transfer of a UMP group from UDP-glucose to galactose-1-phosphate (22). Thus, galactose supplementation might be able to increase the intracellular level of UDP-Gal. Translocation of UDP-Gal from the cytosol to Golgi lumen occurs through the UDP-Gal transporter (UGT), which is an antiporter that mediates the exchange of cytosolic UDP-Gal and luminal UMP across the Golgi membrane. Two Golgi UDP-Gal transporters have been identified so far, UGT1 and UGT2 (23).

Although these transporters could play a role in the UDP-Gal Golgi luminal increase after galactose treatment, the import is strictly dependent on a UMP exchange (24, 25). In galactose-treated cells, we can reasonably hypothesize that the Golgi luminal UMP concentration, due to impaired Golgi galactose transporter activities, is too low to create a gradient sufficient to import UDP-Gal. Similarly, in a human disorder of UDP-Gal transport (SLC35A2 defect) treatment with galactose restores glycosylation and improves clinical symptoms in patients (19).

Another possibility is that cellular galactose entry is linked to Mn2+ entry. In that case, the glycosylation normalization observed under galactose treatment would be linked to a corresponding increase in cellular Mn2+. Our results show that this is unlikely, because glycolipid biosynthesis was altered after galactose or Mn2+ treatment in TMEM165-deficient cells.

The UGT transporters probably do not play any role in this process, because galactose treatment of CHO-Lec8 cells defective in UDP-Gal import in the Golgi increases galactosylation (19). One can hypothesize that UDP-Gal reaches the Golgi via the secretory pathway by using a UDP-Gal transporter localised in the endoplasmic reticulum (ER). Although no UDP-Gal transporters have clearly been identified in the ER so far, there are some promising candidates. In *Arabidopsis thaliana*, it was shown that AtUTr1 is a UDP-Gal/UDP-Glc transporter transporting UDP-Glc 200 times faster than UDP-Gal (26). Another interesting potential candidate is the UDP-galactose transporter-related protein 1 SLC35B1 that localizes to the ER membrane. It is possible that the cytosolic UDP-Gal increase favors the ER UDP-Gal entry by such transporters and its

transport toward the Golgi via the secretory pathway (27). Besides, it has also been shown that there is an association of the Golgi UDP-galactose transporter with UDP-galactose:ceramide galactosyltransferase, localized in the ER. This allows UDP-galactose entry in the ER that can be transported to the Golgi apparatus (28).

Park et al. (17) showed a robust effect of galactose supplementation in SLC39A8-deficient patients with manganese deficiency as an underlying cause of their glycosylation defect. As in TMEM165, supplementing manganese completely rescued the defect while there was only a partial restitution on galactose treatment. In this process, the most likely enzymatic step is β-1,4-galactosyltransferase, a manganese-dependent enzyme essential for glycan synthesis. Along these lines, we hypothesize that in TMEM165-CDG, the improvement due to galactose therapy is through a combination of increased cellular galactose uptake (via GLUT1), increased transport of UDP-Gal to the Golgi, and an increased activity of intraluminal galactosyltransferases, such as B4GALT1.

In conclusion, the beneficial effects of oral galactose supplementation on glycosylation adds TMEM165 deficiency to the list of CDG treatable by galactose.

Acknowledgements

We thank Dr. Dominique Legrand, Research Federation FRABio (Université Lille, CNRS, FR 3688, FRABio, Biochimie Structurale et Fonctionnelle des Assemblages Biomoléculaires), for providing the scientific and technical environment conducive to achieving this work. EURO-CDG-2 has received funding from the European Union's Horizon 2020 research and innovation program under the ERA-NET Cofund action No. 643578.

Funding

This work was supported by the French National Research Agency (SOLV-CDG to F.F); the Mizutani Foundation for Glycoscience (grant to F.F.); and, in part, by the Hayward Foundation and by the National Institute of General Medical Sciences of the National Institutes of Health, which funds the Louisiana Clinical and Translational Science Center (GrantNo. 1 U54 GM104940 to E.M.). P.W. is supported by the Clinical Research Foundation of UZ Leuven, Belgium.

Conflict of interests

None.

References

1. Foulquier F, Amyere M, Jaeken J, Zeevaert R, Schollen E, Race V, Bammens R, Morelle W, Rosnoblet C, Legrand D, Demaegd D, Buist N, Cheillan D, Guffon N, Morsomme P, Annaert W, Freeze HH, Van Schaftingen E, Vikkula M, Matthijs G. TMEM165 deficiency causes a congenital disorder of glycosylation. Am J Hum Genet. 2012;91(1):15–26.
2. Van Scherpenzeel M, Steenbergen G, Morava E, Wevers RA, Lefeber DJ. High-resolution mass spectrometry glycoprofiling of intact transferrin for diagnosis and subtype identification in the congenital disorders of glycosylation. Transl Res. 2015;166(6): 639–649.e1.
3. Potelle S, Morelle W, Dulary E, Duvet S, Vicogne D, Spriet C, Krzewinski-Recchi M-A, Morsomme P, Jaeken J, Matthijs G, De Bettignies G, Foulquier F. Glycosylation abnormalities in Gdt1p/TMEM165 deficient cells result from a defect in Golgi manganese homeostasis. Hum Mol Genet. 016;25(8):1489–1500.
4. Brown JR, Yang F, Sinha A, Ramakrishnan B, Tor Y, Qasba PK, Esko JD. Deoxygenated disaccharide analogs as specific inhibitors of beta1-4-galactosyltransferase 1 and selectin-mediated tumor metastasis. J Biol Chem. 2009;284(8):4952–4959.
5. Ramasamy V, Ramakrishnan B, Boeggeman E, Ratner DM, Seeberger PH, Qasba PK. Oligosaccharide preferences of beta1,4-galactosyltransferase-I: crystal structures of Met340His mutant of human beta1,4-galactosyltransferase-I with a pentasaccharide and trisaccharides of the N-glycan moiety. J Mol Biol. 2005;353(1): 53–67.
6. Ramakrishnan B, Ramasamy V, Qasba PK. Structural snapshots of beta-1,4-galactosyltransferase-I along the kinetic pathway. J Mol Biol. 2006;357(5):1619–1633.
7. Schroeder AS, Kappler M, Bonfert M, Borggraefe I, Schoen C, Reiter K. Seizures and stupor during intravenous mannose therapy in a patient with CDG syndrome type 1b (MPI-CDG). J Inherit Metab Dis. 2010;33(Suppl 3):S497–S502.
8. Park J-S, Ji IJ, An HJ, Kang M-J, Kang S-W, Kim D-H, Yoon S-Y. Disease-associated mutations of TREM2 alter the processing of Nlinked oligosaccharides in the Golgi apparatus. Traffic; 2015;16(5): 510–518.
9. Schindelin J, Arganda-Carreras I, Frise E, Kaynig V, Longair M, Pietzsch T, Preibisch S, Rueden C, Saalfeld S, Schmid B, Tinevez JY, White DJ, Hartenstein V, Eliceiri K, Tomancak P, Cardona A. Fiji: an open-source platform for biological-image analysis. Nat Methods. 2012;9(7):676–682.
10. Morelle W, Michalski J-C. Analysis of protein glycosylation by mass spectrometry. Nat Protoc. 2007;2(7):1585–1602.
11. Zeevaert R, de Zegher F, Sturiale L, Garozzo D, Smet M, Moens M, Matthijs G, Jaeken J. Bone dysplasia as a key feature in three patients with a novel congenital disorder of glycosylation (CDG) type II due to a deep intronic splice mutation in TMEM165. JIMD Rep. 2013;8:145–152.
12. De Smet E, Rioux J-P, Ammann H, Déziel C, Quérin S. FSGS permeability factor-associated nephrotic syndrome: remission after oral galactose therapy. Nephrol Dial Transplant 2009;24(9): 2938–2940.
13. Scott K, Gadomski T, Kozicz T, Morava E. Congenital disorders of glycosylation: new defects and still counting. J Inherit Metab Dis. 2014;37(4):609–617.
14. Freeze HH. Understanding human glycosylation disorders: biochemistry leads the charge. J Biol Chem. 2013;288(10):6936–6945.
15. Jaeken J. Congenital disorders of glycosylation. Handb Clin Neurol. 2013;113:1737–1743.
16. Krasnewich D. Human glycosylation disorders. Cancer Biomark. 2014;14(1):3–16.

17. Park JH, Hogrebe M, Grüneberg M, DuChesne I, von der Heiden AL, Reunert J, Schlingmann KP, Boycott KM, Beaulieu CL, Mhanni AA, Innes AM, Hörtnagel K, Biskup S, Gleixner EM, Kurlemann G, Fiedler B, Omran H, Rutsch F, Wada Y, Tsiakas K, Santer R, Nebert DW, Rust S, Marquardt T. SLC39A8 deficiency: a disorder of manganese transport and glycosylation. Am J Hum Genet. 2015; 97(6):894–903.

18. Morava E. Galactose supplementation in phosphoglucomutase-1 deficiency; review and outlook for a novel treatable CDG. Mol Genet Metab. 2014;112(4):275–279.

19. Dörre K, Olczak M, Wada Y, Sosicka P, Grüneberg M, Reunert J, Kurlemann G, Fiedler B, Biskup S, Hörtnagel K, Rust S, Marquardt T. A new case of UDP-galactose transporter deficiency (SLC35A2-CDG): molecular basis, clinical phenotype, and therapeutic approach. J Inherit Metab Dis. 2015;38(5):931–940.

20. Tegtmeyer LC, Rust S, van Scherpenzeel M, Ng BG, Losfeld M-E, Timal S, Raymond K, He P, Ichikawa M, Veltman J, Huijben K, Shin YS, Sharma V, Adamowicz M, Lammens M, Reunert J, Witten A, Schrapers E, Matthijs G, Jaeken J, Rymen D, Stojkovic T, Laforêt P, Petit F, Aumaître O, Czarnowska E, Piraud M, Podskarbi T, Stanley CA, Matalon R, Burda P, Seyyedi S, Debus V, Socha P, Sykut-Cegielska J, van Spronsen F, de Meirleir L, Vajro P, DeClue T, Ficicioglu C, Wada Y, Wevers RA, Vanderschaeghe D, Callewaert N, Fingerhut R, van Schaftingen E, Freeze HH, Morava E, Lefeber DJ, Marquardt T. Multiple phenotypes in phosphoglucomutase 1 deficiency. N Engl J Med. 2014;370(6):533–542.

21. Cura AJ, Carruthers A. Role of monosaccharide transport proteins in carbohydrate assimilation, distribution, metabolism, and homeostasis. Compr Physiol. 2012;2(2):863–914.

22. McDonald AG, Hayes JM, Davey GP. Metabolic flux control in glycosylation. Curr Opin Struct Biol. 2016;40:97–103.

23. Kawakita M, Ishida N. UDP-Gal transporter-1 and -2. In Taniguchi N, Honke K, Kukuda M, Narimatsu H, Yamiguchi Y, Angata T (eds). Handbook of Glycosyltransferases and Related Genes. Tokyo, Japan: Springer Japan; 2002: 511–517.

24. Kuhn NJ, White A. Evidence for specific transport of uridine diphosphate galactose across the Golgi membrane of rat mammary gland. Biochem J. 1976;154(1):243–244.

25. Guillen E, Abeijon C, Hirschberg CB. Mammalian Golgi apparatus UDP-N-acetylglucosamine transporter: molecular cloning by phenotypic correction of a yeast mutant. Proc Natl Acad Sci USA. 1998;95(14):7888–7892.

26. Reyes F, Marchant L, Norambuena L, Nilo R, Silva H, Orellana A. AtUTr1, a UDP-glucose/UDP-galactose transporter from Arabidopsis thaliana, is located in the endoplasmic reticulum and upregulated by the unfolded protein response. J Biol Chem. 2006; 281(14):9145–9151.

27. Dejima K, Murata D, Mizuguchi S, Nomura KH, Gengyo-Ando K, Mitani S, Kamiyama S, Nishihara S, Nomura K. The ortholog of human solute carrier family 35 member B1 (UDP-galactose transporter-related protein 1) is involved in maintenance of ER homeostasis and essential for larval development in Caenorhabditis elegans. FASEB J. 2009;23(7):2215–2225.

28. Sprong H, Degroote S, Nilsson T, Kawakita M, Ishida N, van der Sluijs P, van Meer G. Association of the Golgi UDP-galactose transporter with UDP-galactose:ceramide galactosyltransferase allows UDP-galactose import in the endoplasmic reticulum. Mol Biol Cell. 2003;14(8):3482–3493.

Supplementary figures

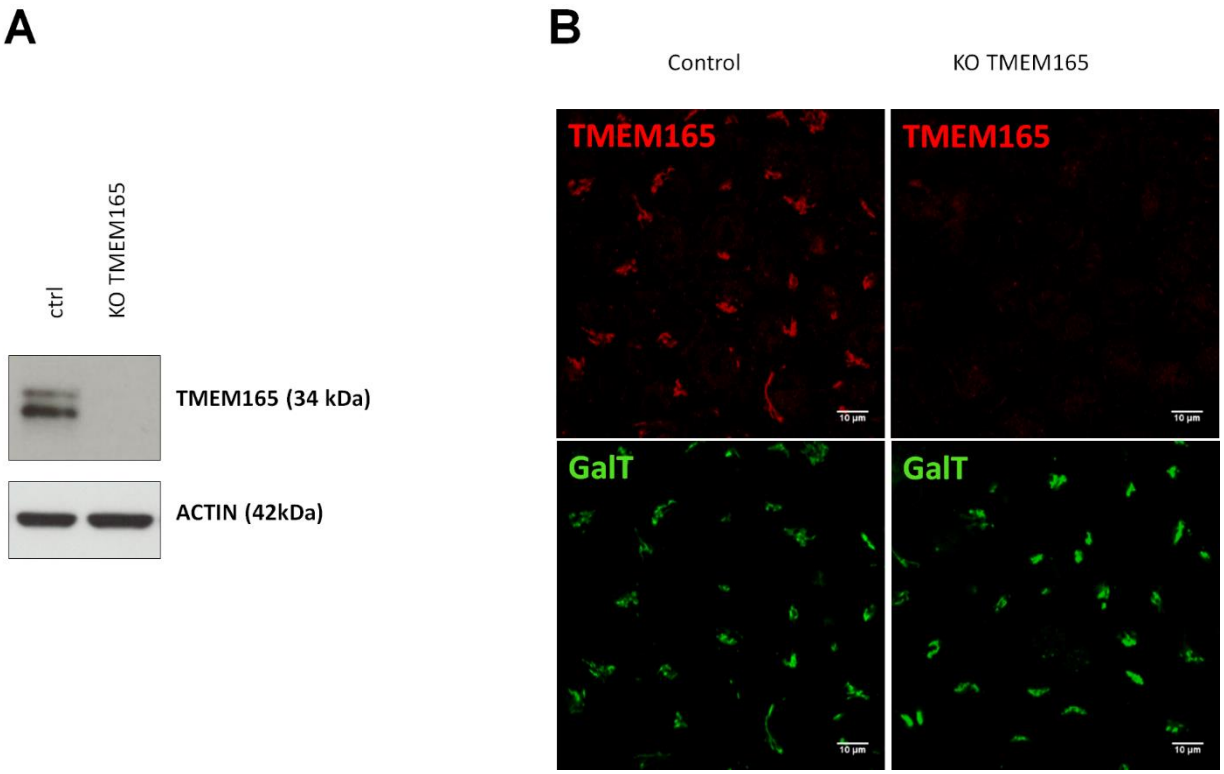

Supplementary figure 1: Verification of TMEM165 knockout by CRISPR-Cas9 on HEK293 cells. (A) Steady state cellular level of TMEM165. Total cell lysates were prepared, subjected to SDS-PAGE and Western blot with the indicated antibodies. **(B)** Control and KO TMEM165 cells were fixed and labeled with antibodies against TMEM165 and GalT (β4GalT1) before confocal microscopy visualization.

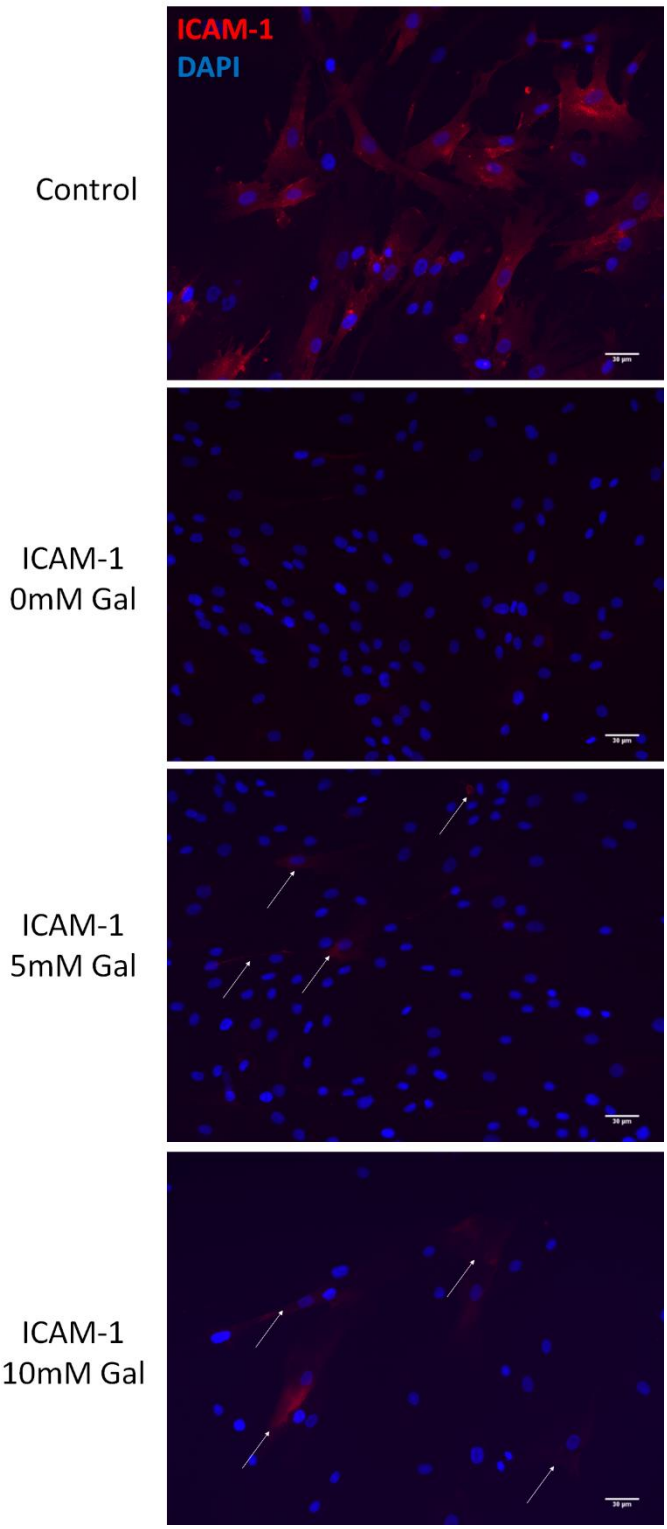

Supplementary figure 2: ICAM-1 levels increased in-vitro on galactose treatment of TMEM165-CDG patient fibroblasts. Control cells and TMEM165-CDG patient cells were treated for five days with the indicated galactose concentration. Cells were then fixed and labeled with antibodies against ICAM-1 before confocal microscopy visualization. DAPI staining was performed and shows the nucleus.

2.3. Complementary results

In addition to LAMP2, we have also analysed TGN46 migration profile by western blot in the same experimental conditions as the ones decribed for LAMP2 (Figure 37).

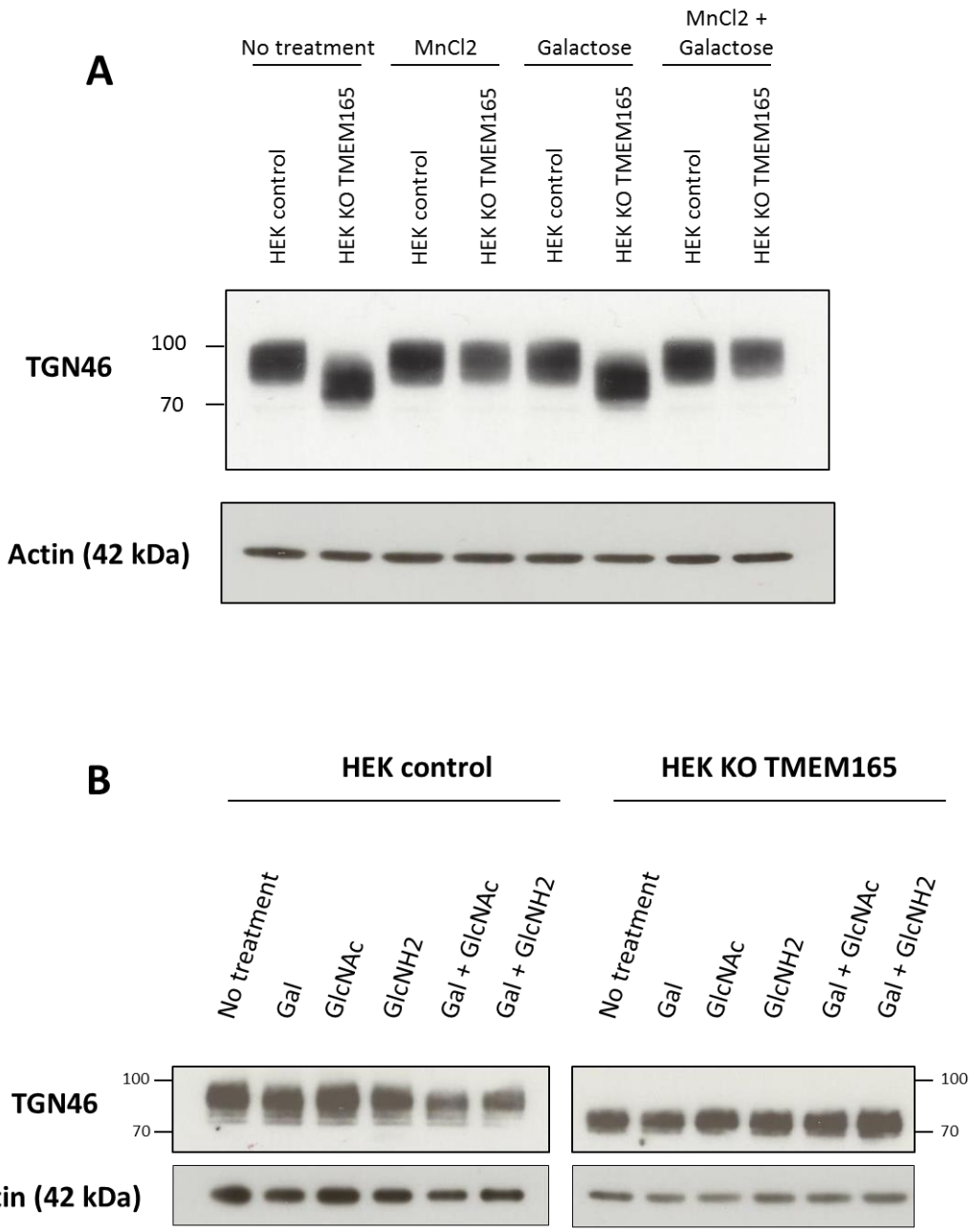

Figure 37. Galactose does not suppresses the observed TGN46 glycosylation defect in HEK TMEM165 KO cells. (A) Steady-state cellular level and gel mobility of TGN46. Control and TMEM165 KO HEK293 cells were cultured in absence or presence of galactose (1 mM), MnCl2 (100 µM), or galactose (1mM) + MnCl2 (100µM) for 18 hours; cell lysates were prepared, subjected to SDS-PAGE, and western blot with the indicated antibodies. (B) Steady-state cellular level and gel mobility of TGN46. Control and TMEM165 KO HEK293 cells were cultured in absence or presence of galactose (1 mM), glucosamine (5 mM), or N-acetylglucosamine (5 mM) for 36 hours. Cell lysates were prepared, subjected to SDS-PAGE, and western blot with the indicated antibodies.

Control and KO TMEM165 HEK293 cells were cultured without or with galactose supplementation in the culture medium. Consistent with our previous reports, a dramatic change in the TGN46 gel mobility was observed in TMEM165 KO HEK293 cells, indicating a severely defective glycosylation (Figure 37A). As expected, MnCl2 treatment completely restored normal TGN46 gel mobility in TMEM165 KO HEK293 cells. Interestingly, unlike LAMP2, TGN46 gel mobility was not normalised by 1mM galactose supplementation. Other monosaccharides were also tested, but none had any effect on the gel mobility of TGN46 in TMEM165 KO HEK293 cells (Figure 37B). These results demonstrate that D-galactose is unable to normalise TGN46 gel mobility.

2.4. Discussion

2.4.1. Deciphering the mechanism of galactose supplementation

In this study, we have demonstrated that Golgi glycosylation defects due to deficiency in TMEM165 improved on galactose supplementation. As a basic scientist, the main following is how does galactose supplementation rescue the galactosylation defect? Several possibilities came to our mind.

Galactose is known to be imported into the cells by several Glc transporters such as GLUT1, GLUT3, and GLUT4. Within the cytosol, Gal is phosphorylated into Gal-1-phosphate then converted in UDP-Gal by the Gal-1-phosphate uridylyltransferase (GALT). Thus, Gal supplementation might increase the cytosolic level of UDP-Gal, then boosting the Golgi uptake of UDP-Gal by SLC35A2. Finally, this will lead to an increase of UDP-Gal in the Golgi, which is the donor substrate for galactosyltransferases. However, UDP-Gal import in the Golgi is strictly dependent on a UMP exchange and we can reasonably think that in galactose-treated cells, the Golgi luminal UMP concentration is too low to create a gradient sufficient to highly increase the UDP-Gal uptake. Besides, in SLC35A2-CDG, treatment with galactose restores glycosylation and improves clinical symptoms in patients, proving that UDP-Gal Golgi uptake is not only linked to SLC35A2 function.

Therefore, one can hypothesize that UDP-Gal can reach the Golgi by using an ER UDP-Gal transporter. Although no UDP-Gal transporters have clearly been identified in the ER so far, there

are some promising candidates. For example, in *Arabidopsis thaliana*, it was shown that AtUTr1 is a UDP-Gal/UDP-Glc transporter in the ER transporting UDP-Glc 200 times faster than UDP-Gal [304]. A potential candidate in human is the UDP-galactose transporter-related protein 1 (SLC35B1) that localizes to the ER membrane and that is thought to be a UDP-Gal transporter. It is then conceivable that an increase in cytosolic UDP-Gal allows UDP-Gal entry in the ER by such transporters that will finally reach the Golgi via the secretory pathway. In addition, it has also been shown that there is an association of the Golgi UDP-Gal transporter with the UDP-galactose:ceramide galactosyltransferase, localized in the ER [305]. This also suggest a UDP-Gal entry in the ER that can then be transported to the Golgi apparatus.

Another possibility suggested by Park and collaborators for SLC39A8-CDG, is that galactose entry is linked to Mn2+ entry. In that case, the glycosylation normalization observed under galactose treatment would be linked to a corresponding increase in cellular Mn2+. Our results show that this is unlikely, because glycolipid biosynthesis was not fully normalized after galactose treatment. Indeed, we also observed a GalNAc defect that was only completely rescued after Mn2+ treatment.

2.4.2. Different effect of galactose and MnCl2 on LAMP2 and TGN46 gel mobility

Surprisingly, unlike LAMP2, TGN46 abnormal gel mobility was not normalized by galactose supplementation (Figure 37). Besides, LAMP2 gel mobility was improved but not totally normalized after galactose treatment (Figure 1 of the paper). In fact, TGN46 and LAMP2 both carry N-glycans but also mucin-type O-glycans, as described in the introduction of the first paper. As presented in the chapter 4 of the introduction, the first step of mucin-type O-glycosylation is likely to be affected by TMEM165 deficiency. Indeed, the transfer of the GalNAc residue by ppGalNAcT is Mn2+ dependent. Therefore, this step is only enhanced by Mn2+ supplementation and not by galactose treatment. Thus, the gel mobility differences observed on LAMP2 after MnCl2 or galactose treatment are probably due to the presence of O-glycans that are not normalized after galactose treatment.

Interestingly, TGN46 gel mobility does not seem to be normalized at all by galactose treatment. There are two explanations to this observation in our assay: either TGN46 N-glycosylation is

somehow not affected in TMEM165 depleted cells, or TGN46 is rather a marker of mucin-type O-glycosylation than a N-glycosylation marker.

Consequently, although classically used as quick readout for N-glycosylation, it is important to note that these two proteins also carry O-glycans that can have an impact on the interpretation of the results.

2.4.3. Galactose and Mn treatment in CDG

Dietary supplementation of galactose has already been reported to be successful in patients with PGM1 deficiency and SLC35A2 deficiency. However, in the case of PGM1-CDG, galactose supplementation also presented some limitations. Indeed, galactose was unable to permanently correct the glycosylation defect and did not improved growth rate in a PGM1-CDG patient [306]. More recently, Park and collaborators have shown that oral galactose supplementation resulted in complete normalization of glycosylation in SLC39A8-CDG. However, since SLC39A8 is an electroneutral $Mn2+/HCO3^{2-}$ and $Zn2+/HCO3^{2-}$ transporter at the plasma membrane, galactose supplementation can only treat symptoms attributable to hypogalactosylation and does not correct malfunction of other manganese-dependent enzymes. Therefore, authors have also tested the effects of Mn2+ on two SLC39A8-CDG patients. They noticed that Mn2+ can easily replace galactose to normalize transferrin glycosylation. They also observed a normalization of all biochemical parameters that were abnormal and some clinical parameters improved. Interestingly, no accumulation of Mn in the brain and no symptoms of manganism were observed after brain MRI.

These observations show that in the case of glycosylation defects due to Mn homeostasis disturbance, manganese supplementation represents a better therapeutic approach than galactose by its ability to correct all biochemical abnormalities that have been detected so far. It encourages us to try in Mn therapy on TMEM165-CDG patients in the near future. However, Mn treatment was not attempted as first therapeutic approach for several reasons. First, patients had normal blood levels of manganese and Mn supplementation could potentially be highly toxic for those patients. Second, compared to the normal daily intake of 1-2mg manganese in adults, the therapeutic dose is much higher to be efficient. Therefore, it requires to be carefully monitor with brain MRI check-ups to prevent manganism and thus Mn therapy is more difficult to setup than galactose therapy, already used in CDG.

2.5. Abstract in French

Contexte: TMEM165-CDG est une maladie multisystémique sévère qui se manifeste par une atteinte métabolique, endocrine et squelettique. Une déficience en TMEM165 conduit à un type de troubles congénitaux de la glycosylation (CDG), un groupe de maladies héréditaires dans lesquelles le processus de glycosylation est altéré. Un défaut de galactosylation a été observé chez les patients après analyse des N-glycanes sériques. Il y a à ce jour plus de 100 CDG, mais seuls certains CDG peuvent être traités.

Objectif: Le galactose s'est révélé bénéfique comme traitement dans d'autres types de CDG avec une galactosylation anormale. L'objectif de cette étude est de caractériser les effets d'une supplémentation en galactose sur la glycosylation golgienne dans les cellules HEK293 déficientes en TMEM165, ainsi que chez deux patients atteints de TMEM165-CDG.

Conception et mise en œuvre: La glycosylation a été évaluée par spectrométrie de masse, par western blot (de LAMP2 et ICAM-1) et par isoélectrofocalisation de la transferrine.

Résultats: Nous avons analysé les N-glycanes et glycolipides dans des cellules HEK293 déficientes en TMEM165, révélant des hypogalactosylations sévères et des défauts de transfert de GalNAc. Bien que ces défauts aient été complètement corrigés par l'addition de Mn2+, nous avons démontré que le défaut de N-glycosylation observé pouvait également être corrigé par une supplémentation en galactose. Nous avons ensuite montré que la supplémentation en galactose par voie orale chez les patients atteints de TMEM165-CDG a amélioré les paramètres biochimiques et cliniques, y compris une amélioration de la fonction endocrinienne et des paramètres de coagulation. Enfin, un début de normalisation du profil de glycosylation de la transferrine a été observé.

Conclusion: à notre connaissance, c'est la première fois qu'est décrite une glycosylation anormale des lipides due à une déficience en TMEM165. C'est également la première description d'un traitement oral efficace dans le cas d'une déficience en TMEM165. Nous recommandons donc l'utilisation de D-galactose par voie orale dans les cas de TMEM165-CDG.

[3] MANGANESE-INDUCED TURNOVER OF TMEM165

3.1. Introduction

In the first paper, we showed that TMEM165 was involved in Golgi Mn2+ homeostasis and then hypothesized that TMEM165 could be a novel Golgi Mn2+/Ca2+ antiporter. Although progresses have been made in identifying cellular Mn2+ transporters in mammals, the mechanisms of Mn2+ homeostasis maintenance are still unclear.

In 2005, Culotta and collaborators have published a review about Mn transport and trafficking in yeast. They present two members of the Nramp family of metal transporters (Smf1p and Smf2p) involved in intracellular trafficking of manganese [307]. Smf1p has been observed to localize to the plasma membrane of *S. cerevisiae* but its contribution in Mn2+ homeostasis seems limited under physiological conditions. Smf2p shares 50% identity with Smf1p but is localized in intracellular Golgi-like vesicles. Interestingly, these proteins are upregulated when yeasts are starved for manganese and targeted to vacuolar degradation when manganese levels become toxic. In fact, studies of Mn2+ homeostasis in yeasts have indicated that most of the proteins involved in Mn2+ homeostasis are differentially targeted and/or degraded in response to Mn2+ [307,308]. Besides, Dambach and collaborators have stated that the UPF0016 family certainly comprises proteins regulated by Mn2+ [309]. Moreover, in mammals, there is a protein named GPP130 that is known to be a specific Golgi Mn2+ sensor [299]. In presence of 500µM $MnCl_2$, GPP130 was shown to be targeted to lysosomal degradation via a Rab7 dependent mechanism.

Altogether, these publications led us to test the impact of high extracellular Mn2+ concentrations on the subcellular localisation and stability of TMEM165.

This study involves a combination of immunofluorescence and western blot experiments. We have once again employed GPP130 as a Golgi Mn2+ sensor. Cell surface biotinylation was performed to observe the putative TMEM165 fraction at the plasma membrane. TMEM165-CDG patient fibroblasts with E108G or R126H mutations and plasmid coding for TMEM165-E108G variants were also used in the study.

3.2. Publication

Manganese-induced turnover of TMEM165

Sven Potelle[1], Eudoxie Dulary[1], Leslie Climer[2], Sandrine Duvet[1], Willy Morelle[1], Dorothée Vicogne[1], Elodie Lebredonchel[1], Marine Houdou[1], Corentin Spriet[1], Marie-Ange Krzewinski-Recchi[1], Romain Peanne[3], André Klein[1], Geoffroy de Bettignies[1], Pierre Morsomme[4], Gert Matthijs[3], Thorsten Marquardt[5], Vladimir Lupashin[2] and François Foulquier[1]

[1]CNRS, UMR 8576 – UGSF – Unité de Glycobiologie Structurale et Fonctionnelle, Université de Lille, Lille F-59000, France;

[2]Department of Physiology and Biophysics, College of Medicine, University of Arkansas for Medical Sciences, Biomed 261-2, Slot 505, 200 South Cedar St., Little Rock, AR 72205, U.S.A.;

[3]Center for Human Genetics, KU Leuven, Leuven, Belgium;

[4]Institut des Sciences de la Vie, Université catholique de Louvain, Louvain-la-Neuve B-1348, Belgium;

[5]Klinik und Poliklinik für Kinder- und Jugendmedizin, Universitätsklinikum Münster, Albert-Schweitzer-Campus 1, Gebäude A 1, Münster 48149, Germany

Correspondance: François Foulquier (francois.foulquier@univ-lille1.fr)

Abstract

TMEM165 deficiencies lead to one of the congenital disorders of glycosylation (CDG), a group of inherited diseases where the glycosylation process is altered. We recently demonstrated that the Golgi glycosylation defect due to TMEM165 deficiency resulted from a Golgi manganese homeostasis defect and that Mn2+ supplementation was sufficient to rescue normal glycosylation. In the present paper, we highlight TMEM165 as a novel Golgi protein sensitive to manganese. When cells were exposed to high Mn2+ concentrations, TMEM165 was degraded in lysosomes. Remarkably, while the variant R126H was sensitive upon manganese exposure, the variant E108G, recently identified in a novel TMEM165-CDG patient, was found to be insensitive. We also showed that the E108G mutation did not abolish the function of TMEM165 in Golgi glycosylation. Altogether, the present study identified the Golgi protein TMEM165 as a novel Mn2+-sensitive protein in mammalian cells and pointed to the crucial importance of the glutamic acid (E108) in the cytosolic ELGDK motif in Mn2+-induced degradation of TMEM165.

Introduction

Manganese is a trace element essential for life. It is involved in the catalytic domain of many enzymes such as Golgi glycosyltransferases, mitochondrial enzymes, and DNA and RNA polymerases. Regulation of its homeostasis is therefore particularly important. Manganese overexposure has been shown to induce neurological symptoms that can result in a Parkinson-like disorder called manganism [1–3]. On the contrary, a decrease in cellular Mn2+ has recently been shown to cause congenital disorders of glycosylation (CDG). Mutations in SLC39A8, a putative plasma membrane manganese transporter, lead to severe glycosylation defects [4]. We recently reported that TMEM165 deficiency was also linked with Golgi Mn2+ homeostasis [5]. Although progress has been made in identifying cellular Mn2+ transporters in mammals, the mechanisms of Mn2+ homeostasis are still unclear. Several different transporters have been involved in manganese transport mechanisms, including the divalent metal transporter 1 (DMT1/NRAMP2/SLC11A2) [1,6], NRAMP1 [7], the transferrin receptor, and the transporters SLC30A10/ZNT8 [8], SLC39A8/ZIP8 [4], and SLC30A14/ZIP14 [9,10]. At the cellular level, most of these transporters are localized at the plasma membrane and/or in endosomes. The secretory pathway consisting of the ER, the Golgi and associated vesicles is also crucial in regulating cellular

Mn2+ homeostasis. In addition, the secretory pathway requires luminal Mn2+ concentration for quality control, proper targeting and processing of proteins. Current knowledge supports that this supply is realized via the action of SPCA1 (secretory pathway Ca-ATPase 1: ATP2C1) and SPCA2 (ATP2C2). SPCA1 is ubiquitously expressed and mediates the import of Ca2+/Mn2+ into the Golgi lumen [11,12]. The tissue expression of SPCA2 is more restricted. However, the importance of the dual transport function in cellular processes is not yet completely deciphered [11]. Overexpression of SPCA1 has been shown to facilitate Mn2+ accumulation into the Golgi [13] and it was thus proposed that SPCA1 was a way to detoxify cytosolic Mn2+ accumulation by sequestering it into the secretory pathway.

In 2012, we identified TMEM165 as a novel Golgi transmembrane protein causing CDG [14]. It belongs to an uncharacterized family of membrane proteins named UPF0016 (Uncharacterized Protein Family 0016; Pfam PF01169). We recently demonstrated that the observed Golgi glycosylation defect resulted from Golgi Mn2+ homeostasis impairment [5]. Based on these results, we hypothesized that TMEM165 could be a novel Golgi Mn2+ transporter. As studies of Mn2+ homeostasis in yeasts have indicated that most of the proteins involved in regulating intracellular Mn2+ concentrations are differentially targeted and/or degraded in response to Mn2+, the role of TMEM165 was tested. The aim of the present study was to decipher the impact of high extracellular Mn2+ concentrations on the subcellular localization and stability of TMEM165. The present study demonstrates that high concentrations of extracellular Mn2+ lead to a rapid lysosomal degradation of TMEM165. We identified the glutamic acid (E108) in the highly conserved motif ELGDK, oriented toward the cytosol, as being crucial in the Mn-induced degradation of TMEM165.

Results

TMEM165 is rapidly and specifically degraded in response to Mn2+

Our previous work highlighted a link between TMEM165 and Golgi Mn2+ homeostasis [5]. As many proteins involved in regulating intracellular Mn2+ homeostasis are directly impacted in their stability by cellular Mn2+ homeostasis changes, the effect of Mn2+ on TMEM165 was tested. For this, a concentration of 500 µM of MnCl2 was first used for different times and the stability of TMEM165 was assessed both by western blot and immunofluorescence experiments. We observed that in response to Mn2+, TMEM165 levels were significantly reduced (Figure 1A,

B). Interestingly, the same sensitivity to Mn2+ was observed for Gdt1p, the yeast ortholog of TMEM165 (Figure 1D). The effects of other ions were also tested (Supplementary Figure S1). Remarkably, we observed that TMEM165 degradation only occurred after MnCl2 exposure, pointing to the specificity of TMEM165 for Mn2+. As GPP130 has also been shown to be sensitive to high Mn2+ concentrations, we compared its time course degradation with TMEM165 (Figure 1A–C). Quantification indicated that TMEM165 loss exceeded 95% after 8 h of Mn2+ treatment, while only a 40% decrease was seen for GPP130. To further tackle the minimal Mn2+ concentration able to induce a loss of TMEM165, we analyzed the stability of TMEM165 with low MnCl2 concentrations (1–50 µM). While 100 µM MnCl2 was sufficient to induce GPP130 degradation [15], our results showed that 1–25 µM of Mn2+ was already sufficient to induce a destabilization of TMEM165 (Figure 1B). Altogether these results indicate that TMEM165, compared with GPP130, is more sensitive to manganese and probably suggests the existence of different degradation mechanisms in response to Mn2+. The impact of Mn2+ on TMEM165 was also seen by immunofluorescence where a decrease in TMEM165 fluorescence associated with Golgi was seen (Supplementary Figure S2A, B). We previously demonstrated that TMEM165 could be found at the plasma membrane [14]. To assess the impact of Mn2+ on the plasma membrane targeted form of TMEM165, surface protein biotinylation was performed in the absence and presence of 500 µM of MnCl2. Interestingly biotin-labeled cell surface TMEM165 displayed the same sensitivity to Mn2+ as the cellular TMEM165. This either suggests that the Mn2+-induced degradation mechanism is not only dedicated to the Golgi pool of TMEM165 or that less TMEM165 traffics to the plasma membrane from the Golgi when the Golgi pool of TMEM165 has been depleted upon excess manganese exposure (Figure 2A). Previous studies have also demonstrated that in yeast, high environmental Ca2+ concentrations in *gdt1Δ* led to strong N-glycosylation deficiencies [5]. The impact of Ca2+ on Mn2+-induced degradation of TMEM165 was assessed by western blot and immunofluorescence (Figure 2B, C). Ca2+ alone had no significant effect on the stability of TMEM165. However, its combined presence with Mn2+ clearly decreased the Mn2+-induced degradation of TMEM165 (80% decrease for the Mn2+ treatment alone compared with 40% decrease for both Ca2+ and Mn2+; Figure 2B). This was confirmed by confocal microscopy (Figure 2C).

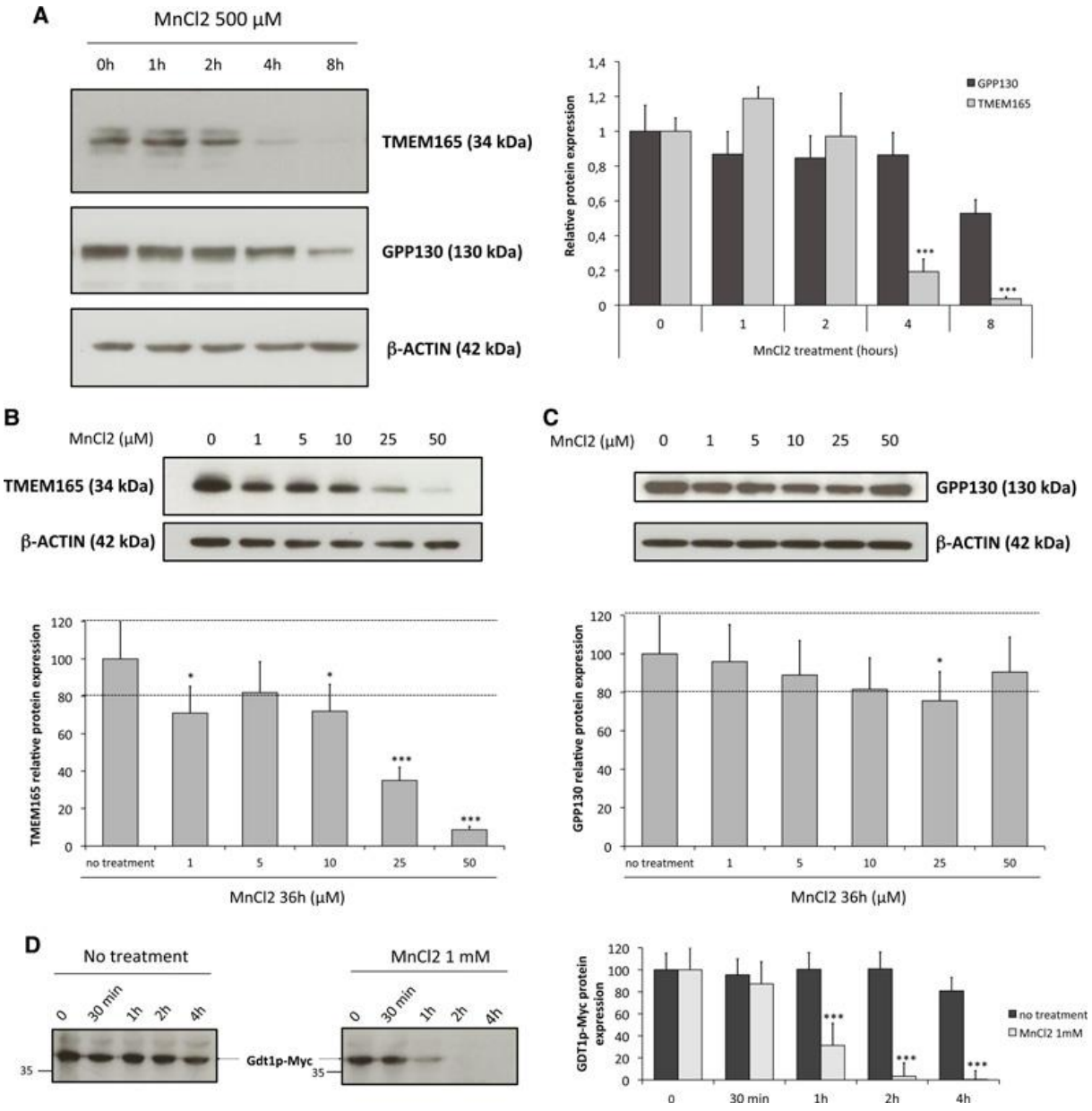

Figure 1. TMEM is rapidly degraded in response to Mn2+. (A) Steady-state cellular level of TMEM165 and GPP130. HeLa cells were treated with MnCl2 500 µM for 0–8 h. Total cell lysates were prepared, and subjected to SDS–PAGE and western blot with the indicated antibodies. Right panel shows the quantification of TMEM165 and GPP130 protein levels after normalization with actin [Number of experiments (N) = 2; ***P-value < 0.001]. (B) Steady-state cellular level of TMEM165. HEK293 cells were treated with MnCl2 from 0 to 50 µM for 36 h. Total cell lysates were prepared, and subjected to SDS–PAGE and western blot with the indicated antibodies. Lower panel shows the quantification of TMEM165 protein levels after normalization with actin (N = 2; ***P-value < 0.001). (C) Steady-state cellular level of GPP130 in the same experimental conditions as described in (B). (D) *Gdt1Δ* yeasts expressing Gdt1p-Myc were cultured in the absence or presence of 1 mM MnCl2. Yeast lysates were then subjected to SDS–PAGE and western blot analysis with the indicated antibodies. Right panel shows the quantification of the Gdt1p-Myc protein levels (N = 2; ***P-value < 0.001).

Lysosomal degradation of TMEM165

As shown by Mukhopadhyay et al. [16], 500 µM MnCl2 treatment induces rapid redistribution of GPP130 in vesicles before their lysosomal degradation. At the opposite of GPP130, no redistribution from the Golgi to peripheral punctate structures was observed for TMEM165 in

response to high Mn2+ concentration (Supplementary Figure S2C). This absence of vesicles could be explained by an extremely fast degradation. To test this hypothesis, the stability of TMEM165 in response to Mn2+ was studied by immunofluorescence in the presence of chloroquine, a lysosomal inhibitor (Figure 3A).

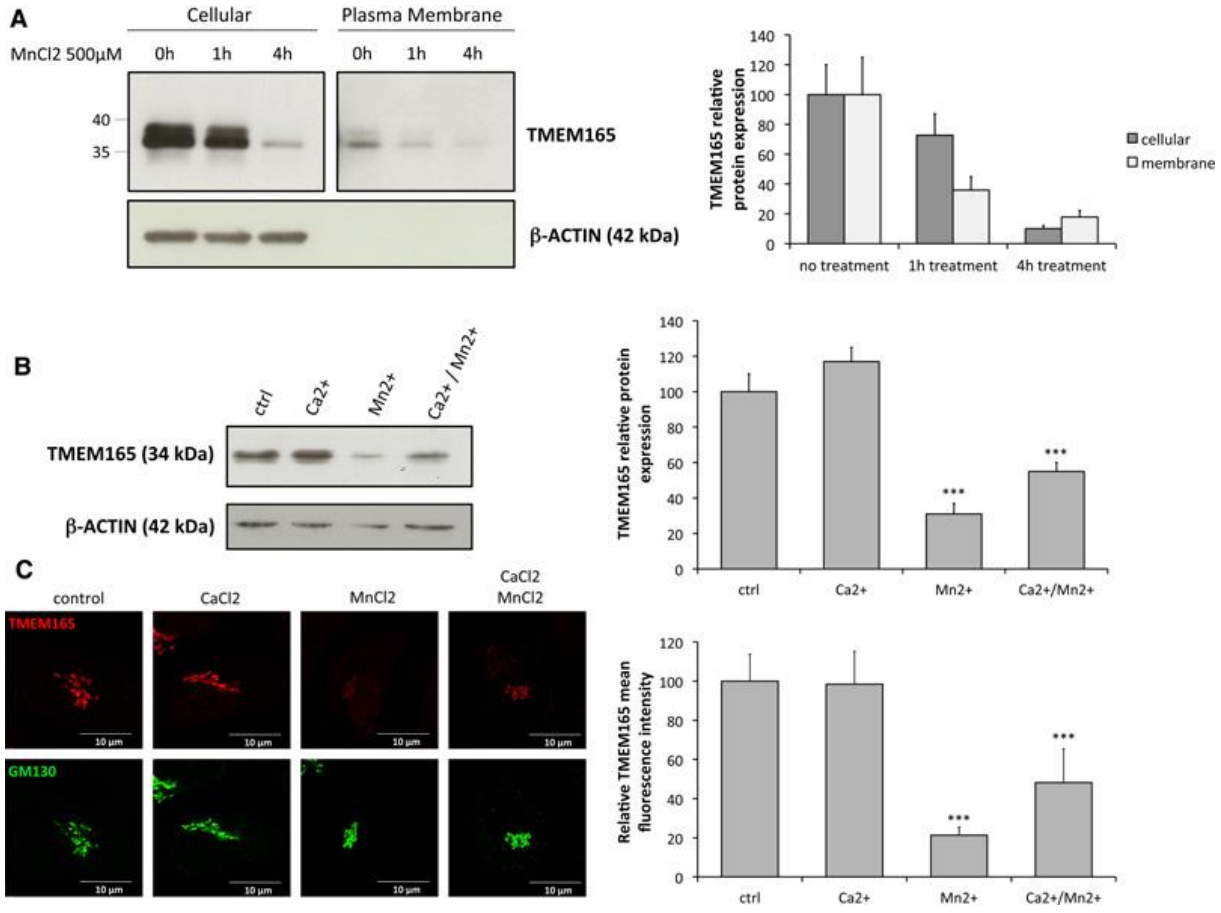

Figure 2. Plasma membrane TMEM165 is also degraded by Mn2+ and Ca2+ compete with Mn2+ for TMEM165 degradation. (A) Cell surface biotinylation was performed in the absence and presence of MnCl2 500 µM. Samples were prepared as described in the materials and methods section and subjected to SDS–PAGE and western blot with the indicated antibodies. Lower panel shows the quantification of TMEM165 protein levels. The plasma membrane panel is separated from the cellular panel as we had to expose films longer to reveal the bands. (B) HEK293 cells were incubated with 500 µM MnCl2 and/or 2 mM CaCl2 for 4 h, and then subjected to SDS–PAGE and western blot with the indicated antibodies. Right panel shows the quantification of TMEM165 protein levels after normalization with actin (N = 2; ***P-value < 0.001). (C) HEK293 cells were incubated with 500 µM MnCl2 and/or 2 mM CaCl2 for 4 h, and then fixed and labeled with antibodies against TMEM165 and GM130 before confocal microscopy visualization (N = 2; ***P-value < 0.001). Right panel shows the quantification of the associated TMEM165 fluorescence intensity (N = 2; n = 50; ***P-value < 0.001).

Although cells treated with Mn2+ alone showed a dramatic loss of TMEM165, those treated in the presence of chloroquine exhibited an accumulation of TMEM165 in punctate structures (Figure 3A). Immunofluorescence experiments with LAMP2, a lysosomal marker, confirmed the presence of TMEM165 in LAMP2-positive structures in chloroquine- and Mn2+ -treated cells. The level of co-localization was determined using Manders' overlap coefficient and revealed a co-

localization of TMEM165 with LAMP2 (72 ± 9%). Same experiments were also done with EEA1 as a specific marker of early endosomes and the quantification revealed no significant co-localization of TMEM165 with EEA1 (7 ± 1%; data not shown). This result shows that TMEM165 is specifically targeted to lysosomal degradation followed Mn2+ exposure. To confirm the lysosomal Mn2+ -induced degradation of TMEM165, an immunoblotting experiment was also performed. As shown in Figure 3B, the Mn-induced degradation of TMEM165 was completely blocked by chloroquine. As chloroquine is known to both shut down endosomal trafficking and inhibit lysosomal proteases, we also tested the effects of leupeptin, a lysosomal protease inhibitor, on the stability of TMEM165 in response to Mn2+ (Supplementary Figure S3). The experiment confirmed the localization of TMEM165 in LAMP2-positive structure as a co-localization of TMEM165 with LAMP2 (62 ± 1%) and the absence of co-localization of TMEM165 with EEA1 (3 ± 1%; data not shown) was observed.

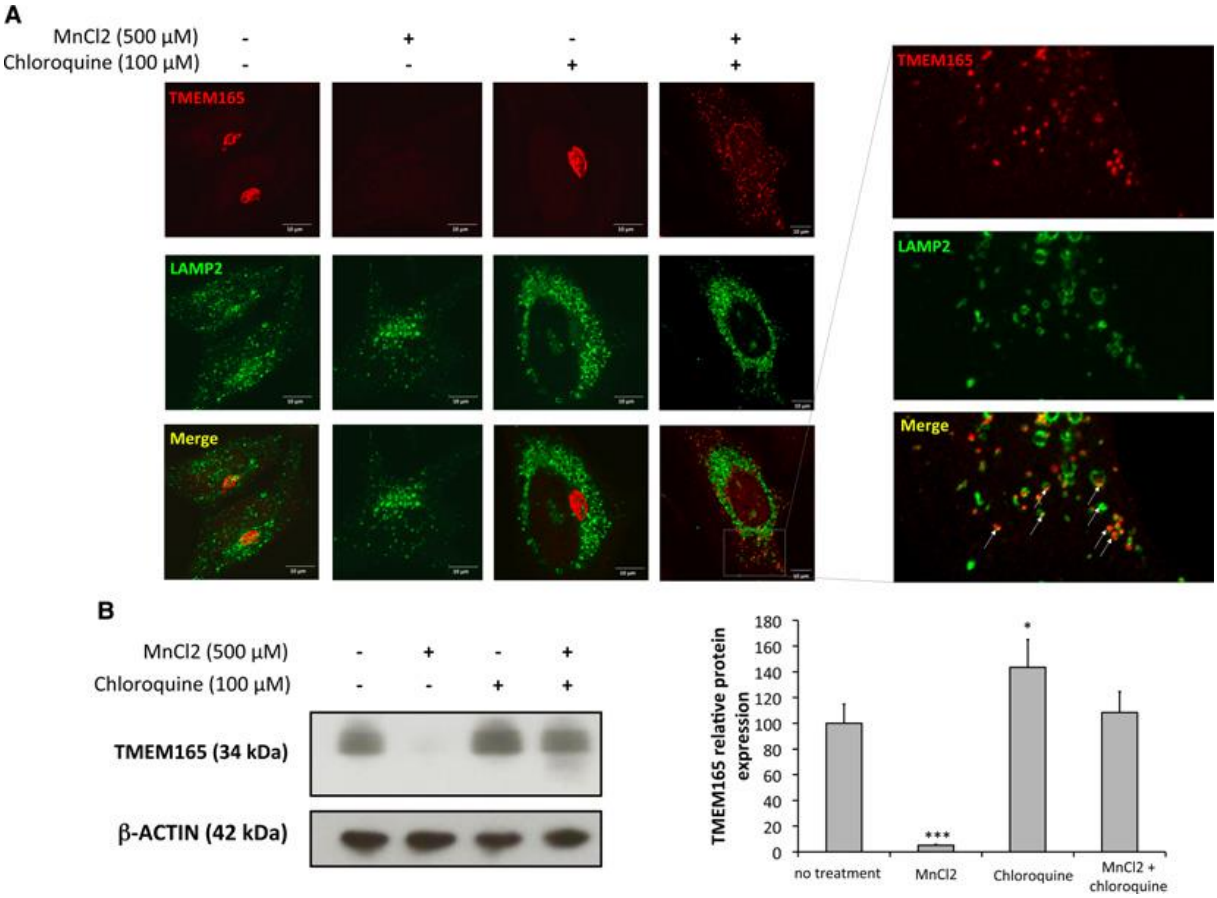

Figure 3. TMEM165 is targeted to lysosomal degradation after Mn2+ exposure. (A) HeLa cells were treated for 8 h with 500 µM MnCl2 and/or 100 µM chloroquine, and fixed and labeled with antibodies against TMEM165 (upper panels) and LAMP2 (middle panels) before confocal microscopy visualization. (B) Western blot analysis of the same experiment described in (A). Total cell lysates were prepared, and subjected to SDS–PAGE and western blot with the indicated antibodies. Right panel shows the quantification of the TMEM165 protein level after normalization with actin (N = 2; ***P-value < 0.001).

The amino acid E108 of the ELGDK motif is involved in Mn2+-induced degradation of TMEM165

To gain more insight into the TMEM165 Mn2+-induced degradation mechanism, we wondered whether the reported missense mutations (pE108G and pR126H) found in TMEM165-deficient CDG patients could impact the TMEM165 Mn2+ sensitivity. To test the putative role of these mutations in TMEM165 Mn2+ responsiveness, immunofluorescence and western blot experiments were performed in the absence and presence of MnCl2 (Figure 4A,B). The missense mutation c.323 A>G (p.E108G) found in two newly TMEM165 deficient siblings was first tested [17]. As observed for wt-TMEM165, the mutant form is Golgi-localized in fibroblasts for the two siblings. This indicates that the mutation does not disturb the subcellular localization of the mutated form of TMEM165 (Figure 4B). The impact of Mn2+ treatment was then investigated during an 8 h time course by western blot and immunofluorescence experiments (Figure 4A, B). As expected, the wild-type (wt) TMEM165 was very sensitive to Mn2+ exposure (Figure 4A). However, the mutated form of TMEM165 (E108G) remained stable (Figure 4A, B). No changes were observed in localization or stability by immunofluorescence. Quantification of the western blot results indicated that wt-TMEM165 loss exceeded 95% at the 6 h time point, while only 20% loss was observed for the mutated form p.E108G. To demonstrate the distinctive feature of this mutation, fibroblasts from another TMEM165-CDG patient, carrying the R126H mutation, were also tested for Mn2+ sensitivity by western blot and confocal microscopy (Figure 5). Although the steady-state level of TMEM165, compared with control fibroblasts, is lower in the R126H patients' fibroblasts, our results highlighted that this mutation did not prevent the Mn2+ -induced TMEM165 (R126H) degradation. It is also important to note that its localization is not altered, neither at the steady-state level nor after chloroquine and Mn2+ exposure (Supplementary Figure S5). After Mn2+ and chloroquine exposure, the co-localization between TMEM165 and LAMP2/EEA1 was determined for both control and patient fibroblasts. For control fibroblasts, we observed a co-localization of TMEM165 with LAMP2 (59 ± 5%) and no significant co-localization of TMEM165 with EEA1 (6 ± 1%). For patient fibroblasts (R126H), the results were the same. A co-localization of TMEM165 with LAMP2 (58 ± 11%) but no significant co-localization of TMEM165 with EEA1 (5 ± 1%) was observed. Interestingly, the western blot results showed that the R126H variant is stabilized upon Mn2+ and chloroquine exposure (Supplementary Figure S5C). This clearly demonstrates that this allele is constitutively able to traffic to the lysosomes upon Mn2+ exposure. In summary, our results support the evidence that the glutamic acid (E) of the highly conserved ELGDK motif is crucial in mediating the lysosomal degradation of TMEM165

in response to Mn2+. To determine whether the E108G mutation could also affect the function of TMEM165, the glycosylation status of LAMP2 was assessed in TMEM165 KO HEK293 cells generated by CRISPR-Cas9 (Figure 4C and Supplementary Figure S4). Both the expression of the wt-TMEM165 and the E108G mutant complemented the observed glycosylation defect. Compared with the expression of the wt TMEM165, the expression of the E108G mutant in rescuing the LAMP2 glycosylation is less efficient. This result suggests, nevertheless, that the E108G mutant remains functional and that the activity of TMEM165 then appears independent of the Mn2+ -induced degradation mechanism.

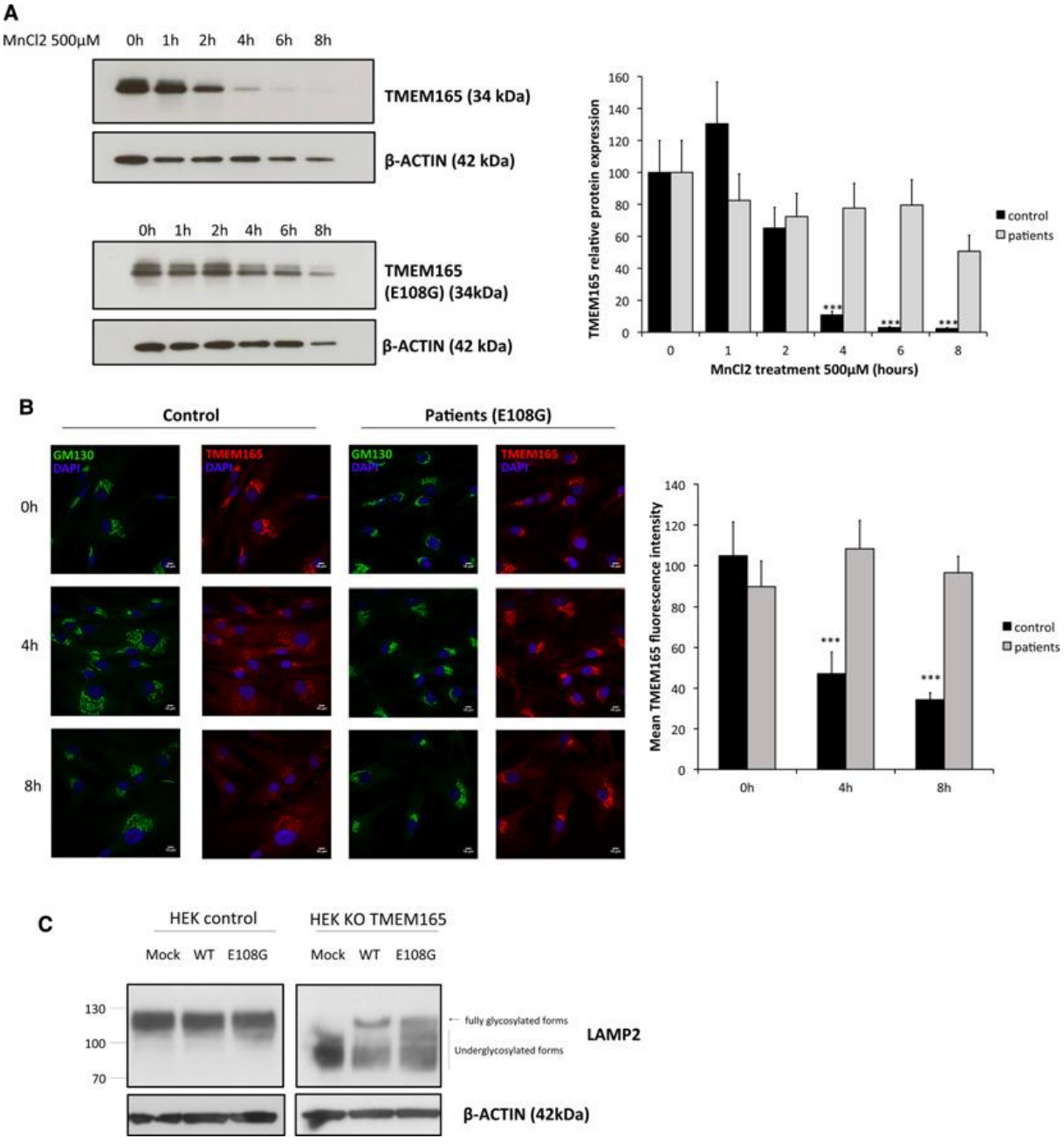

Figure 4. The glutamic acid (E108) in the ELDGK motif is crucial for Mn2+ sensitivity. (A) Healthy skin fibroblasts (upper left) and patients' skin fibroblasts (lower left) carrying E108G mutation were treated with 500 µM MnCl2 for 0–8 h. Total cell lysates were

prepared, and subjected to SDS–PAGE and western blot with the indicated antibodies. Right panel shows the quantification of TMEM165 protein levels after normalization with actin (N = 2; ***P-value < 0.001). (B) Healthy skin fibroblasts and patients' skin fibroblasts carrying E108G mutation were treated with 500 µM MnCl2 for 0, 4, and 8 h. Cells were then fixed and labeled with antibodies against TMEM165 and GM130 before confocal microscopy visualization (N = 2; ***P-value < 0.001). Lower panel shows the quantification of the associated TMEM165 fluorescence intensity (N = 2; n = 30; ***P-value < 0.001). (C) HEK293 control cells and HEK293 KO TMEM165 cells were transfected with empty-vector, wt or E108G plasmid for 36 h. Total cell lysates were prepared, and subjected to SDS–PAGE and western blot with the indicated antibodies.

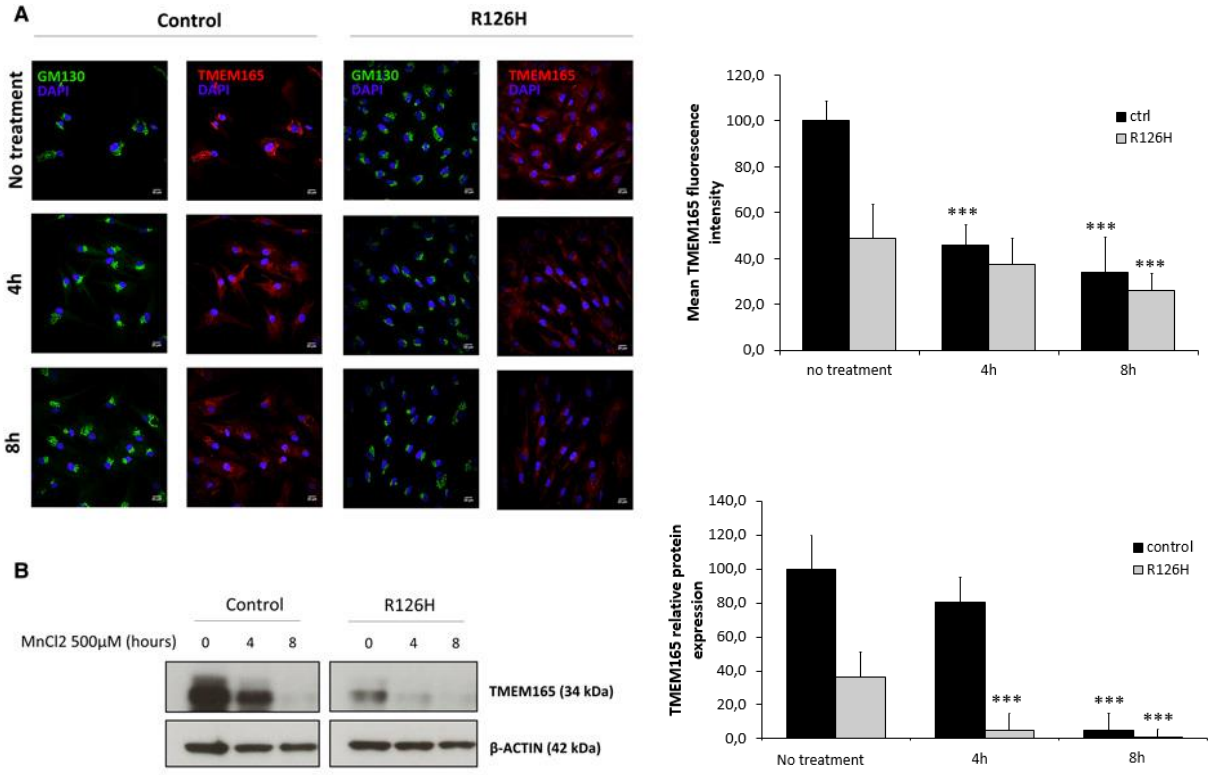

Figure 5. TMEM165 Mn2+-induced degradation also occurs in fibroblasts carrying R126H mutation. (A) Control skin fibroblasts and patient skin fibroblasts carrying R126H mutation were treated with 500 µM MnCl2 for 0–8 h and then fixed and labeled with antibodies against TMEM165 and GM130 before confocal microscopy visualization. Right panel shows the quantification of the associated TMEM165 fluorescence intensity [N = 2; number of cells (n) = 30; ***P-value < 0.001]. (B) Steady-state cellular level of TMEM165. Fibroblasts were treated as described in (A). Total cell lysates were prepared, and subjected to SDS–PAGE and western blot with the indicated antibodies. Right panel shows the quantification of TMEM165 protein levels after normalization with actin (N = 2; ***P-value < 0.001).

Validation of a predicted topology of TMEM165

Human TMEM165 encodes a 7-transmembrane spanning protein of 324 amino acids. To validate a predicted topology of TMEM165 and thus the orientation of the ELGDK motif, we used the two available commercial antibodies against TMEM165, each recognizing two differentially oriented epitopes: the Sigma antibodies recognizing the immunogenic sequence (aa176–aa229) and the antibodies provided by Thermo Fischer directed against the immunogenic sequence (aa17–aa45;

Figure 6A). The topology was determined by selective membrane permeabilization and immunofluorescence analysis (Figure 6B). Under conditions that allowed antibody access to all cellular compartments, both epitopes were detectable and showed co-localization with the Golgi marker GM130 (Figure 6B). Selective permeabilization of the plasma membrane with low concentrations of digitonin allowed visualization of the cytosolic epitope only recognized by the Sigma antibody. On the basis of these results, we can propose a model where the loop encompassing the aa 176–229 is cytosolic and where the ELGDK motif is facing the cytosol (Figure 6A).

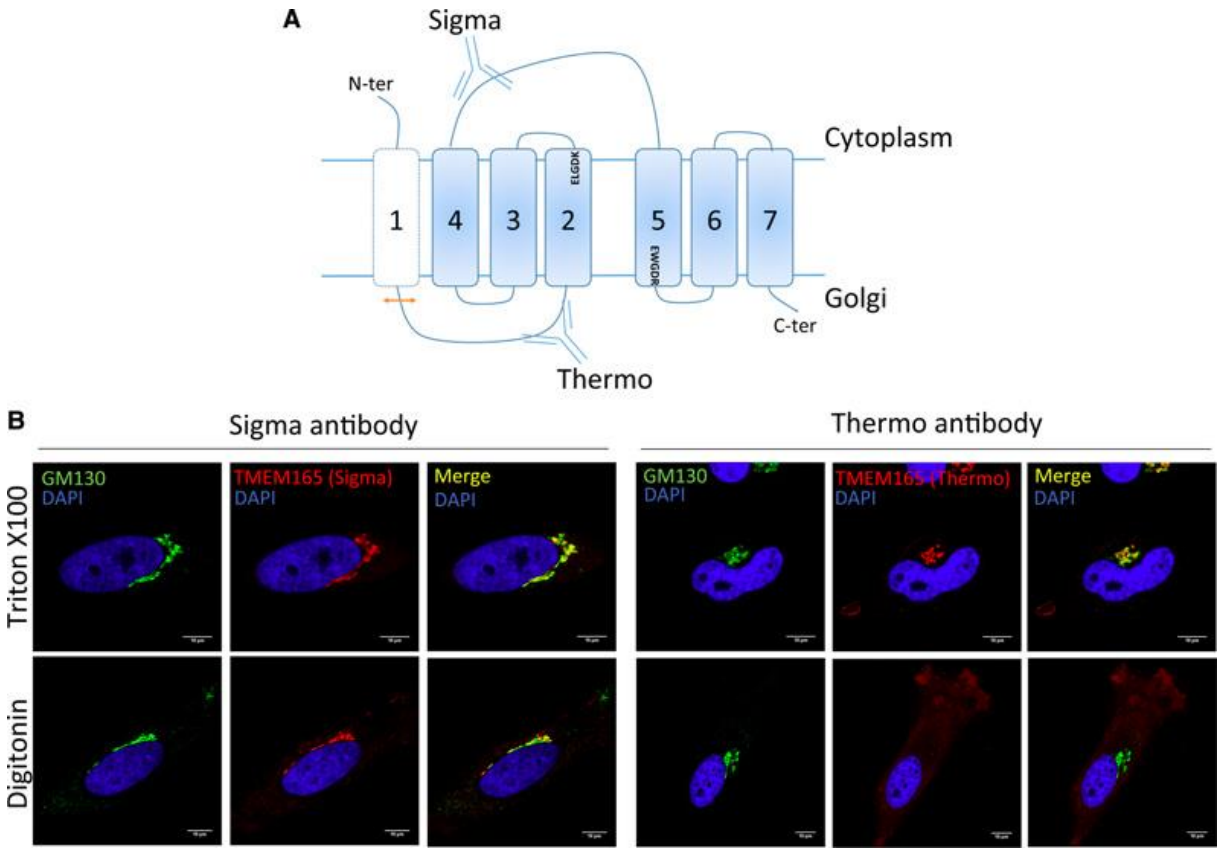

Figure 6. TMEM165 topology. (A) Representation of TMEM165 predicted topology. The two anti-TMEM165 antibodies (Sigma–Aldrich and Thermo Fisher Scientific) depicted here recognize two different parts of the protein. The Sigma ones recognize the cytoplasmic loop between the fourth and fifth transmembrane domains. The Thermo ones recognize the short luminal loop between the first and the second transmembrane domain. The red double arrows show the predicted location of the signal sequence cleavage. The first TMD is depicted in white and with a dotted line border as it can be absent from the mature protein. (B) Cells were fixed with PAF 4% and treated as described in the materials and methods section. Selective permeabilization was done by using Triton X-100 or digitonin. Cells were labeled with antibodies against TMEM165 and GM130 before confocal microscopy visualization.

SPCA1 knockdown does not prevent TMEM165-induced degradation

Since the ELGDK motif is oriented toward the cytosol, we wished to assess whether TMEM165 responded to changes in cytosolic or Golgi luminal Mn2+. To tackle this point, we tested the contribution of SPCA1 (known to be one of the major Golgi Mn2+ importers) in the Mn2+-induced degradation of TMEM165. The impacts of knockdown of SPCA1 on the Mn2+-induced degradation of TMEM165 were assessed. SiRNA depletion of SPCA1 was very efficient as 85% of the protein was depleted compared with untreated cells. Interestingly, knockdown of SPCA1 did not abolish the Mn2+-induced degradation of TMEM165 (Figure 7). The results showed that TMEM165 loss exceeded 80% after 8 h of Mn2+ treatment both in siSPCA1 cells and untreated cells. This highly strengthens the fact that the degradation of TMEM165 is not dependent on Golgi luminal Mn2+ changes.

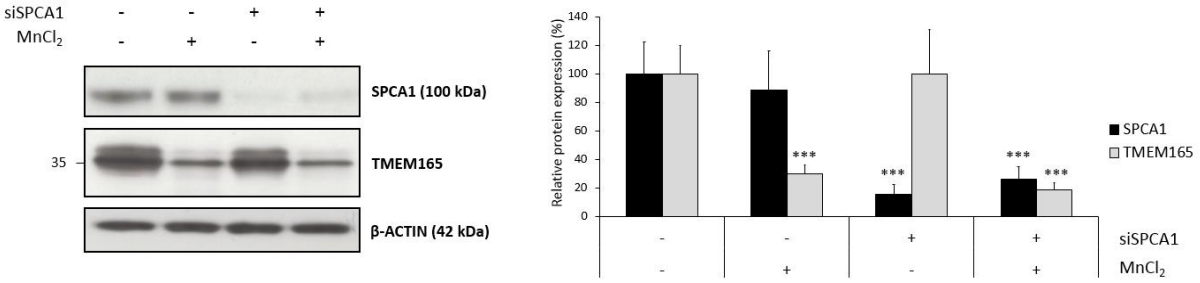

Figure 7. SPCA1 knockdown does not prevent the Mn-induced degradation of TMEM165. (A) Steady-state cellular level of TMEM165 and SPCA1 in control and siSPCA1 HeLa cells. Control and siSPCA1 HeLa cells were cultured in the absence or presence of MnCl2 (500 µM, 8 h); total cell lysates were then prepared, and subjected to SDS–PAGE and western blot with the indicated antibodies. Right panel shows the quantification of TMEM165 and SPCA1 protein levels after normalization with actin (N = 3; ***P-value < 0.001).

Discussion

Our previous work has shown that the observed Golgi glycosylation defect due to a lack of Gdt1p/TMEM165 resulted from a Golgi Mn2+ homeostasis defect, then leading to strong Golgi glycosylation abnormalities. Interestingly, we demonstrated that such defects could totally be suppressed by manganese supplementation, strongly suggesting that TMEM165 could somehow be involved in the Golgi transport of Mn2+. It has been shown in yeast that Smf1p and Smf2p, members of the Nramp family of metal transporters, are tightly regulated by different intracellular Mn2+ concentrations [18–20]. When cells are exposed to toxic Mn2+ concentrations, Smf1p and Smf2p are targeted to the vacuole for degradation, thus stopping the Mn2+ cellular entry. To test whether TMEM165 falls under the same regulation, TMEM165 stability for Mn2+ was tested. Our results showed that TMEM165 was highly sensitive to Mn2+ as manganese supplementation targets TMEM165 under the way of lysosomal degradation.

Although, intriguingly, the molecular mechanisms by which TMEM165 is degraded following Mn2+ exposure are currently not known, the Mn2+ -induced degradation of Gdt1p-Myc in yeasts demonstrated that this mechanism is conserved during evolution. Another mammalian Golgi protein GPP130 has been reported to be sensitive to Mn2+ [16]. While the obtained results are very similar to the one observed for GPP130, several lines of evidences tend to prove that the molecular mechanisms could be different. First, the manganese sensitivity is different as 25 µM manganese is sufficient to engage TMEM165 in the lysosomal degradation pathway, while at this concentration GPP130 is stable. We cannot, however, avoid the fact that this observed difference in manganese sensitivity is coming from the different binding affinities of manganese for these two proteins. Second, the manganese-induced degradation rate of TMEM165 is faster than that of GPP130, as TMEM165 accumulation was never seen in punctate structures under Mn2+ supplementation. Because GPP130 and TMEM165 present high sensitivity to manganese, we cannot exclude a functional link between these two Golgi proteins. Interestingly, while the R126H mutation remains Mn2+ responsive, the glutamic acid (E108) in the highly conserved ELGDK motif was shown to be insensitive to Mn2+ exposure and then crucial in TMEM165 Mn2+-induced degradation. One can suppose that these two mutations act differently on the Mn2+-induced degradation mechanisms of TMEM165. Our data also show that the E108G TMEM165 mutant form is able to rescue the glycosylation defect, although less efficiently than the wt-TMEM165 form. This suggests that the Mn2+-induced degradation mechanism is independent of the function of TMEM165 in Golgi glycosylation. According to the prediction of TMEM165 membrane topology, this motif is oriented towards the cytosol and located between the second and the third transmembrane domains of TMEM165. Our results show that TMEM165 responds to changes in cytosolic Mn2+ and not Golgi luminal changes. Although the R126H mutation reduces basal TMEM165 expression, the protein remains Mn responsive.

The other important question is, why is TMEM165 degraded by high cytosolic Mn2+ concentration? While we currently do not have the answer, our data raise several hypotheses. As a slight fraction of TMEM165 can be found at the plasma membrane, the degradation could be a mechanism to prevent Mn2+ entry through the plasma membrane. As mammalian cells can, however, transport the metal by other plasma membrane transporters, this hypothesis is not likely. When cells are exposed to high manganese concentrations, the plasma membrane transporters import the dangerous metal in the cytosol where it accumulates and impairs many fundamental cellular processes. It is critical for the cell to detoxify the cytosol. The detoxification

is crucial to avoid the impairment of many fundamental cellular processes. It is known that SPCA1, the Golgi P-type ATPase essential to import cytosolic Ca2+ but also Mn2+ inside the Golgi lumen, is the major way for eliminating the surplus of cytosolic Mn2+ from the cell. As TMEM165 is degraded when the manganese level becomes toxic, we can hypothesize that this mechanism participates in detoxification. This is still unclear how TMEM165 participates in such a process, but one can think that TMEM165, in the presence of high Mn2+ concentration in the Golgi, could transport back the Mn2+ into the cytosol. In that case, the specific degradation of TMEM165 in response to Mn2+ would prevent the Mn2+ from the Golgi to be recaptured back into the cytosol, a mechanism that would definitely annihilate the efforts made by SPCA1. Overall, our studies highlight TMEM165 as a novel Golgi Mn2+ sensitive protein in mammalian cells. This discovery sheds light on a novel actor involved in the regulation of intracellular Mn2+ homeostasis and the pathophysiological mechanisms in TMEM165-CDG patients.

Material and methods

Antibodies and other reagents

Anti-TMEM165 and anti-β Actin antibodies were from Sigma–Aldrich (St Louis, MO, U.S.A.). The other anti-TMEM165 antibody was purchased from Thermo Fisher Scientific (Waltham, MA, U.S.A.). Anti-SPCA1 antibody was purchased from Abcam (Cambridge, U.K.). Anti-GM130 antibody was from BD Biosciences (Franklin lakes, NJ, U.S.A.). Anti-GPP130 antibody was purchased from Covance (Princeton, NJ, U.S.A.). Anti-myc (9E10) was purchased from Santa Cruz Biotechnology (Dallas, TX, U.S.A.). Goat anti-rabbit or goat anti-mouse immunoglobulins HRP-conjugated were purchased from Dako (Glostrup, Denmark). Polyclonal goat anti-rabbit or goat anti-mouse conjugated with Alexa Fluor were purchased from Thermo Fisher Scientific (Waltham, MA, U.S.A.). Manganese (II) chloride tetrahydrate was from Riedel-de-Haën (Seelze, Germany). All other chemicals were from Sigma–Aldrich unless otherwise specified.

Constructs, vector engineering and mutagenesis

Plasmids, pcDNA3.1 derivatives expressing either wt-TMEM165 or p.E108G version of TMEM165 (c.A323G mutation), have been generated by Ezyvec (Lille, France). Generation of TMEM165 knockouts HEK293T cells (ATTC) were grown in Dulbecco's Modified Eagle's Medium (DMEM)/F12 medium (Thermo Scientific) supplemented with 10% fetal bovine serum (FBS; Atlas Biologicals). Cells were maintained at 37° and 5% CO2 in a 90% humidified incubator. HEK293T

TMEM165 stable knockouts were generated using the CRISPR technique [21–24]. gRNA sequences were purchased from Genecopoeia (Catalog No. HCP214780-SG01-3). HEK293T cells were transfected with plasmid containing gRNA and a separate plasmid containing Cas9 and mCherry. HEK293 cells were transfected in a 6-well plate at 70% confluence using Lipofectamine 2000 in Opti-MEM (Thermo Scientific). Cells were incubated with the lipid-DNA complexes for 5 h after which the cells were supplemented with DMEM/F12 with FBS at a final concentration of 5%. The medium was changed to DMEM/F12 with 10% FBS 24 h after transfection. Twelve days after transfection, cells were single-cell sorted and knockout colonies were identified by immunofluorescence and western blot using antibodies to TMEM165 (Sigma). Sequencing of knockouts identified deletions in exon 1.

Cell culture and transfections

All cell lines were maintained in DMEM supplemented with 10% FBS (Lonza, Basel, Switzerland), at 37°C in a humidity-saturated 5% CO2 atmosphere. Transfections were performed using Lipofectamine 2000® (Thermo Scientific) according to the manufacturer's guidelines. For drug treatments, incubations were done as described in each figure.

Immunofluorescence staining

Cells were seeded on coverslips for 12–24 h, washed once in Dulbecco's Phosphate Buffer Saline (DPBS, Lonza) and fixed either with 4% paraformaldehyde (PAF) in PBS (pH 7.3) for 30 min at room temperature or with ice-cold methanol for 10 min at room temperature. Coverslips were then washed three times with PBS. Only if the fixation had been done with PAF, cells were permeabilized with 0.5% Triton X-100 in PBS for 15 min and then washed three times with PBS. Coverslips were then put in saturation for 1 h in blocking buffer [0.2% gelatin, 2% Bovine Serum Albumin (BSA), 2% FBS (Lonza) in PBS], followed by incubation for 1 h with primary antibody diluted at 1:100 in blocking buffer. After washing with PBS, cells were incubated for 1 h with Alexa 488-, Alexa 568-, or Alexa 700-conjugated secondary antibody (Life Technologies) diluted at 1:600 in blocking buffer. After washing three times with PBS, coverslips were mounted on glass slides with Mowiol. Fluorescence was detected through an inverted Zeiss LSM780 confocal microscope. Acquisitions were done using the ZEN pro 2.1 software (Zeiss, Oberkochen, Germany). For selective membrane permeabilization, we have used digitonin at 5 µg/ml. Stock

solution was prepared at 5 mg/ml in absolute ethanol, 0.3 M sucrose 0.1 M KCl, 2.5 mM MgCl2 , 1 mM EDTA, 10 mM HEPES, pH 6.9. Permeabilization was done at 4°C for 15 min.

Image analyses

Immunofluorescence images were analyzed using TisGolgi, a home-made imageJ (http://imagej.nih.gov/ij) plugin developed by TISBio and available upon request. Basically, the program automatically detects and discriminates Golgi and vesicles, based on morphological parameters such as size and sphericity. Then, the program calculates for each image the number of detected objects, their size and mean fluorescence intensity. Co-localization analyses were done using JACoP plugin and performed according to the guidelines suggested by Bolte et al. [25].

Western blotting

Cells were scraped in DPBS and then centrifuged at 4500 rpm for 3 min. Supernatant was discarded and cells were then resuspended in RIPA buffer [Tris/HCl 50 mM (pH 7.9), NaCl 120 mM, NP40 0.5%, EDTA 1 mM, Na3 VO4 1 mM, NaF 5 mM] supplemented with a protease cocktail inhibitor (Roche Diagnostics, Penzberg, Germany). Cell lysis was done by passing the cells several times through a syringe with a 26G needle. Cells were centrifuged for 30 min at 20 000g. The supernatant containing protein was estimated with the Micro BCA Protein Assay Kit (Thermo Scientific). A 20 µg aliquot of total protein lysate was put in NuPAGE LDS sample buffer (Invitrogen) (pH 8.4) supplemented with 4% β-mercaptoethanol (Fluka). Samples were heated for 10 min at 95°C, then separated on 4– 12% Bis– Tris gels (Invitrogen) and transferred to nitrocellulose membrane Hybond ECL (GE Healthcare, Little Chalfont, U.K.). The membranes were blocked in blocking buffer (5% milk powder in TBS-T [1X TBS with 0.05% Tween20]) for 1 h at room temperature, then incubated over night with the primary antibodies (used at a dilution of 1:1000, except for anti-myc, used at 1:200) in blocking buffer, and washed three times for 5 min in TBS-T. The membranes were then incubated with the peroxidase conjugated secondary goat anti-rabbit or goat anti-mouse antibodies (Dako; used at a dilution of 1:10 000) in blocking buffer for 1 h at room temperature and later washed three times for 5 min in TBS-T. Signal was detected with chemiluminescence reagent (ECL 2 Western Blotting Susbtrate, Thermo Scientific on imaging film (GE Healthcare, Little Chalfont, U.K.).

Yeast strains, media and lysis

Yeast strains originating from BY4741 background were used for the experiments (*gdt1Δ*: Mata his3Δ 1 leu2Δ 0 ura3Δ 0 *gdt1Δ*::KanMX4). Yeasts were cultured at 30°C. Cultures in liquid media are done under light shaking. Rich medium, named YEP medium, contains yeast extract (10 g/l, Difco), Bacto-peptone (20 g/l, Difco); YPD medium is a YEP medium supplemented with 2% D - glucose (Sigma– Aldrich). Before any analysis, a preculture in YPD medium is done and a volume equivalent to 10 OD600 nm unit is transferred into a bigger volume of YPD medium. Culture begins at a volume equivalent to 6 OD600 nm unit until 18 OD600 nm. MnCl2 was added at this step at the indicated concentration and yeasts were harvested at the indicated times. Yeasts were centrifuged for 5 min at 3500 g. The supernatant was discarded and the pellet was kept frozen at − 20°C. Yeast lysis was performed as described by Ballou et al [26]. Western blot experiments were done as described above.

Cell surface biotinylation

Cells were plated to reach 70– 80% confluence on the day of the experiment. Cells were kept on ice all the time. Cells were washed four times with PBS+ /+ (containing Ca and Mg), pH8. An aliquot of 1.5 ml PBS+ /+ (pH 8) with 7.5 µl biotin was added per dish [Biotin: EZ Link Sulfo-NHS-SS-Biotin (Life Technologies, Carlsbad, CA, U.S.A.), final concentration of 0.5 mg/ml in DMSO]. Cells were then incubated 30 min in a cold room on slow rocking and then washed three times with PBS+ /+ (pH8). Cells were quenched 15 min with 1.5 ml of PBS+/+ glycine 100 mM, BSA 0.5% in a cold room on slow rocking and then washed three times with PBS+ /+ glycine. Cells were scraped in 200 µl of lysis buffer [50 mM HEPES (pH 7.2), 100 mM NaCl, 1% Triton X-100, protease inhibitors], incubated 20 min on ice and centrifuged for 15 min at 20 000g at 4°C. The supernatant was kept and the protein concentration was measured. For the pull-down, put the maximum amount of protein, ideally 500 µg in 1 ml final (lysis buffer) + 30 µl streptavidin beads. Incubate 4h at 4°C on a wheel and then centrifuge at 4000g for 1 min at 4°C. Wash three times with 1 ml of lysis buffer (not supplemented with protease inhibitors) and mix well by inverting the tubes 30 times. Centrifuge at 4000g for 1 min at 4°C and remove the supernatant with a flat end tip. Add NuPAGE LDS sample buffer (Invitrogen) pH 8.4 supplemented with 4% β-mercaptoethanol (Fluka). Samples are boiled at 70°C for 10 min (do not boil if one wishes to

reveal TMEM165 on western blot afterwards) and then centrifuged at 1000g for 1 min, and the supernatant was collected. Samples were frozen at − 20°C. Samples are ready to load on gel.

Statistical analysis

Comparisons between groups were performed using Student's t -test for two variables with equal or different variances, depending on the result of the F -test.

Abbreviations

BSA, bovine serum albumin; CDG, congenital disorders of glycosylation; DMEM, Dulbecco's Modified Eagle's Medium; DPBS, Dulbecco's Phosphate Buffer Saline; FBS, fetal bovine serum; PAF, paraformaldehyde; SPCA1, secretory pathway Ca-ATPase 1; wt, wild-type.

Author Contribution

F.F. obtained financial support to design this study and he wrote the paper. F.F. and S.P. coordinated the study. S.P. and E.D. performed and analyzed most of the experiments. L.C. and V.L. performed the CRISPR-cas9 TMEM165 cells. M.H. performed the experiment in Figure 7. C.S. provided technical assistance for colocalisation studies. D.V. performed immunofluorescence microscopy experiments. E.L. and A.K. performed and analysed the experiment in Figure 4C. R.P. provided technical assistance on surface biotinylation. S.D., W.M. and M.A.K. provided advices. G.D.B. and P.M. reviewed the yeast results. G.M. reviewed the paper and provided us the R126H deficient CDG patients. T.M. provided us the E108G TMEM165 deficient patients.

Funding

This work was supported by the French National Research Agency [SOLV-CDG to F.F] and the Mizutani Foundation for Glycoscience [to F.F.] and EURO-CDG-2 that has received funding from the European Union's Horizon 2020 research and innovation program under the ERA-NET Cofund action N° 643578. V.L. was supported by the NIH grants [GM083144 and U54 GM105814].

Acknowledgements

We are indebted to Dr Dominique Legrand of the Research Federation FRABio (Univ. Lille, CNRS, FR 3688, FRABio, Biochimie Structurale et Fonctionnelle des Assemblages Biomoléculaires) for providing the scientific and technical environment conducive to achieving this work. We thank the BioImaging Center of Lille, especially Christian Slomianny and Elodie Richard, for the use of the Leica LSM70.

Competing Interests

The Authors declare that there are no competing interests associated with the manuscript

References

1 Au, C., Benedetto, A. and Aschner, M. (2008) Manganese transport in eukaryotes: the role of DMT1. Neurotoxicology 29, 569–576 doi:10.1016/j.neuro.2008.04.022

2 Perl, D.P. and Olanow, C.W. (2007) The neuropathology of manganese-induced Parkinsonism. J. Neuropathol. Exp. Neurol. 66, 675–682 doi:10.1097/nen.0b013e31812503cf

3 Squitti, R., Gorgone, G., Panetta, V., Lucchini, R., Bucossi, S., Albini, E. et al. (2009) Implications of metal exposure and liver function in Parkinsonian patients resident in the vicinities of ferroalloy plants. J. Neural. Transm. 116, 1281–1287 doi:10.1007/s00702-009-0283-0

4 Park, J.H., Hogrebe, M., Grüneberg, M., DuChesne, I., Heiden, A.L. von der Reunert, J. et al. (2015) SLC39A8 deficiency: a disorder of manganese

transport and glycosylation. Am. J. Hum. Genet. 97, 894–903 doi:10.1016/j.ajhg.2015.11.003

5 Potelle, S., Morelle, W., Dulary, E., Duvet, S., Vicogne, D., Spriet, C. et al. (2016) Glycosylation abnormalities in Gdt1p/TMEM165 deficient cells result from a defect in Golgi manganese homeostasis. Hum. Mol. Genet. 25, 1489–1500 doi:10.1093/hmg/ddw026

6 Garrick, M.D., Dolan, K.G., Horbinski, C., Ghio, A.J., Higgins, D., Porubcin, M. et al. (2003) DMT1: a mammalian transporter for multiple metals. Biometals 16, 41–54 doi:10.1023/A:1020702213099

7 Forbes, J.R. and Gros, P. (2003) Iron, manganese, and cobalt transport by Nramp1 (Slc11a1) and Nramp2 (Slc11a2) expressed at the plasma membrane. Blood 102, 1884–1892 doi:10.1182/blood-2003-02-0425

8 Chen, P., Bowman, A.B., Mukhopadhyay, S. and Aschner, M. (2015) SLC30A10: a novel manganese transporter. Worm 4, e1042648 doi:10.1080/21624054.2015.1042648

9 Chen, P., Chakraborty, S., Mukhopadhyay, S., Lee, E., Paoliello, M.M.B., Bowman, A.B. et al. (2015) Manganese homeostasis in the nervous system. J. Neurochem. 134, 601–610 doi:10.1111/jnc.13170

10 Girijashanker, K., He, L., Soleimani, M., Reed, J.M., Li, H., Liu, Z. et al. (2008) Slc39a14 gene encodes ZIP14, a metal/bicarbonate symporter: similarities to the ZIP8 transporter. Mol. Pharmacol. 73, 1413–1423 doi:10.1124/mol.107.043588

11 Dode, L., Andersen, J.P., Vanoevelen, J., Raeymaekers, L., Missiaen, L., Vilsen, B. et al. (2006) Dissection of the functional differences between human secretory pathway Ca2+/Mn2+-ATPase (SPCA) 1 and 2

isoenzymes by steady-state and transient kinetic analyses. J. Biol. Chem. 281, 3182–3189 doi:10.1074/jbc.M511547200

12 He, W. and Hu, Z. (2012) The role of the Golgi-resident SPCA Ca2+/Mn2+ pump in ionic homeostasis and neural function. Neurochem. Res. 37, 455–468 doi:10.1007/s11064-011-0644-6

13 Mukhopadhyay, S. and Linstedt, A.D. (2011) Identification of a gain-of-function mutation in a Golgi p-type ATPase that enhances Mn2+ efflux and protects against toxicity. Proc. Natl Acad. Sci. U.S.A. 108, 858–863 doi:10.1073/pnas.1013642108

14 Foulquier, F., Amyere, M., Jaeken, J., Zeevaert, R., Schollen, E., Race, V. et al. (2012) TMEM165 deficiency causes a congenital disorder of glycosylation. Am. J. Hum. Genet. 91, 15–26 doi:10.1016/j.ajhg.2012.05.002

15 Masuda, M., Braun-sommargren, M., Crooks, D. and Smith, D.R. (2013) Golgi phosphoprotein 4 (GPP130) is a sensitive and selective cellular target of manganese exposure. Synapse 67, 205–215 doi:10.1002/syn.21632

16 Mukhopadhyay, S., Bachert, C., Smith, D.R. and Linstedt, A.D. (2010) Manganese-induced trafficking and turnover of the cis-Golgi glycoprotein GPP130. Mol. Biol. Cell 21, 1282–1292 doi:10.1091/mbc.E09-11-0985

17 Schulte Althoff, S., Grüneberg, M., Reunert, J., Park, J.H., Rust, S., Mühlhausen, C. et al. (2015) TMEM165 deficiency: postnatal changes in glycosylation. JIMD Rep. 26, 21–29 doi:10.1007/8904_2015_455

18 Culotta, V.C., Yang, M. and Hall, M.D. (2005) Manganese transport and trafficking: lessons learned from Saccharomyces cerevisiae. Eukaryot. Cell 4, 1159–1165 doi:10.1128/EC.4.7.1159-1165.2005

19 García-Rodríguez, N., Manzano-López, J., Muñoz-Bravo, M., Fernández-García, E., Muñiz, M. and Wellinger, R.E. (2015) Manganese redistribution by calcium-stimulated vesicle trafficking bypasses the need for P-type ATPase function. J. Biol. Chem. 290, 9335–9347 doi:10.1074/jbc.M114.616334

20 Reddi, A.R., Jensen, L.T. and Culotta, V.C. (2009) Manganese homeostasis in Saccharomyces cerevisiae. Chem. Rev. 109, 4722–4732 doi:10.1021/cr900031u

21 Bailey Blackburn, J., Pokrovskaya, I., Fisher, P., Ungar, D. and Lupashin, V.V. (2016) COG complex complexities: detailed characterization of a complete set of HEK293T cells lacking individual COG subunits. Front. Cell Dev. Biol. 4, 23 doi:10.3389/fcell.2016.00023

22 Cong, L., Ran, F.A., Cox, D., Lin, S., Barretto, R., Habib, N. et al. (2013) Multiplex genome engineering using CRISPR/Cas systems. Science 339, 819–823 doi:10.1126/science.1231143

23 Jinek, M., Chylinski, K., Fonfara, I., Hauer, M., Doudna, J.A. and Charpentier, E. (2012) A programmable dual-RNA-guided DNA endonuclease in adaptive bacterial immunity. Science 337, 816–821 doi:10.1126/science.1225829

24 Mali, P., Yang, L., Esvelt, K.M., Aach, J., Guell, M., DiCarlo, J.E. et al. (2013) RNA-guided human genome engineering via Cas9. Science 339, 823–826 doi:10.1126/science.1232033

25 Bolte, S. and Cordelières, F.P. (2006) A guided tour into subcellular colocalization analysis in light microscopy. J. Microsc. 224, 213–232 doi:10.1111/j. 1365-2818.2006.01706.x

26 Ballou, C.E. (1990) [36] isolation, characterization, and properties of Saccharomyces cerevisiae mnn mutants with nonconditional protein glycosylation defects. Methods. Enzymol. 185, 440–470 doi:10.1016/0076-6879(90)85038-P

Supplementary figures

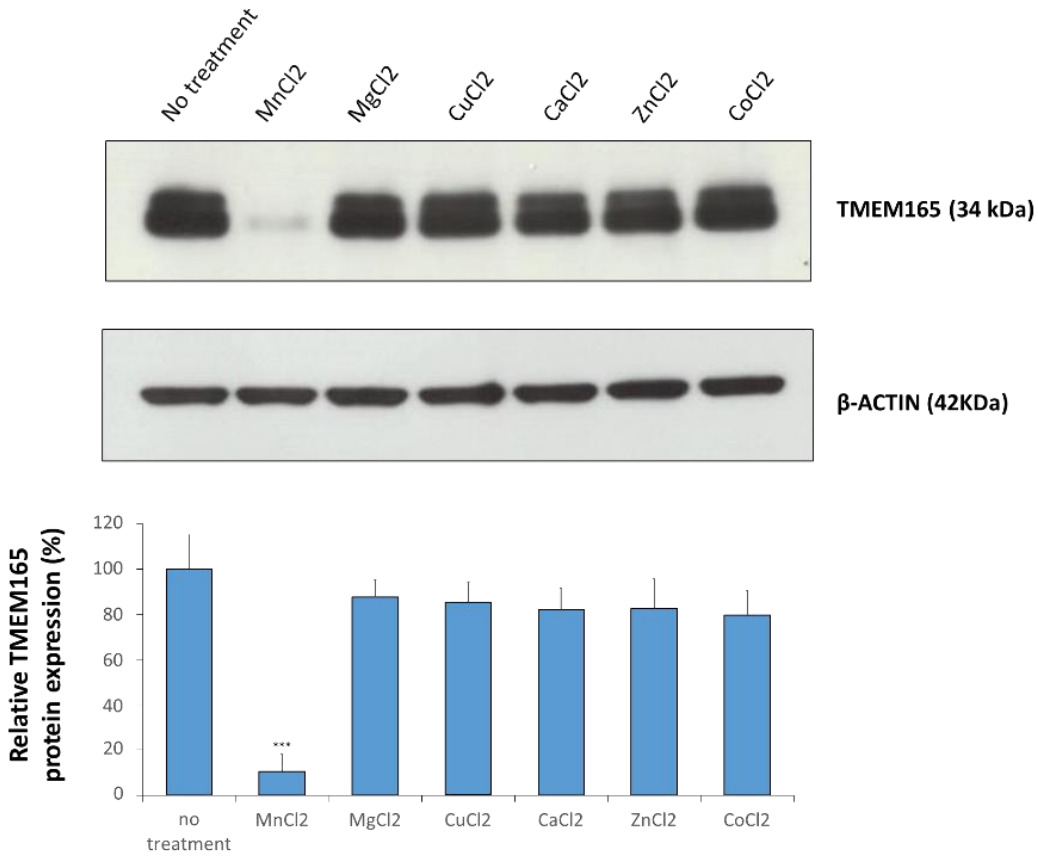

Supplementary Figure 1. TMEM is specifically degraded in response to Mn2+. Steady state cellular level of TMEM165. HeLa cells were treated with the indicated solution at 500 µM for 8h. Total cell lysates were prepared, subjected to SDS-PAGE and Western blot with the indicated antibodies. Lower panel shows the quantification of TMEM165 protein level after normalization with actin (Number of experiments (N) = 3; *** = P value < 0,001).

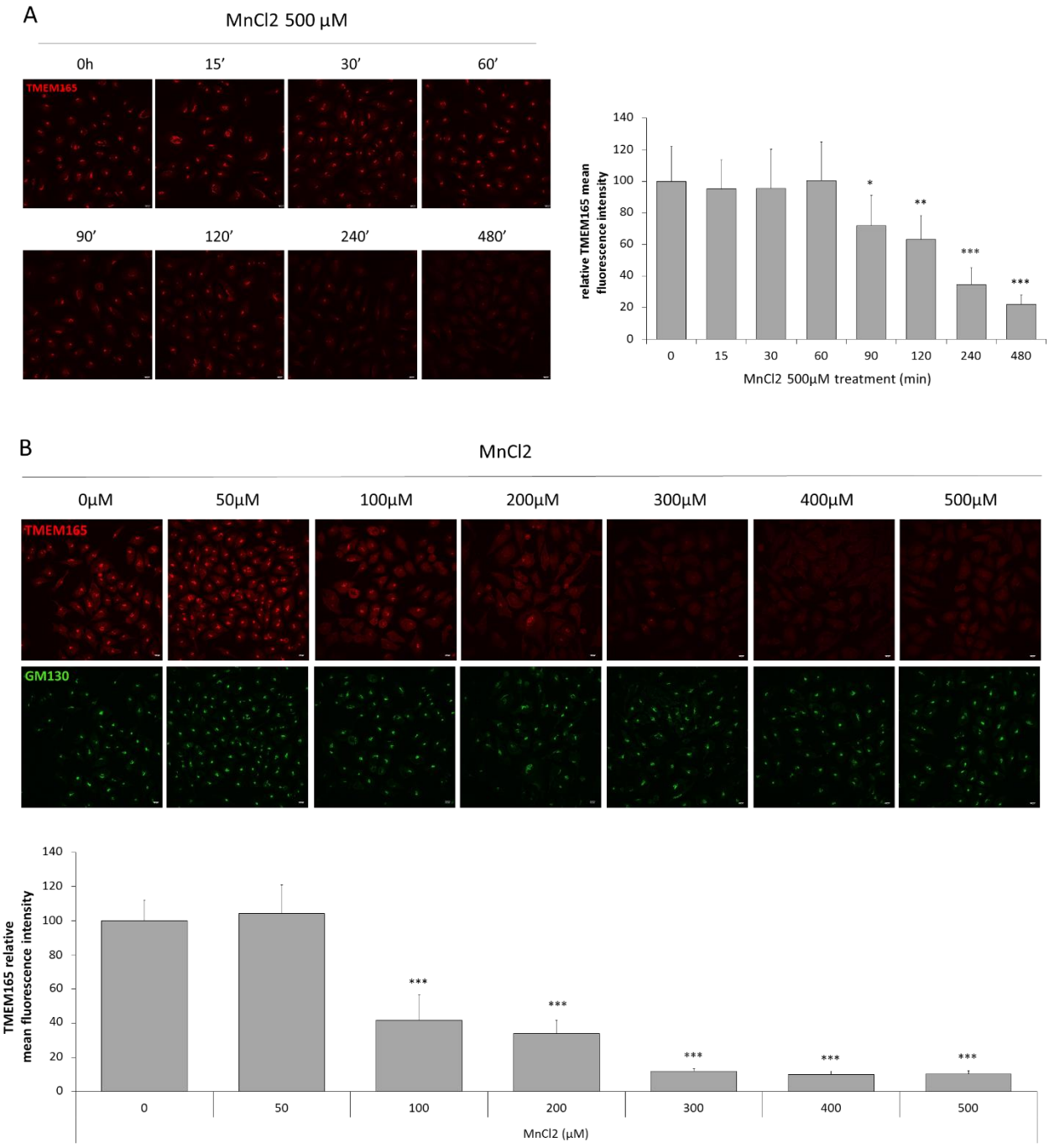

Supplementary Figure 2. Confirmation of TMEM165 degradation by immunofluorescence experiments (A) HeLa cells were incubated with MnCl2 500 µM for 0 to 8h, fixed and labeled with antibodies against TMEM165 before confocal microscopy visualization. Right panel shows the quantification of the associated TMEM165 fluorescence intensity (N = 3; number of cells (n) = 50; *** = P value < 0,001). **(B)** HeLa cells were treated with MnCl2 for 8h at different concentrations, then fixed and labeled with antibodies against TMEM165 and GM130 before confocal microscopy visualization. Lower panel shows the quantification of the associated TMEM165 fluorescence intensity (N = 2; n = 50; *** = P value < 0,001). **(C)** HeLa cells were incubated with MnCl2 500 µM for 1 and 4h, fixed and labeled with antibodies against TMEM165, GPP130 and GM130 before confocal microscopy visualization. White arrows point to some GPP130 positive vesicles.

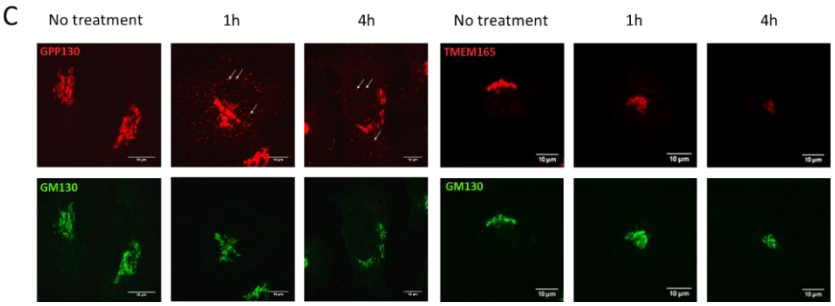

Supplementary Figure 2. *Continued*

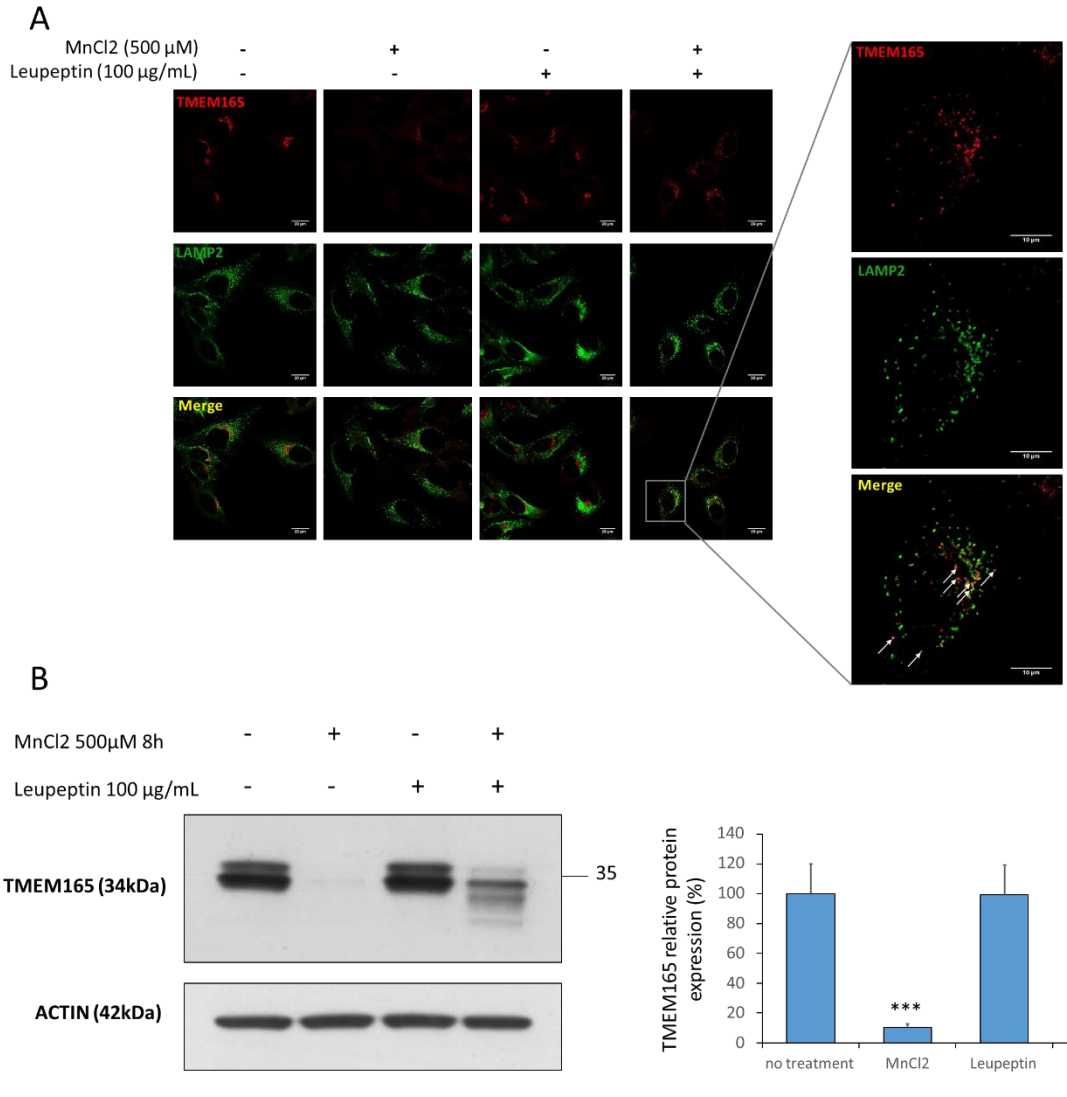

Supplementary figure 3. Leupeptin also prevents TMEM165 induced lysosomal degradation after Mn2+ exposure. (A) HeLa cells were treated for 8h with MnCl2 500 µM and/or leupeptin 100 µg/mL, fixed and labeled with antibodies against TMEM165 (upper panels) and LAMP2 (middle panels) before confocal microscopy visualization. For leupeptin, a pretreatment for 24h has been done. **(B)** Western blot analysis of the same experiment described in (A). Total cell lysates were prepared, subjected to SDS-PAGE and Western blot with the indicated antibodies. Right panel shows the quantification of TMEM165 protein level after normalization with actin (N = 2; *** = P value < 0,001).

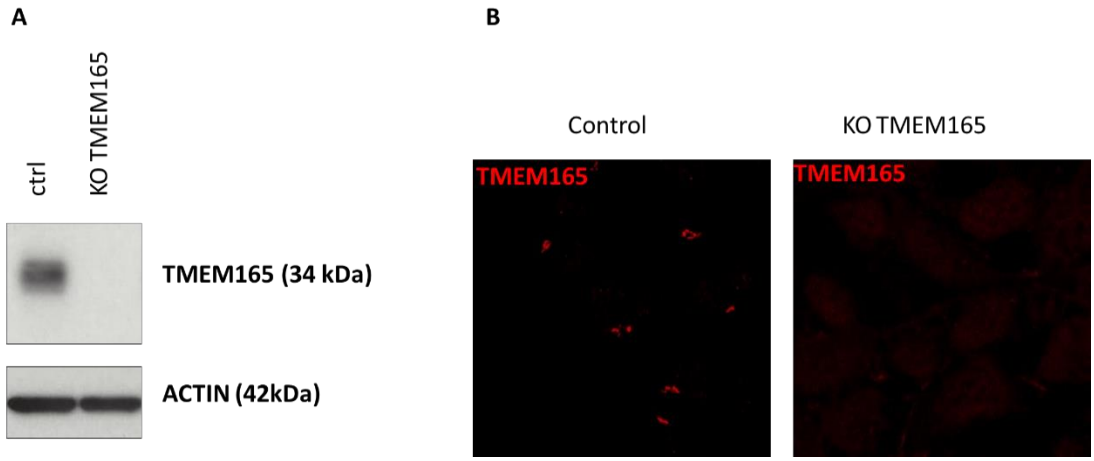

Supplementary Figure 4. Generation and characterization of knockdown HEK293 cells by crispr-cas9. (A) Steady-state cellular level of TMEM165. Total cell lysates were prepared, subjected to SDS–PAGE and western blot with the indicated antibodies. (B) Control and knockout HEK293 cells were fixed and labeled with antibodies against TMEM165 before confocal microscopy visualization.

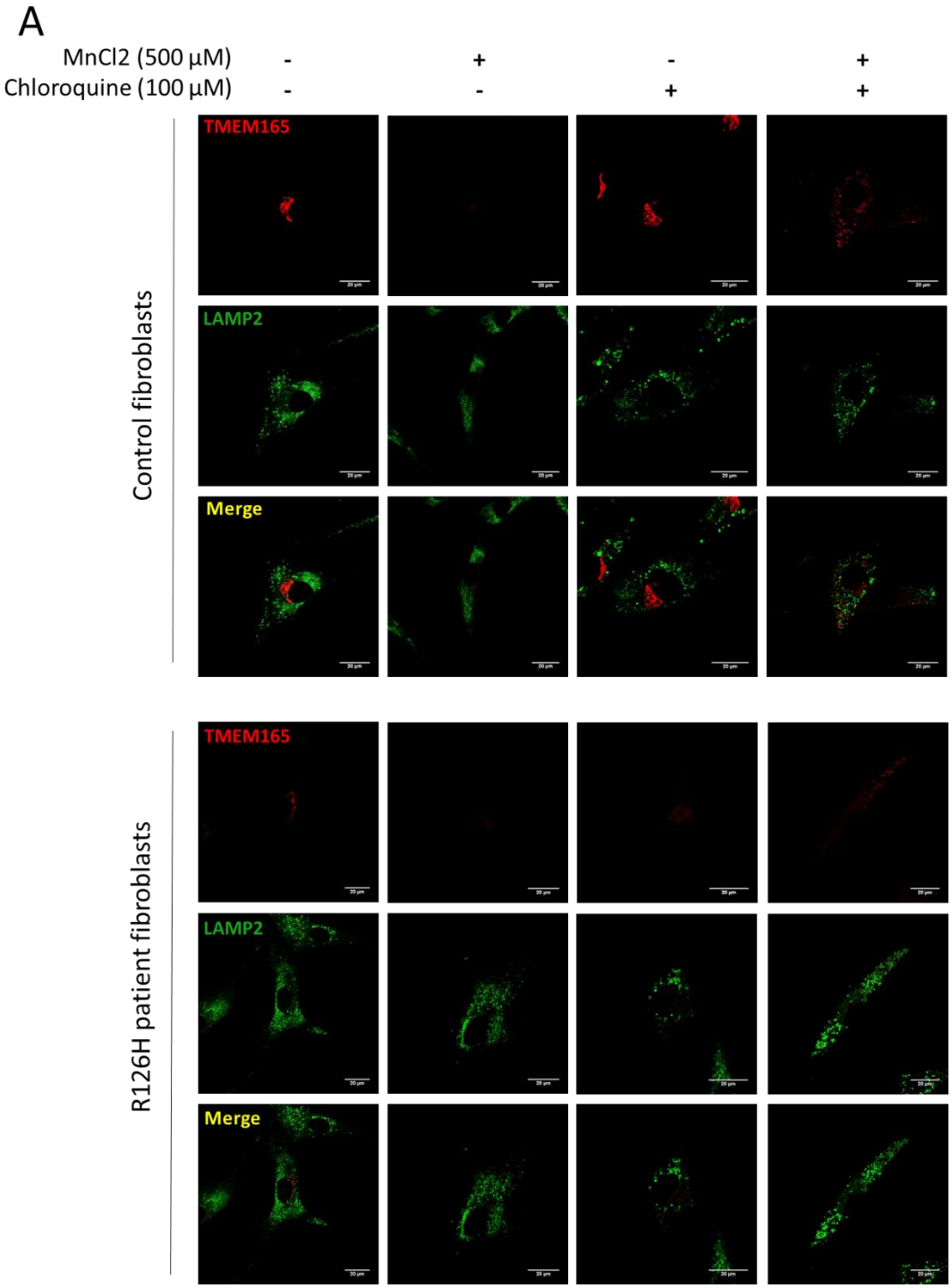

Supplementary figure 5. The R126H mutation does not affect the TMEM165 lysosomal targeting upon Mn2+ and chloroquine exposure. (A) Healthy skin fibroblasts (upper panels) and patients skin fibroblasts (lower panels) carrying R126H mutation were treated for 8h with MnCl2 500 µM and/or chloroquine 100 µM, fixed and labeled with antibodies against TMEM165 and LAMP2 before confocal microscopy visualization. **(B)** Healthy skin fibroblasts (upper panels) and patients skin fibroblasts (lower panels) carrying R126H mutation were treated for 8h with MnCl2 500 µM and/or chloroquine 100 µM, fixed and labeled with antibodies against TMEM165 and EEA1 before confocal microscopy visualization. **(C)** Control and R126H fibroblasts were treated for 8h with MnCl2 500 µM and/or chloroquine 100 µM. Total cell lysates were prepared, subjected to SDS-PAGE and Western blot with the indicated antibodies.

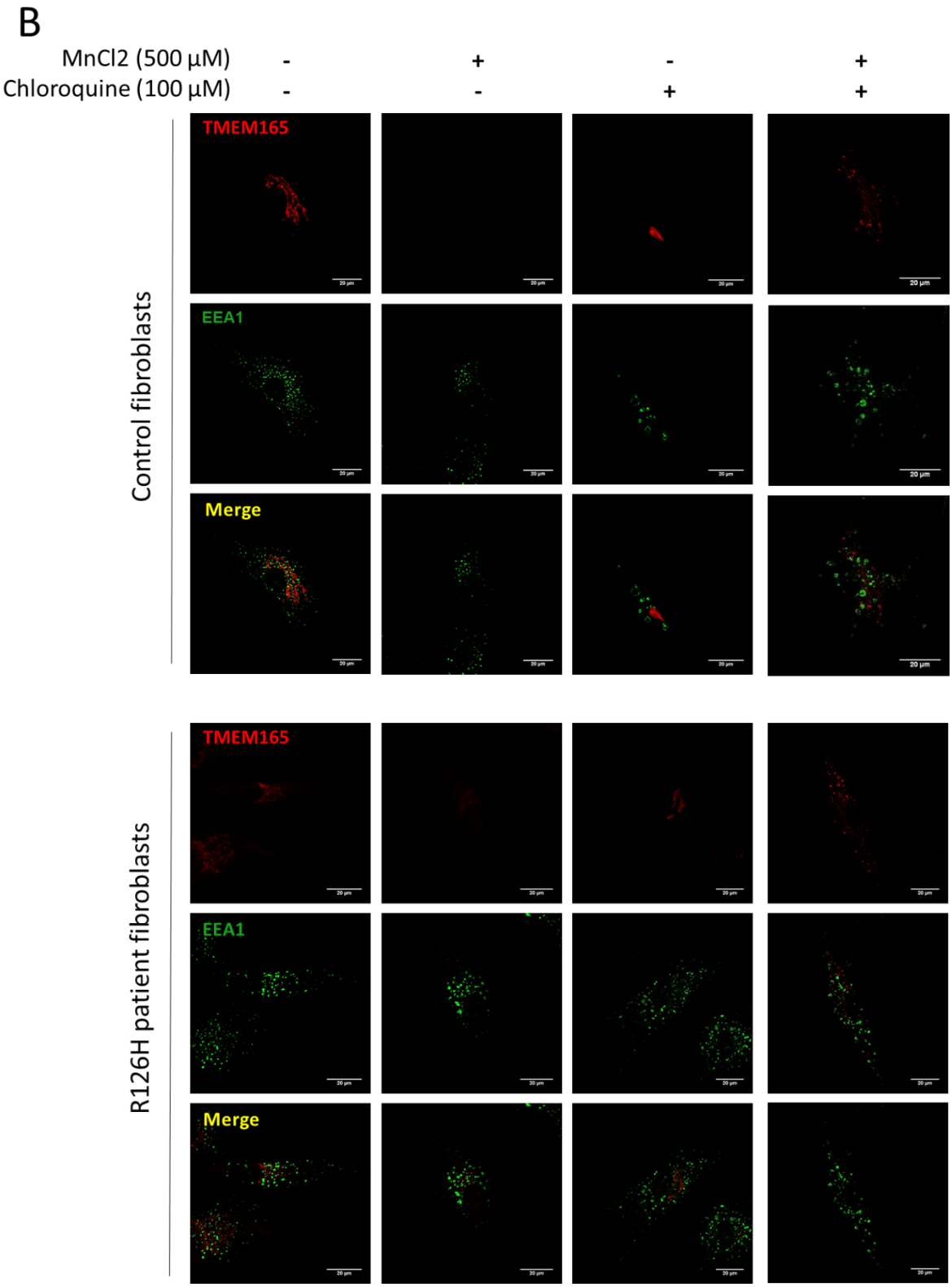

Supplementary figure 5. *Continued*

C

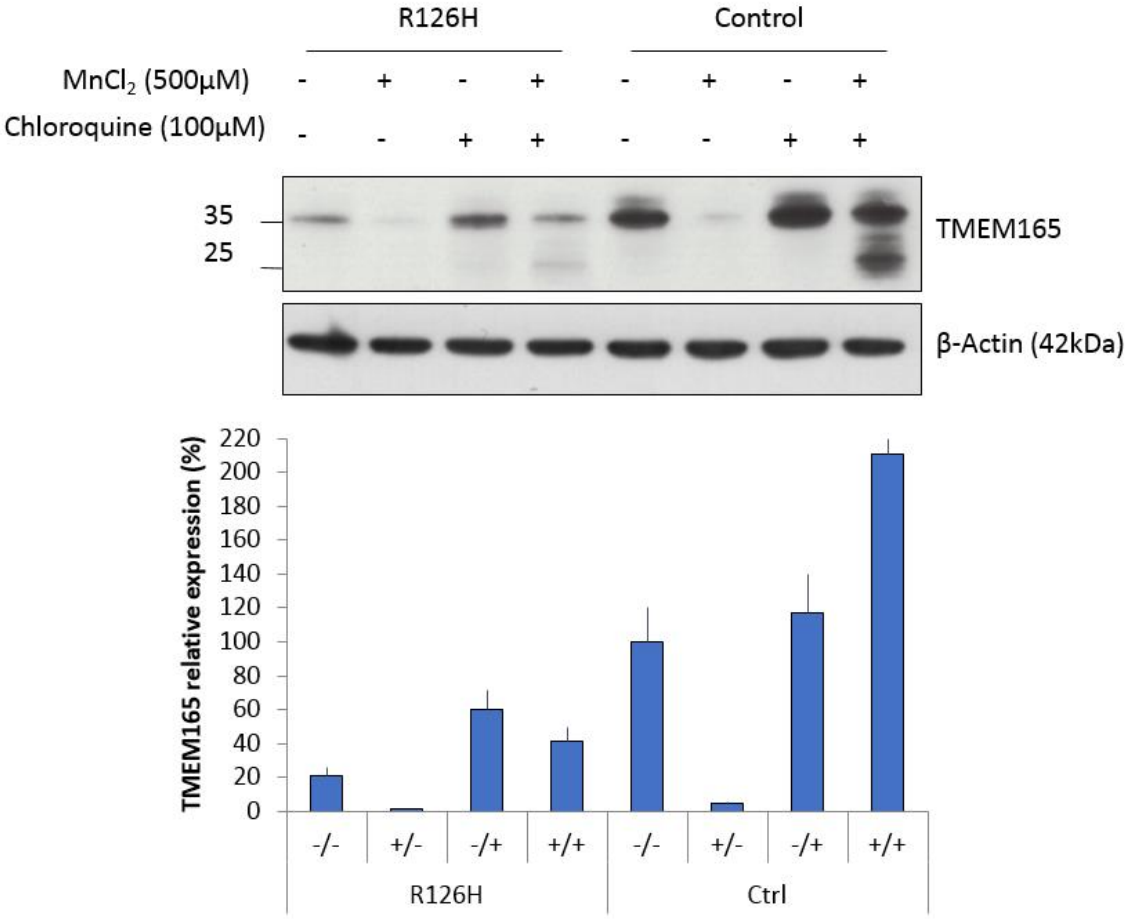

Supplementary figure 5. *Continued*

3.3. Complementary results

Given the similarity between the Mn2+ induced degradation of GPP130 and TMEM165, the rab5 and rab7-dependent pathways were examined using the dominant negative Rab7 (Rab7 T22N) that inhibits the trafficking from multi vesicular bodies (MVBs) to lysosomes [310,311] and the constitutively active form of Rab5 (Q79L) that produces giant MVBs by causing fusion of early endosomes (EEs) and MVBs [312]. To assess the involvement of these two different pathways, we examined the Mn2+ induced TMEM165 degradation in cells either expressing Rab7 T22N or Rab5 Q79L forms (Figure 38). Interestingly, in cells expressing either Rab7 T22N-GFP or Rab5Q79L-GFP, the Mn2+-induced degradation was not prevented and similar to the one observed in non-transfected cells. Overall, our results demonstrate that extracellular Mn2+ induces the lysosomal degradation of TMEM165 via a Rab7 and Rab5 independent pathways, suggesting a direct targeting of TMEM165 from the Golgi to lysosomes. In parallel, the GGA1 pathway was also examined using the pEGFP-C2 GGA1 plasmid, encoding GGA1 lacking the GAE domain, crucial for GGA1 function. We examined the Mn2+ induced TMEM165 degradation in cells expressing this GGA1 mutant named GGA1-DN (Figure 39). Similar to Rab-DN experiments, GGA1-DN did not prevent TMEM165 Mn2+ induced degradation. However, these results should be interpreted carefully, since we did not checked that each pathway was indeed clearly blocked.

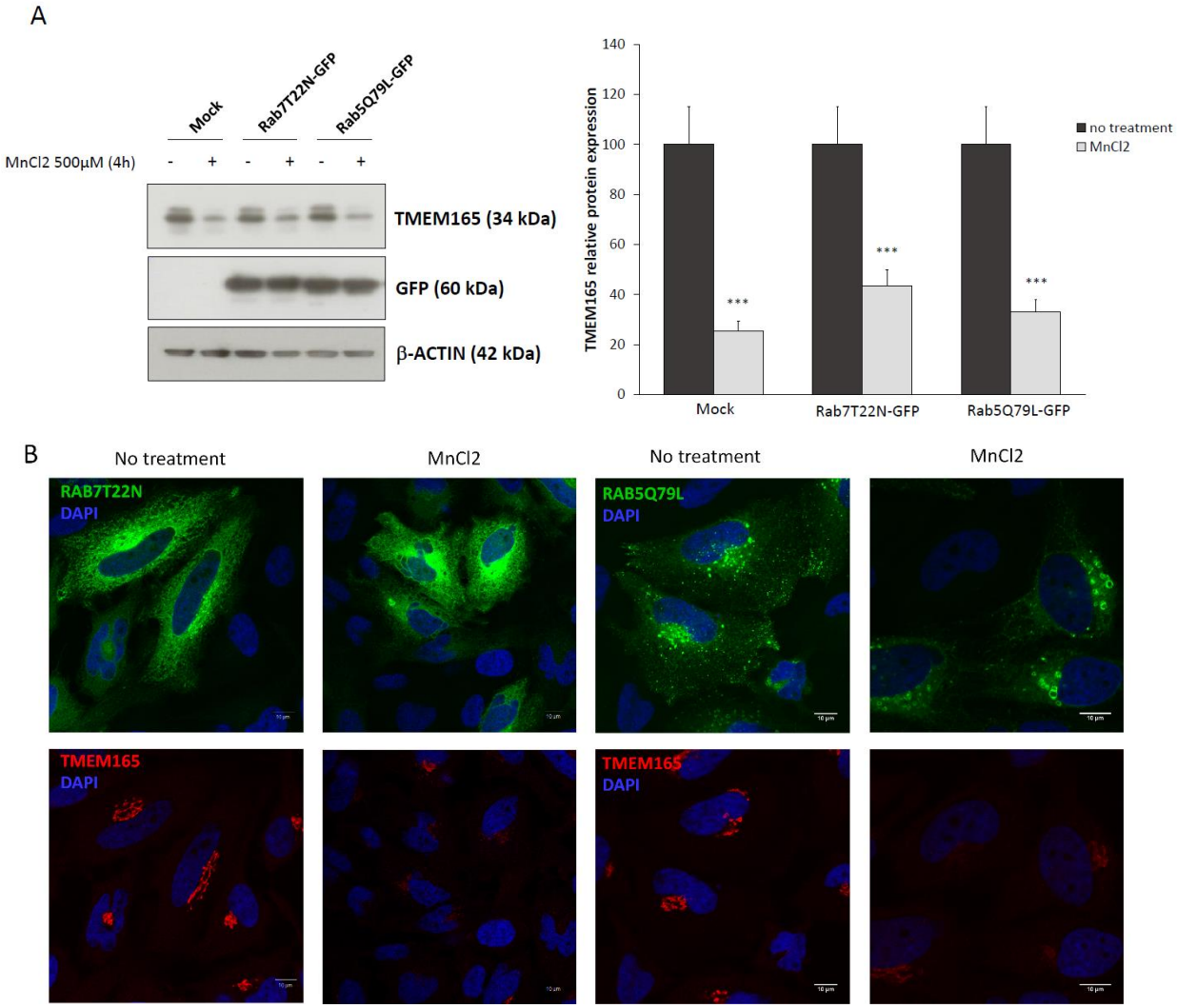

Figure 38. TMEM165 lysosomal degradation is Rab7 and Rab5 independent. HeLa cells were transfected with empty vector (mock), Rab7T22N-GFP or Rab5Q79L-GFP. 36H after transfection, cells were treated or not for 4h with MnCl2 500 µM. **(A)** Total cell lysates were prepared, subjected to SDS-PAGE and Western blot with the indicated antibodies. Right panel shows the quantification of TMEM165 protein levels after normalization with actin (N = 2; *** = P value < 0,001). **(B)** Immunofluorescence analysis by confocal microscopy of the same experiments as described in (A) (N = 2 ; n= 50).

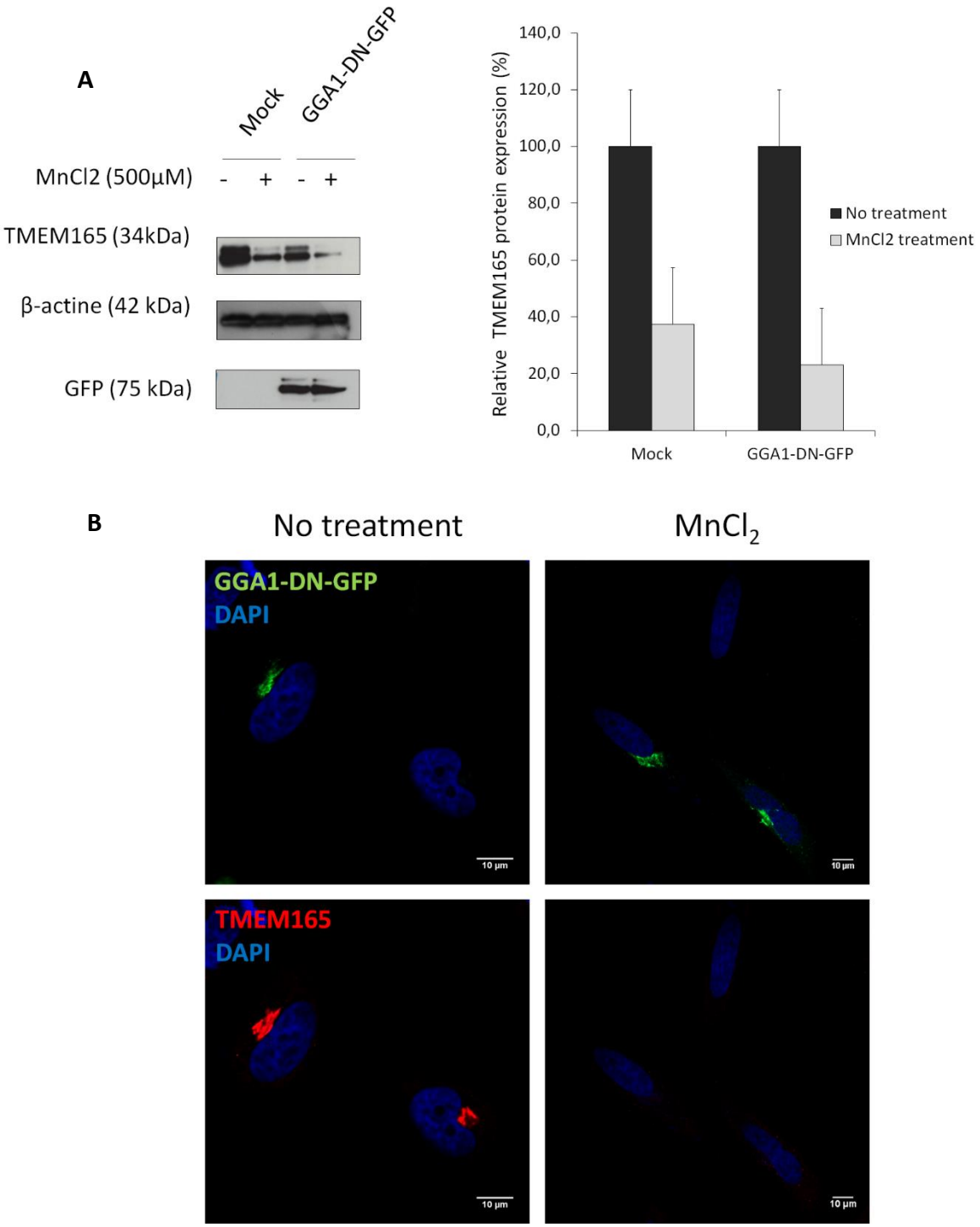

Figure 39. TMEM165 lysosomal degradation is GGA1 independent. HeLa cells were transfected with empty vector (mock) or pEGFP-C2 GGA1 encoding GGA1-DN. 36H after transfection, cells were treated or not for 4h with MnCl2 500 µM. **(A)** Total cell lysates were prepared, subjected to SDS-PAGE and Western blot with the indicated antibodies. Right panel shows the quantification of TMEM165 protein levels after normalization with actin **(B)** Immunofluorescence analysis by confocal microscopy of the same experiments as described in (A).

3.4. Discussion

The main result of this study is that TMEM165 is highly sensitive to Mn2+ since manganese addition in the cell media targets TMEM165 to lysosomal degradation. Interestingly, the Mn2+-induced degradation is conserved in yeast as Gdt1p-Myc is also targeted to degradation after Mn2+ exposure.

We also compared TMEM165 and GPP130 degradation after Mn2+ exposure. TMEM165 revealed to be sensitive to lower Mn2+ concentrations than GPP130 and also that its degradation is faster than GPP130, suggesting that the molecular mechanisms could be different for these two proteins. Nevertheless, we cannot exclude that this observed difference in manganese sensitivity is coming from different binding affinities for manganese.

3.4.1. Deciphering the pathways and mechanisms of TMEM165 induced degradation

3.4.1.1. Pathways possibly involved in TMEM165 induced degradation

The trafficking pathways by which TMEM165 is degraded following Mn2+ exposure are currently not known. Several pathways exist for TGN to lysosomes trafficking (Figure 40). A protein can leave the Golgi apparatus to reach early endosomes (EE) or can bypass EE to directly reach late endosomes. In certain conditions, a direct TGN to lysosomes trafficking has also been reported [313].

Besides, GPP130 is known to be targeted to lysosomal degradation via a Rab7 dependent pathway after Mn2+ exposure. We therefore examined the involvement of the rab5, rab7 and GGA1-dependent pathways using plasmid encoding dominant negative version of these proteins. A simplified view of the roles of these proteins in Golgi to lysosomes trafficking is shown in Figure 40. Interestingly, our complementary results seem to show that extracellular Mn2+ induces lysosomal degradation of TMEM165 via a Rab7, Rab5 and GGA1 independent pathway. However, these results should be interpreted very carefully, since we did not check that each pathway was indeed clearly blocked.

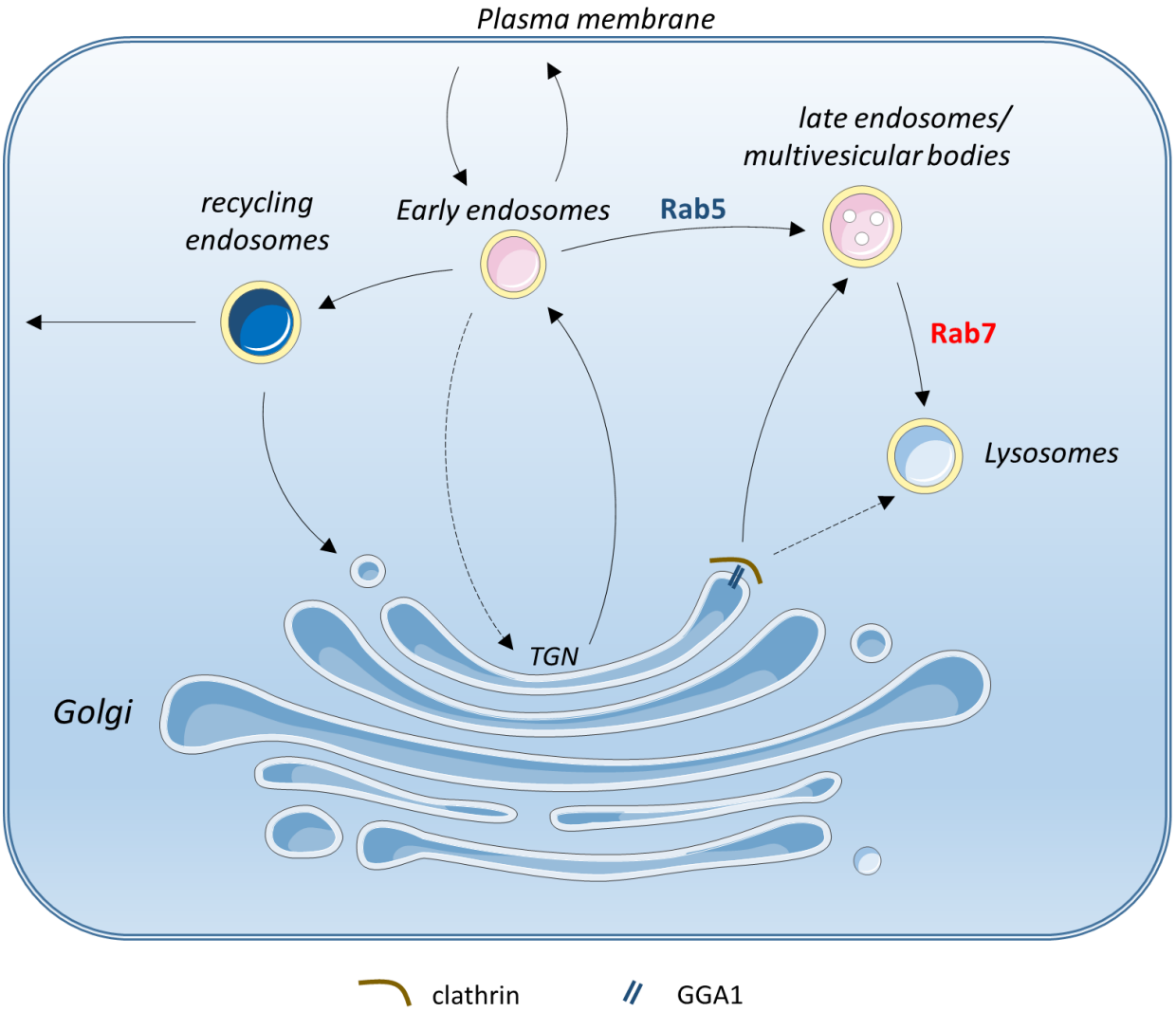

Figure 40. Roles of Rab5, Rab7, GGA1 and clathrin in vesicular trafficking from Golgi to lysosomes. Rab5 localizes to early endosomes (EE) where it is involved in the maturation from EE to late endosomes. Rab7 is required for trafficking from late endosomes to lysosomes and for the formation of functionally mature lysosomes. GGA1 is involved in the recruitment of clathrin to the TGN. Clathrin is a protein that plays a major role in the formation of coated vesicles.

3.4.1.2. Proteins involved in TMEM165 induced degradation

In addition, the proteins involved in the molecular mechanism of TMEM165 induced degradation are currently not known.

Recently, Venkat and collaborators have shown that manganese-induced trafficking and turnover of GPP130 was mediated by a protein called sortilin [314]. Sortilin is known to be a TGN-to-lysosome sorting receptor with a lumenal domain able to bind diverse cargo and a cytoplasmic domain that engages both GGA1 and clathrin [315]. However, there are both sortilin-dependent and sortilin-independent mechanisms to target Golgi proteins for lysosomal degradation. These

authors have shown that after Mn2+ exposure, sortilin binds GPP130 luminal stem domain, leading to the formation of reversible oligomers. This oligomerization then triggers GPP130 exit from the Golgi directly to MVB and then to lysosomes, where it is degraded. This pathway requires GGA1, clathrin and Rab7, but not Rab5. Finally, they have shown that TMEM165 redistribution into lysosomes after Mn2+ exposure was also sortilin dependent, exactly like GPP130. However, the role of oligomerization was not tested. Their result differs from ours, since they observed that TMEM165 induced degradation relies on sortilin and thus GGA1 to be targeted to lysosomes.

In addition, we showed that SPCA1 knockdown did not prevent TMEM165 induced degradation and thus we hypothesised that TMEM165 responds to changes in cytosolic Mn2+ concentrations. This result differs from GPP130 induced degradation, which has been shown to be blocked by SPCA1 knockdown [316].

3.4.2. TMEM165 domains involved in Mn2+ sensitivity

Since TMEM165 induced degradation is not blocked by SPCA1 knockdown, we hypothesied that TMEM165 responds to changes in cytosolic Mn2+. However, sortilin is a Golgi protein that binds cargo in the lumen of the GA. Therefore, regarding the recent results obtained by Venkat and collaborators, we hypothesized that increasing cytosolic Mn2+ concentration likely causes a change in TMEM165 conformation, making it competent to bind degradation partners in the Golgi lumen such as sortilin that will ultimately lead to its targeting to lysosomal degradation.

We thus propose a mechanistic binding model in which TMEM165 is a Ca2+/Mn2+ antiporter using the Ca2+ electrochemical gradient from the Golgi lumen to import Mn2+ from the cytosol into the Golgi lumen (Figure 41). In this model, Ca2+ and Mn2+ binding induces TMEM165 conformational changes. The conformational change triggered by Mn2+ allows TMEM165 to be recognised in the Golgi lumen by the sortilin. This recognition ultimately leads to TMEM165 lysosomal degradation.

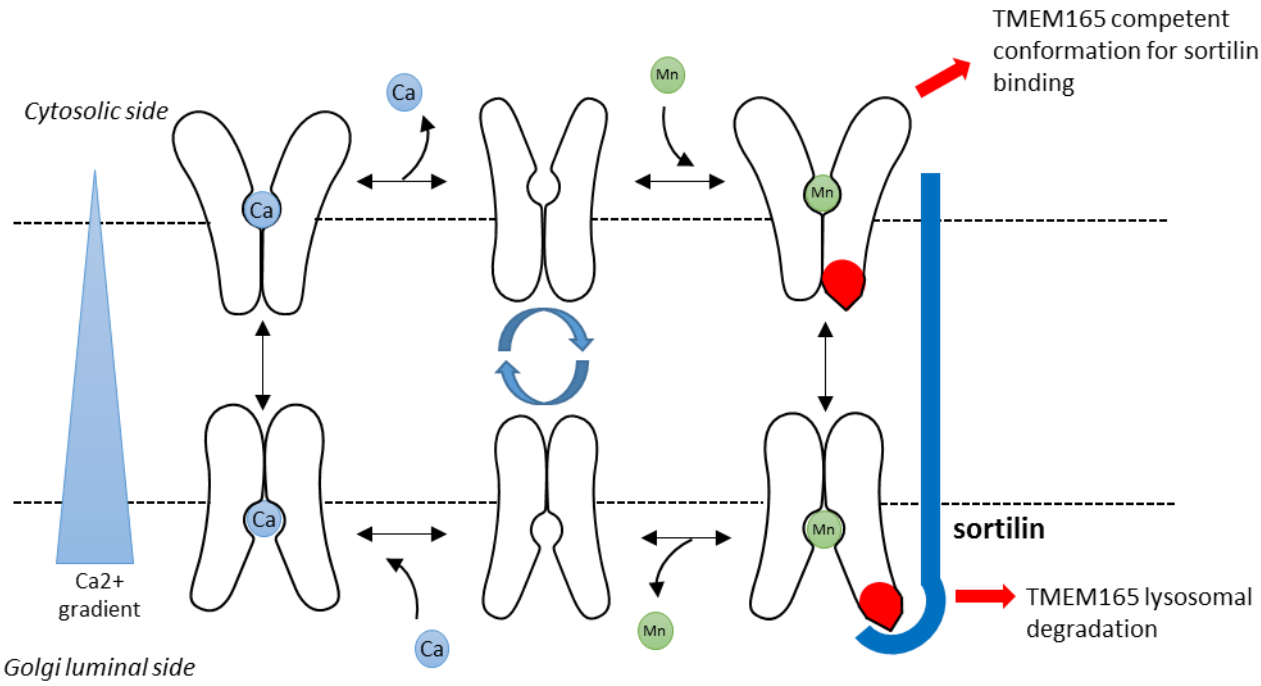

Figure 41. Mechanistic binding model for TMEM165 Mn2+-induced degradation. TMEM165 imports Mn2+ inside the Golgi lumen using the Ca2+ electrochemical gradient from the Golgi lumen. In this model, Ca2+ and Mn2+ binding induces TMEM165 conformational changes, with the conformational change triggered by Mn2+ allowing TMEM165 to be recognised in the Golgi lumen by the sortilin. This recognition ultimately leads to TMEM165 lysosomal degradation. The red part of TMEM165 symbolises the conformational change triggered by cytosolic Mn2+. This model reconciles our results and the recent results in the literature.

We have also tested the effect of two TMEM165 patient mutations on the Mn2+-induced degradation. Interestingly, while the R126H mutation remains Mn2+ sensitive, the glutamic acid (E108) in the highly conserved ELGDK motif was shown to be insensitive to Mn2+ exposure and therefore crucial in TMEM165 Mn2+-induced degradation. According to TMEM165 topology, this ELGDK motif is oriented towards the cytosol and located between the second and the third transmembrane domains of TMEM165. This result shows that the ELGDK motif is crucial for Mn2+ sensitivity and reinforces the fact that TMEM165 responds to changes in cytosolic Mn2+ and not Golgi luminal changes.

In order to explain the differences between the E108G and the R126H mutations, we could raise several hypotheses. First, the E108G mutation could force TMEM165 to adopt a conformation unable to bind degradation partners. In that case, the protein is stable in presence of high Mn2+ concentrations. In the other way around, it could be that the R126H mutation would facilitate the conformational change triggered by Mn2+, thus making the protein more accessible to

degradation partners. Finally, it could be that the E108 is crucial for sortilin binding but not the R126. The R126 could either be not part of the binding motif or not crucial for sortilin recognition.

Our data also show that the E108G TMEM165 mutant is able to rescue the glycosylation defect on LAMP2, although less efficiently than the wt-TMEM165 form. Strong of these observations on the E108G mutant, we decided to answer two related questions: What are the crucial amino acids for TMEM165 function in glycosylation? What are the crucial amino acids for TMEM165 Mn-induced degradation? To address these questions, we generated a lot of TMEM165 mutants with single point mutations. The goal is to understand of this approach is to understand if there is a link between TMEM165 function and its degradation induced by Mn2+. In other words, does TMEM165 need to be functional to be degraded by Mn2+? In addition, these mutants will help us to fully map the TMEM165 domain(s) responsible for its Mn2+-induced degradation. This study is only at the beginning therefore no early results will be presented here.

3.4.3. The purpose of TMEM165 induced degradation

Another important question to address is the purpose of this degradation after high Mn2+ concentrations exposure. While we currently do not have the answer, our data raise several hypotheses.

First, as a slight fraction of TMEM165 can be found at the plasma membrane, the degradation could be a mechanism to prevent an excess of Mn2+ entry at the plasma membrane. But as we have seen that mammalian cells mostly import Mn2+ by other plasma membrane transporters, this hypothesis is not likely true.

Our idea is that there is an interplay between TMEM165 and SPCA1 for Mn2+ handling at the Golgi level (Figure 42). In physiological conditions, we think that TMEM165 is the major Mn2+ importer in the Golgi. Indeed, SPCA1 needs energy to work, and then mostly transports Ca2+ as TMEM165 can import Mn2+ into the Golgi following the Ca2+ gradient generated by SPCA1.

However, an excess of cytosolic Mn2+ is known to be toxic because it can impair many fundamental cellular processes. It is thus critical for the cell to prevent the cytosol from Mn2+ accumulation. It is known in the literature that SPCA1 is involved in Mn2+ detoxification when Mn2+ cytosolic concentrations increase. In fact, in Mn2+ excess, SPCA1 can import Mn2+ inside the Golgi lumen and Mn2+ will be removed from the cell via the secretory pathway. As TMEM165

is degraded when the manganese level becomes toxic, we can hypothesize that this degradation somehow participates in detoxification. One can think that TMEM165, in the presence of high Mn2+ concentration in the Golgi, could transport the Golgi Mn2+ back to the cytosol due to its passive antiporter nature. In that case, the presence of TMEM165 will annihilate all efforts made by SPCA1 to get rid of cytosolic Mn2+. Thus, TMEM165 is degraded to prevent any Mn2+ leak in the cytosol, and SPCA1 can thus continue the Mn2+ detoxification.

Finally, we propose this model to explain the TMEM165 induced degradation (Figure 42). However, we do not exclude that TMEM165 can also use intraluminal Golgi proton to import Mn2+ inside the Golgi lumen.

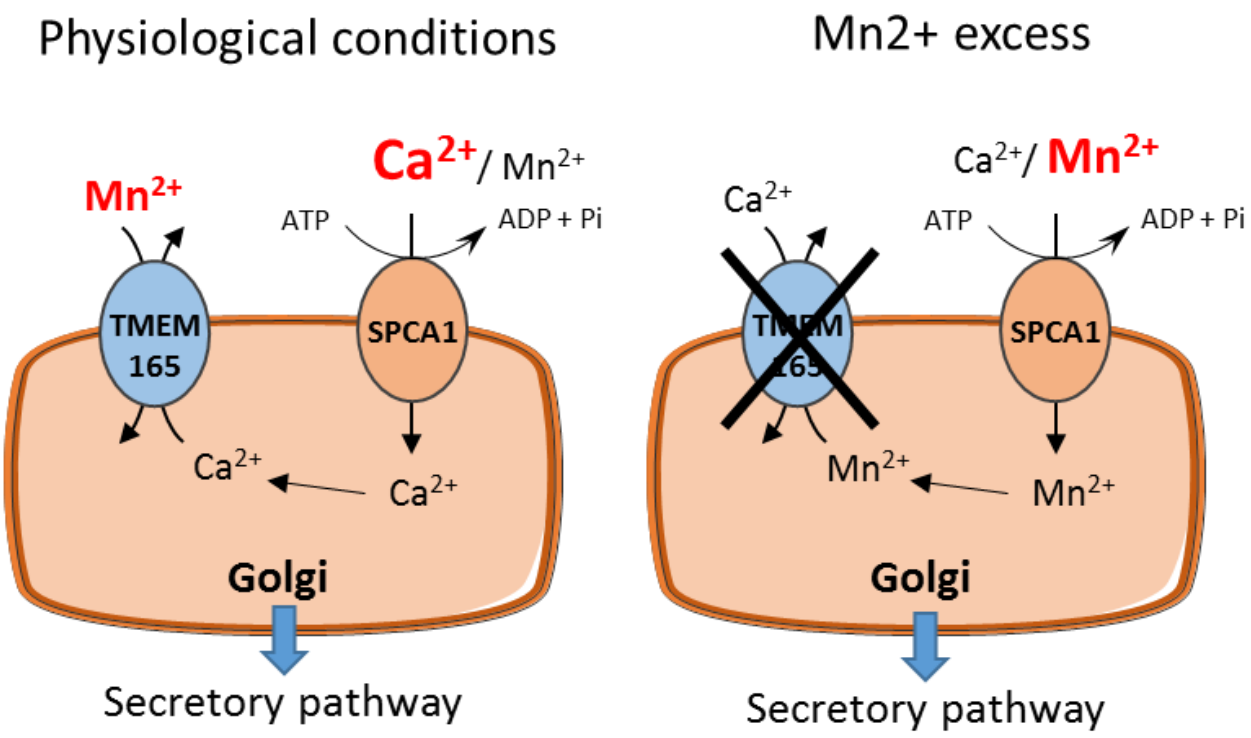

Figure 42. TMEM165 model for ion transport. TMEM165 is a passive antiporter that can import cytosolic Mn2+ inside the Golgi lumen in exchange for Ca2+ release in the cytosol. In physiological conditions, SPCA1 transports Ca2+ and TMEM165 can import Mn2+ into the Golgi following the Ca2+ gradient generated by SPCA1. In Mn2+ excess, SPCA1 can import Mn2+ inside the Golgi lumen. Due to its passive antiporter nature, TMEM165 is degraded to prevent the transport of Mn2+ back to the cytosol.

3.5. Abstract in French

Les déficiences en TMEM165 conduisent à un type de troubles congénitaux de la glycosylation (CDG), un groupe de maladies héréditaires dans lesquelles le processus de glycosylation est altéré. Nous avons récemment démontré que le défaut de glycosylation golgien dû à une déficience en TMEM165 résultait d'un défaut d'homéostasie du Mn2+ au niveau de l'appareil de Golgi. Nous avons également montré qu'une supplémentation en Mn2+ était suffisante pour rétablir une glycosylation normale. Dans cette étude, nous mettons en évidence que TMEM165 est une nouvelle protéine golgienne sensible au manganèse. Lorsque les cellules ont été exposées à des concentrations élevées de Mn2+, TMEM165 a été envoyé aux lysosomes pour être dégradé. De façon remarquable, alors que le mutant R126H reste sensible au manganèse, le mutant E108G, récemment identifié chez un nouveau patient atteint de TMEM165-CDG, est lui insensible. Dans l'ensemble, cette étude a identifié TMEM165 comme étant une nouvelle protéine golgienne sensible au Mn2+ et souligne l'importance cruciale de l'acide glutamique (E108) du motif ELGDK dans la dégradation de TMEM165 induite par le Mn2+.

[4] REVIEWS PUBLISHED

During my PhD, I also published two reviews, one as a first author, and the other as a first co-author.

The first review is an overview of all the post-translational modifications that occur at the Golgi level. We focused on Golgi PTM that can lead to diseases if disrupted. Glycosylation is indeed one of them but many others are also described in this review, such as methylation, palmitoylation, acetylation and so on.

The second review aims at summarizing all the data on TMEM165 and its ortholog in yeast Gdt1p. The goal of this review is to list clues and evidences that will help us to understand the roles of TMEM165 in Golgi glycosylation and ion homeostasis.

4.1. Golgi post-translational modifications and associated diseases

Golgi post-translational modifications and associated diseases

Sven Potelle[1], André Klein[2] and François Foulquier[1*]

1. CNRS-UMR 8576, Structural and Functional Glycobiology unit, FRABIO, University of Lille, 59655 Villeneuve d'Ascq, France.

2. Centre de Biologie et Pathologies, UAM de glycopathologies, CHRU de Lille, University of Lille, 59000 Lille.

*Address correspondence should be sent to: François Foulquier (francois.foulquier@univ-lille1.fr)

Tel. + 33 3 20 43 44 30

Fax. +33 3 20 43 65 55

E-mail. Francois.foulquier@univ-lille1.fr

Abstract

For non-specialists, Golgi is a very well-known subcellular compartment involved in secretion and correct targeting of soluble and transmembrane proteins. Nevertheless, Golgi is also specifically involved in many different and diverse post-translational modifications. Through its diverse functions, Golgi is not only able to modify secreted and transmembrane proteins but also cytoplasmic proteins. The Golgi apparatus research field is so broad that an exhaustive review of this organelle is not doable here. The goal of this review is to cover the main post-translational modifications occurring at the Golgi level and present the identified associated diseases.

Golgi, a brief overview:

Golgi is a cellular organelle composed of several flattened stacks of membranes devoid of ribosomes. These stacks are functionally different and reflect the specific compartmentalization of Golgi enzymes/ transporters involved in the modifications of proteins and lipids. The GA stacks are classically delimited as cis, median, trans and trans-Golgi network (TGN) [38,39]. Present in all animal cells and plants, Golgi is a part of a highly integrated and regulated endomembrane system [40]. Golgi constantly receives incoming material from the endoplasmic reticulum (ER) and sort specific cargo to their correct cellular destination such as the endosomal-lysosomal compartments, the plasma membrane or extracellular space. The cargo movement through the stacks is still controversial and has been suggested to occur in vesicles, in maturing cisternae, or by tubular connections between cisternae [41]. The overall Golgi structure and its plasticity are tightly controlled and crucial for maintaining its functions. As Golgi manufactures and modifies most of the cargo molecules passing through the different stacks, this organelle is considered to be the main contributor to post-translational modifications (PTM) of lipids and proteins. In this review, we will mainly focus on Golgi PTM of proteins in which gene defects have been linked to human diseases. However, many others lead to Golgi PTM associated diseases without being directly involved in PTM. One can think that this last class will certainly constitute in a near future the next booming field of PTM associated diseases.

PTM occurring at the Golgi level and associated diseases:

1. Glycosylation

Glycosylation is a major post-translational modification of proteins and lipids. The main glycosylation types are classified according to the linkage of the sugar moieties to the amino acid, asparagine (N-glycosylation), serine or threonine (O-glycosylation) and ceramide for glycolipids. Some of them begin directly in the ER lumen and continue at the Golgi level (N-glycosylation, O-mannosylation, O-glucosylation, O-fucosylation and glycolipids) (Figure 1). Nevertheless, certain types are entirely performed at the Golgi level (O-N-acetylgalactosaminylation (mucin types) and O-xylosylation (glycosaminoglycans)). Golgi glycosylation mainly consists in the elongation of the sugar chain(s) by addition of specific sugars such as galactose, N-acetylglucosamine, N-acetylgalactosamine, fucose, sialic acids etc. N-glycosylation is an exception to this process where

before further elongation, mannose removal might occur, a process extremely well documented in several reviews [42–44].

The sugar additions at the Golgi level rely on the existence of specific nucleotide sugar transporters and specific Golgi enzymes named glycosyltransferases (GT). Defects in these genes have been first identified in human diseases called CDG for Congenital Disorders of Glycosylation [45]. Nevertheless, a constantly growing subgroup of CDG indirectly affects glycosylation pathways through alterations of Golgi structure, vesicular trafficking and Golgi homeostasis. Today, more than 110 different CDGs have been reported [7] and approximately a third of them disturbs Golgi glycosylation [46]. The identification of these patients was performed via the main screening diagnostic test based on transferrin isoelectrofocalisation pattern, although this test only detects patients with N-glycosylation defects [47,48].

Defects in genes directly involved in glycosylation

Given the excellent recent reviews about CDGs, this part will only describe the identified CDGs from the last two years [1,3,7,46,49–53]. Four new CDGs directly affecting Golgi glycosylation have been identified: MAN1B1-CDG [54], SLC35A1-CDG [55,56], SLC35A2-CDG [57,58] and SLC35A3-CDG. The clinical phenotypes of these pathologies are summarized in table 1.

MAN1B1 is presumed (still controversial) to be a Golgi α1,2 mannosidase involved in the processing of the terminal mannose residues. The clinic is classically mild with observed mental retardation associated with slight facial dysmorphism, and truncal obesity [54]. However, some patients also show more serious phenotypes, including severe intellectual disabilities and a global developmental delay [59].

Three other deficiencies affecting sugar nucleotide transporters were also recently identified. Alterations of SLC35A1, which is the CMP-sialic acid transporter, leads to an autosomal recessive disorder characterized by seizures, ataxia, intellectual disabilities, multiple bleeding episodes and recurrent infections [55]. Similarly, defects in SLC35A2, an X-linked disorder, affect the UDP-galactose transporter. The patients also present intellectual disabilities and seizures and in some cases, ocular and skeletal abnormalities [58]. Recently, defects in SLC35A3, the main UDP-N-Acetylglucosamine transporter, have been linked to a syndrome characterized by arthrogryposis, mental retardation and seizures (AMRS) [60]. All these transporter deficiencies

affect the Golgi luminal pool of nucleotide sugars and consequently different glycosylation pathways. This might explain the severity of the observed phenotypes (table 1).

Defects in genes indirectly involved in glycosylation: defects in vesicular transport

There are more than a hundred genes involved indirectly in PTM. These genes can either be responsible for the structure, the organization and the homeostasis of the Golgi apparatus, or can also mediate the intracellular destination of vesicular transport. The defect of the Golgi function results in abnormal transport of cargo molecules and/or defective PTM. In this chapter, we will describe some examples of diseases in which the gene defect has consequences on the PTM, with a particular focus on glycosylation. The lack of assay exploring the different PTM as well as the unavailability of the tissues for clinical testing (i.e. nervous system) make the biochemical diagnosis of this group of disorders quite difficult. In a great number of diseases only the genetic diagnosis is indeed available and the potential alteration of the PTM has not been studied so far.

COG complex

In 2004, the discovery of the COG7 deficient CDG patients has opened completely new molecular mechanisms of Golgi glycosylation defects [11,61]. For the first time, the field of vesicular trafficking was connected to Golgi glycosylation. COG is indeed a multimeric cytoplasmic complex of 8 subunits (Cog1 to Cog8) known to be involved in the tethering of vesicles to the target compartments such as Golgi. Since 2004, many COG deficient CDG patients have been discovered and detailed in several reviews [62–64]. To date and except for the Cog3 subunit, mutations in all Cog subunits have been described responsible for CDGs [11–14,65–67].The recently identified COG defect was in Cog2, and as for the other COG deficient CDG patients, both N- and O-mucin type glycosylation defects were observed. The clinical manifestations are broad including microcephaly, developmental delay, intellectual disability, seizures, facial dysmorphism and liver dysfunctions [68].

COPII complex

Sec23B is involved in the formation of COPII vesicles from the ER and has been lately identified deficient in 2009 by Schwarz and collaborators in Congenital dyserythropoietic anemia type II

(CDAII) also known as the hereditary erythroblastic multinuclearity with a positive acidified-serum lysis test (HEMPAS) [69]. This autosomal recessive disorder is characterized by bi- and multinucleated erythroblasts. The biochemical characteristic of the disease was a sharper band 3 in the analysis of erythrocyte ghost extracts. This was the consequence of an impaired N-glycosylation of erythrocyte membrane proteins. The glycan structures were elucidated and showed the presence of immature oligosaccharides like high mannose, hybrid, and truncated complex type oligosaccharides [70]. The expression of the defect only in the erythroid lineage is due to the expression levels of *SEC23A* and *SEC23B* genes. The *SEC23A* paralog is indeed expressed in all other tissues, excepted in erythroid cells.

Golgin proteins

Golgi microtubule associated protein 210 (GMAP-210) is encoded by the thyroid hormone receptor interactor 11 gene (*TRIP11*). This protein is a member of the Golgin family, proteins that capture vesicles carrying Rab proteins and maintain the Golgi architecture [71]. The N-terminal part of GMAP-210 interacts with the curved membranes of the vesicles while its C-terminal domain interacts with flat Golgi membranes through interaction with the small guanine nucleotide binding protein Arf1 [72]. Fibroblasts and chondrocytes lacking GMAP-210 presented modifications of proteoglycan glycosylation, with incomplete glycan structures terminated with N-Acetylglucosamine (GlcNAc) residues. A specific retention of Perlecan in the endoplasmic reticulum has also been shown. The study also demonstrated that mutations in *TRIP11* led to achondrogenesis type 1A, a lethal human disease characterized by abnormal ossifications and distinctive histological features of the cartilage [73].

Defects in genes indirectly involved in glycosylation: defects in Golgi homeostasis

Another growing class of identified defects affects Golgi homeostasis in terms of pH and or cations homeostasis. While the impact of such defects on Golgi glycosylation is still controversial, one could think that some specific Golgi glycosyltransferases are extremely sensible to pH/ Cations changes.

E3 ubiquitin ligase

UBE3A encodes the E3 ubiquitin ligase Ube3a, this gene is epigenetically imprinted throughout neuronal brain cells, [74]. Ube3a attaches ubiquitin to diverse substrates and modifies the

function and/ or the turn-over of the ubiquitinylated proteins among which, a certain number of Golgi proteins. Angelman Syndrome is caused by mutations or deletions of the maternally inherited *UBE3A* gene, because the paternal allele of *UBE3A* is epigenetically silenced in neurons. The clinical features of the disease consists of intellectual disability, lack of speech, seizures, and a characteristic behavioral profile. A recent study has demonstrated that the lack of Ubiquitin protein ligase E3A increases the intraluminal Golgi pH with a concomitant reduction in protein sialylation and a distended Golgi phenotype. The mechanism by which Ube3a regulates Golgi pH remains undetermined [75].

Interestingly, two other Golgi proteins (ATP6V0A2 and TMEM165) have been linked to CDGs by impairing Golgi pH and or cation homeostasis. This has been extensively highlighted in recent reviews [7,46,52].

2. Acetylation

Acetylation is an enzymatic reaction that consists in the substitution of an active hydrogen atom by an acetyl group (COCH3) from the donor acetyl coenzyme A (Ac-CoA) (Figure 1). The Ac-CoA is synthesized in the cytosol, then imported into the ER lumen for the subsequent acetylation reaction via SLC33A1 (solute carrier family 33), its specific transporter [76]. The way for Ac-CoA to reach the GA lumen is currently unknown since no Golgi specific Ac-CoA transporter has been identified [76,77]. A vesicular transport is however not excluded. Two main types of acetylation have been identified at the Golgi level: the N-terminal acetylation of proteins and acetylation of specific monosaccharides [78–80]. Concerning the N-terminal acetylation, only HAT4 (Histone Acetyltransferase Type B Protein 4) localizes in the GA membranes and has been shown to be specifically involved in the acetylation of free histone H4 at the cytoplasmic face of the GA [80]. At the opposite, sugar acetylation occurs in the lumen of Golgi. Sialic acids residues can for example be O-acetylated at the 4, 7, 8 and/or 9 position [81] by specific Golgi acetyl transferases [82,83]. The exact physiological roles of *O*-acetylation of sialic acid however, remain to be fully elucidated.

Defects in genes involved in acetylation

No direct defects in Golgi acetyltransferases have been identified so far. Nevertheless, *SLC33A1* has been shown to be mutated in patients from a Chinese population affected by autosomal dominant spastic paraplegia-42 (SPG42) [84,85]. Although the molecular mechanisms leading to

the pathology are not currently known, one can suggest that a global acetylation loss should be seen, as well as a specific loss of O-acetylated glycoconjugates at the Golgi level.

3. Sulfation

Sulfation is a common PTM only occurring in the GA lumen (Figure 1). This PTM is catalyzed by specific sulfotransferases and consists in a transfer of sulfate from the universal sulfate donor 3'-phosphoadenosine-5'-phosphosulfate (PAPS) to the hydroxyl group of an acceptor (a tyrosine on a protein or a sugar chain) [86–88]. The import of PAPS in the Golgi lumen is facilitated by two Golgi-resident PAPS transporters, PAPST1 and PAPST2 [89,90].

Defects in genes involved in sulfation

Macular corneal dystrophy (MCD) type II, an autosomal recessive hereditary disease affecting the cornea, is known to be due to mutations in the promoter region of the corneal-specific sulfotransferase GlcNAc6ST (*CHST6*) gene [87]. These mutations abolish the expression of *CHST6* only in corneal cells, leading to the formation of unsulfated keratan sulfate in the cornea [91]. As a result, patients suffer from a progressive opacification of the cornea. Besides, some mutations on the coding region of *CHST6* have been described in patients suffering from MCD type I [92]. Several other defects listed in the table 1 have also been identified.

4. Phosphorylation

Phosphorylation is a largely distributed PTM and consists in the addition of a phosphate (PO_4^{3-}) group to any acceptor molecule (Figure 1). This modification is highly dynamic and reversible. At the cis-Golgi level, phosphorylation of mannose residues carried by newly synthesized lysosomal enzymes is a crucial step for their recognition by mannose-6-phosphate receptors and their correct targeting to lysosomes [93,94]. Phosphorylation at the Golgi level also occurs via FAM20C on secretory calcium-binding phosphoproteins (SCPP) family (including casein) and many secreted proteins involved in biomineralization, including the small integrin binding ligand N-linked glycoproteins (SIBLING proteins) [95,96]. While many different specific kinases are present within Golgi lumen, these enzymes are however poorly characterized. Finally, phosphorylation on the GA can take place on xylose residues carried by proteoglycans, via the action of FAM20B [97].

Defects in genes involved in phosphorylation

Among other proteins, the mannose-6-phosphate pathway is composed of the GlcNAc-1-phosphotransferase and the uncovering enzyme, which are in charge of the phosphorylation of mannose residues in the cis-Golgi [94]. GlcNAc-1-phosphotransferase deficiencies cause mucolipidosis II and III, two lysosomal storage diseases (LSD) which are characterized by missorting and cellular loss of lysosomal enzymes, and lysosomal accumulation of storage materials [98]. Mucolipidosis II, also referred as I-cell disease, is the most severe one and affected individuals most often die in early childhood [99,100]. Misrouting of lysosomal enzymes can cause numerous pathologies, including many LSD. Interestingly, a genetic linkage analysis has underlined the link between stuttering and mannose-6-phosphate pathway genes [101]. The other phosphorylation identified defects are mentioned in table 1.

5. Methylation

Methylation is a form of alkylation where a methyl group replace a hydrogen atom (Figure 1). With the exception of DNA methylation, protein methylation generally occurs on lysine residues and is not restricted to Golgi. At the Golgi level, methylation is an enzymatic PTM taking place at the cytosolic face of the organelle and using *S*-adenosylmethionine (SAM) as substrate. This modification generally occurs on N-terminal arginines of specific resident Golgi and cargo proteins (Wu et al. 2004a; Zhou et al. 2010), excepted for calmodulin where the methylation (trimethylation) occurs on lysine 115 [104,105]. Interestingly, methylation has been shown to be crucial in the maintenance of Golgi structure [103].

Defects in genes involved in methylation

Calmodulin can be trimethylated by calmodulin-lysine N-methyltransferase (CAMKMT) [105]. In normal individuals, there are 2 isoforms of CAMKMT: the first one is localized in the cytoplasm and the nucleus and the second one is strictly localized in Golgi. 2p21 deletion syndrome is caused by a homozygous deletion which includes SLC3A1, PREPL, PPM1B and the first exon of CAMKMT leading to a loss of its expression [106]. This syndrome consists of cystinuria, neonatal seizures, hypotonia, severe somatic and developmental delay, facial dysmorphism, and reduced activity of all the respiratory chain enzymatic complexes that are encoded in the mitochondria [106]. Authors have demonstrated that the patients suffering from 2p21 deletion syndrome accumulate hypomethylated calmodulin in lysates from their lymphoblastoid cells [105]. As a

result, there is still no way to know if calmodulin hypomethylation is due to a loss of the Golgi isoform. However, no direct defects in Golgi methylation have been reported to date.

6. Palmitoylation

Protein S-palmitoylation describes the covalent but reversible attachment of palmitate onto cysteine residues (Figure 1). Palmitoylation is a highly dynamic PTM, catalysed by palmitoyl aceyltransferases (PAT), that add the palmitate from palmitoyl-CoA anchored on membranes, and their counterpart the acyl protein thioesterases that remove the fatty acid [107]. At the Golgi level, palmitoylation mainly takes place at the cytosolic trans face of the organelle. Interestingly, 12 of the 23 known human PAT localize in the GA [108], making the GA an emerging center for peripheral membrane protein palmitoylation [107].

Defects in genes involved in palmitoylation

Palmitoylation deficiencies have been linked to several neuropsychiatric disorders [109]. Zinc finger, DHHC domain like containing 8 (ZDHHC8) mutations have been clearly linked to schizophrenia [110], ZDHHC15 loss and ZDHHC9 mutations have also been found in patients with X-linked mental retardation [111,112]. Moreover, mutations in Palmitoyl-Protein Thioesterase 1 (PPT1) gene lead to infantile neuronal ceroid lipofuscinosis, a well-described neurodegenerative phenotype in infants [113].

7. Proteolytic cleavage

Proteolytic processing is a PTM that occurs when a protease cleaves a target protein to modify its activity (Figure 1). Several peptides (i.e. peptide hormones) and proteins like growth factors, transcription factors, plasma membrane receptors are synthesized as precursors and must undergo proteolytic cleavage in Golgi lumen to be active [114]. Many Golgi endoproteases such as site 1 protease (S1P), site 2 protease (S2P) and furin have been identified [115–117]. *MBTPS2* is the gene encoding S2P, a Golgi membrane bound protease involved in cholesterol metabolism [116]. S2P substrates in the Golgi includes SREBP transcription factors (SREBP-1a, SREBP 1-c and SREBP-2) and other membrane bound transcription factors requiring a two step cleavage for activation [118].

Defects in genes involved in proteolytic cleavage

Even if there is a real lack of data related to S2P in humans, *MBTPS2* defects have been linked to several human X-linked skin diseases. *MBTPS2* has been shown mutated in the Olmsted syndrome [119], a rare keratinization disorder characterized by the combination of periorificial keratotic plaques and bilateral palmoplantar transgredient keratoderma [120]. The second pathology linked to mutations in *MBTPS2* is the IFAP (ichthyosis follicularis with atrichia and photophobia) syndrome [121–123]. Finally, *MBTPS2* has also been linked to keratosis follicularis spinulosa decalvans (KFSD) disease [124].

Conclusion

Apart from its cellular targeting roles, this review highlights Golgi as the main cellular factory for post-translational modifications. We have seen that these modifications could be essential for the stability, activity, trafficking and proper subcellular localization of many proteins. Several human different diseases due to genes directly involved in the biochemical reaction of post-translational modification have been reported. However and according to the huge number of proteins involved in the Golgi structure and function maintenance (transporters/ vesicular proteins (Rabs, tethering factors, SNAREs, complex associated proteins)/ microtubule associated proteins/ structural proteins), there are no doubts that the integrity of many different PTM is affected. The current lack of tools to explore the different PTM as well as the unavailability of the tissue for clinical testing (i.e. nervous system) complicates such analysis.

Acknowledgements

We would like to dedicate this work to our colleague Pr. Christian Körner who suddenly passed away early in January. The work was supported by a grant from the grant ERARE 11-135 (EURO-CDG) of the ERA-Net for Research Programmes on Rare Diseases Joint Transnational Call 2011 to F.F.

Conflict of Interest:

None

Animal rights:

This article does not contain any studies with human or animal subjects performed by the any of the authors.

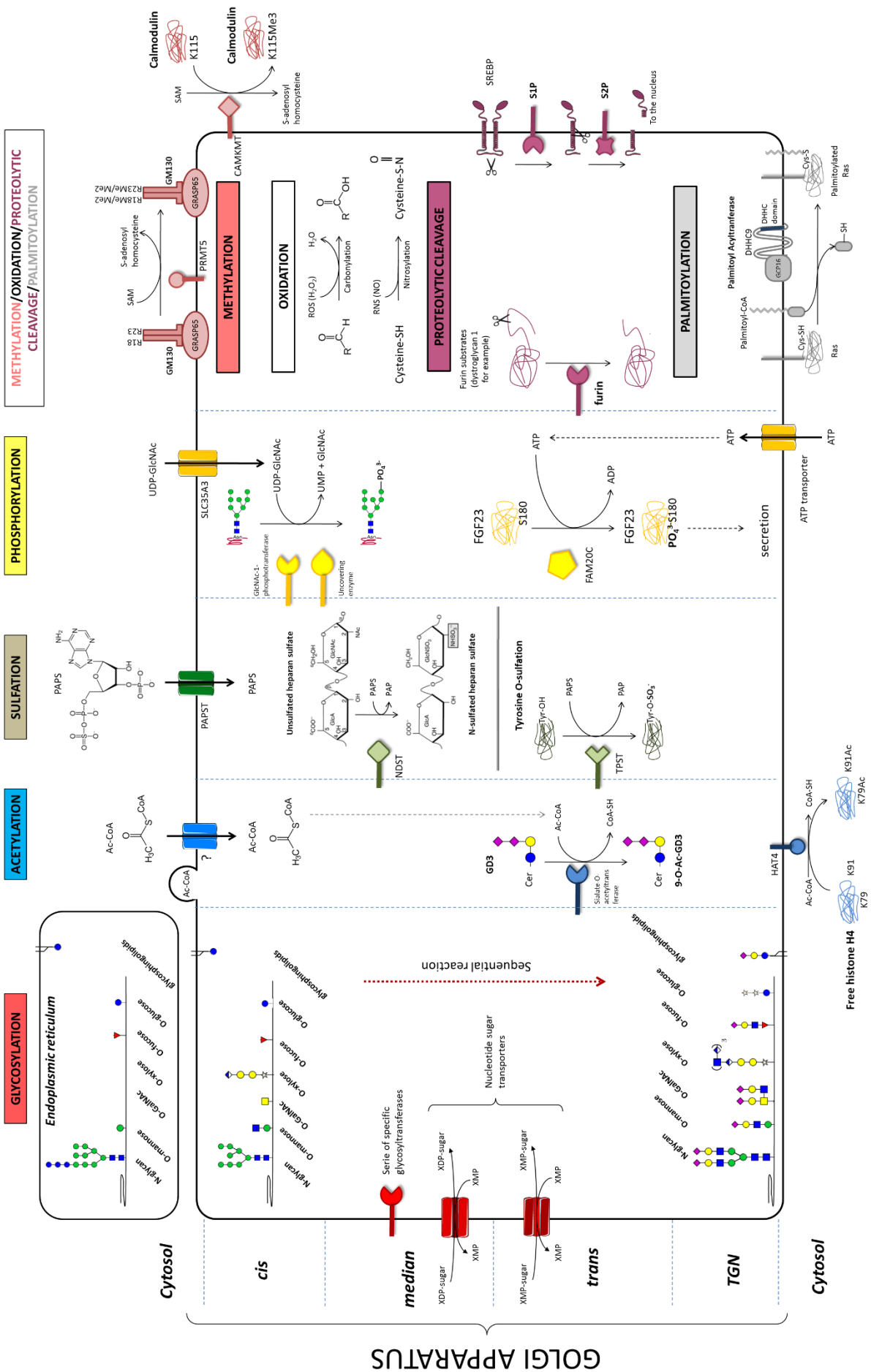

Fig. 1. PTM occurring at the Golgi level. The represented PTMs are the ones in which gene defects linked to human pathologies have been found. Each PTM is located on the specific Golgi cisternae according to the known location. The case of sugar sulfation is a little more complex. Indeed, sulfation of heparan sulfate is a sequential process (N-sulfation, then 2-O, 6-O and finally 3-O sulfation) taking place at the Golgi level but the enzymes are not clearly localized so far. XDP/XMP: Nucleotide di/mono phosphate. NDST: *N-deacetylase*/N-sulfotransferase ; TPST : Tyrosylprotein sulfotransferase. UDP/UMP: Uridine di/monophosphate. FGF23: Fibroblast growth factor 23. PRMT5: protein arginine methyltransferase 5. SAM: S-adenosyl methionine. SREBP: *Sterol Regulatory Element-Binding Proteins.*

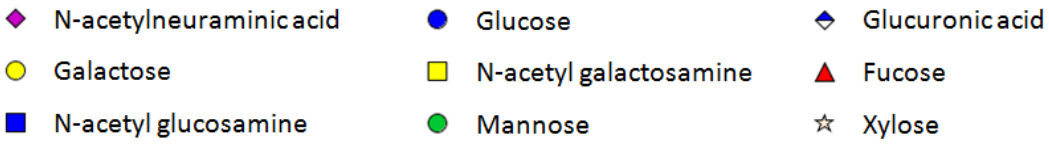

Affectedgene	Protein	AffectedPTM	Disease	Major clinical manifestations	Gene OMIM entry	Disease OMIM entry
MAN1B1	α 1,2 mannosidase	glycosylation	MAN1B1-CDG	severe mental retardation, delayed speech	604346	614202
SLC35A1	CMP-sialic acid transporter	glycosylation	SLC35A1-CDG	seizures, intellectual disability, ataxia, bleeding	605634	603585
SLC35A2	UDP-galactose transporter	glycosylation	SLC35A2-CDG	intellectual disability, seizures, skeletal abnormalities	314375	300896
SLC35A3	UDP-GlcNAc transporter	glycosylation	Arthrogryposis, mental retardation and seizures	autism spectrum disorder, hypotonia, epilepsy, and arthrogryposis	605632	615553
SEC23B	Sec23 homolog B	glycosylation	Dyserythropoietic anemia, congenital, type II	erythroblastic anemia: splenomegaly, gallstones, and iron overload potentially with liver cirrhosis or cardiac failure.	610512	224100
TRIP11	Golgi microtubule associated protein 210	glycosylation	Achondrogenesis type 1A	severe chondrodysplasia, lethal before or shortly after birth	604505	200600
UBE3A	Ubiquitin ligase E3A	glycosylation	Angelman syndrome	intellectual disability, seizures, lack of speech, and characteristic abnormal behavior	601623	105830
COG2	Component of oligomeric Golgi complex 2	glycosylation	COG2-CDG	microcephaly, developmental delay, intellectual disability, seizures, facial dysmorphism, liver dysfunction	606974	no entry yet
SLC33A1	Solute carrier family 33 (acetyl-CoA transporter), member 1	acetylation	Spastic paraplegia-42	spastic gait, increased lower limb tone, weakness and atrophy of the lower limb muscles, pes cavus	603690	612539
CHST3	Chondroitin 6-O-sulfotransferase	sulfation	Spondylo-epiphyseal dysplasia with joint dislocations	unusual skeletal dysplasia	603799	143095
CHST6	Corneal N-acetylglucosamine-6-O-sulfotransferase	sulfation	Macular corneal distrophy type II	progressive corneal opacification and reduced corneal sensitivity	605294	217800
CHST8	GalNAc-4-O sulfotransferase I	sulfation	Peeling skin syndrome	general skin peeling	610190	270300
CHST14	Dermatan sulfate GalNAc-4-O sulfotransferase I	sulfation	Ehlers-Danlos syndrome musculocontractural type 1	craniofacial dysmorphism, congenital contractures of thumbs and fingers, clubfeet, severe kyphoscoliosis	608429	601776
ARSE	Arylsulfatase E	sulfation	Chondrodysplasia punctata 1	stippled epiphyses, brachytelephalangy, nasomaxillary hypoplasia	300180	302950
PAPPS2	PAPS synthase	sulfation	Brachyolmia type 4	short-trunk stature, rectangular vertebral bodies, precocious calcification of rib cartilages, short femoral neck. Early death for severe cases.	603005	612847
SLA26A2	Sulfate anion transporter	sulfation	Achondrogenesis type 1B	severe chondrodysplasia, early death of respiratory failure	606718	600972
			Atelosteogenesis type 2	pulmonary hypoplasia, lethal in infants	606718	256050
			Epiphyseal dysplasia multiple 4	joint pain, scoliosis, malformations of the hands, feet, and knees	606718	226900
			Diastrophic dysplasia	scoliosis, clubfeet, malformed pinnae with calcification of the cartilage, cleft palate in some cases	606718	222600
GNTPG	N-acetylglucosamine-1-phosphotransferase gamma subunit	phosphorylation	Mucolipidosis III gamma	short stature, skeletal abnormalities, cardiomegaly, and developmental delay	607838	252605

Table 1. Golgi PTMs and associated diseases. This table summarizes all the human disorders linked to Golgi PTMs presented in this review.

Table 1 (continued)

Affected gene	Protein	Affected PTM	Disease	Major clinical manifestations	Gene OMIM entry	Disease OMIM entry
GNTPAB	N-acetylglucosamine-1-phosphotransferase alpha and beta subunits	phosphorylation	Mucolipidosis II and III	Hip dislocation, gingival hyperplasian, thoracic deformities and hernia soon after birth. Delayed psychomotor development. Same clinical features for mucolipidosis III as described just above.	607840	252500 252600
IMPAD1	Golgi-resident PAP phosphatase	phosphorylation	Chondrodysplasia with joint dislocations	short stature, chondrodysplasia with brachydactyly, congenital joint dislocations, micrognathia, cleft palate, and facial dysmorphism	614010	614078
INPP5E	Inositol polyphosphate-5-phosphatase	phosphorylation	Morm syndrome	Mental retardation, truncal obesity, retinal dystrophy, and micropenis	613037	610156
		phosphorylation	Joubert syndrome 1	Heterogenous: hypoplasia of the cerebellar vermis with the characteristic neuroradiologic molar tooth sign , dysregulation of breathing pattern and developmental delay.	613037	213300
AKAP9	A-kinase anchor protein 9	phosphorylation	Long QT syndrome-11	recurrent syncope, seizure, or sudden death	604001	611820
FAM20C	Golgi kinase (family with sequence similarity 20, member C)	phosphorylation	Raine syndrome	neonatal osteosclerotic bone dysplasia, increased ossification of the skull	611061	259775
CAMKMT	Calmodulin-lysine N-methyltransferase	methylation	2p21 deletion syndrome	cystinuria, neonatal seizures, hypotonia, severe somatic and developmental delay, facial dysmorphism	609559	606407
MBTPS2	Site-2 protease	proteolytic cleavage	IFAP syndrome with or without BRESHECK syndrome	ichthyosis follicularis, atrichia, and photophobia	300294	308205
			Olmsted syndrome, X-linked	periorificial keratotic plaques and bilateral palmoplantar transgredient keratoderma	300294	300918
			keratosis follicularis spinulosa decalvans, X-linked	keratosis pilaris, progressive cicatricial alopecia of the scalp, eyebrows, and eyelashes	300294	308800
ZDHHC8	Zinc finger, DHHC-type containing 8	palmitoylation	Schizophrenia susceptibility	hallucinations and delusions, inappropriate emotional responses, disordered thinking and concentration, erratic behavior	608784	181500
ZDHHC9	Zinc finger, DHHC-type containing 9	palmitoylation	X-linked mental retardation (Raymond type)	general intellectual limitations associated with impairments in adaptive behavior	300646	300799
ZDHHC15	Zinc finger, DHHC-type containing 15	palmitoylation	X-linked mental retardation-91	general intellectual limitations associated with impairments in adaptive behavior	300576	300577
PPT1	Palmitoyl-protein thioesterase 1	palmitoylation	Neuronal ceroid lipofuscinosis 1	Heterogenous: progressive dementia, seizures, and progressive visual deficiency. The cellular phenotype includes intracellular accumulation of autofluorescent lipopigment storage material.	600722	256730

References

Akama TO, Nishida K, Nakayama J, et al (2000) Macular corneal dystrophy type I and type II are caused by distinct mutations in a new sulphotransferase gene. Nat Genet 26:237–241. doi: 10.1038/79987

Aten E, Brasz LC, Bornholdt D, et al (2010) Keratosis Follicularis Spinulosa Decalvans is caused by mutations in MBTPS2. Hum Mutat 31:1125–1133. doi: 10.1002/humu.21335

Braulke T, Bonifacino JS (2009) Sorting of lysosomal proteins. Biochim Biophys Acta 1793:605–614. doi: 10.1016/j.bbamcr.2008.10.016

Carchon HA, Ndosimao CN, Aerschot SV, Jaeken J (2006) Use of Serum on Guthrie Cards in Screening for Congenital Disorders of Glycosylation. Clin Chem 52:774–775. doi: 10.1373/clinchem.2005.063305

Cathey SS, Leroy JG, Wood T, et al (2010) Phenotype and Genotype in Mucolipidoses II and III alpha/beta: A Study of 61 Probands. J Med Genet 47:38–48. doi: 10.1136/jmg.2009.067736

Chamberlain SJ, Lalande M (2010) Angelman syndrome, a genomic imprinting disorder of the brain. J Neurosci Off J Soc Neurosci 30:9958–9963. doi: 10.1523/JNEUROSCI.1728-10.2010

Condon KH, Ho J, Robinson CG, et al (2013) The Angelman syndrome protein Ube3a/E6AP is required for Golgi acidification and surface protein sialylation. J Neurosci Off J Soc Neurosci 33:3799–3814. doi: 10.1523/JNEUROSCI.1930-11.2013

Coutinho MF, Prata MJ, Alves S (2012) Mannose-6-phosphate pathway: A review on its role in lysosomal function and dysfunction. Mol Genet Metab 105:542–550. doi: 10.1016/j.ymgme.2011.12.012

Cylwik B, Lipartowska K, Chrostek L, Gruszewska E (2013a) Congenital disorders of glycosylation. Part II. Defects of protein O-glycosylation. Acta Biochim Pol 60:361–368.

Cylwik B, Naklicki M, Chrostek L, Gruszewska E (2013b) Congenital disorders of glycosylation. Part I. Defects of protein N-glycosylation. Acta Biochim Pol 60:151–161.

Denecke J, Kranz C, Nimtz M, et al (2008) Characterization of the N-glycosylation phenotype of erythrocyte membrane proteins in congenital dyserythropoietic anemia type II (CDA II/HEMPAS). Glycoconj J 25:375–382. doi: 10.1007/s10719-007-9089-1

Ding YG, Wang JY, Qiao JJ, et al (2010) A novel mutation in MBTPS2 causes ichthyosis follicularis, alopecia and photophobia (IFAP) syndrome in a Chinese family. Br J Dermatol 163:886–889. doi: 10.1111/j.1365-2133.2010.09890.x

Drin G, Morello V, Casella J-F, et al (2008) Asymmetric tethering of flat and curved lipid membranes by a golgin. Science 320:670–673. doi: 10.1126/science.1155821

Dunphy WG, Rothman JE (1985) Compartmental organization of the Golgi stack. Cell 42:13–21.

Edvardson S, Ashikov A, Jalas C, et al (2013) Mutations in SLC35A3 cause autism spectrum disorder, epilepsy and arthrogryposis. J Med Genet 50:733–739. doi: 10.1136/jmedgenet-2013-101753

Farquhar MG (1985) Progress in unraveling pathways of Golgi traffic. Annu Rev Cell Biol 1:447–488. doi: 10.1146/annurev.cb.01.110185.002311

Foulquier F (2009) COG defects, birth and rise! Biochim Biophys Acta 1792:896–902. doi: 10.1016/j.bbadis.2008.10.020

Foulquier F, Ungar D, Reynders E, et al (2007) A new inborn error of glycosylation due to a Cog8 deficiency reveals a critical role for the Cog1-Cog8 interaction in COG complex formation. Hum Mol Genet 16:717–730. doi: 10.1093/hmg/ddl476

Foulquier F, Vasile E, Schollen E, et al (2006) Conserved oligomeric Golgi complex subunit 1 deficiency reveals a previously uncharacterized congenital disorder of glycosylation type II. Proc Natl Acad Sci U S A 103:3764–3769. doi: 10.1073/pnas.0507685103

Freeze HH (2013) Understanding human glycosylation disorders: biochemistry leads the charge. J Biol Chem 288:6936–6945. doi: 10.1074/jbc.R112.429274

Freeze HH, Chong JX, Bamshad MJ, Ng BG (2014) Solving glycosylation disorders: fundamental approaches reveal complicated pathways. Am J Hum Genet 94:161–175. doi: 10.1016/j.ajhg.2013.10.024

Glick BS, Luini A (2011) Models for Golgi traffic: a critical assessment. Cold Spring Harb Perspect Biol 3:a005215. doi: 10.1101/cshperspect.a005215

Hackler R, Arndt T, Helwig-Rolig A, et al (2000) Investigation by isoelectric focusing of the initial carbohydrate-deficient transferrin (CDT) and non-CDT transferrin isoform fractionation step involved in determination of CDT by the ChronAlcoI.D. assay. Clin Chem 46:483–492.

Haghighi A, Scott CA, Poon DS, et al (2013) A Missense Mutation in the MBTPS2 Gene Underlies the X-Linked Form of Olmsted Syndrome. J Invest Dermatol 133:571–573. doi: 10.1038/jid.2012.289

Hennet T (2012) Diseases of glycosylation beyond classical congenital disorders of glycosylation. Biochim Biophys Acta 1820:1306–1317. doi: 10.1016/j.bbagen.2012.02.001

Hirabayashi Y, Nomura KH, Nomura K (2013) The acetyl-CoA transporter family SLC33. Mol Aspects Med 34:586–589. doi: 10.1016/j.mam.2012.05.009

Honke K, Taniguchi N (2002) Sulfotransferases and sulfated oligosaccharides. Med Res Rev 22:637–654. doi: 10.1002/med.10020

Jaeken J (2011) Congenital disorders of glycosylation (CDG): it's (nearly) all in it! J Inherit Metab Dis 34:853–858. doi: 10.1007/s10545-011-9299-3

Jaeken J, Matthijs G (2001) Congenital disorders of glycosylation. Annu Rev Genomics Hum Genet 2:129–151. doi: 10.1146/annurev.genom.2.1.129

Jonas MC, Pehar M, Puglielli L (2010) AT-1 is the ER membrane acetyl-CoA transporter and is essential for cell viability. J Cell Sci 123:3378–3388. doi: 10.1242/jcs.068841

Kamiyama S, Sasaki N, Goda E, et al (2006) Molecular cloning and characterization of a novel 3'-phosphoadenosine 5'-phosphosulfate transporter, PAPST2. J Biol Chem 281:10945–10953. doi: 10.1074/jbc.M508991200

Kamiyama S, Suda T, Ueda R, et al (2003) Molecular cloning and identification of 3'-phosphoadenosine 5'-phosphosulfate transporter. J Biol Chem 278:25958–25963. doi: 10.1074/jbc.M302439200

Kang C, Drayna D (2011) Genetics of speech and language disorders. Annu Rev Genomics Hum Genet 12:145–164. doi: 10.1146/annurev-genom-090810-183119

Kehoe JW, Bertozzi CR (2000) Tyrosine sulfation: a modulator of extracellular protein-protein interactions. Chem Biol 7:R57–61.

Klein A, Roussel P (1998) O-Acetylation of sialic acids. Biochimie 80:49–57. doi: 10.1016/S0300-9084(98)80056-4

Kodera H, Ando N, Yuasa I, et al (2014) Mutations in COG2 encoding a subunit of the conserved oligomeric golgi complex cause a congenital disorder of glycosylation. Clin Genet. doi: 10.1111/cge.12417

Kodera H, Nakamura K, Osaka H, et al (2013) De novo mutations in SLC35A2 encoding a UDP-galactose transporter cause early-onset epileptic encephalopathy. Hum Mutat 34:1708–1714. doi: 10.1002/humu.22446

Koike T, Izumikawa T, Tamura J-I, Kitagawa H (2009) FAM20B is a kinase that phosphorylates xylose in the glycosaminoglycan-protein linkage region. Biochem J 421:157–162. doi: 10.1042/BJ20090474

Kranz C, Ng BG, Sun L, et al (2007) COG8 deficiency causes new congenital disorder of glycosylation type IIh. Hum Mol Genet 16:731–741. doi: 10.1093/hmg/ddm028

Krasnewich D (2014) Human glycosylation disorders. Cancer Biomark Sect Dis Markers 14:3–16. doi: 10.3233/CBM-130374

Lin P, Li J, Liu Q, et al (2008) A missense mutation in SLC33A1, which encodes the acetyl-CoA transporter, causes autosomal-dominant spastic paraplegia (SPG42). Am J Hum Genet 83:752–759. doi: 10.1016/j.ajhg.2008.11.003

Liu H, Abecasis GR, Heath SC, et al (2002) Genetic variation in the 22q11 locus and susceptibility to schizophrenia. Proc Natl Acad Sci U S A 99:16859–16864. doi: 10.1073/pnas.232186099

Lübbehusen J, Thiel C, Rind N, et al (2010) Fatal outcome due to deficiency of subunit 6 of the conserved oligomeric Golgi complex leading to a new type of congenital disorders of glycosylation. Hum Mol Genet 19:3623–3633. doi: 10.1093/hmg/ddq278

Magen S, Magnani R, Haziza S, et al (2012) Human calmodulin methyltransferase: expression, activity on calmodulin, and Hsp90 dependence. PloS One 7:e52425. doi: 10.1371/journal.pone.0052425

Magnani R, Dirk LMA, Trievel RC, Houtz RL (2010) Calmodulin methyltransferase is an evolutionarily conserved enzyme that trimethylates Lys-115 in calmodulin. Nat Commun 1:43. doi: 10.1038/ncomms1044

Mandal C, Mandal C, Chandra S, et al (2012) Regulation of O-acetylation of sialic acids by sialate-O-acetyltransferase and sialate-O-acetylesterase activities in childhood acute lymphoblastic leukemia. Glycobiology 22:70–83. doi: 10.1093/glycob/cwr106

Mansouri MR, Marklund L, Gustavsson P, et al (2005) Loss of ZDHHC15 expression in a woman with a balanced translocation t(X;15)(q13.3;cen) and severe mental retardation. Eur J Hum Genet EJHG 13:970–977. doi: 10.1038/sj.ejhg.5201445

Mao F, Li Z, Zhao B, et al (2015) Identification and Functional Analysis of a SLC33A1: c.339T>G (p.Ser113Arg) Variant in the Original SPG42 Family. Hum Mutat 36:240–249. doi: 10.1002/humu.22732

Miller VJ, Ungar D (2012) Re'COG'nition at the Golgi. Traffic Cph Den 13:891–897. doi: 10.1111/j.1600-0854.2012.01338.x

Mohamed M, Ashikov A, Guillard M, et al (2013) Intellectual disability and bleeding diathesis due to deficient CMP--sialic acid transport. Neurology 81:681–687. doi: 10.1212/WNL.0b013e3182a08f53

Mollenhauer HH, Morré DJ (1974) Polyribosomes associated with the Golgi apparatus. Protoplasma 79:333–336.

Nakazawa K, Hassell JR, Hascall VC, et al (1984) Defective processing of keratan sulfate in macular corneal dystrophy. J Biol Chem 259:13751–13757.

Nalbant D, Youn H, Nalbant SI, et al (2005) FAM20: an evolutionarily conserved family of secreted proteins expressed in hematopoietic cells. BMC Genomics 6:11. doi: 10.1186/1471-2164-6-11

Neufeld EF (1974) The biochemical basis for mucopolysaccharidoses and mucolipidoses. Prog Med Genet 10:81–101.

Ng BG, Buckingham KJ, Raymond K, et al (2013) Mosaicism of the UDP-galactose transporter SLC35A2 causes a congenital disorder of glycosylation. Am J Hum Genet 92:632–636. doi: 10.1016/j.ajhg.2013.03.012

Ng BG, Kranz C, Hagebeuk EEO, et al (2007) Molecular and clinical characterization of a Moroccan Cog7 deficient patient. Mol Genet Metab 91:201–204. doi: 10.1016/j.ymgme.2007.02.011

Oeffner F, Fischer G, Happle R, et al (2009) IFAP syndrome is caused by deficiency in MBTPS2, an intramembrane zinc metalloprotease essential for cholesterol homeostasis and ER stress response. Am J Hum Genet 84:459–467. doi: 10.1016/j.ajhg.2009.03.014

Paesold-Burda P, Maag C, Troxler H, et al (2009) Deficiency in COG5 causes a moderate form of congenital disorders of glycosylation. Hum Mol Genet 18:4350–4356. doi: 10.1093/hmg/ddp389

Parvari R, Gonen Y, Alshafee I, et al (2005) The 2p21 deletion syndrome: characterization of the transcription content. Genomics 86:195–211. doi: 10.1016/j.ygeno.2005.04.001

Planey SL, Zacharias DA (2009) Palmitoyl acyltransferases, their substrates, and novel assays to connect them (Review). Mol Membr Biol 26:14–31. doi: 10.1080/09687680802646703

Rawson RB (2013) The site-2 protease. Biochim Biophys Acta 1828:2801–2807. doi: 10.1016/j.bbamem.2013.03.031

Rawson RB, Zelenski NG, Nijhawan D, et al (1997) Complementation cloning of S2P, a gene encoding a putative metalloprotease required for intramembrane cleavage of SREBPs. Mol Cell 1:47–57.

Raymond FL, Tarpey PS, Edkins S, et al (2007) Mutations in ZDHHC9, which encodes a palmitoyltransferase of NRAS and HRAS, cause X-linked mental retardation associated with a Marfanoid habitus. Am J Hum Genet 80:982–987. doi: 10.1086/513609

Reynders E, Foulquier F, Annaert W, Matthijs G (2011) How Golgi glycosylation meets and needs trafficking: the case of the COG complex. Glycobiology 21:853–863. doi: 10.1093/glycob/cwq179

Reynders E, Foulquier F, Leão Teles E, et al (2009) Golgi function and dysfunction in the first COG4-deficient CDG type II patient. Hum Mol Genet 18:3244–3256. doi: 10.1093/hmg/ddp262

Riemersma M, Sandrock J, Boltje TJ, et al (2014) Disease mutations in CMP-sialic acid transporter SLC35A1 result in abnormal α-dystroglycan O-mannosylation, independent from sialic acid. Hum Mol Genet. doi: 10.1093/hmg/ddu742

Rosnoblet C, Peanne R, Legrand D, Foulquier F (2013) Glycosylation disorders of membrane trafficking. Glycoconj J 30:23–31. doi: 10.1007/s10719-012-9389-y

Roth J (2002) Protein N-glycosylation along the secretory pathway: relationship to organelle topography and function, protein quality control, and cell interactions. Chem Rev 102:285–303.

Roth J, Zuber C, Park S, et al (2010) Protein N-glycosylation, protein folding, and protein quality control. Mol Cells 30:497–506. doi: 10.1007/s10059-010-0159-z

Rymen D, Peanne R, Millón MB, et al (2013) MAN1B1 deficiency: an unexpected CDG-II. PLoS Genet 9:e1003989. doi: 10.1371/journal.pgen.1003989

Salaun C, Greaves J, Chamberlain LH (2010) The intracellular dynamic of protein palmitoylation. J Cell Biol 191:1229–1238. doi: 10.1083/jcb.201008160

Schauer R (2004) Sialic acids: fascinating sugars in higher animals and man. Zool Jena Ger 107:49–64. doi: 10.1016/j.zool.2003.10.002

Schwarz K, Iolascon A, Verissimo F, et al (2009) Mutations affecting the secretory COPII coat component SEC23B cause congenital dyserythropoietic anemia type II. Nat Genet 41:936–940. doi: 10.1038/ng.405

Scott K, Gadomski T, Kozicz T, Morava E (2014) Congenital disorders of glycosylation: new defects and still counting. J Inherit Metab Dis 37:609–617. doi: 10.1007/s10545-014-9720-9

Seidah NG, Mowla SJ, Hamelin J, et al (1999) Mammalian subtilisin/kexin isozyme SKI-1: A widely expressed proprotein convertase with a unique cleavage specificity and cellular localization. Proc Natl Acad Sci U S A 96:1321–1326.

Smits P, Bolton AD, Funari V, et al (2010) Lethal skeletal dysplasia in mice and humans lacking the golgin GMAP-210. N Engl J Med 362:206–216. doi: 10.1056/NEJMoa0900158

Stanley P (2011) Golgi glycosylation. Cold Spring Harb Perspect Biol. doi: 10.1101/cshperspect.a005199

Tagliabracci VS, Engel JL, Wen J, et al (2012) Secreted kinase phosphorylates extracellular proteins that regulate biomineralization. Science 336:1150–1153. doi: 10.1126/science.1217817

Tang L, Liang J, Wang W, et al (2011) A novel mutation in MBTPS2 causes a broad phenotypic spectrum of ichthyosis follicularis, atrichia, and photophobia syndrome in a large Chinese family. J Am Acad Dermatol 64:716–722. doi: 10.1016/j.jaad.2010.02.045

Tiede S, Storch S, Lübke T, et al (2005) Mucolipidosis II is caused by mutations in GNPTA encoding the alpha/beta GlcNAc-1-phosphotransferase. Nat Med 11:1109–1112. doi: 10.1038/nm1305

Van Damme P, Hole K, Pimenta-Marques A, et al (2011) NatF contributes to an evolutionary shift in protein N-terminal acetylation and is important for normal chromosome segregation. PLoS Genet 7:e1002169. doi: 10.1371/journal.pgen.1002169

Van Scherpenzeel M, Timal S, Rymen D, et al (2014) Diagnostic serum glycosylation profile in patients with intellectual disability as a result of MAN1B1 deficiency. Brain J Neurol 137:1030–1038. doi: 10.1093/brain/awu019

Varki A, Diaz S (1985) The transport and utilization of acetyl coenzyme A by rat liver Golgi vesicles. J Biol Chem 260:6600–6608.

Vesa J, Hellsten E, Verkruyse LA, et al (1995) Mutations in the palmitoyl protein thioesterase gene causing infantile neuronal ceroid lipofuscinosis. Nature 376:584–587. doi: 10.1038/376584a0

Vey M, Schäfer W, Berghöfer S, et al (1994) Maturation of the trans-Golgi network protease furin: compartmentalization of propeptide removal, substrate cleavage, and COOH-terminal truncation. J Cell Biol 127:1829–1842.

Wise RJ, Barr PJ, Wong PA, et al (1990) Expression of a human proprotein processing enzyme: correct cleavage of the von Willebrand factor precursor at a paired basic amino acid site. Proc Natl Acad Sci U S A 87:9378–9382.

Wu CC, MacCoss MJ, Mardones G, et al (2004a) Organellar proteomics reveals Golgi arginine dimethylation. Mol Biol Cell 15:2907–2919. doi: 10.1091/mbc.E04-02-0101

Wu X, Steet RA, Bohorov O, et al (2004b) Mutation of the COG complex subunit gene COG7 causes a lethal congenital disorder. Nat Med 10:518–523. doi: 10.1038/nm1041

Yaghoobi R, Omidian M, Sina N, et al (2007) Olmsted syndrome in an Iranian family: report of two new cases. Arch Iran Med 10:246–249. doi: 07102/AIM.0022

Yang X, Yu W, Shi L, et al (2011) HAT4, a Golgi apparatus-anchored B-type histone acetyltransferase, acetylates free histone H4 and facilitates chromatin assembly. Mol Cell 44:39–50. doi: 10.1016/j.molcel.2011.07.032

Yang Y-S, Wang C-C, Chen B-H, et al (2015) Tyrosine Sulfation as a Protein Post-Translational Modification. Mol Basel Switz 20:2138–2164. doi: 10.3390/molecules20022138

Young FB, Butland SL, Sanders SS, et al (2012) Putting proteins in their place: palmitoylation in Huntington disease and other neuropsychiatric diseases. Prog Neurobiol 97:220–238. doi: 10.1016/j.pneurobio.2011.11.002

Yu I-M, Hughson FM (2010) Tethering factors as organizers of intracellular vesicular traffic. Annu Rev Cell Dev Biol 26:137–156. doi: 10.1146/annurev.cellbio.042308.113327

Zhou Z, Sun X, Zou Z, et al (2010) PRMT5 regulates Golgi apparatus structure through methylation of the golgin GM130. Cell Res 20:1023–1033. doi: 10.1038/cr.2010.56

Abstract in French

Pour les non spécialistes, l'appareil de Golgi est un compartiment subcellulaire très connu pour être impliqué dans la sécrétion et l'adressage des protéines solubles et transmembranaires. Néanmoins, le Golgi est également impliqué dans de nombreuses modifications post-traductionnelles essentielles pour la cellule. Grâce à ses fonctions diverses, le Golgi n'est pas seulement capable de modifier les protéines sécrétées et transmembranaires, mais aussi les protéines cytoplasmiques via des enzymes golgiennes dont le site catalytique est tourné vers le cytosol. La recherche dans le domaine de l'appareil de Golgi est tellement large qu'une revue exhaustive de cet organe n'est pas possible ici. L'objectif de cette revue est de couvrir les principales modifications post-traductionnelles survenant au niveau de l'appareil Golgi et de présenter les maladies associées à des défauts dans ces modifications post-traductionnelles.

4.2. TMEM165 deficiencies in Congenital Disorders of Glycosylation type II (CDG-II): clues and evidences for roles of the protein in Golgi functions and ion homeostasis.

TMEM165 deficiencies in Congenital Disorders of Glycosylation type II (CDG-II): clues and evidences for roles of the protein in Golgi functions and ion homeostasis.

Eudoxie Dulary*, Sven Potelle*, Dominique Legrand‡ and François Foulquier‡

Univ. Lille, CNRS, UMR 8576 – UGSF - Unité de Glycobiologie Structurale et Fonctionnelle, F-59000 Lille, France

* contributed equally to this work

‡ Corresponding authors:

Dr. François Foulquier / Dr. Dominique Legrand

Univ. Lille, CNRS, UMR 8576 – UGSF - Unité de Glycobiologie Structurale et Fonctionnelle, F-59000 Lille, France

Tel. + 33 3 20 43 44 30

Fax. + 33 3 20 43 65 55

E-mail. francois.foulquier@univ-lille1.fr / dominique.legrand@univ-lille1.fr

Abstract

Congenital Disorders of Glycosylation (CDG) are rare inherited diseases causing glycosylation defects responsible for severe growth and psychomotor retardations in patients. Whereas most genetic defects affect enzymes directly involved in the glycosylation process, like glycosyltransferases or sugar transporters, recent findings revealed the impact of gene mutations on proteins implicated in both Golgi vesicular trafficking and ion homeostasis. TMEM165 is one of these deficient Golgi proteins found in CDG patients whose function in the secretory pathway has been deduced from several recent studies using TMEM165 deficient mammalian cells or yeast cells deficient in Gtd1p, the yeast TMEM165 ortholog. These studies actually confirm previous observations based on both sequence and predicted topology of this transmembrane protein and the phenotypes of human and yeast cells, namely that TMEM165 is very probably a transporter involved in ion homeostasis. Whereas the exact function of TMEM165 remains to be fully characterized, several studies hypothesize that TMEM165 could be a Golgi localized Ca^{2+}/ H^{+} antiporter. However, recent data also support the role of TMEM165 in Golgi Mn^{2+} homeostasis then arguing for a putative role of Mn^{2+} transporter for TMEM165 essential to achieve the correct N-glycosylation process of proteins in the secretory pathway. This manuscript is a review of the current state of knowledge on TMEM165 deficiencies in Congenital Disorders of Glycosylation as well as new data on function of TMEM165 and some speculative models on TMEM165/Golgi functions are discussed.

Highlights

- TMEM165 is a Golgi ion transporter.
- TMEM165 is involved in Golgi manganese homeostasis.
- TMEM165 deficiency causes major Golgi glycosylation defects.
- Manganese supplementation rescues glycosylation defects.

Keywords

TMEM165, Gdt1p, congenital disorders of glycosylation, N-glycosylation, manganese and calcium Golgi homeostasis.

Abbreviations

CDG: Congenital Disorders of Glycosylation; UPF0016: Uncharacterized Protein Family 0016; Ca^{2+}: calcium; Mn^{2+}: manganese; GAG: glycosaminoglycans; IEF: isoelectrofocalisation; COG: Conserved Oligomeric Golgi;

Acknowledgements

We are indebted to the Research Federation FRABio (Univ. Lille, CNRS, FR 3688, FRABio, Biochimie Structurale et Fonctionnelle des Assemblages Biomoléculaires) for providing the scientific and technical environment conducive to achieving this work. This Research was carried out within the scope of the International Associated Laboratory “Laboratory for the Research on Congenital Disorders of Glycosylation – from cellular mechanisms to cure – GLYCOLAB4CDG”.

1. Introduction

Congenital Disorders of Glycosylation (CDG) are rare and severe inherited disorders in which glycosylation is affected. CDGs are divided into two groups: CDG type I characterized by defects in N-linked protein glycosylation due to deficiencies in the assembly of the dolichylpyrophosphate linked oligosaccharides and/or their transfer to asparagine residues on the nascent polypeptides; and CDG type II where defects are in the processing of N-glycans (Aebi et al., 1999). The CDG family comprises nearly one hundred disorders (Freeze et al., 2014). CDG type II group not only includes defects in enzymes or transporters involved in glycosylation but also in vesicular trafficking and/or Golgi pH homeostasis caused by deficiencies in key proteins like the COG complex or the vesicular H^+-ATPase subunit ATP6V0A2 (Wu et al., 2004; Foulquier et al., 2006; Kranz et al., 2007; Kornak et al., 2008; Paesold-Burda et al., 2009). More recently, Foulquier et al. (2012) identified a new disorder, namely TMEM165-CDG, caused by a primarily uncharacterized Golgi protein whose role(s) in Golgi homeostasis, protein trafficking and glycosylation is (are) now being unravelled in several recent studies. This paper aims to review our current knowledge on the structure/function relationships, the localization, the expression and the putative functions of TMEM165 in Golgi functions.

2. Sequence and topology of TMEM165 and of its yeast ortholog Gdt1p

TMEM165 is a human hydrophobic protein of 324 amino acids containing 7 predicted transmembrane domains (Foulquier et al., 2012) (Figure 1 and Figure 2A). This protein belongs to the Uncharacterized Protein Family 0016 (UPF0016), family of integral membrane proteins of unknown function. According to the database, the members of this family are composed by one or two EXGDK/R motifs (X is any hydrophobic residue) flanked by two hydrophobic regions at the end of the second and the fifth transmembrane domains with an antiparallel orientation (Figure 2A). Both ELGDK and EWGDR motifs contain acidic residues that could play a role in putative cation recognition and these two homologous regions are probably due to a duplication gene event (Demaegd et al., 2014). TMEM165 also presents a cytosolic central loop organized in a coiled-coil domain encompassing 52 amino acids several of which are acidic (Rosnoblet et al., 2013). This central loop contains one leucine pair ($L_{209}L_{210}$), found in a non-canonical [DE]XXXL[LI] signal (Figure 2A). Some studies of the central loop in another member of the UPF0016 family, Vcxp1, suggests that the acidic loop may have a Ca^{2+}-dependent regulatory function (Gifford et al., 2007). In addition, the first cytosolic loop contains a putative lysosomal-targeting sequence

$Y_{124}NRL_{127}$ (belonging to the classical YXXØ lysosomal targeting signal) (Braulke and Bonifacino, 2009) (Figure 2A).

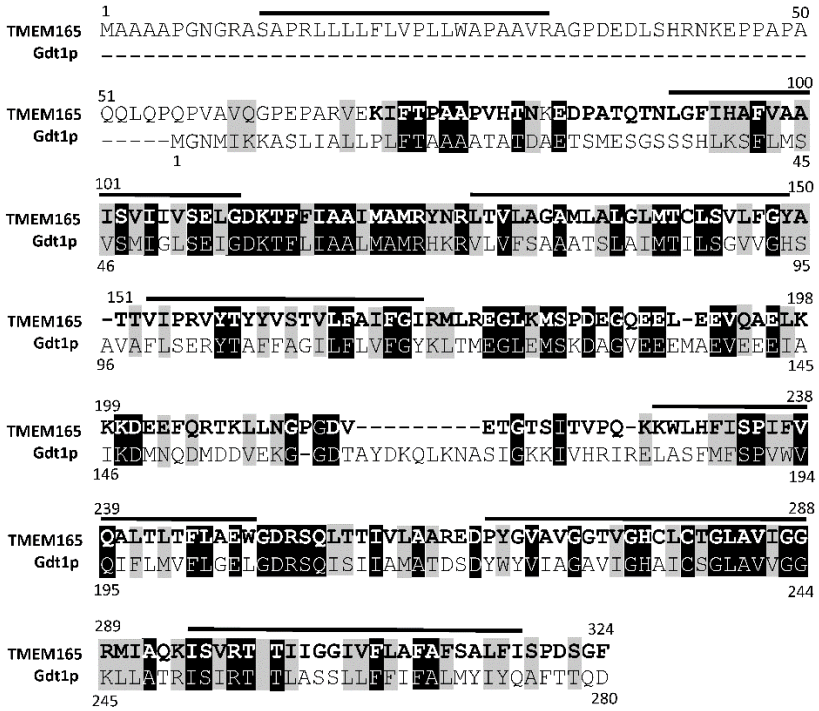

Figure 1: Protein sequence alignment of TMEM165 and Gdt1p. Black boxes indicate the amino acid residues which are identical in both sequences whereas grayed boxes show the homologous amino acid residues. The bold characters in TMEM165 sequence correspond to the amino acid residues which are found conserved in the sequences of the full-length TMEM165 sequences of mammals (SwissProt Database) using the Cobalt-NCBI multiple alignment tool (NCBI). The thick horizontal bars on the top of the sequences indicate the amino acid stretches which are predicted as potential transmembrane domains (TMHMM v2.0 server tool).

TMEM165 is well conserved between prokaryotes (919 different species) and eukaryotes (409 species) (Demaegd et al., 2013). Some orthologs of TMEM165 have been identified and used to study the function of this protein such as the yeast ortholog, Gdt1p (Gcr1 dependent translation factor 1). Gdt1p is a 280 amino acid residues membrane protein whose sequence identity with TMEM165 reaches 38%, concerning more particularly the transmembrane domains and the two EXGDK/R motifs (Figure 1). The two major differences between TMEM165 and Gdt1p lie in both the N-terminus and the central loop. Indeed, the first 55 amino acid residues containing the first transmembrane domain is absent in Gdt1p, whereas the central loop is 10 amino acid residues longer in Gdt1p than in TMEM165 (Figure 1). According to the predictions, the central loop was demonstrated to be in the cytosol (Demaegd et al., 2014; Potelle et al., 2016, submitted).

3. TMEM165/Gdt1p expression and localization in wild type tissues and cells

Database analyses of TMEM165 expression (BioGPS Database) indicate that TMEM165 is ubiquitously expressed with an observed higher expression in smooth muscle, small intestine and colon. In mice, Reinhardt et al. (2014) have demonstrated a distinct pattern of TMEM165 with increased expression during lactation returning to baseline during mammary involution.

While the amino acid sequence of TMEM165/Gdt1p does not contain any ER-retention KDEL/ HDEL signal, its cellular localization presents a Golgi distribution in both mammalian and yeast cells. Unlike Gdt1p which localizes in the cis- and medial Golgi of yeast (Demaegd et al., 2014), TMEM165 colocalizes with the beta 1,4 galactosyltransferase, a glycosyltransferase located in the trans-Golgi better than with GM130, a cis-medial marker (Foulquier et al., 2012). In addition, TMEM165 may also be found, in a lower extent, in late endosomes/lysosomes and at the plasma membrane (Rosnoblet et al., 2013; Demaegd et al., 2013).

4. TMEM165 deficiencies in CDG-II: impact on patients and on the cellular expression, localization and stability of the protein

In 2012, five patients with a CDG-II IEF transferrin pattern were identified in TMEM165-CDG (Foulquier et al., 2012). These patients have similarities in their phenotypes (Foulquier et al, 2012; Zeevaert et al., 2013). Patient 1 is a boy from a Georgian Jewish family with no consanguinity. He was affected by growth retardation with severe dwarfism, psychomotor retardation, osteoporosis, epi-, meta- and diaphyseal dysplasia, muscular weakness, fat excess, joint laxity and hepatosplenomegaly. Patient 2, the sister of patient 1, presented the similar phenotype as her brother but had also fever episodes. The third patient showed the same clinical, biochemical and radiological features as cases 1 and 2. In all three patients, mutation (c.792+182G>A) of TMEM165 was identified (Figure 2B). This mutation activates a cryptic splice donor site and leads to two isoforms: the wild-type one and an additional one resulting in the replacement of exon 4 with a 117 bp intronic sequence. As a consequence, a decreased TMEM165 protein expression was observed in the fibroblasts of these three patients. Patient 4 is a Turkish boy with consanguinity in his family. Although this patient grew normally without hepatosplenomegaly, epilepsy or skeletal abnormalities, he suffered severe psychomotor retardation. This patient possessed a homozygous missense mutation (c.377G>A) that leads to the substitution of an arginine to a histidine [p.Arg126His] in TMEM165 (Figure 2B). Interestingly, whereas the expression level of TMEM165 was found decreased in fibroblasts, striking disturbances of the protein localization was observed with the R126H TMEM165-GFP fusion

protein as it colocalized predominantly with dense lysosomal/endosomal compartments. The last patient (patient 5) is an American girl presenting the same clinical features than patients 1-3 with dwarfism, abnormal fat distribution and skeletal abnormalities such as osteoporosis. In this patient, two mutations in TMEM165 were found: a heterozygous missense mutation (c.377C>T) which leads to a distinct missense mutation [p.Arg126Cys] and a missense mutation (c.910G>A [p.Gly304Arg]) (Foulquier et al., 2012) (Figure 2B). In fibroblasts of patient 5, TMEM165 expression was slightly decreased and its localization was exclusively found at the Golgi level. Moreover, patients with the splice mutation displayed no expression level of TMEM165 and thus have more severe phenotypes than the others (Zeevaert et al., 2013). Interestingly, TMEM165-deficient zebrafish generated by a morpholino strategy were recently used to analyze the consequences of disruption in TMEM165 expression. This study demonstrates defects in morphant structures and more particularly abnormalities in craniofacial phenotypes (alterations in the growth and development of the head and facial bones). These are similar to malformations observed in human patients (Bammens et al., 2014). More recently, a new TMEM165-CDG patient was described (Althoff et al., 2015). This patient was the second child of consanguineous parents. Their first child had died from TMEM165 deficiency at the age of 5 months. The patient presents facial dysmorphism, nephrotic syndrome, cardiac defects, enlarged cerebral ventricles and neurological involvement. In this patient (patient 6), a new mutation [p.Glu108Gly] was found in the conserved ELGDK sequence of TMEM165 (Figure 2B). Interestingly, strong glycosylation defects only appeared in this patient after a few weeks, thus highly suggesting mother's protecting effect on neonatal glycosylation.

From the mutations found in TMEM165-deficient patients, it appears that not only a decreased level of expression of TMEM165 has severe consequences on cells and tissues physiology, but also that several sequence motifs of the protein are crucial for its cellular localization and hence presumably for its stability and function(s). Importance of these sequence motifs, most particularly the putative lysosomal-targeting sequence $_{124}$YNRL$_{127}$, were confirmed by Rosnoblet et al. (2013) through experiments with HeLa cells overexpressing mutated TMEM165 GFP-tagged protein forms. They indeed demonstrated that mutations R126H and R126C lead to preferential TMEM165 targeting to the lysosomal/endosomal compartments and also to the plasma membrane. They also demonstrated that Y124 is crucial for TMEM165 exit from the Golgi, whereas R126 is involved in protein internalization from the plasma membrane.

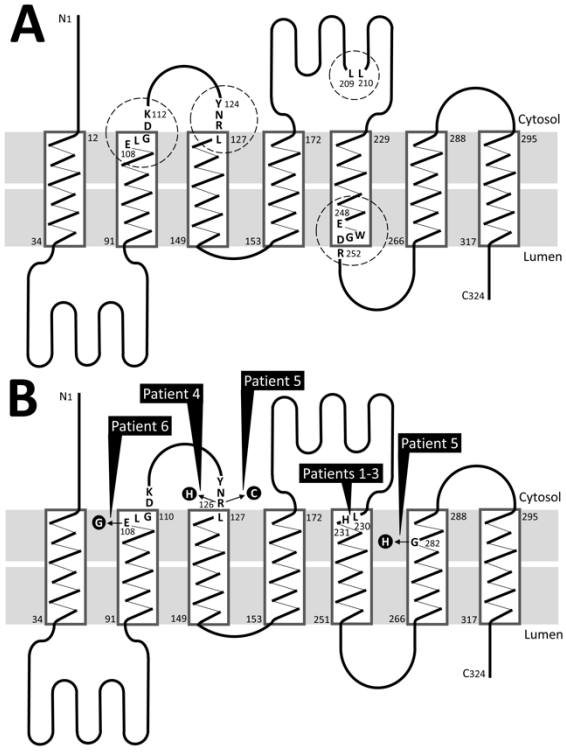

Figure 2: Predicted transmembrane TMEM165 topology showing (A) the sequence motifs which may play roles in both function and intracellular targeting of the protein (see text), and (B) the protein mutations identified in the six TMEM165-CDG patients discovered so far (see text). The seven predicted transmembrane helices are mapped in rectangles spanning the membrane (in gray). Numbers indicate the positions of amino acid residues on the predicted topology model. The topology model was predicted using the TMHMM v2.0 server tool.

TMEM165 deficiencies in CDG-II: impact on Golgi glycosylation

At the Golgi level, different glycosylation processes coexist: N-, O-glycosylation and glycosaminoglycans (GAG) and glycolipids synthesis (Moremen et al., 2012). Most of these processes were found altered in TMEM165-deficient cells.

First, TMEM165-CDG patients exhibit abnormal isoelectrofocalisation (IEF) transferrin patterns revealing defects in the maturation of N-glycans in the Golgi (Foulquier et al., 2012; Zeevaert et al., 2013). This technique is based on the separation of transferrin glycoforms differing from each other by the number of negative charges caused by sialic acids (Jaeken et al., 1984). Plasma transferrin is indeed known to contain two N-glycosylation sites fully occupied by bi-triantennary sialylated N-glycan structures in control individuals. In a normal profile, 4-, 5- and 6-sialo transferrin glycoforms may be detected. In all TMEM165-CDG patients, there are both an increase of 0-, 1-, 2-, and 3-sialo transferrin glycoforms and a concomitant decrease of 6-, 5-, and 4-sialo transferrin glycoforms then arguing for a severe Golgi processing defects. To confirm this decrease of N-glycosylation, experiments in siRNA TMEM165 HEK293 cells were conducted with

fluorescent lectins, more particularly SNA (*Sambicus nigra* lectin) that recognizes the terminal sialic acid. Compared to control cells, a strong decrease in sialylation was revealed (Foulquier et al., 2012). To identify the affected structures, analyses by MALDI-TOF mass spectrometry of glycoproteins from patient serum were performed. Results showed an increase in the undersialylated and undergalactosylated glycans (Foulquier et al., 2012 ; Zeevaert et al., 2013 ; Xia et al., 2013 ; van Scherpenzeel et al., 2015), in fucosylation (Zeevaert et al., 2013), and an in high-mannose type N-glycans suggesting a decrease in N-glycans maturation (Xia et al., 2013). Such accumulation of undergalactosylated glycan structures was also observed in the last discovered TMEM165-CDG patient (Althoff et al., 2015). Very recently, a detailed analysis of N-linked glycans from glycoproteins of TMEM165 depleted HEK293 cells by MALDI-TOF MS confirmed a severe disruption of the galactosylation process of the N-linked glycan structures (Potelle et al., 2016). This galactosylation defect has been shown to be general by affecting the different other glycosylation processes such as the O-glycosylation as well as the glycolipids glycosylation and GAGs synthesis. Moreover, and besides this galactosylation defect, we also demonstrate that the transfer of Gal/ GalNAc residues on glycolipids is severely impaired in TMEM165 depleted cells where a strong accumulation of Glc-Cer is observed. These recent data highlight the crucial involvement of TMEM165 in both the galactosylation glycosylation process and the transfer of GalNAc residues on glycoconjugates.

Second, TMEM165-CDG patients exhibit potential defects in protein O-glycosylation, as assessed by IEF assay of Apolipoprotein-C-III (Apo CIII). This glycoprotein possesses a single O-glycan terminally modified by up to two sialic acids (Wopereis et al., 2003). Using the standard IEF assay, a defect in O-glycans was demonstrated in Apo CIII, with both a decrease of the monosialo- and an increase of the asialo-forms of the protein (Foulquier et al., 2012). This defect was confirmed by LC-MS/MS analyses showing a significant increase in T-antigen (Galβ1-3GalNAc-α-Ser/Thr), slightly/mildly reduced ST-antigen (NeuAcα-2,3-Galβ-1,3-GalNAc-α-Ser/Thr) and increased T/ST-antigen ratio suggesting O-glycan undersialylation (Xia et al., 2013).

At last, the glycosaminoglycans also seem to be affected by TMEM165 defect. Indeed, in TMEM165-knockdown zebrafish, analyses by immunohistochemical staining of cartilage demonstrated alterations in chondroitin sulfate proteoglycan expression with changes in either core protein expression or GAG chain composition (Bammens et al., 2015). These results thus suggest that TMEM165 defect also impairs GAG synthesis.

All together, these results indicate disruption in Golgi glycosylation in TMEM165-CDG with alterations in N-, O-glycosylation and in GAG synthesis, thus confirming the importance of TMEM165 in Golgi glycosylation process.

Recently, the gel mobility of secreted invertase, a protein exclusively N-glycosylated, was assessed in *gdt1*Δ null mutants. A defect in invertase mobility was only observed in the presence of high Ca^{2+} chloride concentration, arguing for an increase in underglycosylated forms (Potelle et al., 2016; Colinet et al., 2016).

5. Role(s) of TMEM165/Gdt1p in Golgi structure and functions

Significant alterations of Golgi morphology were found in fibroblasts of TMEM165-CDG patients using immunofluorescence labeling and Golgi markers like TGN46 for trans-Golgi network, and GM130 for cis- median-Golgi. The Golgi apparatus was indeed found dilated, and the trans-Golgi network markedly fragmented (Foulquier et al., 2012). Such disturbances in Golgi morphology were also reported in CDG patients with defects in the Conserved Oligomeric Golgi (COG) complex that is known to be involved in the vesicular Golgi retrograde trafficking (Ungar et al., 2002). Although it could not be totally excluded that TMEM165 may influence Golgi trafficking, like COG, no direct effect of TMEM165 deficiency on Golgi trafficking has been demonstrated to date.

Both topology predicted from the amino acid sequence of TMEM165 and compared phylogeny strongly suggest that TMEM165 is an ion transporter, most probably a cation and/or proton transporter (Foulquier et al., 2012). A couple of experimental evidences concerning both TMEM165 and its yeast ortholog Gdt1p came early in support to the hypothesis that the proteins are involved in Ca^{2+} and pH homeostasis (Demaegd et al., 2013). It was indeed demonstrated that *gdt1*Δ yeast cells display a strong growth defect when cultured in the presence of high concentrations of Ca^{2+} chloride (700 mM). Interestingly, a truncated version of TMEM165, lacking the first 55 amino acid residues, partially restored yeast growth in presence of Ca^{2+}, suggesting that these proteins have similar functions in their respective hosts. Electrophysiological assessment of Ca^{2+} efflux in yeast overexpressing Gdt1p but not expressing Pmr1p, the Golgi Ca^{2+}/Mn^{2+}-ATPase responsible for the Ca^{2+} supply in the secretory pathway, actually showed that Gdt1p regulates the rate of the Ca^{2+} uptake from the cytosol. In human cells, when TMEM165 is overexpressed and reaches the plasma membrane, patch-clamp analyses showed currents which could be due to cation efflux from cells, whereas the concentration of Ca^{2+} in the cytosol of those

TMEM165 overexpressing cells is lower than in normal cells (Demaegd et al., 2013). In addition to putatively regulate Ca^{2+} homeostasis, TMEM165/Gdt1p was reported to influence pH homeostasis, and hence it was proposed as a Ca^{2+}/H^{+} antiporter. In support to this assertion is the observation that TMEM165 deficiency in patient fibroblasts and siRNA targeted HeLa cells strongly disturb lysosomes/late endosomes pH homeostasis (Demaegd et al., 2013). In addition, Colinet et al. (2016), demonstrated a pH dependent Ca^{2+} uptake activity by using a heterologous expression of Gdt1p in *Lactococus lactis*.

Although many clues indicate that TMEM165 could play an important role in Ca^{2+} and pH homeostasis thus explaining both osteoporosis and bone dysplasia found in TMEM165-CDG patients (Zeevaert et al., 2013), the hypothesis that TMEM165/Gdt1p itself could be a Ca^{2+}/H^{+} antiporter is questioned by a very recent study. This study indeed demonstrated a link between Golgi glycosylation abnormalities due to TMEM165/Gdt1p deficiencies, and a defect in Golgi Mn^{2+} homeostasis (Potelle et al., 2016). The experiments were conducted in both yeasts and mammalian TMEM165/Gdt1p knockdown cells. To evaluate the glycosylation status in *gdt1Δ* knock-out yeast, the electrophoretic mobility of invertase, a heavily-glycosylated protein, was studied. Interestingly, it revealed a glycosylation defect of invertase at high Ca^{2+} concentration (500 mM) which was totally cancelled in a medium supplemented with 1 mM $MnCl_2$, whereas other cations were ineffective. Similar effects were observed in mammalian TMEM165-depleted cells by studying the glycosylation defect of LAMP2 and TGN46, two heavily glycosylated proteins, and by mass spectrometry comparative analysis of N-glycans. Moreover, the Golgi protein GPP130, the stability of which is strictly dependent on the Golgi Mn^{2+} concentration, was used as a specific Mn^{2+} sensor in these cells. Taken as a whole, the experiments thus strongly suggest that the Golgi Mn^{2+} homeostasis is impaired in TMEM165 depleted cells, therefore perturbing the glycosylation process. Mn^{2+} is actually an essential cofactor of several glycosyltransferases using UDP sugars as donors such as galactosyltransferases in mammalian cells (Bai et al., 2006) and mannosyltransferases MNN1, MNN2 and MNN5 in yeasts (Wiggins and Munro, 1998; Rayner and Munro, 1998). These results open the way to the use of therapeutic Mn^{2+} trials in TMEM165-deficient patients (Potelle et al., 2016).

To add an extra layer of complexity, recent results highlighted that low concentrations of extracellular Mn^{2+} lead to a rapid lysosomal degradation of TMEM165. We demonstrate that the ELGDK motif, one of the two EXGDK/R highly-conserved sequences (Figure 2A), is the key motif conferring the Mn^{2+} sensitivity. These data not only reinforce the link between TMEM165 and

Mn^{2+} but also confer a new cellular function of TMEM165 as a novel Mn^{2+} cytosolic sensor of mammalian cells (Potelle et al., 2016, submitted).

6. Putative role of TMEM165/Gdt1p in Golgi ion transport

In yeasts, it was clearly demonstrated that Gdt1p was involved in Ca^{2+} homeostasis (Demaegd et al., 2013) while in human TMEM165 was recently shown to be involved in Golgi Mn^{2+} homeostasis maintenance (Potelle et al., 2016). Although the exact cellular function of TMEM165/ Gdt1p remains to be fully characterized, the results on yeast and mammalian cells bring us to hypothesize that TMEM165/Gdt1p could be somehow a Golgi Ca^{2+}/Mn^{2+} antiporter (Figure 3, A and B). The direction of ion transport is however still controversial and may depend on the ion concentration gradient between the cytosol and the Golgi compartment. Concerning Ca^{2+} and Mn^{2+} ions, their intake in the Golgi lumen is accomplished by SPCA1 and SPCA2 in mammalian cells. These SPCA proteins are Golgi P-type ATPase proteins whose tissue expression is different. While SPCA1 is ubiquitously expressed, SPCA2 is interestingly restricted to some specific tissues. Similarly, Pmr1p is the Golgi P-type ATPase known to import cytosolic Ca^{2+} and Mn^{2+} inside the Golgi lumen in yeasts (Van baelen et al., 2001). As such, we could expect that this Ca^{2+} gradient, generated by SPCA/Pmr1p, could be used for Golgi Mn^{2+} import. In the other way, around and if SPCA/Pmr1p for some reasons mainly pumps Mn^{2+} instead of Ca^{2+}, we could expect that TMEM165/Gdt1p would use the generated Golgi Mn^{2+} gradient to then import Ca^{2+} inside the Golgi lumen. Further experiments are needed to solve. This could explain why TMEM165 is degraded by extracellular concentrations of Mn^{2+}. It is indeed well known that accumulation of cytosolic Mn^{2+} is toxic for the cells (Olanow, 2004; Milatovic et al., 2009). TMEM165 degradation caused by an increased cytosolic Mn^{2+} concentration would thus prevent the action of TMEM165 in the opposite way, and then provoke the Ca^{2+} Golgi exit into the cytosol. This degradation would then engage SPCA in the way of cytosolic Mn^{2+} detoxification. This would also prevent the recapture of the Golgi Mn^{2+} back into the cytosol that would definitely annihilate the SPCA1 efforts.

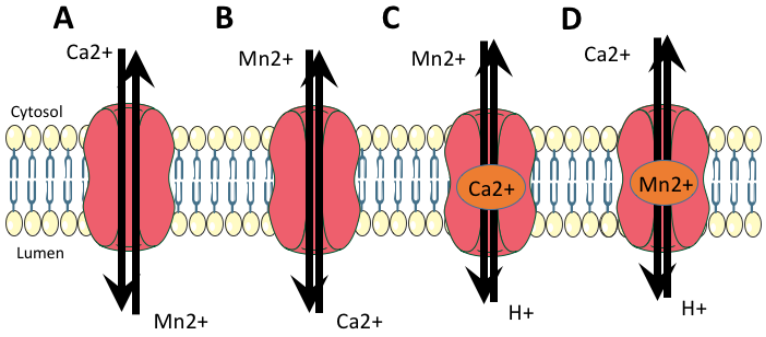

Figure 3: Hypotheses on the role of TMEM165/Gdt1p in ion homeostasis. According to the current experimental results (see text), the scheme illustrates the four possible functions of TMEM165 as ion transporter: TMEM165 could be an antiporter either importing Ca^{2+} into the Golgi while exporting Mn^{2+} in the cytosol (A) or the contrary (B), or TMEM165 could be a Mn^{2+}/H^{+} (C) or Ca^{2+}/H^{+} (D) antiporter whose function is dependent on Ca^{2+} or Mn^{2+}, respectively.

While elegant, these working models do not take into account the pH hypothesis. To unify the different observations, we could imagine a more complicated model where the used counter ion is H^{+}, thus involving the pH gradient generated by the Golgi V0-ATPase. Hence, it could be hypothesized that TMEM165/ Gdt1p would serve as a Golgi Mn^{2+} and or Ca^{2+} importer by using the Golgi pH gradient. One could imagine, this is pure speculation, that this transport (Ca^{2+}/ H^{+} or Mn^{2+}/ H^{+}) could also be regulated by either Mn^{2+} or Ca^{2+} respectively (figure 3, C and D).

7. Conclusion

Complex glycosylation is one of the major functions of the Golgi compartment. It requires not only the right enzymes and substrates at the right places but also correct pH and ionic conditions for which TMEM165 is, without a doubt, plays an important role. Although the function of TMEM165 in controlling Golgi ion homeostasis is still not fully elucidated, strong evidences indicate that it plays a key role in Mn^{2+} homeostasis and also probably influences Ca^{2+} and pH homeostasis. Since Mn^{2+} is a cofactor of galactosyltransferases and that TMEM165 deficiency leads to severe galactosylation defect, it may be assumed that the glycosylation defect in TMEM165 deficient patients is a consequence of an impaired Golgi Mn^{2+} homeostasis. Figure 4 thus illustrates the possible links between the Mn^{2+} concentration in Golgi, in the presence or absence of functional TMEM165, and its impact on protein N- glycosylation. Much needs to be done to fully characterize the putative antiporter or transporter function of TMEM165 for Mn^{2+}, Ca^{2+} and H^{+}. Interestingly, the recent discovery that Mn^{2+} may rescue the glycosylation defects in TMEM-CDG patients opens the way to future therapies for these patients.

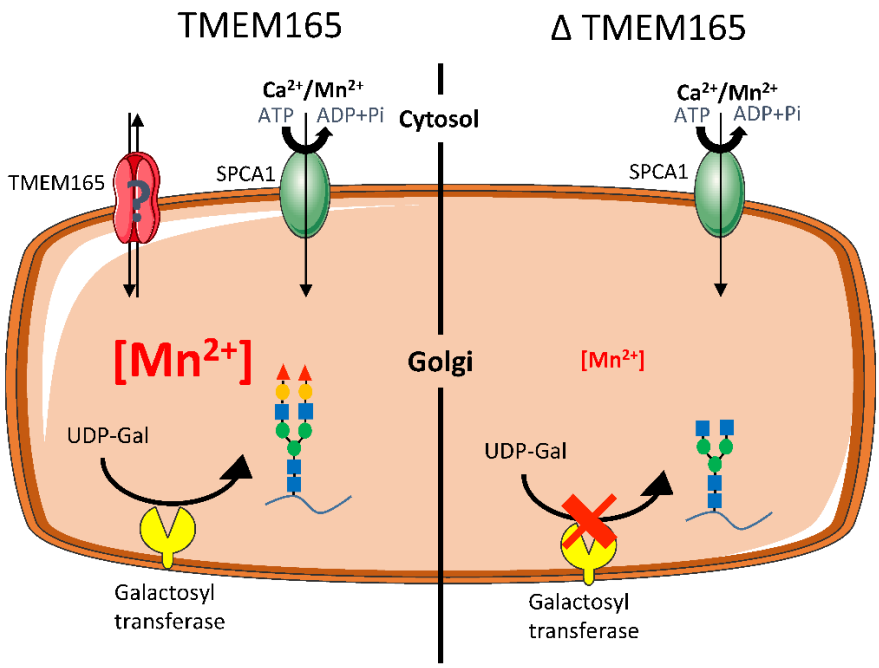

Figure 4: Schematic representation of the impact of TMEM165 deficiency on Golgi Mn^{2+} homeostasis and N-glycosylation defects. The left part of the scheme shows the normal situation where TMEM165 may function, together with the Ca^{2+}/Mn^{2+} ATPase SPCA1, as an ion transporter regulating Golgi Mn^{2+} homeostasis. In this case, the Mn^{2+} concentration in the Golgi permits the Mn^{2+}-dependent galactosyltransferases to transfer galactose residues from UDP-Gal to the N-glycans of proteins. The right part of the scheme illustrates the impact of a TMEM165 deficiency on the entry of Mn^{2+} in the Golgi. The lower Mn^{2+} concentration in the Golgi thus results in a decreased activity of the galactosyltransferases and the undergalactosylation of N-glycoproteins. Blue square: N-acetylglucosamine; green circle: Mannose; yellow circle: Galactose; red triangle: N-Acetylneuraminic acid.

References

Aebi, M., Helenius, A., Schenk, B., Barone, R. Fiumara, A., Berger, E.G., Hennet, T., Imbach, T., Stutz, A., Bjursell, C., Uller, A., Wahlstrom, J.G., Briones, P., Cardo, E., Clayton, P., Winchester, B., Cormier-Dalre, V., de Lonlay, P., Cuer, M., Dupre, T., Seta, N., de Koning, T., Dorland, L., de Loos, F., Kupers, L., 1999. Carbohydrate-deficient glycoprotein syndromes become congenital disorders of glycosylation: an updated nomenclature for CDG. First International Workshop on CDGS. Glycoconj. J. 16, 669–671.

Althoff, S.S., Grüneberg, M., Reunert, J., Park, J.H., Rust, S., Mühlhausen, C., Wada, Y., Santer, R., Marquardt, T., 2015. TMEM165 Deficiency: Postnatal Changes in Glycosylation. JIMD Rep. 26, 2-29.

Bai, C., Xu, X.L., Chan, F.Y., Lee, R.T.H., Wang, Y., 2006. MNN5 encodes an iron- regulated alpha-1,2-mannosyltransferase important for protein glycosylation, cell wall integrity, morphogenesis, and virulence in Candida albicans. Eukaryot. Cell 5, 238–247.

Bammens, R., Mehta, N., Race, V., Foulquier, F., Jaeken, J., Tiemeyer, M., Steet, R., Matthijs, G., Flanagan-Steet, H. 2015. Abnormal cartilage development and altered N-glycosylation in Tmem165-deficient zebrafish mirrors the phenotypes associated with TMEM165-CDG. Glycobiology 25, 669–682.

Braulke, T., Bonifacino, J.S., 2009. Sorting of lysosomal proteins. Biochim. Biophys. Acta 1793, 605–614.

Colinet, A.S., Sengottaiyan, P. Deschamps, A., Colsoul, M.L., Thines, L., Demaegd, D., Duchêne, M.C., Foulquier, F., Hols, P., Morsomme, P., 2016. Yeast Gdt1 is a Golgi-localized calcium transporter required for stress-induced calcium signaling and protein glycosylation. Sci. Rep. 6, 24282.

Demaegd, D., Colinet, A.S., Deschamps, A., Morsomme, P., 2014. Molecular Evolution of a Novel Family of Putative Calcium Transporters. PLoS ONE 9, e100851.

Demaegd, D., Foulquier, F., Colinet, A.S., Gremillon, L., Legrand, D., Mariot, P., Peiter, E., Van Schaftingen, E., Matthijs, G., Morsomme, P., 2013. Newly characterized Golgi-localized family of proteins is involved in calcium and pH homeostasis in yeast and human cells. Proc. Natl. Acad. Sci. USA. 110, 6859–6864.

Foulquier, F., Amyere, M., Jaeken, J., Zeevaert, R., Schollen, E., Race, V., Bammens, R., Morelle, W., Rosnoblet, C., Legrand, D., Demaegd, D., Buist, N., Cheillan, D., Guffon, N., Morsomme, P., Annaert, W., Freeze, H.H., Van Schaftingen, E., Vikkula, M., Matthijs, G., 2012. TMEM165 Deficiency Causes a Congenital Disorder of Glycosylation. Am. J. Hum. Genet. 91, 15–26.

Foulquier, F., Vasile, E., Schollen, E., Callewaert, N., Raemaekers, T., Quelhas, D., Jaeken, J., Mills, P., Winchester, B., Krieger, M., Annaert, W., Matthijs, G., 2006. Conserved oligomeric Golgi complex subunit 1 deficiency reveals a previously uncharacterized congenital disorder of glycosylation type II. Proc. Natl. Acad. Sci. U. S. A. 103, 3764–3769.

Freeze, H.H., Chong, J.X., Bamshad, M.J., Ng, B.G., 2014. Solving glycosylation disorders: fundamental approaches reveal complicated pathways. Am. J. Hum. Genet. 94, 161–175.

Gifford, J.L., Walsh, M.P., Vogel, H.J., 2007. Structures and metal-ion-binding properties of the Ca^{2+}-binding helix-loop-helix EF-hand motifs. Biochem. J. 405, 199–221.

Jaeken, J., van Eijk, H. G., van der Heul, C., Corbeel, L., Eeckels, R., Eggermont, E., 1984. Sialic Acid-Deficient Serum and Cerebrospinal Fluid Transferrin in a Newly Recognized Genetic Syndrome. Clin. Chim. Acta 144, 245–247.

Kornak, U., Reynders, E., Dimopoulou, A., van Reeuwijk, J., Fischer, B., Rajab, A., Budde, B., Nürnberg, P., Foulquier, F., ARCL Debré-type Study Group, Lefeber, D., Urban, Z., Gruenewald, S., Annaert, W., Brunner, H.G., van Bokhoven, H., Wevers, R., Morava, E., Matthijs, G., Van Maldergem, L., Mundlos, S., 2008. Impaired glycosylation and cutis laxa caused by mutations in the vesicular H^+-ATPase subunit ATP6V0A2. Nat Genet. 40, 32-34.

Kranz, C., Ng, B.G., Sun, L., Sharma, V., Eklund, E.A., Miura, Y., Ungar, D., Lupashin, V., Winkel, R.D., Cipollo, J.F., Costello, C.E., Loh, E., Hong, W., Freeze, H.H., 2007. COG8 deficiency causes new congenital disorder of glycosylation type IIh. Hum. Mol. Genet. 16, 731–741.

Milatovic, D., Zaja-Milatovic, S., Gupta, R.C., Yu, Y., Aschner, M., 2009. Oxidative damage and neurodegeneration in manganese-induced neurotoxicity. Toxicol. Appl. Pharmacol. 240, 219–225.

Moremen, K.W., Tiemeyer, M., Nairn, A.V., 2012. Vertebrate protein glycosylation: diversity, synthesis and function. Nat. Rev. Mol. Cell Biol. 13, 448–462.

Olanow, C.W., 2004. Manganese-induced parkinsonism and Parkinson's disease. Ann. N. Y. Acad. Sci. 1012, 209–223.

Paesold-Burda, P., Maag, C., Troxler, H., Foulquier, F., Kleinert, P., Schnabel, S., Baumgartner, M., Hennet, T., 2009. Deficiency in COG5 causes a moderate form of congenital disorders of glycosylation. Hum. Mol. Genet. 18, 4350–4356.

Potelle, S., Morelle, W., Dulary, E., Duvet, S., Vicogne, D., Spriet, C., Krzewinski-Recchi, M.A., Morsomme, P., Jaeken, J., Matthijs, G., de Bettignies, G., Foulquier, F., 2016. Glycosylation abnormalities in Gdt1p/TMEM165 deficient cells result from a defect in Golgi manganese homeostasis. Hum. Mol. Genet. 25, 1489-500.

Rayner, J.C., Munro, S., 1998. Identification of the MNN2 and MNN5 mannosyltransferases required for forming and extending the mannose branches of the outer chain mannans of Saccharomyces cerevisiae. J. Biol. Chem. 273, 26836–26843.

Reinhardt, T.A., Lippolis, J.D., Sacco, R.E., 2014. The Ca^{2+}/H^{+} antiporter TMEM165 expression, localization in the developing, lactating and involuting mammary gland parallels the secretory pathway Ca^{2+} ATPase (SPCA1). Biochem. Biophys. Res. Comm. 445, 417–421

Rosnoblet, C., Legrand, D., Demaegd, D., Hacine-Gherbi, H., de Bettignies, G., Bammens, R., Borrego, C., Duvet, S., Morsomme, P., Matthijs, G., Foulquier, F., 2013. Impact of disease-causing mutations on TMEM165 subcellular localization, a recently identified protein involved in CDG-II. Hum. Mol. Genet. 22, 2914–2928.

Ungar, D., Oka, T., Brittle, E.E., Vasile, E., Lupashin, V.V., Chatterton, J.E., Heuser, J.E., Krieger, M., Waters, M.G., 2002. Characterization of a Mammalian Golgi-Localized Protein Complex, COG, that Is required for normal Golgi morphology and function. J. Cell Biol. 157, 405–415.

Van Baelen, K., Vanoevelen, J., Missiaen, L., Raeymaekers, L., Wuytack, F., 2001. The Golgi PMR1 P-type ATPase of Caenorhabditis elegans. Identification of the gene and demonstration of calcium and manganese transport. J. Biol. Chem. 276, 10683–10691.

Van Scherpenzeel, M., Steenbergen, G., Morava, E., Wevers, R.A., Lefeber, D.J., 2015. High-resolution mass spectrometry glycoprofiling of intact transferrin for diagnosis and subtype identification in the congenital disorders of glycosylation. Transl. Res. 166, 639-649.

Wiggins, C.A., Munro, S., 1998. Activity of the yeast MNN1 α-1,3-mannosyltransferase requires a motif conserved in many other families of glycosyltransferases. Proc. Natl. Acad. Sci. USA 95, 7945–7950.

Wopereis, S., Grünewald, S., Morava, E., Penzien, J.M., Briones, P., García-Silva, M.T., Demacker, P.N., Huijben, K.M., Wevers, R.A., 2003. Apolipoprotein C-III Isofocusing in the Diagnosis of Genetic Defects in O-Glycan Biosynthesis. Clin. Chem. 49, 1839–1845.

Wu, X., Steet, R.A., Bohorov, O., Bakker, J., Newell, J., Krieger, M., Spaapen, L., Kornfeld, S., Freeze, H.H., 2004. Mutation of the COG complex subunit gene COG7 causes a lethal congenital disorder. Nat. Med. 10, 518–523.

Xia, B., Zhang, W., Li, X., Jiang, R., Harper, T., Liu, R., Cummings, R.D., He, M., 2013. Serum N-Glycan and O-Glycan Analysis by Mass Spectrometry for Diagnosis of Congenital Disorders of Glycosylation. Anal. Biochem. 442, 178–85.

Zeevaert, R., de Zegher, F., Sturiale, L., Garozzo, D., Smet, M., Moens, M., Matthijs, G., Jaeken, J., 2013. Bone Dysplasia as a Key Feature in Three Patients with a Novel Congenital Disorder of Glycosylation (CDG) Type II Due to a Deep Intronic Splice Mutation in TMEM165. JIMD Reports 8, 145–152.

Abstract in French

Les troubles congénitaux de la glycosylation (CDG) sont des maladies héréditaires rares qui provoquent des défauts de glycosylation fréquemment responsables d'un défaut de croissance et de retards psychomoteurs chez les patients atteints. Alors que la plupart des défauts génétiques affectent les enzymes directement impliquées dans le processus de glycosylation, comme les glycosyltransférases ou les transporteurs de nucléotide sucre, des études récentes ont souligné l'impact de mutations génétiques au niveau de gènes codant des protéines impliquées dans l'homéostasie ionique et/ou dans le trafic vésiculaire au niveau de l'appareil de Golgi. TMEM165 est une protéine golgienne retrouvée mutée chez des patients CDG. Sa fonction hypothétique a été déduite de plusieurs études récentes en utilisant des cellules de mammifères déficientes de TMEM165 ou des cellules de levure déficientes en Gtd1p, l'orthologue de TMEM165 chez la levure. Ces études ont permis de poser l'hypothèse que TMEM165 serait très probablement un transporteur impliqué dans l'homéostasie ionique du Golgi. Alors que la fonction précise de TMEM165 reste inconnue à ce jour, des auteurs ont émis l'hypothèse que TMEM165 pourrait être un antiporteur Ca2+/H+ de l'appareil de Golgi. Cependant, des données plus récentes soulignent le rôle de TMEM165 dans l'homéostasie golgienne du Mn2+. Cette récente étude met en évidence le rôle clé de TMEM165 dans le processus de N-glycosylation des protéines et pose l'hypothèse que TMEM165 serait en fait impliqué dans l'import de Mn2+ dans l'appareil de Golgi. Cette revue a pour but de dresser l'état actuel des connaissances sur une déficience en TMEM165 dans les CDG ainsi que de présenter de nouvelles données sur la fonction de TMEM165. Pour terminer, certains modèles sur les fonctions de TMEM165 au niveau de l'appareil de Golgi seront discutés.

[5] GENERAL DISCUSSION AND PERSPECTIVES

This section has several objectives. The first one is to sum-up the major results I have obtained during my PhD. The second one is to propose ideas for future work on the subject. Finally, the last important goal is to widen the discussion initiated in each paper to a more general view.

5.1. Roles of TMEM165 in glycosylation

At the beginning of the project, TMEM165 was considered as a putative Ca2+/H+ Golgi antiporter and several hypotheses could explain the observed glycosylation defects in TMEM165-CDG patients.

First, a lack of TMEM165 could prevent the proton leak from the Golgi, therefore resulting in an overacidification of the Golgi, since no H+ leak channel have been identified in the Golgi in mammals. This pH decrease might explain the glycosylation defect since it could lead to an inactivation or at least a decreased activity of specific glycosyltransferases. An overacidification could also induces a premature activation of lysosomal hydrolases in the Golgi such as neuraminidases.

The Ca2+ hypothesis, on the contrary, cannot explain the glycosylation defect since there is no evidence for a role of Ca2+ in glycosylation. However, a disturbance in Golgi Ca2+ homeostasis could explain the skeletal abnormalities observed in TMEM165-CDG patients. Indeed, although Ca2+ is known to be handled carefully by a plethora of transporters and pumps, a disturbance in Ca2+ homeostasis might lead to an abnormal bone development. However, our recent discovery that TMEM165 was involved in Golgi Mn2+ homeostasis led us to rethink and reformulate our hypotheses.

5.1.1. TMEM165 deficiency leads to N-glycosylation and glycolipid defects

We have demonstrated that TMEM165 deficiency led to strong glycosylation defects presumably due to Golgi Mn2+ disturbance. Given the central role of Mn2+ in glycosylation, the link between TMEM165 and glycosylation then all made sense.

We have observed that TMEM165 deficiency led to a strong N-glycosylation defect and that galactosylation was mainly affected. The link between TMEM165 and Mn2+ homeostasis thus

explains the galactosylation defect on N-glycans, since the β-1,4-galactosyltransferase 1 (β4GalT1) strictly requires Mn2+ to be fully active (Figure 19).

Glycolipids, mainly gangliosides, were also analysed by MALDI-MS in control and KO TMEM165 HEK293 cell lines. Our results showed that KO TMEM165 cells barely contains any gangliosides, excepted traces of GM3 and GM2, compared to control cells that expressed diverse pattern of gangliosides, including GM3, GM2, GM1, GD2 and GD1. This indicated a severe glycolipid glycosylation defect in KO TMEM165 cells in addition to an N-glycan galactosylation defect. These results were not surprising, since several enzymes involved in the biosynthesis of gangliosides are Mn2+ dependent, and particularly β4GalNAcT1 (GM2/GD2 synthase), involved in the early steps of gangliosides biosynthesis (table 6). Therefore, all the following steps in the biosynthesis are also disrupted.

Some insights into a potential O-glycosylation defect was reported in the literature. Indeed, Xia and collaborators observed an increase of T antigen (Galβ-1,3-GalNAcα-Ser/Thr) and a decrease of sialylT antigen (Siaα-2,3-Galβ-1,3-GalNAcα-Ser/Thr), suggesting a mucin-type O-glycan undersialylation in TMEM165-CDG patients [296]. In TMEM165 depleted cells, we have observed that TGN46 gel mobility was altered and attributed to a potential O-glycosylation defect, as explained in the section 2.4.2 of the results. Although interesting, these observations are indirect and did not reveal a clear and general O-glycosylation defect.

5.1.2. Mn2+ and galactose supplementation in TMEM165 deficient cells

Interestingly, Mn2+ supplementation has been shown to be able to suppress the glycosylation defect on N-glycans and glycolipids. On the contrary, galactose supplementation was only able to suppress the glycosylation defect on N-glycans but glycolipid glycosylation was only found partially normalized. Indeed, GM3 species were restored but GM2 species were not, since increasing the pool of UDP-Gal by galactose supplementation had no effect on β4GalNAcT1 activity, which requires UDP-GalNAc as nucleotide sugar donor. However, β4GalNAcT1 is Mn2+ dependent, thus explaining why Mn2+ supplementation was able to completely suppress the glycosylation defect on glycolipids. Altogether, these results showed that TMEM165 deficiency led to a galactosylation defect both on N-glycans and glycolipids, but also to a GalNAcylation defect on glycolipids.

5.1.3. Differences between Gdt1p and TMEM165 functions in glycosylation

A major difference was observed between TMEM165 roles in glycosylation and its ortholog in yeast Gdt1p. Indeed, although a lack of TMEM165 leads to glycosylation defect, yeast gdt1Δ strain does not display any glycosylation defect, unless they are exposed to high Ca2+ concentrations, suggesting divergent role of TMEM165 and gdt1p in glycosylation. In the Golgi apparatus in human and yeast, there is also another pump that can potentially play a role in glycosylation: SPCA1 in human and its ortholog Pmr1p in yeast. Interestingly, yeast *pmr1Δ* strain presents a strong and well characterized glycosylation defect that has been shown to be linked to Golgi Mn2+ homeostasis disturbance [317]. However, no link between SPCA1 and glycosylation has been reported to date. These discrepancies between human and yeast regarding glycosylation led us to this hypothesis: in human, TMEM165 is the major Mn2+ importer in the Golgi crucial for glycosylation; in yeast on the contrary, Gdt1p is essential for glycosylation only when Pmr1p is defective for Mn2+ transport (Figure 43).

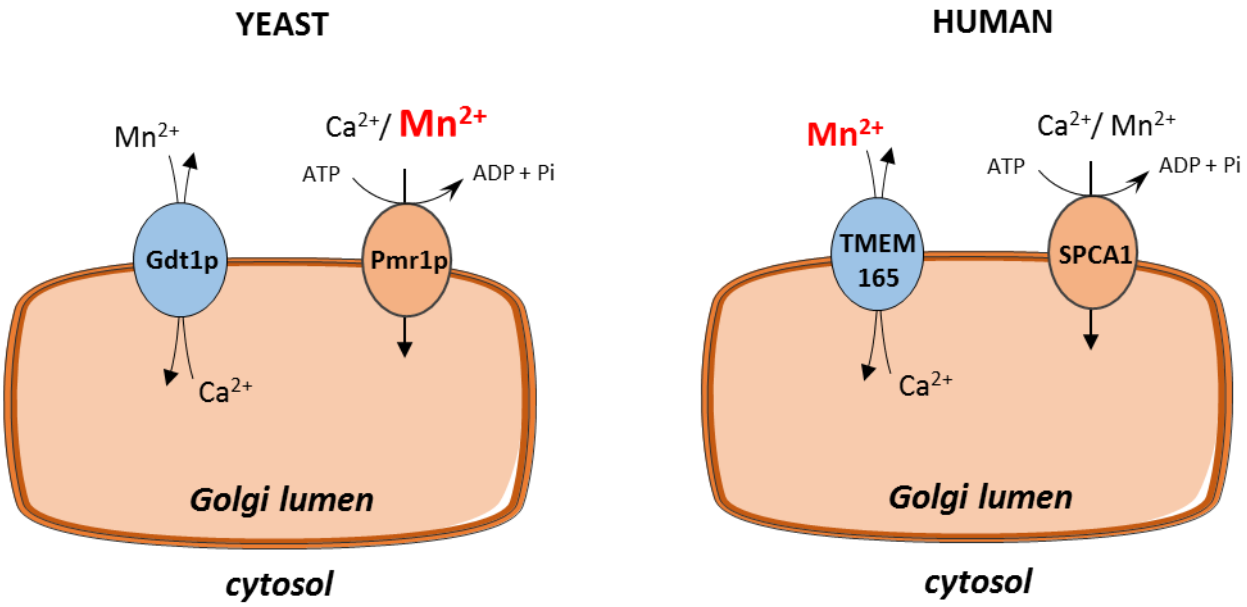

Figure 43. Models showing differences between gdt1p and TMEM165 roles in glycosylation. TMEM165 is the major Mn2+ importer in human and crucial for glycosylation. Gdt1p is a dispensable Mn2+ importer for glycosylation in yeast.

This hypothesis has been supported by a recent publication in our group in which I took part. In this study, we have transformed *pmr1Δ* and *gdt1Δ/pmr1Δ* double knockout strains with Pmr1p mutants defective for transport of either Ca2+ ions (Pmr1pD53A), Mn2+ ions (Pmr1pQ783A) or both (Pmr1pD778A), in order to decipher the origin of the glycosylation defect observed in those two strains (Figure 44). With these tools and the combined use of invertase and NMR, we showed

that the observed Golgi glycosylation defect in the *gdt1Δ/pmr1Δ* double knockout strains only resulted from a lack of intraluminal Golgi Mn2+. We confirmed that the well-known glycosylation defect in the *pmr1Δ* strain also resulted from a lack of Golgi Mn2+ [317]. Our results also revealed that the activity of Gdt1p in Golgi glycosylation becomes essential when Prm1p is defective for Mn2+ transport and only transports Ca2+. Since the glycosylation defect was due to a lack of intraluminal Golgi Mn2+, our results strongly suggest that when Pmr1p only transports Ca2+, Gdt1p is strictly required to import Mn2+ inside the Golgi lumen to sustain Golgi glycosylation.

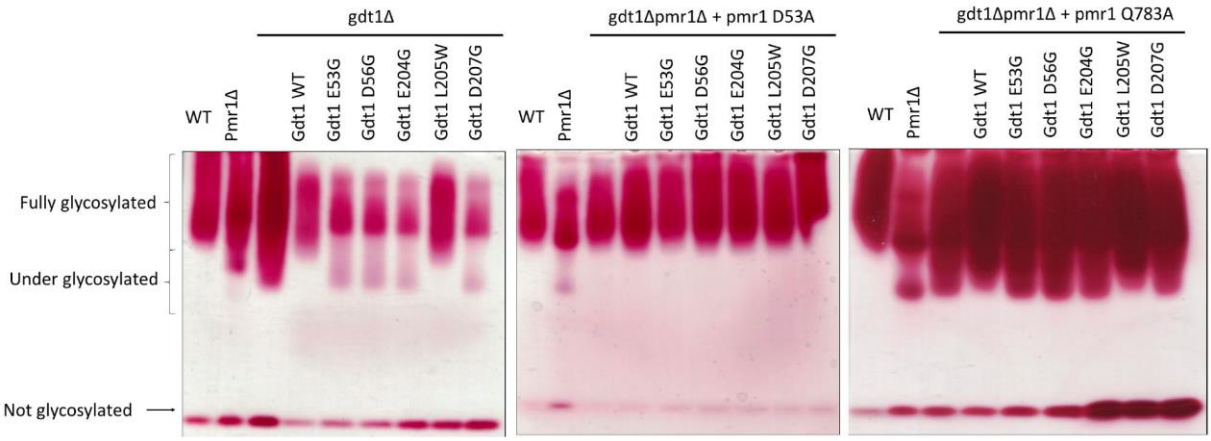

Figure 44. Gdt1p is essential for glycosylation when Pmr1p only imports Ca2+. *gdt1Δpmr1Δ* strains were transformed with pRS41N-pmr1pD53A (left panel) and pRS41N-pmr1p- Q783A (middle panel) and with pRS41H-gdt1p mutants (Gdt1p-E53G, Gdt1p-D56G, Gdt1p-E204G, Gdt1p-L205W and Gdt1p-D207G). Yeasts were grown in YPR medium. gdt1Δ strains were transformed with pRS41H-gdt1p mutants (Gdt1p-E53G, Gdt1p-D56G, Gdt1p-E204G, Gdt1p-L205W and Gdt1p-D207G) (right panel) and yeasts were grown in a YPR media supplemented with 200 mM CaCl2. From Dulary, Yu *et al*, 2018.

Our model also explains the strong N-glycosylation defect observed in *gdt1Δ* cultured with high Ca2+ concentrations. Indeed, a high Ca2+ concentration will cause a cytosolic Ca2+ increase that switches Pmr1p ion transport preference towards Ca2+ instead of Mn2+. The Mn2+ Golgi luminal pool is then rapidly decreased if Gdt1p is not there to efficiently import Mn2+ inside the Golgi lumen. However, since the *pmr1Δ* strain presents a strong Golgi glycosylation defect, one can suggest that in physiological conditions, Pmr1p preferentially import Mn2+ rather than Ca2+ into the Golgi lumen. In such conditions, the role of Gdt1p in Golgi glycosylation is dispensable.

Altogether, these results clearly show that on one hand, TMEM165 is required for a proper Golgi glycosylation in human. On the other hand, Gdt1p is dispensable for yeast Golgi glycosylation. Therefore, we can suggest that Gdt1p plays other roles in yeast unrelated to glycosylation, for example in Ca2+ homeostasis.

5.1.4. Perspectives

Despite all these interesting results, much remains to be done. We first need to obtain a complete mass spectrometry profiling of the glycome in our cell lines, in the absence or presence of Mn2+. These data will gives us more detailed structural information about the glycosylation defect and the rescue by Mn2+. So far, only N-glycans and glycolipids have been analysed. Therefore, we still need to analyse at least glycosaminoglycans, and mucin-type O-glycans. GAG analyses will especially be very interesting, since XYLT1, the first enzyme involved in the biosynthesis of the tetrasaccharidic core of CD/DS/HS, is known to specifically require Mn2+ to be fully active (Figure 19). As described in the introduction, other crucial enzymes involved in GAG biosynthesis are also Mn2+ dependent. Therefore, GAG biosynthesis is likely to be affected by a lack of Golgi Mn2+ due to TMEM165 deficiency.

In parallel, to go further into deciphering the differences between TMEM165 and gdt1p functions in glycosylation, we generated a lot of TMEM165 and gdt1p mutants with single point mutations, to determine the crucial amino acids for their function in glycosylation. LAMP2 glycosylation profile will be assessed in KO TMEM165 cells transfected with TMEM165 mutants. In parallel, invertase glycosylation analysis will be performed in gdt1Δ strains transformed with gdt1p mutants, in the presence of high Ca2+ concentration. The first results obtained in yeast show that acidic residue in gdt1p are crucial for its function in glycosylation.

The fact that Mn2+ supplementation could suppress the observed glycosylation defect, at least on N-glycans and glycolipids, was very interesting and promising for the TMEM165-CDG patients. Still, one important question remains to be addressed: how does extracellular Mn2+ supplementation rescues the glycosylation in KO TMEM165 cells? In parallel, galactose supplementation also improved glycosylation and was tested on TMEM165-CDG patients. Again, the same question should be addressed for galactose supplementation: how does it rescue the galactosylation defect? Although several possibilities came to our mind to explain the glycosylation rescue by Mn2+ and galactose, actual experiments needs to be done in a near future to clarify this. In parallel, we should keep going with therapeutic trials using galactose and we should also try to setup a Mn2+ therapeutic trial following the protocol performed for SLC39A8-CDG.

5.2. The link between TMEM165 deficiency and skeletal abnormalities in TMEM165-CDG patients

One main objective of my thesis was to decipher the molecular mechanisms leading to a glycosylation defect in TMEM165-CDG patients. Although it is now clear that the glycosylation defect in TMEM165 deficient cells is linked to Golgi Mn2+ homeostasis disturbance, some work still need to be done to understand the skeletal abnormalities observed in TMEM165-CDG patients.

Indeed, at the moment, we still need to discover the mechanism leading to skeletal abnormalities in TMEM165-CDG patients. Animal models proved to be useful in that way since TMEM165 deficient zebrafish also developed skeletal abnormalities. We will also take advantage of the available TMEM165 knockout mice in order to answer that question.

Despite a large work on human bone diseases and animal models, the relationship between skeletal development and defects in the ECM are largely understudied. Usually, the defect in skeletal development is mainly due to an abnormal regulation of chondrocyte proliferation and maturation in the cartilage growth plate. Normal endochondral ossification also depends on distinct and complex ECM compounds comprising cartilage proteoglycans that act as regulators of signalling molecules mainly via their glycosaminoglycan chains.

Interestingly, we previously pointed out that several glycosyltransferases (i.e XYLT1) involved in the synthesis of glycosaminoglycan chains of proteoglycans strictly require Mn2+ in their active site to be fully active. Therefore, alteration in Golgi Mn2+ homeostasis due to TMEM165 deficiency could lead to a GAG defect that could thus be the trigger of the skeletal abnormalities observed in TMEM165-CDG patients. Indeed, GAG are key glycan structures of proteoglycans from the ECM. Due to their ability to attract water, GAG form a gel and provide mechanical support to the tissue. In bone ECM, GAG also act as a scaffold for mineral deposit and play a protective role by preventing ECM destruction by proteases. Moreover, GAG are crucial key signalling component during chondrocyte maturation. In case of GAG defect due to TMEM165 deficiency, one could think that bone homeostasis will be disrupted and skeletal development may probably be strongly altered.

5.3. Unravelling TMEM165 ion transport

To decipher TMEM165 ion transport, two non-exclusive methods are possible. The first one is to monitor ion homeostasis in control and TMEM165 deficient cells and will be discussed in 5.3.1 to 5.3.3. However, this approach is indirect and data obtained should be carefully interpreted. The other possibility is to perform direct current measurement on membrane expressing TMEM165 (see 5.3.4). In each section, the discussion about the role of TMEM165 in each ion homeostasis will be accompanied by perspectives to help drawing reliable conclusions.

5.3.1. The role of TMEM165 in H+ homeostasis

When TMEM165 was discovered, it was proposed that TMEM165 was a putative Ca2+/H+ exchanger, able to import Ca2+ in exchange for intraluminal Golgi H+. As described in the introduction, several hypotheses supported a role of TMEM165 in H+ exit from the Golgi. However, the only reported experiments rely on the use of two lysosomal dyes (lysotracker and lysosensor DND189) that become more fluorescent in acidic compartments. Authors showed that lysosomal pH became more acidic in 3 out the 5 patients and in HeLa siTMEM165 cells. Although convincing, no effect of TMEM165 on Golgi pH was assessed. To tackle this, we propose to use pHluorin GFP tagged Golgi proteins to directly monitor Golgi pH in control and TMEM165 deficient cells, as first described by Miesenböck [83]. A role of TMEM165 in Golgi pH homeostasis is not excluded but pH measurement should be redone carefully before drawing conclusions.

5.3.2. The role of TMEM165 in Ca2+ homeostasis

As described in the publication of Demaegd and collaborators, TMEM165 is thought to be involved in Ca2+ entry at the Golgi level. However, their experiments introduced several bias. To measure TMEM165 effect on Ca2+ levels, they had to overexpress a tagged version of TMEM165 that localised in the plasma membrane, since endogenous TMEM165 is mostly localized in the Golgi apparatus and thus was not sufficient to generate current at the plasma membrane. In addition, they measured calcium cytosolic levels using Fura2, known to be quenched by Mn2+ [318]. The experiments performed in yeast also suffer from the same problem, since they used aequorin, also known to be quenched by Mn2+. Therefore, the intensity differences they measured with the probes could also be due to Mn2+ variations.

Besides, we recently hypothesised that TMEM165 is in fact involved in Ca2+ exit from the Golgi apparatus instead of Ca2+ uptake. Therefore, further analyses need to be performed to conclude

about the role of TMEM165 in Ca2+ homeostasis. For example, we are currently using classical electrophysiological measurement to monitor whole cell and Golgi Ca2+ levels in control and KO TMEM165 cells, to insure TMEM165 role in Ca2+ homeostasis. Another possibility is to use GFP-based Ca2+ probe specifically targeted to the Golgi apparatus, as described by Wong and collaborators [319]. These probe could be helpful to measure Golgi Ca2+ levels in control and KO TMEM165 cells.

The importance of Ca2+ exit from the Golgi has been highlighted by the presence of IP3R and RyR. These proteins are able to release intraluminal Golgi Ca2+ in response to specific stimuli, therefore triggering signalling events. Thus, if TMEM165 is indeed involved in Ca2+ exit in the Golgi, we need to understand the precise function of TMEM165 in Ca2+ handling. IP3R and RyR only release luminal Golgi Ca2+ in response to stimuli. It could thus be interesting for a cell to be equipped with a passive antiporter like TMEM165 in order to slowly release Ca2+ in absence of stimulus. Moreover, some cell types do not express RyR and IP3R are known to be absent or only slightly expressed in the TGN. Therefore, in that case, TMEM165 might be crucial for Ca2+ exit from the Golgi lumen.

5.3.3. The role of TMEM165 in Mn2+ homeostasis

We have recently shown that TMEM165 was linked to Mn2+ homeostasis and hypothesised that TMEM165 imports Mn2+ into the Golgi lumen. However, monitoring precisely Golgi Mn2+ homeostasis is extremely difficult, since Mn2+ is a trace element and tools are lacking to measure Mn2+ concentrations. Our Mn2+ measurements using GPP130 as a Golgi Mn2+ sensor were indeed interesting as a first approach but also indirect and not quantitative. Therefore, we try to develop new approaches using for example electronic microscopy or Inductively Coupled Plasma Mass Spectrometry (ICP-MS) to finely measure intracellular or even Golgi Mn2+ concentrations. It is also possible to use electronic microscopy or atomic force spectroscopy to measure Mn signature. A method has also been developed to measure Mn with fura2 used in very specific conditions, taking advantage of the quenching by the Mn2+ [320]. In any case, these approaches require expertise, high end technology and several months of optimisation. Therefore, collaborations should be done to address this point.

5.3.4. Direct measurement of TMEM165 ion transport

Besides these crucial experiments to monitor TMEM165 role in the maintenance of Golgi homeostasis, deciphering direct TMEM165 transport functions will also be important. Indeed, although strongly suggested, there is no clear evidence that TMEM165 is indeed an ion transporter nor if it really transports Mn2+ and Ca2+ as we suggested. As TMEM165 might be electrogenic, excepted if it exchanges 1 Mn2+ against 1 Ca2+, we propose to perform electrophysiological recording in cRNA-injected Xenopus oocytes to characterize its activity. We may also artificially change Mn2+, Ca2+ and H+ levels to measure the transport function of TMEM165 and to determine the stoichiometry of the ion transport. Mutated versions of TMEM165 could also be used to determine the crucial amino acids involved in the transport function. Although these experiments are crucial to understand TMEM165 function, we will need to collaborate on that task as no one in our lab is able to perform such experiments.

5.4. TMEM165 is a Golgi Mn2+ sensitive protein

Finally, we observed that TMEM165 was targeted to lysosomal degradation after high Mn2+ concentrations exposure. This was surprising but interesting as it raised a lot of questions to address in the future. We need to decipher the molecular mechanism underlying TMEM165 lysosomal degradation in the presence of Mn2+. We thus need to find the proteins involved in TMEM165 induced degradation. In addition, we still do not understand the reason behind TMEM165 degradation after Mn2+ exposure. The fact that this mechanism is conserved in yeast and human suggests that it confers an important selective advantage, for example a protection against Mn toxicity.

It is worth noting that tens of thousands years ago, the first Homo sapiens were living in caves and were subjected to high Mn exposure in the soil. For example, human paintings in the Lascaux cave were mainly done with manganese oxide, meaning that Homo sapiens at that time were exposed to high Mn concentration in their environment. These ancestors used to mostly rely on harvesting fruits and vegetables to eat. They particularly ate a lot of nuts, which are known to be a high dietary source of Mn, especially for hazelnuts and walnuts. Therefore, the existence of such induced degradation mechanism during this era was then logic and useful to prevent Mn toxicity. At that time, their lifestyle involved a high Mn intake and Mn induced degradation systems were then crucial to insure their survival. Therefore, nature slowly selected people having in their genome all the players intervening in these processes.

These days, however, humans are not really exposed to high Mn concentrations, excepted for workers in mine, industrial workers, welders or people living near mining areas. Our lifestyle is very different from our ancestors and we are now aware that chronic Mn overexposure can cause manganism. This pathological condition did not exist back in that time since the life expectancy of our ancestors was drastically shorter than ours. As a matter of fact, we nowadays tend to avoid being in contact with manganese and Mn^{2+} is even removed from our drinking water. As a consequence, why do we still keep such ancestral mechanisms in our cells since our Mn intake is extremely low compared to our ancestors? Even if I still do not have the answer, one can think that this TMEM165 induced degradation is more than just involved in Mn detoxification.

Since our Mn intake is extremely low and that Mn is an essential ion for several crucial cellular processes, it is tempting to ask the following question: do we have a sufficient Mn intake during our entire life? Indeed, we live longer than our ancestors and as we age, our ability to absorb vitamins and minerals decreases together with the activity of our enzymes (i.e glycosyltransferases). Therefore, seniors may require more Mn^{2+} to overcome the decrease in GT activity in order to have a fully functional glycosylation for example. Thus, Mn intake should probably be adapted and increased as we grew older. However, Mn detoxification systems also work slower in seniors, making them more susceptible to Mn toxicity. Hence, there is always a thin balance between fully functional biological processes and toxicity.

CONCLUSION

Four classes of molecules are required to build a cell: DNA, proteins, lipids and glycans. Although the importance of DNA and proteins were known for a long time, the role of lipids and above all glycans were blurry and unknown. Glycans were first seen as decorative elements without biological relevance. It was shown later that glycoconjugates were in fact involved in a broad range of essential functions taking place at cellular interfaces. Glycans also confer physicochemical properties to the protein moiety and regulate glycoconjugates localisation. The birth of the glycobiology field and the discovery of the first CDG-patients in 1980 put glycans and glycosylation back on the biology map.

Glycosylation is indeed a fundamental cellular process that involves several actors such as glycosyltransferases, glycosidases and nucleotide sugar transporters. These proteins also require a specific environment and GT are especially known to require divalent cations, mainly Mn2+, to be fully active. The link between Mn2+ and glycosylation in human was established in 1974 [6], but the discovery of a CDG due to Mn2+ homeostasis defect was only reported in 2015, more than 40 years later [7]. CDG primarily encompass genes defects in enzymes directly involved in glycosylation, but a significant subgroup of newly discovered CDG affect Golgi homeostasis, marking a new era in the CDG field. To date, more than 110 CDG subtypes have been described, illustrating the crucial importance of the glycosylation process.

In 2012, the discovery of CDG patients carrying TMEM165 mutations, a putative Golgi cation antiporter, added a new layer of complexity to the field of CDG. My PhD focused on unravelling the functions of TMEM165 and establishing the link between TMEM165 deficiency and the glycosylation defects observed in TMEM165-CDG patients.

In our first study, we highlighted that Golgi Mn2+ homeostasis was impaired in TMEM165 depleted cells, suggesting a Mn2+ entry problem at the Golgi level and therefore questioning TMEM165 putative function as a Ca2+/H+ antiporter. We next demonstrated a general and severe glycosylation defect, with galactosylation especially affected. Interestingly, Mn2+ supplementation almost totally suppressed the observed glycosylation defect. In conclusion, we have demonstrated that the underlying pathological mechanism of TMEM165 deficiency is linked to Golgi Mn2+ homeostasis defect and that the impaired Golgi glycosylation could totally be rescued by the addition of Mn2+.

Since galactosylation was affected, we designed a therapeutic approach using galactose and tested it on TMEM165 deficient cell lines and TMEM165-CDG patients. We demonstrated that Golgi glycosylation defects due to deficiency in TMEM165 also improves on galactose supplementation. However, glycolipid biosynthesis was not fully normalized after galactose treatment. Indeed, there is also a GalNAc defect that was only completely rescued after Mn2+ treatment.

In the last study, we have observed that TMEM165 is a Golgi protein sensitive to Mn2+. Indeed, TMEM165 was rapidly and specifically targeted to lysosomal degradation when cells were exposed to high Mn2+ concentrations. However, the reason behind this phenomenon is still not clear and need to be unravelled.

We propose a model for TMEM165 transport function, in which TMEM165 is able to import cytosolic Mn2+ inside the Golgi lumen against Ca2+ (Figures 43 and 44). The direction of ion transport is still controversial and may depend on the ion concentration gradient between the cytosol and the Golgi. In addition, we do not exclude that TMEM165 can also use Golgi H+ to import Mn2+ inside the Golgi lumen. Moreover, TMEM165 could be a Mn2+/H+ or Ca2+/H+ antiporter whose function is dependent on Ca2+ or Mn2+, respectively.

Finally, in a world where fundamental research is slowly neglected and eclipsed by applied science, it is important to emphasize that without our basic science studies, no treatment for TMEM165-CDG would have been found. Indeed, although screening molecular compounds as potential treatment can be an interesting approach, understanding the precise molecular mechanism of human diseases are always an added value to design therapeutic trials.

REFERENCE LIST

1. Essentials of Glycobiology, Last updated 2009, Accessed on 2009.
2. Zacchi LF, Schulz BL (2016) N-glycoprotein macroheterogeneity: biological implications and proteomic characterization. *Glycoconj J* **33**: 359–376.
3. Foulquier F (2009) COG defects, birth and rise! *Biochim Biophys Acta* **1792**: 896–902.
4. Stanley P (2011) Golgi glycosylation. *Cold Spring Harb Perspect Biol* **3**:.
5. Breton C, Snajdrová L, Jeanneau C, Koca J, Imberty A (2006) Structures and mechanisms of glycosyltransferases. *Glycobiology* **16**: 29R–37R.
6. Khatra BS, Herries DG, Brew K (1974) Some kinetic properties of human-milk galactosyl transferase. *Eur J Biochem* **44**: 537–560.
7. Park JH, Hogrebe M, Grüneberg M, DuChesne I, von der Heiden AL, Reunert J, Schlingmann KP, Boycott KM, Beaulieu CL, Mhanni AA, et al. (2015) SLC39A8 Deficiency: A Disorder of Manganese Transport and Glycosylation. *Am J Hum Genet* **97**: 894–903.
8. Jaeken J (2013) Congenital disorders of glycosylation. *Handb Clin Neurol* **113**: 1737–1743.
9. Freeze HH (2013) Understanding human glycosylation disorders: biochemistry leads the charge. *J Biol Chem* **288**: 6936–6945.
10. Scott K, Gadomski T, Kozicz T, Morava E (2014) Congenital disorders of glycosylation: new defects and still counting. *J Inherit Metab Dis* **37**: 609–617.
11. Krasnewich D (2014) Human glycosylation disorders. *Cancer Biomark Sect Dis Markers* **14**: 3–16.
12. Kornak U, Reynders E, Dimopoulou A, van Reeuwijk J, Fischer B, Rajab A, Budde B, Nürnberg P, Foulquier F, Lefeber D, et al. (2008) Impaired glycosylation and cutis laxa caused by mutations in the vesicular H+-ATPase subunit ATP6V0A2. *Nat Genet* **40**: 32–34.
13. Patel RY, Balaji PV (2007) Length and composition analysis of the cytoplasmic, transmembrane and stem regions of human Golgi glycosyltransferases. *Protein Pept Lett* **14**: 601–609.
14. Hassan H, Reis CA, Bennett EP, Mirgorodskaya E, Roepstorff P, Hollingsworth MA, Burchell J, Taylor-Papadimitriou J, Clausen H (2000) The lectin domain of UDP-N-acetyl-D-galactosamine: polypeptide N-acetylgalactosaminyltransferase-T4 directs its glycopeptide specificities. *J Biol Chem* **275**: 38197–38205.
15. Fritz TA, Raman J, Tabak LA (2006) Dynamic association between the catalytic and lectin domains of human UDP-GalNAc:polypeptide alpha-N-acetylgalactosaminyltransferase-2. *J Biol Chem* **281**: 8613–8619.
16. Herscovics A, Orlean P (1993) Glycoprotein biosynthesis in yeast. *FASEB J Off Publ Fed Am Soc Exp Biol* **7**: 540–550.
17. Aebi M (2013) N-linked protein glycosylation in the ER. *Biochim Biophys Acta BBA - Mol Cell Res* **1833**: 2430–2437.
18. Breitling J, Aebi M (2013) N-Linked Protein Glycosylation in the Endoplasmic Reticulum. *Cold Spring Harb Perspect Biol* **5**:.
19. Moremen KW, Tiemeyer M, Nairn AV (2012) Vertebrate protein glycosylation: diversity, synthesis and function. *Nat Rev Mol Cell Biol* **13**: 448–462.
20. Defaus S, Gupta P, Andreu D, Gutiérrez-Gallego R (2014) Mammalian protein glycosylation--structure versus function. *The Analyst* **139**: 2944–2967.
21. Schreiner R, Schnabel E, Wieland F (1994) Novel N-glycosylation in eukaryotes: laminin contains the linkage unit beta-glucosylasparagine. *J Cell Biol* **124**: 1071–1081.
22. Valliere-Douglass JF, Eakin CM, Wallace A, Ketchem RR, Wang W, Treuheit MJ, Balland A (2010) Glutamine-linked and non-consensus asparagine-linked oligosaccharides present in human recombinant antibodies define novel protein glycosylation motifs. *J Biol Chem* **285**: 16012–16022.
23. McCaffrey K, Braakman I (2016) Protein quality control at the endoplasmic reticulum. *Essays Biochem* **60**: 227–235.
24. Henrissat B, Bairoch A (1996) Updating the sequence-based classification of glycosyl hydrolases. *Biochem J* **316 (Pt 2)**: 695–696.
25. Stanley P (2016) What Have We Learned from Glycosyltransferase Knockouts in Mice? *J Mol Biol* **428**: 3166–3182.
26. Schachter H (1991) The 'yellow brick road' to branched complex N-glycans. *Glycobiology* **1**: 453–461.
27. Moremen KW, Robbins PW (1991) Isolation, characterization, and expression of cDNAs encoding murine alpha-mannosidase II, a Golgi enzyme that controls conversion of high mannose to complex N-glycans. *J Cell Biol* **115**: 1521–1534.
28. Bhide GP, Colley KJ (2017) Sialylation of N-glycans: mechanism, cellular compartmentalization and function. *Histochem Cell Biol* **147**: 149–174.

29. Morelle W, Michalski J-C (2007) Analysis of protein glycosylation by mass spectrometry. *Nat Protoc* **2**: 1585–1602.
30. Yang X, Qian K (2017) Protein O-GlcNAcylation: emerging mechanisms and functions. *Nat Rev Mol Cell Biol* **18**: 452–465.
31. Hart GW, Kreppel LK, Comer FI, Arnold CS, Snow DM, Ye Z, Cheng X, DellaManna D, Caine DS, Earles BJ, et al. (1996) O-GlcNAcylation of key nuclear and cytoskeletal proteins: reciprocity with O-phosphorylation and putative roles in protein multimerization. *Glycobiology* **6**: 711–716.
32. Sakaidani Y, Ichiyanagi N, Saito C, Nomura T, Ito M, Nishio Y, Nadano D, Matsuda T, Furukawa K, Okajima T (2012) O-linked-N-acetylglucosamine modification of mammalian Notch receptors by an atypical O-GlcNAc transferase Eogt1. *Biochem Biophys Res Commun* **419**: 14–19.
33. Hallgren P, Lundblad A, Svensson S (1975) A new type of carbohydrate-protein linkage in a glycopeptide from normal human urine. *J Biol Chem* **250**: 5312–5314.
34. Rabbani SA, Mazar AP, Bernier SM, Haq M, Bolivar I, Henkin J, Goltzman D (1992) Structural requirements for the growth factor activity of the amino-terminal domain of urokinase. *J Biol Chem* **267**: 14151–14156.
35. Müller J, Rana NA, Serth K, Kakuda S, Haltiwanger RS, Gossler A (2014) O-fucosylation of the notch ligand mDLL1 by POFUT1 is dispensable for ligand function. *PloS One* **9**: e88571.
36. Sheikh MO, Wells L (2017) Whoa man! Unexpected protein O-mannosylation pathways in mammals. *J Biol Chem* **292**: 11599–11600.
37. Chiba A, Matsumura K, Yamada H, Inazu T, Shimizu T, Kusunoki S, Kanazawa I, Kobata A, Endo T (1997) Structures of sialylated O-linked oligosaccharides of bovine peripheral nerve alpha-dystroglycan. The role of a novel O-mannosyl-type oligosaccharide in the binding of alpha-dystroglycan with laminin. *J Biol Chem* **272**: 2156–2162.
38. Wells L (2013) The o-mannosylation pathway: glycosyltransferases and proteins implicated in congenital muscular dystrophy. *J Biol Chem* **288**: 6930–6935.
39. Larsen ISB, Narimatsu Y, Joshi HJ, Yang Z, Harrison OJ, Brasch J, Shapiro L, Honig B, Vakhrushev SY, Clausen H, et al. (2017) Mammalian O-mannosylation of cadherins and plexins is independent of protein O-mannosyltransferases 1 and 2. *J Biol Chem* **292**: 11586–11598.
40. Moloney DJ, Shair LH, Lu FM, Xia J, Locke R, Matta KL, Haltiwanger RS (2000) Mammalian Notch1 is modified with two unusual forms of O-linked glycosylation found on epidermal growth factor-like modules. *J Biol Chem* **275**: 9604–9611.
41. Camiruaga A, Usabiaga I, Insausti A, Cocinero EJ, León I, Fernández JA (2017) Understanding the role of tyrosine in glycogenin. *Mol Biosyst*.
42. Schegg B, Hülsmeier AJ, Rutschmann C, Maag C, Hennet T (2009) Core Glycosylation of Collagen Is Initiated by Two β(1-O)Galactosyltransferases. *Mol Cell Biol* **29**: 943–952.
43. Hanisch FG (2001) O-glycosylation of the mucin type. *Biol Chem* **382**: 143–149.
44. Jensen PH, Kolarich D, Packer NH (2010) Mucin-type O-glycosylation--putting the pieces together. *FEBS J* **277**: 81–94.
45. Brockhausen I, Stanley P (2015) O-GalNAc Glycans. In Varki A, Cummings RD, Esko JD, Stanley P, Hart GW, Aebi M, Darvill AG, Kinoshita T, Packer NH, Prestegard JH, et al. (eds.), *Essentials of Glycobiology*. Cold Spring Harbor Laboratory Press, Cold Spring Harbor (NY).
46. Bennett EP, Mandel U, Clausen H, Gerken TA, Fritz TA, Tabak LA (2012) Control of mucin-type O-glycosylation: a classification of the polypeptide GalNAc-transferase gene family. *Glycobiology* **22**: 736–756.
47. Esko JD, Kimata K, Lindahl U (2009) Proteoglycans and Sulfated Glycosaminoglycans. In Varki A, Cummings RD, Esko JD, Freeze HH, Stanley P, Bertozzi CR, Hart GW, Etzler ME (eds.), *Essentials of Glycobiology*. Cold Spring Harbor Laboratory Press, Cold Spring Harbor (NY).
48. Lauder RM (2009) Chondroitin sulphate: a complex molecule with potential impacts on a wide range of biological systems. *Complement Ther Med* **17**: 56–62.
49. Mikami T, Kitagawa H (2013) Biosynthesis and function of chondroitin sulfate. *Biochim Biophys Acta* **1830**: 4719–4733.
50. Shriver Z, Capila I, Venkataraman G, Sasisekharan R (2012) Heparin and heparan sulfate: analyzing structure and microheterogeneity. *Handb Exp Pharmacol* 159–176.
51. Funderburgh JL (2000) Keratan sulfate: structure, biosynthesis, and function. *Glycobiology* **10**: 951–958.
52. Freeze HH, Chong JX, Bamshad MJ, Ng BG (2014) Solving glycosylation disorders: fundamental approaches reveal complicated pathways. *Am J Hum Genet* **94**: 161–175.
53. Degroote S, Wolthoorn J, van Meer G (2004) The cell biology of glycosphingolipids. *Semin Cell Dev Biol* **15**: 375–387.

54. Schnaar RL, Kinoshita T (2015) Glycosphingolipids. In Varki A, Cummings RD, Esko JD, Stanley P, Hart GW, Aebi M, Darvill AG, Kinoshita T, Packer NH, Prestegard JH, et al. (eds.), *Essentials of Glycobiology*. Cold Spring Harbor Laboratory Press, Cold Spring Harbor (NY).
55. Groux-Degroote S, Guérardel Y, Delannoy P (2017) Gangliosides: Structures, Biosynthesis, Analysis, and Roles in Cancer. *Chembiochem Eur J Chem Biol* **18**: 1146–1154.
56. Maccioni HJ, Daniotti JL, Martina JA (1999) Organization of ganglioside synthesis in the Golgi apparatus. *Biochim Biophys Acta* **1437**: 101–118.
57. Nishie T, Hikimochi Y, Zama K, Fukusumi Y, Ito M, Yokoyama H, Naruse C, Ito M, Asano M (2010) Beta4-galactosyltransferase-5 is a lactosylceramide synthase essential for mouse extra-embryonic development. *Glycobiology* **20**: 1311–1322.
58. Furukawa K, Tokuda N, Okuda T, Tajima O, Furukawa K (2004) Glycosphingolipids in engineered mice: insights into function. *Semin Cell Dev Biol* **15**: 389–396.
59. Bexiga MG, Simpson JC (2013) Human Diseases Associated with Form and Function of the Golgi Complex. *Int J Mol Sci* **14**: 18670–18681.
60. Bekier ME, Wang L, Li J, Huang H, Tang D, Zhang X, Wang Y (2017) Knockout of the Golgi stacking proteins GRASP55 and GRASP65 impairs Golgi structure and function. *Mol Biol Cell*.
61. Dippold HC, Ng MM, Farber-Katz SE, Lee S-K, Kerr ML, Peterman MC, Sim R, Wiharto PA, Galbraith KA, Madhavarapu S, et al. (2009) GOLPH3 bridges phosphatidylinositol-4- phosphate and actomyosin to stretch and shape the Golgi to promote budding. *Cell* **139**: 337–351.
62. Cheong FY, Sharma V, Blagoveshchenskaya A, Oorschot VMJ, Brankatschk B, Klumperman J, Freeze HH, Mayinger P (2010) Spatial regulation of Golgi phosphatidylinositol-4-phosphate is required for enzyme localization and glycosylation fidelity. *Traffic Cph Den* **11**: 1180–1190.
63. Tran DT, Ten Hagen KG (2013) Mucin-type O-Glycosylation during Development. *J Biol Chem* **288**: 6921–6929.
64. Albrecht S, Unwin L, Muniyappa M, Rudd PM (2014) Glycosylation as a marker for inflammatory arthritis. *Cancer Biomark Sect Dis Markers* **14**: 17–28.
65. Ashkani J, Naidoo KJ (2016) Glycosyltransferase Gene Expression Profiles Classify Cancer Types and Propose Prognostic Subtypes. *Sci Rep* **6**:.
66. Ruan S, Raj BK, Lloyd KO (1999) Relationship of glycosyltransferases and mRNA levels to ganglioside expression in neuroblastoma and melanoma cells. *J Neurochem* **72**: 514–521.
67. Wu Y-M, Nowack DD, Omenn GS, Haab BB (2009) Mucin glycosylation is altered by pro-inflammatory signaling in pancreatic-cancer cells. *J Proteome Res* **8**: 1876–1886.
68. Chaney W, Sundaram S, Friedman N, Stanley P (1989) The Lec4A CHO glycosylation mutant arises from miscompartmentalization of a Golgi glycosyltransferase. *J Cell Biol* **109**: 2089–2096.
69. Hassinen A, Rivinoja A, Kauppila A, Kellokumpu S (2010) Golgi N-glycosyltransferases form both homo- and heterodimeric enzyme complexes in live cells. *J Biol Chem* **285**: 17771–17777.
70. Kellokumpu S, Hassinen A, Glumoff T (2016) Glycosyltransferase complexes in eukaryotes: long-known, prevalent but still unrecognized. *Cell Mol Life Sci CMLS* **73**: 305–325.
71. Eckert ESP, Reckmann I, Hellwig A, Röhling S, El-Battari A, Wieland FT, Popoff V (2014) Golgi Phosphoprotein 3 Triggers Signal-mediated Incorporation of Glycosyltransferases into Coatomer-coated (COPI) Vesicles. *J Biol Chem* **289**: 31319–31329.
72. Berninsone PM, Hirschberg CB (2000) Nucleotide sugar transporters of the Golgi apparatus. *Curr Opin Struct Biol* **10**: 542–547.
73. Puthenveedu MA, Linstedt AD (2005) Subcompartmentalizing the Golgi apparatus. *Curr Opin Cell Biol* **17**: 369–375.
74. Spessott W, Uliana A, Maccioni HJF (2010) Defective GM3 synthesis in Cog2 null mutant CHO cells associates to mislocalization of lactosylceramide sialyltransferase in the Golgi complex. *Neurochem Res* **35**: 2161–2167.
75. Podos SD, Reddy P, Ashkenas J, Krieger M (1994) LDLC encodes a brefeldin A-sensitive, peripheral Golgi protein required for normal Golgi function. *J Cell Biol* **127**: 679–691.
76. Smith RD, Lupashin VV (2008) Role of the conserved oligomeric Golgi (COG) complex in protein glycosylation. *Carbohydr Res* **343**: 2024–2031.
77. Hirschberg CB, Robbins PW, Abeijon C (1998) Transporters of nucleotide sugars, ATP, and nucleotide sulfate in the endoplasmic reticulum and Golgi apparatus. *Annu Rev Biochem* **67**: 49–69.
78. Hadley B, Maggioni A, Ashikov A, Day CJ, Haselhorst T, Tiralongo J (2014) Structure and function of nucleotide sugar transporters: Current progress. *Comput Struct Biotechnol J* **10**: 23–32.
79. Xu Y-X, Liu L, Caffaro CE, Hirschberg CB (2010) Inhibition of Golgi apparatus glycosylation causes endoplasmic reticulum stress and decreased protein synthesis. *J Biol Chem* **285**: 24600–24608.

80. Toyoda H, Kinoshita-Toyoda A, Selleck SB (2000) Structural analysis of glycosaminoglycans in Drosophila and Caenorhabditis elegans and demonstration that tout-velu, a Drosophila gene related to EXT tumor suppressors, affects heparan sulfate in vivo. *J Biol Chem* **275**: 2269–2275.
81. Wang TF, Guidotti G (1998) Golgi localization and functional expression of human uridine diphosphatase. *J Biol Chem* **273**: 11392–11399.
82. Abeijon C, Yanagisawa K, Mandon EC, Häusler A, Moremen K, Hirschberg CB, Robbins PW (1993) Guanosine diphosphatase is required for protein and sphingolipid glycosylation in the Golgi lumen of Saccharomyces cerevisiae. *J Cell Biol* **122**: 307–323.
83. Miesenböck G, De Angelis DA, Rothman JE (1998) Visualizing secretion and synaptic transmission with pH-sensitive green fluorescent proteins. *Nature* **394**: 192–195.
84. Thorens B, Vassalli P (1986) Chloroquine and ammonium chloride prevent terminal glycosylation of immunoglobulins in plasma cells without affecting secretion. *Nature* **321**: 618–620.
85. Campbell BJ, Rowe GE, Leiper K, Rhodes JM (2001) Increasing the intra-Golgi pH of cultured LS174T goblet-differentiated cells mimics the decreased mucin sulfation and increased Thomsen-Friedenreich antigen (Gal beta1-3GalNac alpha-) expression seen in colon cancer. *Glycobiology* **11**: 385–393.
86. Axelsson MA, Karlsson NG, Steel DM, Ouwendijk J, Nilsson T, Hansson GC (2001) Neutralization of pH in the Golgi apparatus causes redistribution of glycosyltransferases and changes in the O-glycosylation of mucins. *Glycobiology* **11**: 633–644.
87. Rivinoja A, Hassinen A, Kokkonen N, Kauppila A, Kellokumpu S (2009) Elevated Golgi pH impairs terminal N-glycosylation by inducing mislocalization of Golgi glycosyltransferases. *J Cell Physiol* **220**: 144–154.
88. Audry M, Jeanneau C, Imberty A, Harduin-Lepers A, Delannoy P, Breton C (2011) Current trends in the structure-activity relationships of sialyltransferases. *Glycobiology* **21**: 716–726.
89. Powell JT, Brew K (1976) Metal ion activation of galactosyltransferase. *J Biol Chem* **251**: 3645–3652.
90. Ramakrishnan B, Ramasamy V, Qasba PK (2006) Structural snapshots of beta-1,4-galactosyltransferase-I along the kinetic pathway. *J Mol Biol* **357**: 1619–1633.
91. Bauvois B, Cartron JP, Nurden A, Caen J (1981) Glycoprotein-sialyltransferase activity of normal human, thrombasthenic and Bernard-Soulier platelets. *Vox Sang* **40**: 71–78.
92. Chatterjee S, Castiglione E (1987) UDPgalactose:glucosylceramide β1 → 4-galactosyltransferase activity in human proximal tubular cells from normal and familial hypercholesterolemic homozygotes. *Biochim Biophys Acta BBA - Gen Subj* **923**: 136–142.
93. Chen YA, Scales SJ, Patel SM, Doung YC, Scheller RH (1999) SNARE complex formation is triggered by Ca2+ and drives membrane fusion. *Cell* **97**: 165–174.
94. Jena BP (2009) Membrane fusion: role of SNAREs and calcium. *Protein Pept Lett* **16**: 712–717.
95. Cheng PW, DeVries A (1986) Mucin biosynthesis. Enzymic properties of human-tracheal epithelial GDP-L-fucose:beta-D-galactoside alpha-(1----2)-L-fucosyltransferase. *Carbohydr Res* **149**: 253–261.
96. Iannotti MJ, Figard L, Sokac AM, Sifers RN (2014) A Golgi-localized mannosidase (MAN1B1) plays a non-enzymatic gatekeeper role in protein biosynthetic quality control. *J Biol Chem* **289**: 11844–11858.
97. Tempel W, Karaveg K, Liu Z-J, Rose J, Wang B-C, Moremen KW (2004) Structure of mouse Golgi alpha-mannosidase IA reveals the molecular basis for substrate specificity among class 1 (family 47 glycosylhydrolase) alpha1,2-mannosidases. *J Biol Chem* **279**: 29774–29786.
98. Murray BW, Takayama S, Schultz J, Wong CH (1996) Mechanism and specificity of human alpha-1,3-fucosyltransferase V. *Biochemistry (Mosc)* **35**: 11183–11195.
99. Jeon US (2008) Kidney and Calcium Homeostasis. *Electrolytes Blood Press E BP* **6**: 68–76.
100. Berridge MJ, Lipp P, Bootman MD (2000) The versatility and universality of calcium signalling. *Nat Rev Mol Cell Biol* **1**: 11–21.
101. Demaurex N (2002) pH Homeostasis of Cellular Organelles. *Physiology* **17**: 1–5.
102. Berridge MJ, Bootman MD, Roderick HL (2003) Calcium: Calcium signalling: dynamics, homeostasis and remodelling. *Nat Rev Mol Cell Biol* **4**: 517.
103. Chandra S, Kable EP, Morrison GH, Webb WW (1991) Calcium sequestration in the Golgi apparatus of cultured mammalian cells revealed by laser scanning confocal microscopy and ion microscopy. *J Cell Sci* **100 (Pt 4)**: 747–752.
104. Pizzo P, Lissandron V, Capitanio P, Pozzan T (2011) Ca2+ signalling in the Golgi apparatus. *Cell Calcium* **50**: 184–192.
105. Lissandron V, Podini P, Pizzo P, Pozzan T (2010) Unique characteristics of Ca2+ homeostasis of the trans-Golgi compartment. *Proc Natl Acad Sci U S A* **107**: 9198–9203.
106. Krebs J, Agellon LB, Michalak M (2015) Ca2+ homeostasis and endoplasmic reticulum (ER) stress: An integrated view of calcium signaling. *Biochem Biophys Res Commun* **460**: 114–121.
107. Clapham DE (2007) Calcium Signaling. *Cell* **131**: 1047–1058.

108. Van Baelen K, Dode L, Vanoevelen J, Callewaert G, De Smedt H, Missiaen L, Parys JB, Raeymaekers L, Wuytack F (2004) The Ca2+/Mn2+ pumps in the Golgi apparatus. *Biochim Biophys Acta* **1742**: 103–112.
109. Xiang M, Mohamalawari D, Rao R (2005) A novel isoform of the secretory pathway Ca2+,Mn(2+)-ATPase, hSPCA2, has unusual properties and is expressed in the brain. *J Biol Chem* **280**: 11608–11614.
110. Vanoevelen J, Dode L, Van Baelen K, Fairclough RJ, Missiaen L, Raeymaekers L, Wuytack F (2005) The secretory pathway Ca2+/Mn2+-ATPase 2 is a Golgi-localized pump with high affinity for Ca2+ ions. *J Biol Chem* **280**: 22800–22808.
111. Smaardijk S, Chen J, Wuytack F, Vangheluwe P (2017) SPCA2 couples Ca(2+) influx via Orai1 to Ca(2+) uptake into the Golgi/secretory pathway. *Tissue Cell* **49**: 141–149.
112. Demaegd D, Foulquier F, Colinet A-S, Gremillon L, Legrand D, Mariot P, Peiter E, Van Schaftingen E, Matthijs G, Morsomme P (2013) Newly characterized Golgi-localized family of proteins is involved in calcium and pH homeostasis in yeast and human cells. *Proc Natl Acad Sci* **110**: 6859–6864.
113. Foulquier F, Amyere M, Jaeken J, Zeevaert R, Schollen E, Race V, Bammens R, Morelle W, Rosnoblet C, Legrand D, et al. (2012) TMEM165 Deficiency Causes a Congenital Disorder of Glycosylation. *Am J Hum Genet* **91**: 15–26.
114. Taylor RS, Jones SM, Dahl RH, Nordeen MH, Howell KE (1997) Characterization of the Golgi complex cleared of proteins in transit and examination of calcium uptake activities. *Mol Biol Cell* **8**: 1911–1931.
115. Pinton P, Pozzan T, Rizzuto R (1998) The Golgi apparatus is an inositol 1,4,5-trisphosphate-sensitive Ca2+ store, with functional properties distinct from those of the endoplasmic reticulum. *EMBO J* **17**: 5298–5308.
116. Aulestia FJ, Alonso MT, Garcia-Sancho J (2014) Differential calcium handling by the cis and trans regions of the Golgi apparatus. *Biochem J*.
117. Paroutis P, Touret N, Grinstein S (2004) The pH of the Secretory Pathway: Measurement, Determinants, and Regulation. *Physiology* **19**: 207–215.
118. Schapiro FB, Grinstein S (2000) Determinants of the pH of the Golgi Complex. *J Biol Chem* **275**: 21025–21032.
119. Rivinoja A, Pujol FM, Hassinen A, Kellokumpu S (2012) Golgi pH, its regulation and roles in human disease. *Ann Med* **44**: 542–554.
120. Casey JR, Grinstein S, Orlowski J (2010) Sensors and regulators of intracellular pH. *Nat Rev Mol Cell Biol* **11**: 50–61.
121. Weisz OA (2003) Organelle Acidification and Disease. *Traffic* **4**: 57–64.
122. Jefferies KC, Cipriano DJ, Forgac M (2008) Function, structure and regulation of the vacuolar (H+)-ATPases. *Arch Biochem Biophys* **476**: 33–42.
123. Glickman J, Croen K, Kelly S, Al-Awqati Q (1983) Golgi membranes contain an electrogenic H+ pump in parallel to a chloride conductance. *J Cell Biol* **97**: 1303–1308.
124. Maeda Y, Ide T, Koike M, Uchiyama Y, Kinoshita T (2008) GPHR is a novel anion channel critical for acidification and functions of the Golgi apparatus. *Nat Cell Biol* **10**: 1135–1145.
125. Barasch J, Kiss B, Prince A, Saiman L, Gruenert D, al-Awqati Q (1991) Defective acidification of intracellular organelles in cystic fibrosis. *Nature* **352**: 70–73.
126. Barasch J, al-Awqati Q (1993) Defective acidification of the biosynthetic pathway in cystic fibrosis. *J Cell Sci Suppl* **17**: 229–233.
127. Holappa K, Suokas M, Soininen P, Kellokumpu S (2001) Identification of the full-length AE2 (AE2a) isoform as the Golgi-associated anion exchanger in fibroblasts. *J Histochem Cytochem Off J Histochem Soc* **49**: 259–269.
128. Nagasawa M, Kanzaki M, Iino Y, Morishita Y, Kojima I (2001) Identification of a novel chloride channel expressed in the endoplasmic reticulum, golgi apparatus, and nucleus. *J Biol Chem* **276**: 20413–20418.
129. Gentzsch M, Cui L, Mengos A, Chang X-B, Chen J-H, Riordan JR (2003) The PDZ-binding chloride channel ClC-3B localizes to the Golgi and associates with cystic fibrosis transmembrane conductance regulator-interacting PDZ proteins. *J Biol Chem* **278**: 6440–6449.
130. Wu MM, Grabe M, Adams S, Tsien RY, Moore HP, Machen TE (2001) Mechanisms of pH regulation in the regulated secretory pathway. *J Biol Chem* **276**: 33027–33035.
131. Vollet K, Haynes EN, Dietrich KN (2016) Manganese Exposure and Cognition Across the Lifespan: Contemporary Review and Argument for Biphasic Dose–Response Health Effects. *Curr Environ Health Rep* 1–13.
132. Au C, Benedetto A, Aschner M (2008) Manganese transport in eukaryotes: the role of DMT1. *Neurotoxicology* **29**: 569–576.
133. Perl DP, Olanow CW (2007) The neuropathology of manganese-induced Parkinsonism. *J Neuropathol Exp Neurol* **66**: 675–682.
134. Squitti R, Gorgone G, Panetta V, Lucchini R, Bucossi S, Albini E, Alessio L, Alberici A, Melgari JM, Benussi L, et al. (2009) Implications of metal exposure and liver function in Parkinsonian patients resident in the vicinities of ferroalloy plants. *J Neural Transm Vienna Austria 1996* **116**: 1281–1287.

135. O'Neal SL, Zheng W (2015) Manganese Toxicity Upon Overexposure: a Decade in Review. *Curr Environ Health Rep* **2**: 315–328.
136. Goullé J-P, Mahieu L, Castermant J, Neveu N, Bonneau L, Lainé G, Bouige D, Lacroix C (2005) Metal and metalloid multi-elementary ICP-MS validation in whole blood, plasma, urine and hair. Reference values. *Forensic Sci Int* **153**: 39–44.
137. Gibbons RA, Dixon SN, Hallis K, Russell AM, Sansom BF, Symonds HW (1976) Manganese metabolism in cows and goats. *Biochim Biophys Acta* **444**: 1–10.
138. Roth JA (2006) Homeostatic and toxic mechanisms regulating manganese uptake, retention, and elimination. *Biol Res* **39**: 45–57.
139. Fitsanakis VA, Zhang N, Garcia S, Aschner M (2010) Manganese (Mn) and iron (Fe): interdependency of transport and regulation. *Neurotox Res* **18**: 124–131.
140. Gammella E, Buratti P, Cairo G, Recalcati S (2017) The transferrin receptor: the cellular iron gate. *Met Integr Biometal Sci*.
141. Morgan EH (1972) The role of transferrin in iron metabolism. *Med J Aust* **2**: 322–325.
142. van Renswoude J, Bridges KR, Harford JB, Klausner RD (1982) Receptor-mediated endocytosis of transferrin and the uptake of fe in K562 cells: identification of a nonlysosomal acidic compartment. *Proc Natl Acad Sci U S A* **79**: 6186–6190.
143. Garrick MD, Singleton ST, Vargas F, Kuo H-C, Zhao L, Knöpfel M, Davidson T, Costa M, Paradkar P, Roth JA, et al. (2006) DMT1: which metals does it transport? *Biol Res* **39**: 79–85.
144. Gunshin H, Mackenzie B, Berger UV, Gunshin Y, Romero MF, Boron WF, Nussberger S, Gollan JL, Hediger MA (1997) Cloning and characterization of a mammalian proton-coupled metal-ion transporter. *Nature* **388**: 482–488.
145. Kambe T, Tsuji T, Hashimoto A, Itsumura N (2015) The Physiological, Biochemical, and Molecular Roles of Zinc Transporters in Zinc Homeostasis and Metabolism. *Physiol Rev* **95**: 749–784.
146. Chen P, Chakraborty S, Mukhopadhyay S, Lee E, Paoliello MMB, Bowman AB, Aschner M (2015) Manganese homeostasis in the nervous system. *J Neurochem* **134**: 601–610.
147. Jeong J, Eide DJ (2013) The SLC39 family of zinc transporters. *Mol Aspects Med* **34**: 612–619.
148. Clayton PT (2017) Inherited disorders of transition metal metabolism: an update. *J Inherit Metab Dis*.
149. He L, Girijashanker K, Dalton TP, Reed J, Li H, Soleimani M, Nebert DW (2006) ZIP8, member of the solute-carrier-39 (SLC39) metal-transporter family: characterization of transporter properties. *Mol Pharmacol* **70**: 171–180.
150. Tuschl K, Meyer E, Valdivia LE, Zhao N, Dadswell C, Abdul-Sada A, Hung CY, Simpson MA, Chong WK, Jacques TS, et al. (2016) Mutations in SLC39A14 disrupt manganese homeostasis and cause childhood-onset parkinsonism-dystonia. *Nat Commun* **7**: 11601.
151. Xin Y, Gao H, Wang J, Qiang Y, Imam MU, Li Y, Wang J, Zhang R, Zhang H, Yu Y, et al. (2017) Manganese transporter Slc39a14 deficiency revealed its key role in maintaining manganese homeostasis in mice. *Cell Discov* **3**: 17025.
152. Crossgrove JS, Yokel RA (2005) Manganese distribution across the blood-brain barrier. IV. Evidence for brain influx through store-operated calcium channels. *Neurotoxicology* **26**: 297–307.
153. Crossgrove JS, Allen DD, Bukaveckas BL, Rhineheimer SS, Yokel RA (2003) Manganese distribution across the blood-brain barrier. I. Evidence for carrier-mediated influx of managanese citrate as well as manganese and manganese transferrin. *Neurotoxicology* **24**: 3–13.
154. Lockman PR, Roder KE, Allen DD (2001) Inhibition of the rat blood-brain barrier choline transporter by manganese chloride. *J Neurochem* **79**: 588–594.
155. Erikson KM, John CE, Jones SR, Aschner M (2005) Manganese accumulation in striatum of mice exposed to toxic doses is dependent upon a functional dopamine transporter. *Environ Toxicol Pharmacol* **20**: 390–394.
156. He W, Hu Z (2012) The role of the Golgi-resident SPCA Ca^{2+}/Mn^{2+} pump in ionic homeostasis and neural function. *Neurochem Res* **37**: 455–468.
157. Cohen Y, Megyeri M, Chen OCW, Condomitti G, Riezman I, Loizides-Mangold U, Abdul-Sada A, Rimon N, Riezman H, Platt FM, et al. (2013) The yeast p5 type ATPase, spf1, regulates manganese transport into the endoplasmic reticulum. *PloS One* **8**: e85519.
158. Chiesi M, Inesi G (1980) Adenosine 5'-triphosphate dependent fluxes of manganese and and hydrogen ions in sarcoplasmic reticulum vesicles. *Biochemistry (Mosc)* **19**: 2912–2918.
159. Chiesi M, Inesi G (1981) Mg2+ and Mn2+ modulation of Ca2+ transport and ATPase activity in sarcoplasmic reticulum vesicles. *Arch Biochem Biophys* **208**: 586–592.
160. Yonekura S-I, Toyoshima C (2016) Mn2+ transport by Ca2+-ATPase of sarcoplasmic reticulum. *FEBS Lett* **590**: 2086–2095.

161. Fleming SM, Santiago NA, Mullin EJ, Pamphile S, Karkare S, Lemkuhl A, Ekhator OR, Linn SC, Holden JG, Aga DS, et al. (2017) The effect of manganese exposure in Atp13a2-deficient mice. *Neurotoxicology*.
162. Nishito Y, Tsuji N, Fujishiro H, Takeda T-A, Yamazaki T, Teranishi F, Okazaki F, Matsunaga A, Tuschl K, Rao R, et al. (2016) Direct Comparison of Manganese Detoxification/Efflux Proteins and Molecular Characterization of ZnT10 Protein as a Manganese Transporter. *J Biol Chem* **291**: 14773–14787.
163. Qin Y, Dittmer PJ, Park JG, Jansen KB, Palmer AE (2011) Measuring steady-state and dynamic endoplasmic reticulum and Golgi Zn2+ with genetically encoded sensors. *Proc Natl Acad Sci U S A* **108**: 7351–7356.
164. Schweigel-Röntgen M, Kolisek M (2014) SLC41 transporters--molecular identification and functional role. *Curr Top Membr* **73**: 383–410.
165. Sahni J, Scharenberg AM (2013) The SLC41 family of MgtE-like magnesium transporters. *Mol Aspects Med* **34**: 620–628.
166. de Baaij JHF, Hoenderop JGJ, Bindels RJM (2015) Magnesium in man: implications for health and disease. *Physiol Rev* **95**: 1–46.
167. Kim H, Wu X, Lee J (2013) SLC31 (CTR) family of copper transporters in health and disease. *Mol Aspects Med* **34**: 561–570.
168. Venkatesan M, Kuntz DA, Rose DR (2009) Human lysosomal alpha-mannosidases exhibit different inhibition and metal binding properties. *Protein Sci Publ Protein Soc* **18**: 2242–2251.
169. Suzuki T, Hara I, Nakano M, Shigeta M, Nakagawa T, Kondo A, Funakoshi Y, Taniguchi N (2006) Man2C1, an alpha-mannosidase, is involved in the trimming of free oligosaccharides in the cytosol. *Biochem J* **400**: 33–41.
170. Yamamoto H, Tobisawa Y, Inubushi T, Irie F, Ohyama C, Yamaguchi Y (2017) A mammalian homolog of the zebrafish transmembrane protein 2 (TMEM2) is the long-sought-after cell-surface hyaluronidase. *J Biol Chem* **292**: 7304–7313.
171. Pak JE, Arnoux P, Zhou S, Sivarajah P, Satkunarajah M, Xing X, Rini JM (2006) X-ray crystal structure of leukocyte type core 2 beta1,6-N-acetylglucosaminyltransferase. Evidence for a convergence of metal ion-independent glycosyltransferase mechanism. *J Biol Chem* **281**: 26693–26701.
172. Tsopanakis AD, Herries DG (1978) Bovine galactosyl transferase. Substrate.managanese complexes and the role of manganese ions in the mechanism. *Eur J Biochem* **83**: 179–188.
173. Arnold SM, Fessler LI, Fessler JH, Kaufman RJ (2000) Two homologues encoding human UDP-glucose:glycoprotein glucosyltransferase differ in mRNA expression and enzymatic activity. *Biochemistry (Mosc)* **39**: 2149–2163.
174. Wandall HH, Hassan H, Mirgorodskaya E, Kristensen AK, Roepstorff P, Bennett EP, Nielsen PA, Hollingsworth MA, Burchell J, Taylor-Papadimitriou J, et al. (1997) Substrate Specificities of Three Members of the Human UDP-N-Acetyl-α-d-galactosamine:Polypeptide N-Acetylgalactosaminyltransferase Family, GalNAc-T1, -T2, and -T3. *J Biol Chem* **272**: 23503–23514.
175. Kubota T, Shiba T, Sugioka S, Furukawa S, Sawaki H, Kato R, Wakatsuki S, Narimatsu H (2006) Structural basis of carbohydrate transfer activity by human UDP-GalNAc: polypeptide alpha-N-acetylgalactosaminyltransferase (pp-GalNAc-T10). *J Mol Biol* **359**: 708–727.
176. Willer T, Inamori K-I, Venzke D, Harvey C, Morgensen G, Hara Y, Beltrán Valero de Bernabé D, Yu L, Wright KM, Campbell KP (2014) The glucuronyltransferase B4GAT1 is required for initiation of LARGE-mediated α-dystroglycan functional glycosylation. *eLife* **3**:.
177. Inamori K, Willer T, Hara Y, Venzke D, Anderson ME, Clarke NF, Guicheney P, Bönnemann CG, Moore SA, Campbell KP (2014) Endogenous glucuronyltransferase activity of LARGE or LARGE2 required for functional modification of α-dystroglycan in cells and tissues. *J Biol Chem* **289**: 28138–28148.
178. Minamida S, Aoki K, Natsuka S, Omichi K, Fukase K, Kusumoto S, Hase S (1996) Detection of UDP-D-xylose: alpha-D-xyloside alpha 1-->3xylosyltransferase activity in human hepatoma cell line HepG2. *J Biochem (Tokyo)* **120**: 1002–1006.
179. Palma AS, Morais VA, Coelho AV, Costa J (2004) Effect of the manganese ion on human alpha3/4 fucosyltransferase III activity. *Biometals Int J Role Met Ions Biol Biochem Med* **17**: 35–43.
180. Vries D, Theodora, Storm J, Rotteveel F, Verdonk G, van Duin M, Eijnden VD, H D, Joziasse DH, Bunschoten H (2001) Production of soluble human α3-fucosyltransferase (FucT VII) by membrane targeting and in vivo proteolysis. *Glycobiology* **11**: 711–717.
181. Takeya A, Hosomi O, Kogure T (1987) Identification and characterization of UDP-GalNAc: NeuAc alpha 2-3Gal beta 1-4Glc(NAc) beta 1-4(GalNAc to Gal)N-acetylgalactosaminyltransferase in human blood plasma. *J Biochem (Tokyo)* **101**: 251–259.
182. Malagolini N, Dall'Olio F, Di Stefano G, Minni F, Marrano D, Serafini-Cessi F (1989) Expression of UDP-GalNAc:NeuAc alpha 2,3Gal beta-R beta 1,4(GalNAc to Gal) N-acetylgalactosaminyltransferase involved in the synthesis of Sda antigen in human large intestine and colorectal carcinomas. *Cancer Res* **49**: 6466–6470.

183. Persson M, Letts JA, Hosseini-Maaf B, Borisova SN, Palcic MM, Evans SV, Olsson ML (2007) Structural effects of naturally occurring human blood group B galactosyltransferase mutations adjacent to the DXD motif. *J Biol Chem* **282**: 9564–9570.
184. Müller S, Schöttler M, Schön S, Prante C, Brinkmann T, Kuhn J, Götting C, Kleesiek K (2005) Human xylosyltransferase I: functional and biochemical characterization of cysteine residues required for enzymic activity. *Biochem J* **386**: 227–236.
185. Götting C, Müller S, Schöttler M, Schön S, Prante C, Brinkmann T, Kuhn J, Kleesiek K (2004) Analysis of the DXD motifs in human xylosyltransferase I required for enzyme activity. *J Biol Chem* **279**: 42566–42573.
186. Yada T, Sato T, Kaseyama H, Gotoh M, Iwasaki H, Kikuchi N, Kwon Y-D, Togayachi A, Kudo T, Watanabe H, et al. (2003) Chondroitin sulfate synthase-3. Molecular cloning and characterization. *J Biol Chem* **278**: 39711–39725.
187. Yada T, Gotoh M, Sato T, Shionyu M, Go M, Kaseyama H, Iwasaki H, Kikuchi N, Kwon Y-D, Togayachi A, et al. (2003) Chondroitin sulfate synthase-2. Molecular cloning and characterization of a novel human glycosyltransferase homologous to chondroitin sulfate glucuronyltransferase, which has dual enzymatic activities. *J Biol Chem* **278**: 30235–30247.
188. Kakuda S, Shiba T, Ishiguro M, Tagawa H, Oka S, Kajihara Y, Kawasaki T, Wakatsuki S, Kato R (2004) Structural basis for acceptor substrate recognition of a human glucuronyltransferase, GlcAT-P, an enzyme critical in the biosynthesis of the carbohydrate epitope HNK-1. *J Biol Chem* **279**: 22693–22703.
189. Tsutsui Y, Ramakrishnan B, Qasba PK (2013) Crystal Structures of β-1,4-Galactosyltransferase 7 Enzyme Reveal Conformational Changes and Substrate Binding. *J Biol Chem* **288**: 31963–31970.
190. Li J, Rancour DM, Allende ML, Worth CA, Darling DS, Gilbert JB, Menon AK, Young WW (2001) The DXD motif is required for GM2 synthase activity but is not critical for nucleotide binding. *Glycobiology* **11**: 217–229.
191. Okajima T, Nakamura Y, Uchikawa M, Haslam DB, Numata SI, Furukawa K, Urano T, Furukawa K (2000) Expression cloning of human globoside synthase cDNAs. Identification of beta 3Gal-T3 as UDP-N-acetylgalactosamine:globotriaosylceramide beta 1,3-N-acetylgalactosaminyltransferase. *J Biol Chem* **275**: 40498–40503.
192. Amado M, Almeida R, Carneiro F, Levery SB, Holmes EH, Nomoto M, Hollingsworth MA, Hassan H, Schwientek T, Nielsen PA, et al. (1998) A family of human beta3-galactosyltransferases. Characterization of four members of a UDP-galactose:beta-N-acetyl-glucosamine/beta-nacetyl-galactosamine beta-1,3-galactosyltransferase family. *J Biol Chem* **273**: 12770–12778.
193. Zhou D, Dinter A, Gutiérrez Gallego R, Kamerling JP, Vliegenthart JF, Berger EG, Hennet T (1999) A beta-1,3-N-acetylglucosaminyltransferase with poly-N-acetyllactosamine synthase activity is structurally related to beta-1,3-galactosyltransferases. *Proc Natl Acad Sci U S A* **96**: 406–411.
194. Lin A, Mu J, Yang J, Roach PJ (1999) Self-glucosylation of glycogenin, the initiator of glycogen biosynthesis, involves an inter-subunit reaction. *Arch Biochem Biophys* **363**: 163–170.
195. Gibbons BJ, Roach PJ, Hurley TD (2002) Crystal Structure of the Autocatalytic Initiator of Glycogen Biosynthesis, Glycogenin. *J Mol Biol* **319**: 463–477.
196. Nilsson J, Halim A, Larsson E, Moslemi A-R, Oldfors A, Larson G, Nilsson J (2014) LC–MS/MS characterization of combined glycogenin-1 and glycogenin-2 enzymatic activities reveals their self-glucosylation preferences. *Biochim Biophys Acta BBA - Proteins Proteomics* **1844**: 398–405.
197. Chen W, Unligil UM, Rini JM, Stanley P (2001) Independent Lec1A CHO glycosylation mutants arise from point mutations in N-acetylglucosaminyltransferase I that reduce affinity for both substrates. Molecular consequences based on the crystal structure of GlcNAc-TI. *Biochemistry (Mosc)* **40**: 8765–8772.
198. Boix E, Zhang Y, Swaminathan GJ, Brew K, Acharya KR (2002) Structural basis of ordered binding of donor and acceptor substrates to the retaining glycosyltransferase, alpha-1,3-galactosyltransferase. *J Biol Chem* **277**: 28310–28318.
199. Pedersen LC, Dong J, Taniguchi F, Kitagawa H, Krahn JM, Pedersen LG, Sugahara K, Negishi M (2003) Crystal structure of an alpha 1,4-N-acetylhexosaminyltransferase (EXTL2), a member of the exostosin gene family involved in heparan sulfate biosynthesis. *J Biol Chem* **278**: 14420–14428.
200. Kaufman RJ, Swaroop M, Murtha-Riel P (1994) Depletion of Manganese within the Secretory Pathway Inhibits O-Linked Glycosylation in Mammalian Cells. *Biochemistry (Mosc)* **33**: 9813–9819.
201. Crowell CK, Grampp GE, Rogers GN, Miller J, Scheinman RI (2007) Amino acid and manganese supplementation modulates the glycosylation state of erythropoietin in a CHO culture system. *Biotechnol Bioeng* **96**: 538–549.
202. Saito F, Sakamoto I, Kanatani A, Chiba Y (2016) Manganese ion concentration affects production of human core 3 O-glycan in Saccharomyces cerevisiae. *Biochim Biophys Acta*.

203. Gramer MJ, Eckblad JJ, Donahue R, Brown J, Shultz C, Vickerman K, Priem P, van den Bremer ETJ, Gerritsen J, van Berkel PHC (2011) Modulation of antibody galactosylation through feeding of uridine, manganese chloride, and galactose. *Biotechnol Bioeng* **108**: 1591–1602.
204. Hossler P, Khattak SF, Li ZJ (2009) Optimal and consistent protein glycosylation in mammalian cell culture. *Glycobiology* **19**: 936–949.
205. Manya H, Chiba A, Yoshida A, Wang X, Chiba Y, Jigami Y, Margolis RU, Endo T (2004) Demonstration of mammalian protein O-mannosyltransferase activity: coexpression of POMT1 and POMT2 required for enzymatic activity. *Proc Natl Acad Sci U S A* **101**: 500–505.
206. Rodríguez P, Durante P (1990) Characterization of a protein: Glucosyltransferase activity in human platelets. *Biochem Med Metab Biol* **43**: 147–158.
207. Shah SN, Raghupathy E (1977) Differential effects of EDTA, metal ions, and nucleotides on glycoprotein sialyltransferase activity of serum and liver. *Proc Soc Exp Biol Med Soc Exp Biol Med N Y N* **155**: 516–518.
208. Kitazume-Kawaguchi S, Kabata S, Arita M (2001) Differential Biosynthesis of Polysialic or Disialic Acid Structure by ST8Sia II and ST8Sia IV. *J Biol Chem* **276**: 15696–15703.
209. Tewari R, Bachert C, Linstedt AD (2015) Induced oligomerization targets Golgi proteins for degradation in lysosomes. *Mol Biol Cell* **26**: 4427–4437.
210. Ramakrishnan B, Boeggeman E, Ramasamy V, Qasba PK (2004) Structure and catalytic cycle of beta-1,4-galactosyltransferase. *Curr Opin Struct Biol* **14**: 593–600.
211. Qasba PK, Ramakrishnan B, Boeggeman E (2008) Structure and function of beta -1,4-galactosyltransferase. *Curr Drug Targets* **9**: 292–309.
212. Jaeken J, van Eijk HG, van der Heul C, Corbeel L, Eeckels R, Eggermont E (1984) Sialic acid-deficient serum and cerebrospinal fluid transferrin in a newly recognized genetic syndrome. *Clin Chim Acta Int J Clin Chem* **144**: 245–247.
213. Van Schaftingen E, Jaeken J (1995) Phosphomannomutase deficiency is a cause of carbohydrate-deficient glycoprotein syndrome type I. *FEBS Lett* **377**: 318–320.
214. Sharma V, Ichikawa M, Freeze HH (2014) Mannose metabolism: more than meets the eye. *Biochem Biophys Res Commun* **453**: 220–228.
215. Jaeken J, Péanne R (2017) What is new in CDG? *J Inherit Metab Dis*.
216. Grünewald S (2009) The clinical spectrum of phosphomannomutase 2 deficiency (CDG-Ia). *Biochim Biophys Acta* **1792**: 827–834.
217. Jaeken J, Lefeber D, Matthijs G (2014) Clinical utility gene card for: Phosphomannomutase 2 deficiency. *Eur J Hum Genet EJHG* **22**:.
218. Monticelli M, Ferro T, Jaeken J, Dos Reis Ferreira V, Videira PA (2016) Immunological aspects of congenital disorders of glycosylation (CDG): a review. *J Inherit Metab Dis*.
219. Marques-da-Silva D, Dos Reis Ferreira V, Monticelli M, Janeiro P, Videira PA, Witters P, Jaeken J, Cassiman D (2017) Liver involvement in congenital disorders of glycosylation (CDG). A systematic review of the literature. *J Inherit Metab Dis* **40**: 195–207.
220. Freeze HH, Eklund EA, Ng BG, Patterson MC (2012) Neurology of inherited glycosylation disorders. *Lancet Neurol* **11**: 453–466.
221. Vantyghem M-C, Dobbelaere D, Mention K, Wemeau J-L, Saudubray J-M, Douillard C (2012) Endocrine manifestations related to inherited metabolic diseases in adults. *Orphanet J Rare Dis* **7**: 11.
222. Rymen D, Jaeken J (2014) Skin manifestations in CDG. *J Inherit Metab Dis* **37**: 699–708.
223. Coman D, Irving M, Kannu P, Jaeken J, Savarirayan R (2008) The skeletal manifestations of the congenital disorders of glycosylation. *Clin Genet* **73**: 507–515.
224. Jaeken J, Matthijs G (2007) Congenital disorders of glycosylation: a rapidly expanding disease family. *Annu Rev Genomics Hum Genet* **8**: 261–278.
225. Wu X, Steet RA, Bohorov O, Bakker J, Newell J, Krieger M, Spaapen L, Kornfeld S, Freeze HH (2004) Mutation of the COG complex subunit gene COG7 causes a lethal congenital disorder. *Nat Med* **10**: 518–523.
226. Foulquier F, Vasile E, Schollen E, Callewaert N, Raemaekers T, Quelhas D, Jaeken J, Mills P, Winchester B, Krieger M, et al. (2006) Conserved oligomeric Golgi complex subunit 1 deficiency reveals a previously uncharacterized congenital disorder of glycosylation type II. *Proc Natl Acad Sci U S A* **103**: 3764–3769.
227. Kranz C, Ng BG, Sun L, Sharma V, Eklund EA, Miura Y, Ungar D, Lupashin V, Winkel RD, Cipollo JF, et al. (2007) COG8 deficiency causes new congenital disorder of glycosylation type IIh. *Hum Mol Genet* **16**: 731–741.
228. Paesold-Burda P, Maag C, Troxler H, Foulquier F, Kleinert P, Schnabel S, Baumgartner M, Hennet T (2009) Deficiency in COG5 causes a moderate form of congenital disorders of glycosylation. *Hum Mol Genet* **18**: 4350–4356.
229. Reynders E, Foulquier F, Leão Teles E, Quelhas D, Morelle W, Rabouille C, Annaert W, Matthijs G (2009) Golgi function and dysfunction in the first COG4-deficient CDG type II patient. *Hum Mol Genet* **18**: 3244–3256.

230. Fisher P, Ungar D (2016) Bridging the Gap between Glycosylation and Vesicle Traffic. *Membr Traffic* 15.
231. Climer LK, Dobretsov M, Lupashin V (2015) Defects in the COG complex and COG-related trafficking regulators affect neuronal Golgi function. *Front Neurosci* **9**: 405.
232. Rosnoblet C, Peanne R, Legrand D, Foulquier F (2013) Glycosylation disorders of membrane trafficking. *Glycoconj J* **30**: 23–31.
233. Reynders E, Foulquier F, Annaert W, Matthijs G (2011) How Golgi glycosylation meets and needs trafficking: the case of the COG complex. *Glycobiology* **21**: 853–863.
234. Potelle S, Klein A, Foulquier F (2015) Golgi post-translational modifications and associated diseases. *J Inherit Metab Dis*.
235. Miller VJ, Ungar D (2012) Re'COG'nition at the Golgi. *Traffic Cph Den* **13**: 891–897.
236. Lefeber DJ, Morava E, Jaeken J (2011) How to find and diagnose a CDG due to defective N-glycosylation. *J Inherit Metab Dis* **34**: 849–852.
237. Freeze HH (2007) Congenital Disorders of Glycosylation: CDG-I, CDG-II, and beyond. *Curr Mol Med* **7**: 389–396.
238. Babovic-Vuksanovic D, O'Brien JF (2007) Laboratory diagnosis of congenital disorders of glycosylation type I by analysis of transferrin glycoforms. *Mol Diagn Ther* **11**: 303–311.
239. Park JH, Zühlsdorf A, Wada Y, Roll C, Rust S, Du Chesne I, Grüneberg M, Reunert J, Marquardt T (2014) The novel transferrin E592A variant impairs the diagnostics of congenital disorders of glycosylation. *Clin Chim Acta Int J Clin Chem* **436**: 135–139.
240. Zühlsdorf A, Park JH, Wada Y, Rust S, Reunert J, DuChesne I, Grüneberg M, Marquardt T (2015) Transferrin variants: pitfalls in the diagnostics of Congenital disorders of glycosylation. *Clin Biochem* **48**: 11–13.
241. Hackler R, Arndt T, Helwig-Rolig A, Kropf J, Steinmetz A, Schaefer JR (2000) Investigation by isoelectric focusing of the initial carbohydrate-deficient transferrin (CDT) and non-CDT transferrin isoform fractionation step involved in determination of CDT by the ChronAlcoI.D. assay. *Clin Chem* **46**: 483–492.
242. Carchon HA, Ndosimao CN, Aerschot SV, Jaeken J (2006) Use of Serum on Guthrie Cards in Screening for Congenital Disorders of Glycosylation. *Clin Chem* **52**: 774–775.
243. Lefeber DJ (2016) Protein-Specific Glycoprofiling for Patient Diagnostics. *Clin Chem* **62**: 9–11.
244. van Scherpenzeel M, Steenbergen G, Morava E, Wevers RA, Lefeber DJ High-resolution mass spectrometry glycoprofiling of intact transferrin for diagnosis and subtype identification in the congenital disorders of glycosylation. *Transl Res*.
245. Jaeken J, Hennet T, Matthijs G, Freeze HH (2009) CDG nomenclature: time for a change! *Biochim Biophys Acta* **1792**: 825–826.
246. Harms HK, Zimmer KP, Kurnik K, Bertele-Harms RM, Weidinger S, Reiter K (2002) Oral mannose therapy persistently corrects the severe clinical symptoms and biochemical abnormalities of phosphomannose isomerase deficiency. *Acta Paediatr Oslo Nor 1992* **91**: 1065–1072.
247. de Lonlay P, Seta N (2009) The clinical spectrum of phosphomannose isomerase deficiency, with an evaluation of mannose treatment for CDG-Ib. *Biochim Biophys Acta* **1792**: 841–843.
248. Schroeder AS, Kappler M, Bonfert M, Borggraefe I, Schoen C, Reiter K (2010) Seizures and stupor during intravenous mannose therapy in a patient with CDG syndrome type 1b (MPI-CDG). *J Inherit Metab Dis* **33 Suppl 3**: S497-502.
249. Janssen MCH, de Kleine RH, van den Berg AP, Heijdra Y, van Scherpenzeel M, Lefeber DJ, Morava E (2014) Successful liver transplantation and long-term follow-up in a patient with MPI-CDG. *Pediatrics* **134**: e279-283.
250. Jansen JC, Cirak S, van Scherpenzeel M, Timal S, Reunert J, Rust S, Pérez B, Vicogne D, Krawitz P, Wada Y, et al. (2016) CCDC115 Deficiency Causes a Disorder of Golgi Homeostasis with Abnormal Protein Glycosylation. *Am J Hum Genet* **98**: 310–321.
251. Koch J, Mayr JA, Alhaddad B, Rauscher C, Bierau J, Kovacs-Nagy R, Coene KLM, Bader I, Holzhacker M, Prokisch H, et al. (2017) CAD mutations and uridine-responsive epileptic encephalopathy. *Brain J Neurol* **140**: 279–286.
252. Morava E (2014) Galactose supplementation in phosphoglucomutase-1 deficiency; review and outlook for a novel treatable CDG. *Mol Genet Metab* **112**: 275–279.
253. Dörre K, Olczak M, Wada Y, Sosicka P, Grüneberg M, Reunert J, Kurlemann G, Fiedler B, Biskup S, Hörtnagel K, et al. (2015) A new case of UDP-galactose transporter deficiency (SLC35A2-CDG): molecular basis, clinical phenotype, and therapeutic approach. *J Inherit Metab Dis*.
254. Kapusta L, Zucker N, Frenckel G, Medalion B, Ben Gal T, Birk E, Mandel H, Nasser N, Morgenstern S, Zuckermann A, et al. (2013) From discrete dilated cardiomyopathy to successful cardiac transplantation in congenital disorders of glycosylation due to dolichol kinase deficiency (DK1-CDG). *Heart Fail Rev* **18**: 187–196.

255. Dauber A, Ercan A, Lee J, James P, Jacobs PP, Ashline DJ, Wang SR, Miller T, Hirschhorn JN, Nigrovic PA, et al. (2014) Congenital disorder of fucosylation type 2c (LADII) presenting with short stature and developmental delay with minimal adhesion defect. *Hum Mol Genet* **23**: 2880–2887.
256. Almeida A, Layton M, Karadimitris A (2009) Inherited glycosylphosphatidyl inositol deficiency: a treatable CDG. *Biochim Biophys Acta* **1792**: 874–880.
257. Stray-Pedersen A, Backe PH, Sorte HS, Mørkrid L, Chokshi NY, Erichsen HC, Gambin T, Elgstøen KBP, Bjørås M, Wlodarski MW, et al. (2014) PGM3 mutations cause a congenital disorder of glycosylation with severe immunodeficiency and skeletal dysplasia. *Am J Hum Genet* **95**: 96–107.
258. Argov Z, Caraco Y, Lau H, Pestronk A, Shieh PB, Skrinar A, Koutsoukos T, Ahmed R, Martinisi J, Kakkis E (2016) Aceneuramic Acid Extended Release Administration Maintains Upper Limb Muscle Strength in a 48-week Study of Subjects with GNE Myopathy: Results from a Phase 2, Randomized, Controlled Study. *J Neuromuscul Dis* **3**: 49–66.
259. Yuste-Checa P, Brasil S, Gámez A, Underhaug J, Desviat LR, Ugarte M, Pérez-Cerdá C, Martinez A, Pérez B (2016) Pharmacological Chaperoning: A Potential Treatment For PMM2-CDG. *Hum Mutat*.
260. Foulquier F, Ungar D, Reynders E, Zeevaert R, Mills P, García-Silva MT, Briones P, Winchester B, Morelle W, Krieger M, et al. (2007) A new inborn error of glycosylation due to a Cog8 deficiency reveals a critical role for the Cog1-Cog8 interaction in COG complex formation. *Hum Mol Genet* **16**: 717–730.
261. Reynders E, Foulquier F, Leão Teles E, Quelhas D, Morelle W, Rabouille C, Annaert W, Matthijs G (2009) Golgi function and dysfunction in the first COG4-deficient CDG type II patient. *Hum Mol Genet* **18**: 3244–3256.
262. Lübbehusen J, Thiel C, Rind N, Ungar D, Prinsen BHCMT, de Koning TJ, van Hasselt PM, Körner C (2010) Fatal outcome due to deficiency of subunit 6 of the conserved oligomeric Golgi complex leading to a new type of congenital disorders of glycosylation. *Hum Mol Genet* **19**: 3623–3633.
263. Shestakova A, Zolov S, Lupashin V (2006) COG complex-mediated recycling of Golgi glycosyltransferases is essential for normal protein glycosylation. *Traffic Cph Den* **7**: 191–204.
264. Pokrovskaya ID, Willett R, Smith RD, Morelle W, Kudlyk T, Lupashin VV (2011) Conserved oligomeric Golgi complex specifically regulates the maintenance of Golgi glycosylation machinery. *Glycobiology* **21**: 1554–1569.
265. Cohen MM, Hall BD, Smith DW, Graham CB, Lampert KJ (1973) A new syndrome with hypotonia, obesity, mental deficiency, and facial, oral, ocular, and limb anomalies. *J Pediatr* **83**: 280–284.
266. Duplomb L, Duvet S, Picot D, Jego G, El Chehadeh-Djebbar S, Marle N, Gigot N, Aral B, Carmignac V, Thevenon J, et al. (2014) Cohen syndrome is associated with major glycosylation defects. *Hum Mol Genet* **23**: 2391–2399.
267. Zhao S, Li CM, Luo XM, Siu GKY, Gan WJ, Zhang L, Wu WKK, Chan HC, Yu S (2017) Mammalian TRAPPIII Complex positively modulates the recruitment of Sec13/31 onto COPII vesicles. *Sci Rep* **7**: 43207.
268. DeRossi C, Vacaru A, Rafiq R, Cinaroglu A, Imrie D, Nayar S, Baryshnikova A, Milev MP, Stanga D, Kadakia D, et al. (2016) trappc11 is required for protein glycosylation in zebrafish and humans. *Mol Biol Cell*.
269. Matalonga L, Bravo M, Peinado CS, García-Pelegrí E, Ugarteburu O, Vidal S, Llambrich M, Quintana E, Fuster-Jorge P, Gonzalez-Bravo MN, et al. (2016) Mutations in TRAPPC11 are Associated with a Congenital Disorder of Glycosylation. *Hum Mutat*.
270. Fujiwara T, Oda K, Yokota S, Takatsuki A, Ikehara Y (1988) Brefeldin A causes disassembly of the Golgi complex and accumulation of secretory proteins in the endoplasmic reticulum. *J Biol Chem* **263**: 18545–18552.
271. Doms RW, Russ G, Yewdell JW (1989) Brefeldin A redistributes resident and itinerant Golgi proteins to the endoplasmic reticulum. *J Cell Biol* **109**: 61–72.
272. Fischer B, Dimopoulou A, Egerer J, Gardeitchik T, Kidd A, Jost D, Kayserili H, Alanay Y, Tantcheva-Poor I, Mangold E, et al. (2012) Further characterization of ATP6V0A2-related autosomal recessive cutis laxa. *Hum Genet* **131**: 1761–1773.
273. Morava E, Wopereis S, Coucke P, Gillessen-Kaesbach G, Voit T, Smeitink J, Wevers R, Grünewald S (2005) Defective protein glycosylation in patients with cutis laxa syndrome. *Eur J Hum Genet EJHG* **13**: 414–421.
274. Van Damme T, Gardeitchik T, Mohamed M, Guerrero-Castillo S, Freisinger P, Guillemyn B, Kariminejad A, Dalloyaux D, van Kraaij S, Lefeber DJ, et al. (2017) Mutations in ATP6V1E1 or ATP6V1A Cause Autosomal-Recessive Cutis Laxa. *Am J Hum Genet* **100**: 216–227.
275. Jansen EJR, Martens GJM (2012) Novel insights into V-ATPase functioning: distinct roles for its accessory subunits ATP6AP1/Ac45 and ATP6AP2/(pro) renin receptor. *Curr Protein Pept Sci* **13**: 124–133.
276. Jansen EJR, Timal S, Ryan M, Ashikov A, van Scherpenzeel M, Graham LA, Mandel H, Hoischen A, Iancu TC, Raymond K, et al. (2016) ATP6AP1 deficiency causes an immunodeficiency with hepatopathy, cognitive impairment and abnormal protein glycosylation. *Nat Commun* **7**: 11600.

277. Jansen JC, Timal S, van Scherpenzeel M, Michelakakis H, Vicogne D, Ashikov A, Moraitou M, Hoischen A, Huijben K, Steenbergen G, et al. (2016) TMEM199 Deficiency Is a Disorder of Golgi Homeostasis Characterized by Elevated Aminotransferases, Alkaline Phosphatase, and Cholesterol and Abnormal Glycosylation. *Am J Hum Genet* **98**: 322–330.
278. Vanbeselaere J, Vicogne D, Matthijs G, Biot C, Foulquier F, Guerardel Y (2013) Alkynyl monosaccharide analogues as a tool for evaluating Golgi glycosylation efficiency: application to Congenital Disorders of Glycosylation (CDG). *Chem Commun Camb Engl* **49**: 11293–11295.
279. Péanne R, Vanbeselaere J, Vicogne D, Mir A-M, Biot C, Matthijs G, Guérardel Y, Foulquier F (2013) Assessing ER and Golgi N-glycosylation process using metabolic labeling in mammalian cultured cells. *Methods Cell Biol* **118**: 157–176.
280. Park JH, Hogrebe M, Fobker M, Brackmann R, Fiedler B, Reunert J, Rust S, Tsiakas K, Santer R, Grüneberg M, et al. (2017) SLC39A8 deficiency: biochemical correction and major clinical improvement by manganese therapy. *Genet Med Off J Am Coll Med Genet*.
281. Riley LG, Cowley MJ, Gayevskiy V, Roscioli T, Thorburn DR, Prelog K, Bahlo M, Sue CM, Balasubramaniam S, Christodoulou J (2016) A SLC39A8 variant causes manganese deficiency, and glycosylation and mitochondrial disorders. *J Inherit Metab Dis*.
282. Boycott KM, Beaulieu CL, Kernohan KD, Gebril OH, Mhanni A, Chudley AE, Redl D, Qin W, Hampson S, Küry S, et al. (2015) Autosomal-Recessive Intellectual Disability with Cerebellar Atrophy Syndrome Caused by Mutation of the Manganese and Zinc Transporter Gene SLC39A8. *Am J Hum Genet* **97**: 886–893.
283. Demaegd D, Colinet A-S, Deschamps A, Morsomme P (2014) Molecular evolution of a novel family of putative calcium transporters. *PloS One* **9**: e100851.
284. Krzewinski-Recchi M-A, Potelle S, Mir A-M, Vicogne D, Dulary E, Duvet S, Morelle W, de Bettignies G, Foulquier F (2017) Evidence for splice transcript variants of TMEM165, a gene involved in CDG. *Biochim Biophys Acta BBA - Gen Subj* **1861**: 737–748.
285. Rosnoblet C, Legrand D, Demaegd D, Hacine-Gherbi H, de Bettignies G, Bammens R, Borrego C, Duvet S, Morsomme P, Matthijs G, et al. (2013) Impact of disease-causing mutations on TMEM165 subcellular localization, a recently identified protein involved in CDG-II. *Hum Mol Genet* **22**: 2914–2928.
286. Braulke T, Bonifacino JS (2009) Sorting of lysosomal proteins. *Biochim Biophys Acta* **1793**: 605–614.
287. Hoecker N, Leister D, Schneider A (2017) Plants contain small families of UPF0016 proteins including the PHOTOSYNTHESIS AFFECTED MUTANT71 transporter. *Plant Signal Behav* 0.
288. Schneider A, Steinberger I, Herdean A, Gandini C, Eisenhut M, Kurz S, Morper A, Hoecker N, Rühle T, Labs M, et al. (2016) The Evolutionarily Conserved Protein PHOTOSYNTHESIS AFFECTED MUTANT71 is Required for Efficient Manganese Uptake at the Thylakoid Membrane in Arabidopsis. *Plant Cell*.
289. Gandini C, Schmidt SB, Husted S, Schneider A, Leister D (2017) The transporter SynPAM71 is located in the plasma membrane and thylakoids, and mediates manganese tolerance in Synechocystis PCC6803. *New Phytol* **215**: 256–268.
290. Brandenburg F, Schoffman H, Kurz S, Krämer U, Keren N, Weber APM, Eisenhut M (2017) The Synechocystis Manganese Exporter Mnx Is Essential for Manganese Homeostasis in Cyanobacteria. *Plant Physiol* **173**: 1798–1810.
291. Demaegd D, Foulquier F, Colinet A-S, Gremillon L, Legrand D, Mariot P, Peiter E, Van Schaftingen E, Matthijs G, Morsomme P (2013) Newly characterized Golgi-localized family of proteins is involved in calcium and pH homeostasis in yeast and human cells. *Proc Natl Acad Sci U S A* **110**: 6859–6864.
292. Colinet A-S, Thines L, Deschamps A, Flémal G, Demaegd D, Morsomme P (2017) Acidic and uncharged polar residues in the consensus motifs of the yeast Ca(2+) transporter Gdt1p are required for calcium transport. *Cell Microbiol*.
293. Colinet A-S, Sengottaiyan P, Deschamps A, Colsoul M-L, Thines L, Demaegd D, Duchêne M-C, Foulquier F, Hols P, Morsomme P (2016) Yeast Gdt1 is a Golgi-localized calcium transporter required for stress-induced calcium signaling and protein glycosylation. *Sci Rep* **6**: 24282.
294. Zeevaert R, de Zegher F, Sturiale L, Garozzo D, Smet M, Moens M, Matthijs G, Jaeken J (2013) Bone Dysplasia as a Key Feature in Three Patients with a Novel Congenital Disorder of Glycosylation (CDG) Type II Due to a Deep Intronic Splice Mutation in TMEM165. *JIMD Rep* **8**: 145–152.
295. Althoff SS, Grüneberg M, Reunert J, Park JH, Rust S, Mühlhausen C, Wada Y, Santer R, Marquardt T (2015) TMEM165 Deficiency: Postnatal Changes in Glycosylation. *JIMD Rep*.
296. Xia B, Zhang W, Li X, Jiang R, Harper T, Liu R, Cummings RD, He M (2013) Serum N-glycan and O-glycan analysis by mass spectrometry for diagnosis of congenital disorders of glycosylation. *Anal Biochem* **442**: 178–185.

297. Bammens R, Mehta N, Race V, Foulquier F, Jaeken J, Tiemeyer M, Steet R, Matthijs G, Flanagan-Steet H (2015) Abnormal Cartilage Development and Altered N-Glycosylation in Tmem165-Deficient Zebrafish Mirrors the Phenotypes Associated with TMEM165-CDG. *Glycobiology*.
298. Reinhardt TA, Lippolis JD, Sacco RE (2014) The Ca(2+)/H(+) antiporter TMEM165 expression, localization in the developing, lactating and involuting mammary gland parallels the secretory pathway Ca(2+) ATPase (SPCA1). *Biochem Biophys Res Commun* **445**: 417–421.
299. Mukhopadhyay S, Bachert C, Smith DR, Linstedt AD (2010) Manganese-induced trafficking and turnover of the cis-Golgi glycoprotein GPP130. *Mol Biol Cell* **21**: 1282–1292.
300. Leyva-Illades D, Chen P, Zogzas CE, Hutchens S, Mercado JM, Swaim CD, Morrisett RA, Bowman AB, Aschner M, Mukhopadhyay S (2014) SLC30A10 is a cell surface-localized manganese efflux transporter, and parkinsonism-causing mutations block its intracellular trafficking and efflux activity. *J Neurosci Off J Soc Neurosci* **34**: 14079–14095.
301. Lu L, Hong W (2014) From endosomes to the trans-Golgi network. *Semin Cell Dev Biol*.
302. Burd CG (2011) Physiology and pathology of endosome-to-Golgi retrograde sorting. *Traffic Cph Den* **12**: 948–955.
303. Potelle S, Morelle W, Dulary E, Duvet S, Vicogne D, Spriet C, Krzewinski-Recchi M-A, Morsomme P, Jaeken J, Matthijs G, et al. (2016) Glycosylation abnormalities in Gdt1p/TMEM165 deficient cells result from a defect in Golgi manganese homeostasis. *Hum Mol Genet* **25**: 1489–1500.
304. Reyes F, Marchant L, Norambuena L, Nilo R, Silva H, Orellana A (2006) AtUTr1, a UDP-glucose/UDP-galactose transporter from Arabidopsis thaliana, is located in the endoplasmic reticulum and up-regulated by the unfolded protein response. *J Biol Chem* **281**: 9145–9151.
305. Sprong H, Degroote S, Nilsson T, Kawakita M, Ishida N, van der Sluijs P, van Meer G (2003) Association of the Golgi UDP-Galactose Transporter with UDP-Galactose:Ceramide Galactosyltransferase Allows UDP-Galactose Import in the Endoplasmic Reticulum. *Mol Biol Cell* **14**: 3482–3493.
306. Nolting K, Park JH, Tegtmeyer LC, Zühlsdorf A, Grüneberg M, Rust S, Reunert J, Du Chesne I, Debus V, Schulze-Bahr E, et al. (2017) Limitations of galactose therapy in phosphoglucomutase 1 deficiency. *Mol Genet Metab Rep* **13**: 33–40.
307. Culotta VC, Yang M, Hall MD (2005) Manganese transport and trafficking: lessons learned from Saccharomyces cerevisiae. *Eukaryot Cell* **4**: 1159–1165.
308. Reddi AR, Jensen LT, Culotta VC (2009) Manganese Homeostasis in Saccharomyces cerevisiae. *Chem Rev* **109**: 4722–4732.
309. Dambach M, Sandoval M, Updegrove TB, Anantharaman V, Aravind L, Waters LS, Storz G (2015) The ubiquitous yybP-ykoY riboswitch is a manganese-responsive regulatory element. *Mol Cell* **57**: 1099–1109.
310. Bucci C, Thomsen P, Nicoziani P, McCarthy J, van Deurs B (2000) Rab7: A Key to Lysosome Biogenesis. *Mol Biol Cell* **11**: 467–480.
311. Progida C, Cogli L, Piro F, Luca AD, Bakke O, Bucci C (2010) Rab7b controls trafficking from endosomes to the TGN. *J Cell Sci* **123**: 1480–1491.
312. Stenmark H, Parton RG, Steele-Mortimer O, Lütcke A, Gruenberg J, Zerial M (1994) Inhibition of rab5 GTPase activity stimulates membrane fusion in endocytosis. *EMBO J* **13**: 1287–1296.
313. Gu F, Crump CM, Thomas G (2001) Trans-Golgi network sorting. *Cell Mol Life Sci CMLS* **58**: 1067–1084.
314. Venkat S, Linstedt AD (2017) Manganese-induced trafficking and turnover of GPP130 is mediated by sortilin. *Mol Biol Cell*.
315. Canuel M, Libin Y, Morales CR (2009) The interactomics of sortilin: an ancient lysosomal receptor evolving new functions. *Histol Histopathol* **24**: 481–492.
316. Mukhopadhyay S, Linstedt AD (2011) Identification of a gain-of-function mutation in a Golgi P-type ATPase that enhances Mn2+ efflux and protects against toxicity. *Proc Natl Acad Sci U S A* **108**: 858–863.
317. Dürr G, Strayle J, Plemper R, Elbs S, Klee SK, Catty P, Wolf DH, Rudolph HK (1998) The medial-Golgi ion pump Pmr1 supplies the yeast secretory pathway with Ca2+ and Mn2+ required for glycosylation, sorting, and endoplasmic reticulum-associated protein degradation. *Mol Biol Cell* **9**: 1149–1162.
318. Fasolato C, Hoth M, Penner R (1993) Multiple mechanisms of manganese-induced quenching of fura-2 fluorescence in rat mast cells. *Pflugers Arch* **423**: 225–231.
319. Wong AKC, Capitanio P, Lissandron V, Bortolozzi M, Pozzan T, Pizzo P (2013) Heterogeneity of Ca2+ handling among and within Golgi compartments. *J Mol Cell Biol* **5**: 266–276.
320. Kwakye GF, Li D, Kabobel OA, Bowman AB (2011) Cellular fura-2 manganese extraction assay (CFMEA). *Curr Protoc Toxicol* **Chapter 12**: Unit12.18.

APPENDIX I

Investigating the function of Gdt1p in yeast Golgi glycosylation

Eudoxie Dulary*[1,2], Shin-Yi Yu*[1], Geoffroy de Bettignies[1,2], Valérie Decool[3], **Sven Potelle**[1,2], Sandrine Duvet[1,2], Marie-Ange Krzewinski-Recchi[1,2], Anne Garat[3], Gert Matthijs[2,4], Yann Guerardel[1] and François Foulquier[1,2]

1 Univ. Lille, CNRS, UMR 8576 – UGSF - Unité de Glycobiologie Structurale et Fonctionnelle, F-59000 Lille, France ; LIA GLYCOLAB4CDG France/ Belgium (International Associated Laboratory

2 LIA GLYCOLAB4CDG France/Belgium (International Associated Laboratory) " Laboratory for the Research on Congenital Disorders of Glycosylation – from cellular mechanisms to cure".

3 Univ. Lille, CHU Lille, Institut Pasteur de Lille, EA 4483 – IMPECS – IMPact de l'Environnement Chimique sur la Santé humaine, F-59000 Lille, France

4 Center for Human Genetics, KU Leuven, Leuven, Belgium

Address correspondence should be sent to: François Foulquier (francois.foulquier@univ-lille1.fr)

* These authors have equally contributed

Address: Univ. Lille, CNRS, UMR 8576 – UGSF - Unité de Glycobiologie Structurale et Fonctionnelle, F-59000 Lille, France

Tel. + 33 3 20 43 44 30

Fax. +33 3 20 43 65 55

E-mail. Francois.foulquier@univ-lille1.fr

Abstract

The Golgi ion homeostasis is tightly regulated to ensure essential cellular processes such as glycosylation, yet our understanding of this regulation remains incomplete. Gdt1p is a member of the conserved Uncharacterized Protein Family (UPF0016). Our previous work suggested that Gdt1p may function in the Golgi by regulating Golgi Ca^{2+}/ Mn^{2+} homeostasis. NMR structural analysis of the polymannan chains showed that the *gdt1Δ* mutant cultured in presence of high Ca^{2+} concentration, as well as the *prm1Δ* and *gdt1Δ/pmr1Δ* strains presented strong late Golgi glycosylation defects with a lack of α-1,2 mannoses substitution- and α-1,3 mannoses termination. The addition of Mn^{2+} confirmed the suppression of these defects. Interestingly, our structural data confirmed that the glycosylation defect in *prm1Δ* could also completely be suppressed by the addition of Ca^{2+}. The use of Pmr1p mutants either defective for Ca^{2+} or Mn^{2+} transport or both revealed that the suppression of the observed glycosylation defect in *pmr1Δ* strains by the intraluminal Golgi Ca^{2+} requires the activity of Gdt1p. These data support the hypothesis that Gdt1p, in order to sustain the Golgi glycosylation process, import Mn^{2+} inside the Golgi lumen when Prm1p exclusively transports Ca^{2+}. Our results also reinforce the functional link between Gdt1p and Pmr1p as we highlighted that Gdt1p was a Mn^{2+} sensitive protein whose abundance was directly dependent on the nature of the ion transported by Pmr1p. Finally, this study demonstrated that the acidic residues of the two conserved motifs E-x-G-D-[KR], likely constituting the cation binding sites of Gdt1p, play a crucial role in Golgi glycosylation and hence in Mn^{2+} transport.

Keywords: Gdt1p, Prm1p, Golgi glycosylation, Mn^{2+} homeostasis

1. Introduction

In 2012, we highlighted TMEM165 as the first member of the Uncharacterized Protein Family 0016 (UPF0016) related to human diseases. Defects in TMEM165 lead to a rare inherited disorders named CDG for Congenital Disorders of Glycosylation in which Golgi glycosylation process is affected. Found in bacteria, archaea, yeast, plants and animals, members of the UPF0016 family share two highly conserved regions as signatures motifs: E-x-G-D-[KR] (Foulquier et al. 2012). Many evidences show that these two motifs form the pore of the protein and then the functionality of the UPF0016 members. Currently, the precise cellular functions of these proteins remain to be fully characterized and are under debate. In yeasts, it was previously reported that Gdt1p was involved in Ca2+ transport then playing an important role in Ca2+ signaling and Golgi protein glycosylation thereby supporting the hypothesis that Gdt1p would act as Ca2+/H+ antiporter in the Golgi apparatus (Demaegd et al. 2013; Colinet et al. 2016). The role of TMEM165 as a Golgi Ca2+/H+ antiporter can however be questioned. We recently highlighted that the observed glycosylation defect due to TMEM165 deficiencies resulted from a defect in Golgi Mn2+ homeostasis (Potelle et al. 2016). Moreover, we demonstrated that TMEM165 was a novel Golgi protein sensitive to Mn2+ as exposition to high Mn2+ concentrations lead to lysosomal degradation of TMEM165 (Potelle et al. 2017). These data reinforced the hypothesis of TMEM165 as being involved in Mn2+ transport. This is also currently emphasized by several other studies. In Arabidopsis thaliana, the homologous protein photosynthesis affected mutant 71 PHOTOSYNTHESIS AFFECTED MUTANT 71 (PAM71) has been shown to be required for efficient Mn2+ uptake at the thylakoid membrane (Schneider et al. 2016). Moreover, the Mnx protein of the cyanobacterial model strain *Synechocystis sp.* PCC 6803, also belonging to the UPF0016 family, was recently demonstrated as a Mn exporter (Brandenburg et al. 2017). Altogether these data cast doubt about the substrate specificity of the UPF0016 members. From a general point of view, the mechanisms by which yeast cells regulate Golgi Ca2+ and Mn2+ homeostasis, both critical for many cellular processes and in particular Golgi glycosylation, are not completely deciphered yet.

In this paper we have investigated more into details the contribution of Gdt1p, Pmr1p and both in Golgi glycosylation processes. We have demonstrated that inactivation of Pmr1 led to strong Golgi glycosylation defects fully reversed by the addition of both Ca2+ and Mn2+.

Interestingly, in the *gdt1Δ/pmr1Δ* double knock-out strain, only the addition of Mn2+ was able to suppress the observed Golgi glycosylation defect thus pointing the critical role of Gdt1p in suppressing the Golgi glycosylation defect in *pmr1Δ* strains supplemented with Ca2+. We have also shown that the abundance and function of Gdt1p in Golgi glycosylation was dependent on the function of Pmr1p. By using mutants of Pmr1p specifically defective for transport of either Ca2+ ions (Pmr1pD53A), Mn2+ ions (Pmr1pQ783A) or both (Pmr1pD778A), our results evidenced that in the case where Pmr1p only transport Ca2+ from the cytosol to the Golgi lumen, Gdt1p was necessary to import Mn2+ inside the Golgi lumen to suppress the observed Golgi glycosylation defect. Finally, this paper demonstrated that the acidic residues of the two conserved motifs E-x-G-D-[KR] of Gdt1p are involved in Golgi glycosylation.

2. Material and methods

Yeast strains and media

Yeast strains used for the experiments are listed below:

Wild-type (WT) Mata his3Δ1 leu2Δ0 ura3Δ0

pmr1Δ Mata his3Δ1 leu2Δ0 ura3Δ0 *pmr1Δ*::KanMX4

gdt1Δ Mata his3Δ1 leu2Δ0 ura3Δ0 *gdt1Δ*::KanMX4

gdt1Δ/pmr1Δ Mata his3Δ1 leu2Δ0 ura3Δ0 *gdt1Δ*::KanMX4 *pmr1Δ*::KanMX4

Yeast were cultured at 30°C. Cultures in liquid media are done under a light shaking. Rich media, named YEP media, contains yeast extract (10 g.L-1, Difco), Bacto-peptone (20 g.L-1, Difco). YPD media is a YEP media supplemented with 2% D-glucose (Sigma-Aldrich). YPR is YEP supplemented with 2% raffinose (Euromedex). Selection antibiotics were added at 100 µg.mL-1 for nourseothricine, 200 µg.mL-1 for G418 and 300 µg.mL-1 for hygromycin.

Constructs, vector engineering and mutagenesis

Plasmids, pRS41H derivatives (wt, E53G, D56G, E204G, L205W and D207G mutated version of *GDT1*) and pRS41N derivatives (wt, D53A, D778A and Q783A mutated version of *PMR1*) have been generated by E-zyvec (Lille, France).

Extraction and isolation of mannan from yeast

The equivalent of 50 g yeast was suspended in 300 mL of 0.02 M citrate buffer (pH 7), autoclaved at 125°C, 90 min. The solid pellet was then removed by centrifugation and the supernatant collected. An equivalent volume of Fehling solution was added to the supernatant and stirred at room temperature until precipitates form. The precipitates are collected and dissolved with 100 mL of 3N HCl. 300 mL of ethanol are then added to precipitated mannan. The mannan are then dissolved in 50mL water and dialyzed (MWCO 3500) against water overnight at 4°C. The dialyzed mannans are then dried and lyophilized.

Invertase glycosylation analysis

Before any analysis, a preculture in YPD media is done and a volume equivalent to 15 OD600nm units is centrifuged for 3 minutes at 3500 rpm. The supernatant is discarded and the pellet is

suspended in YPR media to induce invertase expression. Calcium, manganese and other ions were added at this step at the indicated concentration. After a 20h culture in YPR, yeasts were centrifuged for 5 minutes at 3500 rpm. Supernatant was discarded and the pellet was kept frozen at -20°C. The cells were then resuspensed and lysed by glass-bead agitation in cold TBP buffer (5.52 g of diethylbarbituric acid and 1 g of Tris base per liter of water, pH 7.0; to 100 ml, add 1 ml of stock PMSF (0.174 g of phenylmethanesulfonyl fluoride in 10 ml of absolute ethanol) just before use]. 3µL of the supernatant are loaded on native gel. For the revelation of the invertase activity, the gel is then soaked into a 4°C sucrose solution (0.1 M pure sucrose in 0.1 M sodium acetate, pH 5.1) for 10 min and then immediately transferred into a 37°C sucrose solution for 10 min to hydrolyze the substrate. The gel is then quickly rinsed twice with water and transferred to a Pyrex dish containing 50 ml of TTC (50 mg of 2,3,5- triphenyltetrazolium chloride (TTC) in 50 ml of 0.5 M NaOH). The dish is boiled until the color appears. To stop the coloration and neutralize the NaOH, the gel is washed with water and stored in 10% acetic acid until imaging.

Western Blotting

Yeasts were centrifuged for 5 minutes at 3500 rpm. Supernatant was discarded and cells were then resuspended in TBP buffer supplemented with a protease cocktail inhibitor (Roche Diagnostics, Penzberg, Germany). Cell lysis was induced by vortexing the cells with beads 1h at 4°C. Cells were centrifuged for 5 min at 3500g. The protein concentration of supernatant was estimated with the micro BCA Protein Assay Kit (Thermo Scientific). 20 µg of total protein lysates were dissolved in NuPAGE LDS sample buffer (Invitrogen) pH 8.4 supplemented with 4% β-mercaptoethanol (Fluka). Samples were heated 10 min at 95°C and then separated on 4%-12% Bis- Tris gels (Invitrogen) and transferred to nitrocellulose membrane Hybond ECL (GE Healthcare, Little Chalfont, UK). The membranes were incubated in blocking buffer (5% milk powder in TBS-T [1X TBS with 0.05% Tween20]) for 1 h at room temperature, then incubated overnight with the anti-HA (Santa Cruz; used at a dilution of 1:200) in blocking buffer, and washed three times for 5 min in 156 TBS-T. The membranes were then incubated with the peroxidase-conjugated secondary goat anti-rabbit (Dako; used at a dilution of 1:10,000) in blocking buffer for 1 h at room temperature and later washed three times for 5 min in TBS-T. Signal was detected with chemiluminescence reagent (ECL 2 Western Blotting Susbtrate, Thermo Scientific) on imaging film (GE Healthcare, Little Chalfont, UK).

Whole cell Mn measurement by ICP-MS

Yeasts were grown in YPD medium and a volume equivalent to 15 OD600nm units was centrifuged for 3 minutes at 3500 rpm. The supernatant was discarded and the pellet was suspended in YPD media containing or not 50 µM MnCl2. After 20h, a volume equivalent to 25 OD600nm units is centrifuged for 3 minutes at 3500 rpm. Yeasts are washed twice with EDTA 1 µM and 3 times with water. Yeasts were suspended in 500 µL of HNO3 30% and heat at 65°C in a light shaking during 20h. 500 µL of water were added to the mixture. 300 µL were analyzed by ICP-MS (Inductively Coupled Plasma - Mass Spectrometer). Mn analyses were done in the Toxicology Laboratory of the Lille University Hospital. Samples were diluted 50 times with 1.5% (v/v) nitric acid (ultrapure quality 69.5%, Carlo Erba Reagents, Val de Reuil, France) solution in ultrapure water (Purelab Option-Q, Veolia Water, Antony, France) containing 0.1% triton®X-100 (Euromedex, Souffelweyersheim, france), 0.2% butan-1-ol (VWR Chemicals, Fontenay-sous-Bois, France), and 0.5µg/L rhodium (Merk, Darmstadt, Germany). Assays were performed on an ICP-MS THERMO ICAPTM Q (Thermo Scientific, Courtaboeuf Cedex, France). The limit of

quantification was 0.2µg/L).

NMR analyses

All NMR experiments were acquired on Avance II Bruker spectrometer equipped with BBO 5mm probe resonating at 400 MHz for ^{1}H, 100.6 MHz for ^{13}C. Mannans were dissolved in 500 µL $^{2}H2O$ (99.96% ^{2}H, Eurisotop), and then transferred into 5 mm Shigemi tubes (Allision Park, USA). NMR experiments were performed at 293K for Mannan. The ^{1}H chemical shifts were expressed in ppm related to the methyl signal of acetone (δ ^{1}H 2.225 and δ ^{13}C 31.55 ppm) as internal standards. The COSY90, $^{1}H/^{13}C$-HSQC experiments were performed by using Bruker standard sequences and optimized for each experiment.

Monosaccharide analyses

10 µg of inositol (taken as internal standard) and 10 µg of target mannan were mixed. The monosaccharide composition was established by GC and GC/MS as alditol-acetate derivatives. Briefly, samples were hydrolyzed in 4 M trifluoroacetic acid (TFA) for 4 h at 100°C and then reduced with sodium borohydride in 0.05 M NaOH for 4 h. Reduction was stopped by dropwise addition of acetic acid until pH 6 was reached and borate salts were co-distilled by repetitive evaporation in dry methanol. Peracetylation was performed in acetic anhydride at 100°C for 2 h. The derivatized monosaccharides were dissolved in 1 mL of chloroform, and 1 µL of sample was injected into GC-MS (TRACE GC Ultra, Thermo Fisher Scientific). The capillary column is SOLGEL-1MS (Part No. 054795, 30m x 0.25 mm x 0.25 µm). The initial oven temperature was held at 120°C, increased to 230°C at 3°C/min, and then, 270°C for 10 min. The derivatized monosaccharides were well separated into individual peaks, and identified by MS. However, the signal of GlcNAc was very low due to the very low percentage of GlcNAc in mannan. Therefore, selected ion monitor (SIM) was applied to increase sensitivity and quantify the amount of Man and GlcNAc. We took the same amount of authentic standards which are inositol, Man, GlcNAc to estimate the response factor of each monosaccharide in this method. Ions at *m/z* 168, 187, and 144 were used as indicative fragment ions for inositol, Man, and GlcNAc, respectively. The size of isolation window was set 0.2 Da, and the scan time of selected ion was 0.2 sec. The response factor of inositol was set to 1. In this system, response factors of Man and GlcNAc were established to 0.48 and 0.28, respectively. The amount (µg) of mannose in different Mannan samples was calculated by the formula [(Peak area of selected ion at *m/z* 187 for Man/0.48)/Peak area of selected ion at *m/z* 168 for inositol *10]. Similar calculation was applied to GlcNAc, which is [(Peak area of selected ion at *m/z* 144 for GlcNAc/0.28)/Peak area of selected ion at *m/z* 168 for inositol *10]. We assumed most of mannan is located on *N*-glycans. Therefore, the number of Man per *N*-glycan was established as [molar of Man/(molar of GlcNAc*2)].

3. Results

3.1. The suppression of the glycosylation defect in *pmr1Δ* strains supplemented with Ca2+ is dependent on the activity of Gdt1p

We have previously reported that the increased mobility of secreted invertase activity by zymography (in native polyacrylamide gel) was a good reporter of Golgi *N*-glycosylation

deficiency in yeast (Potelle et al. 2016). Using this technique, we have demonstrated that the Golgi *N*-glycosylation defect in *gdt1Δ* strains observed on invertase cultured in presence of high Ca2+ concentration could efficiently be suppressed by the addition of Mn2+. This was also observed for *pmr1Δ* and *gdt1Δ/pmr1Δ* double knock-out strains (Potelle et al. 2016). Although we demonstrated that high environmental Ca2+ concentration in *gdt1Δ* led to strong glycosylation defects, we established here that the addition of Ca2+ rescues the glycosylation defect in *pmr1Δ*. Indeed, 10mM Ca2+ treatment is sufficient to greatly reduce the invertase mobility to a normal value (Fig. 1A). Since Gdt1p and Prm1p are two Golgi proteins involved in the regulation of the Golgi Ca2+/Mn2+ homeostasis, glycosylation defect in *gdt1Δ*/*pmr1Δ* double knock-out strains was analyzed in the absence and the presence of increasing Ca2+ concentrations (from 10mM Ca2+ to 300mM) (Fig. 1A). Although the invertase mobility is strongly affected in the *gdt1Δ*/*pmr1Δ* double knock-out strains, the Ca2+ treatment does not restore it to a normal value (Fig. 1A). By contrast and as previously observed, the addition of 50 µM Mn2+ is sufficient to fully restore the Golgi *N*-glycosylation in the different yeast strains (Supplementary Fig. 1).

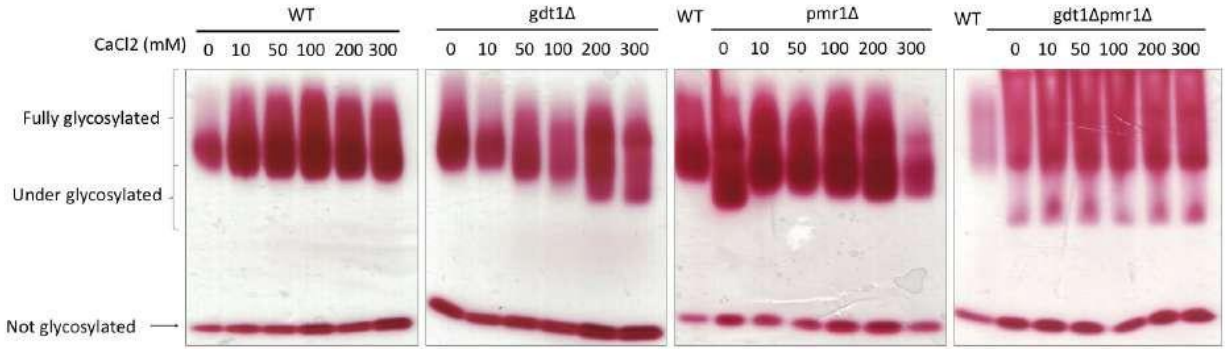

Figure 1: The suppression of the glycosylation defect in *pmr1Δ* strains supplemented with Ca2+ is dependent of the activity of Gdt1p. Wild-type (WT), *gdt1Δ*, *pmr1Δ* and *gdt1Δpmr1Δ* yeasts mutants were grown to an OD600 of 0.8 in a YPD medium. Afterwards, yeasts were transferred in YPR medium with an increase of the indicated CaCl2 concentrations to induce Invertase secretion. N-glycosylated invertase secreted was analyzed in a native gel as indicated by Ballou et al.

These results points to the crucial requirement of Gdt1p activity in the restoration of the glycosylation in *pmr1Δ* strains supplemented with Ca2+. Altogether these results strongly suggest a functional link between Gdt1p and Pmr1p in maintaining Golgi glycosylation homeostasis.

3.2. General structural analysis of the mannans from wild type and different mutants under different supplement of Ca2+/Mn2+

In order to further delineate the nature of the observed overall Golgi N-glycosylation defects, total mannans were isolated from yeast strains cultured under different Ca2+/Mn2+ conditions, followed by detailed structural analyses. So called mannans from most yeasts share similar overall architectures. They are made of $Man_8GlcNAc_2$ N-linked glycans extended by a α-linked polymannoside containing around 200 mannose residues. In *S. cerevisiae*, the polymannoside is composed of a long stretch of (α-1,6)-linked D-mannopyranose units substituted in C2 positions by short side chains of (α-1,2)-linked mannose units that may be further capped by terminal Man(α-1,3) residues (Munro et al. 2001). So called acid-labile mannan domain is further attached to the (α-1,2)- oligomannosides through phospho-di-ester bonds (Nelson et al. 1991). In a first step, we established the structural features of the mannan isolated from WT strain by 1D ^{1}H-NMR experiment (Fig. 2A). Due to its polymeric nature, it is not possible to assign the signals corresponding to all individual monosaccharide residues of mannans. However, five broad signals annotated as I, II, III, IV, V could be detected in the 5.5-4.8 ppm anomeric region, which natures were established by observing their spin systems by ^{1}H-^{1}H COSY, TOCSY and ^{1}H-^{13}C HSQC experiments, based on literature (Vinogradov et al. 1998) (Fig. 2A). They were assigned to five major epitopes (**I**), internal - 2)Man(α-1,2) residues; (**II**), terminal Man(α-1,3) residues; (**III**), -2,6)Man(α-1,6) branched residues; (**IV**), terminal Man(α-1,2) and -3)Man(α-1,2) residues; (**V**), unbranched -6)Man(α-1,6) residues. Furthermore, terminal Man(α-1,2) (**IV.a**, H2 at 4.06 ppm) and -3)Man(α-1,2) residues (**IV.b**, H2 at 4.22 ppm) could be differentiated by COSY90 spectrum as shown in Fig. 2B. Relative quantification of NMR signals I to V provides reliable snapshot of the overall mannan structural features. As shown in Fig. 2C, mannan isolated from WT strain is characterized by a high proportion of (α1-2) substitution on the (α 1-6)-mannoside stretch [2,6)Man / 6)Man = 6,4], leaving few un-substituted -6)Man(α-1,6) residues.

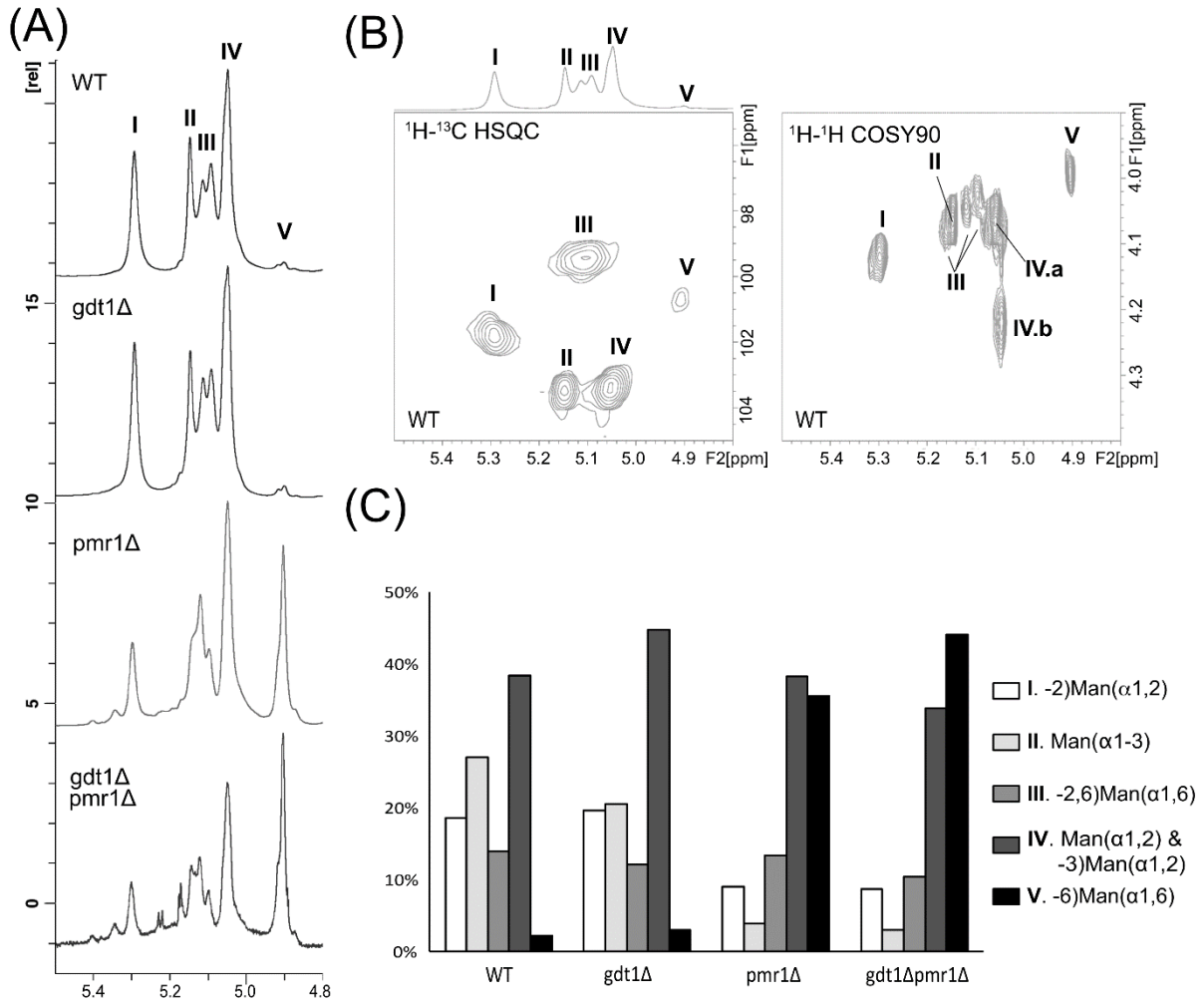

Figure 2: Structural analysis of the mannans from *S. cerevisiae* strains depleted or not in Gdt1 and Pmr1. (A) Comparison of the anomeric regions of ^{1}H-NMR spectra from WT, gdt1Δ, pmr1Δ and gdt1Δ/pmr1Δ strains; (B) details of the ^{1}H-^{13}C HSQC and ^{1}H-^{1}H COSY spectra from WT mannan showing the anomeric positions of mannose residues I-V; (C) relative quantifications of mannose residues based on NMR signals intensities.

In a second step, we compared the structures of mannans isolated from all four strains grown in normal conditions by homo- and heteronuclear NMR. 1D ^{1}H-NMR spectra, of mannans isolated from wild type and gdt1Δ established that these two strains exhibit very similar mannosylation patterns (Fig. 2A). In contrast, distinctive features were observed in the structures of mannans isolated from pmr1Δ and gdt1Δpmr1Δ strains compared to WT, as shown by 1D ^{1}H-NMR spectra (Fig. 2A) and relative quantification of ^{1}H-^{13}C HSQC NMR signals (Fig. 2C). The two most salient features of mannans from pmr1Δ and gdt1Δpmr1Δ strains were (i) a sharp decrease in the proportion of internal (α-1,2) oligomannoside side chains and of (α-1,3) capping mannose residues, which correlated with (ii) a large increase in the proportion of unbranched (α-1,6) polymannoside backbone. Indeed, the proportion of unbranched 6)Man(α-1,6) residues in pmr1Δ and gdt1Δpmr1Δ strains increased by 17 and 28 times compared to WT

mannan. Additionally, COSY90 spectra showed an increased proportion of terminal Man(α-1,2) residues on mannans from pmr1Δ and gdt1Δpmr1Δ strains, which is correlated with a decreased proportion of terminal Man(α-1,3) (data not shown). Altogether, these experiments show that a lack of pmr1 and both gdt1pmr1 leads to a drastic reduction of the branching pattern of (α-1,6) polymannoside domain of the mannan.

In a third step, we screened by 1D ^{1}H-NMR experiments the structural variability of mannans isolated from all four strains following supplementation with 0.5M Ca2+, 0.05mM Mn2+ and 0.5M Ca2+/ 0.05mM Mn2+ with a special focus on their branching patterns. The branching defects were expressed as a % of unbranched -6)Man(α-1,6) residues compared with total residues by quantifying signal V on 1D ^{1}H-NMR spectra (Supp Fig. 1 and Fig 2A). In accordance with the above results, WT and gdt1Δ grown in normal condition contained less than 2% of -6)Man(α-1,6) residues, whereas mannans from pmr1Δ and gdt1Δpmr1Δ contained 21 and 27% of - 6)Man(α-1,6) residues, respectively. This observed branching defect was fully restored in pmr1Δ by the addition of any divalent cation, Ca2+ or Mn2+. Contrarily, the glycosylation defect of gdt1Δpmr1Δ strain which is almost entirely restored in presence of Mn2+ and both Ca2+ and Mn2+ (4% and 7%), is not restored in the sole presence of Ca2+. Then, *gdt1Δ* cultured in presence of 0.5M Ca2+ showed an increased proportion of unbranched -6)Man(α- 1,6) backbone, as well as a decreased number of (α-1,3) mannose capping (data not shown). However, these defects were also completely restored by the addition of Mn2+.

NMR analysis established that a lack of Pmr1p leads to strong defects in the mannan synthesis through the decrease of terminal Man(α-1,3) capping, the decrease of side chains (α-1,2) mannosylation and the increase of the proportion of unbranched 6)Man(α-1,6). These characteristics should result in the change of mannan size. In order to determine the average size of mannan domain of *N*-glycans, we quantified Man and GlcNAc residues in all samples by GC/MS analysis, and deduced the average number of mannose per *N*-glycan based on the presence of the chitobiose core. As shown in Fig. 3B, *N*-glycans isolated from WT and *gdt1Δ* strains grown in normal conditions contained an average of 220-250 Man residues. However, we observed that the size of mannan domain of gdt1Δ strain under Ca2+ , as well as pmr1Δ and gdt1Δpmr1Δ strains in normal conditions and under Ca2+ are drastically reduced (Fig. 3A) down to about 40 Man residues. Under Mn2+ supplementation, the size of mannans from pmr1Δ and

gdt1Δpmr1Δ was restored to average sizes. Altogether, structural analysis by NMR and GC/MS showed that the glycosylation defects are due to a reduced synthesis of -2)Man(α-1,2) side chains that results in the synthesis of polymannosylated *N*-glycans of smaller size compared to that of WT strains. This suggests that a lack of pmr1 and/or gdt1 would affect late Golgi glycosyltransferases such as MMN2/ MNN5/ MNN1. Altogether, these results demonstrate (i) the crucial requirement of Gdt1p in maintaining Golgi glycosylation when cells are cultured in presence of Ca2+ and (ii) that the suppression of the glycosylation defect by the Ca2+ in pmr1Δ strains is strictly dependent on the activity of Gdt1p.

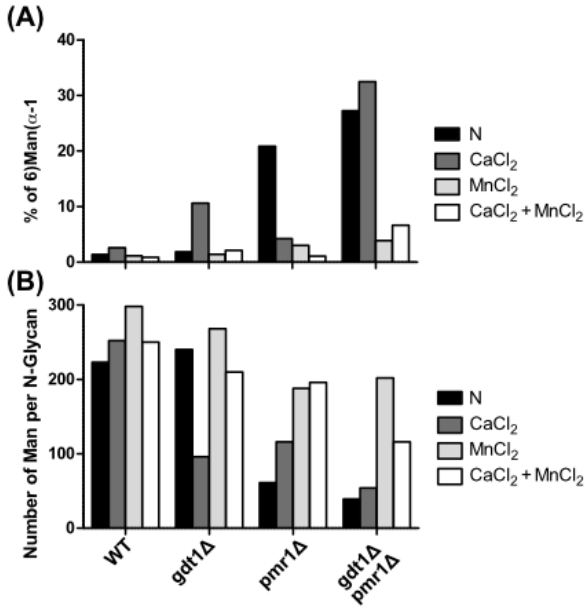

Figure 3: Comparison of mannans isolated from yeasts grown in various conditions: N, non-supplemented; CaCl2, supplemented with 0.5M CaCl2; MnCl2, supplemented with 0.05mM MnCl2; CaCl2+MnCl2, supplemented with CaCl2 0.5M and MnCl2 0.05mM. (A) The branching pattern of the 1,6-linked mannan backbone is expressed as the proportion of 6)Man(α-1,6) residues in mannans and calculated from the relative integration of signal V from 1H-NMR spectra (see Supp Fig. 1). Its increases is indicative a defect in the synthesis of 2)Man(α-1,2) side chains. (B) The overall size of mannans was established as a number of mannose residues per *N*-glycans. The reduction in the size of mannans correlates with the defect in the synthesis of 2)Man(α-1,2) side chains.

3.3. The abundance and function of Gdt1p in glycosylation is dependent on the Prm1p function

To further investigate the contribution of Ca2+ *versus* Mn2+ transport activity of Pmr1p to the observed N-glycosylation defect, we first transfected *PMR1*-deficient cells with three point mutants of Pmr1p that were defective for transport of either Ca2+ ions (Pmr1pD53A), Mn2+

ions (Pmr1pQ783A) or both (Pmr1pD778A) (Wei et al. 1999; Mandal, Woolf, and Rao 2000). Although both Pmr1pD53A and Q783A can suppress the observed initial glycosylation defect, differences can be observed (Fig. 4A). The restoration is total with Prm1pWT and the Pmr1pD53A and only partial with the Pmr1pQ783A (Fig. 4A, left panel). To assess the potential role of Gdt1p in this glycosylation rescue, *gdt1Δpmr1Δ* strains were transfected with the same Pmr1p mutants. While the expression of the D53A completely restored the glycosylation, the Q783A clearly did not (Fig. 4A, right panel). To confirm these results, the invertase mobility in the *pmr1Δ* and *gdt1Δ*/*pmr1Δ* double knock- out strains transfected with the Pmr1pQ783A in the presence of increasing Ca2+ concentrations was evaluated. In the *pmr1Δ* yeast strains transfected with the pmr1Q783A, the invertase mobility is strongly reduced both in absence of Ca2+ and under increasing Ca2+ concentrations (Fig. 4B, left panel). We demonstrated that this effect was due to the activity of Gdt1p, as the Ca2+ treatment in the *gdt1Δ*/*pmr1Δ* double knock-out strains transfected with the pmr1Q783A does not suppress the observed glycosylation defect (Fig 4B, right panel). We then wondered whether the suppression of the glycosylation defect in *pmr1Δ* strains supplemented with Ca2+ could result from Gdt1p expression changes. The cellular abundance of Gdt1p was then evaluated by Western blotting using specific antibodies directed against Gdt1p in *pmr1Δ* strains, transfected or not with the different Pmr1p mutants defective for transport of either Ca2+ ions (Pmr1pD53A), Mn2+ ions (Pmr1pQ783A) or both (Pmr1pD778A). This experience showed that the abundance of Gdt1p was directly linked to the transport function of Pmr1p. In *pmr1Δ*, the abundance of Gdt1p was greatly reduced (-80% compared to WT) (Fig. 4C). Remarkably, the expression of Pmr1Wt in *pmr1Δ* strains greatly restored the Gdt1p abundance. Interestingly, while the expression of the Pmr1pD53A also completely rescue the Gdt1p level, the two other Pmr1p mutants (Q783A and D778A) had no effects on Gdt1p abundance (Fig. 4C). A slight rescue can be seen with the Pmr1pQ783A mutant. These results then proves that the abundance of Gdt1p is dependent of the transport function of Pmr1p and are in accordance with those obtained recently (Potelle et al. 2017) where we highlighted that the abundance of Gdt1p was greatly reduced in response to Mn2+. To go further, we then evaluated the total cellular Mn2+ concentration in the different yeast strains under different conditions by ICP-MS. While under physiological conditions the total cellular Mn2+ concentration is similar in the different mutants, a huge increase is observed followed Mn2+ supplementation in all investigated mutants compared to WT (Fig 4D). After Mn2+ supplementation, a 10-fold increase in Mn2+ concentration is observed in the *gdt1Δ*/*pmr1Δ* double knock-out mutant, a 5 fold increase in the *pmr1Δ* mutant and a 2 fold increase in the

gdt1Δ mutant. These results support the fact that both Prm1 and Gdt1 are involved in total cellular Mn2+ homeostasis.

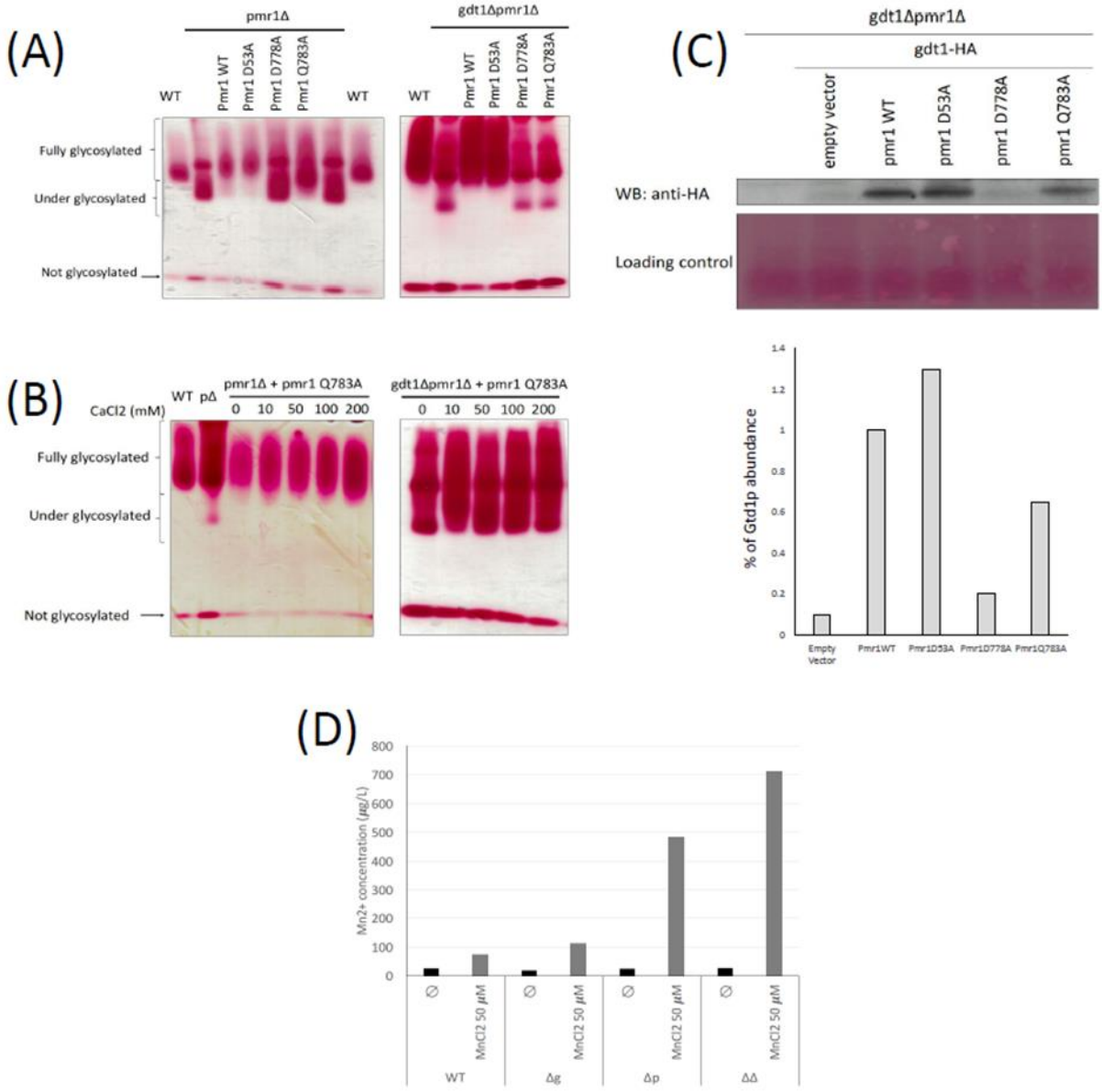

Figure 4: **The function and abundance of Gdt1p in glycosylation is dependent on the Prm1p function** (A) The Glycosylation defect in pmr1p mutants depends on its function. Pmr1Δ and gdt1Δpmr1Δ strains were transformed with pRS41N-pmr1p mutants (pmr1p-WT, pmr1p-D53A, pmr1p-D778A and pmr1p-Q783A). Yeasts were grown in YPR media and N-glycosylated invertase profile was performed (B) Ca2+ uptake by pmr1p influences the Mn2+ uptake by Gdt1p. Yeasts were grown in YPR media supplemented with an increase of the indicated $CaCl_2$ concentrations in the medium and invertase profile was analyzed. (C) Abundance of Gdt1p depends on the Pmr1p function. *gdt1Δpmr1Δ* strains were transformed with pRS41H-Gdt1p-HA and with pRS41N-Pmr1p mutants (pmr1p-WT, pmr1p-D53A, pmr1p-D778A and pmr1p-Q783A). Yeasts were grown in YPD medium and GDT1 expression was performed by western Blot using an anti-HA. Quantification of Gdt1p protein after normalization on ponceau red (N = 3). (D) Cytosolic manganese detoxification needs Pmr1p. Wild-type (WT), *gdt1Δ*, *pmr1Δ* and *gdt1Δpmr1Δ* yeasts mutants were grown to an OD600 of 0.8 in a YPD medium and transferred to a media containing no Mn2+ or 50 μM MnCl2. Total Mn2+ concentrations were analyzed by ICP-MS. Quantification of the cellular Mn2+ concentration (N = 2).

Our results demonstrate that (i) the Golgi glycosylation defect observed in pmr1 deficient cells result from a lack of Golgi intraluminal Mn2+, (ii) that the rescue of the glycosylation defect in *pmr1Δ* strains by the intraluminal Golgi Ca2+ requires the activity of Gdt1p.

3.4. Acidic residues of the conserved motifs of Gdt1p are involved in Golgi glycosylation

As previously published (Foulquier et al. 2012; Demaegd et al. 2014; Dulary et al. 2016), members of the UPF0016 family contain two highly conserved consensus motifs E-ϕ-G-D-[KR]-[TS], predicted to be involved in the transport function of UPF0016 members. Recently these motifs have been shown to be part of the regulatory Ca2+ binding domains. In order to evaluate the importance of these two motifs in the maintenance of Golgi glycosylation homeostasis, mutated versions of Gdt1p have been generated (E53G, D56G, E204G and D207G) and used to complement the observed glycosylation defect in *gdt1Δ* strains cultured in presence of high Ca2+ concentrations. Interestingly none of the mutated Gdt1p, except L205W mutation, complements the observed glycosylation defect demonstrating that these acidic amino acids are essential for the function of Gdt1p in Golgi glycosylation (Fig. 5). We then wondered whether the activity of Gdt1p was required in the case where Prm1p would only transport Mn2+. For that, the same mutated versions were expressed in *gdt1Δ*/*pmr1Δ* strains transformed with Pmr1pD53A and the invertase mobility was followed. As shown in figure 5, the glycosylation was completely restored for all the mutated versions of Gdt1p, demonstrating that Gdt1p is dispensable when Prm1p exclusively transports Mn2+. Similar experiment was then performed in *gdt1Δ*/*pmr1Δ* strains transformed with Pmr1pQ783A. Although the expression of Gdt1p wt partially rescues the invertase glycosylation defect, none of the mutated version suppresses the glycosylation defect (Fig. 5). This result clearly demonstrates that the requirement of Gdt1p for Golgi glycosylation then depends on the nature of the ion transported by Pmr1p.

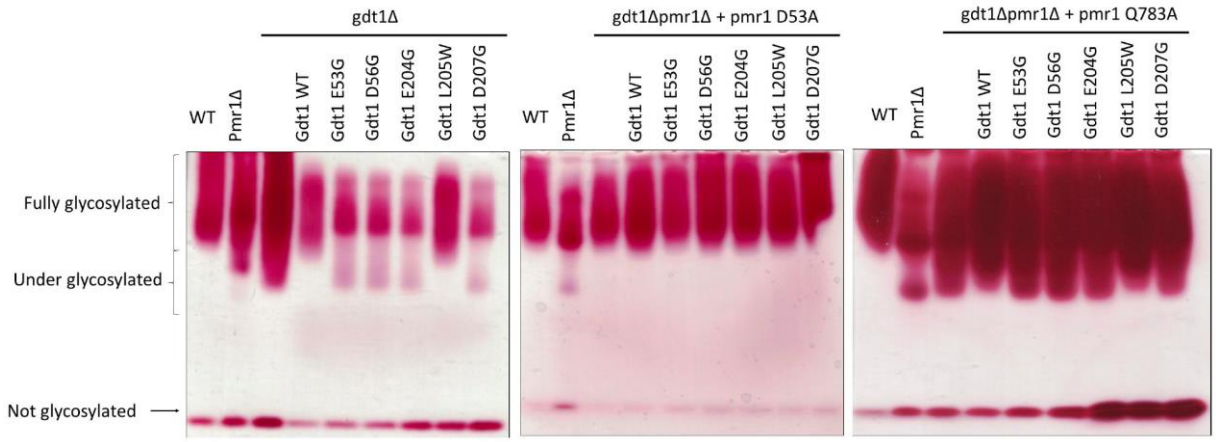

Figure 5: **Acidic residues of the conserved motifs of Gdt1p are involved in Golgi glycosylation**. *gdt1Δpmr1Δ* strains were transformed with pRS41N-pmr1pD53A (left panel) and pRS41N-pmr1p- Q783A (middle panel) and with pRS41H-gdt1p mutants (Gdt1p-E53G, Gdt1p-D56G, Gdt1p-E204G, Gdt1p-L205W and Gdt1p-D207G). Yeasts were grown in YPR medium. *gdt1Δ* strains were transformed with pRS41H-gdt1p mutants (Gdt1p-E53G, Gdt1p-D56G, Gdt1p-E204G, Gdt1p-L205W and Gdt1p- D207G) (right panel) and yeasts were grown in a YPR media supplemented with 200 mM CaCl2.

4. Discussion

The regulation of Ca2+ and Mn2+ concentration in the Golgi apparatus is crucial for many cellular processes particularly the secretion of proteins and the maintenance of Golgi glycosylation. One of the main supplier/regulator of Ca2+/Mn2+ Golgi homeostasis is the Golgi localized P-type ATPase Pmr1p. Our previous work raised the possibility that Gdt1p may also play a crucial role in Golgi ion homeostasis and Golgi glycosylation. Although the precise cellular function of Gdt1p in the Golgi remains unsolved, results cast doubt about its precise function in the transport substrates. In this work we show that Gdt1p is a functionally important Golgi protein playing a unique role in Golgi glycosylation. Compared to mammalian cells, yeasts further maturate the N-linked glycans with the addition of outer chains that may contain up to 300 mannose residues (Munro 2001). These hypermannosylated structures consists in a long backbone of α-1,6-linked mannose residues substituted with α-1,2-linked mannose residues themselves branched with terminal α-1,3-linked mannose residues. Many Golgi mannosyltransferase complexes are involved in generating these specific structures. In this paper we assessed and compared by using NMR the structural details of polymannan chains in the different yeast strains (*gdt1Δ*, *pmr1Δ* and *gdt1Δ*/*pmr1Δ* strains) under different conditions.

The NMR experiments showed strong alteration of the Golgi N-linked glycosylation in the different yeast strains under various conditions. While the backbone of α-1,6-linked mannose residues is not altered, strong defects in α-1,3- and α-1,2- branching are mainly observed in *gdt1Δ* strains cultured in presence of high Ca2+ concentration, *pmr1Δ* and *gdt1Δ*/*pmr1Δ* strains. We also confirmed that addition of Mn2+ was sufficient to completely restore the observed branching defects. Interestingly, our data clearly demonstrated that the suppression of the Golgi glycosylation defects by the Ca2+ in *pmr1Δ* yeast strains was dependent on the activity of Gdt1p. Based on the structural analysis of the polymannan chains, we deduced that the defects mainly affected medial and late Golgi glycosylation as only the α-1,2 substitution- and the α-1,3 termination are affected. This points toward an alteration of Mnn2p/ Mnn5p/ Mnn6p and/or Mnn1p activities. The α-1,6 initiation/ elongation seems not to be altered in our analysis. Taken together, our structural analysis data showed Gdt1p as well as Prm1p to be critical participants in medial and late Golgi glycosylation functions.

The identity of Gdt1p as a potential Golgi transporter controlling both Golgi Ca2+/ Mn2+ homeostasis arose from our studies and others (Colinet et al. 2016; Dulary et al. 2016; Potelle et al. 2016). In this work we further evaluated the potential role of Gdt1p in importing Mn2+ from the cytosol to the Golgi lumen. As first pointed by us (Foulquier et al. 2012) and others (Demaegd et al. 2014; Schneider et al. 2016; Brandenburg et al. 2017) members of the UPF0016 family contain two highly conserved consensus motifs E-ϕ-G-D-[KR]-[TS], predicted to be involved in the transport function of UPF0016 members. Our results show that mutations of the acidic amino acids of these two conserved motifs (E53A, D56A, E204A and D207A) completely abolish the suppression of the glycosylation defect. Interestingly, we demonstrated that an active form of Gdt1p was exclusively required in case where Prm1p mainly transports Ca2+. When Pmr1p mainly imports Mn2+ inside the Golgi lumen, our results show that Gdt1p is completely dispensable for the Golgi glycosylation. We propose that these amino acids constitute the cation binding sites of Gdt1p (one for Ca2+ and one for Mn2+). We can assume that mutations in any of these amino acids completely abolish the transport function of Gdt1p by impairing cation affinity or conformation changes of the pocket.

Moreover, the use of different Pmr1p mutants defective for transport of either Ca2+ ions (Pmr1pD53A), Mn2+ ions (Pmr1pQ783A) or both (Pmr1pD778A) (Wei et al. 1999; Mandal, Woolf, and Rao 2000) showed that the observed Golgi glycosylation defect in the *gdt1Δ*/*pmr1Δ* strains only resulted from a lack of intraluminal Golgi Mn2+ and not Ca2+. Our data suggest that

the activity of Gdt1p in Golgi glycosylation becomes essential only when Prm1p transports Ca2+. It should also be noted that the suppression of the glycosylation defect is more efficient in *pmr1Δ* strains complemented with Pmr1pQ783A under Ca2+ supplementation. Given the fact that the observed Golgi glycosylation defect was due to a lack of intraluminal Golgi Mn2+, our results strongly suggest that when Pmr1p only transports Ca2+ from the cytosol to the Golgi lumen, Gdt1p is necessary to import Mn2+ inside the Golgi lumen by exchanging Ca2+. This model also explain why high environmental Ca2+ concentrations in *gdt1Δ* would lead to strong N-glycosylation deficiencies. When cytosolic Ca2+ concentration increases, Pmr1p favors the transport of Ca2+ in place of Mn2+. The Golgi luminal pool of Mn2+ is then rapidly depleted if Gdt1p is not there to efficiently import Mn2+ inside the Golgi lumen. Given the fact that a lack of Pmr1p leads to strong Golgi glycosylation defects, our results suggest that in physiological conditions, Pmr1p preferentially import Mn2+ rather than Ca2+ into the Golgi lumen. In such conditions, the role of Gdt1p, at least in Golgi glycosylation, is completely dispensable. Would that suggest that Gdt1p use the Golgi Mn2+ gradient generated by Pmr1p to import cytosolic Ca2+ inside the Golgi lumen? The question is completely open. As many antiport transporters can work in reverse if the gradient concentration of the driving ion is reversed, we can reasonably postulate that Gdt1p may also work in both directions. As our results show that the requirement of Gdt1p in Golgi glycosylation depends on the nature of the ion transported by Pmr1p, we then propose that Gdt1p would be the leak channel of Pmr1p.

Figure 6: **Hypothesis on the role of Gdt1p in ion homeostasis.** In this model, Gdt1p would be a Mn2+/Ca2+

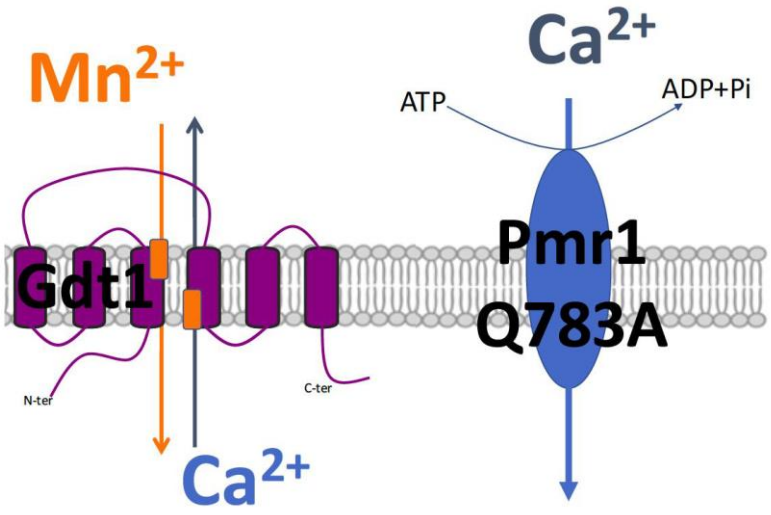

antiporter whose function depends on Pmr1p. When Pmr1p would import Ca2+ to the Golgi lumen, Gdt1p would import Mn2+ by exporting Ca2+.

5. Acknowledgements

This work was supported by grants from Agence Nationale de la Recherche (SOLV-CDG project to F.F.), Mizutani Grant (to F.F.) and EURO-CDG-2 that has received funding from the European Union's Horizon 2020 research and innovation program under the ERA-NET Cofund action N° 643578. We are also indebted to Dr Dominique Legrand for the Research Federation FRABio (Univ. Lille, CNRS, FR 3688, FRABio, Biochimie Structurale et Fonctionnelle des Assemblages Biomoléculaires) for providing the scientific and technical environment conducive to achieving this work.

6. Conflict of interests

None.

7. References

[1] F. Foulquier, M. Amyere, J. Jaeken, R. Zeevaert, E. Schollen, V. Race, R. Bammens, W. Morelle, C. Rosnoblet, D. Legrand, D. Demaegd, N. Buist, D. Cheillan, N. Guffon, P. Morsomme, W. Annaert, H.H. Freeze, E. Van Schaftingen, M. Vikkula, G. Matthijs, TMEM165 deficiency causes a congenital disorder of glycosylation, Am. J. Hum. Genet. 91 (2012) 15–26. doi:10.1016/j.ajhg.2012.05.002.

[2] D. Demaegd, F. Foulquier, A.-S. Colinet, L. Gremillon, D. Legrand, P. Mariot, E. Peiter, E. Van Schaftingen, G. Matthijs, P. Morsomme, Newly characterized Golgi-localized family of proteins is involved in calcium and pH homeostasis in yeast and human cells, Proc. Natl. Acad. Sci. U. S. A. 110 (2013) 6859–6864. doi:10.1073/pnas.1219871110.

[3] A.-S. Colinet, P. Sengottaiyan, A. Deschamps, M.-L. Colsoul, L. Thines, D. Demaegd, M.-C. Duchêne, F. Foulquier, P. Hols, P. Morsomme, Yeast Gdt1 is a Golgi-localized calcium transporter required for stress-induced calcium signaling and protein glycosylation, Sci. Rep. 6 (2016) 24282. doi:10.1038/srep24282.

[4] S. Potelle, W. Morelle, E. Dulary, S. Duvet, D. Vicogne, C. Spriet, M.-A. Krzewinski- Recchi, P. Morsomme, J. Jaeken, G. Matthijs, G. De Bettignies, F. Foulquier, Glycosylation abnormalities in Gdt1p/TMEM165 deficient cells result from a defect in Golgi manganese homeostasis, Hum. Mol. Genet. 25 (2016) 1489–1500. doi:10.1093/hmg/ddw026.

[5] S. Potelle, E. Dulary, L. Climer, S. Duvet, W. Morelle, D. Vicogne, E. Lebredonchelle, M. Houdou, C. Spriet, M.-A. Krzewinski-Recchi, R. Peanne, A. Klein, G. DE Bettignies, P. Morsomme, G. Matthijs, T. Marquardt, V. Lupashin, F. Foulquier, Manganese-induced turnover of TMEM165, Biochem. J. (2017). doi:10.1042/BCJ20160910.

[6] A. Schneider, I. Steinberger, A. Herdean, C. Gandini, M. Eisenhut, S. Kurz, A. Morper, M. Hoecker, T. Rühle, M. Labs, U.I. Flügge, S. Geimer, S.B. Schmidt, S. Husted, A.P.M. Weber, C. Spetea, D. Leister, The Evolutionarily Conserved Protein PHOTOSYNTHESIS AFFECTED MUTANT71 is Required for Efficient Manganese Uptake at the Thylakoid Membrane in Arabidopsis, Plant Cell. (2016) tpc.00812.2015. doi:10.1105/tpc.15.00812.

[7] F. Brandenburg, H. Schoffman, S. Kurz, U. Krämer, N. Keren, A.P.M. Weber, M. Eisenhut, The Synechocystis Manganese Exporter Mnx Is Essential for Manganese Homeostasis in Cyanobacteria, Plant Physiol. 173 (2017) 1798–1810. doi:10.1104/pp.16.01895.

[8] S. Munro, What can yeast tell us about *N* -linked glycosylation in the Golgi apparatus?, FEBS Lett. 498 (2001) 223–227. doi:10.1016/S0014-5793(01)02488-7.

[9] E. Vinogradov, B. Petersen, K. Bock, Structural analysis of the intact polysaccharide mannan from Saccharomyces cerevisiae yeast using 1H and 13C NMR spectroscopy at 750 MHz, Carbohydr. Res. 307 (1998) 177–183.

[10] Y. Wei, V. Marchi, R. Wang, R. Rao, An N-terminal EF hand-like motif modulates ion transport by Pmr1, the yeast Golgi Ca(2+)/Mn(2+)-ATPase, Biochemistry (Mosc.). 38 (1999) 14534–14541.

[11] D. Mandal, T.B. Woolf, R. Rao, Manganese selectivity of pmr1, the yeast secretory pathway ion pump, is defined by residue gln783 in transmembrane segment 6. Residue Asp778 is essential for cation transport, J. Biol. Chem. 275 (2000) 23933–23938. doi:10.1074/jbc.M002619200.

[12] D. Demaegd, A.-S. Colinet, A. Deschamps, P. Morsomme, Molecular evolution of a novel family of putative calcium transporters, PloS One. 9 (2014) e100851. doi:10.1371/journal.pone.0100851.

[13] E. Dulary, S. Potelle, D. Legrand, F. Foulquier, TMEM165 deficiencies in Congenital Disorders of Glycosylation type II (CDG-II): Clues and evidences for roles of the protein in Golgi functions and ion homeostasis, Tissue Cell. (2016). doi:10.1016/j.tice.2016.06.006.

Supplementary figures

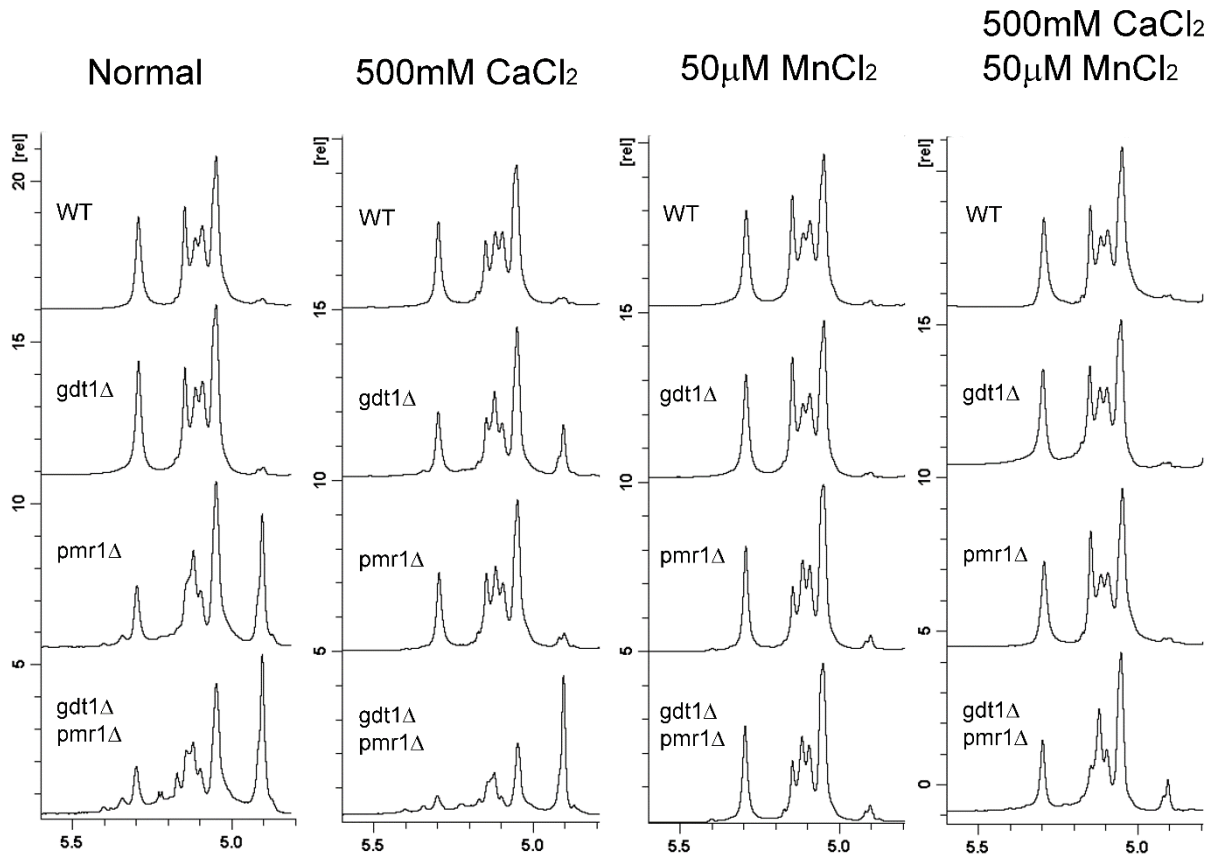

Supplementary Figure 1: Comparison of the anomeric regions of 1H-NMR spectra from WT, gdt1Δ, pmr1Δ and gdt1Δ/pmr1Δ strains in various conditions (0.5M CaCl2, 0.05mM MnCl2; CaCl2 0.5M and MnCl2 0.05mM).